Stony Brook University

Physiological, Histological, and Mechanical Characteristics of

Selected Epaxial Muscles in Primates

A Dissertation Presented

by

Md. Emranul Huq

to

The Graduate School

in Partial Fulfillment of the

Requirements

for the Degree of

Doctor of Philosophy

in

Anthropology

(Physical Anthropology)

Stony Brook University

August 2013

Stony Brook University

The Graduate School

Md. Emranul Huq

We, the dissertation committee for the above candidate for the

Doctor of Philosophy degree, hereby recommend

acceptance of this dissertation.

John G. Fleagle, Ph. D. (Dissertation Advisor)
Professor, Department of Anatomical Sciences

William L. Jungers, Ph. D. (Chairperson of Defense)
Professor, Department of Anatomical Sciences

Jack T. Stern, Jr., Ph. D. (Member)
Professor, Department of Anatomical Sciences

Andrea B. Taylor, Ph. D. (Outside Member)
Associate Professor, Department of Community and Family Medicine
Duke University

Christine E. Wall, Ph. D. (Outside Member)
Associate Research Professor, Department of Evolutionary Anthropology
Duke University

This dissertation is accepted by the Graduate School

Charles Taber
Interim Dean of the Graduate School

Abstract of the Dissertation

Physiological, Histological, and Mechanical Characteristics of

Selected Epaxial Muscles in Primates

by

Md. Emranul Huq

Doctor of Philosophy

in

Anthropology

(Physical Anthropology)

Stony Brook University

2013

The spine is the central element of the locomotor skeleton, acting as a link between the head and limbs. However, despite well-documented differences in spinal morphology among primates, we have comparatively little quantitative documentation on the structural characteristics of muscles that move the spine. The primary goals of this investigation were: (i) to identify and characterize morphological and related physiological, histological, and mechanical aspects of selected epaxial muscles in two groups of related but behaviorally distinct primates; and (ii) to investigate if these features could be interpreted in terms of the degree of spinal mobility during locomotion.

To these ends, thoracic and lumbar segments of three epaxial muscles (iliocostalis, longissimus, and multifidus) were examined for physiological and histological differences in two pairs of primates: (a) *Galago senegalensis* vs *Nycticebus coucang*, and (b) *Chlorocebus aethiops* vs. *Erythrocebus patas*. In pair (a), *G. senegalensis* are habitual leapers, while *N. coucang* are

cautious arboreal quadrupeds. In pair (b), *E. patas* are terrestrial quadrupeds; while *C. aethiops* engage in both terrestrial and arboreal quadrupedalism. Physiological and histological parameters studied were: (i) muscle mass, (ii) angle of pinnation, (iii) fiber length, (iv) tendon length, (v) potential excursion of muscle (*h*), (v) physiological cross-sectional area (PCSA), and (vi) fiber type. Mechanical differences in muscles were studied by investigating characteristics of bony lever arm of lumbar vertebrae of each species.

The results indicate that within the first pair, epaxial muscles of the leaper (*G. senegalensis*) are physiologically and histologically designed for generating high contraction velocity (important for rapid back extension during leaping); while the muscles of the slow-moving *N. coucang* are adapted for postural and stabilizing purposes. Differences in bony lever arm also support these observations. Within the second pair, muscles of *C. aethiops* are physiologically suited for generating higher force relative to those of *E. patas*. Histologically and mechanically, however, muscles of *C. aethiops* are adapted for producing high contraction velocity (relative to those of *E. patas*) required for rapid back extension. These differences can possibly be explained by differences in the respective positional behaviors of the two monkeys.

In sum, these results indicate that differences in spinal mobility pattern are reflected in structural characteristics of epaxial muscles. Future work will focus on more fine-grained analyses of the locomotor role of spine in primates, including in vivo muscle recruitment patterns.

For my mother and father

Table of Contents

List of Tables

Chapter 2

Chapter 3

List of Figures

Chapter 1

Chapter 2

Appendix

Acknowledgments

It is rare for the fruits of one's labor to be the result of a singular effort, and this dissertation is no exception either. A special gratitude is due to the Stony Brook Interdepartmental Doctoral Program in Anthropological Sciences for the incredible learning facility the faculty has created – nowhere could I have learnt better.

First and foremost, I give endless thanks to my advisor Dr. John Fleagle. He was incredibly generous with his time, and I never would have made it through without his help. Throughout my graduate career, he provided support and encouragement during my times of need. I admire him greatly for his intellect, patience, sense of humor, and an uncanny ability to see the big picture at all times. His perspective has helped me pull out of the minutiae on numerous occasions.

I am also indebted to other members of my committee. Dr. Bill Jungers pointed out important statistical and methodological issues, and suggested how to resolve them. He also let me borrow specimens from his private cadaver collection. Dr. Jack Stern spent long hours discussing and explaining details of muscle structure and mechanics. One could not have learnt from a better teacher; and I am grateful to him for reading several drafts of this dissertation, and providing incisive comments. Drs. Andrea Taylor and Chris Wall, my external committee members, held my hands and guided me through data collection at Duke University, and later with the analyses. They also made critical and cogent suggestions to improve my arguments.

My data collection was made possible through the generosity of many individuals. Dr. Fred Anapol (University of Wisconsin – Milwaukee) allowed me to dissect and collect tissues from his collection of cercopithecoid monkeys. Thanks are also due to Linda Gordon (US

National Museum of Natural History), Terry Kensler (Laboratory of Primate Morphology and Genetics, Caribbean Primate Research Center, University of Puerto Rico), Eileen Westwig (American Museum of Natural History), and Dr. Sarah Zehr (Duke Lemur Center) for providing access to specimens. The immunohistological data could not have been collected without the help of Dr. Zuowei Su (Immunohistochemical Laboratory, Dept. of Pathology, Duke University Medical Center). A very special "thank you" goes to Jean Moreau for the countless number of times she has helped me with daunting paperwork and for her reliable smile.

Many friends have supported me during tough times. Ian Wallace and Justin Ledogar helped me survive through the gross anatomy of fall 2007; our joint review sessions were the most enjoyable passages of time I have had at the Stony Brook University. Justin Ledogar was my "muse"; in fact, the inspiration for this dissertation came during one of our conversations. I am also grateful to Ari Grossman, Mark Coleman, Biren Patel, Jonathan Perry, Justin Hall, Anne Su, Andrea Baden, Amanda Kingston, Stephanie Maiolino, Rachel Jacobs, Joseph Sertich, Ashley Gosselin-Ildari, Sara Burch, Kyle Viterbo, Nicholas Holowka, Allison Nesbitt, and Nate Thompson. My "inner circle" of friends in Bangladesh, Adnan Hossain, Ruhul Quddus, and Muhibullah Tanvir; as well as Siddharth Satpathy, April Manalang, and Kelly Reeve have been loyal all along. The company of Bangladeshi graduate students at the Stony Brook University helped me keep my spirits up through various ups and downs.

Last but not the least, my parents, especially my father who did not live long enough to see through the completion of this degree, have endured enormous stress and sacrifice to help me succeed. Words cannot do justice to their contributions. They also had to deal with my characteristic stubbornness. Yet, they supported me through thick and thin, and never forced me to do anything against my wish.

This research was supported by the Stony Brook University, the L. S. B. Leakey Foundation, the Turkana Basin Institute, the US National Institutes of Health (grant # R24 HD050837-01 to Andrea B. Taylor), and the US National Science Foundation (grants # BCS-0452160 to Andrea B. Taylor, and BCS-0094522 to Christine E. Wall). The Caribbean Primate Research Center is supported by the US National Institutes of Health (grant # 8 P40 OD012217-2).

Chapter 1

Introduction

1.1 Form, function, and adaptation

The study of the relationship between form and function, or functional morphology, has long been of interest to anthropological investigators. Within functional morphology, the terms "form" and "function" are heuristic devices that allow the separation of phenomena that are inextricably linked within an organism. In general, "form" refers to shape and size, while "function" refers to how a particular form moves itself and interacts with its surroundings. However, these two definitions do not have any real context unless they are applied to a specific problem involving an organism or a group of organisms (Wainright, 1988).

The relationship between form and function is usually discussed in the context of adaptation. For example, how an organism interacts with and manipulates its surroundings could be used as a measure of individual adaptation. Few topics in functional morphology are as controversial as adaptation (Stern, 1970; Ross et al., 2002). In a very narrow sense, adaptations are phenotypic attributes of organisms that have current utility, that evolved by natural selection to perform their current function, and that are maintained in their lineages by natural selection (e.g., Williams, 1966; Sober, 1984; Coddington, 1988; Baum and Larson, 1991; Harvey and Pagel, 1991). Lauder (1996), for example, defined adaptation as a trait that "enhances fitness and that arose historically as a result of natural selection for its current biological role." A wider, more inclusive approach is to consider adaptation as a trait with a current utility, and that increases the adaptedness (fitness) of its possessor (Bock and von Wahlert, 1965; Kay and Cartmill, 1977; Bock, 1980; Fisher, 1985; Reeve and Sherman, 1983; Anthony and Kay, 1993). Such traits presumably arise through natural selection. Building on these ideas, and extending

them, Brandon (1990) argued that the concept of adaptation should take into account (a) evidence of selection (i.e. whether there is differential reproduction); (b) ecological explanation for selection; (c) evidence of heritability; (d) population structure and gene flow; and (e) phylogeny (i.e. what evolved from what).

In a (living) taxon, the hypothesis that a trait is an adaptation for a specific function can be examined by determining whether the trait actually performs that function, as manifested in an organism's behavior. This approach has been used frequently in the study of primate adaptations (Lockwood and Fleagle, 1999; Ross et al., 2002), and has also been applied to test hypotheses regarding the evolution of specific traits to subsequent adaptive radiations (Farrell, 1998; Hunter and Jernvall, 1995).

One application of this approach explores the relationship between musculoskeletal form and positional behavior. Musculoskeletal morphologies in extant species are products of long and complex interactions of evolutionary changes, developmental processes, and daily activities. It is not easy to determine the extent of individual contributions of these factors to the extant form, as they are interrelated parts of the total functional-morphological complex of an individual organism. Therefore, it is important to apply multiple techniques and perspectives to a specific problem.

As an order, primates engage in a variety of positional behaviors, viz. leaping, arboreal and terrestrial quadrupedalism, suspensory behavior, and bipedalism (Fleagle, 1999). Over the last several decades, functional studies of the musculoskeletal morphology of primate postcrania incorporating comparative anatomy, naturalistic observation, and various experimental approaches have become increasingly abundant (Fulton 1940; Howell 1944; Ankel, 1962; Avis, 1962; Hildebrand 1967; Napier and Napier, 1967; Ripley, 1967; Carpenter and Durham, 1969;

Stern, 1971; Grand, 1972, 1976, 1977, 1978, 1984; Tuttle, 1972; Wilson, 1972; Rose, 1973, 1974, 1993; Fleagle, 1977a, b, 1978; Kimura et al. 1979; Rodman, 1979; Fleagle and Mittermeier, 1980; Rollinson and Martin, 1981; Cant, 1986; Vilensky 1987, 1989; Vilensky et al. 1991; Anemone, 1993; Gál, 1993a, b; Gebo, 1993; Larson, 1993; Shapiro, 1993a; Demes et al. 1994; Dunbar, 1994; Gebo and Chapman, 1995; McGraw, 1996, 1998; Meldrum et al., 1997; Vilensky and O'Connor 1997; Dunbar and Badam, 1998; Larson 1998; Schmitt 1998; Cartmill et al. 2002; Schmitt and Lemelin 2002; Lemelin et al. 2003; Larson and Stern, 2006; Wallace and Demes, 2008). These analyses have been successful in documenting the complex relationship between musculoskeletal form and function within and among diverse group of extant primates, and have led to the acceptance of Oxnard's argument that "the locomotor behavior of an animal is, on a gross level, controlled by the anatomy of the animal" (1975). Such information also has been important in attempts to reconstruct the evolutionary development of the primate postcranial skeleton (e.g., MacLatchy et al., 2000; Bloch and Boyer, 2002; Pilbeam, 2004).

However, these analyses tend to be complicated by factors that are rather difficult to control experimentally. For example, the evolutionary history of the animal(s) studied must be taken into account, because the interaction between form and function is contingent upon the evolutionary background of the organism involved. Natural selection works only on the available materials. Purvis and Webster (1999) argued that variation must be analyzed within clades rather than between them. Comparison should be made between pairs of lineages that differ in the X-variable (in this case, positional behavior), and base such comparisons on phylogeny to control for the influence that phylogeny might have had on these comparisons (Purvis and Webster, 1999). An experimental approach for the study of comparative functional morphology that tries to control for the influence of phylogeny has been delineated by Fleagle (1979). Briefly, this

methodology calls for the careful and quantitative documentation of behavior and musculoskeletal morphology in phylogenetically closely related extant species. Their morphological differences are then to be compared and predictions be based on differences in their behaviors.

Traditionally, the study of functional morphology has primarily been based on analysis of musculoskeletal anatomy (see above for references). However, differences in positional behavior among animals, irrespective of phylogenetic relationship, may be due to morphological features that are less obvious than musculoskeletal characteristics. Such features are those that reflect the dynamics of physiological input to locomotor behavior, e.g. intramuscular, physiologically related morphology, and should be associated with an animal's behavior. If such features cannot be linked with behavior, then this must also be understood. Investigations addressing these issues have focused primarily on non-mammalian vertebrates (e.g., Edman, 1966; Willemse, 1977; Wineksi and Gans, 1984; Magid and Law, 1985) and non-primate mammals (e.g., Burke, 1981; Eisenberg, 1983; Bodine et al., 1987; Hoffer et al., 1987; Gordon et al., 1988; Bang et al., 2006), and to a lesser extent on primates (e.g., Fleagle, 1977a; Anapol and Jungers, 1986; Anapol and Barry, 1996; Organ et al., 2009; Organ, 2010).

The present study attempts to understand the functional morphology of selected intrinsic back muscles in two comparisons of related primate taxa. First, I will compare individuals from two strepsirrhine taxa – *Galago senegalensis* (lesser galago) and *Nycticebus coucang* (slow loris). These two forms are phylogenetically closely related, in that they both belong to the same infraorder (Lorisiformes) as well as superfamily (Lorisoidea); and are distinct from Malagasy strepsirrhines (Yoder et al., 2001; Grubb et al., 2003; Brandon-Jones et al., 2004; Masters et al., 2007; Harrison, 2010). However, they are characterized by quite dissimilar positional behavior,

G. senegalensis being a habitual leaper, while *N. coucang* a cautious arboreal quadruped, which also engages in anti-pronograde suspension and cantilevering (Napier and Walker, 1967; Charles-Dominique, 1977; Charles-Dominique and Bearder, 1979; Sellers, 1996; Nekaris, 2001; Nekaris and Stevens, 2007). In addition, I will also examine back muscles of two cercopithecine taxa – vervet (*Chlorocebus aethiops*) and patas (*Erythrocebus patas*) monkeys – more closely related species (compared to the strepsirrhines which belong to the same superfamily, the two cercopithecine species belong to the same tribe Cercopithicini) with more subtle differences in patterns of positional behavior (see Tosi et al., 2004, for a recent analysis of phylogenetic relationship between these two taxa). Patas monkeys are terrestrial quadrupeds, and vervets engage in both terrestrial and arboreal quadrupedalism (Hall, 1966; Rose, 1979, Gebo and Chapman, 1995). However, during terrestrial galloping, vervet monkeys are reported to exhibit a greater range of spinal movement in the sagittal plane to increase their hindlimb stride length, while patas monkeys have been described as more stiff-backed, but use their longer limbs to achieve the same goal (Vangor, 1979; Hurov, 1987).

1.2 Locomotion and spinal movement

The spine is the central element of the locomotor skeleton, acting as a partially flexible, partially rigid link between the head and limbs. The spine's important role in the locomotor system is attested by its morphological variation among primates that rely on different positional behaviors (Ankel, 1965, 1972; Benton, 1967, 1974; Clauser, 1975, 1980; Donisch, 1973; Erikson, 1960, 1963; Hurov, 1987; Jungers, 1984; Keith, 1902, 1923, 1940; Sanders, 1990, 1991; Schultz, 1938, 1961; Shapiro, 1993a; Slijper, 1946; Ward, 1990, 1993; Washburn and Buettner-Janusch, 1952). However, despite well-documented differences in spinal morphology among primates, we have comparatively little quantitative documentation of the functional role of spinal movement in primate locomotion (see Hurov, 1987; Demes et al. 1990; Vilensky et al. 1994; Schmidt and Fischer, 2000; Shapiro et al. 2001 for some important contributions). Most investigators of spinal kinematics have focused on non-mammalian vertebrates (e.g. Roos, 1964; Sukhanov, 1974; Carrier, 1990; Frolich and Biewener, 1992), while fewer comparative data are available for the mammals (but see Hildebrand, 1959; Gambaryan, 1974; Jenkins, 1974; English, 1980; Schilling and Fischer, 1999; and primate references above). This is surprising, given that an important characteristic of the evolution of mammalian locomotion was an increasing emphasis on sagittal plane, rather than lateral movements of the spine (Hildebrand, 1974).

For many mammals, sagittal bending of the spine increases stride length, particularly when asymmetrical gaits such as galloping are used at faster speeds (Hildebrand, 1959, 1974; Goslow et al. 1973; English, 1980; Hurov, 1987; Sargis, 2001). For example, Taylor (1978) noted that in dogs, a transition from trot to gallop would include an involvement of the bending trunk. Electromyography showed that the iliocostalis lumborum (in dogs) remained inactive at lower speeds, became active at slow gallop, and then went up with increasing acceleration

(Taylor, 1978). This pattern of muscle recruitment has also been supported by EMG data collected in cats (Carlson et al. 1979; English, 1980).

In primates, Hurov (1987) observed a somewhat similar phenomenon during galloping by vervets that used rapid sagittal movement of spine to make their strides longer. This pattern of spinal movement is quite distinct from that of other (non-mammalian) terrestrial tetrapods, which exhibit lateral bending during locomotion (Sukhanov, 1974; Carrier, 1990; Frolich and Biewener, 1992). This basic difference is well known, but studies of mammals, including primates, have also shown that there is variation in spinal flexibility across species, gaits, and speeds (e.g. Hildebrand, 1959; Goslow et al. 1973; English, 1980; Hurov, 1987). For example, Pridmore (1992) demonstrated that lateral bending of the trunk by the opossum (*Monodelphis domestica*) remains an important component of mammalian locomotion, especially at slower walking speeds.

Among arboreal mammals, sagittal flexion-extension of the spine is characteristic of habitual leapers, as this movement allows them to increase leap-length by extending the spine from its flexure at the beginning of take-off phase (as opposed to increasing stride length during running) (Sargis, 2001). Although quantitative data on the role of the spinal movement during leaping is lacking, this process (sagittal movement) has been qualitatively observed in a number of taxa, including primates, e.g. leaping galagines (Hall-Craggs, 1965; Jenkins, 1974; Bennet-Clark, 1977; Aerts, 1998; Sargis, 2001; James et al. 2007), colobine monkeys (Fleagle, 1977a) and pitheciine monkeys (Walker, 2005). On the other hand, arboreal mammals that prioritize cautious quadrupedalism (and possibly anti-pronograde suspension) over agile leaping tend to have a more stable spine, with the range of lateral flexion being greater than that of sagittal flexion (e.g., sloths, Straus and Wislocki, 1932; lorisines, Cartmill and Milton, 1977; Curtis,

1995; Shapiro and Demes, 1996; Shapiro et al., 2001; *Ptilocercus lowii*, Sargis, 2001). In fact, lorisines reportedly use lateral flexion of their spine to increase hindlimb stride length, and the prominence of lateral flexion increases at higher velocities in *Nycticebus coucang*, resembling a pattern seen in amphibians (Shapiro et al. 2001). It, therefore, appears that different taxa use different strategies for increasing their stride lengths. It is reasonable to expect that such variation in back movements will be reflected in the bony and muscular anatomy of the back.

1.3 Mechanical explanation of the role of spinal movement in leaping

Leaping is generally considered a hindlimb-driven locomotor behavior (e.g. for primates, see Hall-Craggs, 1965; Jouffroy et al. 1974; Demes et al. 1994, 1995, 1996, 1999, Aerts, 1998; for non-primate mammals, see Howell, 1932; Badoux, 1965; Alexander and Vernon, 1975; Biewener et al. 1981). Some investigators, however, have made qualitative observations on the movement of the back during leaping by primates (e.g. Hall-Craggs, 1965; Jouffroy et al. 1974; Walker, 2005). Hall-Craggs (1965) observed, for example, that the stance of *G. senegalensis* was a low-crouch, with its back flexed. The take-off phase began with a progressive extension of the back and the trunk. These movements were followed by extensions of the hindlimb segments, leading to an alignment of the trunk and hindlimb in the direction of the trajectory (Fig. 1).

Walker (2005) observed that at the preparatory phase of leaping, the white-faced saki, *Pithecia pithecia*, would lower its body into a crouch by limb and back flexion, to be followed by immediate extensions of the hindlimbs and back to initiate take-off. This extension would result in a highly angled body orientation, to be maintained throughout the take-off phase. At the completion of this phase, and with the body in the air, the hindlimbs would begin to flex. This flexion would continue until the body was tucked into a ball, with the back flexed and hindlimbs flexed at approximately 90^{o} at the hips and knees. As the monkey approached the landing target (midflight 2), an extension of the hindlimb would be immediately followed by an extension of the back. Finally, the animal would land on its hindlimb (Fig. 2).

This description shows that there are similarities between the leaping of *G. senegalensis* and *P. pithecia*, in that in both animals, a crouched stance (with the back flexed) is followed by an extension of the back at the beginning of the take-off phase. This particular movement of the back (flexion, followed by extension, aided by the extensor muscles; Hall-Craggs, 1965) would

be theoretically useful for the propulsive effort during take-off because it would increase the distance or the time for the epaxial muscular force to be applied; although as yet, no quantitative data exist to test this theory.

It should also be noted that *G. senegalensis* has been categorized as a vertical clinger and leaper (Napier and Walker, 1967; Gebo, 1987; Off and Gebo, 2005), and *P. pithecia* tends to take off from a vertically clinging position as well (Walker, 2005). Even when they are taking off from a vertical substrate, their take-off stance is typically a low-crouched position. In such a position, active spinal flexion by abdominal muscles against the resistance of spinal extensors does not take place. However, *P. pithecia* apparently rapidly extends its flexed back at take-off. On the other hand, Fig. 1 shows that rapid back extension (from a prior flexed position) occurs prior to hindlimb extension in the galago. In both cases, back extensor muscles would need to contract rapidly.

1.4 Comparative osteology

One common approach to the study of primate epaxial anatomy has been the measurement of vertebrae and the length of the spinal column to allow computation of a variety of indices that are variably indicative of differing locomotor propensities among closely related taxa (e.g., Schultz, 1938, 1961). Similarly, several workers have considered morphological features of vertebrae and the specificity of these features for particular modes of locomotion (e.g., Rockwell et al., 1938; Ankel, 1972; Rose, 1975; Shapiro, 1995; Organ, 2010). In fact, the differences in vertebral morphology between arboreal leapers and slow-moving arboreal quadrupeds have been relatively well-documented (Sargis, 2001; Shapiro et al. 2005; Shapiro, 2007). These features include differences in the height of the vertebral body, length of the spinous process, position and orientation of the transverse processes, and interzygapophyseal distance. Of interest is how specific characteristics such as these can affect the mechanics of load-bearing, flexibility, and muscle leverage and emphasize either the stabilizing or accelerating capabilities of the back, depending on the specific requirements of a particular behavioral adaptation (Pal and Routal, 1987; Johnson and Shapiro, 1998; Shapiro, 1993a, 1995, 2007; Shapiro and Simons, 2002; Shapiro et al, 2001, 2005). Interpretations derived from these studies have also been applied to fossil vertebral elements (e.g. Shapiro, 1993b; Ward, 1993), and have led to the elucidation of possible locomotor and postural characteristics of extinct primates, including hominins.

1.5 Comparative gross myology

To date, the gross morphological analyses of whole muscles in primates have been primarily concerned with comparative studies of muscle attachments and/or relative muscle weights (e.g. Fleagle, 1977a; Lemelin, 1995; Kumakura et al, 1996; but see Anapol, 1984; Anapol and Jungers, 1986; Anapol and Barry, 1996; Anapol and Gray, 2003; Organ et al., 2009, for some exceptions). Comparisons of the sites of muscle attachments allow comparisons of bony lever arms (the perpendicular distance from the line of action of a muscle to the joint) and some functional implications are possible. For example, small lever arms allow high average velocity of movement; somewhat larger lever arms allow the greatest power (Smith and Savage, 1956). This dichotomy is illustrated by Smith and Savage (1956) in a comparison of the propulsive musculature of cursorial and fossorial mammals. However, Stern (1974) also observed that muscles that were ideal for bringing the limb to a certain position in the least amount of time had substantially larger moment arms than muscles best designed for achieving high velocity of movement at the same position.

Relatively few studies have attempted to investigate the role of the back (and its muscles) in locomotion. In mammals, compared with lower vertebrates, lateral bending and rotation about the long axis of the body (i.e. spine) play a less important role during locomotion compared with limb movements, but still occur at slower and symmetrical gaits such as walk or trot (Gray, 1968; Gambaryan, 1974; Jenkins and Camazine, 1977; van de Graff et al., 1982; Pridmore, 1992; Schilling and Fischer, 1999). Spinal movements gain importance in mammals, however, during faster locomotion using asymmetrical gait (e.g., gallop) (Howell, 1944; Gray, 1968; Hildebrand, 1959; Gambaryan, 1974), during which they contribute about half the stance length (Fischer and Lehmann, 1998; Schilling and Fischer, 1999; Fischer et al., 2002). Smith and Savage (1956)

observed that in some cursorial mammals (e.g., some marsupials and insectivores, almost all rodents and carnivores, and suids and tragulids) adopting a “leaping gallop”, the vertebral column is flexible and the axial musculature plays an important part in leaping by extending the spine from its flexure. However, in mammals with a “horse gallop” (equids and larger ruminants), the spine is relatively rigid, and the axial musculature shows a marked reduction in fleshy elements and a better development of the tendinous ones. These muscles, therefore, are adapted for resisting tension than for shortening.

A number of investigators have measured weights of skeletal muscles (including epaxial ones) of primates and tried to relate them to the positional behavior and back movement. For example, the mass of the mm. erector spinae in the lumbar region is higher in the leaping monkeys relative to that in the arboreal quadrupedal ones (Fleagle, 1977a; Johnson and Shapiro, 1998). These authors have argued that leaping requires a capacity for powerful and flexible sagittal movement of the lumbar region, which would be facilitated by an enhanced mm. erector spinae group. Erector spinae is also particularly well-developed in the hamadryas baboon – a terrestrial quadruped. This feature most likely contributes to the sagittal motion which is required in the terrestrial, bounding-type locomotion characterizing these monkeys (Kumakura et al. 1996). On the other hand, erector spinae is poorly developed in spider monkeys, whose locomotor repertoire includes arboreal quadrupedalism, suspension, brachiation, and climbing (Fleagle, 1999). Clearly, powerful sagittal movement of the back is not a priority for this group of primates, which would explain the weaker structure of their epaxial muscles (Kumakura et al., 1996). Rather, they have relatively shorter, stiffer backs (Erikson, 1963).

1.6 Goals of the study

The primary goals of this study are: (i) to evaluate and compare morphological and related physiological, histological, and mechanical aspects of selected epaxial muscles in two groups of related but behaviorally distinct primates; and (ii) test functional hypotheses about the relationship between morphological (including myological and osteological) features of back muscles and spinal mobility during locomotion.

Iliocostalis, longissimus, and multifidus muscles will be studied. The morphological and mechanical differences among these muscles will be compared in two pairs of primate groups: (a) *Galago senegalensis* vs *Nycticebus coucang*, and (b) *Chlorocebus aethiops* vs. *Erythrocebus patas*. The two taxa in the first pair are phylogenetically closely related but exhibit divergent positional behavior – the former are slow-moving arboreal quadrupeds, while the latter are leapers (see above for references). The taxa in the second pair are also phylogenetically closely related, and they have similar positional behavior (terrestrial quadrupedalism; see above for references). However, there is a subtle difference in the back movement during locomotion between these two monkeys.

It has been argued that leaping involves powerful back extension (Shapiro et al. 2005). However, prior studies on primate leaping have related one or more morphological features (limb proportions, vertebral morphology, etc.) to behavioral considerations at a gross level (e.g. Fleagle, 1977a; Fleagle and Meldrum, 1988; Shapiro, 2007 and references therein), but usually to the exclusion of muscular morphology and physiology (but see Hall-Craggs, 1974; Fleagle, 1977a; Anapol, 1984; Anapol and Jungers, 1986 for notable exceptions). Studies on leaping kinematics tend to focus on the role of the appendicular skeleton as well as the force produced during various phases of the act of leaping (Demes et al. 1996, 1999). For the most part, studies

on primate leaping, working with the notion that leaping is a "hindlimb-driven" locomotor mode have concerned themselves with the role of hind limb. Conspicuously absent from these analyses of leaping is the role of the epaxial region, although several osteological (i.e. vertebral) correlates of leaping (e.g. the elongation of the lumbar segment of the spine, elongation of the spinous process, more lateral projection and greater ventral and cranial orientation of the lumbar transverse process; Shapiro, 2007) have been documented. These features supposedly promote spinal mobility along a sagittal plane, which is important for leaping because it requires rapid sagittal back movement (Fleagle, 1977a; Walker, 2005; Shapiro, 2007). The present study attempts to fill the void in the analysis of leaping in its comprehensive morphological treatment of the epaxial muscle structure and the inclusion of observations from the bony elements of the back (i.e. vertebrae) as a possible reflection of muscle use by the habitual leapers.

To this end, the epaxial musculature in leaping primates assumes a particular significance. It has been observed (Fleagle, 1977a) and speculated (Johnson and Shapiro, 1998) that the erector spinae in leaping primates exhibits relatively greater mass compared to that in the non-leaping ones. Because their function is to extend the spine, the epaxial muscles, therefore, constitute a useful group within which to study the interrelationship of structure and function.

The leaping taxon in this study is represented by *G. senegalensis*, which displays a "striking saltatory mode of progression (Hall-Craggs, 1974). The locomotor profile characteristics of this taxon are reflected by a number of gross anatomical features of its post-cranial musculo-skeletal anatomy, including low intermembral indices (forelimb/hindlimb ratios) (Napier and Walker, 1967); elongated tarsus (Morton, 1924); and relative hypertrophy of hindlimb muscles (quadriceps femoris and triceps surae groups; Hall-Craggs, 1974; Demes et al, 1998).

The choice of *N. coucang* for comparison with *G. senegalensis* is a result of both theoretical and practical considerations. The phylogenetic proximity between the two species (see above for references) is expected to reduce the "phylogenetic noise" that may obscure the true significance of the results of comparison by overestimating differences (e.g., Dolphin et al., 2000). Secondly, the differences in positional behavior between these two taxa are well-documented, and reflected in the locomotor skeleton of each of these two taxa (e.g. Fleagle, 1999). Thirdly, in contrast to the spine of the galagids, vertebral morphology of the lorisids facilitates enhanced stability in a sagittal plane (reduced range of flexion-extension), and relatively greater mobility in a coronal plane (greater range of lateral spinal movement, supposedly useful for bridging, climbing, and reaching) (Shapiro, 2007). These factors, therefore, provide an ideal opportunity to investigate the physiological, histological, and mechanical characteristics of the epaxial muscles in two closely related taxa, with known locomotor differences. This analysis is also expected to demonstrate the relationship between the relative degree of spinal mobility and morphological characteristics of muscles responsible for such mobility.

Compared to the straightforward locomotor differences between the leaping galago and the slow-moving loris, the distinction between *C. aethiops* and *E. patas* is less obvious. While both of these primates practice terrestrial quadrupedalism, their back function varies during locomotion. Hurov (1987) experimentally observed that during galloping, vervet monkeys employ sagittal back extension to increase their stride length, while longer limbs of patas monkeys help them achieve the same goal, without having to extend their spine (also Vangor, 1979). I, therefore, hypothesize that architectural, histological, and osteological characteristics of

the spine and its intrinsic muscles will reflect this difference in spinal movement pattern between these two monkeys.

The present study addresses the general question of how the underlying morphological parameters of muscles reflect their function(s) in an individual. Specific questions to be addressed are:

1) How are the varieties in architecture and histological properties observed among epaxial muscles associated with the range of spinal mobility?
2) Does the variation in leverage based on osteological measurements of vertebrae reflect differences in spinal mobility?

The following features will be examined:

- Muscle mass
- Angle of pinnation
- Fiber length
- Physiological cross-sectional area (PCSA)
- Fiber types
- Cranio-caudal length of the lumbar vertebral bodies
- Position and orientation (ventral/dorsal) of lumbar transverse processes
- Length of lumbar spinous processes
- Interzygapophyseal distance (cranio-caudal)

The functional implications of each of these variables, considered individually, are well-documented. For example, we can calculate the PCSA of muscles and infer their maximum capacity for force generation. Likewise, we have some insights into the osteological features that

reflect spinal mobility and muscle leverage. What is important to know, however, is how the various quantifiable aspects of muscle morphology are interrelated, if at all.

1.7 Significance of the study

Traditionally, considerations of primate epaxial anatomy have emphasized human morphology in an effort to understand the evolution of bipedalism. For example, a consideration of the axial region was a major point in Keith's (1923) argument that a common ancestry involving "brachiation" and "orthograde" posture could explain the morphological similarities between humans and other hominoids. Keith's work on vertebral morphology was a major contribution to research on evolutionary adaptation, but he did not take into account possible functional and morphological distinctions between orthogrady, brachiation, and bipedalism. Subsequent researchers have identified many important and functionally relevant distinctions in the vertebral anatomy among various groups of primates (e.g., Rockwell et al., 1938; Ankel, 1972; Rose, 1975; Pal and Routal, 1987; Shapiro, 1993a, 1995, 2007; Johnson and Shapiro, 1998; Shapiro and Simons, 2002; Shapiro et al, 2001, 2005; Sargis, 2001; Organ, 2010). As a result, we are now in a better position for elucidating the functional morphology and evolutionary development of the primate back; yet many questions remain unanswered.

Although all aspects of the vertebral musculoskeletal system are functionally important, the "-skeletal" half of the musculoskeletal system has received more attention relative to the complementary "muscular" part. A number of studies, however, have looked into the functional relationship between intrinsic back muscles and locomotion in mammals, including primates (e.g. Carlson et al, 1979; English, 1980; Taylor, 1978; Tokuriki, 1973a, b; Shapiro and Jungers, 1988, 1994). These studies support the idea that differences in the habitual gait of an animal may be reflected in the function of the epaxial muscles and thus have underscored the importance of these muscles in relation to locomotion.

However, these studies have their own limitations. While it has been acknowledged that "[t]he structure of … the spinal musculature will depend on the type of gait adopted" (Smith and Savage, 1956), the relationship between a certain locomotor mode and the particular morphological characteristics of the spinal musculature is not well understood. This problem is of critical importance, because the structural characteristics of the epaxial muscles are likely to reflect functional demands (Kumakura and Inokuchi, 1992). Likewise, the architectural and histochemical characteristics of this muscle group in relation to certain habitual locomotor mode (e.g. leaping) have not been adequately documented. Based on the observations on the architectural and histochemical differences in voluntary muscles in relation to their functions, we may expect to find well-defined (and differentiated) architectural configurations in the epaxial muscles of primates exhibiting widely divergent locomtor behavior (e.g., between leapers and cautious arboreal quadrupeds). Third, and related, the extent of spinal mobility in relation to habitual locomotion has rarely been quantified, which makes it difficult to draw meaningful conclusions about the former's impact on muscle properties. Even in those studies that attempted to test such relationships, muscles from homologous regions of the spinal column were not included, thus potentially limiting the utility of their conclusions. Finally, it has been argued that the evolution of habitual bipedalism in humans might have involved a modification in the architecture and mechanical properties of these muscles (Shapiro and Jungers, 1988). The present study is expected to contribute to our understanding of the anatomy and function of the epaxial muscles in relation to positional behavior.

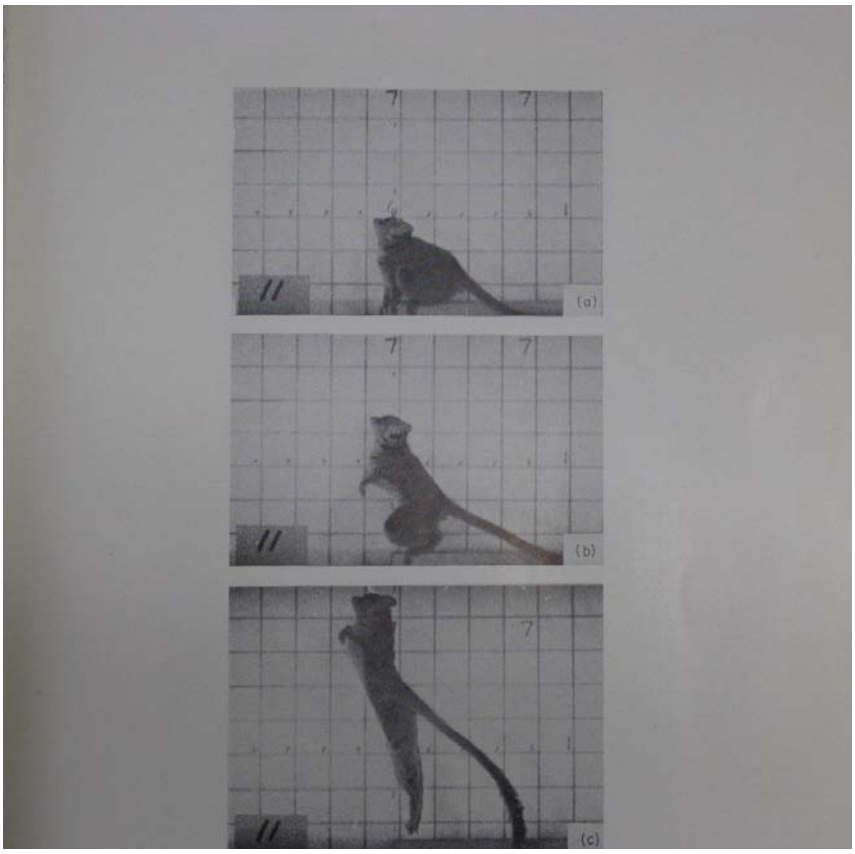

Fig. 1: The leap of *Galago senegalensis*: (top) the preparatory crouch; (middle) the extension of the back; (bottom) the alignment of the trunk and hindlimbs as the animal takes-off (Hall-Craggs, 1965).

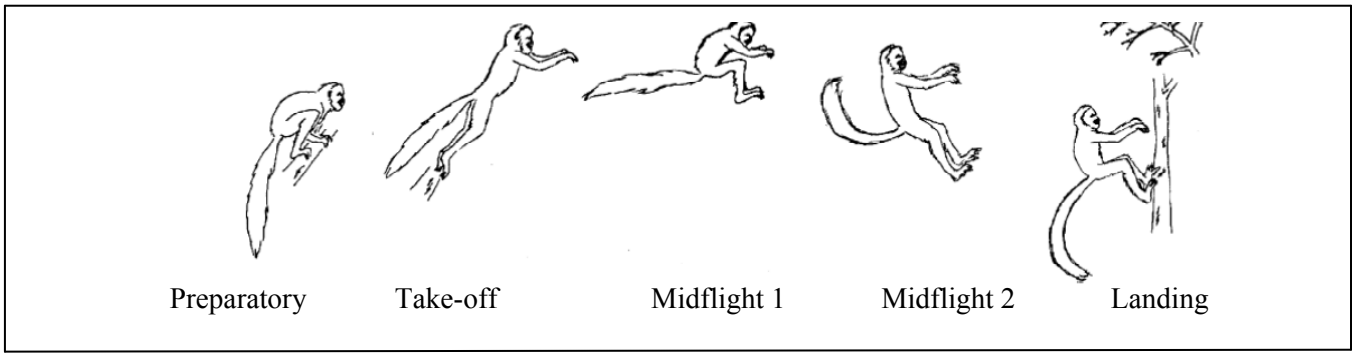

Fig. 2: Phases of leaping in *Pithecia pithecia* (from Walker, 2005)

Chapter 2

Muscle Physiology

2.1 Introduction

Oxnard (1975) argued that "the locomotor behavior of an animal is…controlled by the anatomy of the animal." As the engines that produce movements and drive the skeleton, skeletal muscles represent an appropriate biological example of structure-function relationship. As a result, studies of muscle function are intimately tied to studies of muscle structure. One of the goals of this study is to compare the architecture of epaxial muscles between primates characterized by different spinal movement patterns. The (vertebrate) leapers tend to have a mobile back designed for allowing sagittal plane movement (e.g. Hall-Craggs, 1965; Jouffroy et al. 1974; Walker, 2005), and the anti-gravity axial musculature (i.e. epaxial muscles; Asmussen, 1959) plays an important role in leaping by extending the spine from its flexure at the beginning of the take-off phase (for the role of spinal extension in arboreal leapers, see Hall-Craggs, 1965; Walker, 2005; for the role of the vertebral column and epaxial muscles in spinal mobility in a number of terrestrial and arboreal mammals, see Smith and Savage, 1956; English, 1980; Hurov, 1987; Sargis, 2001). During leaping, an animal will require high peak power output and enhanced maximum shortening velocity which will allow it to accelerate to achieve the all important take-off velocity (Bennet-Clark, 1977). The take-off velocity is determined by work (or impulse), which must be accomplished in a timespan dictated by acceleration. Power supply is critical in determining leaping distance, with most, if not all, specialist leapers using energy storage to some extent to enhance power (James et al, 2007). For many leapers (mammals, non-mammalian vertebrates, and even invertebrates such as insects), their body mass does not allow an increase in the maximum muscle shortening velocity beyond a certain point. These animals,

therefore, need to be able to increase the storage of elastic potential energy prior to the jump, to amplify available muscle power output, enabling them to achieve their desired jump distance (Bennet-Clark, 1977). Amplification of muscle power output occurs when elastic energy is released at an increased rate. This process has been illustrated in Aerts' (1998) study of the vertical jump of *G. senegalensis*. Aerts observed that elastic energy storage increased with countermovement (where a preparatory crouching was followed by an extension of the hind limbs and trunk) jump performance. The use of a countermovement enables force enhancement due to the stretch of active muscles, and time for the extensor muscles to attain high force (and thereby greater momentum) prior to shortening (Gans, 1982; Aerts, 1998).

In contrast to the leaping capability of the galagids, the lorisids are prominent for their slow, cautious quadrupedalism, climbing, and suspensory movement (Walker, 1969; Curtis, 1995; Fleagle, 1999; Shapiro and Simons, 2002). Investigators have noted that the spinal column of the lorisids is designed for extensive lateral flexion, a high range of freedom for transverse movement in the lumbar region, as opposed to the characteristic flexion-extension seen in quadrupedal mammals, as well as a limited range of extension at the thoraco-lumbar junction (Fig. 1; Ankel, 1967; Dykyj, 1980; Demes et al, 1990; Curtis, 1995). In addition, Curtis (1995) has observed a reduced trunk extensor muscle mass in the lorisids, which she has related to the less abrupt movement of the back, and a frequent use of the upside-down suspensory posture in these primates. During such movements, the trunk remains flexed, and active back extension is not required. Another distinctive feature of the locomotion of the lorisids is the use of cantilevering and bridging to move across arboreal gaps (Nekaris and Bearder, 2011), movements that require an enhanced stability of the trunk (Curtis, 1995; Shapiro and Simons, 2002). These peculiarities led Straus and Wislocki (1932) to suggest that the back musculature of

the lorisids is “more adapted to the gross purpose of strength and support than to the finer movements of agility.”

Experimental work on the back movement patterns of the vervet and patas monkeys show that the vervet monkeys (*C. aethiops*) exploit the available spinal flexibility to increase stride length (Gambaryan, 1974; Hurov, 1987). The reduced length of the distal segment of their hindlimbs is likely to restrict their ability to increase stride length and galloping speed. Vervet monkeys compensate for this shortcoming by increasing the range of sagittal back motion (Hurov, 1987). Presumably, this back movement requires an enhanced velocity-generating capability by the intrinsic back muscles. The spinal movement of the patas monkey (*E. patas*) is less diverse than that of the lorisids; but Hurov (1987) observed that during galloping, its back remains relatively stiff and immobile, while the elongated distal segments of the hindlimb facilitate an increase in stride length (Hurov, 1987).

As stated before, muscles are responsible for producing forces and movements associated with locomotion. Architecture refers to the internal arrangement of muscle fibers in relation to its axis of force generation (Lieber, 2010), and differences in architectutral configuration can have profound effect on muscle function (e.g. Gans and Bock, 1965; Gans, 1982; Anapol and Jungers, 1986; Gans and de Vree, 1987; Anapol and Herring, 1989).

Although comprehensive data on epaxial muscle architecture are scant, a number of investigators have used muscle weights to draw conclusions about gross behavioral differences [e.g. braking vs propulsive functions (Haxton, 1947); quadrupedalism vs leaping (Fleagle, 1977)]. Comparative studies of muscle fiber architecture in primates (Taylor and Vinyard, 2009; Organ et al, 2009), other mammals (e.g. rabbits: Taylor et al, 2006), and other vertebrates (e.g. for Harris’ hawk: Marden, 1990; for finches: van der Meij and Bout, 2004, 2006; for catfish:

Herrell et al, 2002; van Wassenberg et al, 2005) have shown functional and adaptive increases in muscle force through increases in muscle weight (~mass). However, isolated muscle weight indices (individual muscles as a proportion of some arbitrarily determined standard) are of questionable interpretability and tend to be inconsistently applied among workers (Stern, 1971).

Importantly, it should be noted that the relationship between muscle mass and force production is not straightforward. The internal arrangement of fibers has important implications for a whole muscle's capacity for generating force and excursion/contraction velocity. Within a whole muscle, the orientation of muscle fibers in relation to the line of action of the muscle influences its functional capabilities. Thus, skeletal muscle architecture has been defined as "the arrangement of muscle fibers relative to the axis of force generation." (Lieber, 2010). Muscle fibers are arranged either in parallel with, or at an angle to (i.e. pinnate muscles) the force-generating axis of the muscle, and both of these types of arrangements exist in a variety of configurations (Gans and Bock, 1965; Gans, 1982; for different configurations of parallel-fibered muscles, see Fig. 2 in Gans, 1982).

The maximum force that can be generated by a muscle is proportional to its physiological cross-sectional area (PCSA) (Lieber, 2010). Theoretically, PCSA represents the sum of the cross-sectional areas of all fibers within a muscle (e.g., Gans and Bock, 1965). The proportional relationship between muscle PCSA and maximum force-generating capacity was empirically demonstrated by Powell et al (1984). The estimate of PCSA takes into account fiber length and the orientation of fibers relative to the force-generating axis of the muscle (i.e. pinnation angle).

The maximum excursion and contraction velocity that a muscle can generate are proportional to fiber length (Lieber, 2010). A muscle fiber comprises a number of sarcomeres arranged in series. The velocity of muscle contraction is a function of excursion over time.

Because all the sarcomeres in a fiber are approximately of the same length and contract more or less the same distance rather simultaneously, so do lengths of fibers and whole muscles in their entirety (Gans, 1982; Anapol et al., 2004; Lieber, 2010). As a result, contraction velocity (distance/time) is proportional to fiber or fasciculus length, i.e. the number of sarcomeres in series (Gans, 1982; Anapol et al., 2004; Lieber, 2010). Bodine et al. (1982) confirmed this principle in an experiment on the semitendinosus muscle of the cat. Bodine et al. (1982) observed that the absolute contraction velocity was determined by fiber length, in that longer fibers were capable of generating greater contraction velocity, and concluded that velocity was a function of the number of sarcomeres in series (Bodine et al., 1982). It should be noted that force and velocity are inversely related, i.e., the higher the load, the slower the velocity of contraction (Hill, 1938).

Thus, to summarize, given two muscles of comparable volume, a parallel-fibered muscle is better suited for greater excursion and higher velocity of contraction (more sarcomeres in series), while pinnate-fibered muscles are suited either for increased force-production or to concentrate force into a smaller allocated area of attachment (more cross-bridges in parallel) (Gans, 1982; Biewener, 1998; Anapol et al., 2004). In vertebrates and mammals, limb flexors tend to comprise more parallel-fibered muscles, while anti-gravity muscles (such as the soleus, medial head of triceps brachii) are short and pinnate-fibered (Anapol and Jungers, 1986; Anapol and Barry, 1996; Biewener, 1998).

In this study, muscle architecture includes whole-muscle mass, fiber length, angle of pinnation (i.e. the extent to which fibers are arranged in parallel to, or angled, relative to the force-generating axis of the muscle), and the muscle cross-sectional area. The many permutations of these components account for much of the functional heterogeneity among

muscles. What is useful about these highly variable architectural components is that they comprise a group of quantifiable morphologic features that are interpretable in physiologic terms (e.g. Gans and Bock, 1965; Gans, 1982; Anapol and Jungers, 1986; Gans and de Vree, 1987; Anapol and Herring, 1989).

Hypotheses to be tested

One may ask how these architectural variables influence the spinal mobility in the species under investigation in this study. For rapid back extension during leaping (galago) and galloping (vervets), velocity should be improved with the contraction of relatively long, parallel fibers, which are capable of a greater range of excursion. On the other hand, both slow loris and patas monkey are characterized by a stable trunk. I, therefore, hypothesize that species which engage in rapid spinal extension (*G. senegalensis* and *C. aethiops*) will have epaxial muscles architecturally suited to generate relatively large excursions and high contraction velocities compared to closely related species which are characterized by greater spinal stability (*N. coucang* and *E. patas*). Specifically, I predict the following:

i) Longer fibers facilitate increased maximum muscle excursion and greater contraction velocity (Lieber, 2010). To promote rapid spinal extension for leaping (*G. senegalensis*) and galloping (*C. aethiops*), *G. senegalensis* and *C. aethiops* will have epaxial muscles comprising relatively longer fibers (relative to thoraco-lumbar spine length and muscle length) and relatively greater *h* (potential excursion of whole muscle relative to muscle length) compared to those of the slow-moving, stable-backed *N. coucang*, and *E. patas*, respectively.

ii) For a given muscle volume, pinnate fibers tend to be shorter than fibers oriented parallel to its force-generating axis (Lieber, 2010). Pinnate-fibered muscles are able

to increase PCSA (and therefore, force) by packing more fibers adjacent to each other in a given space (Gans, 1982; Lieber, 2010). Pinnate-fibered epaxial muscles with a higher PCSA are capable of generating greater maximum muscle force, and would be expected to facilitate maintaining a stable trunk in *N. coucang* for arboreal locomotion, including slow quadrupedalism, cantilevering/bridging, and anti-pronograde suspension. However, I can think of no *a priori* reason to expect that *E. patas* should generate relatively greater maximum epaxial muscle forces compared to *C. aethiops*. Therefore, I preliminarily predict that relatively greater epaxial muscle PCSAs (relative to body mass) in *E. patas* would be an architectural trade-off of their relatively shorter, more pinnate fibers.

In addition to testing these predictions, I explored tendon length as a proportion of muscle fibers to understand the role of tendon in elastic storage in epaxial muscles.

2.2 Materials and methods

Epaxial muscle tissues for *G. senegalensis*, *N. coucang*, *C. aethiops*, and *E. patas* were obtained from various private and museum collections (Table 1). The strepsirrhine specimens were captive, while the cercopithecoid (*C. aethiops* and *E. patas*) specimens were wild-shot. The cadavers were previously fixed and stored in either alcohol or formalin. Because these cadavers had been pre-dissected, and various organs/tissues had been removed, it was not possible to collect reliable measurements of individual body mass.

Tissue collection. All tissues were collected from one side of the cadaver. Skin and the extrinsic back muscles (trapezius, latissimus dorsi, rhomboids, levator scapulae) overlying the epaxial muscles were reflected. The target muscles (iliocostalis, longissimus, and multifidus) were divided between thoracic and lumbar segments, dissected free from their bony attachments, and trimmed of excess tendon and fascia. Upon extraction, whole muscle length (ML) was measured along the long axis of each muscle from its origin to insertion with digital calipers accurate to the nearest 0.01 mm (Anapol et al., 2004). All tissues were collected from between the T1 and the last lumbar vertebrae. The extracted tissues were then stored in 10% formalin solution. After dissection, the length of the thoraco-lumbar vertebral column was measured from the tip of the spinous process of T1 to the tip of the spinous process of the last lumbar vertebra with a measuring tape to the nearest 0.1 mm.

Data collection. Individual weights of each tissue segment were measured to the nearest 0.0001 gm on a digital scale (Meitler-Toledo, Inc.). Before measuring, tissues were blotted dry on paper towels.

Surface pinnation angle (θ') was measured directly with a protractor on the superficial surface of the excised tissue as the angle that muscle fibers made relative to the tendon (Fig. 2).

Depending on the size of the muscle and orientation of its fibers, measurements were taken on multiple sites (cranial, middle, and caudal) of the same tissue sample, and then mean of the observations were computed. For each fasciculus, I also measured the length of the tendon from its proximal attachment to the bone to the proximal myotendinous junction (TP), and the length of the tendon from its distal attachment to the bone to the distal myotendinous junction (TD) (Fig. 3). The sum of TP and TD was the total tendon length (TL) for a muscle fasciculus. A mean value of TL for each muscle was computed, and used in subsequent analysis.

Two different procedures were used to estimate fiber length (Lf), one for small tissues, and one for the larger ones. For smaller tissues, which included all strepsirrhine muscles and multifidus of vervet and patas monkeys, each sample was immersed in 30% nitric acid solution for chemical digestion (Loeb and Gans, 1986; Organ et al. 2009; Taylor and Vinyard, 2009). When properly digested, i.e. when individual fibers could be teased apart without breakage, the tissues were removed from the acid solution, and placed under dissecting microscopes (Olympus-5000 and Nikon SM-1500) for manual dissection.

At least 25 fasciculi were manually teased apart from each muscle belly. Following Rayne and Crawford (1972), I did not separate out individual fibers, as they were likely to tear during the dissection process. Therefore, I use the terms “fiber length” and “measured fasciculus length” interchangeably (Rayne and Crawford, 1972). Only those fasciculi with rounded/squared ends, and that were untwisted and uncurled were measured. Each fascicle group then was mounted on glass slides with a mounting medium, cover slipped, and air-dried. Prior to cover-slipping, each fasciculus was measured with digital calipers to the nearest 0.01 mm. For each tissue sample, at least 10 fasciculi were measured. Prior to acid digestion, a small chunk of tissue (Length = ~3 mm x Width = ~1.5 mm x Thickness = ~1.5 mm) was removed from each segment

and preserved in 70% ethanol solution for subsequent histological analysis. To achieve an accurate measurement of Lf, the length of each removed chunk was added to the raw fiber length.

For the larger muscles, which included vervet and patas iliocostalis and longissimus, I took architectural measurements *in situ*, following the methods of Anapol and Barry (1996). Each muscle was longitudinally bisected, turned on its perpendicular, and pinned to a styrofoam block to facilitate viewing of the fascicule in situ. Three sampling sites (proximal, middle and distal) were chosen for fiber architecture measurement, and at each site, the lengths of 10 neighboring fasciculi (from the proximal myotendinous junction to the distal myotendinous junction; Fig. 4) were measured with digital calipers to the nearest 0.01 mm. After measuring fasciculus length, a small chunk was removed from each tissue segment, and chemically digested, dissected, and mounted on slides in the manner described above. In addition, after measuring fasciculus length, and before chemical digestion, a small chunk of tissue (see above for dimensions) was removed from each segment and preserved in 70% ethanol solution for subsequent histochemical analysis.

Ideally, measurements of fiber length and pinnation angle are taken on muscles that are set at their resting lengths, i.e. the length at which force is of maximum potential. Unfortunately, most available cadavers (including those examined here) were fixed with their trunks either flexed or extended so that the muscles were either shortened or stretched relative to their presumed resting lengths. In addition to the effect of fixation at various postures on fiber lengths and all variables involving fiber lengths, when a pinnate muscle contracts or is stretched, the fibers swivel relative to their attached ends, altering the pinnation angle and the muscles force-generating potential (Anapol and Barry, 1996).

To adjust for the variation in fiber length that occurred because the specimens were fixed in a variety of postures, raw fiber length (Lf) was normalized to a standardized sarcomere length (Felder et al., 2005). Sarcomere length (Ls) for the mounted fibers was measured to the nearest 0.01 μm using laser diffraction, which utilizes incident laser light diffracting through the I-band region of the sarcomere to estimate sarcomere length (Lieber et al., 1984). Values for the Lf, normalized for Ls, were calculated using the following equation (Felder et al. 2005):

$$NLf = Lf\,(2.41\ \mu m/Ls),$$

where NLf = normalized fiber length; Lf = raw fiber length; Ls = measured sarcomere length; 2.41 μm = empirically determined optimum sarcomere length in *Macaca mulatta* limb muscles (Walker and Schrodt, 1974).

NLf was used to restore the average surface pinnation to its resting sarcomere equivalent by the following equation (Organ et al., 2009):

$$\theta = \arcsin\,[Lf \sin(\theta')/NLf],$$

where θ = resting pinnation angle, θ' = measured mean surface pinnation.

Using the aforementioned variables, PCSA was computed using the following equation (Powell et al., 1984):

$$PCSA\ (cm^2) = \text{muscle mass (gm)} \times \cos\theta/[NLf\,(cm) \times 1.0564\ gm/cm^3],$$

where 1.0564 gm/cm^3 is the specific density of the mammalian skeletal muscle (Murphy and Beardsley, 1974).

Estimated potential excursion of a whole muscle (*h*), calculated following Anapol and Gray (2003): $h\ (mm) = NLf\,[\cos\theta - \sqrt{(\cos^2\theta + n^2 - 1)}]$, where n (coefficient of contraction) = 0.769. To account for inter-specimen size differences, *h* for any muscle was standardized by dividing it by the resting length of the belly (Lb), reconstructed from its length at excision (ML),

following Muhl (1982) and Anapol and Gray (2003): Lb ≈ ML + [1.2987(NLf - Lf)]. I also computed the ratio TL/(TL + NLf) for each muscle as an estimate of its capacity for elastic storage; greater value for this ratio would indicate a greater capacity for elastic storage involving tendons (Anapol and Barry, 1996; Anapol et al., 2004).

Data analysis. Descriptive statistics (mean and standard deviation) were computed and evaluated for each of the raw and derived muscle measures (mass, pinnation, NLf, potential excursion of whole muscle (*h*), tendon length, and (TL/(TL + NLf)). Muscle mass was standardized by species mean body mass (Table 1) using the following formula:

(Muscle mass x 100)/Species mean body mass

Muscle length (Lb) and thoraco-lumbar spine length are important biomechanical factors influencing muscle activity and spinal movement. Therefore, shape ratios relative to biomechanical standards for fiber length were created by dividing NLf by both muscle length as well as by thoraco-lumbar spine length. Because in geometrically similar animals, muscle cross-sectional area should be proportional to body mass$^{(2/3)}$ (Thorpe et al., 1999), PCSA was standardized by species mean body mass$^{(2/3)}$ (Thorpe et al., 1999). Species mean body mass data were collected from the literature (Table 1). To understand how sensitive PCSA was to body mass, I computed relative PCSA with (i) species mean body mass, (ii) upper estimate of body mass (Mean + SD), and (iii) lower estimate of body mass (Mean – SD). For each pair of primates, results of these computations were compared both graphically and statistically. Because of small sample sizes, it was unlikely that the assumptions of parametric testing would be met (Sokal and Rohlf, 1995). Therefore, and unless otherwise noted, one-tailed, non-parametric Mann-Whitney U tests were used to test for significant species differences within each pair, and an a priori significance level of $p \leq 0.05$ was set for these and all statistical

analyses. In cases where the one-tailed test resulted in no statistical difference for a particular variable between two species within a pair, I report the result of a two-tailed Mann-Whitney U test to look for an overall difference in the variable between the two species (Zar, 1999; Vinyard et al., 2003). Also, in cases where I did not have any directional prediction, I report the results of a two-tailed Mann-Whitney U test to look for an overall difference in the variable between the two species. A one-way ANOVA with post-hoc LSD test for multiple pairwise comparisons was conducted for each architectural variable for all species. Performing multiple comparisons involving all study species reduces statistical problems associated with comparing only two species (Garland and Adolph, 1994). All statistical analyses were conducted on the SPSS v. 16 software (IBM-SPSS, Inc.).

2.3 Results

Gross morphology of the muscles.

G. senegalensis (lesser galago) and *N. coucang* (slow loris)

Thoracic iliocostalis. In the lesser galago, thoracic iliocostalis attaches cranially to the ribs by fleshy slips. The caudal attachment of its fibers is on the thoracolumbar aponeurosis (Figs. 5-6). In the slow loris, the thoracic iliocostalis attaches cranially to the ribs via slender tendons, and caudally to the thoracolumbar aponeurosis (Figs. 8-9).

Lumbar iliocostalis. The lumbar segments of the m. iliocostalis of the lesser galago (Figs. 5 and 7) and the slow loris (Figs. 8 and 10) do not have a separate cranial attachment relative to the thoracic segment. The fibers of the thoracic segment that attach to the thoracolumbar aponeurosis are continuous with those of the lumbar segment. The lumbar segment attaches caudally to the iliac crest, and differs from the thoracic segment in that it does not attach to the ribs (both species).

Thoracic longissimus. The longissimus muscle of the lesser galago has a caudal attachment on the ventral surface of the thoracolumbar aponeurosis. In the thoracic region, fleshy slips of the m. longissimus attach cranially on the ribs as well as on the transverse processes of the thoracic vertebrae (Fig. 11). In the slow loris, longissimus attaches caudally on the thoracolumbar aponeurosis. Cranially, it attaches to the transverse processes of the thoracic vertebrae between T1 and T16. However, its cranial attachment to the ribs is more complex. In the cranial thoracic region (T1 – T3-4), lonsissimus thoracis does not attach to the ribs. Below that segment, and until T13-14, it attaches to the ribs by fleshy slips (Figs. 14-15).

Lumbar longissimus. Three layers of the m. longissimus were noticed in the lumbar region of the lesser galago, based on the presence of fascial planes. The superficial layer is a

continuation of the thoracic segment of the muscle, and it attaches to the transverse processes of the lumbar vertebrae. The middle and deep layers attach from the lumbar accessory processes. All three layers converge on a tendon that continues caudally (Figs. 12-13). In the lumbar region of the slow loris, longissimus attaches to the transverse processes of the lumbar vertebrae, and more caudally, to the thoracolumbar aponeurosis (Figs. 14 and 16).

Multifidus. There is no clear regional distinction in the multifidus muscle of the lesser galago. In both thoracic and lumbar regions, this muscle attaches caudally to the transverse process by a muscular slip, which crosses 2-4 segments, and attaches cranially to the spinous process by a short tendon (Figs. 17-18). The cranial and caudal attachments of the multifidus in the thoracic and lumbar regions of the slow loris are basically the same as with those of the galago. The only difference is that slips of multifidus in the loris cross 4-5 vertebral segments (Figs. 19-20).

C. aethiops (vervet) and *E. patas* (patas)

There was no noticeable difference in the attachment patterns of epaxial muscles between the two cercopithecoid monkeys. Therefore, in situ photographs of muscles were taken on one species (*E. patas*) only.

Thoracic iliocostalis. The thoracic and lumbar segments of the m. iliocostalis are separable only artificially. The more caudal portion of the thoracic iliocostalis takes its origin as a fleshy slip from the last rib. More cranially, the fleshy slips attach to the upper six (or seven) ribs by narrow tendons (Figs. 21-23).

Lumbar iliocostalis. More caudally, lumbar iliocostalis in both monkeys is partially covered by the thoracolumbar aponeurosis. Its fibers arise from the cranial border of the ilium, as well as from the lateral border of the m. longissimus. Caudal fibers of lumbar iliocostalis insert

on the transverse processes of the lumbar vertebrae. Cranial fibers insert by narrow tendons on ribs 8-12 (Figs. 21, 24-25).

Thoracic longissimus. Caudal fibers of the thoracic longissimus take origin primarily from the deep surface of the thoracolumbar aponeurosis. They insert mostly by tendinous slips on the transverse processes of the lower thoracic vertebrae. More cranially, the tendinous slips insert on both transverse processes and medial parts of ribs (Figs. 26-28).

Lumbar longissimus. Fibers of the lumbar longissimus arise from the medial part of the iliac crest and the deep surface of the thoracolumbar aponeurosis. These fibers pass medially and cranially to insert primarily on the transverse processes of the lumbar vertebrae (Figs. 26, 29-30).

Multifidus. In both thoracic and lumbar regions, individual slips of multifidus bridge two to four vertebral segments. The caudal attachment of each slip is to the transverse process, while cranially, each slip attaches tendinously to the spinous process (Figs. 31-33).

Architectural morphometrics

Summary of results

Prediction 1: G. senegalensis meets the prediction of having epaxial muscles with relatively longer fibers and relatively greater potential excursion capability compared to those of *N. coucang*. Contrary to the prediction, however, epaxial muscles of *C. aethiops* have relatively shorter fibers and relatively smaller potential excursion capability compared to those of *E. patas*.

Prediction 2: Epaxial muscles of *N. coucang* have greater pinnation angles and relatively larger PCSAs compared to those of *G. senegalensis*; this observation supports the prediction. *C. aethiops* also meets the prediction of having more parallel-fibered epaxial muscles compared to those of *E. patas*; the latter have more pinnate-fibered muscles. On the other hand, epaxial

muscles of *C. aethiops* have relatively larger PCSAs compared to those of *E. patas*. This observation does not support the prediction.

Results of the strepsirrhine pair

Absolute muscle mass. Average mass for each muscle segment, except the lumbar iliocostalis, is greater for the larger-bodied slow loris, compared to the smaller-bodied lesser galago (Table 2). However, there is considerable overlap in muscle masses between the two taxa (Figs. 34). There is no significant difference in muscle mass for any segment between the two species (two-tailed Mann-Whitney U test; Table 2).

Relative muscle mass. Mean relative muscle mass for each muscle segment, except the thoracic multifidus, is greater for the lesser galago, compared to those of the slow loris (Table 3). There is also considerable overlap in relative muscle masses between the species (Fig. 35). There is no significant difference in relative muscle mass for any segment between the two species (two-tailed Mann-Whitney U test; Table 3).

Pinnation angle. Average pinnation angles for each muscle segment (except the lumbar multifidus) are greater for the slow loris, compared to those of the lesser galago (Table 4; Fig. 36). However, only the thoracic segments of the iliocostalis, longissimus, and multifidus are significantly more pinnate in the slow loris; in other segments, the differences are not significant (Table 4; one-tailed test).

Resting fiber length (NLf). Compared to *N. coucang*, *G. senegalensis* has longer NLf for all muscle segments (Table 5; Fig. 37). Apart from thoracic iliocostalis and thoracic longissumus, these differences are significant for each muscle segment (Table 5; one-tailed test).

Standardized NLf. When NLf is standardized for thoraco-lumbar spine length (Table 6; Fig. 38) and muscle length (Lb) (Table 7; Fig. 39), lesser galago shows significantly longer fibers for all muscle segments compared to those of the slow loris (Tables 6-7; one-tailed test).

Potential excursion of whole muscle (h). Potential excursion for whole muscle is significantly greater for lesser galago compared to that of the slow loris for all muscle segments, except thoracic iliocostalis and thoracic longissimus (Table 8; Fig. 40; one-tailed test). However, when *h* is standardized by Lb, lesser galago shows significantly greater *h* for each muscle segment relative to that of the slow loris (Table 9; Fig. 41; one-tailed test). Patterns of difference in *h* and relative *h* between the species mirror the ones observed for NLf and relative NLf (standardized for Lb) (Tables 5, 7; Figs. 37, 39).

Tendon length (TL) and *TL/(TL + NLf).* The variables TL and TL/(TL + NLf) are consistently and significantly greater in all muscle segments of *G. senegalensis*, compared to those of *N. coucang* (Tables 10-11; Figs. 42-43; one-tailed test).

Physiological cross-sectional area (PCSA). Slow loris has greater PCSA for each muscle segment compared to that of the lesser galago (Table 12; Fig. 44). However, this difference is significant only for lumbar longissimus (Table 12). When standardized for body size (mean, upper, and lower estimates), lumbar iliocostalis of lesser galago shows greater PCSA compared to that of the slow loris (Tables 13-15; Figs. 45-47). For all other muscle segments, slow loris has greater relative PCSA (Tables 13-15; Figs. 45-47). No significant difference exists between the two species for relative PCSA of any muscle segment (Tables 13-15; one- and two-tailed tests).

Results of the cercopithecoid pair

Absolute muscle mass. Average muscle mass is greater for the vervet monkey in lumbar iliocostalis, thoracic longissimus, and lumbar multifidus, compared to those of the patas monkey

(Table 16; Fig. 48). However, apart from lumbar iliocostalis, there is no significant difference for any other muscle segment between the two species (two-tailed Mann-Whitney U test; Table 16).

Relative muscle mass. Relative muscle masses for all segments are greater for the vervet monkey compared to those of the patas monkey (Table 17; Fig. 49). Differences between the species are significant for all muscle segments except thoracic iliocostalis and thoracic multifidus (two-tailed Mann-Whitney U test; Table 17).

Pinnation angle. Muscles of the patas monkeys are more pinnate than those of the vervet monkeys (Table 18 Fig. 50). Differences in pinnation angles are significant for all muscle segments, except thoracic iliocostalis and thoracic longissimus (Table 18; one-tailed test).

Resting fiber length (NLf). Fiber length, normalized for sarcomere length, is greater in the patas monkey for all muscle segments, except thoracic longissimus (Table 19; Fig. 51). The differences are significant for thoracic iliocostalis, lumbar longissimus, and thoracic and lumbar segments of multifidus (Table 19; one-tailed test).

Standardized NLf. Relative NLf (standardized for thoraco-lumbar spine length) is greater for the patas monkey in all muscle segments, except thoracic longissimus (Table 20; Fig. 52). Apart from lumbar iliocostalis and thoracic longissimus, the differences are significant for all muscle segments (Table 20; one-tailed test). When standardized for muscle length (Lb), relative NLf is still greater for the patas monkey in all muscle segments, except thoracic longissimus (Table 21; Fig. 53). However, differences between the species are significant only in thoracic iliocostalis and lumbar multifidus (Table 21; one-tailed test).

Potential excursion of whole muscle (h). Compared to the vervet monkey, *h* is greater in the patas monkey for all muscle segments, except thoracic longissimus (Table 22; Fig. 54). The differences are significant for all muscle segments, except lumbar iliocostalis and thoracic

longissimus (Table 22; one-tailed test). Relative *h* is also greater in the patas monkey for all muscle segments, except thoracic longissimus (Table 23; Fig. 55). The differences in relative *h* between species are significant only for thoracic iliocostalis and lumbar multifidus (Table 23; one-tailed test). Patterns of difference in *h* and relative *h* between the species mirror the ones observed for NLf and relative NLf (standardized for Lb) (Tables 19, 21; Figs. 51, 53).

Tendon length (TL) and *TL/(TL +NLf).* Apart from lumbar longissimus, TL is greater for all muscle segments of *C. aethiops*, compared to those of *E. patas* (Table 24; Fig. 56). However, no significant difference exists between the species in TL (Table 24; one- and two-tailed tests).

Relative to *E. patas*, TL/(TL + NLf) is greater for all muscle segments, except thoracic longissimus, in *C. aethiops* (Table 25; Fig. 57). Significant difference between the species only exists in thoracic iliocostalis, thoracic multifidus, and lumbar multifidus (Table 25; one-tailed test).

Physiological cross-sectional area (PCSA). Compared to *E. patas*, PCSA is higher for *C. aethiops* in lumbar segments of iliocostalis, longissimus, and multifidus (Table 26; Fig. 58). Differences between the species are significant only in lumbar segments of iliocostalis and multifidus (Table 26; one- and two-tailed tests). When standardized for body size (mean, upper, and lower estimates), relative PCSA is greater for the vervet monkey in all muscle segments (Tables 27-29; Figs. 59-61). Differences in relative PCSA (standardized for mean and upper estimate of body mass; Tables 27-28; one-tailed test) are significant in all muscle segments except thoracic segments of longissimus and multifidus. On the other hand, differences in relative PCSA (standardized for the lower estimate of body mass) are significant only in lumbar segments of iliocostalis and multifidus (Table 29; one-tailed test).

Results of one-way ANOVA and multiple pairwise comparisons.

Results of one-way ANOVA are significant for all variables among the species (Table 30). Results of multiple pairwise comparisons are described below.

Absolute muscle mass (Table 31). There is no significant difference between *G. senegalensis* and *N. coucang* in muscle mass. On the other hand, both the strepsirrhine species show significant differences with each one of the cercopithecoid species. There is also no significant difference between *C. aethiops* and *E. patas* in muscle mass.

Relative muscle mass (Table 32). Significant difference in relative muscle mass exists between *G. senegalensis* and *E. patas*. There is no significant difference in relative muscle mass between *N. coucang* and any of the other three taxa. *C. aethiops* and *E. patas* also show significant difference in relative muscle mass.

Resting pinnation (Table 33). Ranges for pinnation angles in each species are: *G. senegalensis*: $1.77^{o} – 8.35^{o}$; *N. coucang*: $3.11^{o} – 12.55^{o}$; *C. aethiops*: $1.00^{o} – 4.92^{o}$; *E. patas*: $2.41^{o} – 10.12^{o}$. There is no significant difference in pinnation angle between lesser galago and patas monkey. All other differences are significant.

Resting fiber length (NLf) (Table 34). Both strepsirrhine species differ significantly from each of the cercopothecoid species in Lf. However, Lf is not significantly different between the vervet and patas monkeys.

Relative NLf (Tables 35-36). Both strepsirrhine species differ significantly from each of the cercopothecoid species in relative NLf (standardized for thoraco-lumbar spine length and muscle length). However, relative NLf is not significantly different between the vervet and patas monkeys.

Potential excursion of whole muscle (h) (Tables 37-38). Both strepsirrhine species differ significantly from each other, and from each of the cercopothecoid species in *h* and relative *h*. However, neither *h* nor relative *h* are not significantly different between the vervet and patas monkeys.

Tendon length (TL) and *TL/(TL + NLf)* (Tables 39-40). Both strepsirrhine species differ significantly from each other, and from each of the cercopothecoid species in TL. However, TL is not significantly different between the cercopithecoid species (Table 39).

For the ratio TL/(TL + NLf), lesser galago differ significantly from the vervet monkey, but not from the slow loris or the patas monkey. Both slow loris and patas monkey differ significantly from other species. Vervet monkey differed significantly from the slow loris and patas monkey, but not from the lesser galago (Table 40).

Physiological cross-sectional area (PCSA) (Table 41). There is no significant difference in PCSA between the lesser galago and the slow loris. Lesser galago differs significantly from each of the cercopithecoid species. Slow loris differs significantly from the vervet monkey, but not from the patas monkey. PCSA is vervet and patas monkeys does not differ significangly from each other.

Relative PCSA (Tables 42-44). *G. senegalensis* does not differ significantly in relative PCSA (standardized for mean and upper estimate of body mass) from any of the other three species (*N. coucang*, *C. aethiops*, and *E. patas*). *N. coucang* differs significantly from *E. patas*, but not from *G. senegalensis* or *C. aethiops*. *C. aethiops* does not differ significantly from *E. patas* (Tables 42-43). On the other hand, when PCSA is standardized for the lower estimate of body mass, relative PCSA differs significantly between the strepsirrhines, and between *N.*

coucang and *E. patas*. No significant difference exists between the cercopithecoid species; and between *G. senegalensis* and any of the two cercopithecoid species (Table 44).

2.4 Discussion

Trends in fiber architecture within pairs.

Architectural differences in the epaxial muscles between the lesser galago and the slow loris appear to be related to differences in their respective positional behavior. As predicted, the lesser galago has both absolutely and relatively longer fibers, and relatively greater potential excursion of the whole muscle. Relatively greater potential excursion of the whole muscle appears to be the function of relatively longer fibers given both variables were size-standardized with muscle length (Lb). Likewise, as predicted, the slow loris typically displays both absolutely and relatively larger PCSAs for epaxial muscles. Epaxial muscles with relatively longer fibers and relatively greater potential excursion would facilitate rapid back extension during leaping for the lesser galago; while epaxial muscles with greater absolute and relative PCSAs would produce greater force and allow the slow loris to stabilize its trunk during slow arboreal quadrupedalism, bridging, and below-branch hanging.

Between the Old World monkeys, patas is terrestrial, while the vervet monkey engages in both arboreal and terrestrial locomotion. Interspecific differences in architectural characteristics are likely to reflect mechanical demands on their bodies, as created by details of their respective positional behaviors. Contrary to my predictions, the vervet monkey has relatively larger PCSAs for all muscle segments; while patas monkey generally has both absolutely and relatively longer fibers.

Internal differences in muscle architecture

Functional partitioning of a muscle can be enhanced through the alteration of intramuscular morphology, e.g., fiber architecture or fiber types (Herring et al., 1979; Anapol, 1984; Anapol and Jungers, 1986, 1987; Anapol and Barry, 1996). More precise discrimination

among constituent units of a muscle group resulting from variation in these intramuscular morphological features can extend the behavioral range of a synergistic muscle group.

The intermuscular variation present in the epaxial muscles of both these strepsirrhine species may be functionally related to their environmental niche. Being anti-gravity muscles, erector spinae and multifidus stabilizes the trunk against gravity. Consequently, these muscles would be expected to require a high degree of neuromuscular flexibility for control, which must be exercised in the precarious three-dimensional arboreal substrate regularly inhabited by both strepsirrhine species considered here.

As demonstrated in Tables 5-7, and in Figs. 37-39, epaxial muscles of the lesser galago have significantly longer fibers (both absolutely and relatively) than those of the slow loris. Because contraction velocity is a function of excursion over time, and excursion is a function of fiber length, relatively longer muscle fibers indicate lesser galagos are capable of generating both relatively greater excursion and contraction velocity of their epaxial muscles. For the lesser galago, fibers are consistently relatively longer in all of the epaxial muscle segments. In addition, potential excursion of whole muscle (*h*/Lb), is relatively higher for the lesser galago (Table 9; Fig. 41). Thus the role of epaxial muscles in producing relatively high contraction velocities is more pronounced in the habitual leaper with its rapid back extension during the take-off phase than in the slow-moving loris.

By contrast, and as predicted, relative PCSAs in the lesser galago are smaller for all muscle segments (with the exception of lumbar iliocostalis) compared to those in the slow loris. This pattern was generally observed whether using average body mass, or upper and lower estimates of body mass. Taken together, these observations illustrate the importance of generating velocity and maintaining spinal stability in the lesser galago and slow loris,

respectively. In addition, elastic storage capacity is also greater for the habitual leaper (*G. senegalensis*) than the cautious arboreal quadruped (*N. coucang*), as demonstrated by longer tendons and higher TL/(TL + NLf) ratios in the lesser galago compared to those in the slow loris (Tables 10-11; Figs. 42-43).

Results for the vervet and patas monkeys are less straightforward to interpret than those of the strepsirrhines. As previously noted, experimental work (Hurov, 1987) demonstrated that the vervet monkey utilizes its greater range for sagittal mobility in the spine to increase stride length during galloping. However, contrary to predictions, the vervet monkey has relatively shorter fibers, and consequently relatively smaller potential excursion (*h*/Lb) in most of its epaxial muscles, compared to those of the patas monkey (Tables 19-21, 23; Figs. 51-53; 55). Results also show that vervet monkey epaxial muscles tend to have higher TL/(TL + NLf) ratios, compared to those of the patas monkey (Table 25; Fig. 57). Relatively shorter fibers and longer tendons in vervets would allow the tendons of the epaxial muscles of the former to act as passive springs for rapid sagittal spinal movement during galloping. On the other hand, despite maintaining a more stable back (compared to the vervet monkey) during galloping, the epaxial muscles of the patas monkey tend to have relatively longer fibers (except thoracic longissimus), shorter tendons (except lumbar longissimus), and smaller TL/(TL + NLf). Therefore, elastic storage may be less important for these monkeys. Relatively longer fibers are also associated with a reduction in the relative PCSAs for all muscle segments of the patas monkey (Tables 27-29; Figs. 59-61).

Results of multiple pairwise comparisons combining all four species do not show any consistent pattern of differences. For certain variables, such as absolute and relative NLf (Tables 34-36), and absolute and relative *h* (potential excursion of whole muscle; Tables 37-38), the two

strepsirrhine taxa differed significantly from each other, and from each of the cercopithecoid taxa; while there was no significant difference between the two cercopithecoid taxa. On one hand, these observations might reflect the extreme differences in locomotion patterns between the strepsirrhines themselves (habitual leaping by *G. senegalensis* vs. cautious arboreal quadrupedalism/anti-pronograde suspension/cantilevering by *N. coucang*), and between the strepsirrhine and cercopithecoid pairs. On the other hand, the absence of significant differences between the cercopithecoid species might be indicative of more subtle differences (compared to the highly pronounced differences between the strepsirrhines) between these species in spinal movement during locomotion (vervets rapidly extend their spine only during fast terrestrial movement, such as galloping; Hurov, 1987). The importance of tendons in elastic storage in species engaging in rapid sagittal spinal movement (lesser galago and vervet) is possibly reflected in the absence of significant difference between these two species in TL/(TL + NLf) ratio (Table 40). Multiple pairwise comparisons in absolute and relative PCSAs consistently show that there is no significant difference between vervet and patas monkeys (Tables 41-44), again possibly reflecting the subtle difference between the species in their spinal movement patterns.

Interspecific differences in muscle architecture

Relative maximum muscle strength. Muscle PCSA is proportional to the maximum force that can be developed by a muscle. It was predicted that the higher relative PCSAs in the epaxial muscles of the slow loris, in comparison to those of the lesser galago, would indicate an increased emphasis on more exertive activities, such as bridging or below-branch hanging, both of which would require stabilizing the trunk against gravity. This prediction was supported by architectural data. On the other hand, the observation that relative PCSA was greater in the

epaxial muscles of the vervet monkey, compared to those of the patas monkey, does not support my prediction. It may be speculated that the higher relative PCSAs in the epaxial muscles of the vervet monkey are correlated to its preference for arboreal habitats (Fleagle, 1999), where the need for trunk stabilization is at a premium when the supporting substrate is less than the body width of the animal.

Pinnation, especially in the thoracic region, influenced the difference in physiological cross-sectional areas (absolute and relative) between the lesser galago and the slow loris. Epaxial muscles of the slow loris were significantly more pinnate in the thoracic segments, compared to those of the lesser galago, which would allow the muscles in the thoracic region to pack in more fibers, thus also increasing mass. The thoracic region of the spine in primates is designed for producing movement in a coronal plane, i.e. lateral flexion. Lorisid primates tend to have a greater range of lateral, as opposed to sagittal, flexion in their spinal columns (Cartmill and Milton, 1977; Curtis, 1995; Shapiro and Demes, 1996; Shapiro et al. 2001). It has been experimentally observed that lorisids, in a manner similar to the amphibians, use the lateral flexion of their spine to increase hindlimb stride length (Shapiro et al. 2001). Lateral flexion would also be useful during bridging, when the animal would have to reach out to some support/prey with its forelimbs and trunk being suspended in the air. Thus, the relatively larger thoracic PCSAs, comprising of relatively shorter, more pinnate fibers would have allowed the thoracic segments of the epaxial muscles to produce force sufficient enough for maintaining such trunk posture on an unstable substrate.

Relative velocity of contraction. Because the lengths of all sarcomeres in a muscle fiber are essentially equivalent (Burkholder and Lieber, 2001), and the sarcomeres contract the same distance more or less simultaneously (ter Keurs et al., 1978), velocity (distance/time) is

proportional to fiber/fasciculus length. Thus, since parallel-fibered muscles can be expected to comprise of longer fibers, compared to pinnate-fibered muscles of similar volume, parallel-fibered muscles are considered to be suited for speed of contraction, i.e. more sarcomeres in series. The relationship between force and velocity, however, involves a trade-off, i.e. the higher the load, the slower the velocity of contraction (Hill, 1938).

In the present study, all epaxial muscles, without exception, are geared for excursion and velocity in the lesser galago, especially in the lumbar segments, where fibers are longer than those in the thoracic segments (Tables 6-7, 9; Figs. 38-39, 41). In addition, while muscles of the lesser galago have relatively longer fibers and relatively greater potential excursion capability (*h*/Lb) compared to those of the slow loris, the latter species have relatively greater PCSAs in most of its epaxial muscles compared to those of the galago. While relatively longer fibers and relatively greater potential excursion capability would facilitate rapid back extension for the habitually leaping galago, and relatively greater PCSA would allow the slow loris to stabilize trunk against gravity during exertive arboreal locomotion (e.g., cantilevering, anti-pronograde suspension), it may also be argued that these characteristics reflect an architectural trade-off between increased excursion and contraction velocity (longer fibers and greater potential excursion capability in lesser galago) and muscle force (greater PCSA in slow loris), given that both architectural characteristics cannot be enhanced simultaneously (Gans, 1982; Taylor and Vinyard, 2004, 2008; Taylor et al, 2009; Table 45; Figs. 62-67).

Although epaxial muscles of the lesser galago are characterized by their capacity to generate greater contraction velocity, lumbar ilicostalis of lesser galago, with its relatively larger PCSA (Tables 13-15) compared to that of the slow loris, also appears to be suited for producing greater force. Histochemical data show that galago lumbar iliocostalis is overwhelmingly

composed of Type II fibers (93.52%; Chapter 3; Table 5).Type II fibers of galago lumbar iliocostalis are also very large (Chapter 3; Table 18). These observations suggest that lumbar iliocostalis of the lesser galago is capable of generating high tension (because of the overwhelming presence of large Type II fibers; Bodine et al., 1987); while at the same time increasing the muscle's active range of motion and contraction velocity through its relatively longer fibers. It may, therefore, be speculated that in the lesser galago, lumbar iliocostalis plays an as yet unknown special role in spinal extension during leaping. Further investigation of the structure and function of lumbar iliocostalis in a variety of specialized primate leapers, including *G. senegalensis*, would be required to clarify its importance.

The situation is more complicated in the cercopithecoid monkeys. While experimental data show that the vervet monkey has a more sagittally mobile spine relative to the patas monkey (Hurov, 1987), the latter has relatively longer fibers in most of its epaxial muscles (Tables 20-21; Figs. 52-53). In the absence of any *a priori* prediction as to why this should be so, this observation may be interpreted as the outcome of the trade-off between force and velocity (Table 46; Figs. 68-73). The relatively smaller PCSAs of the epaxial muscles of the patas monkey also support this interpretation. It should be noted that being a habitually terrestrial animal, there might be less need for the patas monkey to stabilize its trunk on an unstable substrate, which could also explain the relatively smaller PCSAs, and consequently relatively lower maximum force-producing capabilities, of its epaxial muscles. On the other hand, vervets spend approximately 80% of its time on trees (Fleagle, 1999). On an unstable arboreal surface, epaxial muscles of the vervet monkey would need to be able to exert more force to stabilize the trunk.

Elastic storage capacity. During contraction, only the muscle fibers (not the tendons) consume energy by hydrolyzing ATP. Thus, a greater TL/(TL + NLf) ratio reduces the expense

of contraction without compromising tension. If a muscle-tendon unit is lengthened under increasing force, elastic energy can be preserved. This energy is returned through elastic recoil (Alexander and Bennet-Clark, 1977; Biewener et al., 1981). In the lumbar region of the spine, which is adapted for sagittal plane movements (flexion-extension), the epaxial muscles of a habitual leaper (lesser galago) may need to produce such movements more rapidly (during the take-off phase of leaping, and over a large range of movements) than during movements such as below-branch suspension and bridging, which are associated with the slow loris. The presence of longer tendons in the epaxial muscles of the lesser galago would enable these muscles to act as springs, and increase the storage of elastic potential energy prior to the leap. However, in order for elastic storage in the tendons of epaxial muscles to be effective, the spine of the lesser galago must undergo an active flexion by abdominal muscles against the resistance of contracting spinal extensors (i.e. epaxial muscles). There is no evidence that this happens. On the contrary, available data indicate that the take-off stance of the lesser galago is a low-crouch, where the spine is already flexed and no active preparatory spinal flexion takes place (Hall-Craggs, 1965; Off and Gebo, 2005). In such a case, the significance of elastic storage in epaxial muscles would be minimized; instead, contraction velocity would be generated by longer fibers, which the galagos have.

Between the cercopithecoid monkeys, epaxial muscles of vervet tend to have relatively longer tendons, compared to those of the patas monkey. For rapid movement on the ground (e.g., galloping, where active spinal flexion would seem to occur), vervet monkeys would be able to utilize the elastic storage capacity of their epaxial tendons to produce rapid sagittal spinal movement, and consequently, increase their stride length.

Another possible source of elastic storage is the sarcomeral protein titin. It has been observed that titin is actually capable of storing more elastic energy than tendon (Linari et al., 2003; Telley et al., 2006; Herzog et al., 2012). However, it would be metabolically expensive for an animal that was relying on elastic storage for a specific activity to use sarcomeres to store this energy. Thus, tendons offer muscles a low-cost means of storing elastic energy (Roberts and Azizi, 2011). It is much more cost-effective, if the animal does not require additional range or speed of contraction, to replace sarcomeres with tendons (J. Stern, personal communication).

Muscle architecture differences (Hypothesis tests)

The results demonstrate that, in general, slow loris and vervet monkey have epaxial muscles with relatively larger PCSAs compared to those of the lesser galago and patas monkey. For the slow loris, this characteristic supports my prediction, and can be interpreted as an adaptation for maintaining spinal stability during arboreal locomotion. Previous work (Shapiro, 2007) has demonstrated that the leapers (lesser galago) and cautious arboreal quadrupeds (slow loris) have osteological characteristics that have been functionally linked to their typical spinal movement. Relative differences in fiber length and PCSA can be added to the suite of musculoskeletal features that differentiate these primates.

Contrary to the prediction, the results demonstrate that the epaxial muscles of the vervet monkey are adapted for force production (greater relative PCSA). I speculate that this architectural configuration may allow the vervets to maintain a stable trunk in an arboreal setting, which they tend to use more frequently than the patas monkey (Isbell et al., 1998; Fleagle, 1999). The data also show that relative increase in force production in the epaxial muscles of the vervet monkey is associated with a reduction in its relative fiber length. However, epaxial muscles of the vervet monkey also tend to have relatively longer tendons. Although

vervet and patas monkeys spend an almost equal amount of time running on the ground (Isbell et al., 1998), to overcome the limitation (on increasing stride length for running/galloping) imposed by their relatively shorter limbs (Hurov, 1987), vervet monkeys would be capable of using their epaxial muscles with long tendons as passive springs for rapid sagittal spinal movement, which would enable them to use their spine as the proximal element of the hindlimb, leading to a greater hindlimb stride length.

The data also show that epaxial muscles of the patas monkey, in addition to having relatively longer fibers, are also more pinnate. The implication of this finding is that the muscles of the patas monkey are able to pack in elongated fibers in greater numbers relative to those of the vervet monkey.

The situation whereby the epaxial muscles of the slow loris and the vervet monkey are capable of producing relatively greater maximum muscle forces (compared to lesser galago and patas monkey, respectively) can be compared and contrasted with two case studies. Organ et al. (2009) observed a relative increase in the PCSAs of the caudal muscles of prehensile-tailed compared to non-prehensile-tailed monkeys. Organ et al (2009) functionally linked the relatively larger tail muscle PCSAs to the need for the prehensile-tailed monkeys to generate relatively greater maximum muscle force associated with suspending and supporting their body weight during arboreal locomotion. However, the relatively higher tail muscle PCSAs were achieved by an increase in muscle mass, and not by increases in pinnation angles, or decreases in fiber length.

Taylor and Vinyard (2009) made similar observations of the jaw muscles of *Cebus apella*. They observed relatively greater jaw-closing muscle PCSAs in *Cebus apella* compared to untufted capuchins, and concluded that the relatively larger muscle PCSAs had been primarily driven by greater muscle mass, and not by a concomitant increase in pinnation angle, or a

decrease in relative fiber length. The authors inferred that the increase in muscle mass was achieved by adding more fibers. Taylor and Vinyard (2009) functionally linked the relatively larger muscle PCSAs to the ability of *C. apella* to generate relatively large muscle and bite forces needed to break open hard nuts, but at little expense to relative maximum jaw gape.

In the lesser galago, epaxial muscles with narrower pinnation angles and relatively longer fibers would have allowed muscles to be composed of parallel-oriented, long fibers suited for generating relatively greater excursion/contraction velocity. In the patas monkey, epaxial muscles with wider pinnation angles and relatively longer fibers would allow the muscles to pack relatively longer fibers in greater number; muscles with this configuration would be theoretically capable of producing a relatively higher excursion. Architectural data show that values of *h* (both absolute and relative to the length of whole muscle), as a measure of the potential excursion of whole muscle, are generally higher for the epaxial muscles of the patas monkey, compared to those of the vervet monkey (Tables 22-23; Figs. 54-55).

On the other hand, there is a general reduction in relative tendon length in the epaxial muscles of the patas monkey, suggesting that elastic energy storage, and consequently the use of epaxial muscles as springs may not be an important characteristic of the spinal movement of this monkey. It may be speculated that the relatively elongated limbs of the patas monkey diminish the significance of epaxial muscles in increasing spinal mobility, and consequently stride length. Although behavioral data show that patas monkeys are generally more mobile on the ground than the sympatric vervet monkeys (Isbell et al., 1998), the role of epaxial muscles in the spinal mobility of the patas monkeys has not been fully investigated. It is possible that the spinal movement in patas monkeys is determined primarily by the osseo-ligamentous and/or cartilaginous characteristics of the vertebral column (e.g., thickness of intervertebral disc; Hurov,

1987), with the epaxial muscles playing a more limited role. Further analysis of the function of epaxial muscles in the patas monkey is needed before a conclusion can be made in this regard.

Functional implications

Morphologies of bones, joints, and muscles are factors that affect musculoskeletal adaptation to a particular positional behavior. Among these factors, the bony skeletal configuration seems to be the least plastic one. Significant differences in the skeletal postcranial anatomy between closely related species are found to be strongly associated with specific differences in positional behavior in some primates (e.g., Fleagle, 1977b, 1999; Rodman, 1979; Ward and Sussman, 1979; Fleagle and Meldrum, 1988; Burr et al., 1989; Strasser, 1992).

The more plastic component of musculoskeletal anatomy is muscle morphology. Interspecific differences in muscle architecture and their functional consequences for locomotion have been extensively investigated both theoretically and experimentally. Despite the importance of muscle attachments (in defining the bony lever arm, and implying significant functional consequences for the force-velocity relationship; Smith and Savage, 1956; Stern, 1974), attachment sites ordinarily do not change within the lifetime of the adult (Anapol and Barry, 1996; Zumwalt, 2006). Stern (1971) noted that vasti peripherales in the habitually leaping cebid monkeys were characterized by restricted proximal attachments, implying fewer, but longer muscle fibers. This contrasts to the more extensive proximal attachments (shorter, but more fibers) in the relatively non-leaping prehensile-tailed forms. On the other hand, during a relatively short time span, pinnation and fiber types can change with training or stimulation (Salmons, 1980; Aagaard et al., 2001), and sarcomeres may be added or subtracted to adjust to length requirements (Herring et al., 1984). Changes in pinnation can increase or decrease fiber length (thus velocity) without necessarily altering the area of the attachment site (Anapol and

Jungers, 1986; Anapol and Barry, 1996). Thus, despite the overall reciprocity of the force-velocity relationship, altering fiber architecture can either increase the velocity of high-force muscles or increase the force output of high-velocity muscles.

The apparent greater flexibility in muscles than in bones would seemingly allow a species to respond to selective pressure facultatively, while preserving the bony morphology underlying its more habitual behavior. As Rose (1974) argued, the mobility of the ateline hindlimb is not only useful in their normal suspensory behavior, but also in their proficient postural and locomotor bipedalism, both in the trees and on the ground. Similar adaptations to climbing behavior have been suggested as preadaptive to human bipedalism (Stern, 1975; Fleagle et al., 1981).

Morphological comparisons of the bony vertebral elements between the lesser galago and the slow loris were previously reported and found to be related to differences in their respective positional behavior (Shapiro, 2007). Slow loris was found to be more closely related to other cautious arboreal quadrupeds, such as *Pongo*, which also has reduced spinous processes. What is interesting is that interspecific differences in muscle architecture between the two strepsirrhine taxa are almost as pronounced as are the differences in bony morphology. The differences in muscle morphology between the vervet and patas monkeys are less prominent than those between the strepsirrhines. Thus, it is possible that vertebral morphology might be more important in facilitating the spinal movements of vervet and patas monkeys.

The greater malleability of muscles permits greater flexibility in locomotor behavior of a species than that which might be indicated by an investigation of skeletal morphology alone. This flexibility provides an opportunity to adapt more rapidly to a shift in

behavioral/environmental niche, while allowing functionally significant aspects of the skeleton to evolve more gradually.

Table 1: Comparative sample for muscle physiological analysis

Species	Sample size			Body mass: Species mean ± SD (g)		Sources of specimens
	M	F	Total			
Galago senegalensis	4	0	4	213 ± 32		Collection of Dr. W. L. Jungers, Dept. of Anatomical Sciences, Stony Brook University.
Nycticebus coucang	3	1	4	589 ± 143		Collection of Dr. J. Hanna, West Virginia School of Osteopathic Medicine. Dept. of Mammalogy, US National Museum of Natural History (Specimen nos. 502559, 297828). Duke Lemur Center (Specimen no. 1906m).
Chlorocebus aethiops	1	4	5	4260 ± 680 (♂)	2980 ± 430 (♀)	Collections of Dr. F. Anapol and Dr. N. Tappen, Dept. of Anthropology, University of Wisconsin-Milwaukee.
Erythrocebus patas	2	3	5	12400 ± 3500 (♂)	6500 ± 1000 (♀)	

Sources of body mass:

Galago senegalensis and *Nycticebus coucang*: Jungers and Colson (1985).

Chlorocebus aethiops: Turner et al., 1994; cited in Smith and Jungers, 1997.

Erythrocebus patas: Galat-Luong et al., 1996; cited in Smith and Jungers, 1997.

Table 2: Summary of absolute muscle mass (g) for the strepsirrhines (Mean ± SD)

Species	Iliocostalis		Longissimus		Multifidus	
	Thoracic	Lumbar	Thoracic	Lumbar	Thoracic	Lumbar
G. senegalensis	0.2504 ± 0.1470	0.5234 ± 0.3815	0.5358 ± 0.1951	0.4438 ± 0.1969	0.0411 ± 0.0169	0.0769 ± 0.0353
N. coucang	0.5481 ± 0.4118	0.3511 ± 0.3201	1.3206 ± 0.8624	0.8265 ± 0.6809	0.2005 ± 0.2098	0.0974 ± 0.0898
Mann-Whitney U test result (two-tailed)	NS (p = 0.34)	NS (p = 0.68)	NS (p = 0.2)	NS (p = 0.34)	NS (p = 0.34)	NS (p = 0.88)

Table 3: Summary of relative muscle mass for the strepsirrhines (Mean ± SD)

Species	Iliocostalis		Longissimus		Multifidus	
	Thoracic	Lumbar	Thoracic	Lumbar	Thoracic	Lumbar
G. senegalensis	0.1176 ± 0.0690	0.2457 ± 0.1791	0.2516 ± 0.0916	0.2083 ± 0.0925	0.0193 ± 0.0080	0.0361 ± 0.0166
N. coucang	0.0931 ± 0.0699	0.0596 ± 0.0544	0.2242 ± 0.1464	0.1403 ± 0.1156	0.0340 ± 0.0356	0.0165 ± 0.0152
Mann-Whitney U test result (two-tailed)	NS (p = 0.49)	NS (p = 0.11)	NS (p = 0.69)	NS (p = 0.2)	NS (p = 0.69)	NS (p = 0.11)

Table 4: Summary of resting pinnation angle for the strepsirrhines (Mean ± SD)

Species	Iliocostalis		Longissimus		Multifidus	
	Thoracic	Lumbar	Thoracic	Lumbar	Thoracic	Lumbar
G. senegalensis	4.18 ± 1.20	3.09 ± 1.30	5.72 ± 1.26	4.92 ± 1.06	3.02 ± 0.23	4.42 ± 3.06
N. coucang	7.84 ± 2.64	5.91 ± 2.42	9.04 ± 2.59	6.53 ± 2.16	5.43 ± 1.48	4.36 ± 0.75
Mann-Whitney U test result (one-tailed)	p = 0.01	NS (p = 0.06)	p = 0.03	NS (p = 0.17)	p = 0.01	NS (p = 0.5)
Mann-Whitney U test result (two-tailed)	p = 0.02	NS (p = 0.12)	NS (p = 0.06)	NS (p = 0.34)	p = 0.02	NS (p = 1.00)

Table 5: Summary of NLf (mm) for the strepsirrhines (Mean ± SD)

Species	Iliocostalis		Longissimus		Multifidus	
	Thoracic	Lumbar	Thoracic	Lumbar	Thoracic	Lumbar
G. senegalensis	15.00 ± 4.60	16.91 ± 7.28	13.72 ± 1.18	22.50 ± 3.11	10.43 ± 2.63	10.77 ± 2.17
N. coucang	10.64 ± 3.47	7.90 ± 0.52	10.65 ± 1.98	7.57 ± 1.69	5.98 ± 2.24	3.78 ± 0.83
Mann-Whitney U test result (one-tailed)	NS (p = 0.17)	p = 0.01	NS (p = 0.06)	p = 0.01	p = 0.01	p = 0.01
Mann-Whitney U test result (two-tailed)	NS (p = 0.34)	p = 0.02	NS (p = 0.12)	p = 0.02	p = 0.02	p = 0.02

Table 6: Summary of Relative NLf-1 for the strepsirrhines (Mean ± SD)

Species	Iliocostalis		Longissimus		Multifidus	
	Thoracic	Lumbar	Thoracic	Lumbar	Thoracic	Lumbar
G. senegalensis	14.86 ± 4.21	17.25 ± 9.00	13.74 ± 1.73	22.36 ± 1.77	10.46 ± 2.95	10.84 ± 2.75
N. coucang	6.79 ± 2.27	5.01 ± 0.24	6.78 ± 1.43	4.83 ± 1.25	3.83 ± 1.49	2.39 ± 0.47
Mann-Whitney U test result (one-tailed)	p = 0.01	p = 0.01	p = 0.01	p = 0.01	p = 0.01	p = 0.01

Table 7: Summary of Relative NLf-2 for the strepsirrhines (Mean ± SD)

Species	Iliocostalis		Longissimus		Multifidus	
	Thoracic	Lumbar	Thoracic	Lumbar	Thoracic	Lumbar
G. senegalensis	31.90 ± 7.58	42.84 ± 13.44	23.31 ± 0.84	46.62 ± 4.00	49.48 ± 12.78	63.89 ± 17.25
N. coucang	16.34 ± 4.95	19.32 ± 0.53	11.79 ± 2.36	14.04 ± 4.41	18.74 ± 7.26	13.03 ± 1.41
Mann-Whitney U test result (one-tailed)	p = 0.03	p = 0.01	p = 0.01	p = 0.01	p = 0.01	p = 0.01

Table 8: Summary of *h* for the strepsirrhines (Mean ± SD)

Species	Iliocostalis		Longissimus		Multifidus	
	Thoracic	Lumbar	Thoracic	Lumbar	Thoracic	Lumbar
G. senegalensis	3.48 ± 1.07	3.91 ± 1.68	3.19 ± 0.28	5.22 ± 0.73	2.41 ± 0.61	2.50 ± 0.51
N. coucang	2.50 ± 0.83	1.84 ± 0.12	2.50 ± 0.46	1.76 ± 0.40	1.39 ± 0.52	0.88 ± 0.19
Mann-Whitney U test result (one-tailed)	NS (p = 0.17)	p = 0.01	NS (p = 0.06)	p = 0.01	p = 0.01	p = 0.01
Mann-Whitney U test result (two-tailed)	NS (p = 0.34)	p = 0.02	NS (p = 0.12)	p = 0.02	p = 0.02	p = 0.02

Table 9: Summary of relative *h* for the strepsirrhines (Mean ± SD)

Species	Iliocostalis		Longissimus		Multifidus	
	Thoracic	Lumbar	Thoracic	Lumbar	Thoracic	Lumbar
G. senegalensis	0.074 ± 0.018	0.099 ± 0.031	0.054 ± 0.002	0.108 ± 0.009	0.115 ± 0.03	0.148 ± 0.04
N. coucang	0.038 ± 0.012	0.045 ± 0.001	0.028 ± 0.006	0.033 ± 0.01	0.044 ± 0.02	0.03 ± 0.003
Mann-Whitney U test result (one-tailed)	p = 0.03	p = 0.01	p = 0.01	p = 0.01	p = 0.01	p = 0.01
Mann-Whitney U test result (two-tailed)	NS (p = 0.06)	p = 0.02	p = 0.02	p = 0.02	p = 0.02	p = 0.02

Table 10: Summary of TL (mm) for the strepsirrhines (Mean ± SD)

Species	Iliocostalis		Longissimus		Multifidus	
	Thoracic	Lumbar	Thoracic	Lumbar	Thoracic	Lumbar
G. senegalensis	35.78 ± 5.07	26.77 ± 5.87	37.03 ± 3.47	37.81 ± 3.72	11.90 ± 0.71	10.75 ± 1.7
N. coucang	7.92 ± 2.32	6.89 ± 0.82	8.21 ± 1.64	6.38 ± 1.19	4.96 ± 1.82	3.12 ± 0.56
Mann-Whitney U test result (one-tailed)	p = 0.01	p = 0.01	p = 0.01	p = 0.01	p = 0.01	p = 0.01
Mann-Whitney U test result (two-tailed)	p = 0.02	p = 0.02	p = 0.02	p = 0.02	p = 0.02	p = 0.02

Table 11: Summary of TL/(TL + NLf) for the strepsirrhines (Mean ± SD)

Species	Iliocostalis		Longissimus		Multifidus	
	Thoracic	Lumbar	Thoracic	Lumbar	Thoracic	Lumbar
G. senegalensis	0.7081 ± 0.0514	0.6223 ± 0.0579	0.7287 ± 0.0308	0.6275 ± 0.0228	0.5379 ± 0.0529	0.5009 ± 0.0210
N. coucang	0.4298 ± 0.0157	0.4651 ± 0.0287	0.4349 ± 0.0067	0.4594 ± 0.0435	0.4549 ± 0.0058	0.4535 ± 0.0233
Mann-Whitney U test result (one-tailed)	p = 0.01	p = 0.01	p = 0.01	p = 0.01	p = 0.03	p = 0.01
Mann-Whitney U test result (two-tailed)	p = 0.02	p = 0.02	p = 0.02	p = 0.02	NS (p = 0.06)	p = 0.02

Table 12: Summary of PCSA (cm^2) for the strepsirrhines (Mean ± SD)

Species	Iliocostalis		Longissimus		Multifidus	
	Thoracic	Lumbar	Thoracic	Lumbar	Thoracic	Lumbar
G. senegalensis	0.15 ± 0.06	0.35 ± 0.28	0.37 ± 0.15	0.19 ± 0.10	0.04 ± 0.02	0.07 ± 0.04
N. coucang	0.61 ± 0.68	0.41 ± 0.34	1.26 ± 0.98	1.22 ± 1.27	0.27 ± 0.28	0.24 ± 0.21
Mann-Whitney U test result (one-tailed)	NS (p = 0.17)	NS (p = 0.44)	NS (p = 0.06)	p = 0.01	NS (p = 0.17)	NS (p = 0.17)
Mann-Whitney U test result (two-tailed)	NS (p = 0.34)	NS (p = 0.88)	NS (p = 0.12)	p = 0.02	NS (p = 0.34)	NS (p = 0.34)

Table 13: Summary of relative PCSA-1 for the strepsirrhines (Mean ± SD)

Species	Iliocostalis		Longissimus		Multifidus	
	Thoracic	Lumbar	Thoracic	Lumbar	Thoracic	Lumbar
G. senegalensis	0.004 ± 0.001	0.01 ± 0.008	0.01 ± 0.004	0.005 ± 0.003	0.001 ± 0.0005	0.002 ± 0.001
N. coucang	0.009 ± 0.008	0.006 ± 0.004	0.018 ± 0.014	0.017 ± 0.018	0.004 ± 0.004	0.003 ± 0.003
Mann-Whitney U test result (one-tailed)	NS (p = 0.44)	NS (p = 0.34)	NS (p = 0.44)	NS (p = 0.17)	NS (p = 0.17)	NS (p = 0.34)
Mann-Whitney U test result (two-tailed)	NS (p = 0.88)	NS (p = 0.68)	NS (p = 0.88)	NS (p = 0.34)	NS (p = 0.34)	NS (p = 0.68)

Table 14: Summary of relative PCSA-2 for the strepsirrhines (Mean ± SD)

Species	Iliocostalis		Longissimus		Multifidus	
	Thoracic	Lumbar	Thoracic	Lumbar	Thoracic	Lumbar
G. senegalensis	0.004 ± 0.001	0.01 ± 0.007	0.01 ± 0.004	0.005 ± 0.003	0.001 ± 0.0004	0.002 ± 0.001
N. coucang	0.007 ± 0.007	0.005 ± 0.004	0.015 ± 0.012	0.015 ± 0.015	0.003 ± 0.003	0.003 ± 0.003
Mann-Whitney U test result (one-tailed)	NS (p = 0.44)	NS (p = 0.34)	NS (p = 0.5)	NS (p = 0.17)	NS (p = 0.17)	NS (p = 0.34)
Mann-Whitney U test result (two-tailed)	NS (p = 0.88)	NS (p = 0.68)	NS (p = 1.00)	NS (p = 0.34)	NS (p = 0.34)	NS (p = 0.68)

Table 15: Summary of relative PCSA-3 for the strepsirrhines (Mean ± SD)

Species	Iliocostalis		Longissimus		Multifidus	
	Thoracic	Lumbar	Thoracic	Lumbar	Thoracic	Lumbar
G. senegalensis	0.005 ± 0.001	0.011 ± 0.008	0.011 ± 0.005	0.006 ± 0.003	0.001 ± 0.0005	0.002 ± 0.001
N. coucang	0.01 ± 0.009	0.007 ± 0.006	0.021 ± 0.016	0.02 ± 0.02	0.004 ± 0.004	0.004 ± 0.004
Mann-Whitney U test result (one-tailed)	NS (p = 0.44)	NS (p = 0.34)	NS (p = 0.34)	NS (p = 0.17)	NS (p = 0.17)	NS (p = 0.34)
Mann-Whitney U test result (two-tailed)	NS (p = 0.88)	NS (p = 0.68)	NS (p = 0.68)	NS (p = 0.34)	NS (p = 0.34)	NS (p = 0.68)

Table 16: Summary of absolute muscle mass (g) for the cercopithecoid monkeys (Mean ± SD)

Species	Iliocostalis		Longissimus		Multifidus	
	Thoracic	Lumbar	Thoracic	Lumbar	Thoracic	Lumbar
C. aethiops	1.2901 ± 0.4187	5.1762 ± 1.958	10.6 ± 6.348	9.8 ± 4.55	0.0877 ± 0.01	0.4063 ± 0.182
E. patas	2.1492 ± 1.675	2.558 ± 1.341	9.8 ± 7.43	12.8 ± 10.69	0.1999 ± 0.1255	0.1399 ± 0.027
Mann-Whitney U test result (two-tailed)	NS (p = 0.69)	p = 0.03	NS (p = 0.84)	NS (p = 0.84)	NS (p = 0.34)	NS (p = 0.11)

Table 17: Summary of relative muscle mass for the cercopithecoid monkeys (Mean ± SD)

Species	Iliocostalis		Longissimus		Multifidus	
	Thoracic	Lumbar	Thoracic	Lumbar	Thoracic	Lumbar
C. aethiops	0.0396 ± 0.0101	0.1616 ± 0.0649	0.3134 ± 0.1319	0.3087 ± 0.1581	0.0027 ± 0.0005	0.0124 ± 0.0057
E. patas	0.0247 ± 0.0226	0.0306 ± 0.0189	0.0995 ± 0.0477	0.1296 ± 0.0776	0.0021 ± 0.0014	0.0016 ± 0.0006
Mann-Whitney U test result (two-tailed)	NS (p = 0.22)	p = 0.01	p = 0.01	p = 0.02	NS (p = 0.49)	p = 0.03

Table 18: Summary of resting pinnation angle for the cercopithecoid monkeys (Mean ± SD)

Species	Iliocostalis		Longissimus		Multifidus	
	Thoracic	Lumbar	Thoracic	Lumbar	Thoracic	Lumbar
C. aethiops	4.13 ± 0.65	2.33 ± 0.25	3.036 ± 0.517	2.77 ± 0.74	2.10 ± 0.71	1.83 ± 0.62
E. patas	4.53 ± 1.88	4.186 ± 1.232	5.135 ± 3.012	4.32 ± 1.05	3.29 ± 0.17	4.28 ± 0.60
Mann-Whitney U test result (one-tailed)	NS (p = 0.5)	p = 0.02	NS (p = 0.16)	p = 0.02	p = 0.01	p = 0.01
Mann-Whitney U test result (two-tailed)	NS (p = 1.00)	p = 0.04	NS (p = 0.32)	p = 0.04	p = 0.02	p = 0.02

Table 19: Summary of NLf (mm) for the cercopithecoid monkeys (Mean ± SD)

Species	Iliocostalis		Longissimus		Multifidus	
	Thoracic	Lumbar	Thoracic	Lumbar	Thoracic	Lumbar
C. aethiops	22.18 ± 4.40	35.70 ± 7.21	32.87 ± 11.09	32.82 ± 7.37	8.38 ± 1.98	6.78 ±2.37
E. patas	31.81 ± 7.18	38.99 ± 4.57	25.09 ± 9.08	43.61 ± 10.45	12.30 ± 1.32	13.17 ± 2.43
Mann-Whitney U test result (one-tailed)	p = 0.02	NS (p = 0.27)	NS (p = 0.21)	p = 0.05	p = 0.01	p = 0.01
Mann-Whitney U test result (two-tailed)	p = 0.04	NS (p = 0.54)	NS (p = 0.42)	NS (p = 0.10)	p = 0.02	p = 0.02

Table 20: Summary of Relative NLf-1 for the cercopithecoid monkeys (Mean ± SD)

Species	Iliocostalis		Longissimus		Multifidus	
	Thoracic	Lumbar	Thoracic	Lumbar	Thoracic	Lumbar
C. aethiops	8.144 ± 1.021	13.321 ± 3.299	11.978 ± 3.128	12.115 ± 2.283	3.047 ± 0.789	2.483 ± 0.98
E. patas	11.84 ± 3.46	14.67 ± 3.70	9.23 ± 3.22	15.919 ± 2.964	4.669 ± 0.686	5.125 ± 1.581
Mann-Whitney U test result (one-tailed)	p = 0.02	NS (p = 0.27)	NS (p = 0.11)	p = 0.03	p = 0.01	p = 0.03
Mann-Whitney U test result (two-tailed)	p = 0.04	NS (p = 0.54)	NS (p = 0.22)	NS (p = 0.06)	P = 0.02	NS (p = 0.06)

Table 21: Summary of relative NLf-2 for the cercopithecoid monkeys (Mean ± SD)

Species	Iliocostalis		Longissimus		Multifidus	
	Thoracic	Lumbar	Thoracic	Lumbar	Thoracic	Lumbar
C. aethiops	22.40 ± 2.62	23.93 ± 3.54	28.03 ± 8.59	22.07 ± 4.16	45.38 ± 10.32	33.65 ± 10.24
E. patas	27.87 ± 3.38	31.16 ± 8.05	22.35 ± 5.16	25.29 ± 4.56	52.43 ± 15.04	50.36 ± 8.14
Mann-Whitney U test result (one-tailed)	p = 0.03	NS (p = 0.08)	NS (p = 0.21)	NS (p = 0.21)	NS (p = 0.25)	p = 0.03
Mann-Whitney U test result (two-tailed)	NS (p = 0.06)	NS (p = 0.16)	NS (p = 0.42)	NS (p = 0.42)	NS (p = 0.50)	NS (p = 0.06)

Table 22: Summary of *h* for the cercopithecoid monkeys (Mean ± SD)

Species	Iliocostalis		Longissimus		Multifidus	
	Thoracic	Lumbar	Thoracic	Lumbar	Thoracic	Lumbar
C. aethiops	5.14 ± 1.02	8.25 ± 1.67	7.61 ± 2.57	7.59 ± 1.71	1.94 ± 0.46	1.57 ± 0.55
E. patas	7.38 ± 1.66	9.04 ± 1.05	5.83 ± 2.08	10.11 ± 2.41	2.85 ± 0.31	3.05 ± 0.57
Mann-Whitney U test result (one-tailed)	p = 0.02	NS (p = 0.27)	NS (p = 0.21)	p = 0.05	p = 0.01	p = 0.01
Mann-Whitney U test result (two-tailed)	p = 0.04	NS (p = 0.54)	NS (p = 0.42)	NS (p = 0.10)	p = 0.02	p = 0.02

Table 23: Summary of relative *h* for the cercopithecoid monkeys (Mean ± SD)

Species	Iliocostalis		Longissimus		Multifidus	
	Thoracic	Lumbar	Thoracic	Lumbar	Thoracic	Lumbar
C. aethiops	0.0519 ± 0.006	0.0553 ± 0.008	0.0649 ± 0.0199	0.0511 ± 0.0097	0.1049 ± 0.0234	0.0778 ± 0.0236
E. patas	0.0647 ± 0.008	0.0722 ± 0.0186	0.0519 ± 0.0117	0.0586 ± 0.0105	0.1214 ± 0.0348	0.1168 ± 0.019
Mann-Whitney U test result (one-tailed)	p = 0.03	NS (p = 0.08)	NS (p = 0.21)	NS (p = 0.21)	NS (p = 0.25)	p = 0.01
Mann-Whitney U test result (two-tailed)	NS (p = 0.06)	NS (p = 0.16)	NS (p = 0.42)	NS (p = 0.42)	NS (p = 0.50)	p = 0.02

Table 24: Summary of TL (mm) for the cercopithecoid monkeys (Mean ± SD)

Species	Iliocostalis		Longissimus		Multifidus	
	Thoracic	Lumbar	Thoracic	Lumbar	Thoracic	Lumbar
C. aethiops	60.25 ± 16.44	61.53 ± 7.35	62.08 ± 8.46	59.24 ± 7.80	9.83 ± 1.17	11.31 ± 2.43
E. patas	56.07 ± 12.36	51.20 ± 16.06	49.98 ± 14.76	69.29 ± 11.89	9.82 ± 0.74	10.11 ± 1.95
Mann-Whitney U test result (one-tailed)	NS (p = 0.5)	NS (p = 0.21)	NS (p = 0.11)	NS (p = 0.11)	NS (p = 0.5)	NS (p = 0.34)
Mann-Whitney U test result (two-tailed)	NS (p = 1.00)	NS (p = 0.42)	NS (p = 0.22)	NS (p = 0.22)	NS (p = 1.00)	NS (p = 0.68)

Table 25: Summary of TL/(TL + NLf) for the cercopithecoid monkeys (Mean ± SD)

Species	Iliocostalis		Longissimus		Multifidus	
	Thoracic	Lumbar	Thoracic	Lumbar	Thoracic	Lumbar
C. aethiops	0.723 ± 0.062	0.635 ± 0.033	0.659 ± 0.082	0.645 ± 0.062	0.543 ± 0.077	0.628 ± 0.093
E. patas	0.638 ± 0.025	0.558 ± 0.091	0.669 ± 0.045	0.616 ± 0.016	0.445 ± 0.041	0.435 ± 0.059
Mann-Whitney U test result (one-tailed)	p = 0.01	NS (p = 0.16)	NS (p = 0.5)	NS (p = 0.27)	p = 0.03	p = 0.01
Mann-Whitney U test result (two-tailed)	p = 0.02	NS (p = 0.32)	NS (p = 1.00)	NS (p = 0.54)	NS (p = 0.06)	p = 0.02

Table 26: Summary of PCSA (cm^2) for the cercopithecoid monkeys (Mean ± SD)

Species	Iliocostalis		Longissimus		Multifidus	
	Thoracic	Lumbar	Thoracic	Lumbar	Thoracic	Lumbar
C. aethiops	0.5434 ± 0.1064	1.3493 ± 0.3294	3.079 ± 1.476	2.868 ± 1.46	0.104 ± 0.032	0.588 ± 0.316
E. patas	0.6343 ± 0.466	0.6187 ± 0.3162	4.8397 ± 4.845	2.8472 ± 2.416	0.151 ± 0.099	0.1001 ± 0.0041
Mann-Whitney U test result (one-tailed)	NS (p = 0.35)	p = 0.01	NS (p = 0.5)	NS (p = 0.35)	NS (p = 0.17)	p = 0.01
Mann-Whitney U test result (two-tailed)	NS (p = 0.70)	p = 0.02	NS (p = 1.00)	NS (p = 0.70)	NS (p = 0.34)	p = 0.02

Table 27: Summary of relative PCSA-1 for the cercopithecoid monkeys (Mean ± SD)

Species	Iliocostalis		Longissimus		Multifidus	
	Thoracic	Lumbar	Thoracic	Lumbar	Thoracic	Lumbar
C. aethiops	0.0024 ± 0.0004	0.006 ± 0.001	0.014 ± 0.006	0.013 ± 0.007	0.0005 ± 0.0001	0.0025 ± 0.001
E. patas	0.0014 ± 0.0009	0.0014 ± 0.0008	0.0097 ± 0.008	0.0058 ± 0.004	0.0003 ± 0.0002	0.0002 ± 0.0001
Mann-Whitney U test result (one-tailed)	p = 0.05	p = 0.00	NS (p = 0.16)	p = 0.03	NS (p = 0.17)	p = 0.01
Mann-Whitney U test result (two-tailed)	NS (p = 0.10)	p = 0.00	NS (p = 0.32)	NS (p = 0.06)	NS (p = 0.34)	p = 0.02

Table 28: Summary of relative PCSA-2 for the cercopithecoid monkeys (Mean ± SD)

Species	Iliocostalis		Longissimus		Multifidus	
	Thoracic	Lumbar	Thoracic	Lumbar	Thoracic	Lumbar
C. aethiops	0.0022 ± 0.0004	0.0055 ± 0.0013	0.0124 ± 0.0057	0.0119 ± 0.0066	0.0004 ± 0.0001	0.0023 ± 0.0009
E. patas	0.0012 ± 0.0009	0.0013 ± 0.0007	0.0084 ± 0.0068	0.005 ± 0.003	0.0003 ± 0.0002	0.0002 ± 0.0001
Mann-Whitney U test result (one-tailed)	p = 0.05	p = 0.00	NS (p = 0.16)	p = 0.03	NS (p = 0.17)	p = 0.01
Mann-Whitney U test result (two-tailed)	NS (p = 0.10)	p = 0.00	NS (p = 0.32)	NS (p = 0.06)	NS (p = 0.34)	p = 0.02

Table 29: Summary of relative PCSA-3 for the cercopithecoid monkeys (Mean ± SD)

Species	Iliocostalis		Longissimus		Multifidus	
	Thoracic	Lumbar	Thoracic	Lumbar	Thoracic	Lumbar
C. aethiops	0.0027 ± 0.0004	0.0067 ± 0.0015	0.0152 ± 0.007	0.0145 ± 0.0079	0.0005 ± 0.0001	0.0028 ± 0.0012
E. patas	0.0016 ± 0.0011	0.0017 ± 0.0009	0.0118 ± 0.0104	0.007 ± 0.005	0.0004 ± 0.0002	0.0003 ± 0.0001
Mann-Whitney U test result (one-tailed)	NS (p = 0.08)	p = 0.00	NS (p = 0.16)	NS (p = 0.11)	NS (p = 0.25)	p = 0.01
Mann-Whitney U test result (two-tailed)	NS (p = 0.16)	p = 0.00	NS (p = 0.32)	NS (p = 0.22)	NS (p = 0.50)	p = 0.02

Table 30: One-way ANOVA results (n = 4 species)

Variable	F	P
Absolute muscle mass	7.936	p = 0.00
Relative muscle mass	4.198	p = 0.01
Resting pinnation angle	20.523	p = 0.00
Resting fiber length (NLf)	21.512	p = 0.00
Relative NLf-1	19.134	p = 0.00
Relative NLf-2	21.638	p = 0.00
Potential excursion of whole muscle (*h*)	21.421	p = 0.00
Relative *h*	21.540	p = 0.00
Tendon length (TL)	23.731	p = 0.00
TL/(TL + NLf)	27.409	p = 0.00
PCSA	4.364	p = 0.01
Relative PCSA-1	3.109	p = 0.03
Relative PCSA-2	3.044	p = 0.03
Relative PCSA-3	3.252	p = 0.03

Table 31: Absolute muscle mass: Multiple pairwise comparison

Species	*G. senegalensis*	*N. coucang*	*C. aethiops*	*E. patas*
G. senegalensis	---	NS (p = 0.86)	p = 0.00	p = 0.00
N. coucang	NS (p = 0.86)	---	p = 0.00	p = 0.00
C. aethiops	p = 0.00	p = 0.00	---	NS (p = 0.964)
E. patas	p = 0.00	p = 0.00	NS (p = 0.964)	---

Table 32: Relative muscle mass: Multiple pairwise comparison

Species	*G. senegalensis*	*N. coucang*	*C. aethiops*	*E. patas*
G. senegalensis	---	NS (p = 0.13)	NS (p = 0.93)	p = 0.01
N. coucang	NS (p = 0.13)	---	NS (p = 0.1)	NS (p = 0.19)
C. aethiops	NS (p = 0.93)	NS (p = 0.1)	---	p = 0.00
E. patas	p = 0.01	NS (p = 0.19)	p = 0.00	---

Table 33: Resting pinnation angle: Multiple pairwise comparison

Species	*G. senegalensis*	*N. coucang*	*C. aethiops*	*E. patas*
G. senegalensis	---	p = 0.00	p = 0.00	NS (p = 0.84)
N. coucang	p = 0.00	---	p = 0.00	p = 0.00
C. aethiops	p = 0.00	p = 0.00	---	p = 0.00
E. patas	NS (p = 0.84)	p = 0.00	p = 0.00	---

Table 34: Resting fiber length (NLf): Multiple pairwise comparison

Species	*G. senegalensis*	*N. coucang*	*C. aethiops*	*E. patas*
G. senegalensis	---	p = 0.02	p = 0.00	p = 0.00
N. coucang	p = 0.02	---	p = 0.00	p = 0.00
C. aethiops	p = 0.00	p = 0.00	---	NS (p = 0.12)
E. patas	p = 0.00	p = 0.00	NS (p = 0.12)	---

Table 35: Relative NLf-1: Multiple pairwise comparison

Species	*G. senegalensis*	*N. coucang*	*C. aethiops*	*E. patas*
G. senegalensis	---	p = 0.00	p = 0.00	p = 0.00
N. coucang	p = 0.00	---	p = 0.00	p = 0.00
C. aethiops	p = 0.00	p = 0.00	---	NS (p = 0.17)
E. patas	p = 0.00	p = 0.00	NS (p = 0.17)	---

Table 36: Relative NLf-2: Multiple pairwise comparison

Species	*G. senegalensis*	*N. coucang*	*C. aethiops*	*E. patas*
G. senegalensis	---	p = 0.00	p = 0.00	p = 0.00
N. coucang	p = 0.00	---	p = 0.00	p = 0.00
C. aethiops	p = 0.00	p = 0.00	---	NS (p = 0.11)
E. patas	p = 0.00	p = 0.00	NS (p = 0.11)	---

Table 37: Potential excursion of whole muscle (*h*): Multiple pairwise comparison

Species	*G. senegalensis*	*N. coucang*	*C. aethiops*	*E. patas*
G. senegalensis	---	p = 0.02	p = 0.00	p = 0.00
N. coucang	p = 0.02	---	p = 0.00	p = 0.00
C. aethiops	p = 0.00	p = 0.00	---	NS (p = 0.11)
E. patas	p = 0.00	p = 0.00	NS (p = 0.11)	---

Table 38: Relative *h*: Multiple pairwise comparison

Species	*G. senegalensis*	*N. coucang*	*C. aethiops*	*E. patas*
G. senegalensis	---	p = 0.00	p = 0.00	p = 0.01
N. coucang	p = 0.00	---	p = 0.00	p = 0.00
C. aethiops	p = 0.00	p = 0.00	---	NS (p = 0.11)
E. patas	p = 0.01	p = 0.00	NS (p = 0.11)	---

Table 39: Tendon length (TL): Multiple pairwise comparison

Species	*G. senegalensis*	*N. coucang*	*C. aethiops*	*E. patas*
G. senegalensis	---	p = 0.00	p = 0.00	p = 0.00
N. coucang	p = 0.00	---	p = 0.00	p = 0.00
C. aethiops	p = 0.00	p = 0.00	---	NS (p = 0.54)
E. patas	p = 0.00	p = 0.00	NS (p = 0.54)	---

Table 40: TL/(TL + NLf): Multiple pairwise comparison

Species	*G. senegalensis*	*N. coucang*	*C. aethiops*	*E. patas*
G. senegalensis	---	p = 0.00	NS (p = 0.35)	p = 0.03
N. coucang	p = 0.00	---	p = 0.00	p = 0.00
C. aethiops	NS (p = 0.35)	p = 0.00	---	p = 0.00
E. patas	p = 0.03	p = 0.00	p = 0.00	---

Table 41: PCSA: Multiple pairwise comparison

Species	*G. senegalensis*	*N. coucang*	*C. aethiops*	*E. patas*
G. senegalensis	---	NS (p = 0.33)	p = 0.01	p = 0.00
N. coucang	NS (p = 0.33)	---	NS (p = 0.08)	p = 0.04
C. aethiops	p = 0.01	NS (p = 0.08)	---	NS (p = 0.76)
E. patas	p = 0.00	p = 0.04	NS (p = 0.76)	---

Table 42: Relative PCSA-1: Multiple pairwise comparison

Species	*G. senegalensis*	*N. coucang*	*C. aethiops*	*E. patas*
G. senegalensis	---	NS (p = 0.06)	NS (p = 0.52)	NS (p = 0.31)
N. coucang	NS (p = 0.06)	---	NS (p = 0.19)	p = 0.00
C. aethiops	NS (p = 0.52)	NS (p = 0.19)	---	NS (p = 0.08)
E. patas	NS (p = 0.31)	p = 0.00	NS (p = 0.08)	---

Table 43: Relative PCSA-2: Multiple pairwise comparison

Species	*G. senegalensis*	*N. coucang*	*C. aethiops*	*E. patas*
G. senegalensis	---	NS (p = 0.09)	NS (p = 0.5)	NS (p = 0.25)
N. coucang	NS (p = 0.09)	---	NS (p = 0.27)	p = 0.00
C. aethiops	NS (p = 0.5)	NS (p = 0.27)	---	NS (p = 0.06)
E. patas	NS (p = 0.25)	p = 0.00	NS (p = 0.06)	---

Table 44: Relative PCSA-3: Multiple pairwise comparison

Species	*G. senegalensis*	*N. coucang*	*C. aethiops*	*E. patas*
G. senegalensis	---	p = 0.04	NS (p = 0.55)	NS (p = 0.40)
N. coucang	p = 0.04	---	NS (p = 0.11)	p = 0.00
C. aethiops	NS (p = 0.55)	NS (p = 0.11)	---	NS (p = 0.13)
E. patas	NS (p = 0.40)	p = 0.00	NS (p = 0.13)	---

Table 45: Correlation between absolute NLf (excursion and velocity) and absolute PCSA (force): Strepsirrhines

Correlation statistics	Iliocostalis		Longissimus		Multifidus	
	Thoracic	Lumbar	Thoracic	Lumbar	Thoracic	Lumbar
Pearson's *r*	-0.580	-0.320	-0.818	-0.637	-0.365	-0.517
p (one-tailed)	NS (0.066)	NS (0.220)	0.006	0.045	NS (0.187)	NS (0.095)
p (two-tailed)	NS (0.132)	NS (0.440)	0.012	NS (0.09)	NS (0.374)	NS (0.190)

Table 46: Correlation between absolute NLf (excursion and velocity) and absolute PCSA (force): Cercopithecoids

Correlation statistics	Iliocostalis		Longissimus		Multifidus	
	Thoracic	Lumbar	Thoracic	Lumbar	Thoracic	Lumbar
Pearson's *r*	0.144	-0.075	-0.568	-0.145	0.236	-0.717
p (one-tailed)	NS (0.346)	NS (0.418)	0.044	NS (0.345)	NS (0.287)	0.023
p (two-tailed)	NS (0.692)	NS (0.836)	NS (0.088)	NS (0.690)	NS (0.574)	0.046

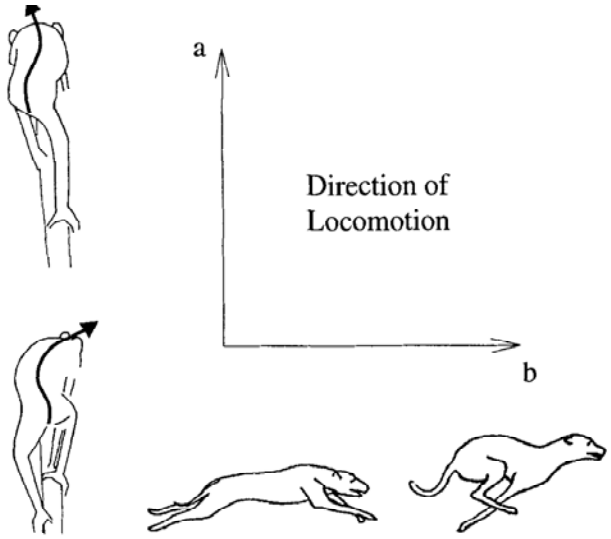

Fig. 1. a: Transverse movement of the trunk in a lorisid primate. b: Two different phases of a leaping gallop in dog; left: back maximally extended; right: back maximally bent. Adapted from Demes et al. (1990); Slijper (1946).

Fig. 2: Schematic representation of a bipinnate muscle. Pinnation angle (θ) is measured as the angle formed between the muscle fiber and the muscle line of action (Organ et al., 2009).

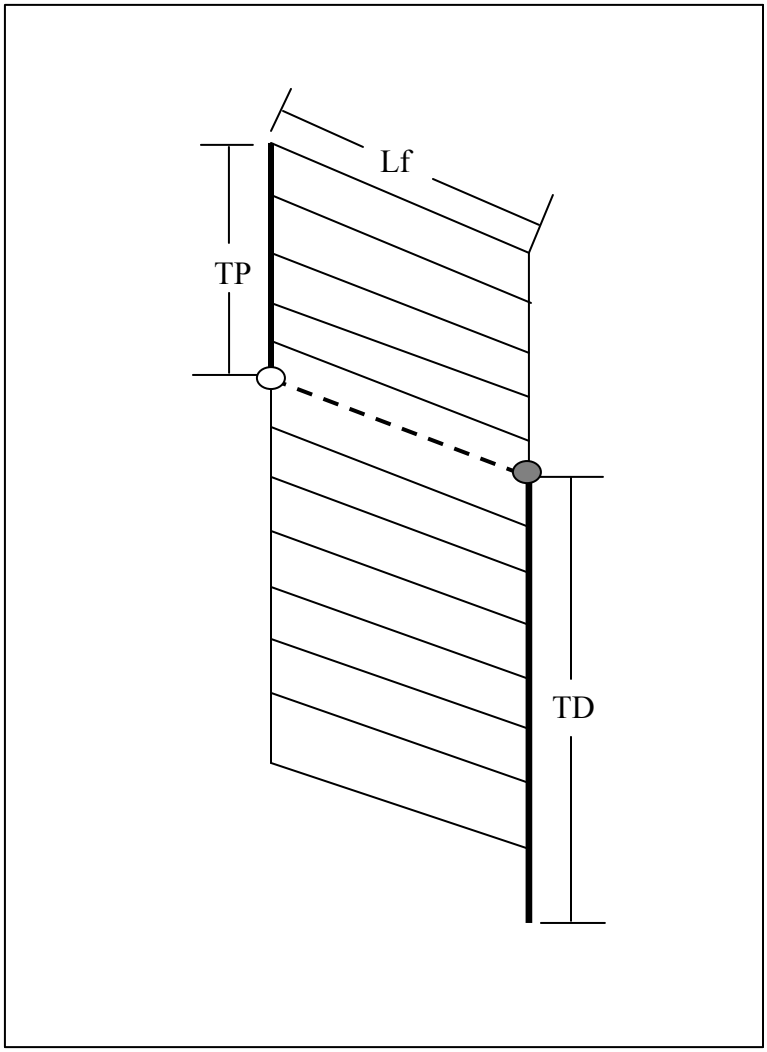

Fig. 3: Measurement of fiber length and tendon length. The dashed line represents a fiber of interest. Lf = Length of muscle fiber. TP = Proximal tendon length, measured as the length of tendon running from the proximal bony attachment to the proximal myotendinous junction. TD = Distal tendon length, measured as the length of tendon from the distal bony attachment to the most distal myotendinous junction. TP + TD = TL (tendon length) (after Anapol and Barry, 1996).

Fig. 4: Fascicle length measurement procedure for certain tissue segments. See “Materials and methods” for details.

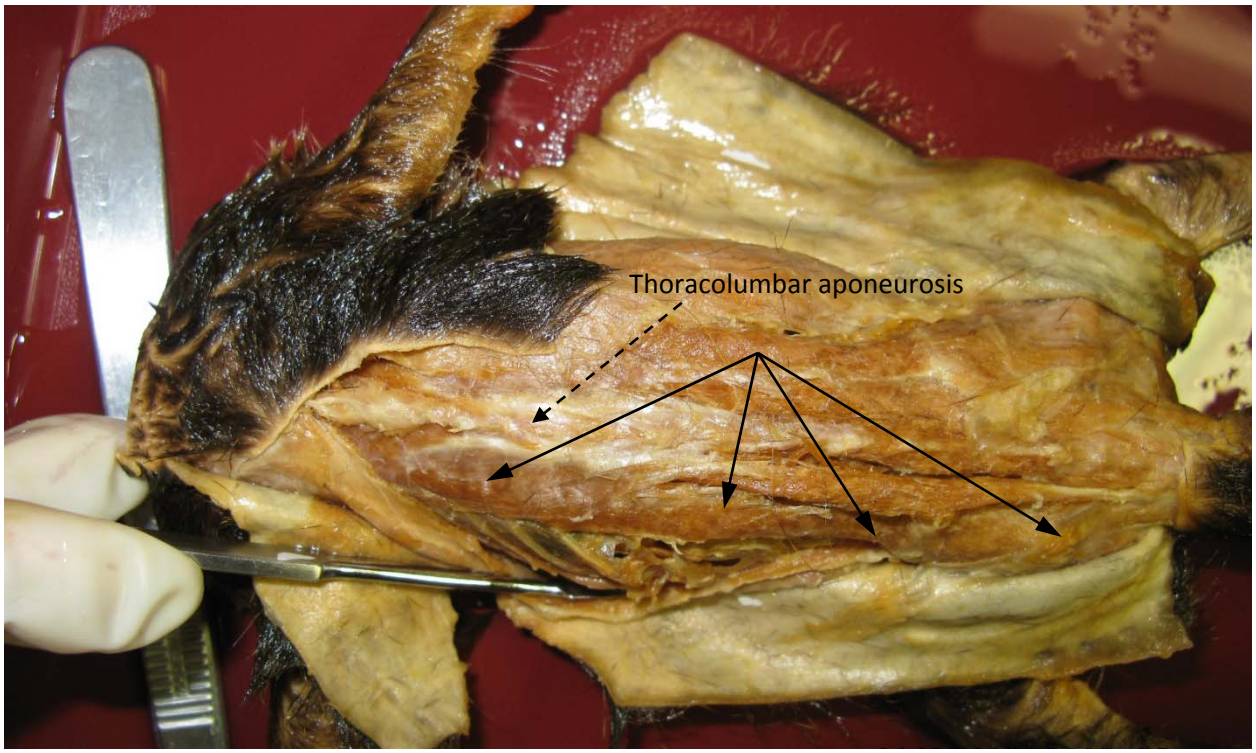

Fig. 5: Arrows indicate the m. iliocostalis of *G. senegalensis in situ*. Caudal is to the right. Dashed arrow points to the thoracolumbar aponeurosis.

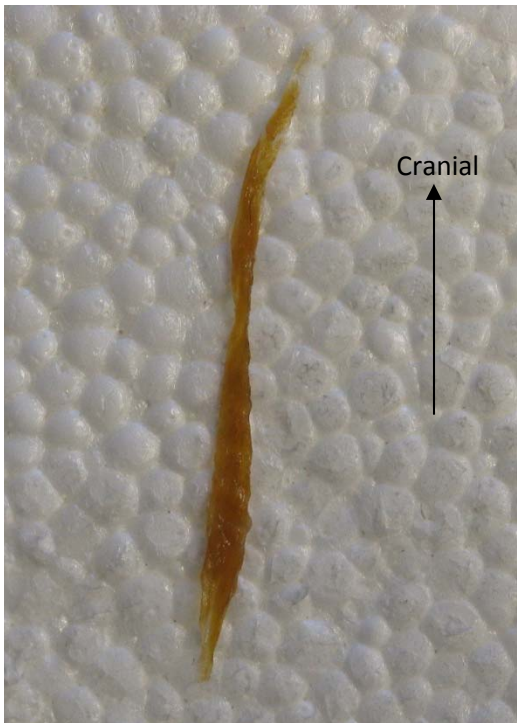

Fig. 6 Thoracic iliocostalis of *G. senegalensis*.

Fig. 7: Lumbar iliocostalis of *G. senegalensis*

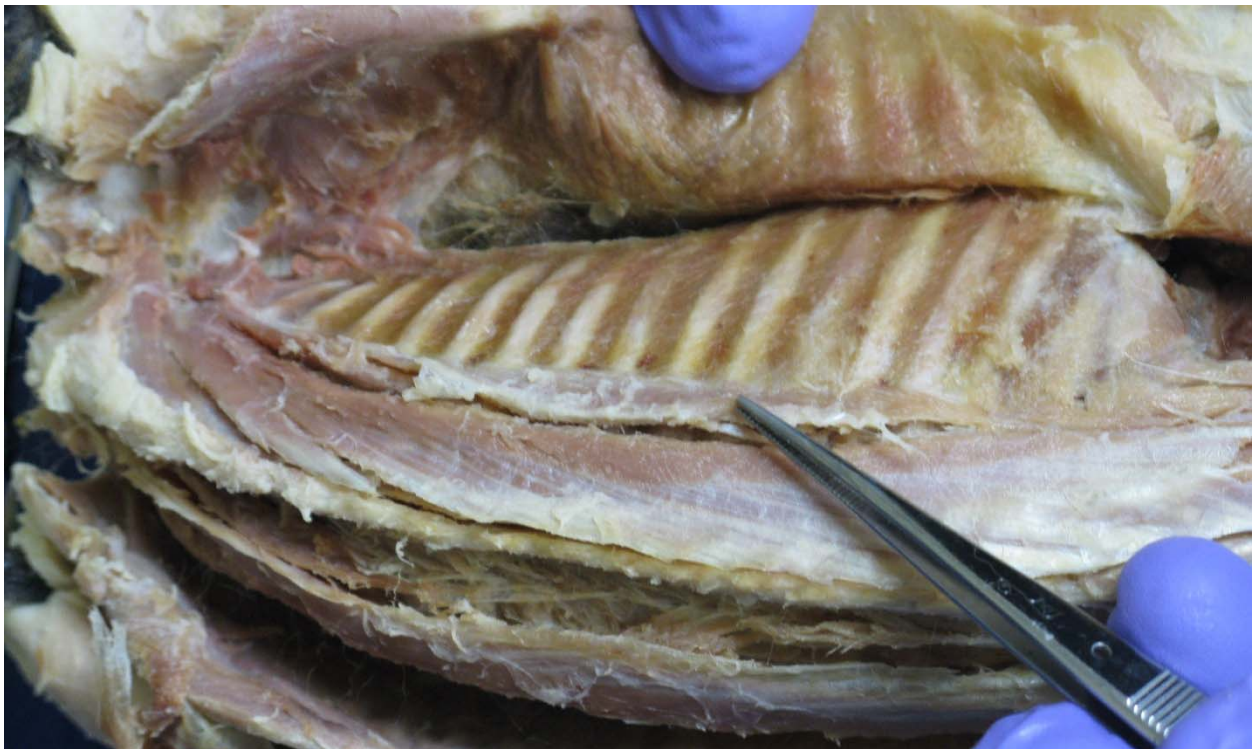

Fig. 8: The tip of the forceps points to the m. iliocostalis of *N. coucang in situ*. Caudal is to the right.

Fig. 9: Thoracic iliocostalis of *N. coucang*.

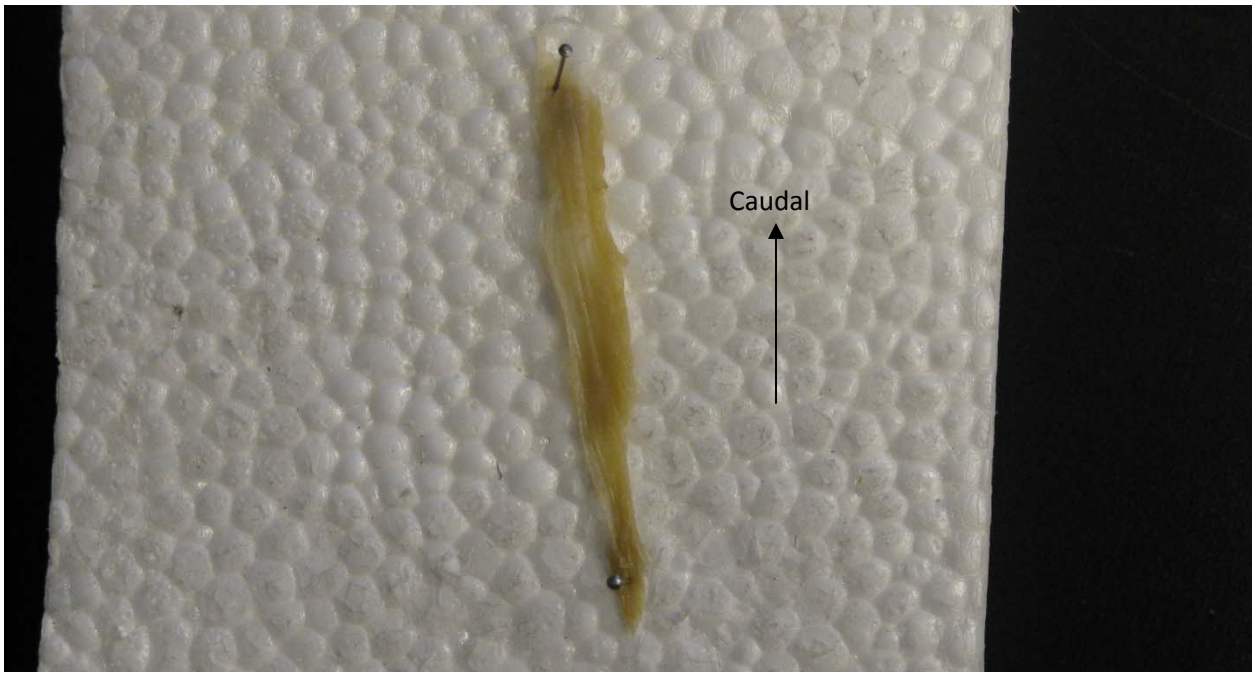

Fig. 10: Lumbar iliocostalis of *N. coucang*.

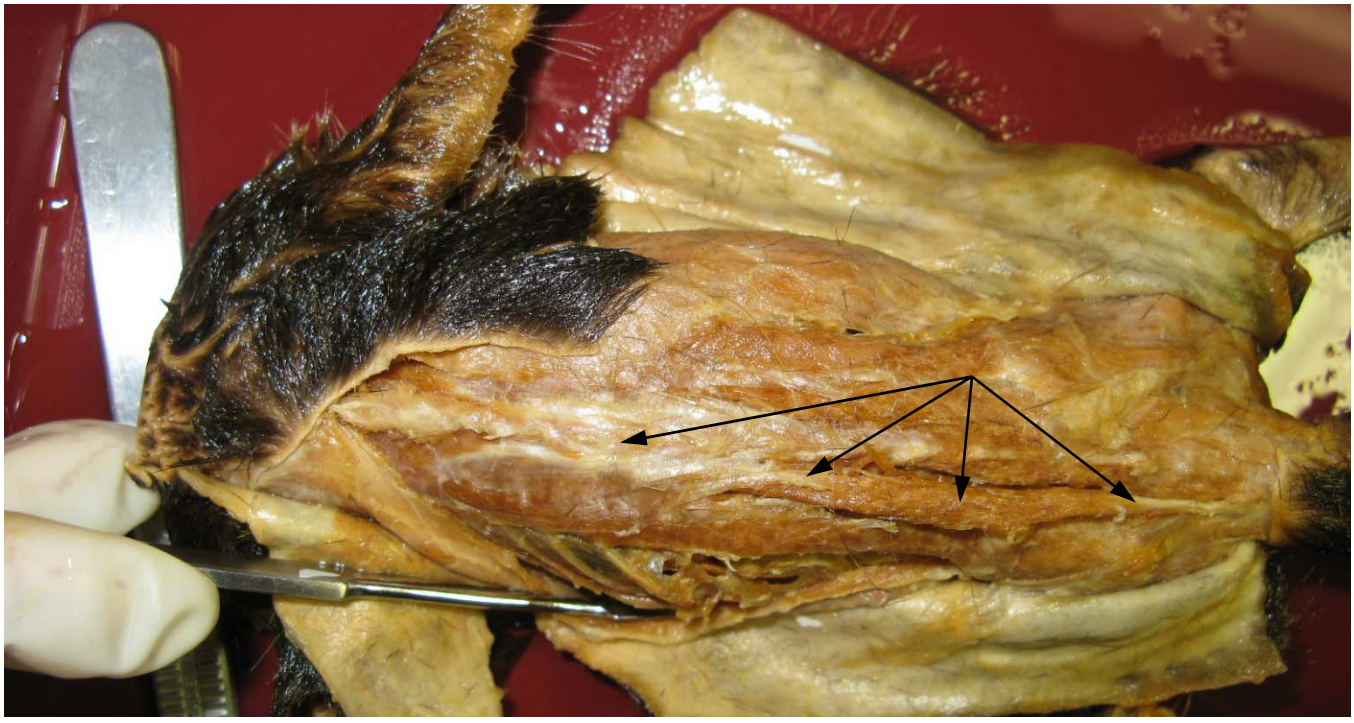

Fig. 11: Arrows indicate m. longissimus of *G. senegalensis in situ*. Caudal is to the right.

Fig. 12: Lumbar longissimus of *G. senegalensis*

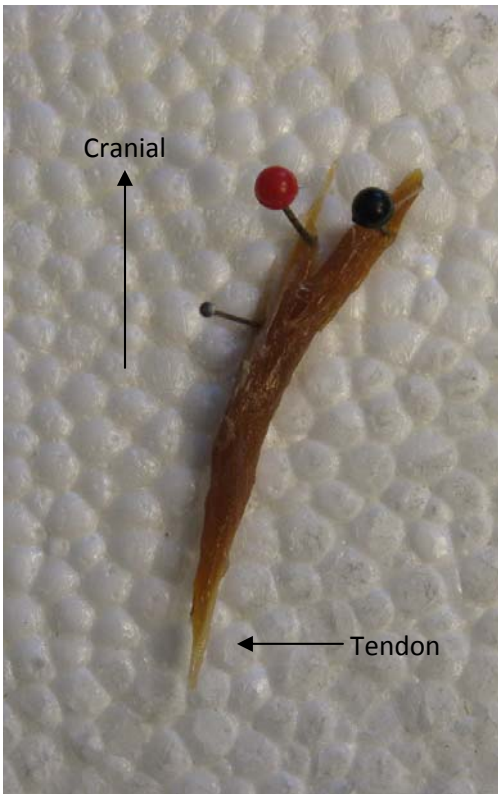

Fig. 13: Three layers of lumbar longissimus of *G. senegalensis* converging on a tendon

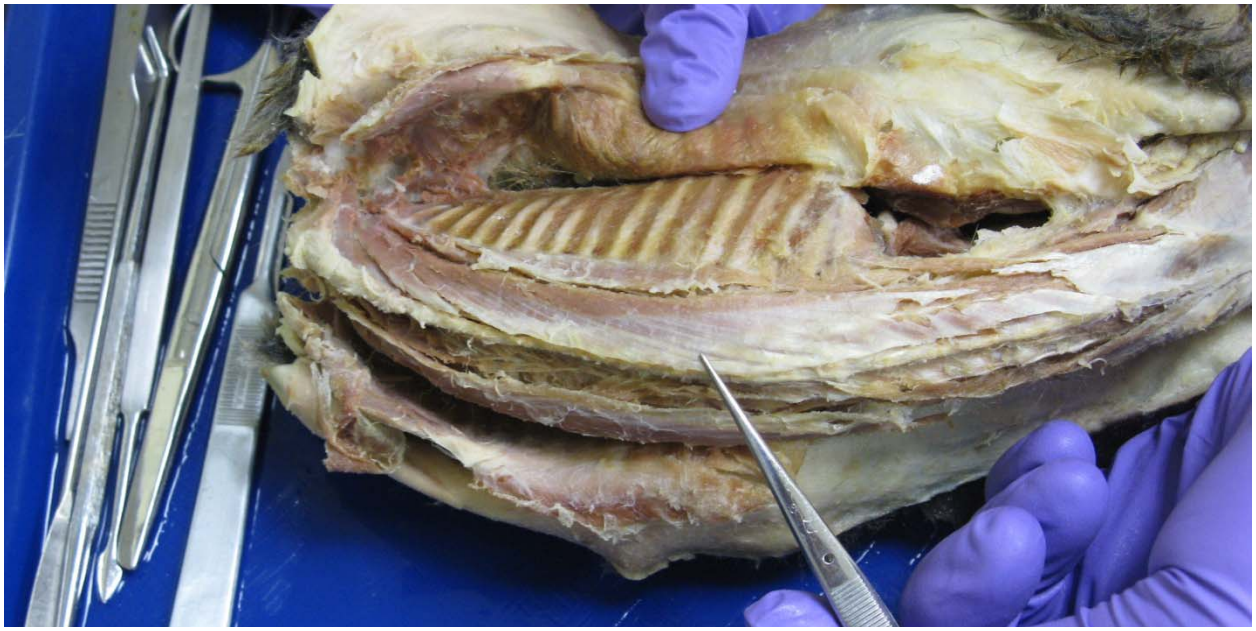

Fig. 14: The tip of the forceps points to the m. longissimus of *N. coucang in situ*. Caudal is to the right.

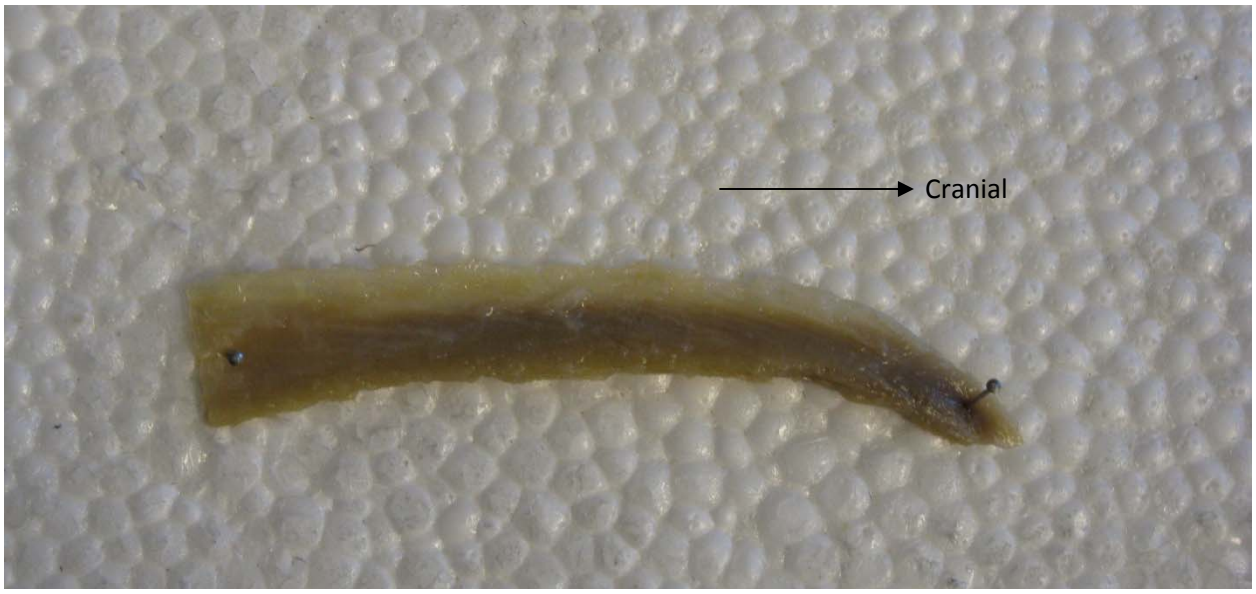

Fig. 15: Thoracic longissimus of *N. coucang*.

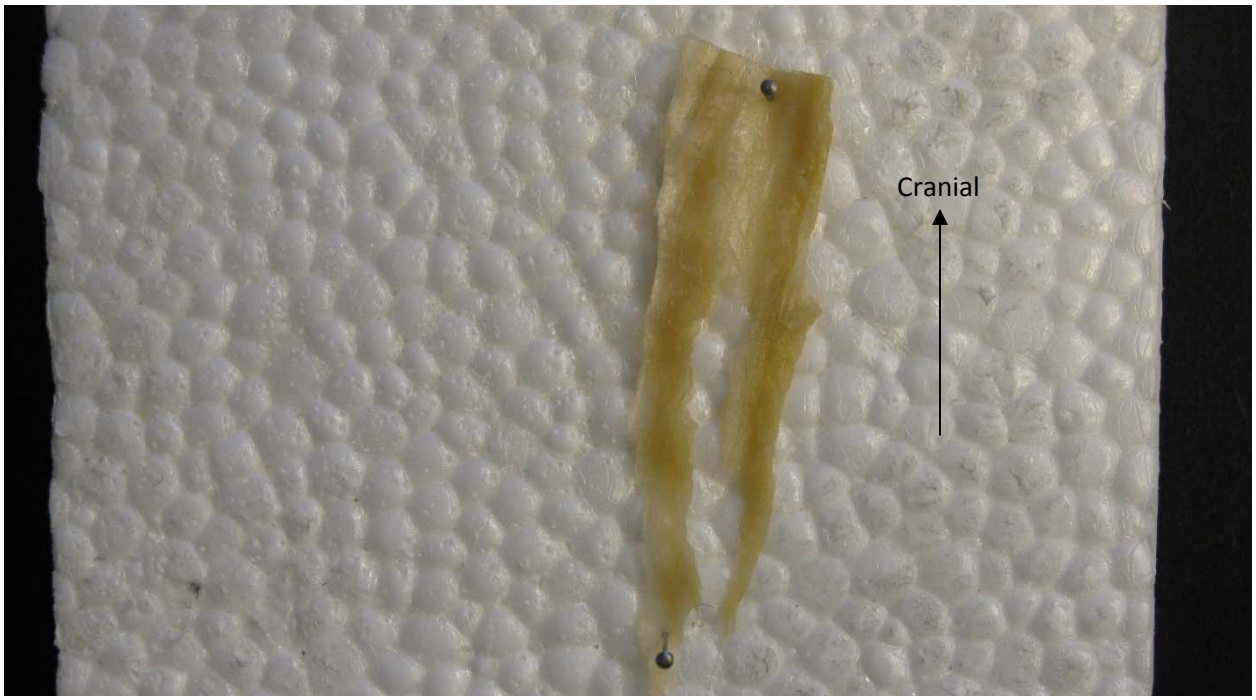

Fig. 16: Lumbar longissimus of *N. coucang*.

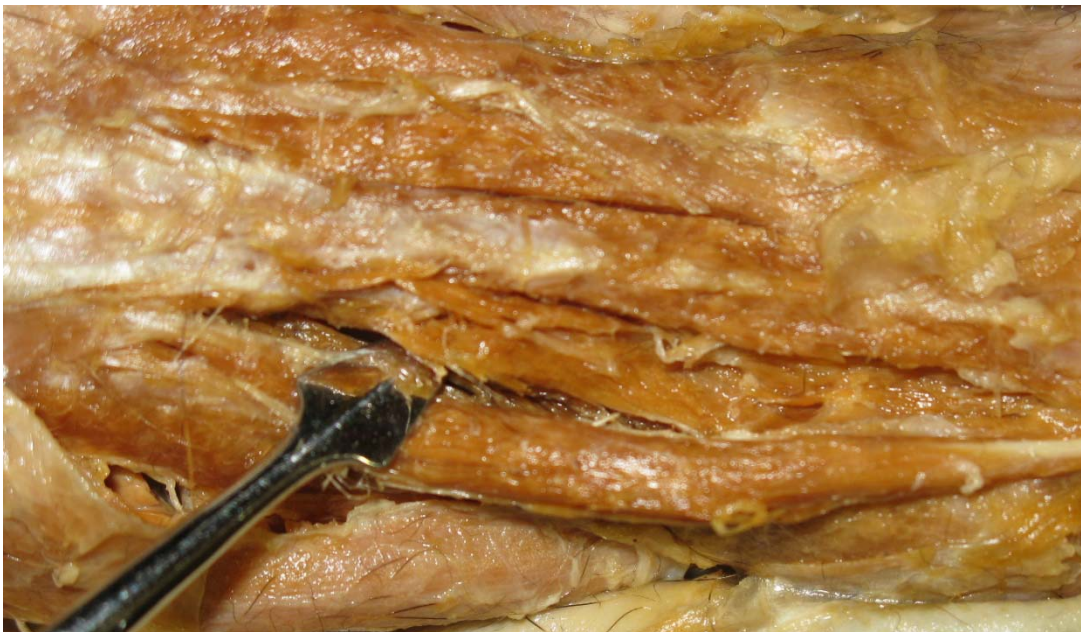

Fig. 17: The tip of the probe points to m. multifidus (lumbar region) of *G. senegalensis in situ*. Caudal is to the right.

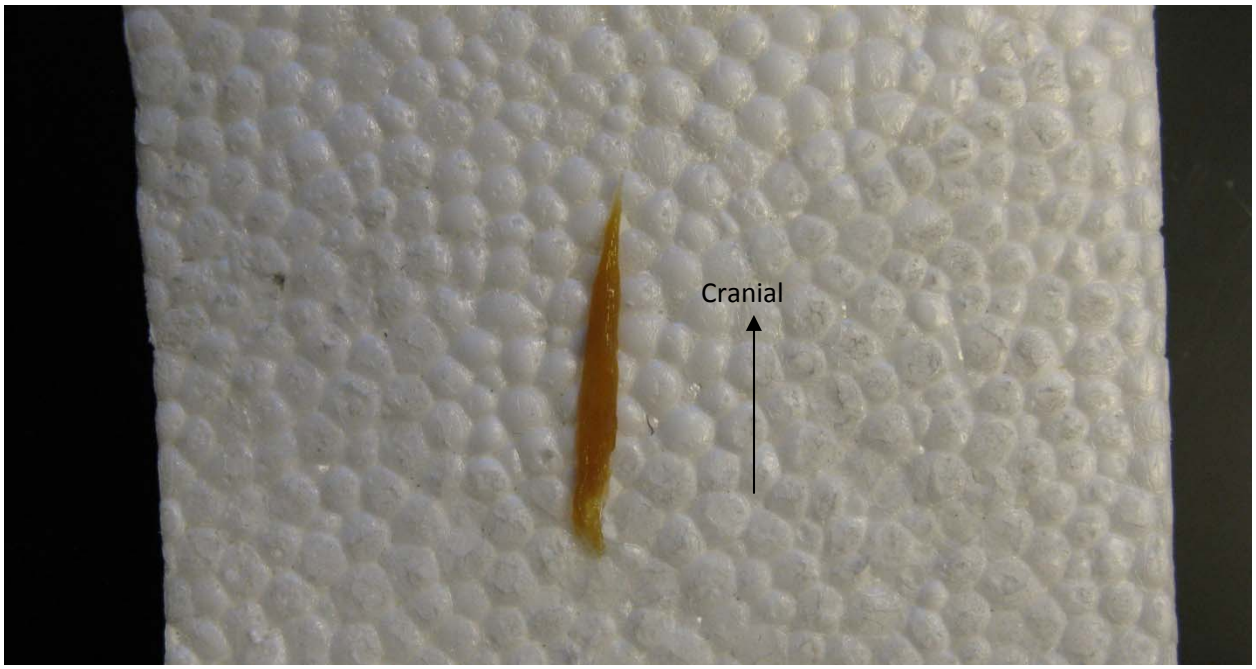

Fig. 18: One slip of m. multifidus of *G. senegalensis*.

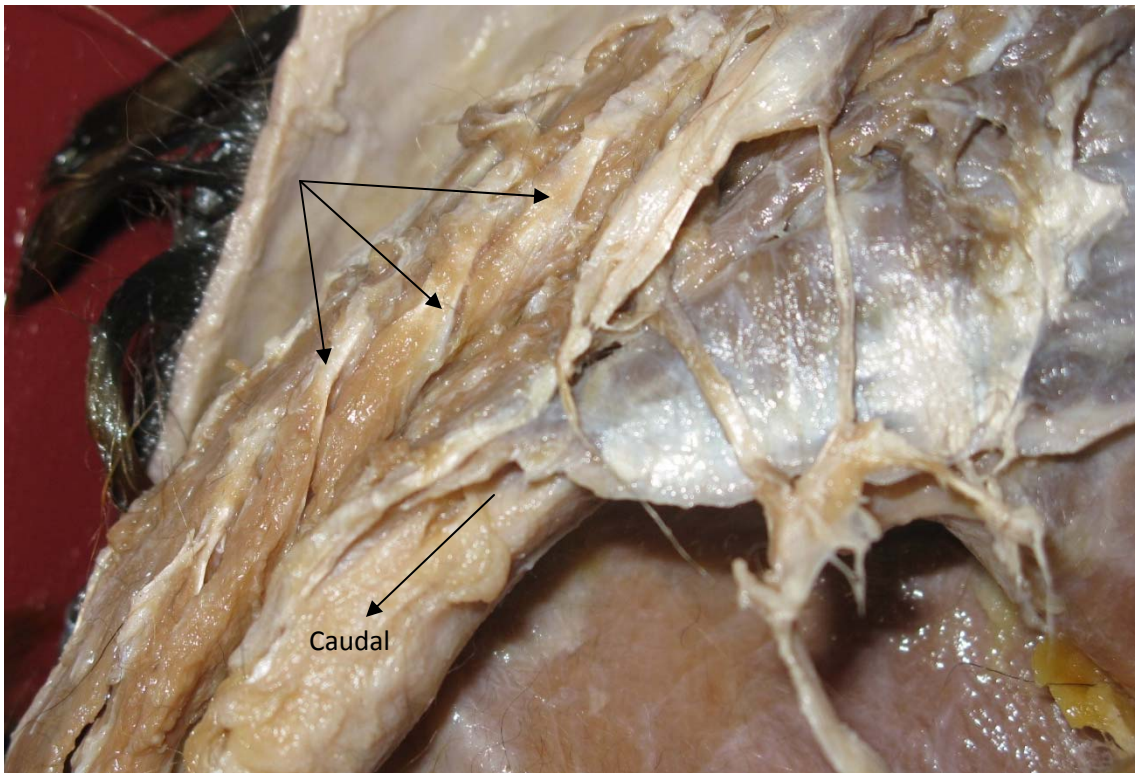

Fig. 19: Arrows point to slips of m. multifidus of *N. coucang in situ*.

Fig. 20: One slip of m. multifidus of *N. coucang*. Cranial is to the left.

Fig. 21: The tip of the forceps points to m. iliocostalis of *E. patas*. Cranial is to the left.

Fig. 22: Thoracic iliocostalis of *C. aethiops*.

Fig. 23: Thoracic iliocostalis of *E. patas*.

Fig. 24: Lumbar iliocostalis of *C. aethiops*.

Fig. 25: Lumbar iliocostalis of *E. patas*.

Fig. 26: The tip of the forceps points to m. longissimus of *E. patas*. Cranial is to the left.

Fig. 27: Thoracic longissimus of *C. aethiops*.

Fig. 28: Thoracic longissimus of *E. patas*.

Fig. 29: Lumbar longissimus of *C. aethiops*.

Fig. 30: Lumbar longissimus of *E. patas*.

Fig. 31: The tip of the forceps points to m. multifidus of *E. patas*. Cranial is to the left.

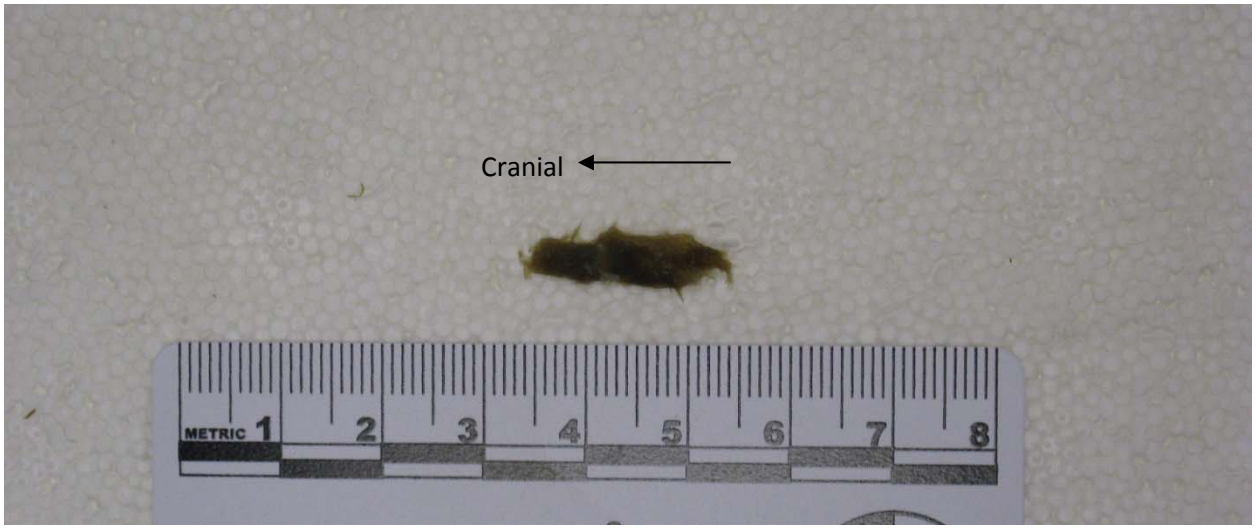

Fig. 32: Multifidus of *C. aethiops*.

Fig. 33: Multifidus of *E. patas*.

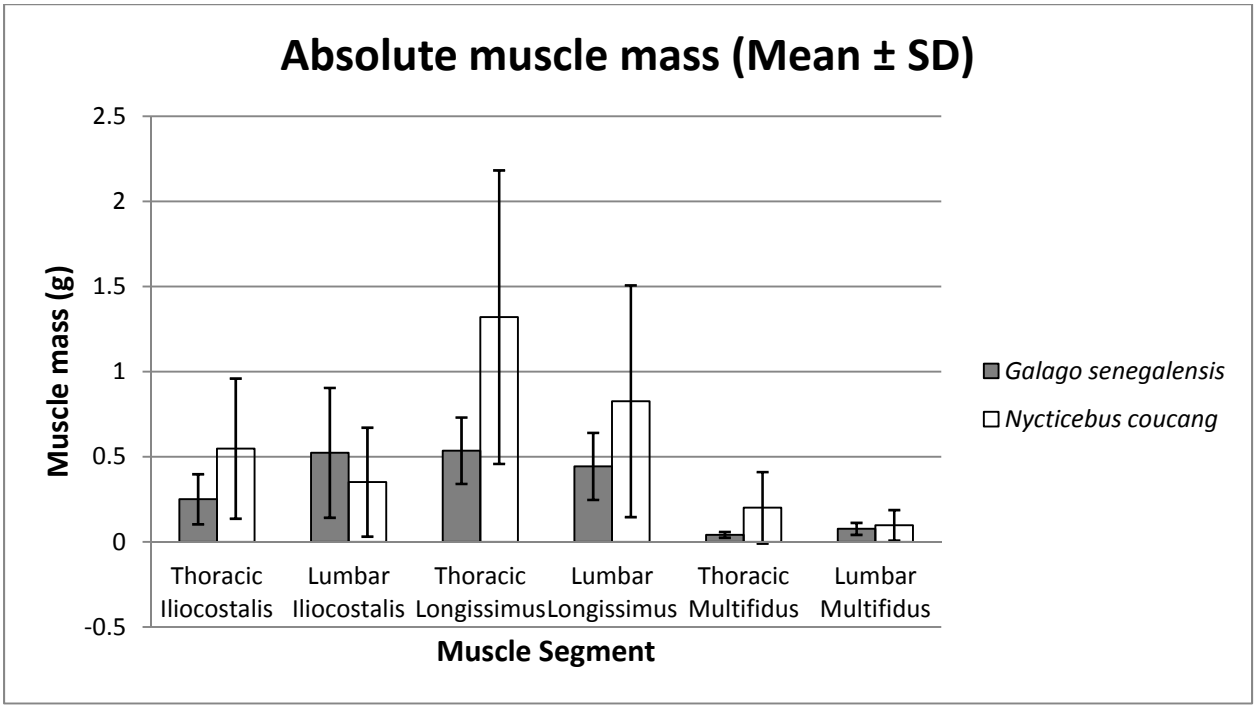

Fig. 34: Mean (± SD) of absolute muscle mass for *G. senegalensis* and *N. coucang*

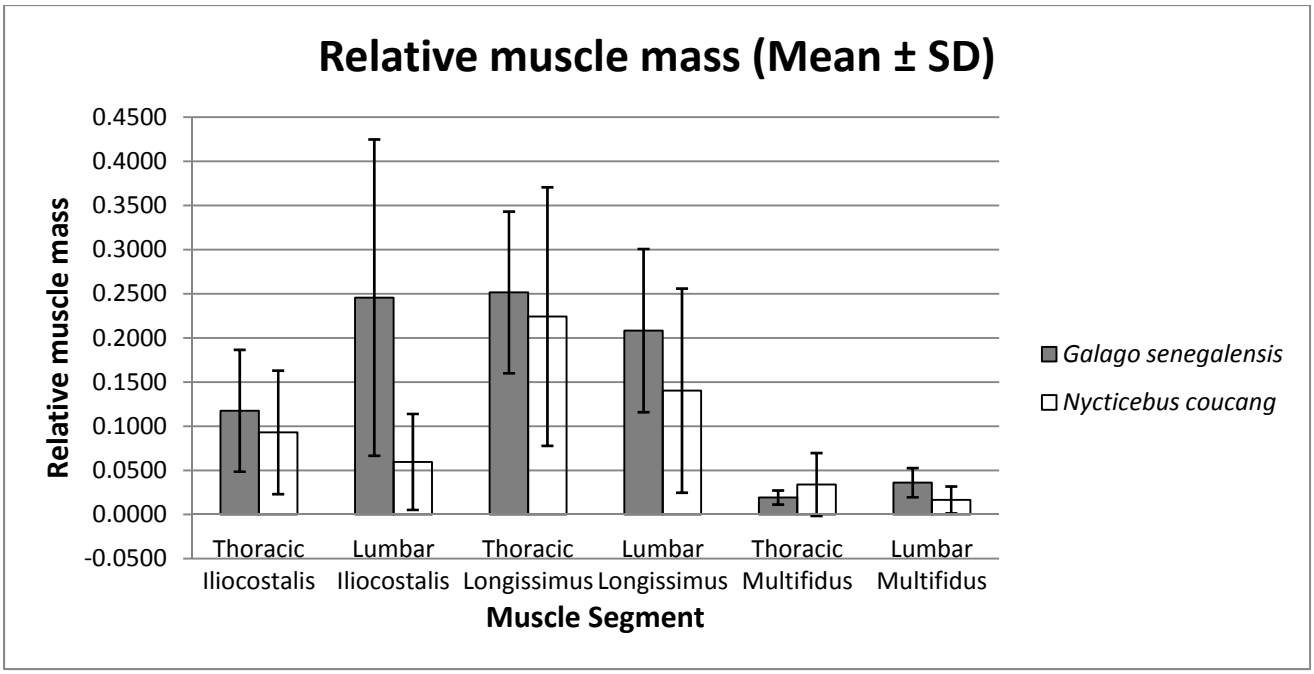

Fig. 35: Mean (± SD) of relative muscle mass for *G. senegalensis* and *N. coucang*

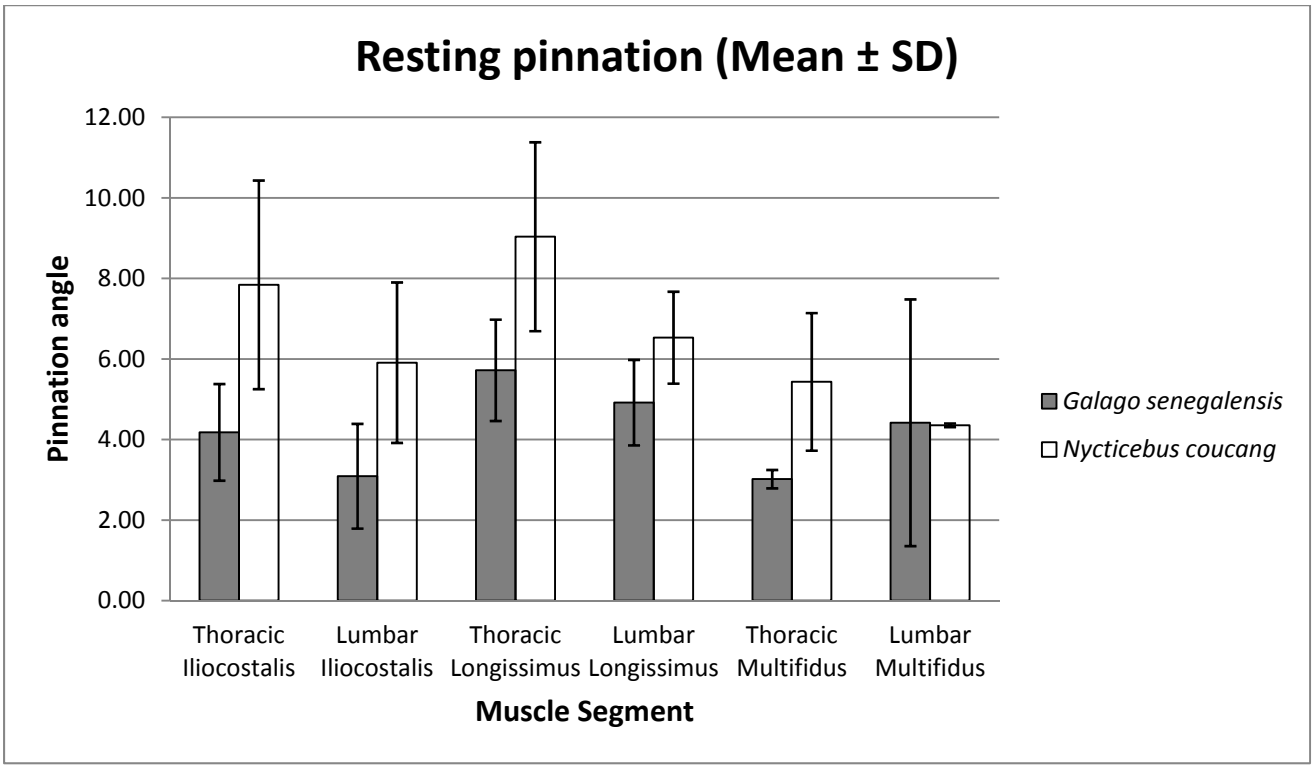

Fig. 36: Mean (± SD) of resting pinnation for *G. senegalensis* and *N. coucang*

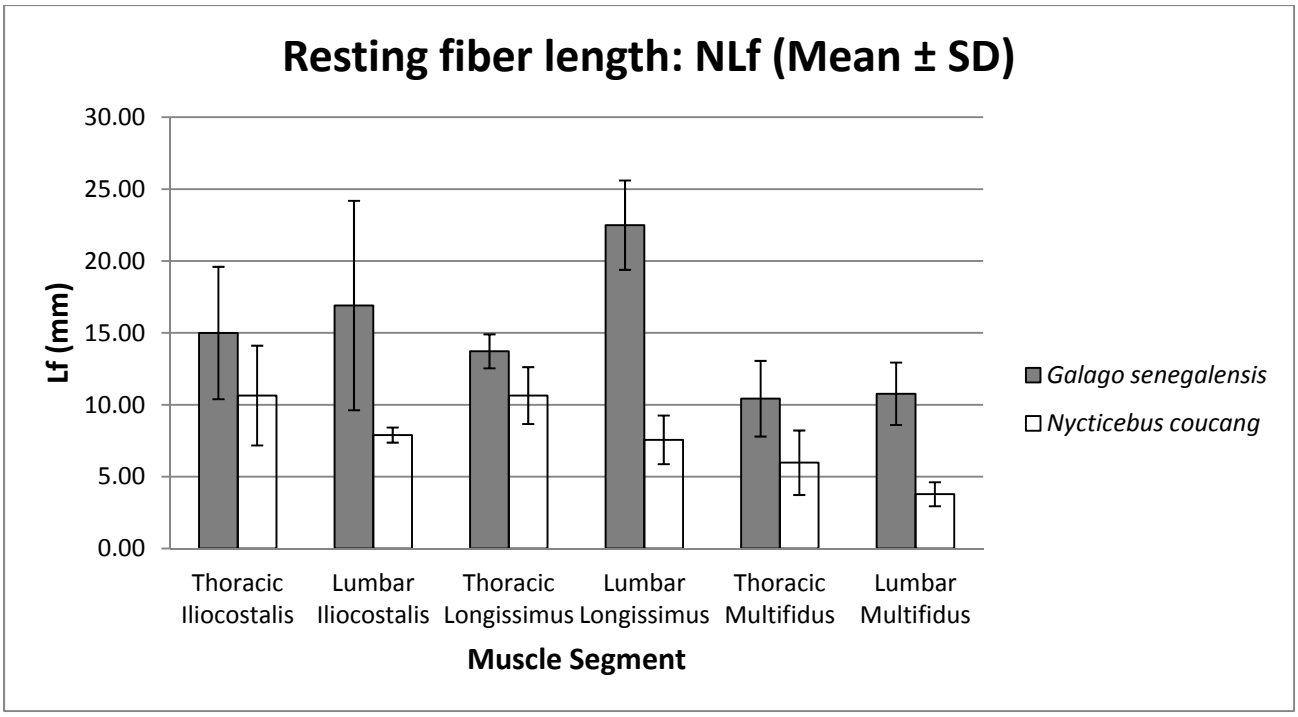

Fig. 37: Mean (± SD) of resting fiber length (NLf) for *G. senegalensis* and *N. coucang*

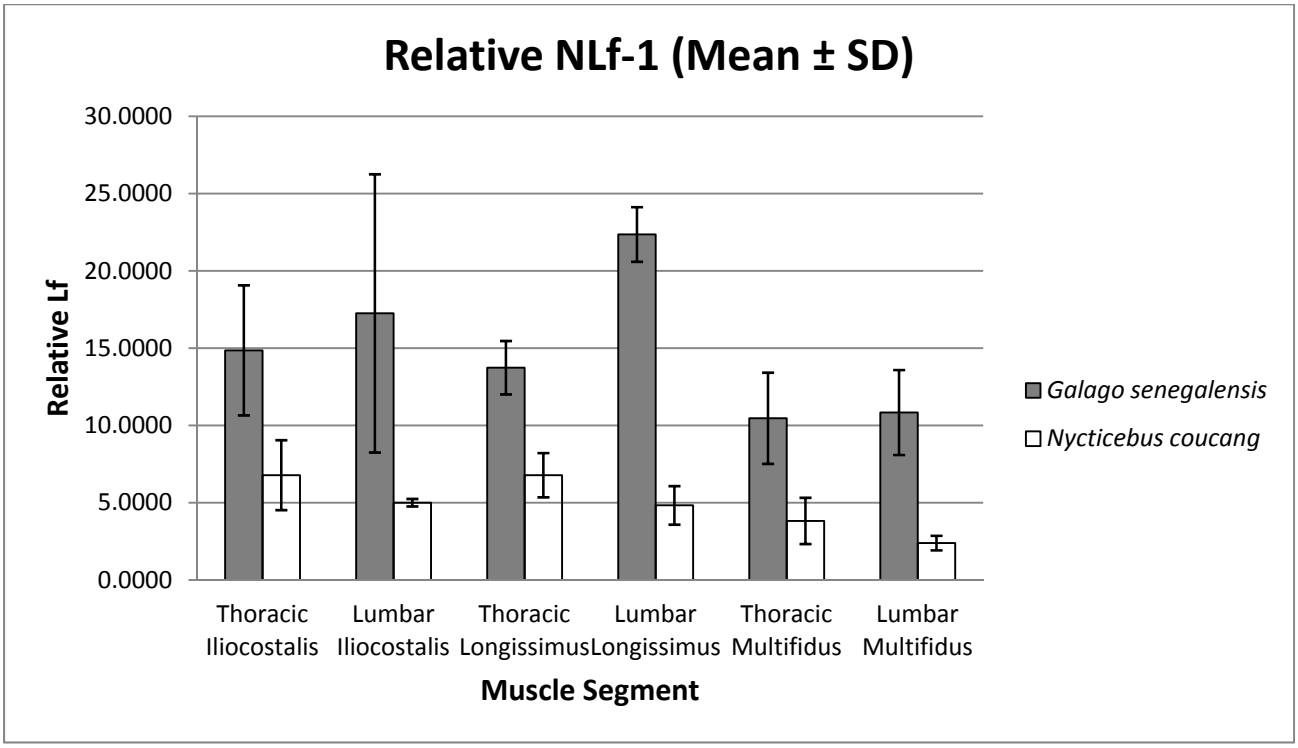

Fig. 38: Mean (± SD) of relative NLf-1 (to thoraco-lumbar spine length) for *G. senegalensis* and *N. coucang*

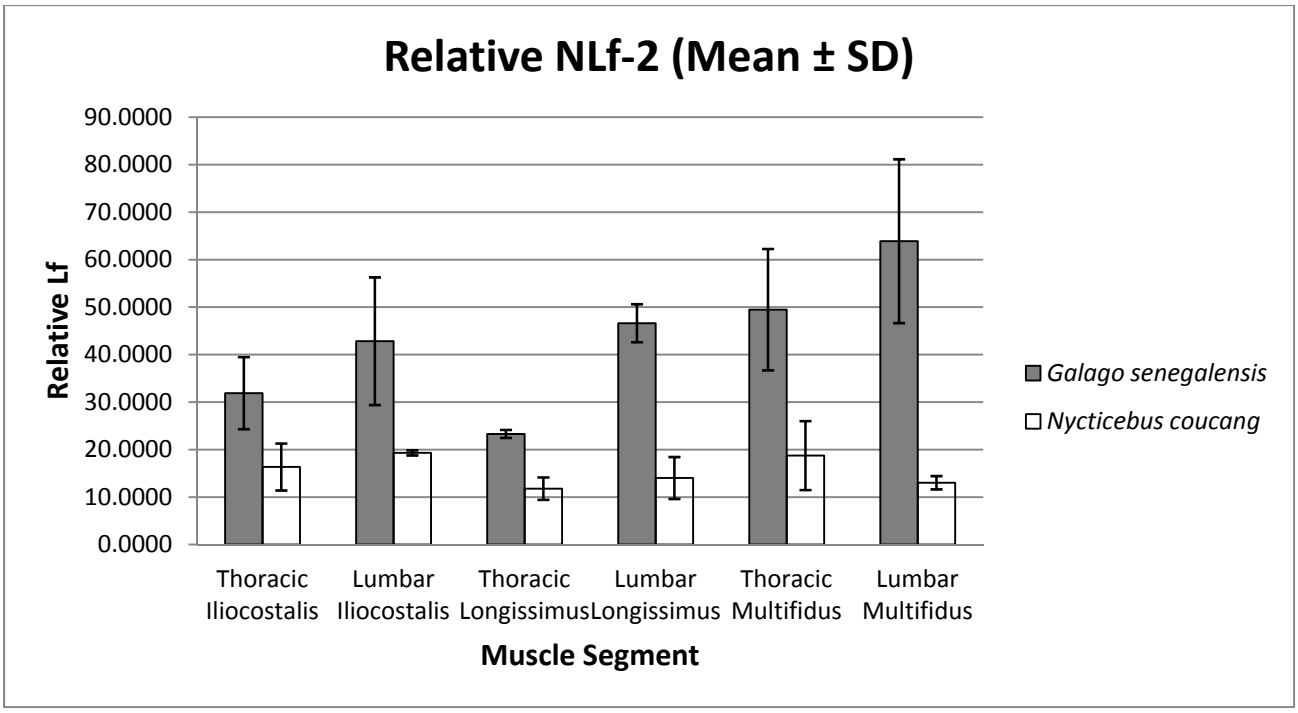

Fig. 39: Mean (± SD) of relative NLf-2 (to resting muscle length) for *G. senegalensis* and *N. coucang*

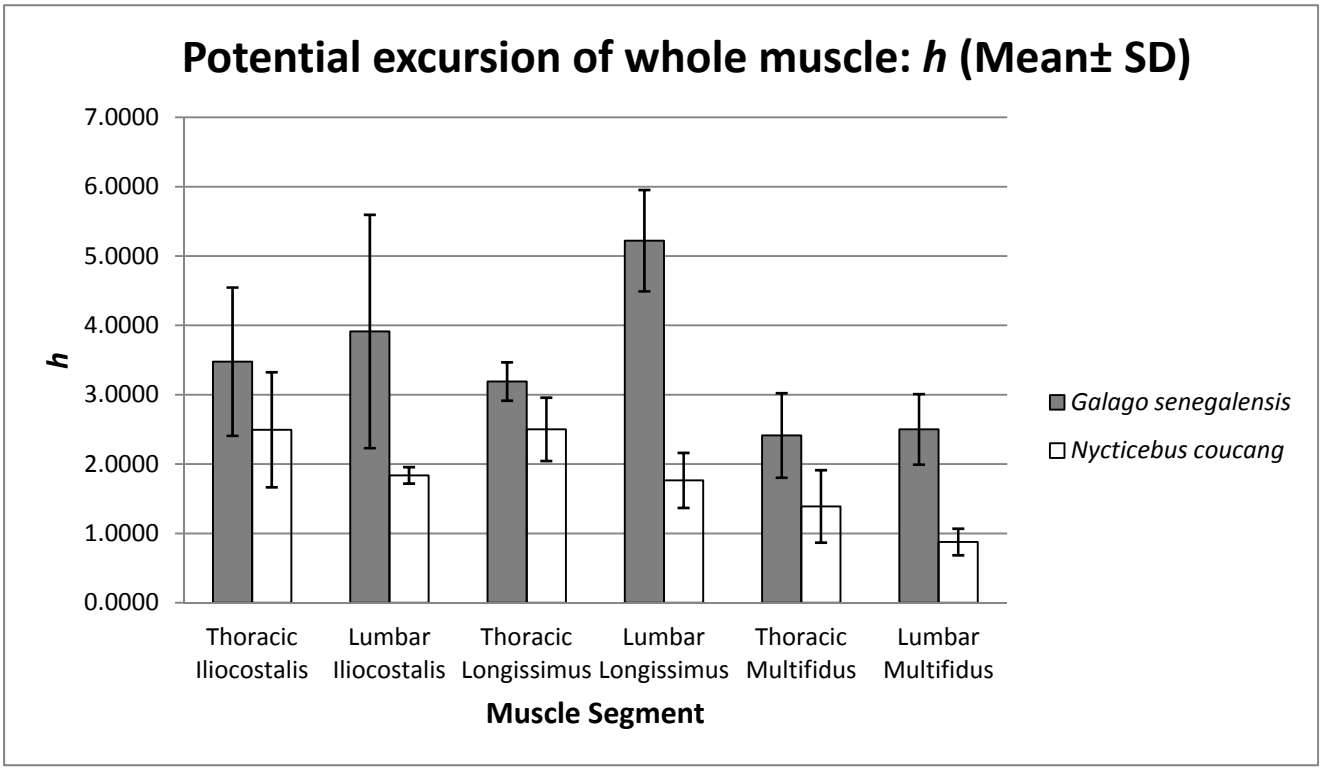

Fig. 40: Mean (± SD) of *h* for *G. senegalensis* and *N. coucang*

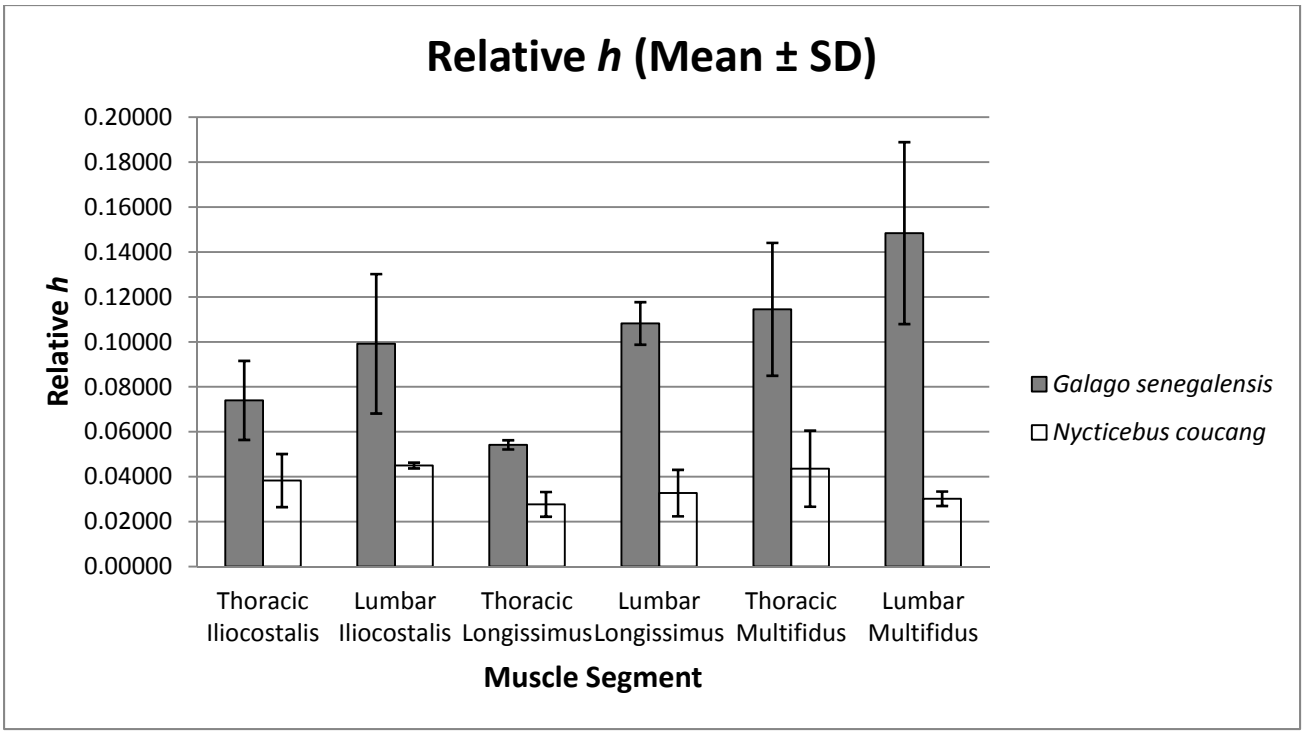

Fig. 41: Mean (± SD) of relative *h* for *G. senegalensis* and *N. coucang*

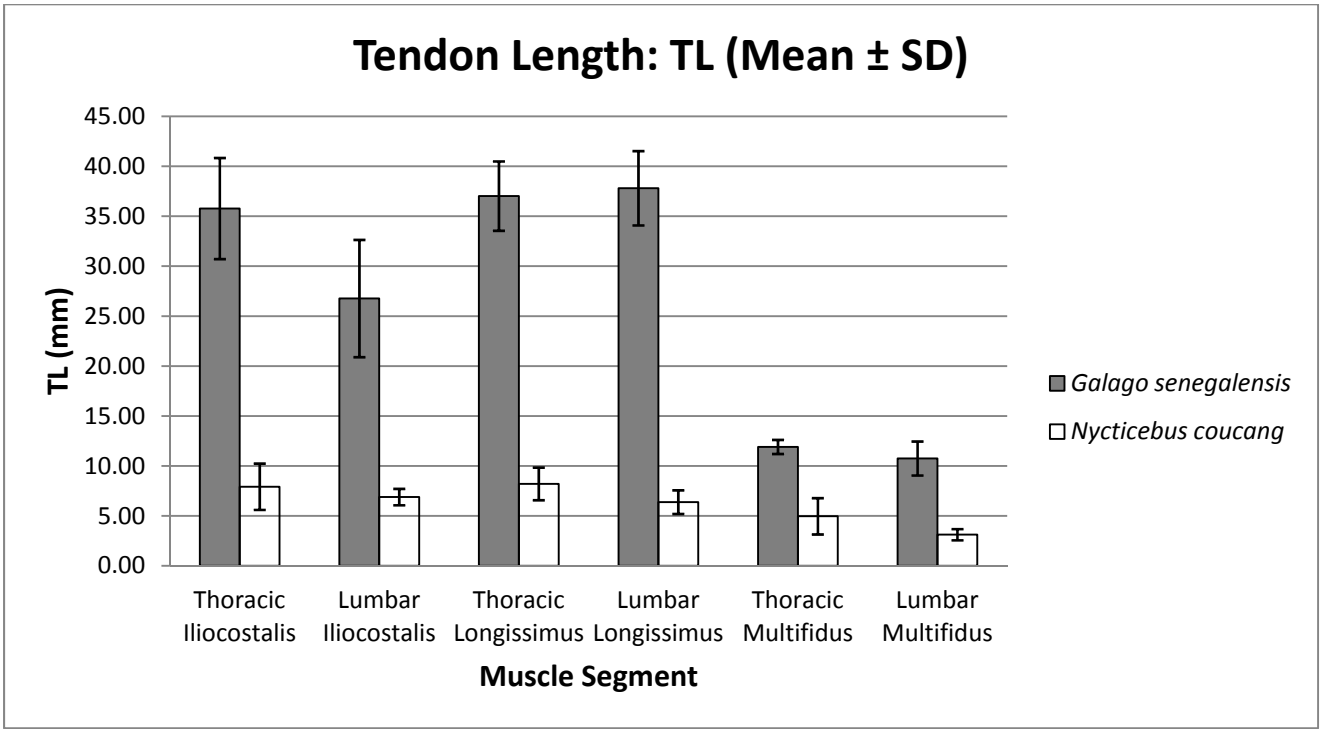

Fig. 42: Mean (± SD) of tendon length (TL) for *G. senegalensis* and *N. coucang*

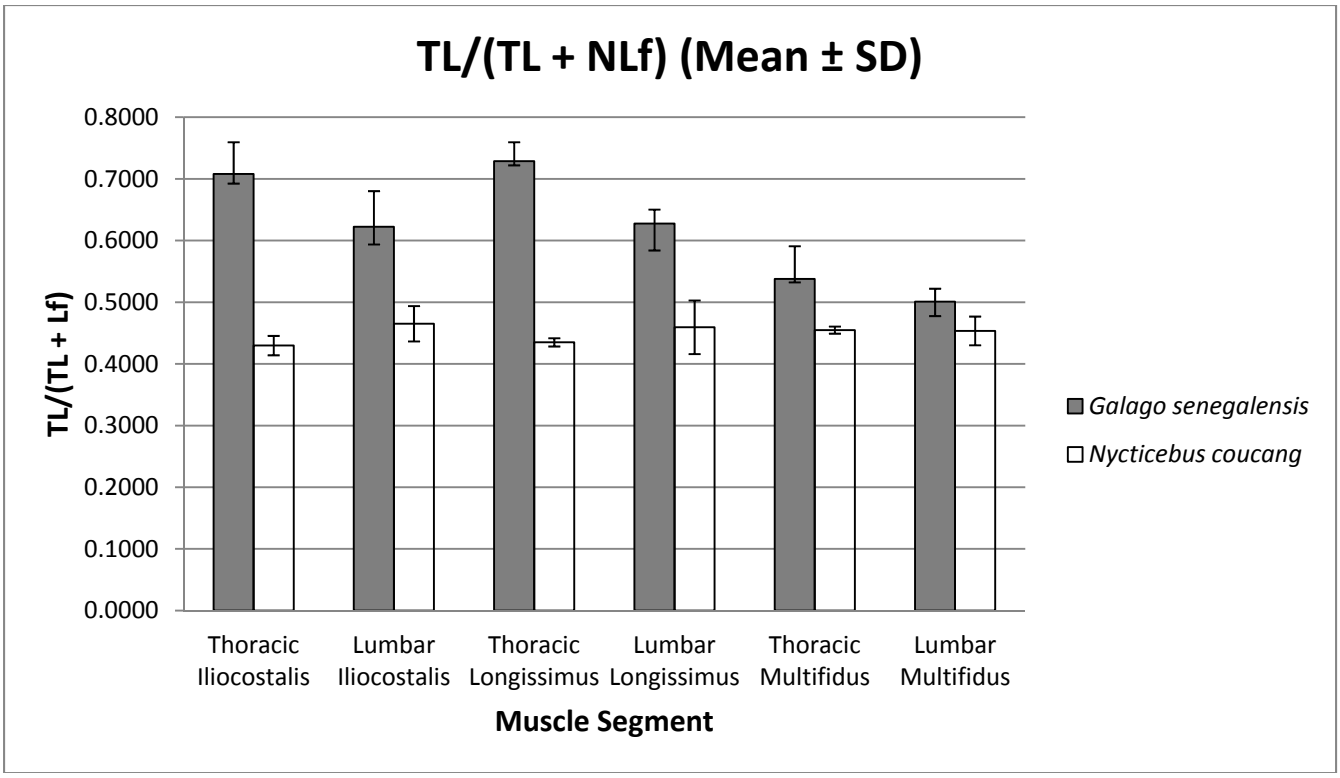

Fig. 43: Mean (± SD) of TL/(TL + NLf) for *G. senegalensis* and *N. coucang*

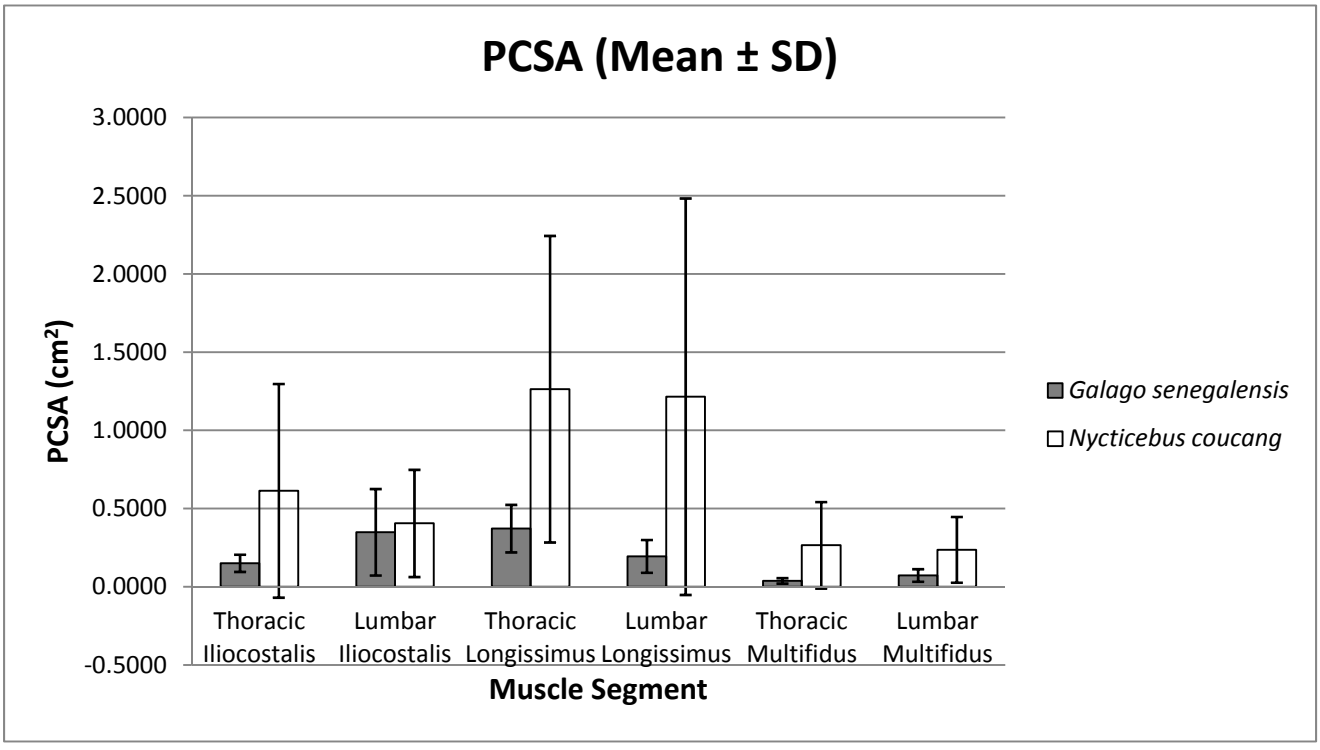

Fig. 44: Mean (± SD) of PCSA for *G. senegalensis* and *N. coucang*

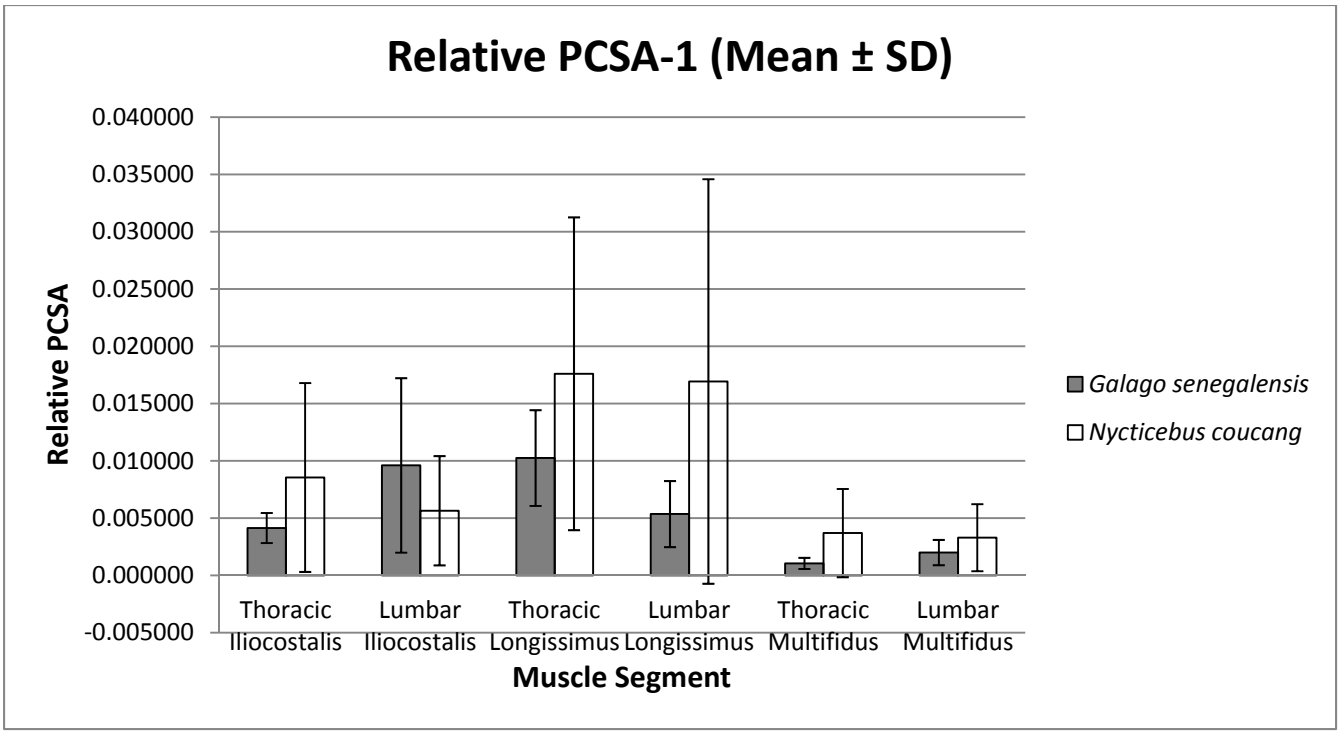

Fig. 45: Mean (± SD) of relative PCSA-1 (to species mean body mass$^{0.67}$) for *G. senegalensis* and *N. coucang*

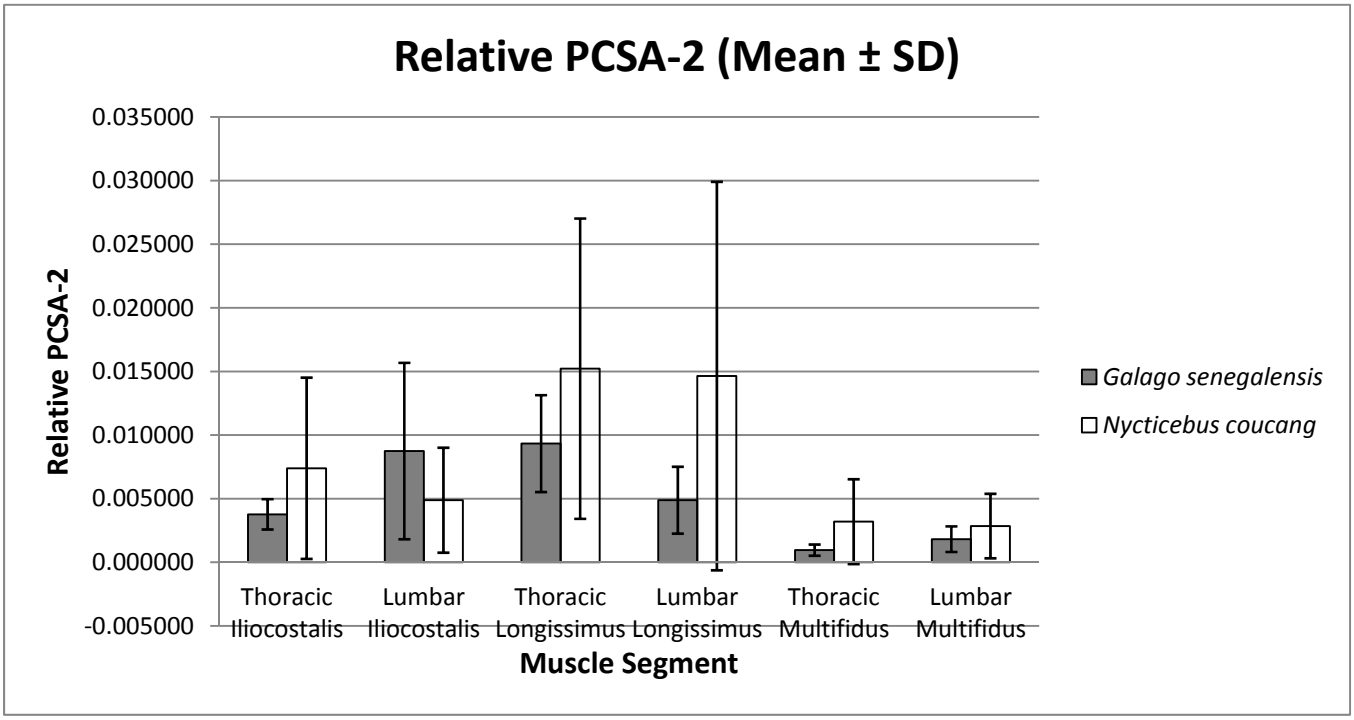

Fig. 46: Mean (± SD) of relative PCSA-2 (to upper estimate of body mass$^{0.67}$) for *G. senegalensis* and *N. coucang*

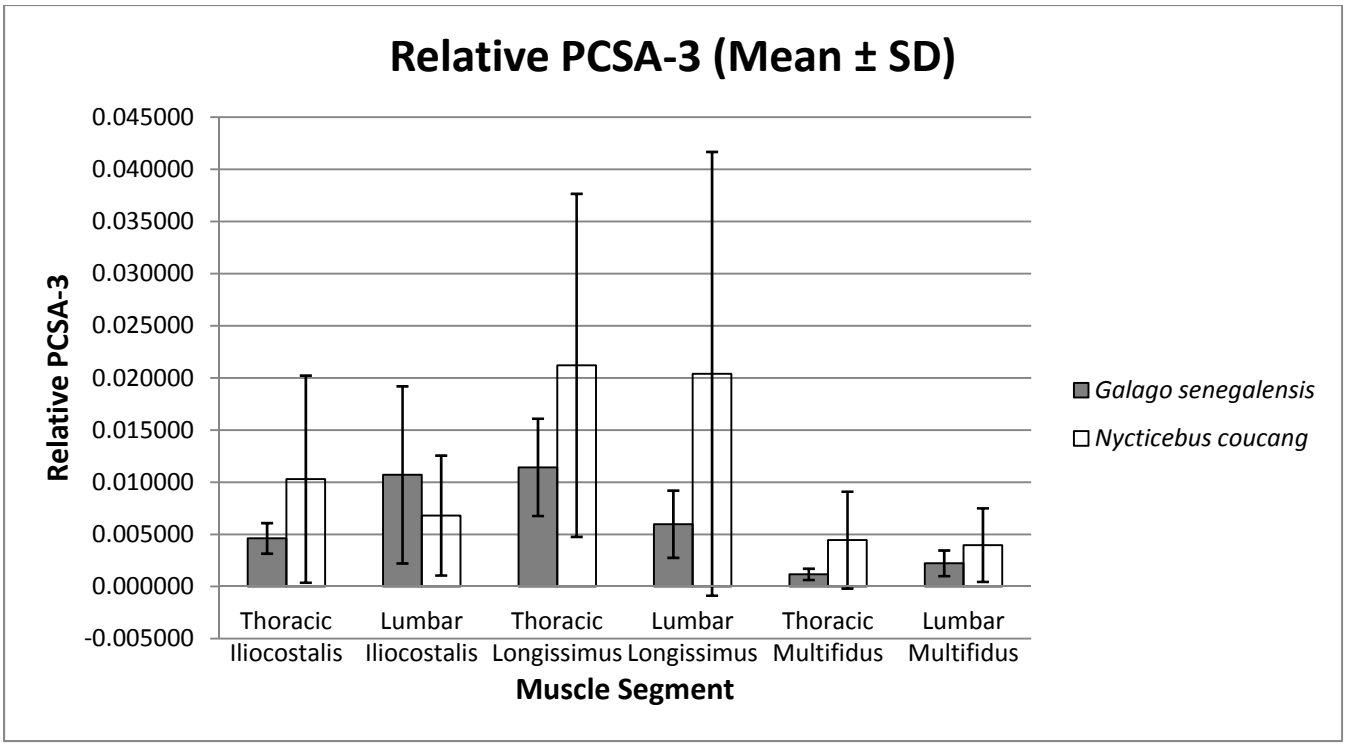

Fig. 47: Mean (± SD) of relative PCSA-3 (to lower estimate of body mass$^{0.67}$) for *G. senegalensis* and *N. coucang*

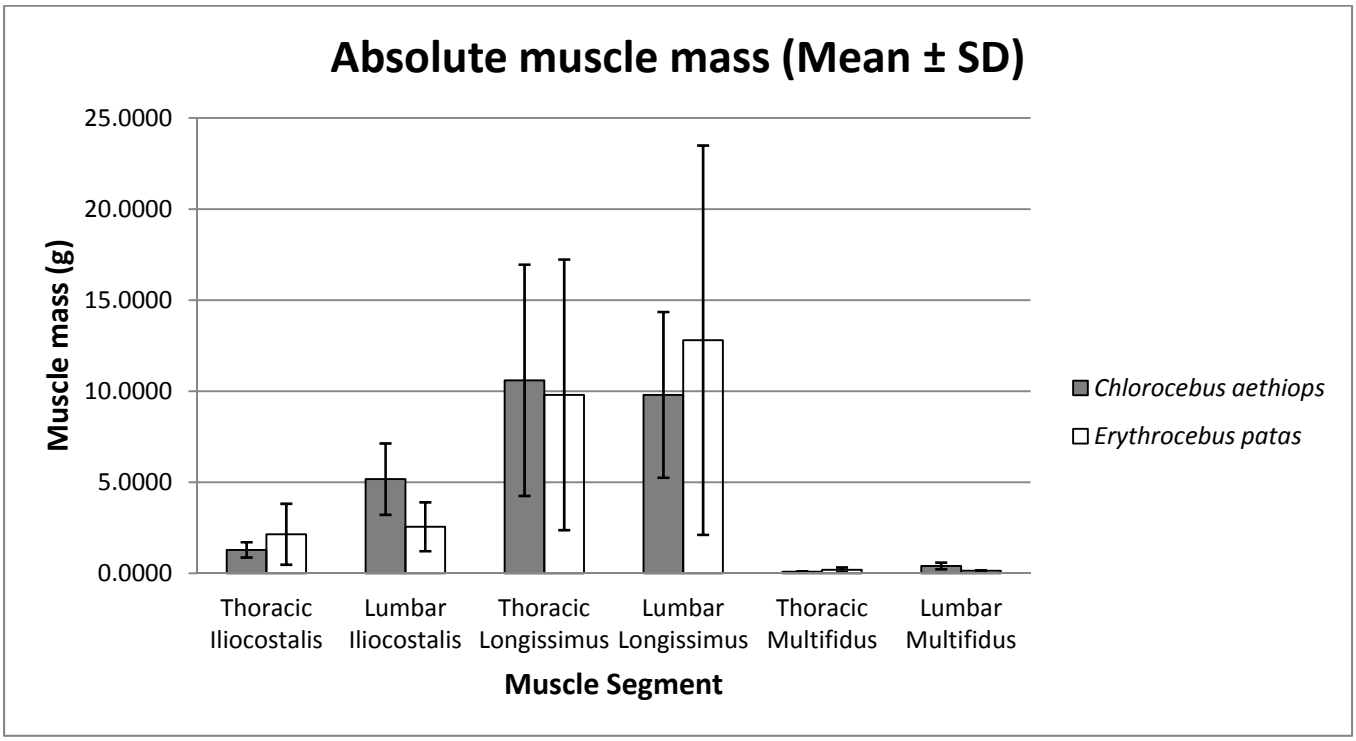

Fig. 48: Mean (± SD) of absolute muscle mass for *C. aethiops* and *E. patas*

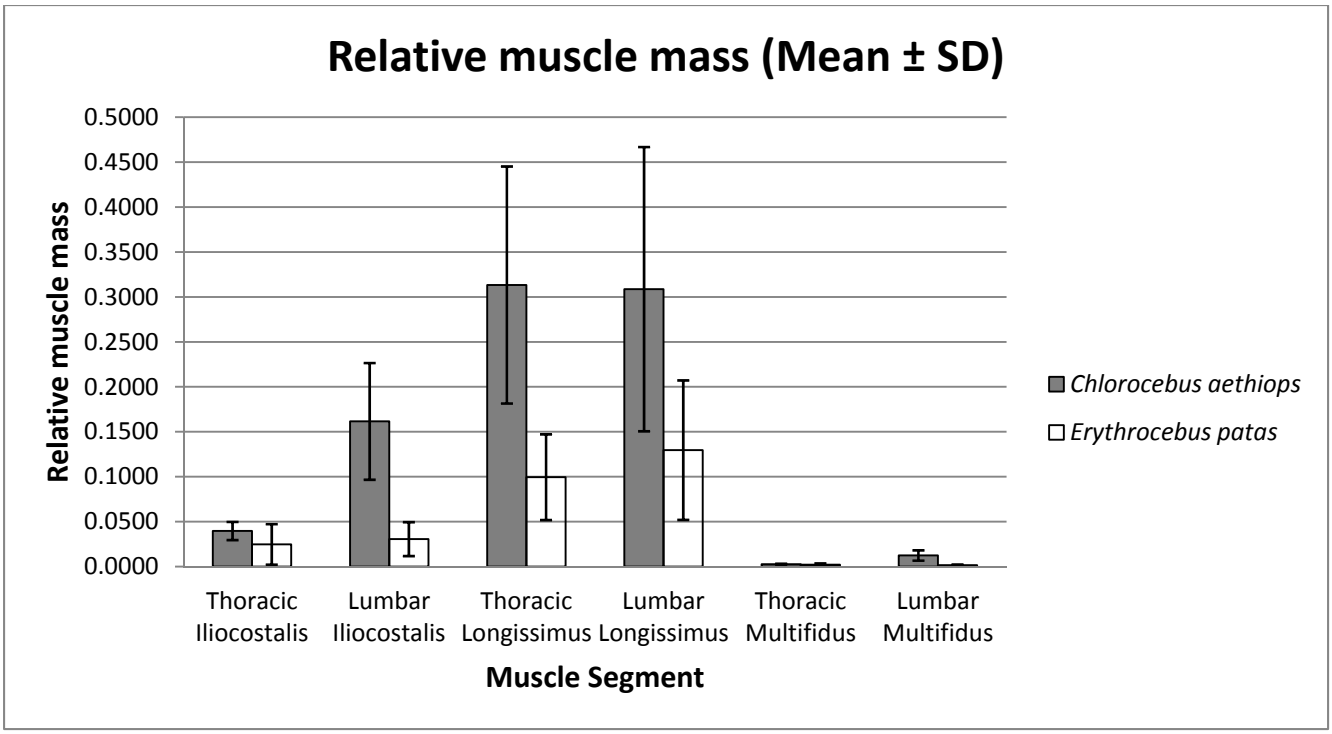

Fig. 49: Mean (± SD) of relative muscle mass for *C. aethiops* and *E. patas*

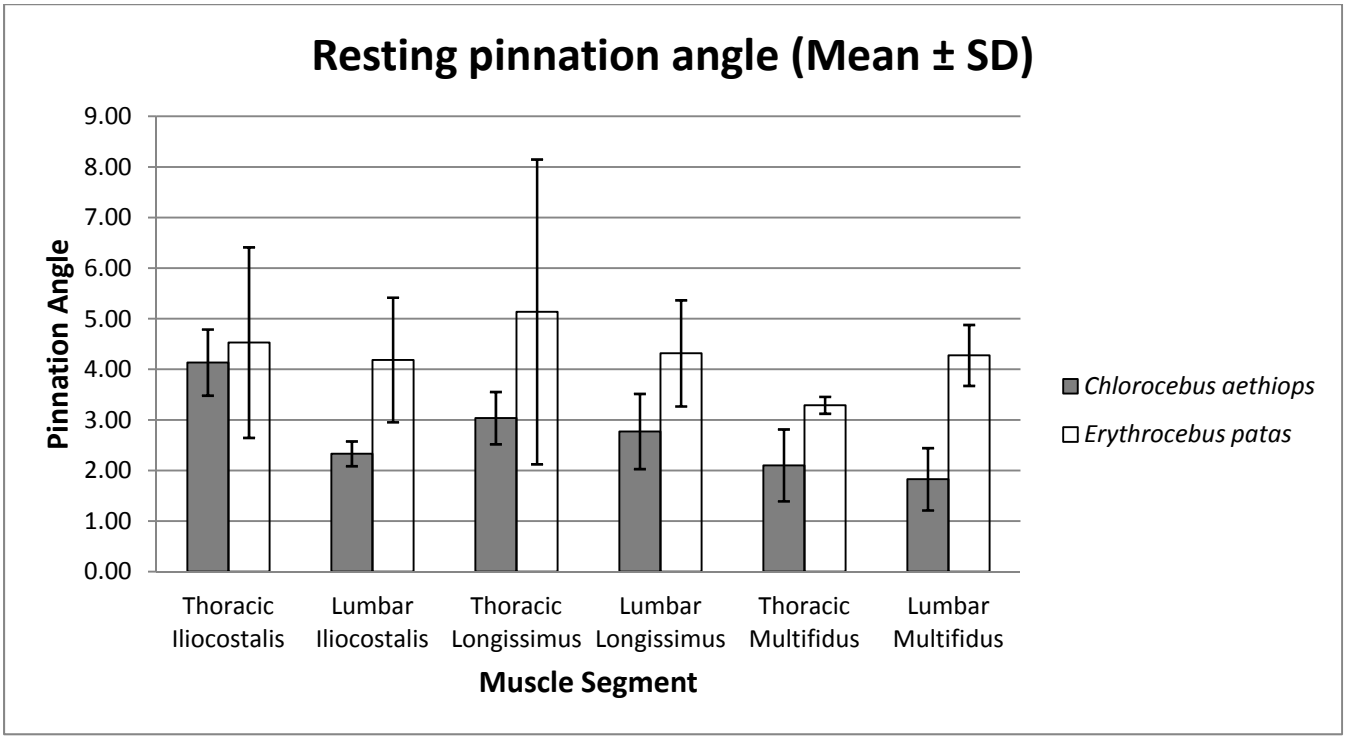

Fig. 50: Mean (± SD) of resting pinnation for *C. aethiops* and *E. patas*

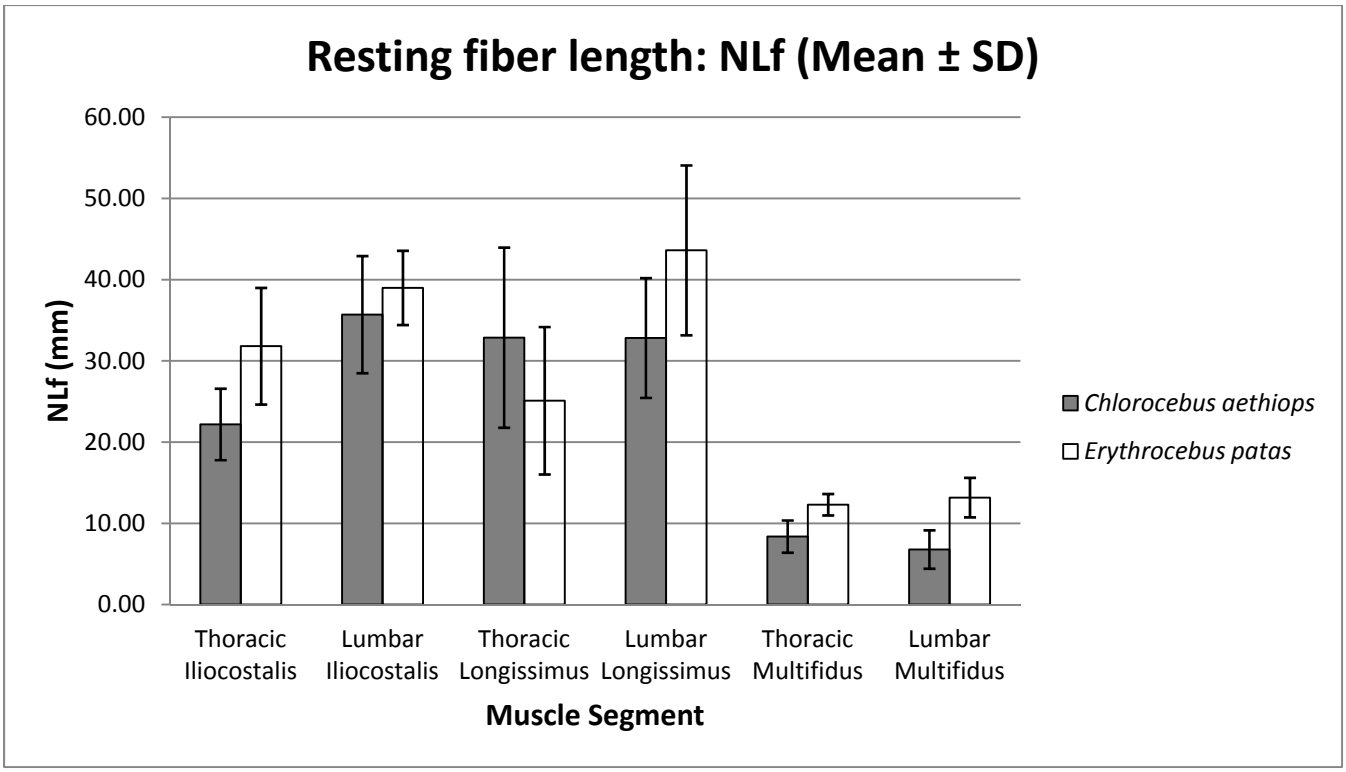

Fig. 51: Mean (± SD) of resting fiber length (NLf) for *C. aethiops* and *E. patas*

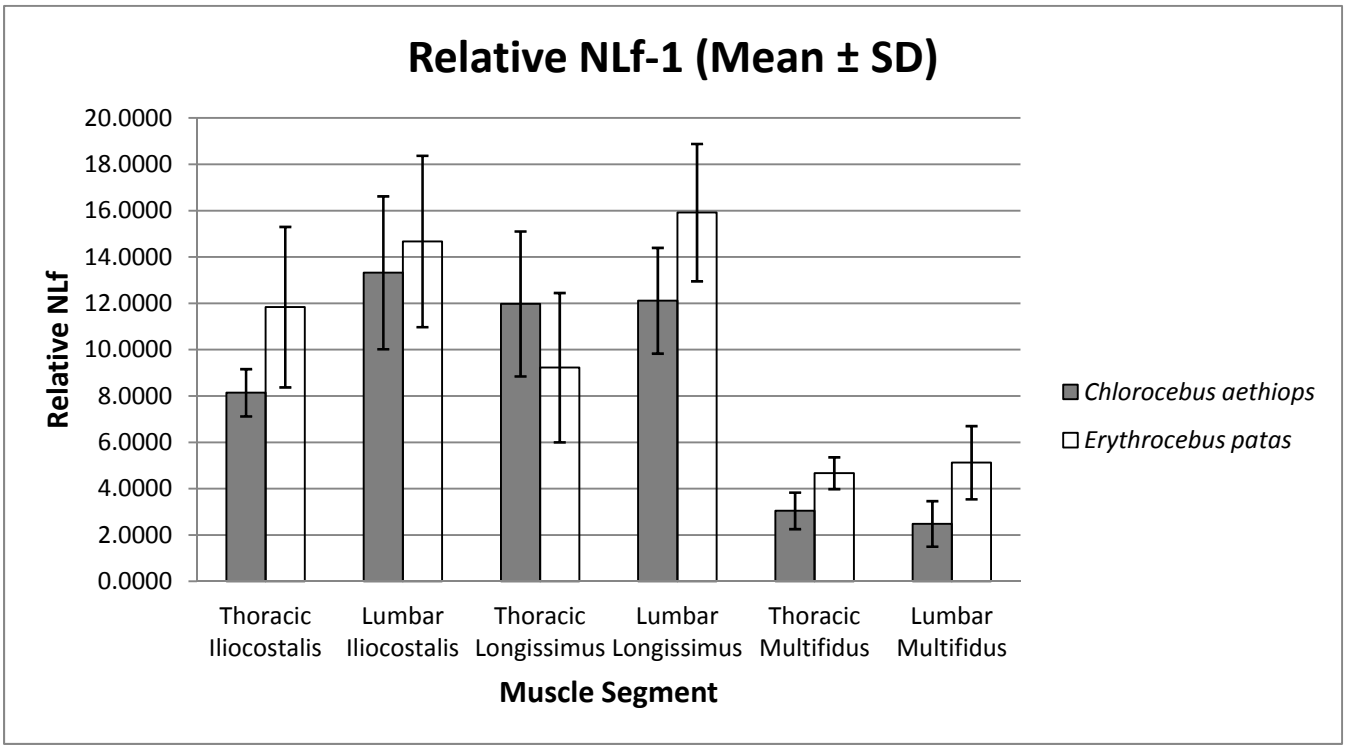

Fig. 52: Mean (± SD) of relative NLf-1 (to thoraco-lumbar spine length) for *C. aethiops* and *E. patas*

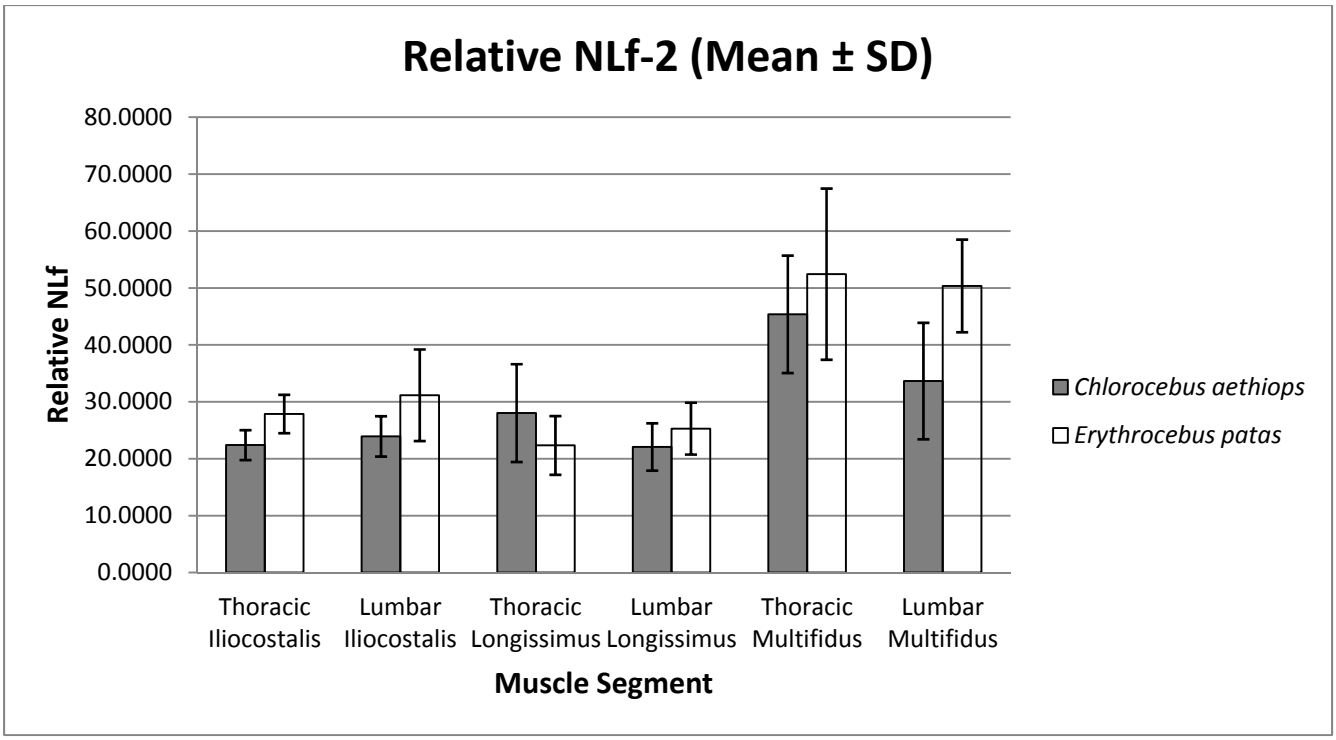

Fig. 53: Mean (± SD) of relative NLf-2 (to resting muscle length) for *C. aethiops* and *E. patas*

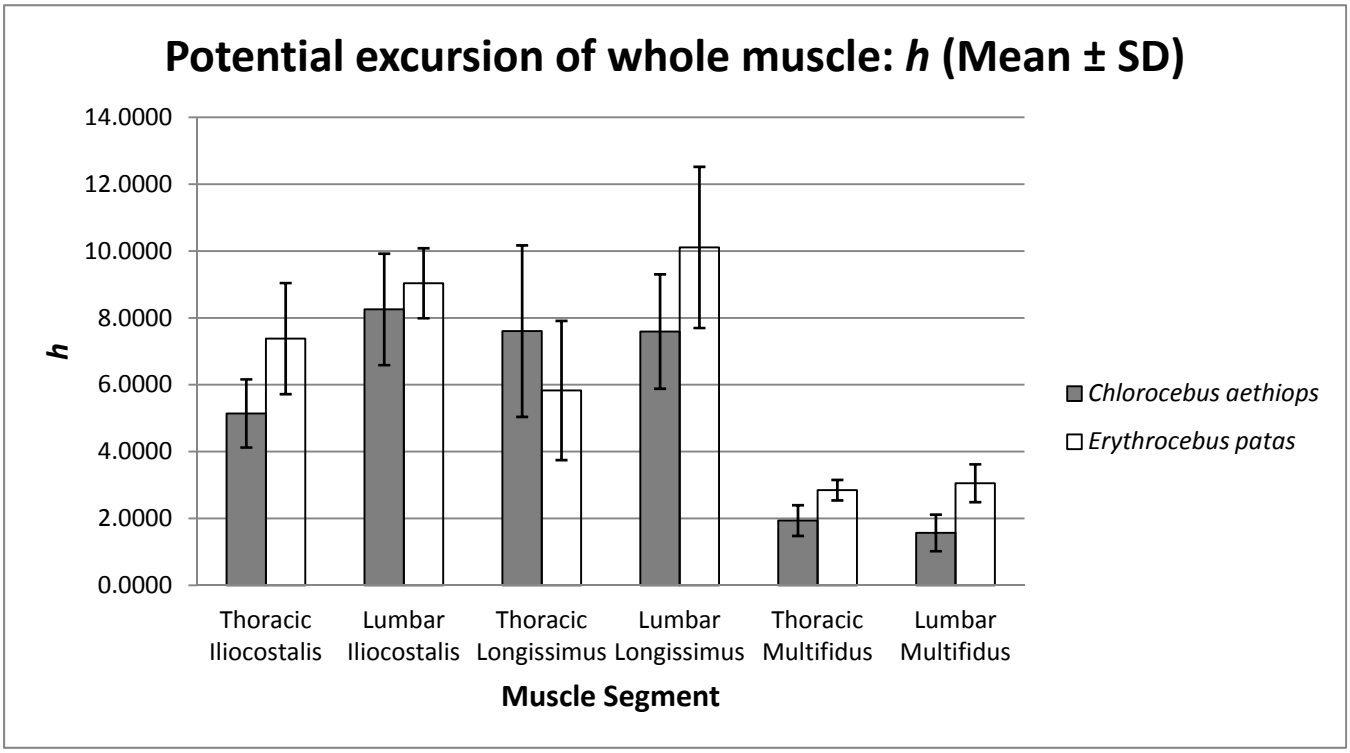

Fig. 54: Mean (± SD) of *h* for *C. aethiops* and *E. patas*

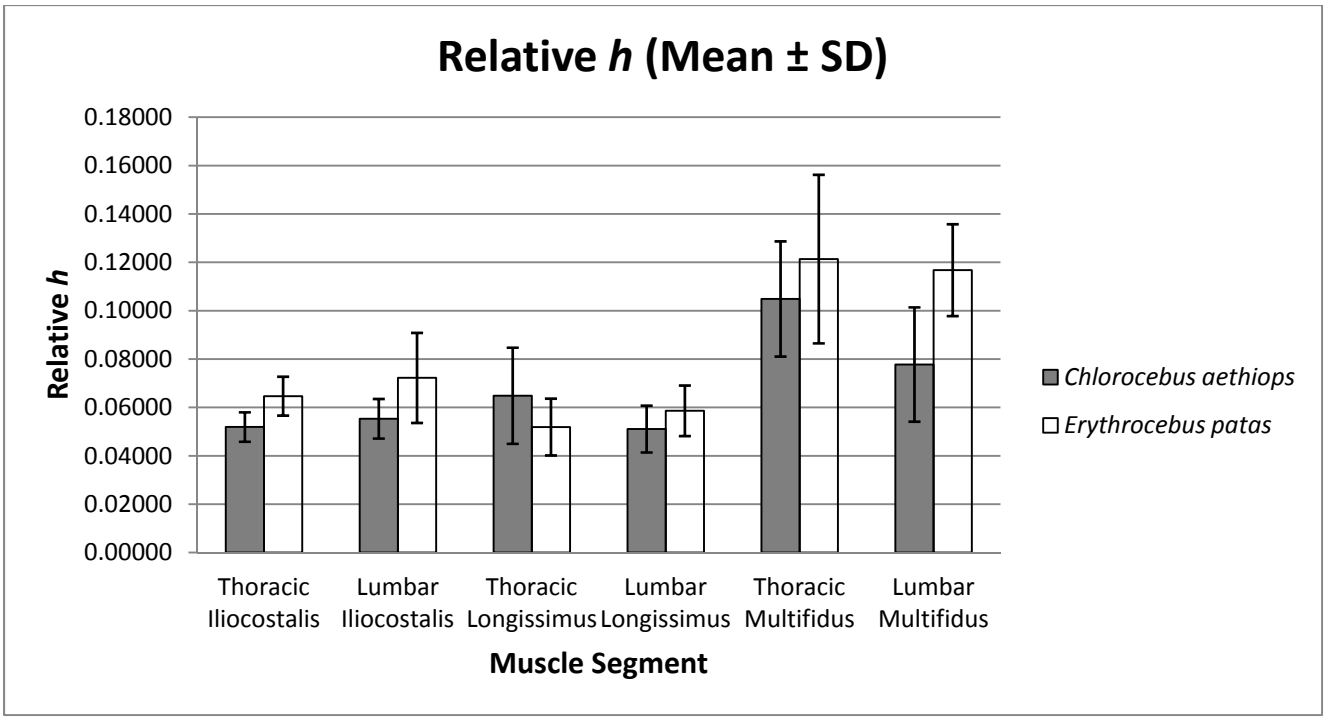

Fig. 55: Mean (± SD) of relative *h* for *C. aethiops* and *E. patas*

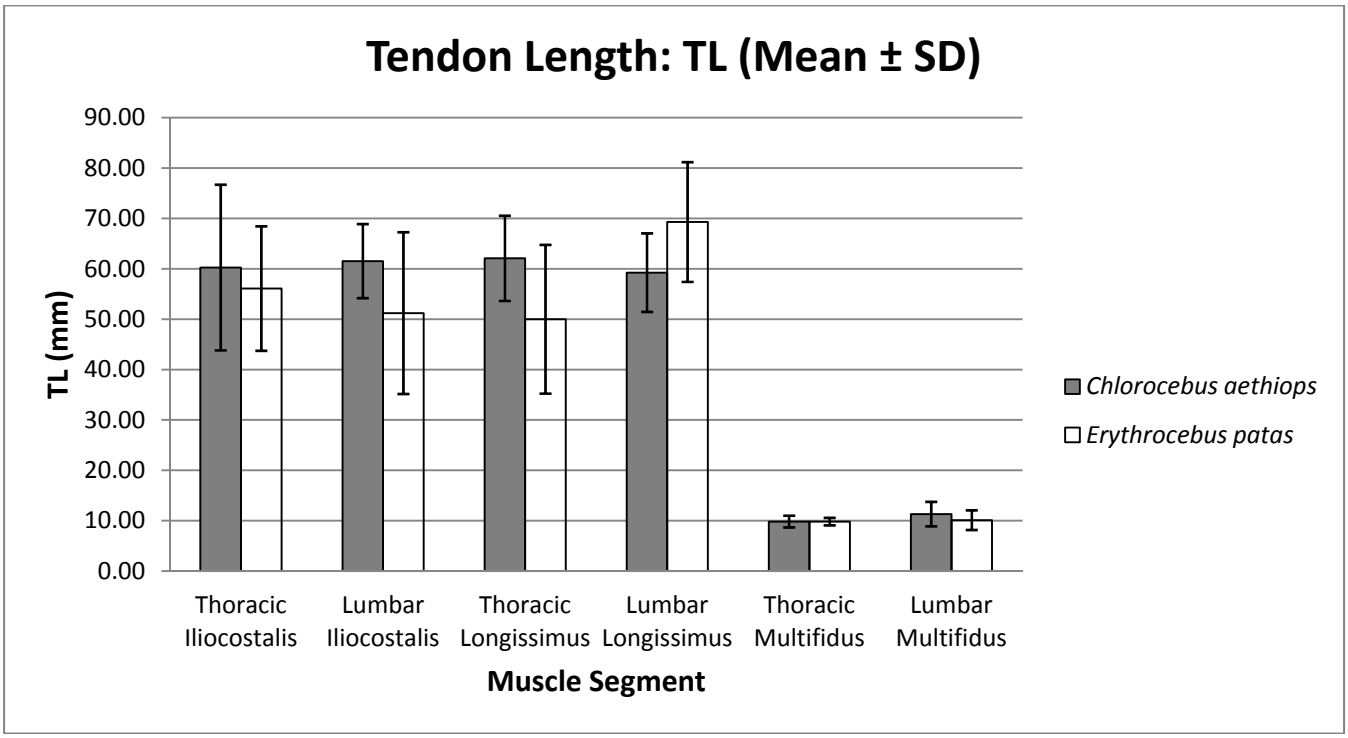

Fig. 56: Mean (± SD) of tendon length (TL) for *C. aethiops* and *E. patas*

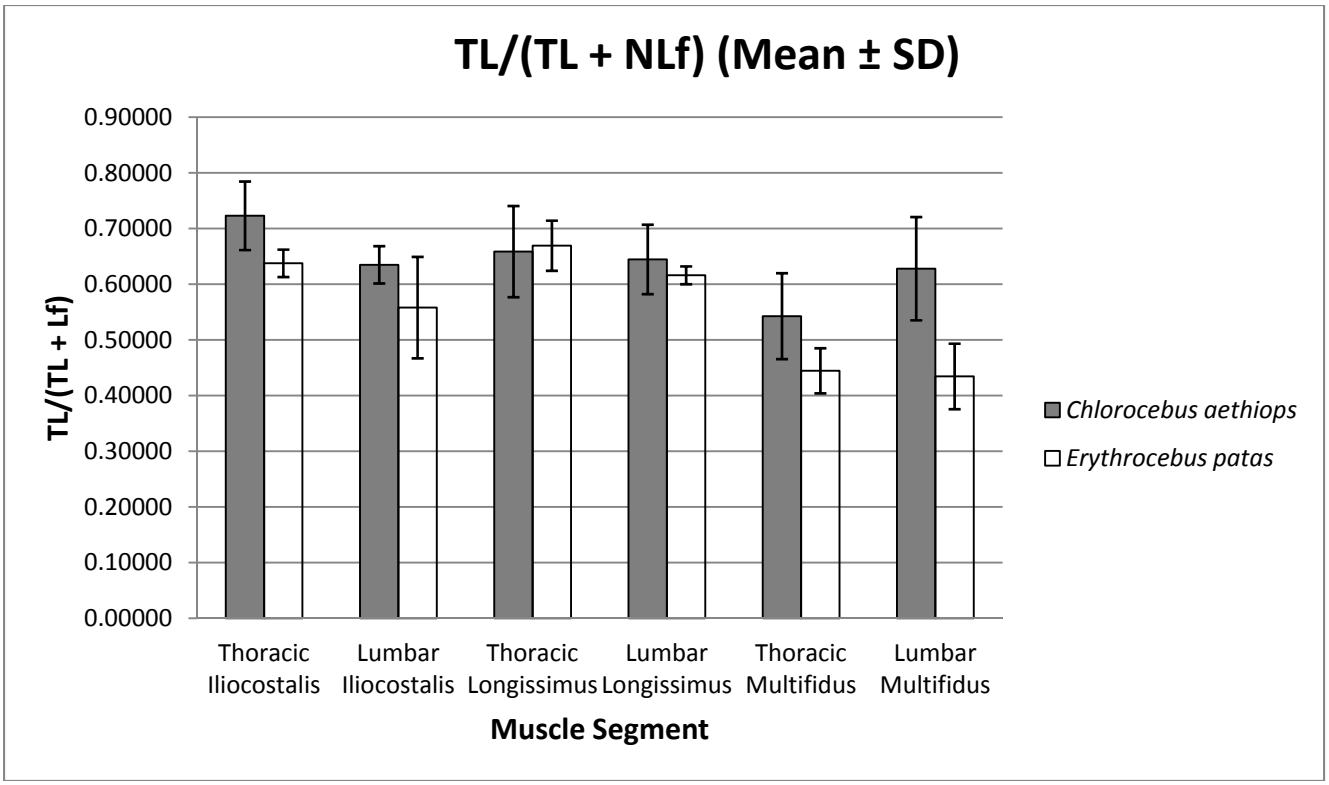

Fig. 57: Mean (± SD) of TL/(TL + NLf) for *C. aethiops* and *E. patas*

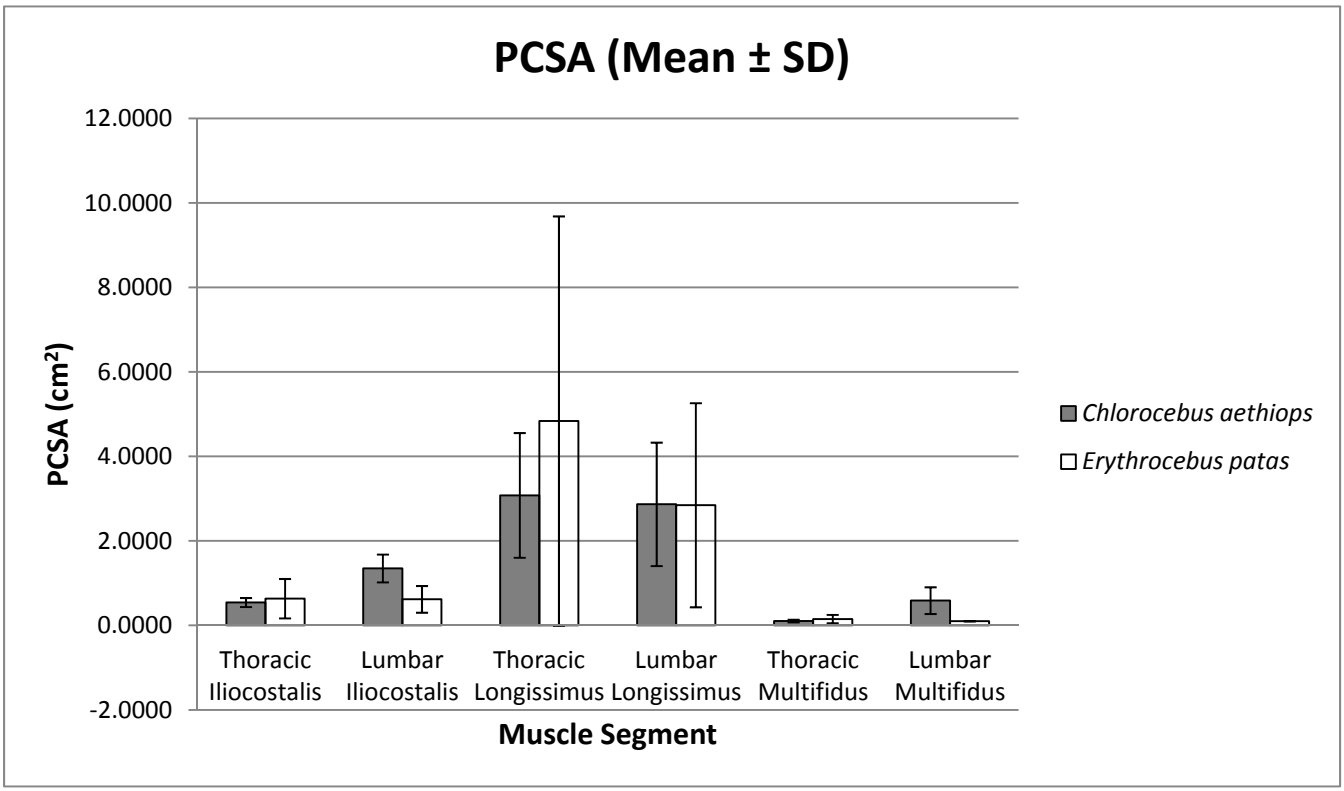

Fig. 58: Mean (± SD) of PCSA for *C. aethiops* and *E. patas*

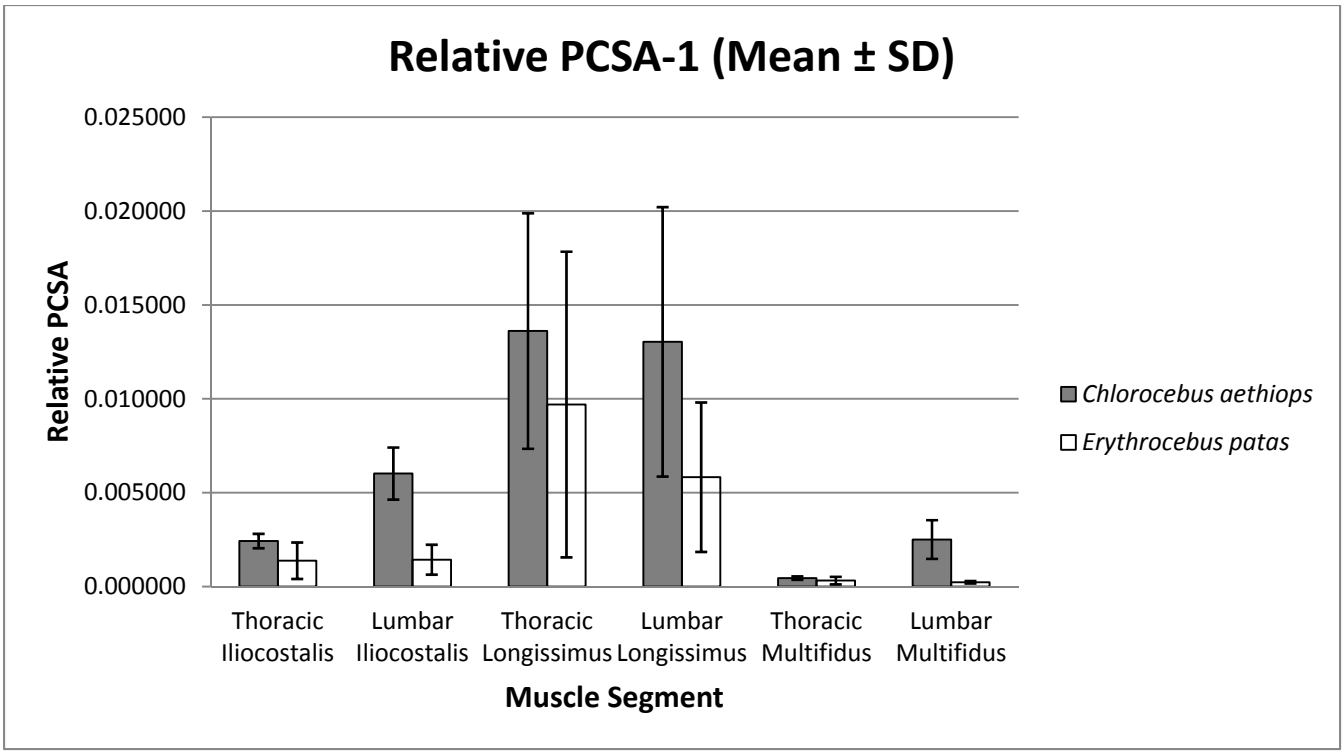

Fig. 59: Mean (± SD) of relative PCSA-1 (to species mean body mass$^{0.67}$) for *C. aethiops* and *E. patas*

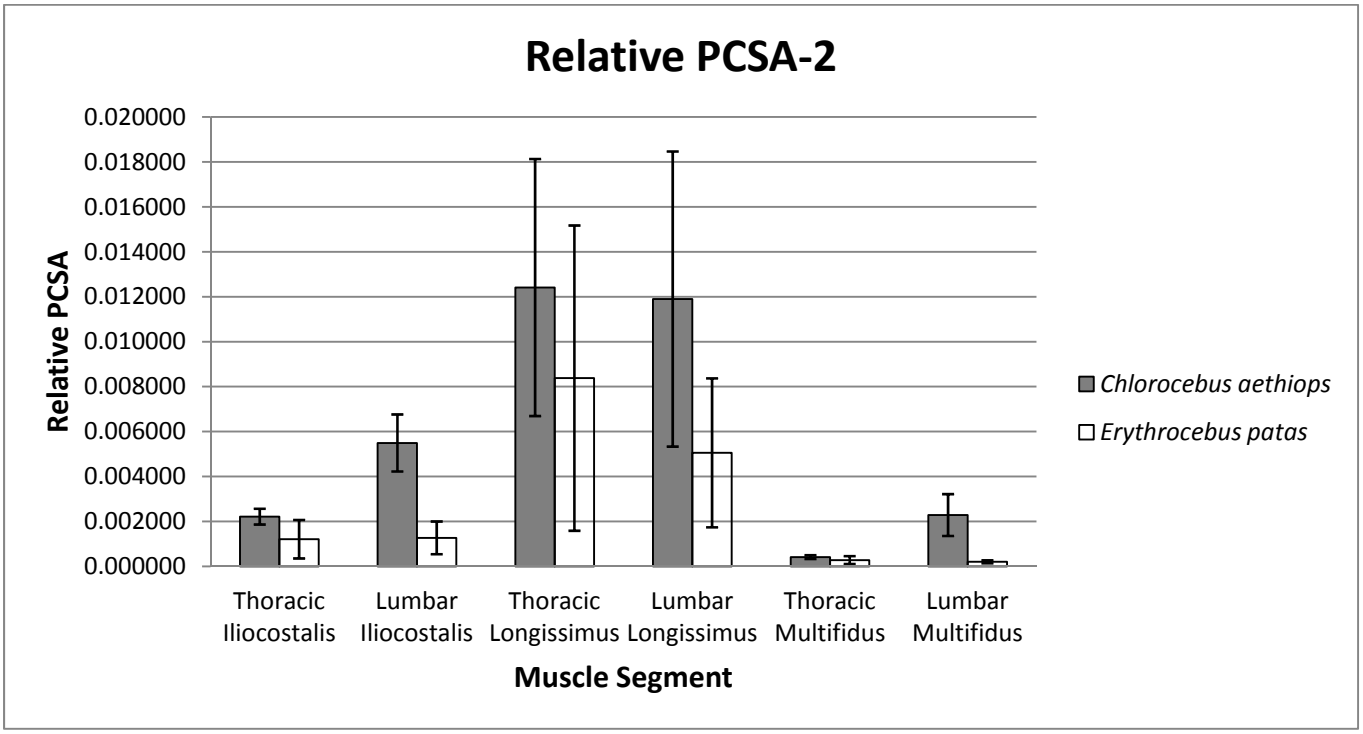

Fig. 60: Mean (± SD) of relative PCSA-2 (to upper estimate of body mass$^{0.67}$) for *C. aethiops* and *E. patas*

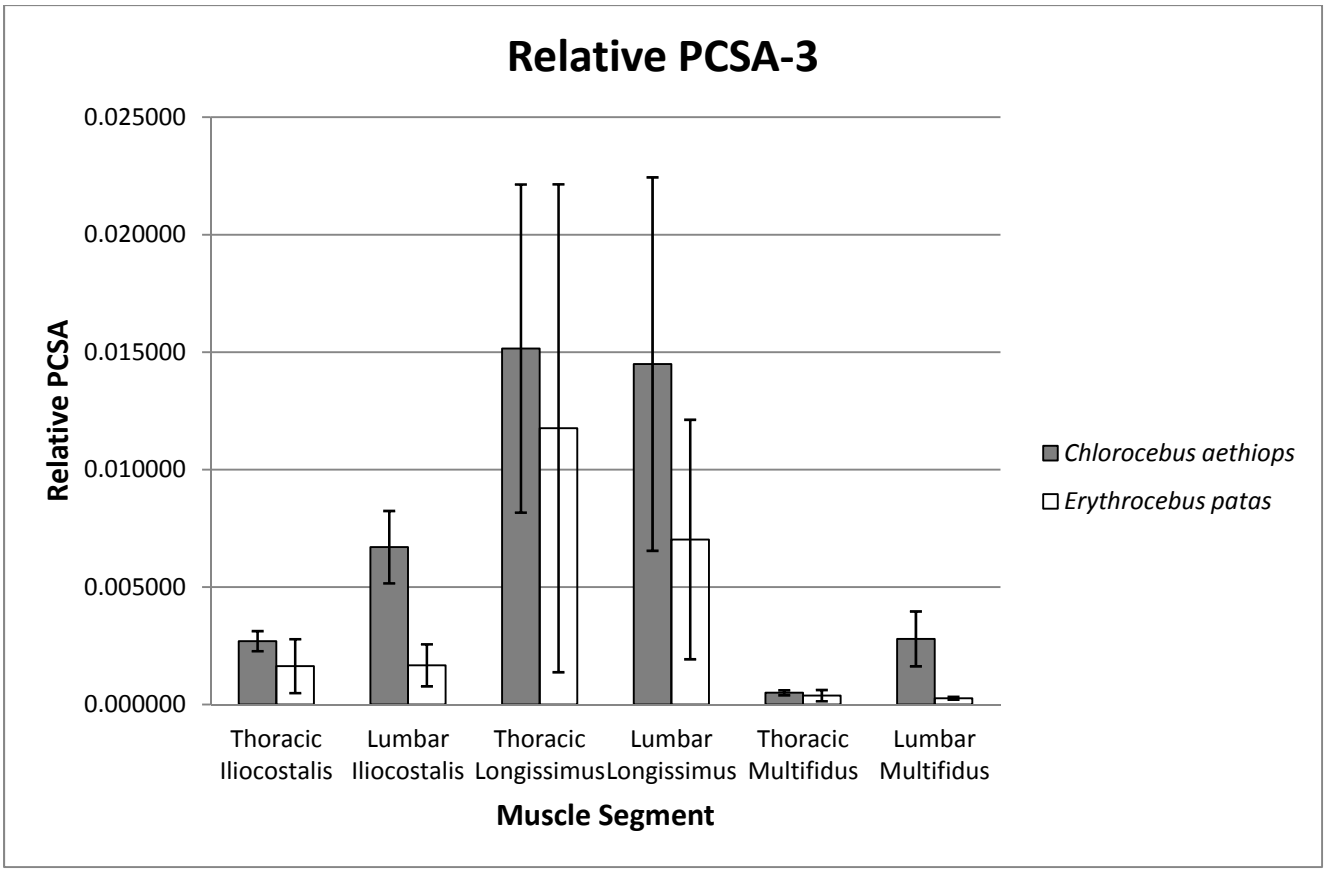

Fig. 61: Mean (± SD) of relative PCSA-3 (to lower estimate of body mass$^{0.67}$) for *C. aethiops* and *E. patas*

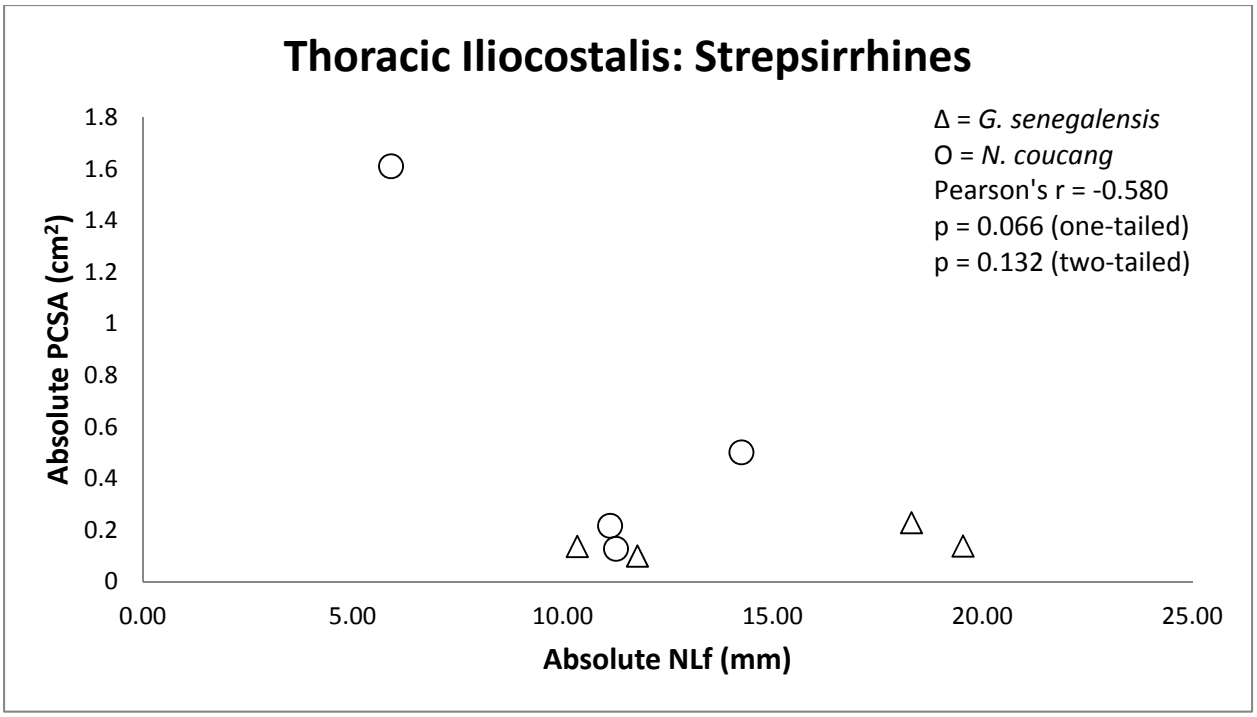

Fig. 62: Bivariate plot demonstrating partial negative correlation (i.e. architectural trade-off) between muscle velocity (NLf) and force (PCSA). This correlation is not significant (see Table 42).

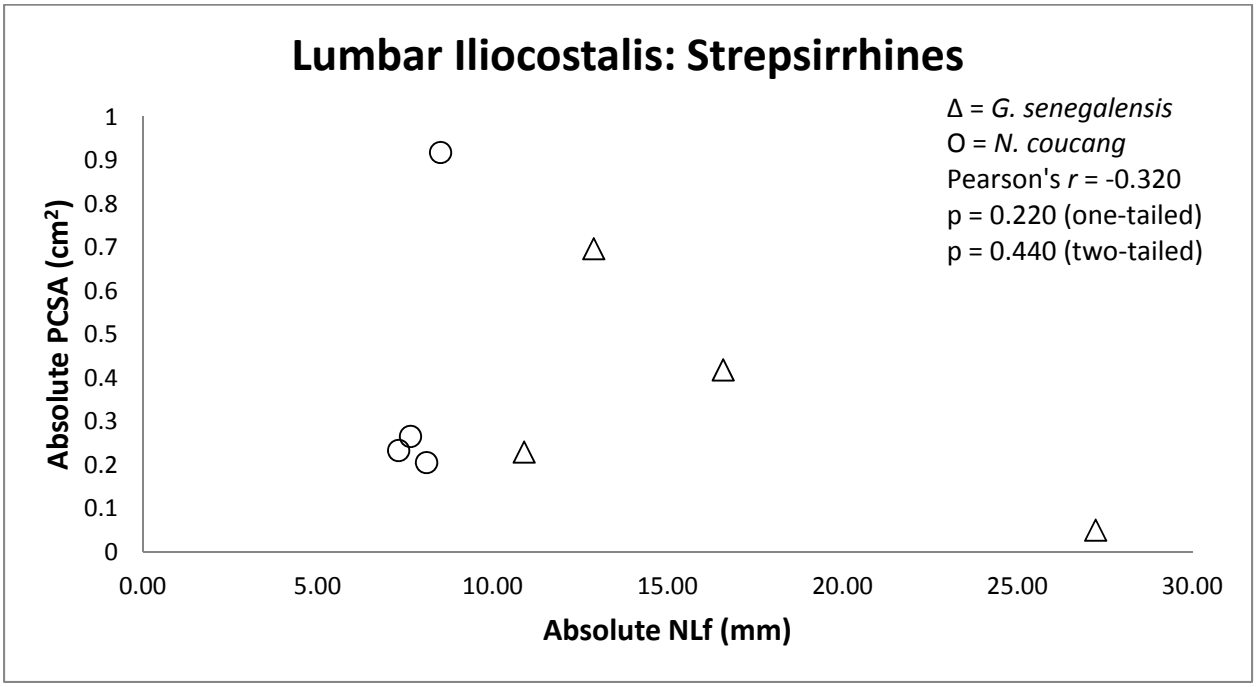

Fig. 63: Bivariate plot demonstrating moderate negative correlation (i.e. architectural trade-off) between muscle velocity (NLf) and force (PCSA). This correlation is not significant (see Table 42).

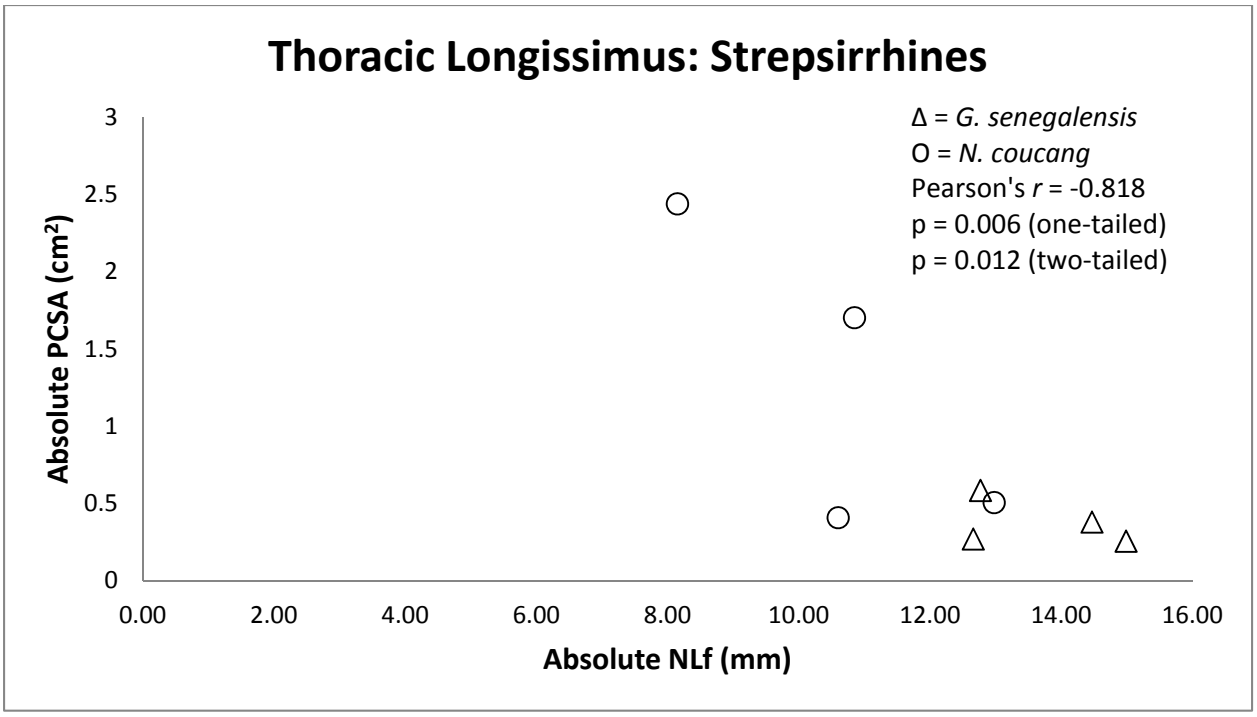

Fig. 64: Bivariate plot demonstrating high negative correlation (i.e. architectural trade-off) between muscle velocity (NLf) and force (PCSA). This correlation is significant (see Table 42).

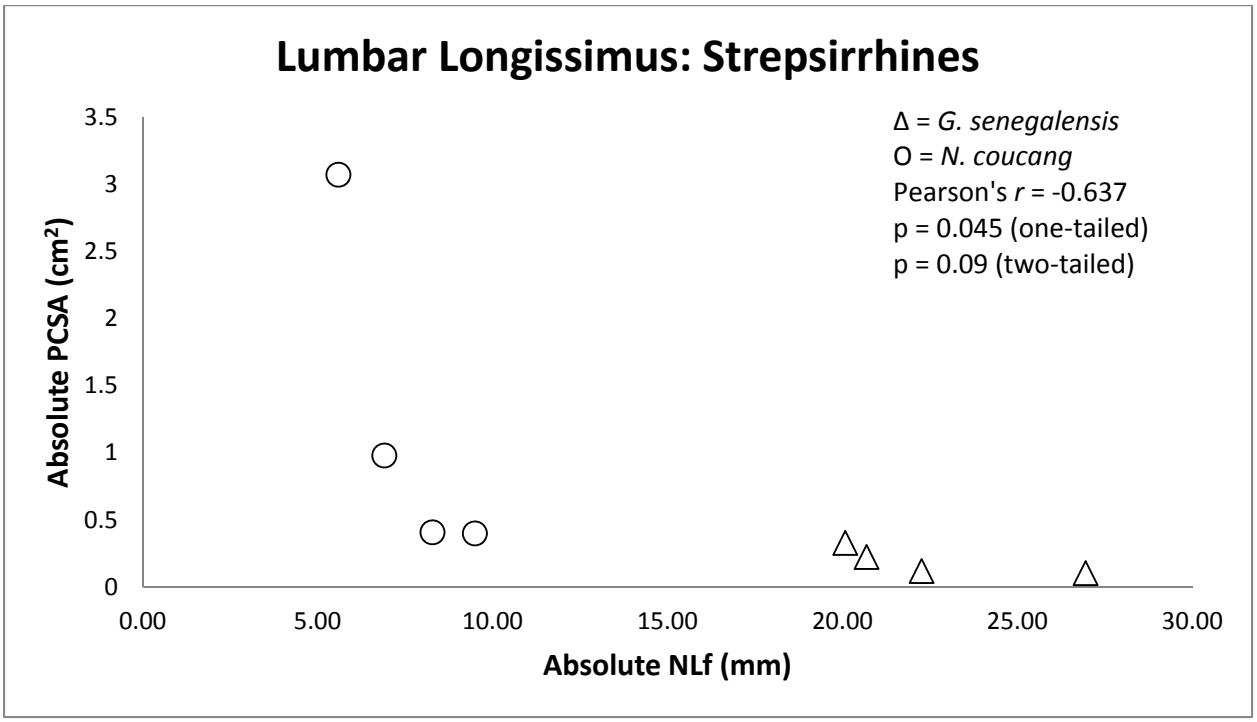

Fig. 65: Bivariate plot demonstrating partial negative correlation (i.e. architectural trade-off) between muscle velocity (NLf) and force (PCSA). The one-tailed correlation is significant (see Table 42).

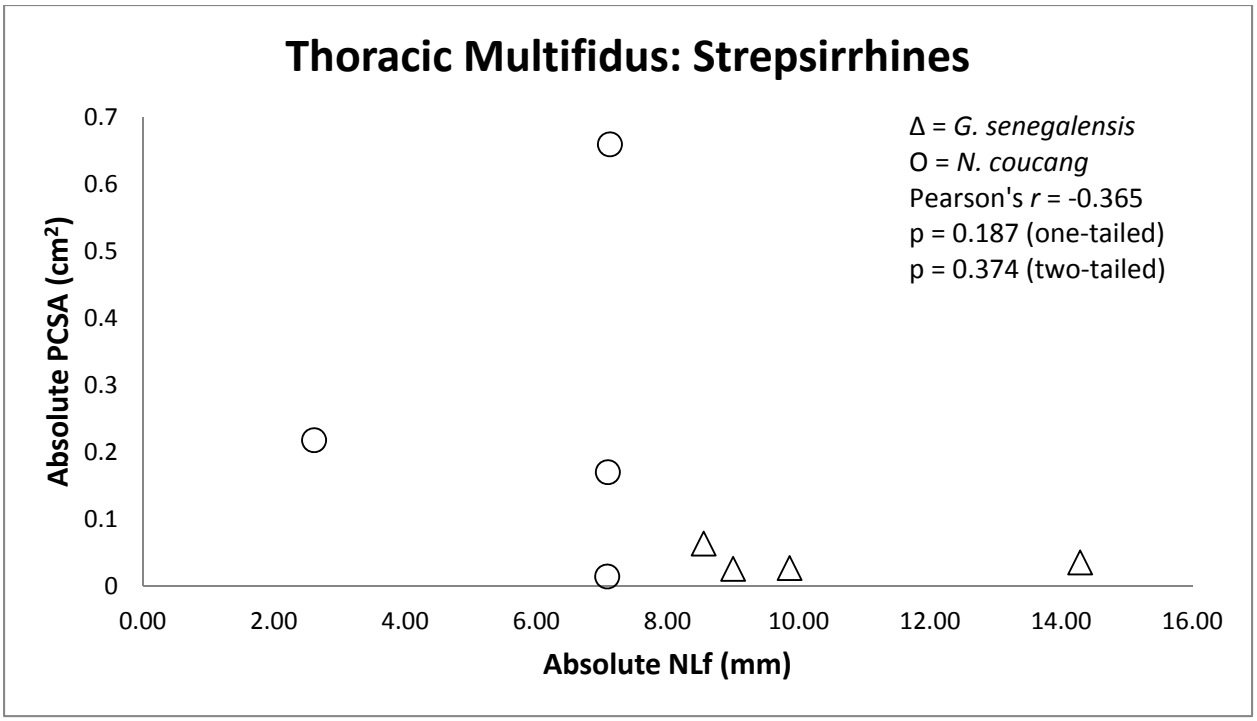

Fig. 66: Bivariate plot demonstrating moderate negative correlation (i.e. architectural trade-off) between muscle velocity (NLf) and force (PCSA). This correlation is not significant (see Table 42).

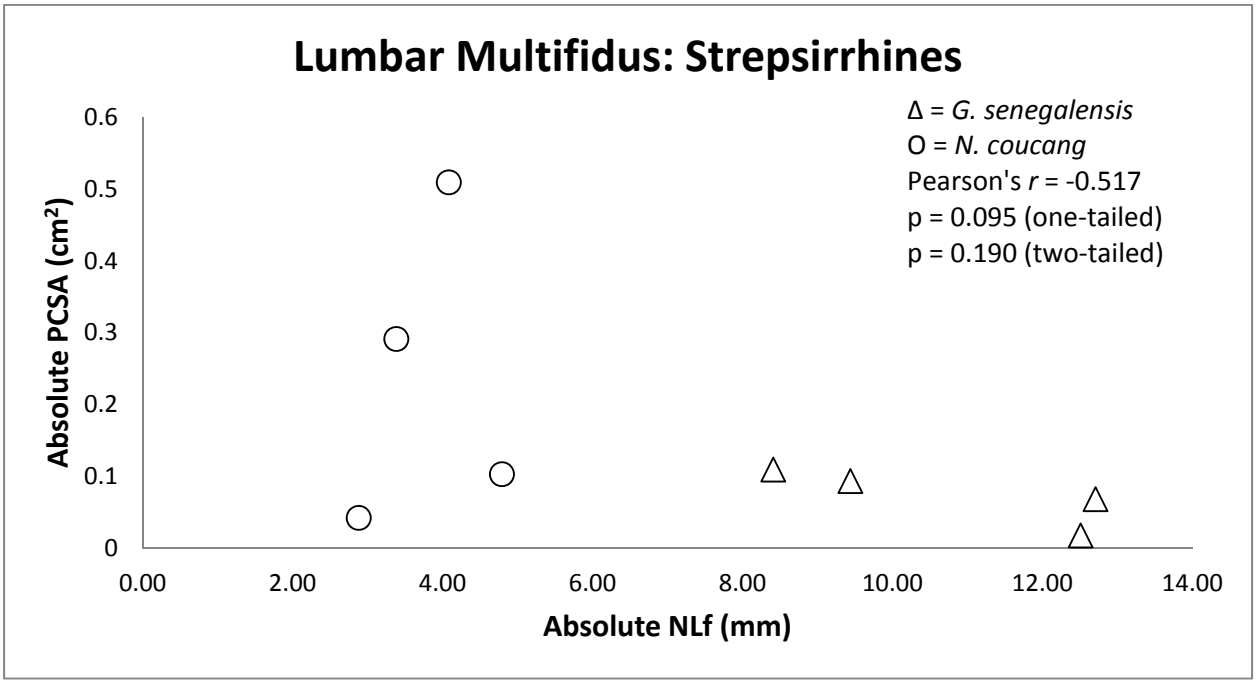

Fig. 67: Bivariate plot demonstrating partial negative correlation (i.e. architectural trade-off) between muscle velocity (NLf) and force (PCSA). This correlation is not significant (see Table 42).

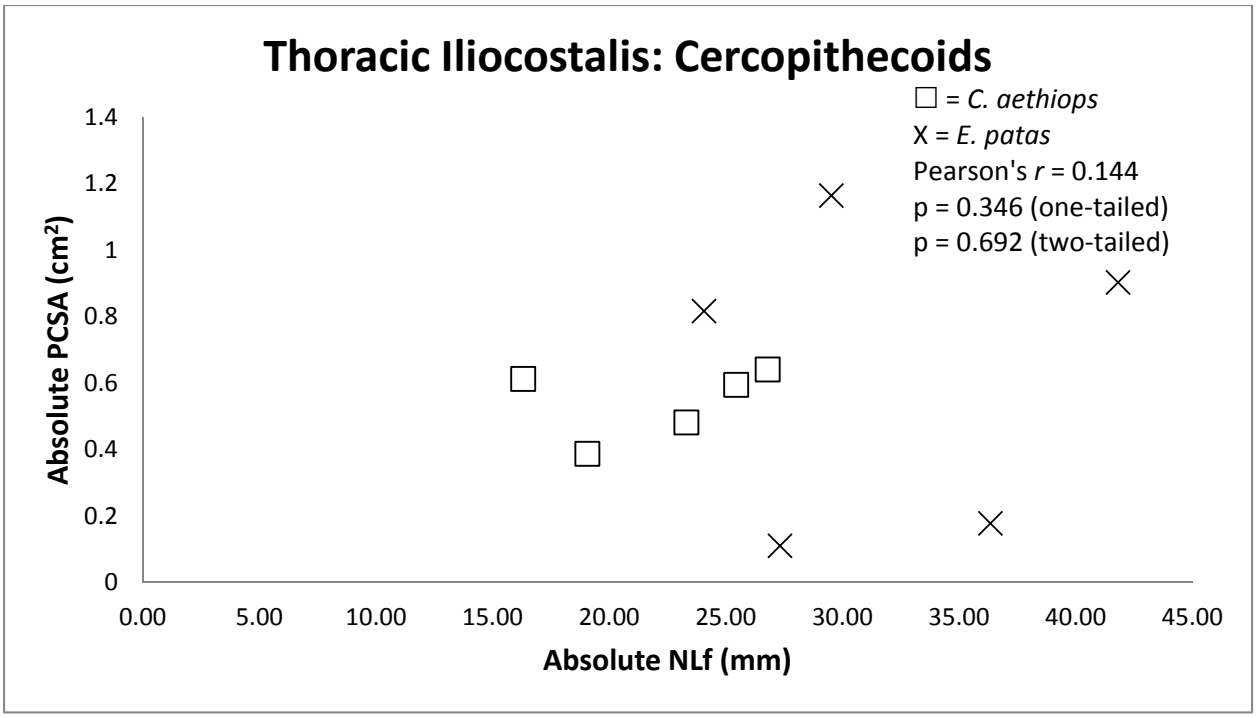

Fig. 68: Bivariate plot demonstrating moderate positive correlation between muscle velocity (NLf) and force (PCSA). This correlation is not significant (see Table 43).

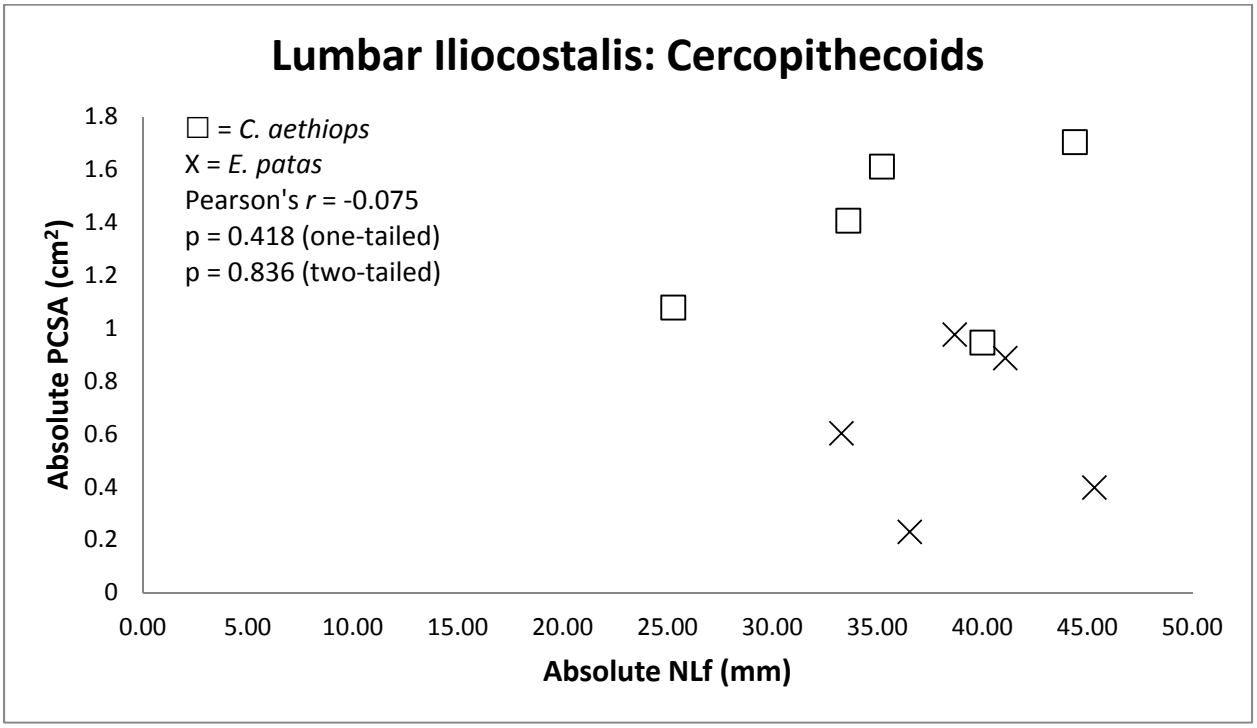

Fig. 69: Bivariate plot demonstrating low negative correlation (i.e. architectural trade-off) between muscle velocity (NLf) and force (PCSA). This correlation is not significant (see Table 43).

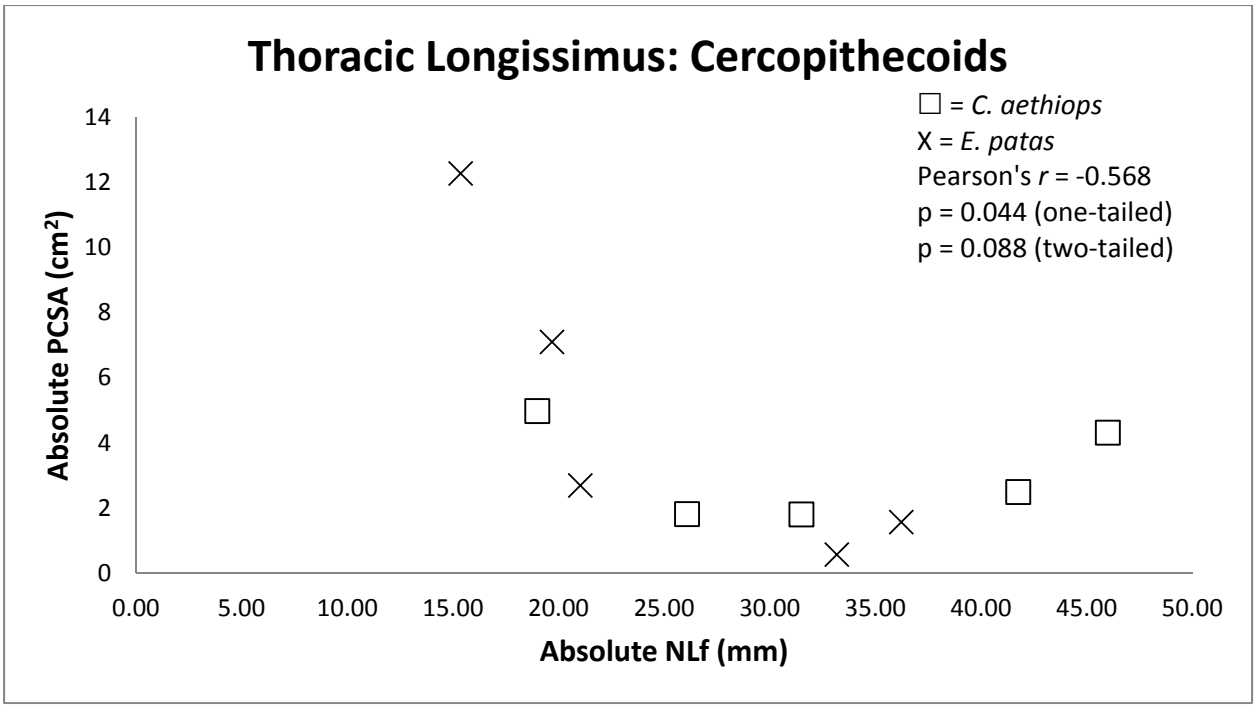

Fig. 70: Bivariate plot demonstrating partial negative correlation (i.e. architectural trade-off) between muscle velocity (NLf) and force (PCSA). The one-tailed correlation is significant (see Table 43).

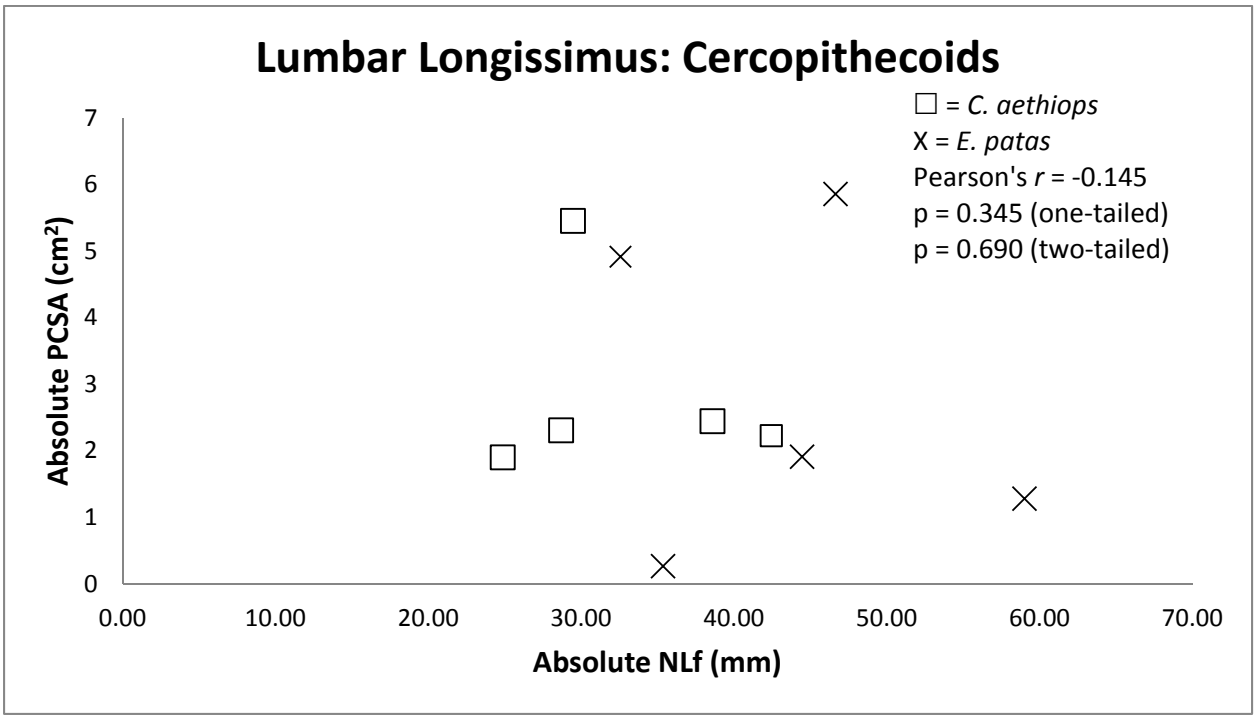

Fig. 71: Bivariate plot demonstrating moderate negative correlation (i.e. architectural trade-off) between muscle velocity (NLf) and force (PCSA). This correlation is not significant (see Table 43).

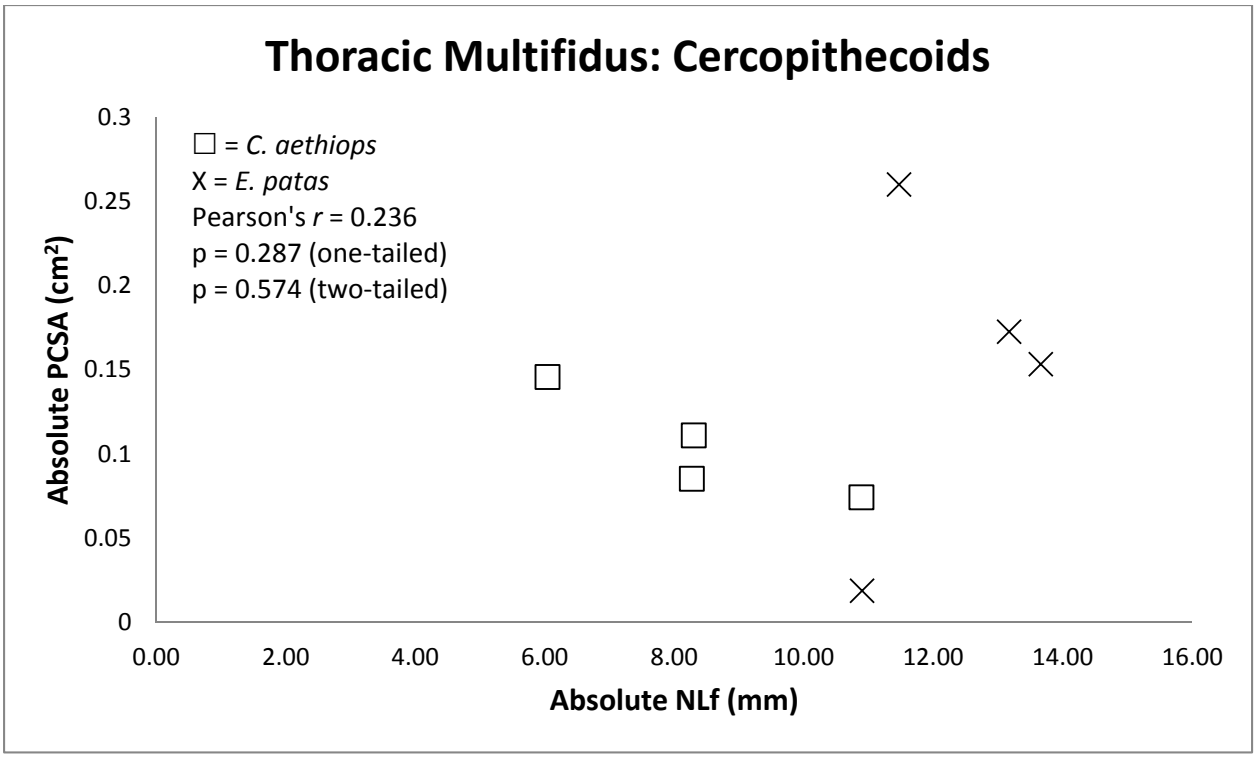

Fig. 72: Bivariate plot demonstrating moderate positive correlation between muscle velocity (NLf) and force (PCSA). This correlation is not significant (see Table 43).

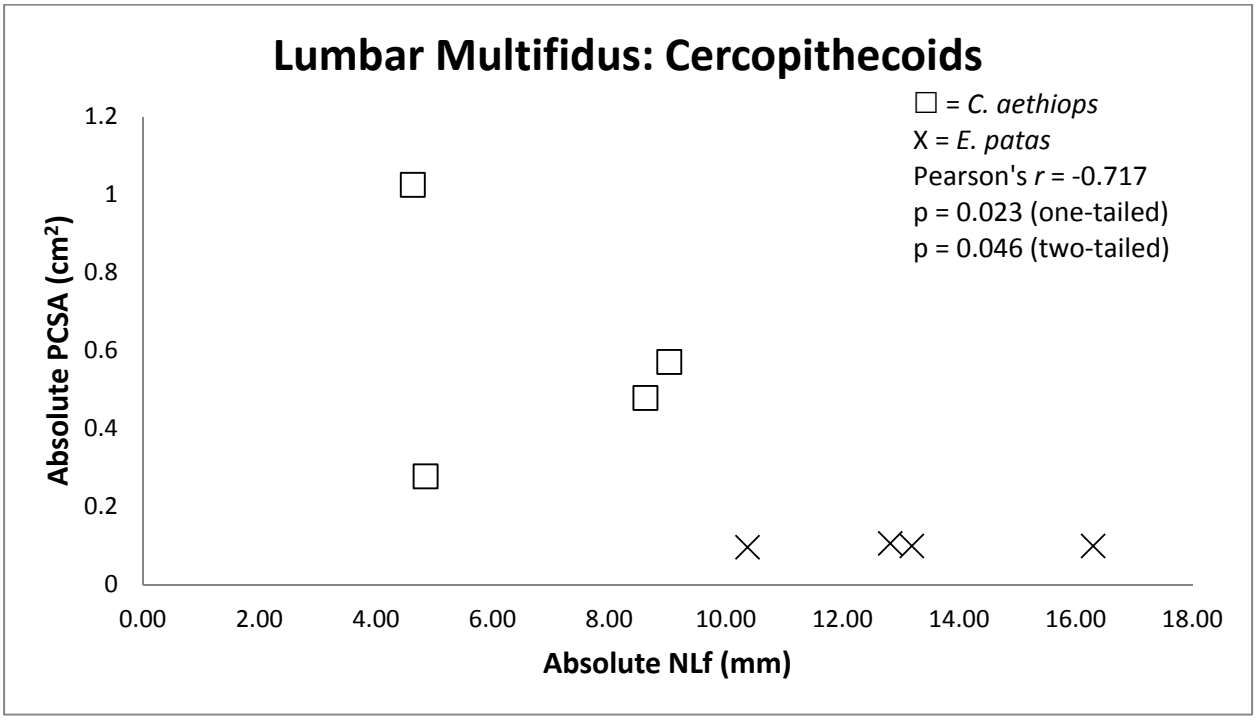

Fig. 73: Bivariate plot demonstrating high negative correlation (i.e. architectural trade-off) between muscle velocity (NLf) and force (PCSA). This correlation is significant (see Table 43).

Chapter 3

Muscle Histology

3.1 Introduction

Mammalian skeletal muscles contain combinations of fibers with different contractile and metabolic properties. The presence of these various fiber types within the same muscle permits it to generate forces over a wide range of shortening velocities with varying degrees of resistance to fatigue. Unlike the muscles of most lower vertebrates and invertebrates, which tend to have more homogeneous fiber compositions, mammalian muscles exhibit a remarkable degree of versatility in meeting their contractile requirements. In fact, the heterogeneous fiber composition of mammalian skeletal muscles reflects the complexity of the neuromuscular developmental process (Lieber, 2010).

Muscles as energy-producing units

Muscle mechanical work is converted from chemical energy, in the form of ATP (adenosine triphosphate), which is derived either from the anaerobic glycolysis of glucose stored as glycogen, or from oxidation. Muscle fibers are specialized and differ in their content of enzymes and substrates of metabolism. As opposed to the glycolytic metabolism that exhausts glycogen stores, the oxidative metabolism provides energy for virtually unlimited periods of time as long as a sufficient blood supply is provided. It suits particularly the requirements of antigravity (postural) muscles (Armstrong et al., 1982). Biochemical approaches to the main function of locomotor muscles are based on the relationships between their contractile and biochemical properties (substrates of metabolism, enzymic and proteinic characteristics).

The concept of histological and functional heterogeneity of mammalian skeletal muscles (mosaic pattern) dates back to the late nineteenth century when Ranvier (cited in Jouffroy and

Médina, 2004) observed that the red and well-vascularized muscles of rabbits contracted slowly whereas the pale and poorly vascularized fibers of the white muscles were fast. As early as 1885, Ehrlich (cited in Jouffroy and Médina, 2004) observed that the oxidative capacity of muscles destined for continuous work was higher than that of muscles destined for rapid movements or short-lasting activities. Further advance did not occur before the 1960s, with improvements in histochemical procedures for demonstrating enzymic activity (oxidative enzymes, ATPase, and phosphorylase).

The "glycogen depletion method" (Edström and Kugelberg, 1968; Kugelberg and Edström; 1968) demonstrated that: (1) all fibers composing a motor unit (innervated by a single motoneuron) are of the same metabolic type; and (2) the maximum speed of contraction and resistance to fatigue of a motor unit is related to the histochemical properties of its muscle fibers. It provided a basis for correlating physiological and biochemical investigation (Burke et al., 1973; Burke and Tsairis, 1974; Dum and Kennedy, 1980; Burke, 1981). According to their physiological properties, motor units have been divided into three main categories: (1) slow (S) units, with slow maximum contraction velocity and high resistance to fatigue; (2) fast fatigable (FF) units, with fast maximum time of contraction and very readily fatigable; and (3) fast fatigue-resistant (FR) units, with intermediate contraction times and resistance to fatigue. In addition, a small group of motor units with intermediate resistance to fatigue between FF and FR were named F(int) (Burke and Tsairis, 1974, 1977; Burke et al., 1976). Owing to the multiplicity of intermediate types of fast fibers, it has been advocated that FF and FR are the extremes of a spectrum rather than discrete categories (Stephens and Stuart, 1974). Identification of myofiber types is based on either enzymic or antigenic protein specificity.

Here, it needs to be noted that different investigators have used different terminology in identifying various myofibers. Table 1 shows several fiber type classification schemes, which will be useful in establishing a terminological equivalence for fiber types (Lieber, 2010).

Enzymic identification of myofibers

Fibers of mammalian skeletal muscles can be classified into two main types based on the stability of their myosin ATPase (mATPase) to alkaline (pH 10.4) conditions: low activity or high activity. Brooke and Kaiser (1970) classified mATPase into two primary types: I and II, with type II having a less acid-stable form IIA and a more acid-stable form IIB. The results were associated with the content of enzymes (NADH [nicotinamide adenine dehydrogenase] and SDH [succinate dehydrogenase]) that reflect the mitochondrial content (an indicator of oxidative metabolism). Peter et al. (1972), by staining serial sections alternately for myosin ATPase and the metabolic enzymes, found that Type I fibers had high oxidative capacity. Because of the positive correlation between muscle contraction velocity and myosin ATPase activity (Barany, 1967), Peter et al. (1972) used the contraction velocity of type I fibers to estimate their myosin ATPase activity rate. They called them "slow-oxidative" fibers (SO). Myosin ATPase associated with type IIA stained darkly for both oxidative and glycolytic enzymes: they were named "fast-oxidative/glycolytic" fibers (FOG). Lastly, type IIB fibers had low oxidative and high glycolytic capacity, and they also had the fastest contraction velocity: they were dubbed "fast-glycolytic" fibers (FG). Later investigations based on mATPase histochemistry delineated four major subtypes: three fast (IIA, IIB, and IIX) and one slow (I) (Schiaffino et al., 1989; Gorza, 1990; Hämäläinen and Pette, 1993). The classifications based on myosin ATPase and oxidative enzymes cannot be strictly equated. However, Pette and Staron (1997) pointed out that a good correlation between types I and SO fibers remains undisputed. This typing scheme has also been

extended to MyHC genes and gene expression. Thus, mammals, including humans, have four MyHC genes in their genome that are commonly expressed in skeletal muscle: beta, 2A, 2X, and 2B (MyHC-beta gene is eventually expressed as Type I fiber; Yoon et al., 1992; Weiss and Leinwand, 1996; Weiss et al., 1999). Although it appears that early MyHC expression patterns define adult fiber types (Weiss and Leinwand, 1996), changes in isoform composition in the latter can occur in response to neuronal (Pette and Vrbova, 1985), hormonal (Izumo et al., 1986), mechanical (Loughna et al., 1990), and electrical (Gorza et al., 1988; Termin et al., 1989; Ausoni et al., 1990) stimuli, as well as with aging (Butler-Brown et al., 1984; Whalen et al., 1984; Larsson et al., 1991) and exercise (Andersen et al., 1994).

The relationships between the functional categories of motor units S, FR, FF, and the enzymic categories of fibers were pointed out by Burke and colleagues (1971, 1974, 1986). They showed that the fatigue-resistant, slow-twitch motor units consist of fibers that stain only weakly for alkaline ATPase and intensely for mitochondrial enzymes (SDH), and conversely for the fast-twitch motor units. Further subtypes of myofibers have been described, mainly fiber types IIC (intermediate between I and IIA: Brooke and Kaiser, 1970) and IIX (see above). Similarly, as regards resistance to fatigue and force output, Edström and Kugelberg (1968) and Burke (1975, 1981) found a small number of motor units (F-int) with intermediate characteristics between FR and FF ("FI" type: McDonagh et al., 1980a, b). These intermediate types are found in small numbers: they are considered as transitional forms expressing fiber plasticity (Gauthier, 1986; Peters, 1989). Their existence, however, does not modify the basic classification of the myofibers into the three main categories, I, IIA, and IIB.

Antigenic protein identification of myofibers

As regards the proteinic diversity of myofibers, immunohistochemical techniques supplement data drawn from enzyme histochemistry. Myosin is the most abundant protein in muscles and makes up the primary component of the thick filament. Its molecule is made up of two heavy chains (MyHCs) and four light chains (MyLCs) (Gauthier, 1986; Peters, 1989). These chains occur as several distinct isoforms (isomyosins). Adult skeletal muscle fibers are composed of different isoforms (slow and fast) of the myosin heavy chains (Gauthier and Lowey, 1977). Myofibers defined as slow or fast by histoenzymic reactions have fundamentally different MyHC (Staron and Pette, 1986). It has been shown that the distinct slow and fast MyHC isoforms correlate with the distinct enzyme patterns of mATPase staining: molecular techniques have revealed a single slow MyHC and three fast MyHCs which correspond to the IIA, IIX/D, and IIB enzyme categories (Gauthier and Lowey, 1977, 1979; Bär and Pette, 1988; Schiaffino et al, 1989; Gorza, 1990; Bottinelli et al, 1994; Graziotti et al, 2001). Antibodies specific for fast MyHC react with the fibers that have high alkali-stable mATPase activity (type II; Brooke and Kaiser, 1970), and conversely antibodies specific for slow MyHC react with type I fibers that have a very low alkali-stable mATPase activity.

According to Pette and Staron (2000), MyHC isoforms represent the most appropriate markers for fiber type delineation. They show an excellent correlation with the classical fiber types I (= SO) and II (= FOG and FG) as assessed by myosin ATPase histoenzymology (Brooke and Kaiser, 1970; Peter et al, 1972). As investigations about muscle immunology have advanced during the last few decades, the number of intermediate fiber types that have been discovered has increased, suggesting a continuum rather than discrete categories. Recent studies have shown that, in addition to "pure" fiber types (Hämäläinen and Pette, 1995) that are characterized by the

expression of a single MyHC isoform, there are "hybrid" fibers that express two or more MyHC isoforms (Gorza, 1990; Hämäläinen and Pette, 1993; Staron and Pette, 1993; Pette and Staron, 1997, 2000, 2001). These hybrid fibers bridge the gaps between the pure fiber types (I/IIA, IIA/IIX, IIX/IIB), hence the appearance of a continuum. The hybrid fibers bridging the gap between types I and IIA fibers can be easily identified, because they react to both categories of antibodies: against slow and fast myosin. Experimental studies have shown that electrical stimuli, mechanical factors (immobilization, loading and unloading, space weightlessness), variations in thyroid hormone levels, etc. induce changes in MyHC expression heading in the direction of either fast-to-slow or the reverse (Hämäläinen & Pette, 1995; Pette & Staron, 1997, 2000, 2001; Sartorius et al, 1998; Kischel et al, 2001; Serrano et al. 2001; Stephenson, 2001). In fact, it has been argued that hybrid fibers enable a muscle to fine-tune its efficiency for the wide range of forces, velocities, levels of endurance, and levels of resistance to fatigue it is required to generate. For example, Vijayan et al (2001) noted that when the chronically unloaded hindlimb muscles of rats had been subjected to eccentric contraction, FOG (≈ Type IIA) fibers were predominantly damaged, and SO (≈ Type I) fibers were least damaged. Damaged hybrid fiber proportions ranged between the two extremes (Vijayan et al., 2001). Williamson et al. (2000, 2001) also observed that after an extended period of progressive resistance training in humans, the proportion of hybrid fibers (type I/IIA) decreased, and pure fibers (types I and IIA) increased. Based on this evidence, it may be argued that in response to the changing loading regime of limb muscles, hybrid fibers provide a buffer between pure fiber types, or they form a reservoir from which fibers can be transformed and added to the already existing pure fiber types.

Support for the idea that hybrid fibers enable a muscle to respond more effectively to functional demands comes from studies of specialized striated muscles as well. For example, all

fibers in rat stapedius are hybrid (Dammeijer et al., 2000), an unusual configuration which would enable the stapedius to contract fast and fatigue slowly (thereby stiffening the middle ear ossicle chain) at acoustic stimulations stronger than 80 dB (Dammeijer et al., 2000).

In short, both enzymehistochemistry and immunohistochemistry are alternative approaches to the analysis of muscle fiber types. However, as opposed to the myosin enzymatic activity, antibody epitopes of the myosin persist in the protein for a longer period of time after death. Muscles preserved in formaldehyde react to antibodies against MyHCs (Jouffroy and Médina, 2004). The persistence of immunoreactivity makes immunohistochemical fiber-typing convenient for the study of preserved cadavers, a useful procedure for comparative zoological investigations (Jouffory and Médina, 1996, 2004; Médina and Jouffroy, 1998; Jouffroy et al., 1999).

Fiber types and recruitment patterns

The distribution of muscle fibers into several categories can help to accommodate the variety of demands placed upon the musculo-skeletal system. Several studies of recruitment patterns, intramuscular motor unit distribution, and muscle mechanics have suggested that each fiber type may be quite specialized in its participation in movement (e.g. Burke and Tsairis, 1973; Hannerz and Grimby, 1973; Gollnick et al. 1974a, b; Armstrong et al. 1977; Botterman et al. 1978; Monster et al. 1978; Sullivan and Armstrong, 1978; Gregor et al. 1979; Maton, 1980). Others have demonstrated discrete compartmentalization within selected limb muscles in cat, both in the differential arrangement of fibers and the distribution of motor units (Gonyea and Ericson, 1977; English and Letbetter 1982; McConathy et al. 1983).

Some investigators have also noted a relationship between body size and expression of MyHC isoforms (i.e. Types I, IIA, IIX, and IIB). For example, skeletal muscles of small

mammals such as mice, which have a relatively fast stride frequency, tend to have a very high proportion of Type IIB fibers (Burkholder et al., 1994). In contrast, larger mammals (e.g., humans) tend to have relatively slower stride frequency, and even though they have the gene for Type IIB MyHC, they typically do not express it. It has been demonstrated, by antibody reactivity and *in situ* hybridization, that fibers in human skeletal muscle that had been traditionally identified as Type IIB, were actually expressing the Type IIX isoform (Smerdu et al., 1994).

It is well known that postural and propulsory limb muscles differ in their fiber type composition. While propulsory muscles or muscle regions possess a primarily homogenous distribution of fast-twitch/Type II fibers, postural muscles or muscle regions contain primarily slow-twitch/Type I fibers (Collatos et al., 1977; Burke, 1981; Armstrong et al., 1982; Fischer, 1999; Schmidt and Schilling, 2007). Based on these observations, designations such as postural or stabilizing, and propulsive or mobilizing are used interchangeably and imply a certain metabolic profile. However, we should remember that a stabilizing role may involve long periods of activation to ensure the structural linking of skeletal elements. This sustained activity requires a high percentage of slow, oxidative, Type I muscle fibers. On the other hand, quick postural responses, such as stabilization of the trunk against rapid loading from extrinsic limb muscles during running/leaping likely necessitate fast muscle fibers.

Muscles are activated based on the motoneuron recruitment in a spinal segment. Fatigue-resistant Type I fibers tend to be recruited earlier than the fatigable Type II fibers (Armstrong, 1980; Burke, 1981; Stuart and Enoka, 1983; Chanaud et al., 1991). A number of studies (Gillespie et al. 1974; Walmsley et al. 1978; Maton, 1980; Smith et al. 1980) have noted that at lower activity levels, particularly those which entail postural, as well as fine, deliberate,

feedback-controlled movement, slow oxidative (Type I) fibers will be recruited (perhaps exclusively). At higher levels of activity, which require faster, more powerful movements, the fast-twitch fibers (Type II) will be recruited, either in addition to, or instead of the slow-twitch fibers previously recruited (Gillespie et al. 1974; Walmsley et al. 1978; Maton, 1980; Smith et al. 1980). In the case of extra-ocular muscles, for a rapid movement of the eyeball, fast-twitch fibers are recruited first, followed by slow-twitch fibers (Rubinstein and Hoh, 2000). Walmsley et al. (1978) observed that only the fatigue-resistant muscle regions of cat limb muscles were recruited at slow-to-moderate walking speed. However, with the increase in walking speed, all muscle regions had been activated. The same principle applies to the differential activation of "slow" and "fast" heads in elbow, knee, and ankle extensors in primates and other mammals (Smith et al., 1980; Anapol and Jungers, 1987; Fischer, 1999). In addition, the percentage of slow fibers in a muscle is positively correlated with the time the muscle is active (either the average percentage of the time a muscle is active at a specific level or the average time the muscle is on, per contraction) (Monster et al. 1978).

During isometric exercise, when a muscle is contracting at tension less than 20% of its maximal voluntary contraction (MVC), only slow-twitch fibers (Type I) are recruited (Gollnick et al. 1974b). During submaximal endurance isotonic exercise (pedaling), fast, Type II fibers are not recruited until the slow are depleted of glycogen. When the energy requirement exceeds the maximal aerobic power, both slow- and fast-twitch fibers become involved in the exercise (Gollnick et al. 1974a).

Assuming that this functional specialization is the rule, closely related animals (even conspecifics) with distinctively different modes of behavior would likely exhibit a disparity in the relative proportions of fiber types within functionally important or critical muscles or muscle

groups. For example, Gunn (1978) compared thoroughbreds and greyhounds to other horses and dogs and found a "high speed selection," i.e. a greater fractional area of high activity-myosin ATPase fibers in certain locomotory and respiratory muscles in these two breeds. Also, Marechal et al. (1976) reported a mixture of slow-twitch and fast-twitch fatigue-resistant fibers (in equal proportions) and the absence of fast-twitch fatiguable fibers in the hindlimbs and diaphragm of *Perodicticus potto*, a slow-climbing strepsirrhine.

Sickles and Pinkstaff (1981b) found that different fiber types predominated in the hindlimb muscles of closely-related animals with different locomotor propensities: fast-twitch oxidative-glycolytic (FOG, Type IIA) fibers in tree shews; fast-twitch glycolytic (FG, Type IIB) in lesser busbaby; and slow-twitch oxidative (SO, Type I) in loris. From these data, they predicted that FOG would predominate in running animals, FG in jumping animals, and SO in the postural muscles of all animals. Whether any fast-fatigable fibers are present in the slow climbing *Nycticebus coucang* is controversial (Ariano et al. 1973; Sickles and Pinkstaff, 1980).

The distribution of fiber types within individual muscles and within groups of muscles seem to be arranged in an even more orderly fashion, and may imply further functional differentiation. Sickles and Pinkstaff (1981b) noted that, in a runner (*Tupaia*), the deeper muscles of a group and the deeper portions of individual large thigh muscles contained higher percentages of S (Type I) fibers than the more superficial muscles and portions of muscles. In contrast, leaping animals (e.g. *Galago*) have predominantly fast (Type II) fibers evenly distributed throughout the hip and leg extensors and the plantar flexors (Sickles and Pinkstaff, 1981b). Finally, the hindlimb muscles of a slow moving animal (*Nycticebus coucang*) were characterized by an absence of glycolytic fast-twitch (Type IIB) fibers (Sickles and Pinkstaff, 1981b). Furthermore, the pattern of recruitment of a specific type of motor unit appears to be

related to the nature of the specific movement being performed. Measuring glycogen depletion in *Galago*, Gillespie et al. (1974) demonstrated that after running, the slow-twitch (Type I) units of vastus lateralis are the most depleted, the FR (Type IIA) units second, and the FF (Type IIB) units least depleted. After jumping, the sequence is reversed.

Other histoenzymic studies of primates have focused on a single genus showing specialized modes of locomotion, e.g. the leapers *Aotus* (Plaghki et al. 1981) and *Eulemur* (Anapol and Jungers, 1986), the suspensory *Hylobates* (Kimura and Inokuchi, 1985), and the arboreal quadruped/leaper *Microcebus* (Petter and Jouffroy, 1993). In their study of *Eulemur fulvus*, Anapol and Jungers (1986) investigated the fiber-type population in the four heads of the quadriceps femoris muscle. They observed that the relatively superficial heads (rectus femoris, vastus medialis, and vastus lateralis) contained a high percentage of fast-twitch (Type II) fibers, while the deep vastus intermedius was almost exclusively composed of slow-twitch (Type I) fibers. The authors argued that vastus intermedius was best suited for postural behavior, indicated by its recruitment and maintenance during walk/run and galloping (although during standing high leaps, the other three heads of the quadriceps femoris showed a higher recruitment ratio). A similar observation was made by Jouffroy et al. (1999), who found one muscle head composed overwhelmingly (85% and above) of slow-twitch fibers (Type I) in the triceps brachii, quadriceps femoris, and triceps surae of *Macaca mulatta.* These muscle heads were specialized for posture, as demonstrated by EMG data that they were recruited at low levels to maintain joint position against the flexing effects of gravity (Jouffroy et al. 1999).

Armstrong (1980) summarized the distribution of physiologically distinctive motor units. In the limbs of terrestrial mammals, extensor groups are characterized by slow-twitch (Type I) fibers predominating in the deepest muscles and decreasing in relative abundance in the more

superficial ones. The flexor groups contain few slow fibers and no deep slow (whole) muscles. Fast (heterogeneous) whole muscles have their slow-twitch fibers closer to the bone. Therefore, muscles (and parts of muscles) closest to the bone have the highest concentration of slow-twitch fibers (Burke, 1980; Armstrong, 1980). Locating slow fibers in the deepest parts of the limb is thought to minimize heat loss when an animal is at rest and reduce their otherwise high cost of maintenance (e.g. high resting blood flow, oxygen extraction) during inactivity (Burke, 1980).

A comprehensive demonstration of the requirement for motor units with functionally distinctive characteristics comes out of works on gait changes during locomotion (Armstrong et al. 1977; Sullivan and Armstrong, 1978; Taylor, 1978; Armstrong, 1980). Armstrong et al. (1977) measured the glycogen depletion rates for specific fiber types in the limbs of young lions during locomotion. While rates of glycogen depletion in whole muscles (biceps femoris and triceps brachii) increased with speed (without discontinuity) at gait transitions, striking discontinuities were observed in the depletion rates of individual fiber types. They concluded that a gait transition did not occur at the maximum tension for either a fiber type or a whole muscle and that different configurations of motor units within an individual muscle may be recruited as the animal changes its gait. These results were supported, in part, by Sullivan and Armstrong (1978) in rats.

Epaxial muscles and fiber types in primates

Studies on muscle fiber types in non-human primates have primarily focused on appendicular musculature, as those are directly related to locomotion. Still, a number of investigators have produced detailed works on the epaxial muscle characteristics (primarily those of macaques) (e.g., Bagnall et al., 1983; Ford et al., 1986; Kojima and Okada, 1996; Kumakura et al., 1996). They observed a lower proportion of slow-twitch (Type I) fibers in the lumbar

region relative to the thoracic region at both superficial and deep levels. It may be argued that the higher percentage of Type II fibers in the lumbar segments of the spinal extensor (i.e., epaxial) muscles would impart greater flexibility, and a capability of rapid sagittal movement of the spine of the macaque.

Roos (1964) argued that in the course of the vertebrate and mammalian evolution, the role of the spine had evolved from producing lateral bending to sagittal bending, with limbs serving as anchors supporting the body's progression. This observation, coupled with the role of the spine during asymmetrical gait in mammals, and the enlargement of erector spinae and transversospinal muscles in mammals (Howell, 1938; Starck, 1978; Jones, 1979), led Schilling (2009) to speculate that fast-twitch (Type II) fibers had been added around the mammalian spine. This development, she argued, would have facilitated the evolution of vigorous sagittal spine oscillations in bounding and galloping (Schilling, 2009). I hypothesize that epaxial muscles of primates with rapid spinal extension will contain more fast-twitch (Type II) fibers; while slow-twitch (Type I) fibers will predominate in those of the dorsostable primates and those without rapid back extension. I predict that

i) There will be a higher proportion of fast-twitch, Type II fibers in the epaxial muscles of *G. senegalensis* (lesser galago); while slow-twitch, Type I fibers will predominate in those of *N. coucang* (slow loris). Likewise, epaxial muscles of *C. aethiops* (vervet monkey) will contain more fast-twitch, Type II fibers relative to those of *E. patas* (patas monkey) (more slow-twitch, Type I fibers).

ii) Relative to the thoracic region, epaxial muscles in the lumbar region of the lesser galago will contain more fast-twitch, Type II fibers. The same pattern will be present in the thoracic and lumbar segments of the epaxial muscles of the vervet

monkey; while in the epaxial muscles of the patas monkey, there will be no noticeable difference in the relative proportion of Type I (slow-twitch) and Type II (fast-twitch) fibers between thoracic and lumbar segments.

3.2 Materials and methods

The sample size for histochemical analysis is presented in Table 2. All cadavers were previously fixed and stored in alcohol and/or formalin.

Immunohistochemical analysis of muscles

A small chunk of tissue (L = ~3 mm X W = ~1.5 mm X Thickness = ~1.5 mm) was removed from each muscle segment and preserved in 70% ethanol solution. These tissue blocks were then transferred to the Immunohistochemistry Laboratory (Dept. of Pathology, Duke University Medical Center). They were embedded in paraffin, and then cut into 5 μm transverse sections on a cryostat.

Sections were pre-treated with 1% bovine serum albumin (BSA, Sigma) dissolved in trisma-buffered saline/0.1% Tween 20 (TBST) for 20 minutes. Then they were incubated for 45 minutes at room temperature with two primary antibodies. Mouse monoclonal antibodies, raised against rabbit skeletal muscle, were used as primary antibodies to slow myosin (MyHC I, Clone NOQ7.5.4D, Sigma-Aldrich, Inc.) and fast myosin (MyHC II, Clone MY-32, Sigma-Aldrich, Inc.). Both of these antibodies were diluted 1:400 in TBST. It is to be noted that the MY-32 antibody does not distinguish among sub-types of Type II (IIA, IIX, and IIB) fibers (Sciote and Morris, 2000).

After washing in TBST, tissue sections were incubated for 30 minutes at room temperature in the biotinylated secondary antibody (horse anti-mouse, Vector), diluted 1:200 in TBST. Following a wash in TBST, Vectastain Elite ABC (Vector) was applied to the sections, and incubated for 30 minutes. After another wash in TBST, DAB Chromagen (Dako) was applied to the sections, and incubated for 5 minutes. The sections were then washed in dH_2O, and rinsed in tap water for 1 minute. The sections were then counterstained in hematoxylin for

30 seconds, and the slides were rinsed in tap water until they became clear. Blue neclei was applied by dipping each section 4 times in ammonium water. After a rinse in tap water for 2 minutes, they were dehydrated, cleared, and cover-slipped. Prior to preparing the sections, this procedure was tested on formalin-preserved human skeletal muscle tissue to determine its effectiveness.

The muscle sections were saved as digital images at 20x magnification using a Zeiss axiocam digital camera attached to a Zeiss Axioskop microscope and AxioVision 4.4 software (Carl Zeiss, Inc.). Microscope fields in serial and contiguous sections were matched by identifying specific muscle cells by their shape and size in contiguous thin sections and using fiducial markers such as fascial planes and blood vessels. Images were printed at 600 dpi on a high resolution color printer to facilitate identification of contiguous and serial sections. Fiber type counts were made from the prints using a hand-held counter. Fibers were counted as dark, moderate, weak, or no stain intensity; dark, moderate, and weak counts were combined for subsequent statistical analysis. Fibers that had stained for both primary antibodies were classified as "hybrid." Depending on the tissue and staining quality, areas of at least 10 fibers were measured for each fiber type from each muscle segment. Fiber areas were measured with ImageJ v. 1.24 software (Abramoff et al., 2004).

All statistical analyses were carried out on Microsoft Excel 2007 (Microsoft™) or SPSS v. 16 (IBM, Inc.). One-tailed Mann-Whitney U tests were conducted to evaluate whether individual muscle segments had significantly different proportions of MyHC-I and MyHC-II isoforms. A G-test of independence was used to test for independence of species and antibody reaction for each muscle segment. A one-way ANOVA with post-hoc LSD test for multiple pairwise comparisons was conducted for fiber-type proportions for all species. For one-way

ANOVA with multiple pairwise analysis, fibers of a particular type in all muscle segments of each individual specimen of a particular species (e.g., type I fibers in all muscle segments of individual no. 1 of *G. senegalensis*) were pooled. Although sex-related data were reported, sex-related significance testing was not conducted because apart from the *E. patas* sample, no other species had more than one individual from each sex. Level of significance for all tests was set at $p \leq 0.05$.

3.3 Results

Proportions and regional distribution of fiber types

In general, all muscle segments contained Type I, Type II, and hybrid fibers, but in varying proportions. Representative sections of stained tissues are shown in Figs. 1-48. G-tests of independence showed that except for thoracic multifidus of the two cercopithecoid species, there was a strong association between species and antibody reaction (Tables 3-4).

Summary of results

Prediction 1. *G. senegalensis* meets the prediction of a higher proportion of Type II fibers compared to *N. coucang* (Tables 5-6; Figs. 49-50). Type II fiber area is notably larger than Type I fiber area in the lesser galago (Table 18; Fig. 62). Type I and Type II fiber areas are more similar to each other in size in the slow loris (Table 19; Fig. 63).

By contrast, *C. aethiops* and *E. patas* have very similar proportions of Type I and Type II fibers, with a slight predominance of Type II fibers seen in both species (Tables 7-8; Figs. 51-52). Type II fiber areas are moderately larger than Type I fiber areas in both species (Tables 20-21; Figs. 64-65).

Prediction 2. G. senegalensis lumbar muscle segments show moderately to slightly higher proportions of Type II fibers than in the thoracic segments (Table 5; Fig. 49). This pattern is also seen in 2 (out of 3) muscles in *C. aethiops* (Table 7; Fig. 51). On the other hand, in 2 (out of 3) muscles of *E. patas*, proportions of Type II fibers are moderately to slightly higher in the thoracic than in the lumbar regions (Table 8; Fig. 52).

Differences in fiber type proportions

Thoracic iliocostalis. In *G. senegalensis*, this muscle was primarily consisted of Type II fibers (78.37%) (Table 5; Fig. 49).

In *N. coucang*, thoracic iliocostalis was overwhelmingly composed of Type I fibers (70.32%) (Table 6; Fig. 50). The difference was significant between *G. senegalensis* and *N. coucang* for Type I, but not for Type II, fibers (Table 9). The female slow loris also had a higher proportion of Type I, and a lower proportion of Type II fibers, than the male (Table 11; Figs. 53-54).

Thoracic ilicostalis in both species of cercopithecoid monkeys contained a higher proportion of Type II fibers, relative to Type I fibers. However, the proportion of Type II fibers was higher in the muscle of *E. patas* (64.96%) relative to that of *C. aethiops* (49.94%) (Tables 7-8; Figs. 51-52). On the other hand, vervet monkey had a higher proportion of Type I fibers (40.03%) relative to patas monkey (25.24%) (Tables 7-8; Figs. 51-52). There was no significant difference in the presence of Type I and of Type II fibers between species (Table 10).

The thoracic iliocostalis of male vervets had a higher proportion of Type I, and lower proportion of Type II fibers (Table 12; Figs. 56-58). On the other hand, the male patas monkeys had a higher proportion of Type II fibers; while the females had more Type I fibers (Table 13; Figs. 59-61).

Lumbar iliocostalis. Overwhelming majority of the fibers in the lumbar iliocostalis of *G. senegalensis* was Type II (Table 5; Fig. 49); on the other hand, Type I fibers (61.54%) predominated in this muscle of *N. coucang* (Table 6; Fig. 50). Significant differences between the species also existed for each of the Types I, II, and hybrid fibers (Table 9).

The lumbar iliocostalis of *C. aethiops* contained more Type II fibers relative to that of the patas monkey (Tables 7-8; Figs. 51-52). In contrast, there was a greater proportion of Type I fibers in the muscle of the *E. patas* (Table 8; Fig. 52). However, the differences between the two species were not significant for any of the types I and II fibers (Table 10).

Lumbar iliocostalis in the male slow loris had a higher proportion of Type I, and lower proportion of Type II, fibers relative to that in the female (Table 11; Figs. 53-55). For the vervet monkey, lumbar iliocostalis in males contained more Type II, and less Type I, fibers relative that in females. The same pattern was also observed between sexes of the patas monkey (Tables 12-13; Figs.56-61).

Thoracic longissimus. In the lesser galago, thoracic longissimus contained a high proportion of Type II fibers (Table 5; Fig. 49). In contrast, thoracic longissimus of the slow loris was overwhelmingly composed of Type I fibers (Table 6; Fig. 50). Significant differences were observed in the distribution of both Types I and II fibers between the two species (Table 9).

Thoracic longissimus had a greater percentage of Type II fibers in the vervet monkey relative to that in the patas monkey (Tables 7-8; Figs. 51-52). On the other hand, patas monkey had a higher proportion of Type I fibers relative to the vervet monkey (Tables 7-8; Figs. 51-52). However, no significant difference was observed in the distribution of either Type I or Type II fibers in thoracic longissimus between the cercopithecoid monkeys (Table 10).

Thoracic longissimus in both male and female slow loris were primarily composed of Type I fibers, although the muscle contained slightly more Type I fibers in males than in females (Table 11; Figs. 53-55). Female vervet monkey had more Types I and II fibers than males (Table 12; Figs. 56-58). In the thoracic longissimus of patas monkey, there were more Type I fibers in the females, and Type II fibers in males (Table 13; Figs. 59-61).

Lumbar longissimus. The lumbar longissimus of *G. senegalensis* had a very high proportion (76.56%) of Type II fibers (Table 5; Fig. 49); while in *N. coucang*, Type I fibers predominated (63.35%) (Table 6; Fig. 50). The differences between the species, for both Type I and Type II fibers, were also significant (Table 9).

In both *C. aethiops* and *E. patas* monkeys, lumbar longissimus consisted of primarily Type II fibers (Tables 7-8; Figs. 51-52). However, there was a higher proportion of Type I fibers in *E. patas* (35.31%) compared to *C. aethiops* (32.25%) (Tables 7-8). However, no significant differences between the two taxa were observed for the presence of either Type I or II fibers (Table 10).

Between the sexes of the slow loris, proportion of Type II fibers was higher in the males than in the female (Table 11; Figs. 53-54). In the vervet monkey, relative to the females, the male had a higher proportion of Type I, and lower proportion of Type II, fibers (Table 12; Figs. 56-58). On the other hand, lumbar longissimus of the patas monkey carried more Type I fibers in females, and Type II fibers in males (Table 13; Figs. 59-61).

Thoracic multifidus. Thoracic multifidus in *G. senegalensis* contained a majority of Type II fibers, relative to Type I fibers (Table 5; Fig. 49). In the *N. coucang*, the opposite pattern was observed (Table 6; Fig. 50), with Type I fibers in the majority. Differences for Type I and II fibers were also significant between the species (Table 9).

Multifidus in vervets (both thoracic and lumbar) could not be analyzed because the antibody was degraded (Figs. 33-36). There were a greater proportion of Type II fibers, relative to Type I, in the thoracic multifidus of patas (Table 8; Fig. 52).

In the male specimens of slow loris, thoracic multifidus contained more Type I, and less Type II fibers, relative to that in the female (Table 11; Figs. 53-54). In the patas monkey, the proportion of Type I fibers was lower in the tissue of the male relative to that in the females, while the latter had less Type II fibers relative to the former (Table 13; Figs. 59-60).

Lumbar multifidus. In the slow loris, lumbar multifidus was composed overwhelmingly of Type I fibers (73.29%); while in the lesser galago, Type II fibers were more prevalent

(68.58%) (Tables 5-6; Figs. 49-50). The differences between the primates were significant for both Types I and II fibers (Table 9).

Majority of the fibers in the lumbar multifidus of the patas monkey were Type II (Table 8; Fig. 52).

Between the sexes of the slow loris, lumbar multifidus contained in males contained a higher proportion of Type I, and lower proportion of Type II, fibers relative to that of the female (Table 11; Figs. 53-54). Type II fibers predominated in both male and female patas monkeys; although females had a higher proportion of Type I fibers, and lower proportion of Type II fibers, than the males (Table 13; Figs.59-60).

ANOVA and multiple pairwise test results

One-way ANOVA test showed significant differences in terms of both count and proportion of different types of fiber among species (Table 14).

Results of the multiple pairwise comparison tests showed that *G. senegalensis* differed significantly from *N. coucang* in terms of both count and proportion of Type I fibers; while between *G. senegalensis* and each of the cercopithecoid monkeys, differences were significant only in proportions, and not counts, of Type I fibers (Table 15). On the other hand, both the count and the proportion of Type I fibers in *N. coucang* differed significantly from all other species (Table 15). There were no significant differences, in terms of either count or proportion of Type I fibers, between *C. aethiops* and *E. patas* (Table 15).

Lesser galago differed significantly from slow loris in both count and proportion of Type II fibers; while from both vervet and patas monkeys, it differed significantly in proportion, but not in count (Table 16). Slow loris differed significantly from lesser galago and patas monkey in both counts and proportions of Type II fibers, but from the vervet monkey, the difference was

significant in proportion, and not in count of Type II fibers (Table 16). Vervet and patas monkeys differed significantly from each other only in count, and not in proportion, of Type II fibers (Table 16).

For hybrid fibers, lesser galago differed significantly from slow loris and patas monkey (count and proportion); but from vervet monkey, it differed significantly in proportion, not in count (Table 17). Slow loris differed significantly from the vervet monkey in both count and proportion of hybrid fibers; but from the patas monkey, the difference was significant only in proportion (Table 17). Vervet and patas monkeys differed significantly from each other in both count and proportion of hybrid fibers (Table 17).

Differences in fiber area

Within each species, fiber area varied more or less consistently between different fiber types. For the lesser galago, Type I fibers had significantly smaller areas than Type II fibers for all muscle segments, except thoracic iliocostalis (Tables 18-19; Fig. 62). However, for the slow loris, the situation was different. Type II fibers of the thoracic longissimus had larger areas relative to Type I fibers; for the remaining tissues, Type I fibers showed greater areas (Table 20; Fig. 63). In addition, there were no significant differences in area between Types I and II fibers for the thoracic longissimus of the slow loris; all other segments showed significant differences (Table 21).

Regarding the difference in fiber area between sexes in the slow loris, Type I fibers of lumbar longissimus of the female had larger areas relative to those of the males (Table 22; Figs. 66). On the other hand, Type II fibers of the lumbar longissimus and thoracic multifidus of the female had larger Type II fibers relative to those of the males (Table 22; Fig. 67).

In the muscles of the vervet monkey, areas of Type II fibers were significantly larger relative to those of Type I fibers for all tissue samples (Tables 23-24; Fig. 64). However, between the sexes, females had larger Type I fibers in lumbar iliocostalis and lumbar longissimus; while areas of Type II fibers were larger for the female individuals in lumbar iliocostalis (Table 25; Figs. 68-69).

Areas of Type II fibers were significantly larger relative to those of Type I fibers in all muscle segments of the patas monkey (Tables 26-27; Fig. 65). Areas of both Types I and II fibers were also larger in males than in females (Table 28; Figs. 70-71).

3.4 Discussion

Fiber types are known to demonstrate a marked degree of plasticity (Salmons, 1980). Depending on the type, intensity, and duration of changes in motoneuron-specific impulse patterns, neuromuscular activity, and mechanical loading, muscle fibers tend to adjust their phenotypes to meet the altered functional demands (reviewed in Pette, 2001). In addition, because a whole muscle consists of numerous discreet motor units, each of a characteristic fiber type, innumerable permutations are available, and the implications for functional variability are profound.

Stabilizing the trunk against gravity is the main function of epaxial muscles (Asmussen, 1959), which are also characterized by a regionalization of the muscle with different proportions of muscle fiber types in different muscle regions, and therefore, different contractile properties (Ariano et al., 1973; Armstrong, 1980; Burke, 1981; Roy et al., 1984; Petter and Jouffroy, 1993; Jouffroy et al., 1999). The fiber type composition of antigravity muscles has been shown to be correlated with positional behavior in various mammalian species (Ariano et al., 1973; Sickles and Pinkstaff, 1981a, b; Kimura and Inokuchi, 1985; Anapol and Jungers, 1986; Hermanson et al., 1993; Jouffory et al., 2003; Watson et al., 2003). The present study shows that the fiber type composition of the epaxial muscles varies with different demands resulting from differences in spinal movement pattern.

Fiber type composition and muscle function

G. senegalensis, although a habitual leaper, has been observed to move quadrupedally at slower speeds (Napier and Walker, 1967). The epaxial muscles, apart from stabilizing the trunk against gravity, are also important for rapid back extension at the beginning of the take-off phase for leaping. This characteristic is reflected in the fiber type composition and fiber area of the

epaxial muscles of the species. The proportions of large, fatigable, but fast-contracting Type II fibers, and (mostly) smaller, fatigue-resistant Type I fibers were inversely related to each other within its epaxial muscles. The percentage of hybrid fibers varied among muscles, and showed no consistent relationship with other fibers. Pairwise comparisons also reflect the importance of Type II fibers in producing rapid movement for a habitual leaper, as evinced by the significant differences in the proportions of Type II fibers between the lesser galago and the rest of the study species.

The differences in fiber type composition between thoracic and lumbar segments of the epaxial muscles of the lesser galago reflect the different roles of these two regions of the spine during leaping. Because (a) rapid extension of the back is required for leaping, and (b) sagittal movement (flexion-extension) takes place at the lumbar region of the spine, the lumbar segments of the epaxial muscles tend to have a higher proportion of Type II fibers compared to the thoracic segments. On the other hand, the epaxial muscles showed a gradient in their proportions of Types I and II fibers from deep to superficial regions in both thoracic and lumbar segments. Thus, the deepest of the muscles in the present study – multifidus – consists of a higher percentage of fatigue-resistant Type I fibers in the lumbar segment; in the thoracic segment, this proportion was only marginally lower than that of thoracic longissimus. This pattern (deeper muscles with more Type I fibers) has also been observed in other mammals (dog: Armstrong et al., 1982; mouse lemur: Petter and Jouffroy, 1993; sheep: Suzuki, 1995; cui and tree shrew: von Mering and Fischer, 1999; rhesus macaque: Singh et al., 2002). In both thoracic and lumbar regions of the lesser galago, longissimus tends to contain less Type II fibers relative to iliocostalis. It should be noted that longissimus is parallel to the spine, and is an almost pure extensor. Ilicostalis, on the other hand, is located more laterally, and should effect as much

lateral flexion (unilateral activation) as extension (bilateral activation). For a habitual leaper, iliocostalis as an extensor would be more important than its role in lateral flexion (J. Fleagle; personal communication). However, apart from speculating that both of these muscles are responsible for rapid spinal extension, it is not possible to make a functional differentiation regarding their respective recruitment patterns at this point.

The slow-moving pattern of *N. coucang* (Napier and Walker, 1967; Walker, 1969) presents a different locomotor scenario for this arboreal quadruped. With at least two limbs grasping the support, the need for rapid acceleration and adaptation to the variety of substrates found among the trees is dramatically reduced. On the other hand, during anti-pronograde suspension and bridging, the premium is on trunk-stabilization. The constituent fiber types in the epaxial muscle of the loris are limited primarily to the fatigue-resistant Type I variety. These muscles would have to remain active for an extended period of time for the animal. Pairwise comparisons also underline the importance of Type I fibers for the slow loris compared to other species.

Similar to the muscles of the lesser galago, lumbar (but not thoracic) multifidus of the slow loris contained more Type I fibers relative to the more superficial tissues in the same spinal region. In addition, contrary to the pattern observed in the lesser galago, Type I fibers in most muscle segments of the slow loris (except thoracic longissimus) had larger areas relative to the Type II fibers. Because of the role of the lumbar region in sagittal movement of the spine, it can be hypothesized that the presence of large, fatigue-resistant fibers in those muscle segments would be useful for the loris' attempt at extending the spine in order to reach an overhead support during bridging (Hanna et al., 2011; J. Hanna, personal communication).

Distribution of fiber types in the epaxial muscles of the cercopithecoid monkeys demonstrates the subtle nature of the differences in their respective spinal mobility pattern. The epaxial muscles of both species contain a high percentage of Type I fibers, which might be important in maintaining trunk stability. However, the higher proportion of Type II fibers in the lumbar region of the vervet monkey would allow for generating high velocity. On the other hand, the proportions of Type II fibers in the lumbar segments of the epaxial muscles of the patas monkey, while high, are still low relative to comparable values for the vervet monkey (although the differences were not significant). The differential distribution of Type II fibers in lumbar muscle segments might be explained by differences in spinal movement during galloping in the two monkeys (Hurov, 1987). A (relatively) higher proportion of smaller, fatigue-resistant Type I fibers would allow the patas monkey to maintain a stable back during galloping; while the greater presence of larger, "high velocity" Type II fibers would be helpful in rapid sagittal movement of the lumbar region of the spine to increase the stride length of the vervet monkey. A higher proportion of hybrid fibers (compared to those in the vervet monkey) in the lumbar epaxial muscle segments of the patas monkey also serves to reduce the proportion of Type II fibers (Tables 7-8; Figs. 51-52). It has been observed that other cercopithecoid monkeys, such as macaques, also have a lower percentage of Type I fibers in the lumbar region relative to the thoracic region (Bagnall et al. 1983).

A comparative analysis of the fiber type distribution between humans and macaques might usefully illustrate the functional differences. Bagnall et al. (1983) observed that in the lumbar longissimus in humans, there were more Type I fibers relative to those in the macaque muscle, which had a correspondingly higher proportion of Type II fibers. This observation might reflect functional differences between epaxial muscles of humans and macaques. The rhesus

macaque, being a pronograde quadruped, has a virtually horizontal spine, while the human attempts to maintain an erect column. Postural tone and balance are, therefore, more important for humans, which may explain the presence of a greater proportion of postural (Type I) fibers in human epaxial muscles. On the other hand, if (lumbar) longissimus (as part of the erector spinae group) is considered to be responsible for the sagittal movement of the spine, it may explain the presence of higher percentage of Type II fibers in the longissimus of the monkey, which would be useful in providing flexibility and movement instead of stability.

Sexual dimorphism and fiber type composition

There does not appear to be any consistent effect of sexual dimorphism on the fiber type composition of the epaxial muscles of the slow loris and vervet monkey. On the other hand, in the patas monkey, fiber type distribution differs with sex. The female patas monkeys have a higher proportion of Type I fibers, while the males tend to have a higher proportion of Type II fibers. The reason for this particular pattern is unclear. It has been reported that female patas monkeys use tall trees for scanning the horizon and detecting predators (Enstam and Isbell, 2004). Isbell et al (1998) have also observed that in response to alarm calls for mammalian carnivore predators, female patas monkeys tend to climb trees more often than the sympatric (female) vervet monkeys. Being a terrestrial species, climbing may be more challenging to the larger patas monkey, than the smaller, more aroboreally adapted vervet monkey. Epaxial muscles with a relatively higher proportion of Type I fibers would be helpful for the former to maintain trunk stability on trees, along with the use of tail as an auxiliary balancing mechanism (Larson and Stern, 2006). In fact, data show that iliocostalis and longissimus (thoracic and lumbar segments) of female patas monkeys contain a greater proportion of Type I fibers compared to those of female vervet monkeys, while the proportions of Type I fibers in the multifidus (thoracic

and lumbar) of the female vervets are only marginally higher than those of the female patas (Tables 15 and 17).

Another hypothesis for the presence of a higher proportion of Type I fibers in the epaxial muscles of patas females, compared to those of patas males, might be advanced on the basis of details of the daily activity and life-history of the species. Patas monkeys forage while walking nearly four times as much as sympatric vervet monkeys. Because of their large home range, and widely dispersed food-sources, patas monkeys also travel three times farther than vervets per unit time, and travel twice the distance of vervets between food sites (Isbell et al., 1998). In addition, patas neonates tend to be quite large (average birth weight = 0.625 kg; Lee, 1995), compared to those of other guenon species (Lee, 1995). It is possible that female patas monkeys carry their infants during foraging; and also spend a considerable amount of time breast-feeding them, while maintaining a sitting posture (the weaning age of *E. patas* is 0.58 year; Ross and Jones, 1995). A high proportion of fatigue-resistant Type I fibers in the epaxial muscles would allow a female patas monkey to carry the additional weight of an infant (either on its back during locomotion, or in its ventrum for feeding) while maintaining a stable trunk. More data on the histochemical profile of epaxial muscles in other cercopithecoid species will be needed to test this hypothesis.

Sexual dimorphism in the distribution of fiber types in epaxial muscles has been observed in humans as well, with females having more Type I fibers than males (Thorstensson and Carlson, 1987; Mannion et al, 1997). However, the human case is not readily comparable to those of the cercopithecoid monkeys in the present study, because of the differences in positional behavior. Being bipeds, the spine has to carry the weight of the entire upper body in humans. It can be speculated that a higher proportion of fatigue-resistant, Type I fibers in the epaxial muscles of human females would be useful for maintaining an erect posture while carrying the

additional load of the developing fetus during pregnancy. In fact, it has been argued that the biomechanical demands of pregnancy might have exerted an early selection pressure on the evolution of lumbar lordosis in bipedal hominins (Whitcome et al., 2007). A greater presence of Type I fibers in the epaxial muscles of human females could be added to the list of characteristics associated with the evolution of human bipedalism.

Functional implications

A greater reliance on the sagittal mobility of the spine was an important aspect of mammalian evolution compared with more primitive vertebrates. Yet, certain quadrupedal mammals have retained the more primitive, reptile-like spinal mobility pattern, which puts more emphasis on lateral bending of the trunk (Roos, 1964). Although data on the histochemical characteristics of epaxial muscles of the amphibians and reptiles are rare, experimental works on the roles of trunk musculature (both epaxial and hypaxial muscles) in reptiles have revealed that the primary role of the epaxial muscles is to stabilize trunk against vertical ground reaction forces, while lateral bending is produced by hypaxial muscles (Ritter, 1995, 1996). It has been argued that the lorisid primates, after the reptilian fashion, use lateral bending of their trunk to increase stride length (Shapiro et al., 2001). It seems plausible that their epaxial muscles would perform the role of trunk stabilizers. This argument is reinforced by the high proportion of Type I fibers in the epaxial muscles of the loris. On the other hand, the greater presence of fast- twitch, Type II fibers in the muscles of the lesser galago and the vervet monkey is explicable on the basis of the rapid back extension at the beginning of leaping for the former, and during galloping for the latter. EMG experiment on the epaxial muscles of cats have revealed that during galloping, the extension of the spine by the epaxial muscles, which act as elastic bodies, serves to increase step length and limb speed; while these muscles tend to stabilize the pelvic girdle during

walking and trotting (English, 1980). (However, when passive tension in a whole muscle through elastic storage by tendons and connective tissues becomes important, it tends to minimize the role of fibers in muscle activation. In addition, Magid and Law (1985) observed that in intact muscle fibers with a sarcomere length of ~3.8 μm, passive tension was produced by the elastic tension of myofibrils. The relationship between passive tension and histochemical characteristics of muscle fibers is yet to be fully understood.) It has been reported that patas monkeys tend to spend a considerable portion of their time walking between widely dispersed food sites (Isbell et al., 1998). It may be argued that the relatively higher proportion of Type I fibers in the lumbar segments of the superficial epaxial muscles (iliocostalis and longissimus) of the patas monkey underscore their primary function as a pelvic stabilizer during walking.

Table 1: Fiber Type Classification Schemes

Basis for scheme	Fiber type spectrum			Authors
Metabolic	SO	FOG	FG	Peter et al. (1972)
Histochemistry	Type 1	Type 2A	Type 2B	Brooke & Kaiser (1970)
Immunohistochemistry	Type 1	Type 2A	Type 2B and 2X	Schiaffiano et al. (1989)

SO = slow oxidative; FOG = fast oxidative glycolytic; FG = fast glycolytic. Type 2X fibers are not consistently distinguishable from type 2B fibers (Schiaffino et al. 1989).

Table 2: Comparative sample for muscle histology

Species	Sample size			Sources
	M	F	Total	
Galago senegalensis	3	0	3	Collection of Dr. W. L. Jungers (Dept. of Anatomical Sciences, Stony Brook University).
Nycticebus coucang	2	1	3	Dept. of Mammalogy, US National Museum of Natural History (specimen nos. 297828, 502559). Duke Lemur Center (specimen no. 1906m)
Chlorocebus aethiops	1	3	4	Collections of Dr. N. Tappen and Dr. F. Anapol (Dept. of Anthropology, University of Wisconsin-Milwaukee).
Erythrocebus patas	2	2	4	

Table 3: G-test of independence for species and antibody reaction: Strepsirrhines

Species	Muscle Segment	G-statistic	P
G. senegalensis (n = 3) vs. *N. coucang* (n = 3)	Thoracic Iliocostalis	630.466	$p < 0.0001$
	Lumbar Iliocostalis	3309.699	$p < 0.0001$
	Thoracic Longissimus	784.731	$p < 0.0001$
	Lumbar Longissimus	1808.891	$p < 0.0001$
	Thoracic Multifidus	123.933	$p < 0.0001$
	Lumbar MUltifidus	431.455	$p < 0.0001$

Table 4: G-test of independence for species and antibody reaction: Cercopithecoids

Species	Muscle Segment	G-statistic	P
C. aethiops (n = 4) v *E. patas* (n = 4)	Thoracic Iliocostalis	101.234	$p < 0.0001$
	Lumbar Iliocostalis	96.545	$p < 0.0001$
	Thoracic Longissimus	65.452	$p < 0.0001$
	Lumbar Longissimus	35.114	$p < 0.0001$
	Thoracic Multifidus	1.768	NS ($p = 0.21$)
	Lumbar MUltifidus	62.39	$p < 0.0001$

Table 5: Fiber type composition of *G. senegalensis* (n = 3)

Muscle segment	Number (%) of fiber types			
	Type I (%)	Type II (%)	Hybrid (%)	Total (%)
Thoracic Iliocostalis	440 (21.43)	1609 (78.37)	4 (0.19)	2053 (100.00)
Lumbar Iliocostalis	115 (5.87)	1832 (93.52)	12 (0.61)	1959 (100.00)
Thoracic Longissimus	412 (31.50)	879 (67.20)	17 (1.30)	1308 (100.00)
Lumbar Longissimus	362 (21.70)	1277 (76.56)	29 (1.74)	1668 (100.00)
Thoracic Multifidus	131 (31.41)	274 (65.71)	12 (2.88)	417 (100.00)
Lumbar Multifidus	131 (28.98)	310 (68.58)	11 (2.43)	452 (100.00)

Table 6: Fiber type composition of *N. coucang* (n = 3)

Muscle segment	Number (%) of fiber types			
	Type I (%)	Type II (%)	Hybrid (%)	Total (%)
Thoracic Iliocostalis	327 (70.32)	90 (19.35)	48 (10.32)	465 (100.00)
Lumbar Iliocostalis	2870 (61.54)	987 (21.16)	807 (17.30)	4664 (100.00)
Thoracic Longissimus	2402 (66.85)	869 (24.19)	322 (8.96)	3593 (100.00)
Lumbar Longissimus	3944 (63.35)	1309 (21.02)	973 (15.63)	6226 (100.00)
Thoracic Multifidus	227 (61.68)	100 (27.17)	41 (11.14)	368 (100.00)
Lumbar Multifidus	1040 (73.29)	230 (16.21)	149 (10.50)	1419 (100.00)

Table 7: Fiber type composition of *C. aethiops* (n = 4)

Muscle segment	Number (%) of fiber types			
	Type I (%)	Type II (%)	Hybrid (%)	Total (%)
Thoracic Iliocostalis	699 (40.03)	872 (49.94)	175 (10.02)	1746 (100.00)
Lumbar Iliocostalis	543 (31.83)	1094 (64.13)	69 (4.04)	1706 (100.00)
Thoracic Longissimus	324 (31.33)	647 (62.57)	63 (6.09)	1034 (100.00)
Lumbar Longissimus	593 (32.25)	1046 (56.88)	200 (10.88)	1839 (100.00)
Thoracic Multifidus	---	---	---	---
Lumbar Multifidus	---	---	---	---

Table 8: Fiber type composition of *E. patas* (n = 4)

Muscle segment	Number (%) of fiber types			
	Type I (%)	Type II (%)	Hybrid (%)	Total (%)
Thoracic Iliocostalis	518 (25.24)	1333 (64.96)	201 (9.80)	2052 (100.00)
Lumbar Iliocostalis	1291 (32.54)	2221 (55.99)	455 (11.47)	3967 (100.00)
Thoracic Longissimus	801 (35.09)	1159 (50.77)	323 (14.15)	2283 (100.00)
Lumbar Longissimus	958 (35.31)	1329 (48.99)	426 (15.70)	2713 (100.00)
Thoracic Multifidus	1044 (32.86)	1513 (47.62)	620 (19.52)	3177 (100.00)
Lumbar Multifidus	347 (26.39)	664 (50.49)	304 (23.12)	1315 (100.00)

Table 9: Mann-Whitney U test summary for the strepsirrhines

Pair	Muscle	Segment	P		
			Type I	Type II	Hybrid
G. senegalensis (n = 3) vs. *N. coucang* (n = 3)	Iliocostalis	Thoracic	p = 0.05	NS (p = 0.35)	p = 0.05
	Iliocostalis	Lumbar	p = 0.05	p = 0.05	p = 0.05
	Longissimus	Thoracic	p = 0.05	p = 0.05	p = 0.05
	Longissimus	Lumbar	p = 0.05	p = 0.05	p = 0.05
	Multifidus	Thoracic	p = 0.05	p = 0.05	p = 0.05
	Multifidus	Lumbar	p = 0.05	p = 0.05	p = 0.05

Table 10: Mann-Whitney U test summary for the cercopithecoid monkeys

Pair	Muscle	Segment	P		
			Type I	Type II	Hybrid
C. aethiops (n = 4) vs. *E. patas* (n = 4)	Iliocostalis	Thoracic	NS (p = 0.1)	NS (p = 0.5)	NS (p = 0.5)
	Iliocostalis	Lumbar	NS (p = 0.5)	NS (p = 0.5)	NS (p = 0.243)
	Longissimus	Thoracic	NS (p = 0.5)	NS (p = 0.243)	p = 0.01
	Longissimus	Lumbar	NS (p = 0.5)	NS (p = 0.443)	NS (p = 0.17)
	Multifidus	Thoracic	---	---	---
	Multifidus	Lumbar	---	---	---

Table 11: Fiber type composition by sex: *N. coucang* (male = 2, female = 1)

Muscle segment	Number (%) of fiber types							
	Type I (%)		Type II (%)		Hybrid (%)		Total (%)	
	M	F	M	F	M	F	M	F
Thoracic Iliocostalis	261 (69.79)	66 (72.53)	74 (19.79)	16 (17.58)	39 (10.43)	9 (9.89)	374 (100)	91 (100)
Lumbar Iliocostalis	1953 (64.07)	917 (56.75)	589 (19.32)	398 (24.63)	506 (16.60)	301 (18.63)	3048 (100)	1616 (100)
Thoracic Longissimus	1499 (67.61)	903 (65.63)	514 (23.18)	355 (25.80)	204 (9.20)	118 (8.58)	2217 (100)	1376 (100)
Lumbar Longissimus	2805 (63.53)	1139 (62.89)	935 (21.18)	374 (20.65)	675 (15.29)	298 (16.45)	4415 (100)	1811 (100)
Thoracic Multifidus	177 (63.21)	50 (61.68)	75 (26.79)	25 (28.41)	28 (10.00)	13 (14.77)	280 (100)	88 (100)
Lumbar Multifidus	914 (76.10)	126 (57.80)	176 (14.65)	54 (24.77)	111 (9.24)	38 (17.43)	1201 (100)	218 (100)

Table 12: Fiber type composition by sex: *C. aethiops* (male = 1, female = 3)

Muscle segment	Number (%) of fiber types							
	Type I (%)		Type II (%)		Hybrid (%)		Total (%)	
	M	F	M	F	M	F	M	F
Thoracic Iliocostalis	122 (43.57)	577 (38.27)	137 (48.93)	735 (50.29)	21 (7.50)	154 (11.44)	280 (100)	1466 (100)
Lumbar Iliocostalis	89 (21.76)	454 (36.08)	299 (73.11)	795 (60.27)	21 (5.13)	48 (3.65)	409 (100)	1297 (100)
Thoracic Longissimus	74 (30.45)	250 (31.07)	150 (61.73)	497 (63.53)	19 (7.82)	44 (5.40)	243 (100)	791 (100)
Lumbar Longissimus	137 (39.03)	456 (29.58)	153 (43.59)	893 (64.30)	61 (17.38)	139 (6.12)	351 (100)	1488 (100)
Thoracic Multifidus	---	---	---	---	---	---	---	---
Lumbar Multifidus	---	---	---	---	---	---	---	---

Table 13: Fiber type composition by sex: *E. patas* (male = 2, female = 2)

Muscle segment	Number (%) of fiber types							
	Type I (%)		Type II (%)		Hybrid (%)		Total (%)	
	M	F	M	F	M	F	M	F
Thoracic Iliocostalis	255 (18.98)	263 (39.52)	1029 (75.35)	304 (42.16)	77 (5.67)	124 (18.32)	1361 (100)	691 (100)
Lumbar Iliocostalis	122 (10.98)	1169 (45.47)	1195 (84.87)	1026 (39.09)	52 (4.15)	403 (15.44)	1369 (100)	2598 (100)
Thoracic Longissimus	297 (22.99)	504 (49.95)	814 (65.77)	345 (33.34)	153 (11.24)	170 (16.71)	1264 (100)	1019 (100)
Lumbar Longissimus	115 (10.91)	843 (49.85)	812 (79.64)	517 (31.06)	100 (9.45)	326 (19.09)	1027 (100)	1686 (100)
Thoracic Multifidus	496 (28.68)	548 (37.90)	986 (57.11)	527 (36.26)	246 (14.21)	374 (25.84)	1728 (100)	1449 (100)
Lumbar Multifidus	141 (21.10)	206 (32.39)	410 (59.83)	254 (39.70)	127 (19.07)	177 (27.91)	678 (100)	637 (100)

Table 14: One-way ANOVA results for differences in fiber type composition among species

Fiber Type Composition					
Type I	Type I (%)	Type II	Type II (%)	Hybrid	Hybrid (%)
$p < 0.05$	$p < 0.05$	$p < 0.05$	$p < 0.05$	$p < 0.05$	$p < 0.05$

Table 15: Multiple pairwise comparisons for Type I fiber

Species	*Galago senegalensis*		*Nycticebus coucang*		*Chlorocebus aethiops*		*Erythrocebus patas*	
	Type I	Type I (%)	Type I	Type I (%)	Type I	Type I (%)	Type I	Type I (%)
G. senegalensis (n=3)	---	---	$p < 0.05$	$p < 0.05$	NS ($p = 0.31$)	$p < 0.05$	NS ($p = 0.08$)	$p < 0.05$
N. coucang (n = 3)	$p < 0.05$	$p < 0.05$	---	---	$p < 0.05$	$p < 0.05$	$p < 0.05$	$p < 0.05$
C. aethiops (n = 4)	NS ($p = 0.31$)	$p < 0.05$	$p < 0.05$	$p < 0.05$	---	---	NS ($p = 0.21$)	NS ($p = 0.21$)
E. patas (n = 4)	NS ($p = 0.08$)	$p < 0.05$	$p < 0.05$	$p < 0.05$	NS ($p = 0.21$)	NS ($p = 0.21$)	---	---

Table 16: Multiple pairwise comparisons for Type II fiber

Species	*Galago senegalensis*		*Nycticebus coucang*		*Chlorocebus aethiops*		*Erythrocebus patas*	
	Type II	Type II (%)	Type II	Type II (%)	Type II	Type II (%)	Type II	Type II (%)
G. senegalensis (n=3)	---	---	$p < 0.05$	$p < 0.05$	NS ($p = 0.06$)	$p < 0.05$	NS ($p = 0.45$)	$p < 0.05$
N. coucang (n = 3)	$p < 0.05$	$p < 0.05$	---	---	NS ($p = 0.34$)	$p < 0.05$	$p < 0.05$	$p < 0.05$
C. aethiops (n = 4)	NS ($p = 0.06$)	$p < 0.05$	NS ($p = 0.34$)	$p < 0.05$	---	---	$p = 0.05$	NS ($p = 0.17$)
E. patas (n = 4)	NS ($p = 0.45$)	$p < 0.05$	$p < 0.05$	$p < 0.05$	$p = 0.05$	NS ($p = 0.17$)	---	---

Table 17: Multiple pairwise comparisons for Hybrid fiber

Species	*Galago senegalensis*		*Nycticebus coucang*		*Chlorocebus aethiops*		*Erythrocebus patas*	
	Hybrid	Hybrid (%)	Hybrid	Hybrid (%)	Hybrid	Hybrid (%)	Hybrid	Hybrid (%)
G. senegalensis (n=3)	---	---	$p < 0.05$	$p < 0.05$	NS ($p = 0.14$)	$p < 0.05$	$p < 0.05$	$p < 0.05$
N. coucang (n = 3)	$p < 0.05$	$p < 0.05$	---	---	$p < 0.05$	$p < 0.05$	NS ($p = 0.08$)	$p < 0.05$
C. aethiops (n = 4)	NS ($p = 0.14$)	$p < 0.05$	$p < 0.05$	$p < 0.05$	---	---	$p < 0.05$	$p < 0.05$
E. patas (n = 4)	$p < 0.05$	$p < 0.05$	NS ($p = 0.08$)	$p < 0.05$	$p < 0.05$	$p < 0.05$	---	---

Table 18: Area for different fiber types: *G. senegalensis* (Mean ± SD)

Muscle	Fiber area (μm^2)	
	Type I	Type II
Thoracic Iliocostalis	670.13 ± 170.96	628.10 ± 166.58
Lumbar Iliocostalis	494.47 ± 137.03	2126.52 ± 535.07
Thoracic Longissimus	496.24 ± 129.55	722.01 ± 199.47
Lumbar Longissimus	515.66 ± 144.34	1388.69 ± 417.08
Thoracic Multifidus	559.13 ± 136.21	953.58 ± 308.39
Lumbar Multifidus	473.11 ± 128.36	1903.20 ± 803.59

Table 19: Mann-Whitney U test result for intra-segmental differences in fiber area: *G. senegalensis*

Muscle	Segment	P (Type I vs. Type II)
Iliocostalis	Thoracic	NS ($p = 0.17$)
Iliocostalis	Lumbar	$p < 0.05$
Longissimus	Thoracic	$p < 0.05$
Longissimus	Lumbar	$p < 0.05$
Multifidus	Thoracic	$p < 0.05$
Multifidus	Lumbar	$p < 0.05$

Table 20: Area for different fiber types: *N. coucang* (Mean ± SD)

Muscle	Fiber area (μm^2)	
	Type I	Type II
Thoracic Iliocostalis	687.43 ± 164.63	528.03 ± 209.39
Lumbar Iliocostalis	1186.55 ± 237.16	805.76 ± 150.98
Thoracic Longissimus	886.33 ± 186.43	930.94 ± 226.32
Lumbar Longissimus	791.72 ± 208.30	716.31 ± 143.63
Thoracic Multifidus	722.62 ± 166.26	565.80 ± 155.54
Lumbar Multifidus	986.14 ± 204.38	717.99 ± 158.68

Table 21: Mann-Whitney U test result for intra-segmental differences in fiber area: *N. coucang*

Muscle	Segment	P (Type I vs. Type II)
Iliocostalis	Thoracic	$p < 0.05$
Iliocostalis	Lumbar	$p < 0.05$
Longissimus	Thoracic	NS ($p = 0.12$)
Longissimus	Lumbar	$p < 0.05$
Multifidus	Thoracic	$p < 0.05$
Multifidus	Lumbar	$p < 0.05$

Table 22: Fiber area (Mean ± SD) by sex: *N. coucang*

Muscle Segment	Fiber area (μm^2)			
	Type I		Type II	
	M	F	M	F
Thoracic Iliocostalis	765.40 ± 176.06	609.46 ± 112.74	439.62 ± 188.86	608.39 ± 201.65
Lumbar Iliocostalis	1190.99 ± 254.75	1181.01 ± 219.59	846.92 ± 178.15	751.31 ± 87.65
Thoracic Longissimus	1006.24 ± 175.97	766.42 ± 100.21	1042.11 ± 220.33	819.76 ± 174.01
Lumbar Longissimus	787.11 ± 257.10	796.33 ± 149.79	706.81 ± 160.52	725.81 ± 127.15
Thoracic Multifidus	727.14 ± 166.59	718.10 ± 169.23	540.97 ± 159.00	590.63 ± 151.08
Lumbar Multifidus	1070.70 ± 209.28	901.58 ± 163.04	757.41 ± 175.92	678.58 ± 131.24

Table 23: Area for different fiber types: *C. aethiops* (Mean ± SD)

Muscle	Fiber area (μm^2)	
	Type I	Type II
Thoracic Iliocostalis	930.98 ± 412.58	2259.87 ± 600.03
Lumbar Iliocostalis	586.59 ± 243.44	1165.98 ± 348.26
Thoracic Longissimus	741.72 ± 293.93	956.20 ± 353.76
Lumbar Longissimus	678.45 ± 157.77	1568.49 ± 320.40
Thoracic Multifidus	---	---
Lumbar Multifidus	---	---

Table 24: Mann-Whitney U test result for intra-segmental differences in fiber area: *C. aethiops*

Muscle	Segment	P (Type I vs. Type II)
Iliocostalis	Thoracic	$p < 0.05$
Iliocostalis	Lumbar	$p < 0.05$
Longissimus	Thoracic	$p < 0.05$
Longissimus	Lumbar	$p < 0.05$
Multifidus	Thoracic	---
Multifidus	Lumbar	---

Table 25: Fiber area (Mean ± SD) by sex: *C. aethiops*

Muscle Segment	Fiber area (μm^2)			
	Type I		Type II	
	M	F	M	F
Thoracic Iliocostalis	1161.69 ± 461.88	700.27 ± 152.70	2402.58 ± 617.86	2117.16 ± 557.58
Lumbar Iliocostalis	523.13 ± 198.58	650.05 ± 270.51	1074.81 ± 277.90	1257.16 ± 391.24
Thoracic Longissimus	773.14 ± 343.16	716.59 ± 252.35	1189.10 ± 358.84	769.88 ± 214.79
Lumbar Longissimus	672.85 ± 145.35	684.05 ± 172.12	1668.64 ± 336.00	1468.34 ± 275.31
Thoracic Multifidus	---	---	---	---
Lumbar Multifidus	---	---	---	---

Table 26: Area for different fiber types: *E. patas* (Mean ± SD)

Muscle	Fiber area (μm^2)	
	Type I	Type II
Thoracic Iliocostalis	474.37 ± 214.74	1191.99 ± 274.61
Lumbar Iliocostalis	984.74 ± 581.46	1135.53 ± 375.99
Thoracic Longissimus	863.13 ± 426.45	1276.47 ± 518.60
Lumbar Longissimus	875.97 ± 482.08	2336.06 ± 907.44
Thoracic Multifidus	781.49 ± 229.39	1219.58 ± 321.69
Lumbar Multifidus	1337.93 ± 772.92	2276.52 ± 1195.85

Table 27: Mann-Whitney U test result for intra-segmental differences in fiber area: *E. patas*

Muscle	Segment	P (Type I vs. Type II)
Iliocostalis	Thoracic	$p < 0.05$
Iliocostalis	Lumbar	$p < 0.05$
Longissimus	Thoracic	$p < 0.05$
Longissimus	Lumbar	$p < 0.05$
Multifidus	Thoracic	$p < 0.05$
Multifidus	Lumbar	$p < 0.05$

Table 28: Fiber area (Mean ± SD) by sex: *E. patas*

Muscle Segment	Fiber area (μm^2)			
	Type I		Type II	
	M	F	M	F
Thoracic Iliocostalis	625.61 ± 175.82	323.12 ± 124.82	1246.23 ± 211.58	1137.75 ± 321.03
Lumbar Iliocostalis	1458.49 ± 443.05	511.00 ± 162.54	1449.71 ± 218.45	821.36 ± 187.78
Thoracic Longissimus	1157.07 ± 412.33	569.19 ± 145.91	1700.15 ± 361.01	852.79 ± 211.69
Lumbar Longissimus	1282.53 ± 323.37	469.41 ± 159.85	3078.71 ± 515.25	1593.42 ± 516.45
Thoracic Multifidus	907.54 ± 191.14	655.43 ± 194.39	1276.20 ± 168.74	1162.95 ± 419.67
Lumbar Multifidus	1972.01 ± 594.19	703.85 ± 170.37	3278.26 ± 795.07	1274.78 ± 443.84

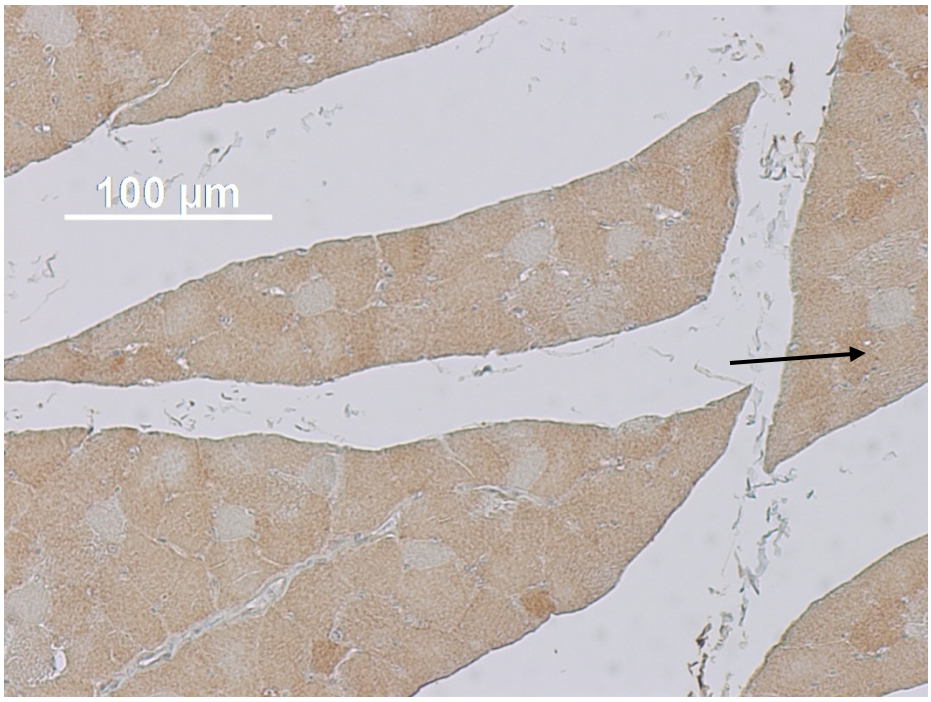

Fig. 1: Immunostained section [MY-32 (= fast) antibody] of thoracic iliocostalis (Type II) of *G. senegalensis*. The arrow points to a muscle cell that reacted positively to the fast antibody.

Fig. 2: Immunostained section [NOQ7.5.4D (= slow) antibody] of thoracic iliocostalis (Type I) of *G. senegalensis*. The arrow points to the identical muscle cell from Fig. 1. Here, this cell reacted negatively to the slow antibody.

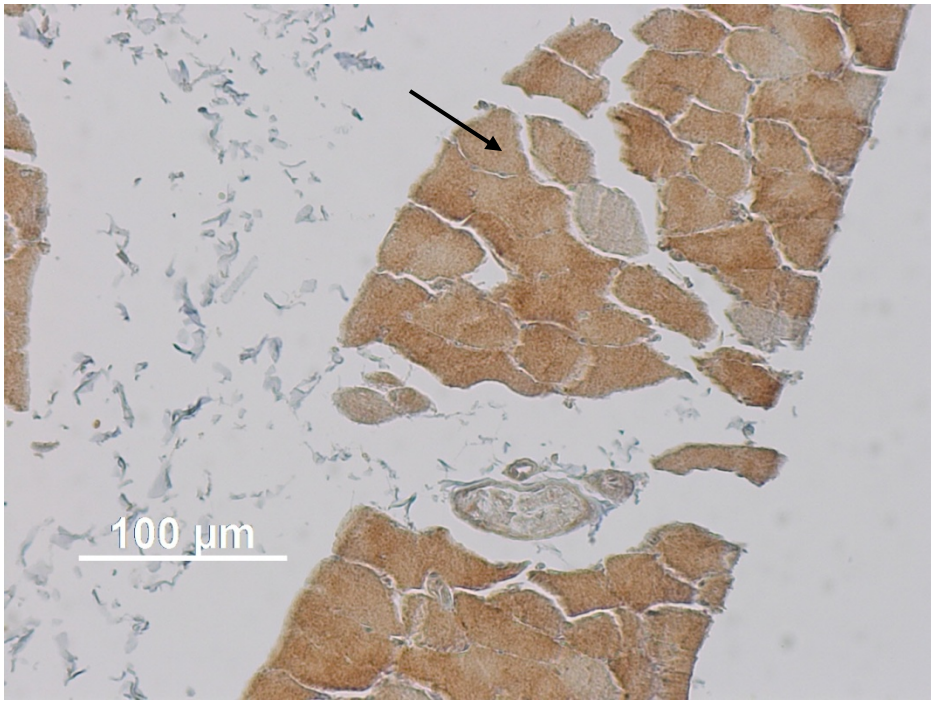

Fig. 3: Immunostained section [MY-32 (= fast) antibody] of lumbar iliocostalis (Type II) of *G. senegalensis*. The arrow points to a muscle cell that reacted positively to the fast antibody.

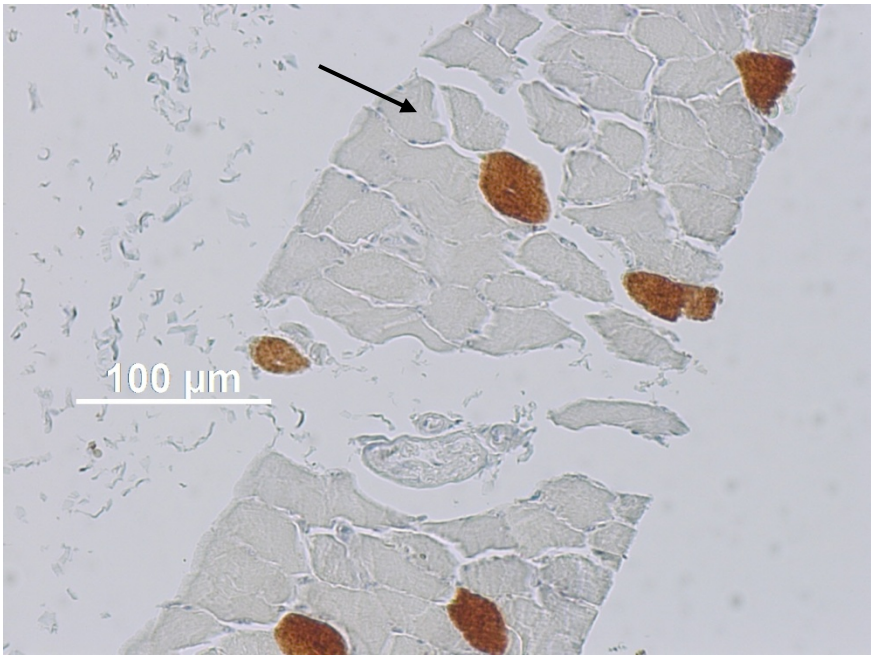

Fig. 4: Immunostained section [NOQ7.5.4D (= slow) antibody] of lumbar iliocostalis (Type I) of *G. senegalensis*. The arrow points to the identical muscle cell from Fig. 3. Here, this cell reacted negatively to the slow antibody.

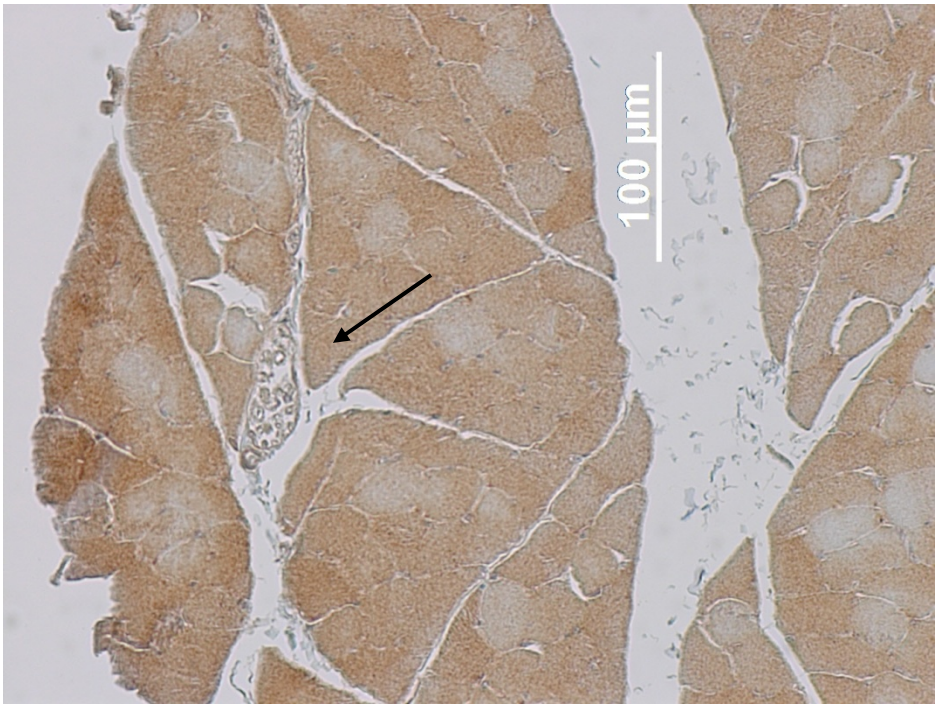

Fig. 5: Immunostained section [MY-32 (= fast) antibody] of thoracic longissimus (Type II) of *G. senegalensis*. The arrow points to a muscle cell that reacted positively to the fast antibody.

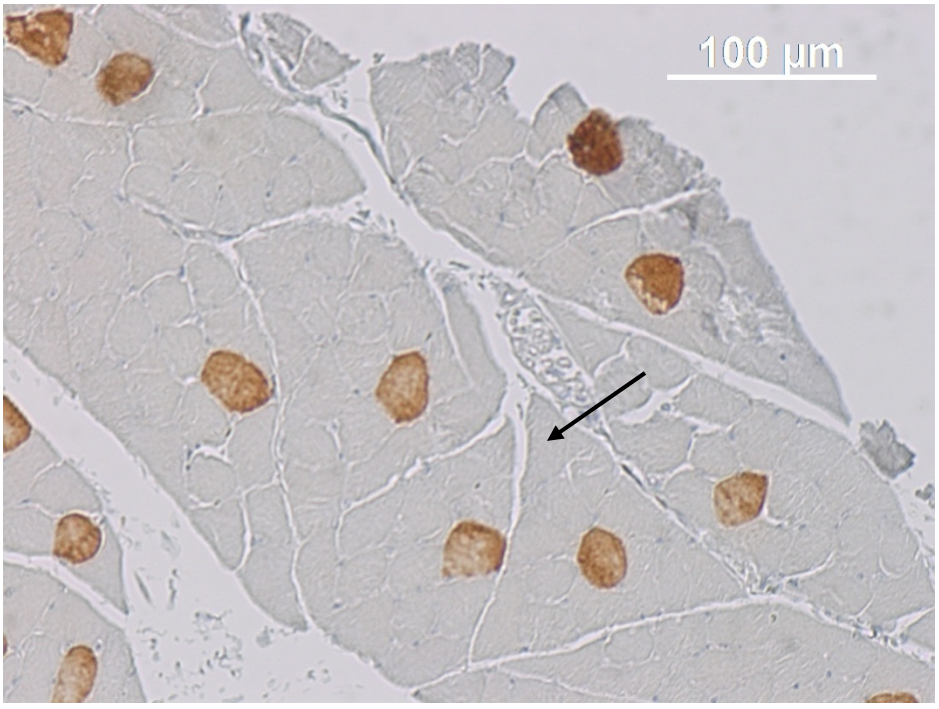

Fig. 6: Immunostained section [NOQ7.5.4D (= slow) antibody] of thoracic longissimus (Type I) of *G. senegalensis*. The arrow points to the identical muscle cell from Fig. 5. Here, this cell reacted negatively to the slow antibody.

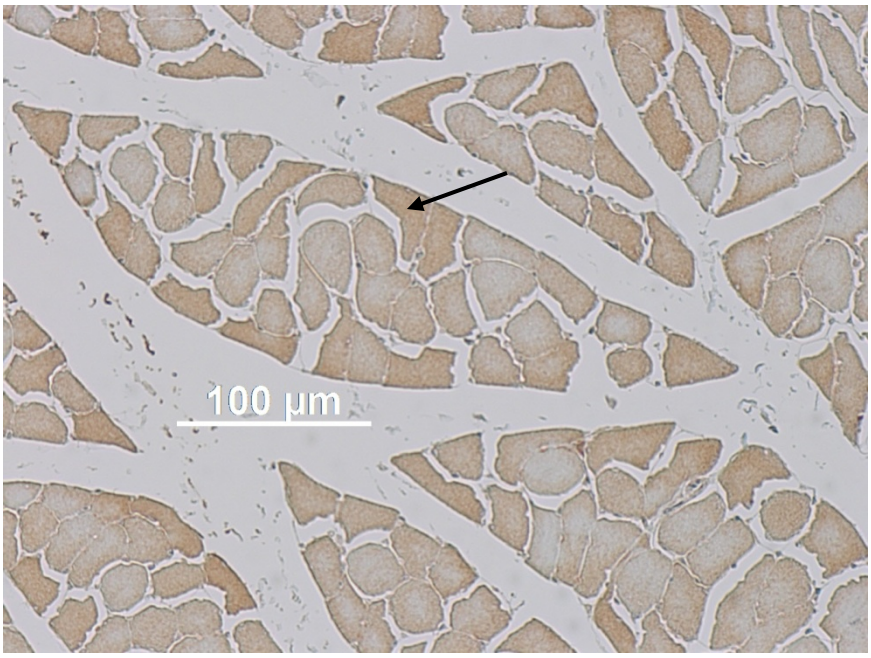

Fig. 7: Immunostained section [MY-32 (= fast) antibody] of lumbar longissimus (Type II) of *G. senegalensis*. The arrow points to a muscle cell that reacted positively to the fast antibody.

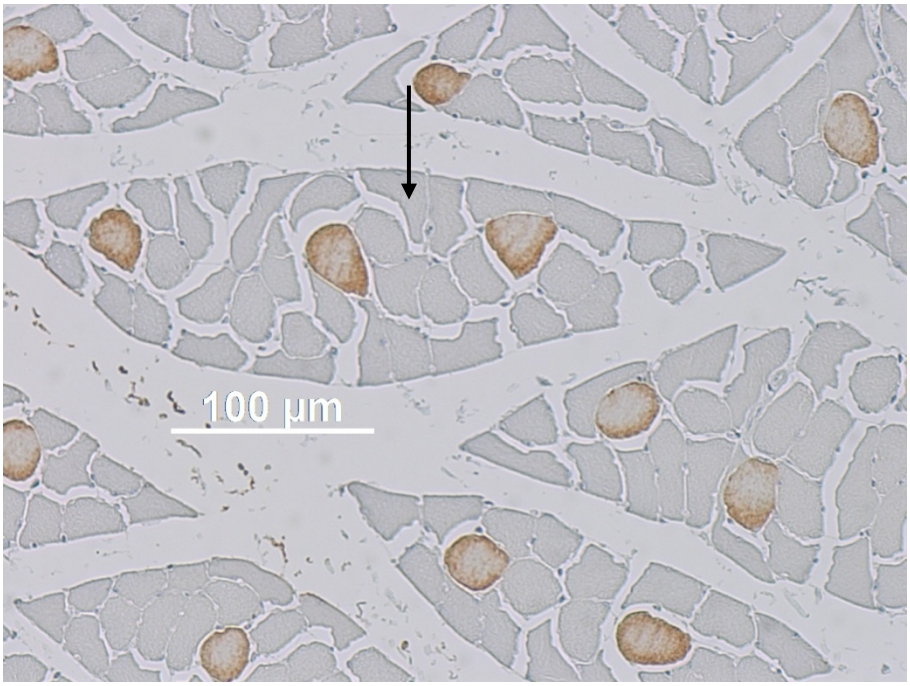

Fig. 8: Immunostained section [NOQ7.5.4D (= slow) antibody] of lumbar longissimus (Type I) of *G. senegalensis*. The arrow points to the identical muscle cell from Fig. 7. Here, this cell reacted negatively to the slow antibody.

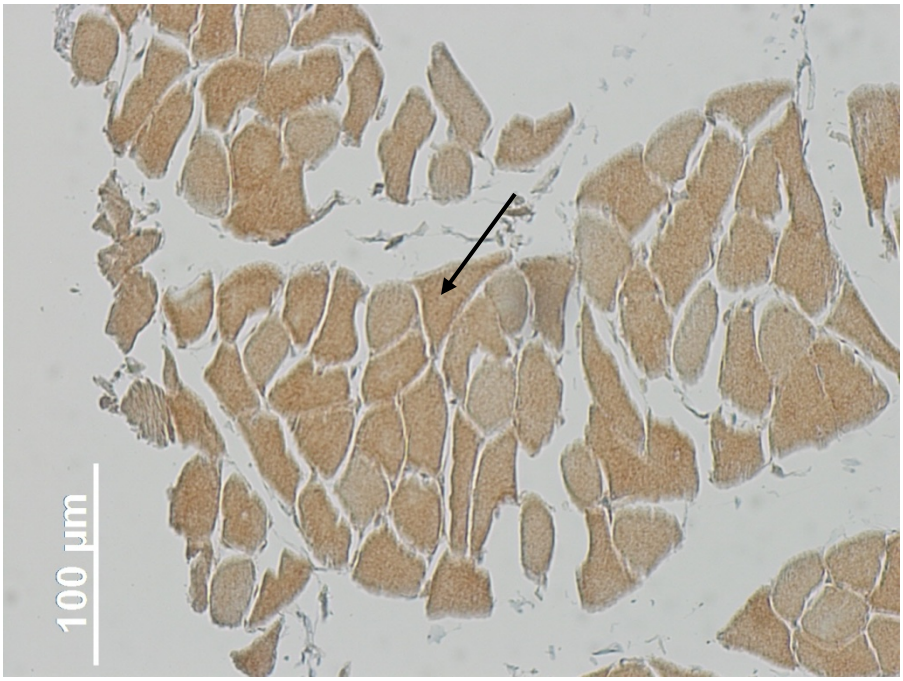

Fig. 9: Immunostained section [MY-32 (= fast) antibody] of thoracic multifidus (Type II) of *G. senegalensis*. The arrow points to a muscle cell that reacted positively to the fast antibody.

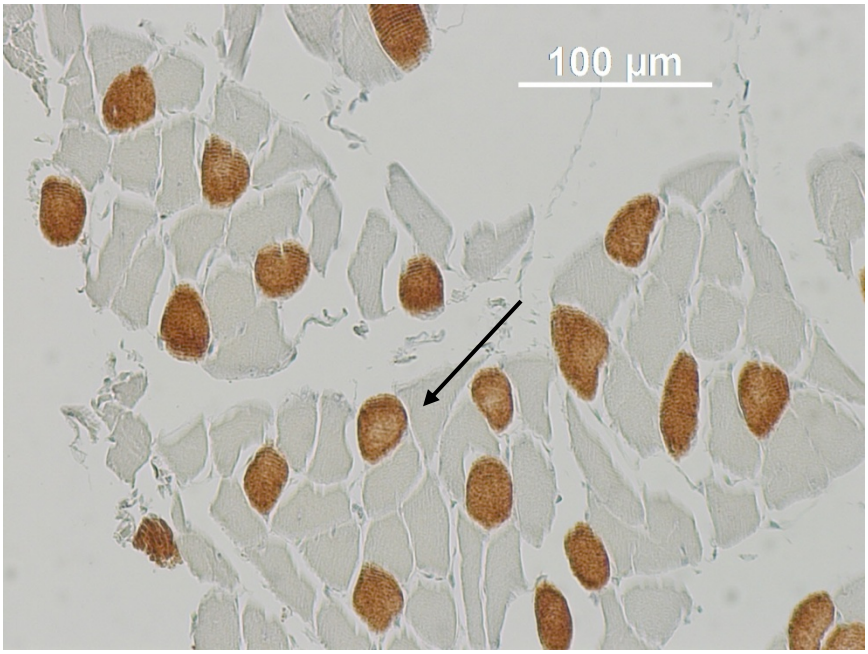

Fig. 10: Immunostained section [NOQ7.5.4D (= slow) antibody] of thoracic multifidus (Type I) of *G. senegalensis*. The arrow points to the identical muscle cell from Fig. 9. Here, this cell reacted negatively to the slow antibody.

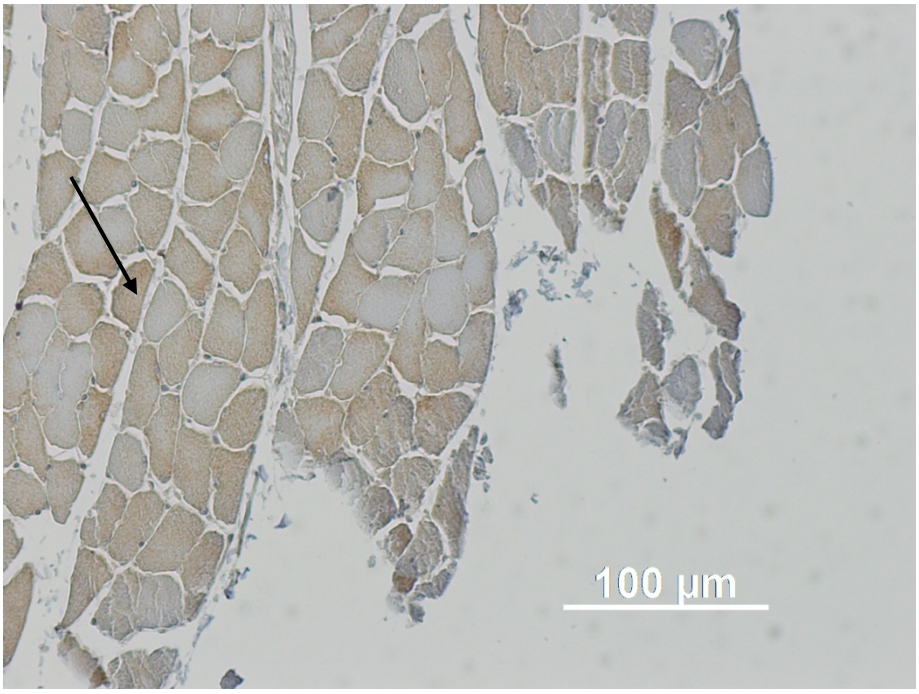

Fig. 11: Immunostained section [MY-32 (= fast) antibody] of lumbar multifidus (Type II) of *G. senegalensis*. The arrow points to a muscle cell that reacted positively to the fast antibody.

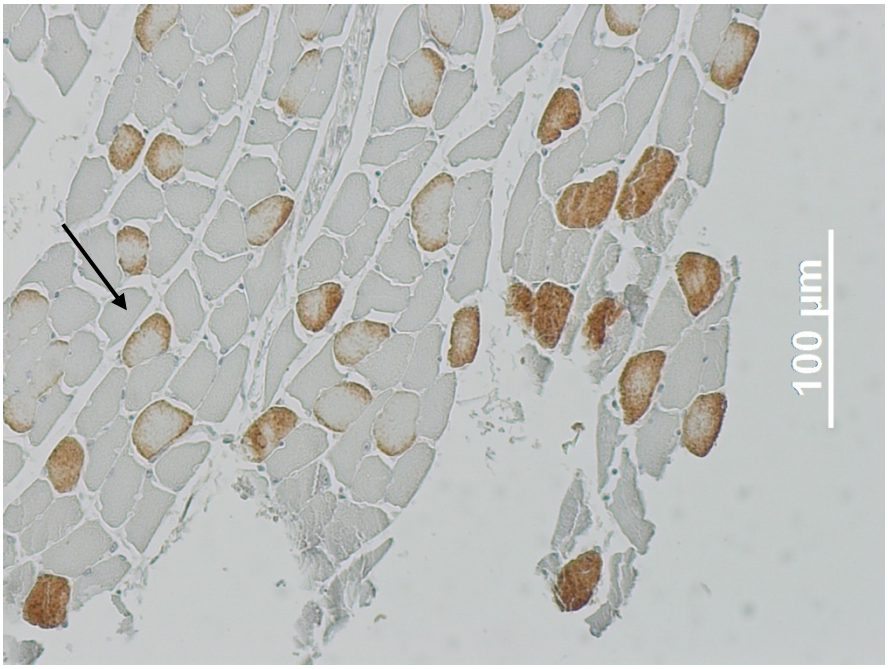

Fig. 12: Immunostained section [NOQ7.5.4D (= slow) antibody] of lumbar multifidus (Type I) of *G. senegalensis*. The arrow points to the identical muscle cell from Fig. 11. Here, this cell reacted negatively to the slow antibody.

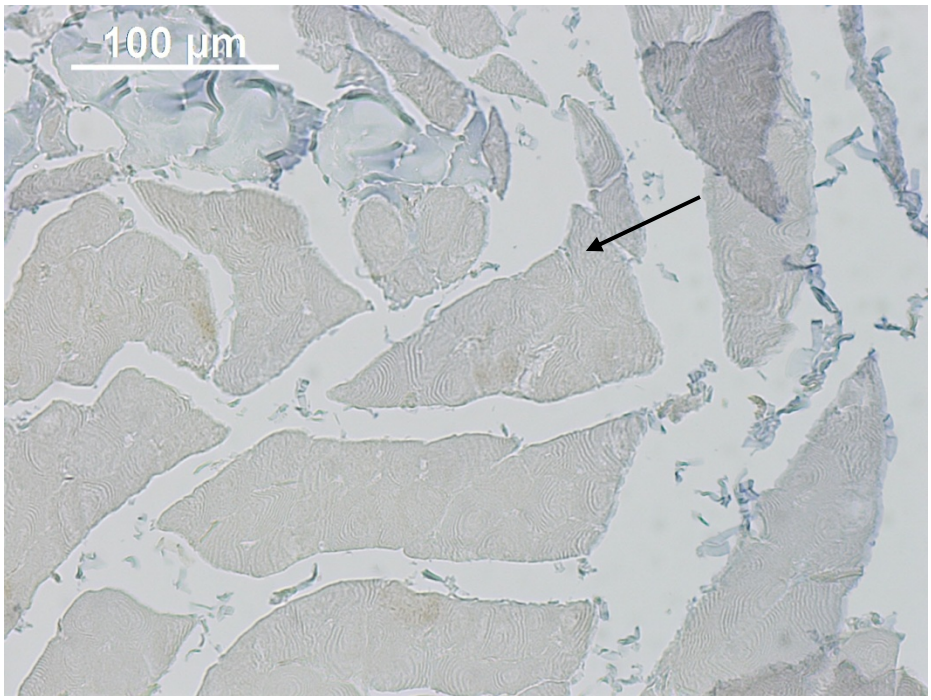

Fig. 13: Immunostained section [MY-32 (= fast) antibody] of thoracic iliocostalis (Type II) of *N. coucang*. The arrow points to a muscle cell that reacted negatively to the fast antibody.

Fig. 14: Immunostained section [NOQ7.5.4D (= slow) antibody] of thoracic iliocostalis (Type I) of *N. coucang*. The arrow points to the identical muscle cell from Fig. 13. Here, this cell reacted positively to the slow antibody.

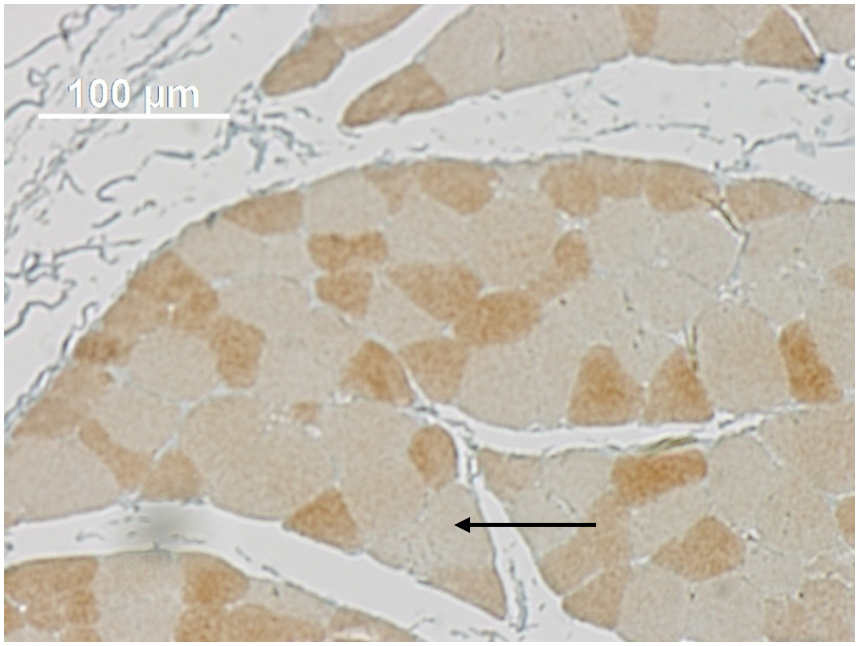

Fig. 15: Immunostained section [MY-32 (= fast) antibody] of lumbar iliocostalis (Type II) of *N. coucang*. The arrow points to a muscle cell that reacted weakly to the fast antibody.

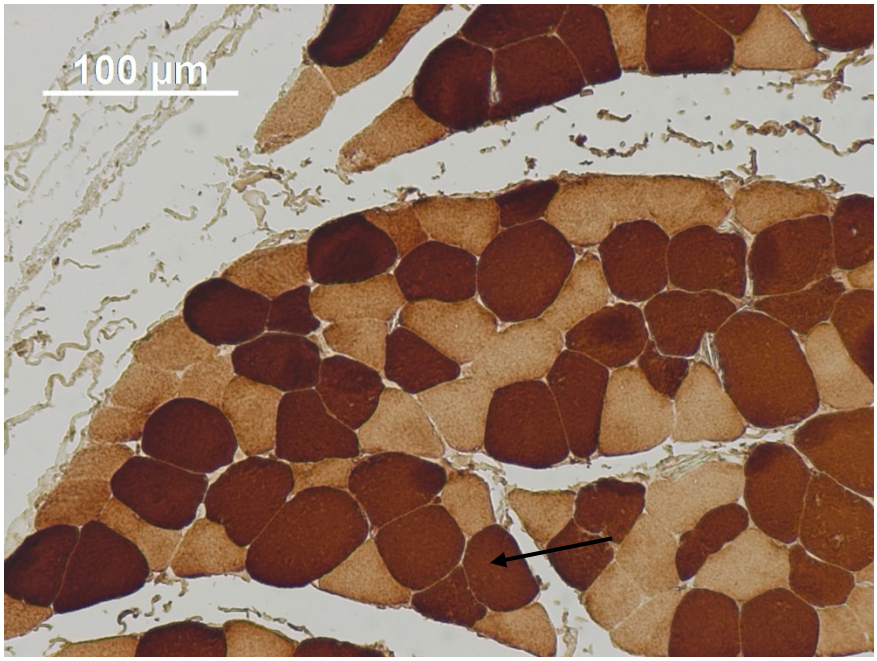

Fig. 16: Immunostained section [NOQ7.5.4D (= slow) antibody] of lumbar iliocostalis (Type I) of *N. coucang*. The arrow points to the identical muscle cell from Fig. 15. Here, this cell reacted strongly to the slow antibody.

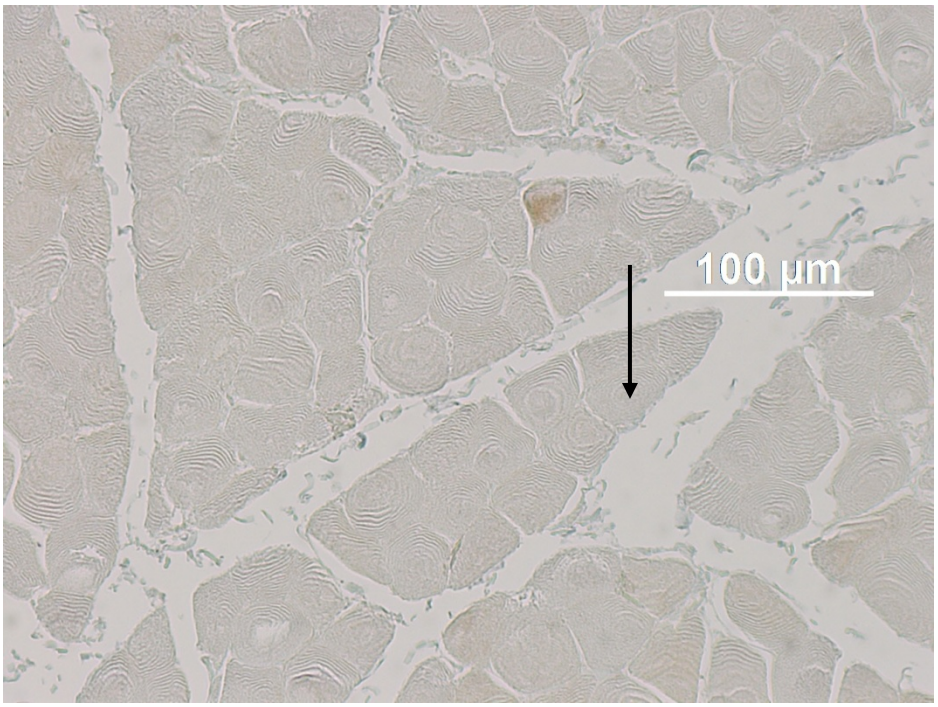

Fig. 17: Immunostained section [MY-32 (= fast) antibody] of thoracic longissimus (Type II) of *N. coucang*. The arrow points to a muscle cell that reacted negatively to the fast antibody.

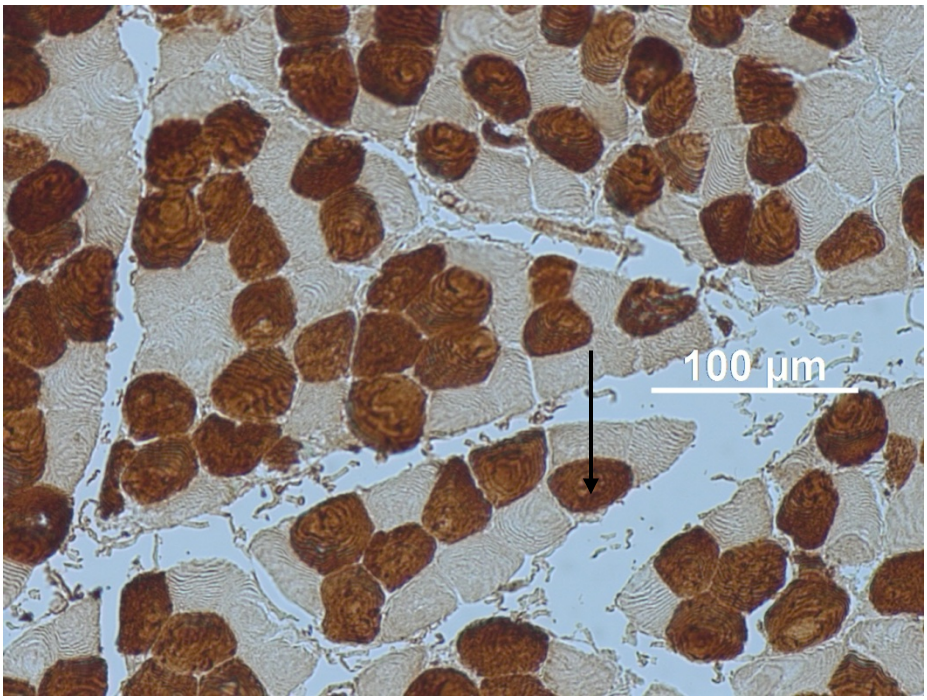

Fig. 18: Immunostained section [NOQ7.5.4D (= slow) antibody] of thoracic longissimus (Type I) of *N. coucang*. The arrow points to the identical muscle cell from Fig. 17. Here, this cell reacted positively to the slow antibody.

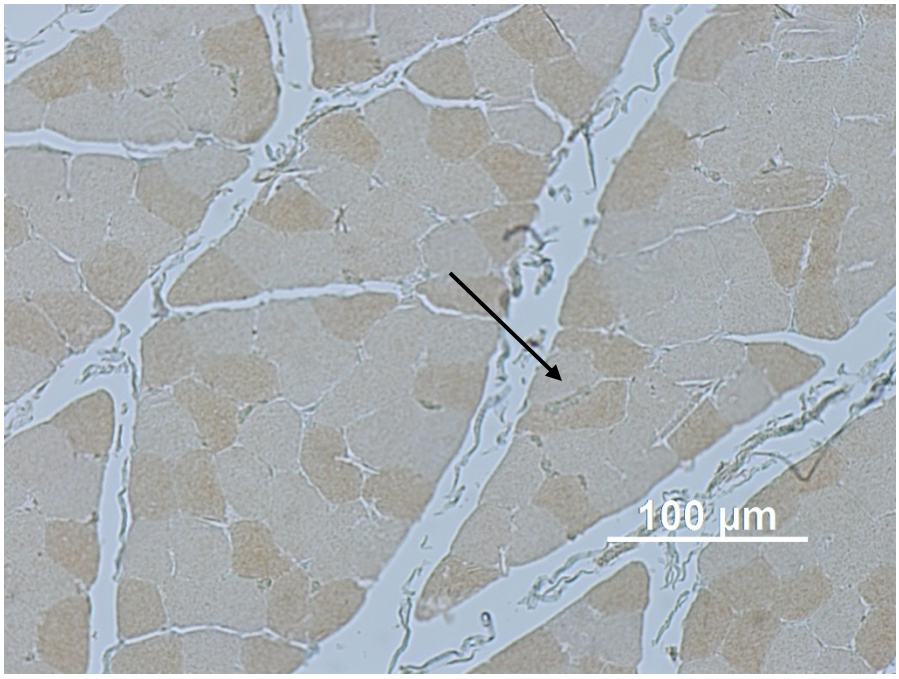

Fig. 19: Immunostained section [MY-32 (= fast) antibody] of lumbar longissimus (Type II) of *N. coucang*. The arrow points to a muscle cell that reacted weakly to the fast antibody.

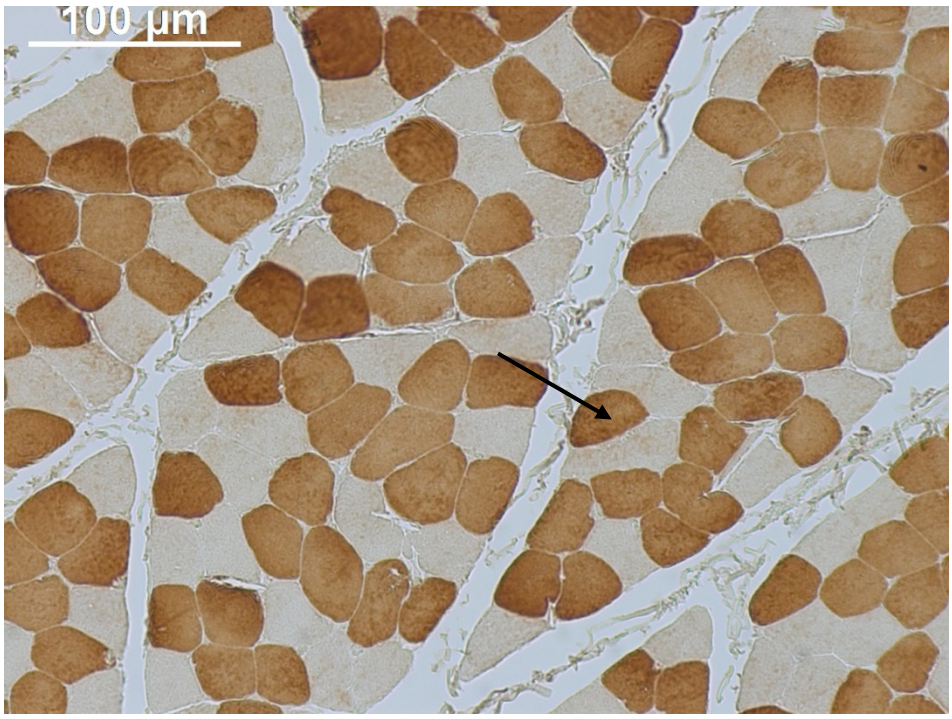

Fig. 20: Immunostained section [NOQ7.5.4D (= slow) antibody] of lumbar longissimus (Type I) of *N. coucang*. The arrow points to the identical muscle cell from Fig. 19. Here, this cell reacted strongly to the slow antibody.

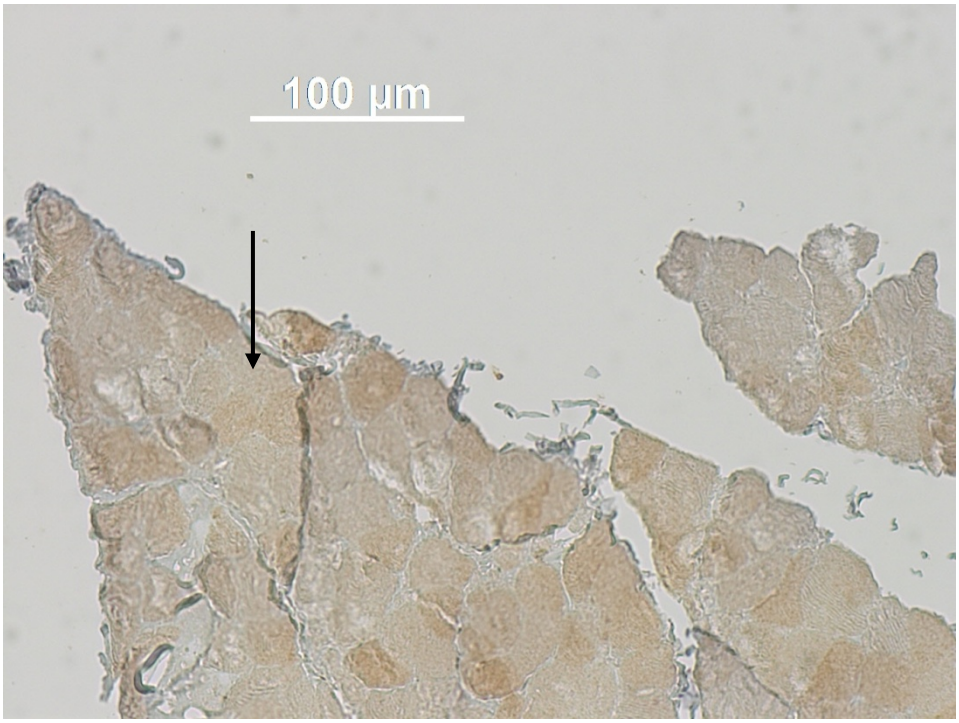

Fig. 21: Immunostained section [MY-32 (= fast) antibody] of thoracic multifidus (Type II) of *N. coucang*. The arrow points to a muscle cell that reacted weakly to the fast antibody.

Fig. 22: Immunostained section [NOQ7.5.4D (= slow) antibody] of thoracic multifidus (Type I) of *N. coucang*. The arrow points to the identical muscle cell from Fig. 21. Here, this cell reacted strongly to the slow antibody.

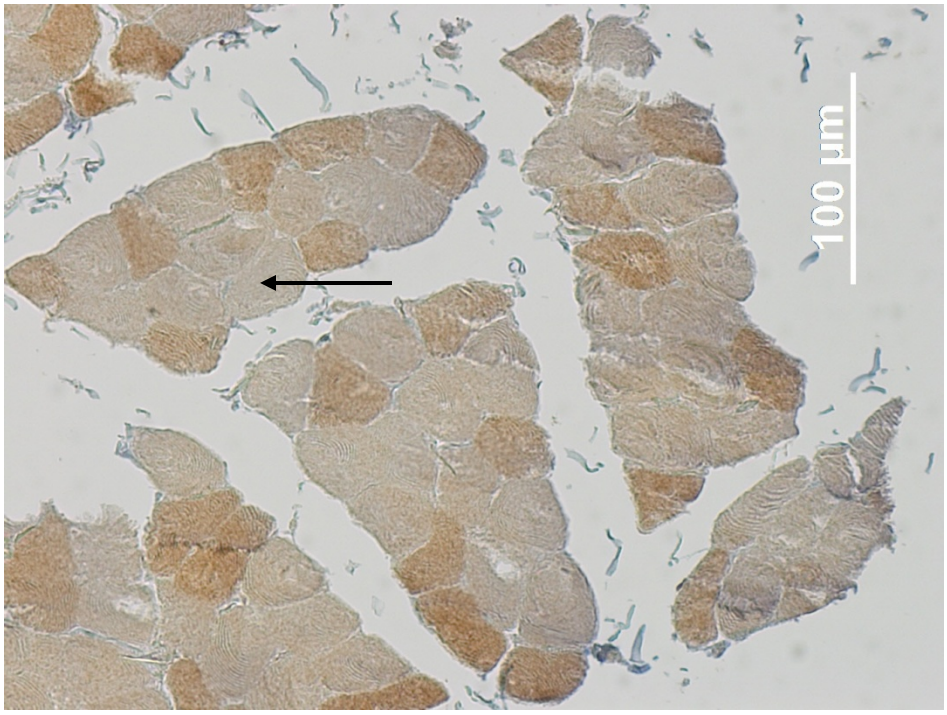

Fig. 23: Immunostained section [MY-32 (= fast) antibody] of lumbar multifidus (Type II) of *N. coucang*. The arrow points to a muscle cell that reacted weakly to the fast antibody.

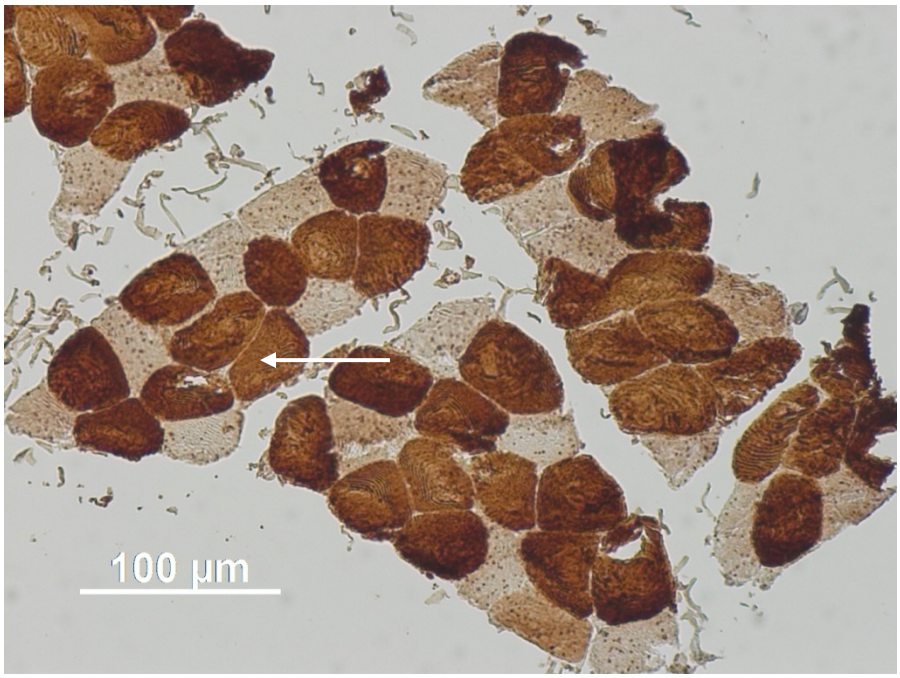

Fig. 24: Immunostained section [NOQ7.5.4D (= slow) antibody] of lumbar multifidus (Type I) of *N. coucang*. The arrow points to the identical muscle cell from Fig. 23. Here, this cell reacted strongly to the slow antibody.

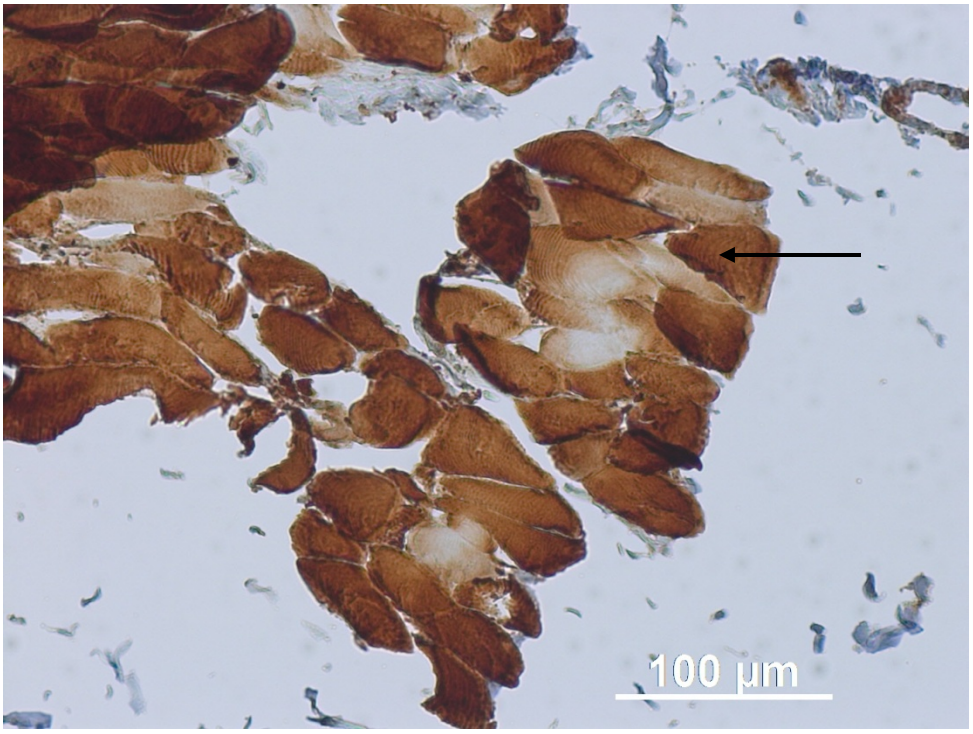

Fig. 25: Immunostained section [MY-32 (= fast) antibody] of thoracic iliocostalis (Type II) of *C. aethiops*. The arrow points to a muscle cell that reacted strongly to the fast antibody.

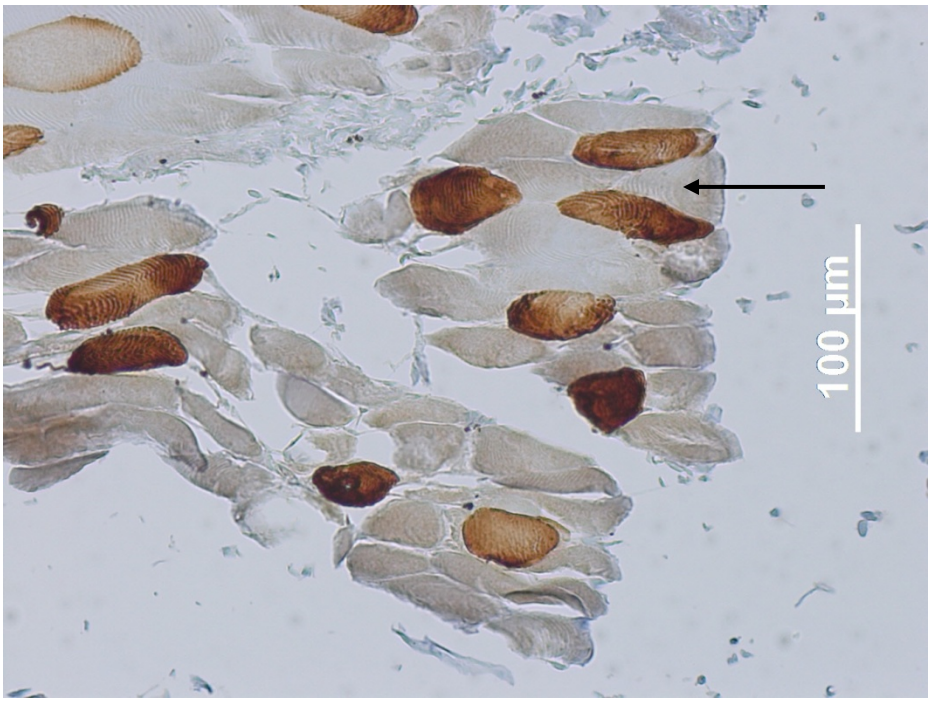

Fig. 26: Immunostained section [NOQ7.5.4D (= slow) antibody] of thoracic iliocostalis (Type I) of *C. aethiops*. The arrow points to the identical muscle cell from Fig. 25. Here, this cell reacted weakly to the slow antibody.

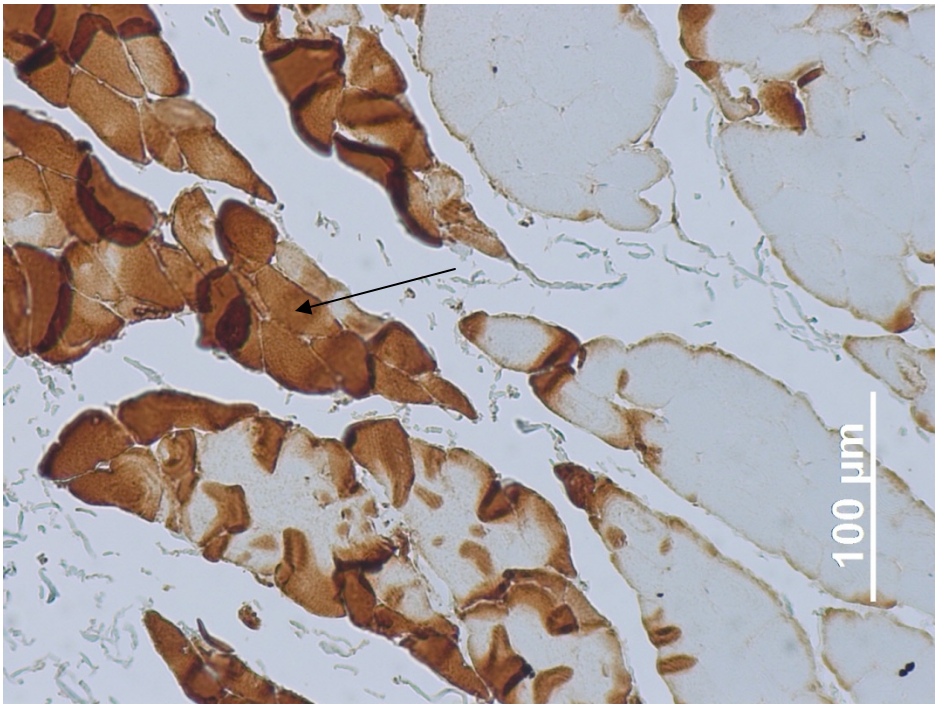

Fig. 27: Immunostained section [MY-32 (= fast) antibody] of lumbar iliocostalis (Type II) of *C. aethiops*. The arrow points to a muscle cell that reacted strongly to the fast antibody.

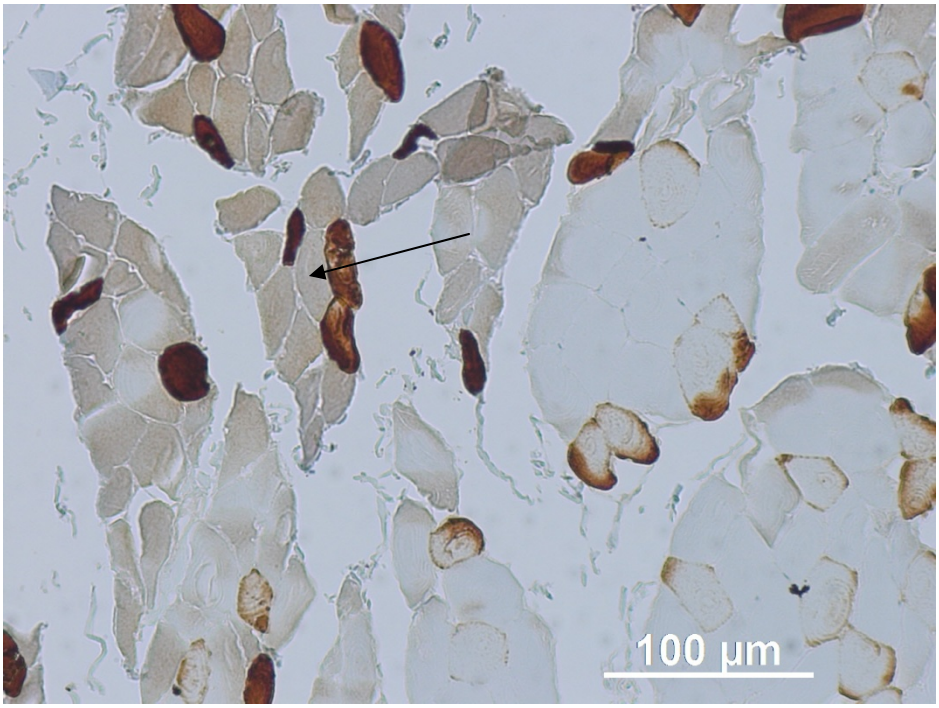

Fig. 28: Immunostained section [NOQ7.5.4D (= slow) antibody] of lumbar iliocostalis (Type I) of *C. aethiops*. The arrow points to the identical muscle cell from Fig. 27. Here, this cell reacted weakly to the slow antibody.

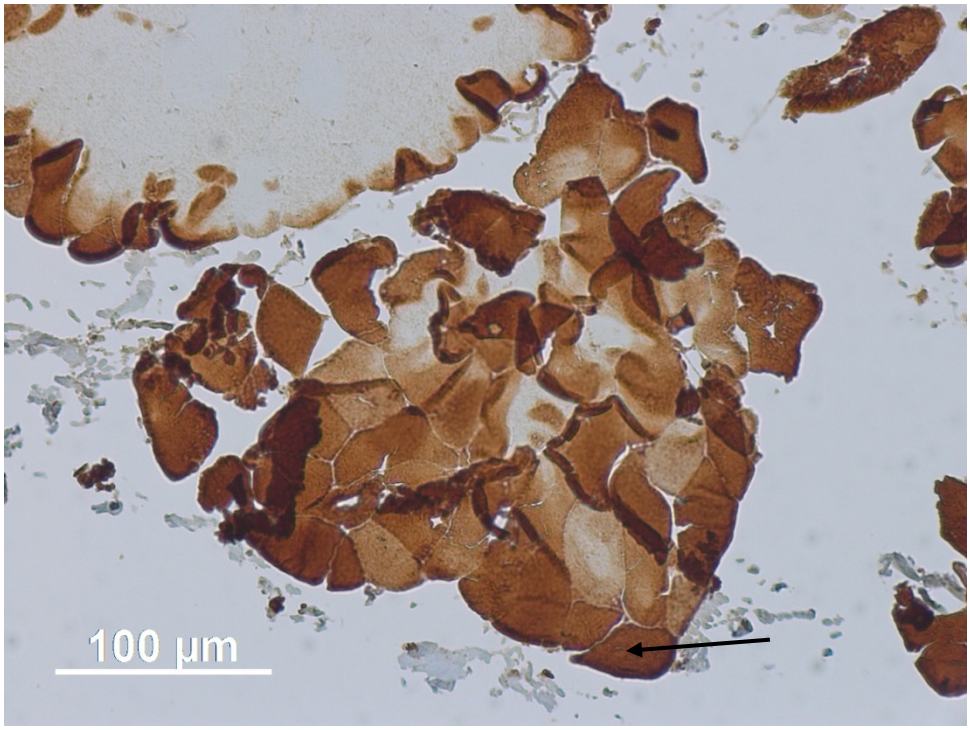

Fig. 29: Immunostained section [MY-32 (= fast) antibody] of thoracic longissimus (Type II) of *C. aethiops*. The arrow points to a muscle cell that reacted positively to the fast antibody.

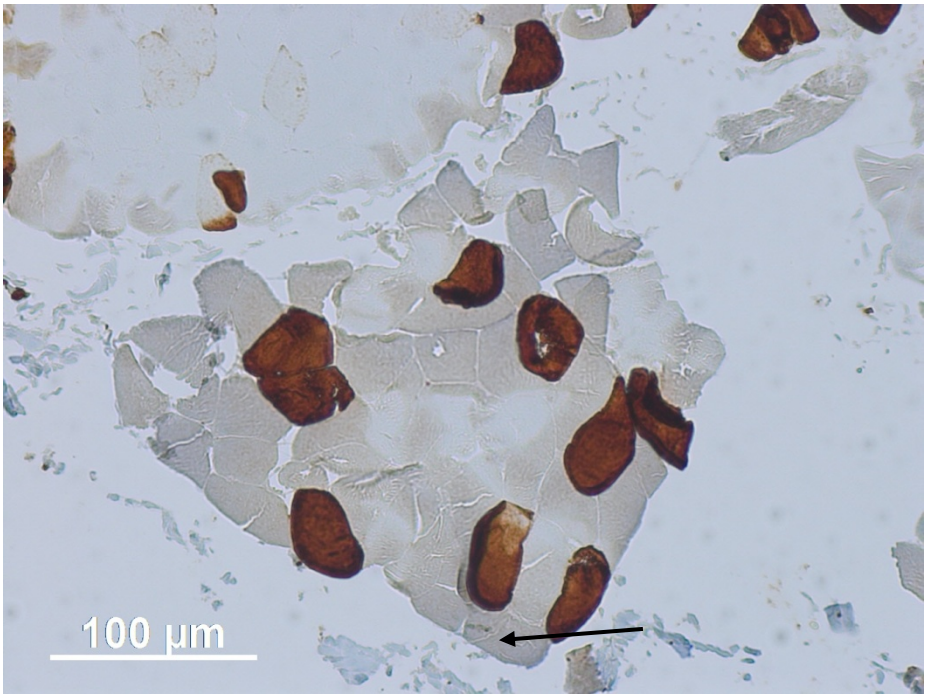

Fig. 30: Immunostained section [NOQ7.5.4D (= slow) antibody] of thoracic longissimus (Type I) of *C. aethiops*. The arrow points to the identical muscle cell from Fig. 29. Here, this cell reacted negatively to the slow antibody.

Fig. 31: Immunostained section [MY-32 (= fast) antibody] of lumbar longissimus (Type II) of *C. aethiops*. The arrow points to a muscle cell that reacted strongly to the fast antibody.

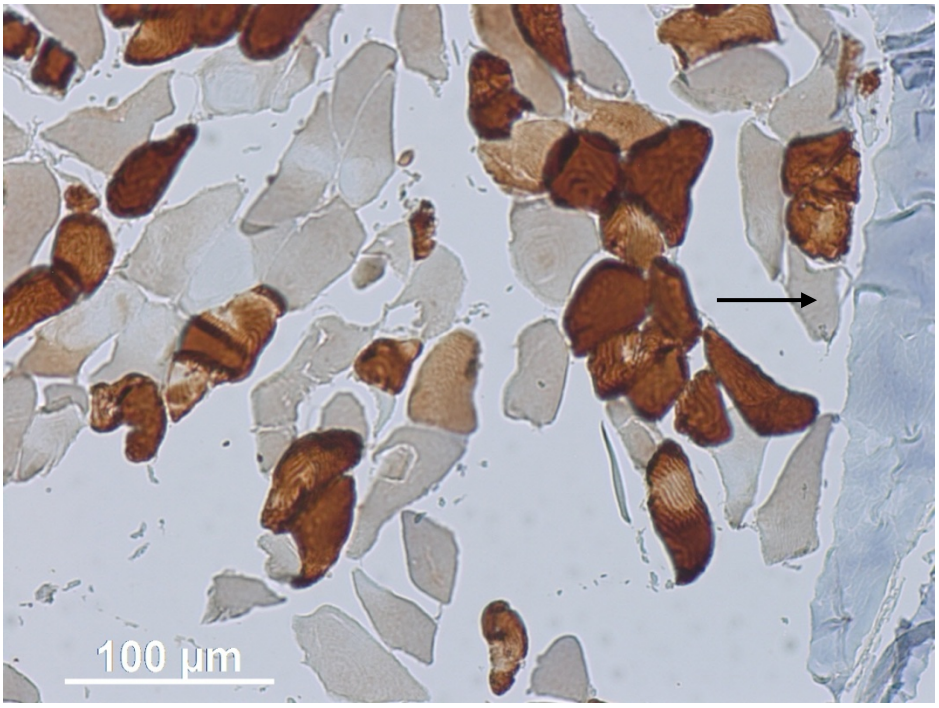

Fig. 32: Immunostained section [NOQ7.5.4D (= slow) antibody] of lumbar longissimus (Type I) of *C. aethiops*. The arrow points to the identical muscle cell from Fig. 31. Here, this cell reacted weakly to the slow antibody.

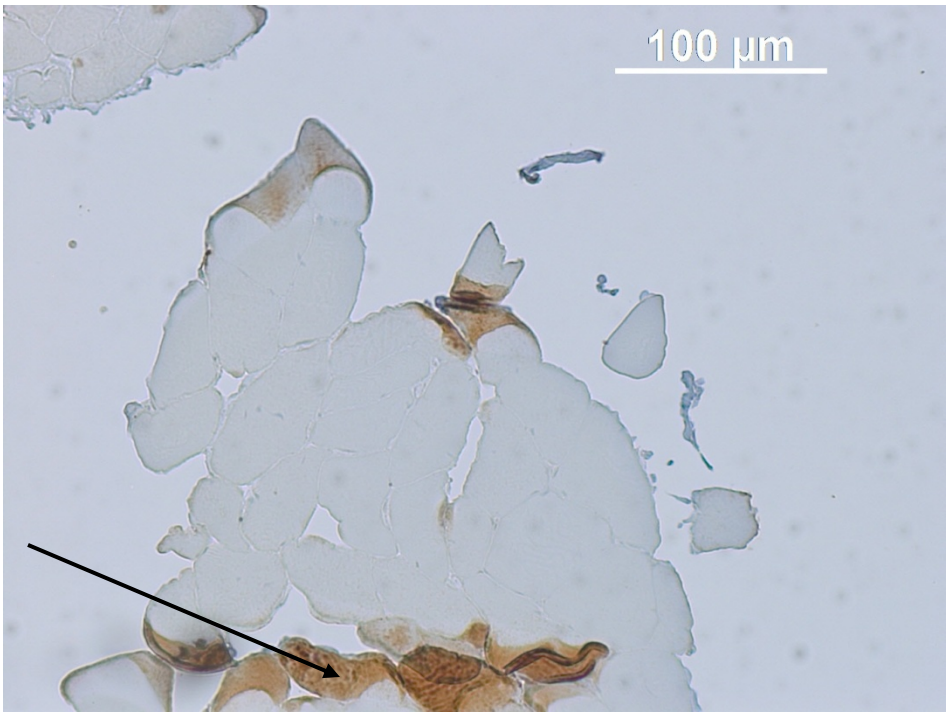

Fig. 33: Immunostained section [MY-32 (= fast) antibody] of thoracic multifidus (Type II) of *C. aethiops*. The arrow points to a muscle cell that reacted positively to the fast antibody.

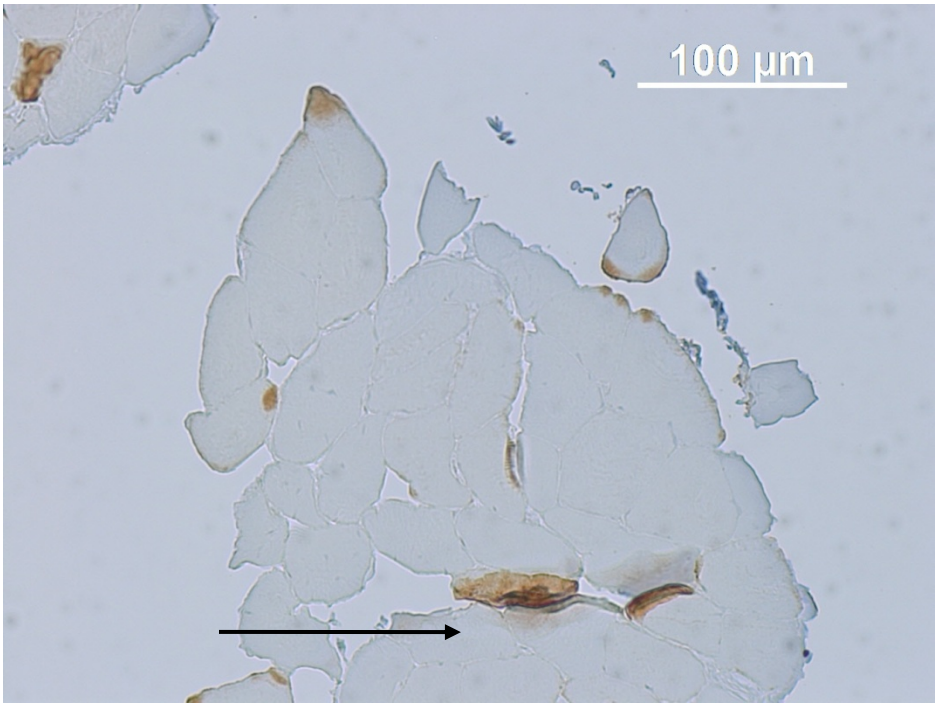

Fig. 34: Immunostained section [NOQ7.5.4D (= slow) antibody] of thoracic multifidus (Type I) of *C. aethiops*. The arrow points to the identical muscle cell from Fig. 33. Here, this cell reacted negatively to the slow antibody.

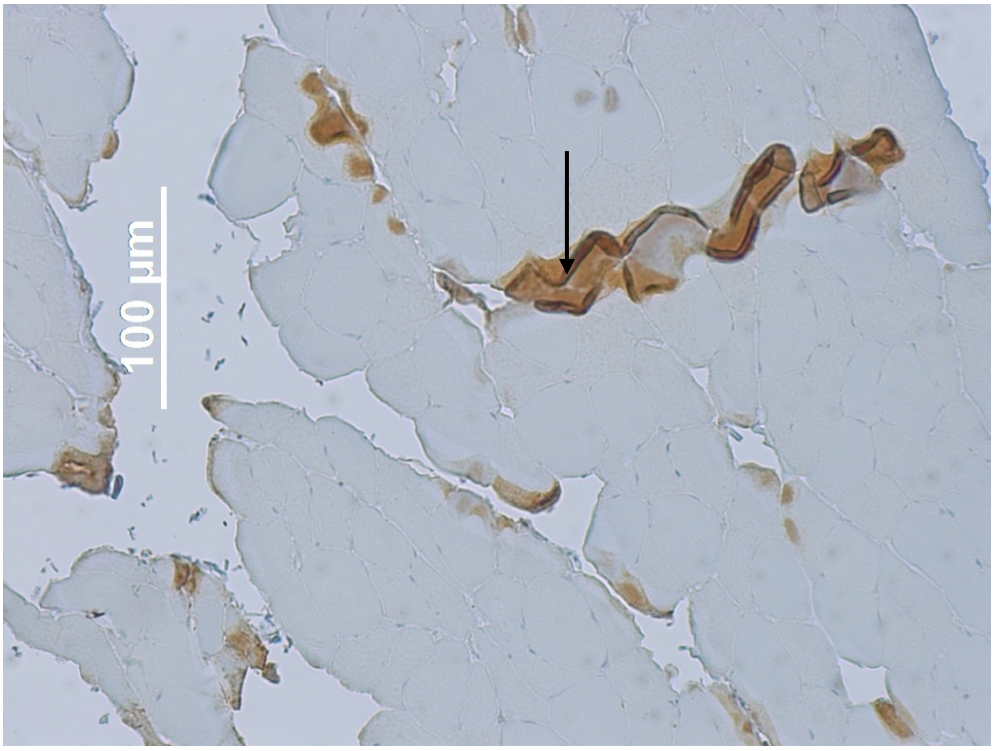

Fig. 35: Immunostained section [MY-32 (= fast) antibody] of lumbar multifidus (Type II) of *C. aethiops*. The arrow points to a muscle cell that reacted positively to the fast antibody.

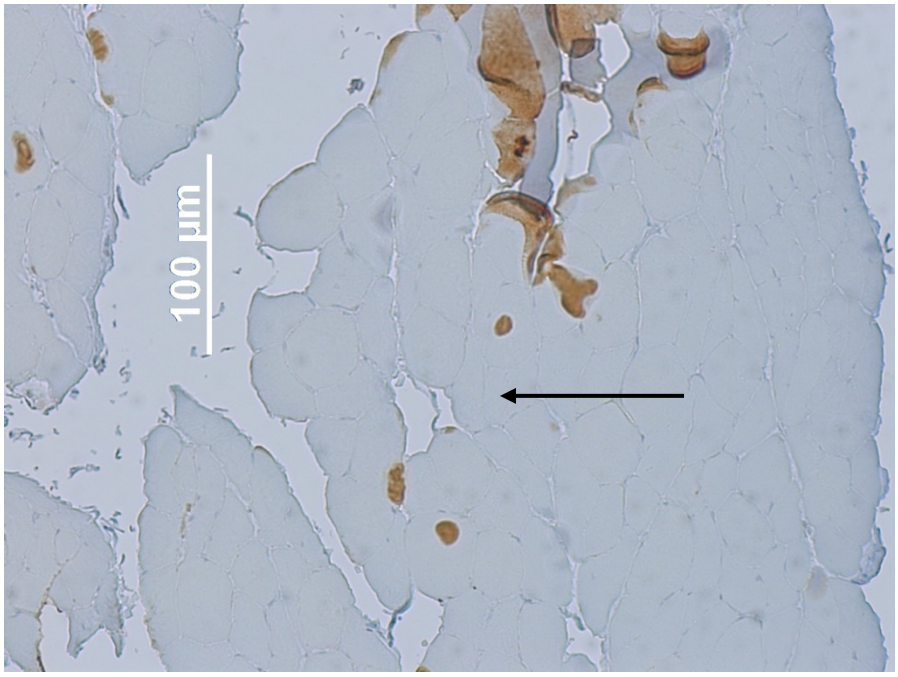

Fig. 36: Immunostained section [NOQ7.5.4D (= slow) antibody] of lumbar multifidus (Type I) of *C. aethiops*. The arrow points to the identical muscle cell from Fig. 35. Here, this cell reacted negatively to the slow antibody.

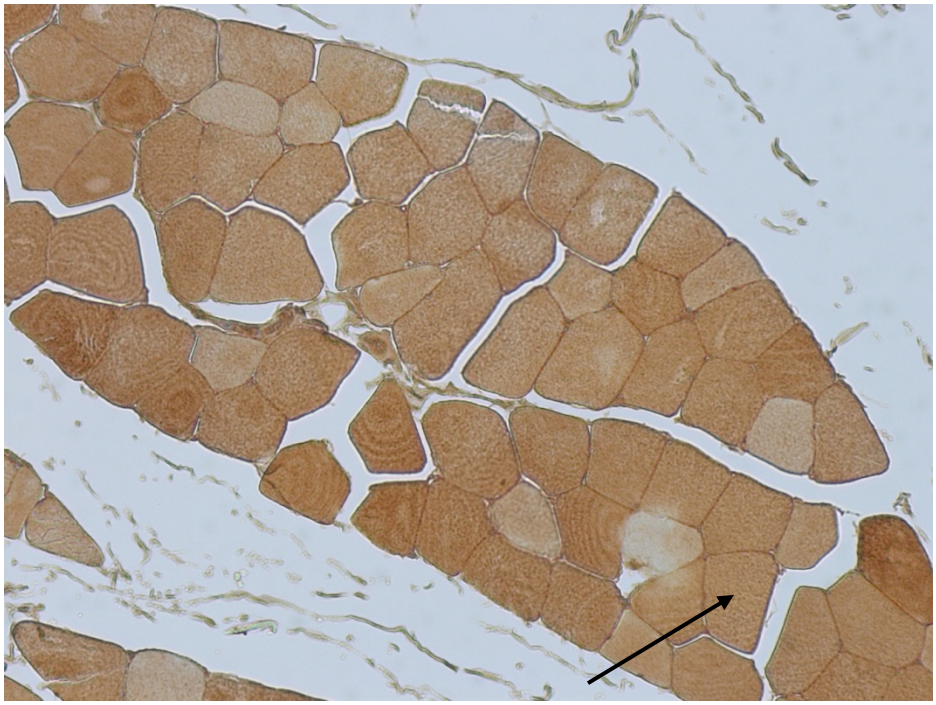

Fig. 37: Immunostained section [MY-32 (= fast) antibody] of thoracic iliocostalis (Type II) of *E. patas*. The arrow points to a muscle cell that reacted strongly to the fast antibody.

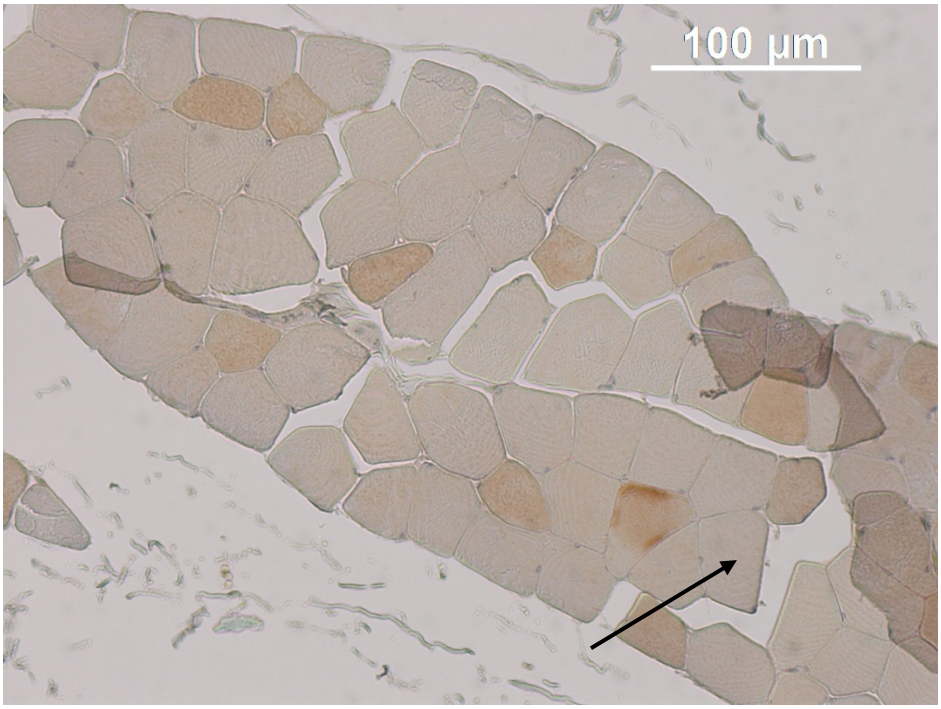

Fig. 38: Immunostained section [NOQ7.5.4D (= slow) antibody] of thoracic iliocostalis (Type I) of *E. patas*. The arrow points to the identical muscle cell from Fig. 37. Here, this cell reacted weakly to the slow antibody.

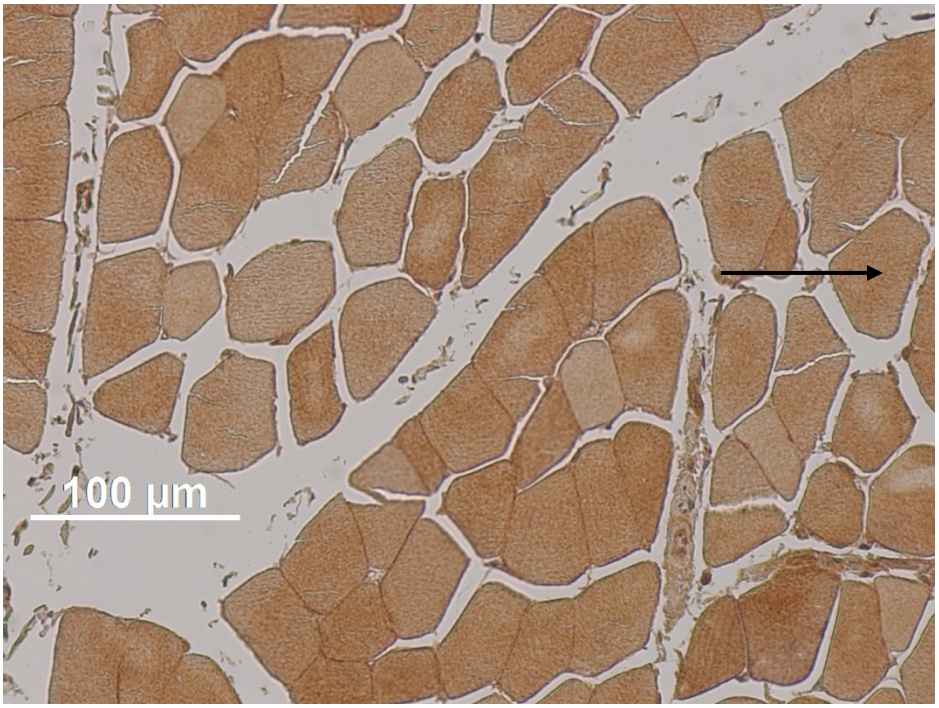

Fig. 39: Immunostained section [MY-32 (= fast) antibody] of lumbar iliocostalis (Type II) of *E. patas*. The arrow points to a muscle cell that reacted strongly to the fast antibody.

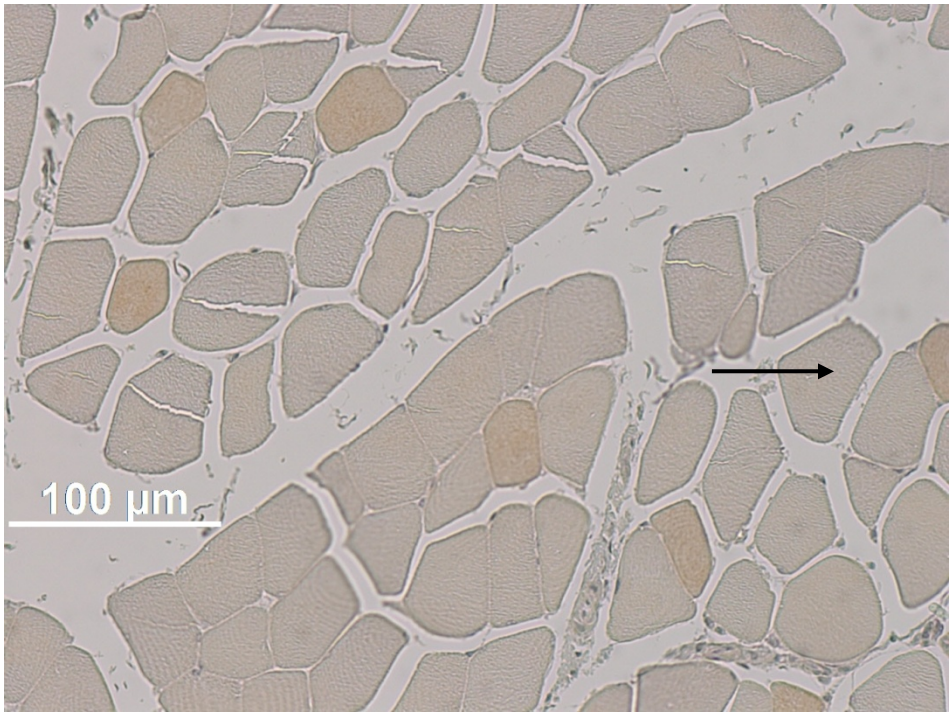

Fig. 40: Immunostained section [NOQ7.5.4D (= slow) antibody] of lumbar iliocostalis (Type I) of *E. patas*. The arrow points to the identical muscle cell from Fig. 39. Here, this cell reacted weakly to the slow antibody.

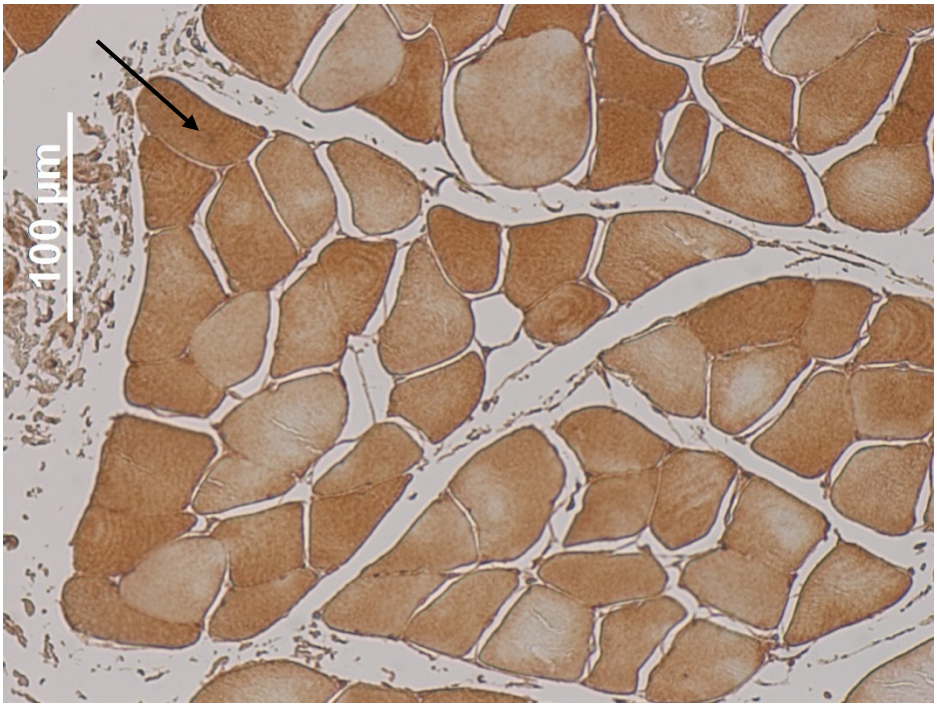

Fig. 41: Immunostained section [MY-32 (= fast) antibody] of thoracic longissimus (Type II) of *E. patas*. The arrow points to a muscle cell that reacted strongly to the fast antibody.

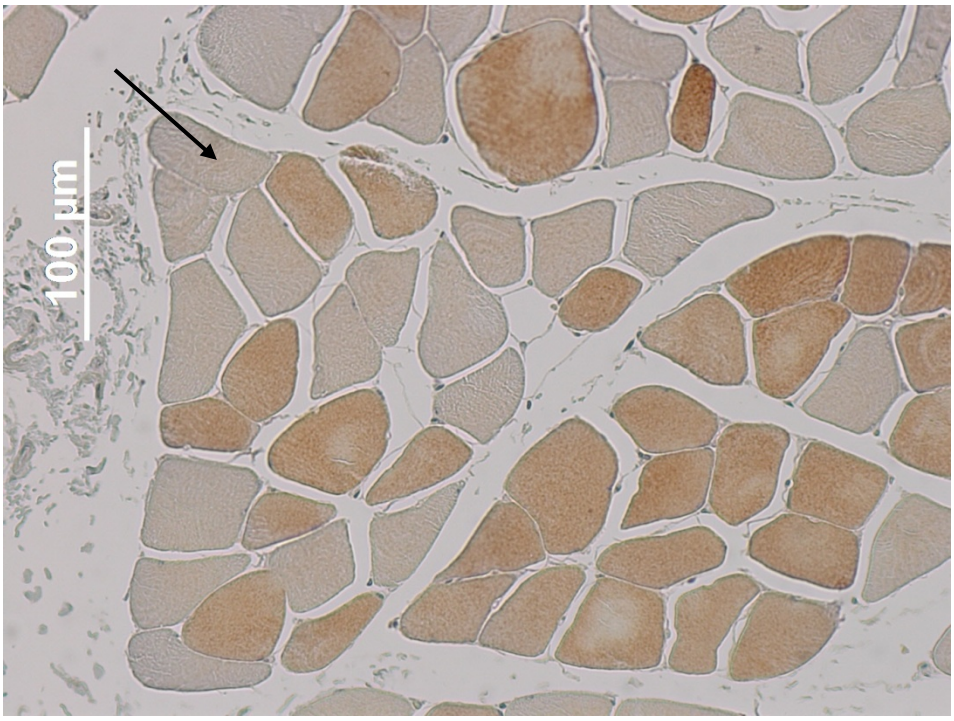

Fig. 42: Immunostained section [NOQ7.5.4D (= slow) antibody] of thoracic longissimus (Type I) of *E. patas*. The arrow points to the identical muscle cell from Fig. 41. Here, this cell reacted weakly to the slow antibody.

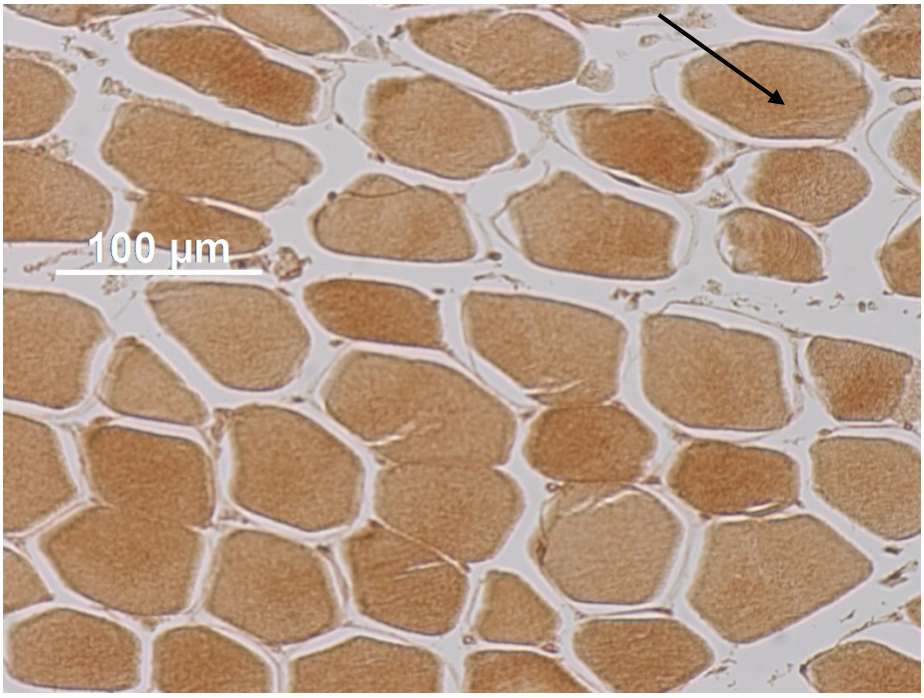

Fig. 43: Immunostained section [MY-32 (= fast) antibody] of lumbar longissimus (Type II) of *E. patas*. The arrow points to a muscle cell that reacted positively to the fast antibody.

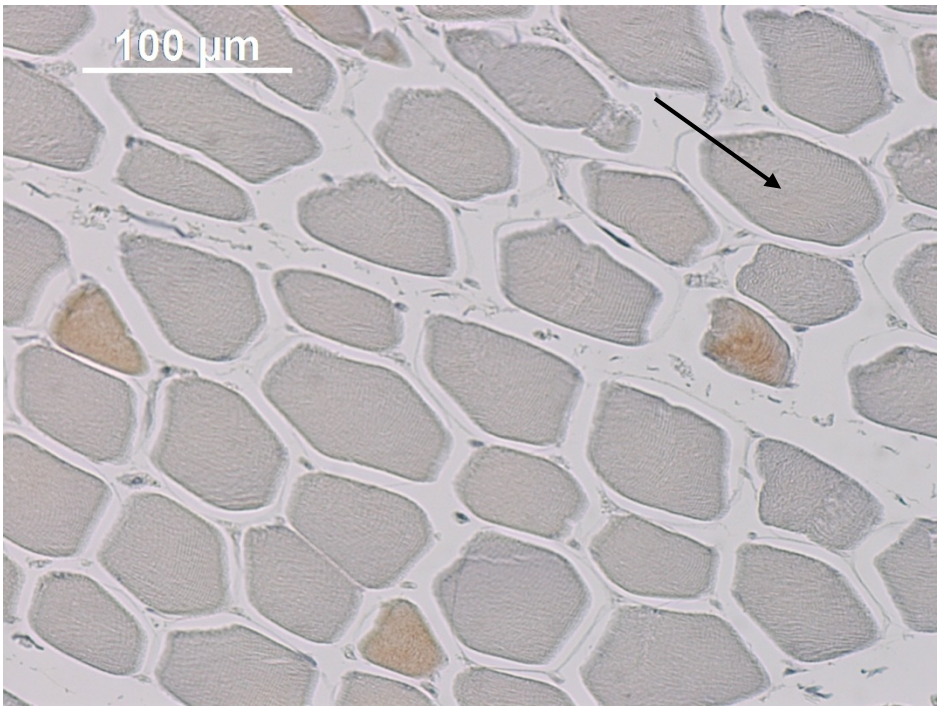

Fig. 44: Immunostained section [NOQ7.5.4D (= slow) antibody] of lumbar longissimus (Type I) of *E. patas*. The arrow points to the identical muscle cell from Fig. 43. Here, this cell reacted negatively to the slow antibody.

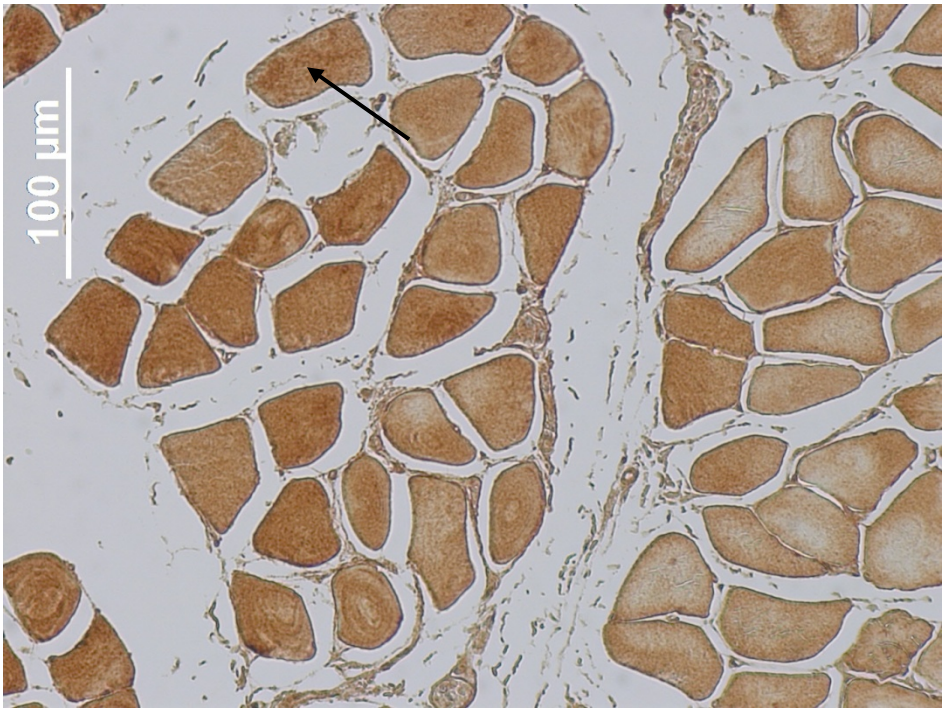

Fig. 45: Immunostained section [MY-32 (= fast) antibody] of thoracic multifidus (Type II) of *E. patas*. The arrow points to a muscle cell that reacted strongly to the fast antibody.

Fig. 46: Immunostained section [NOQ7.5.4D (= slow) antibody] of thoracic multifidus (Type I) of *E. patas*. The arrow points to the identical muscle cell from Fig. 45. Here, this cell reacted weakly to the slow antibody.

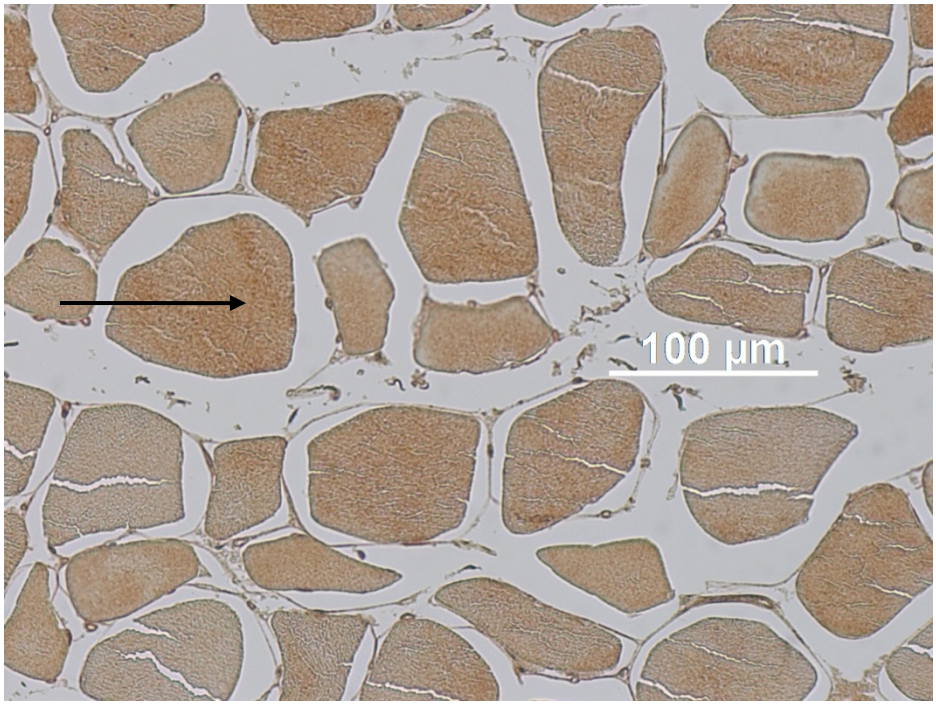

Fig. 47: Immunostained section [MY-32 (= fast) antibody] of lumbar multifidus (Type II) of *E. patas*. The arrow points to a muscle cell that reacted positively to the fast antibody.

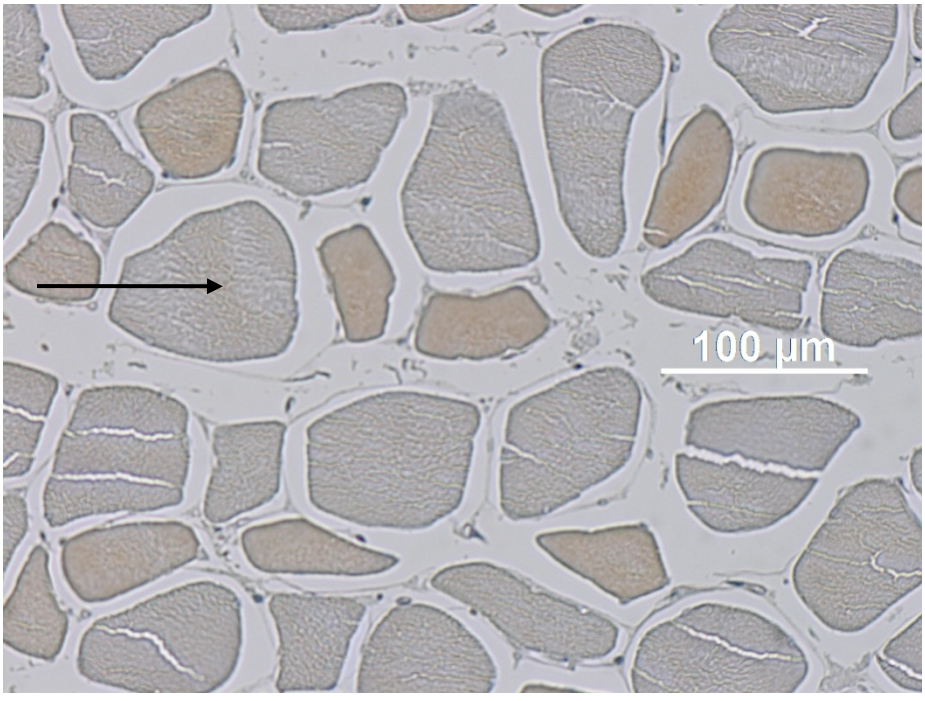

Fig. 48: Immunostained section [NOQ7.5.4D (= slow) antibody] of lumbar multifidus (Type I) of *E. patas*. The arrow points to the identical muscle cell from Fig. 47. Here, this cell reacted negatively to the slow antibody.

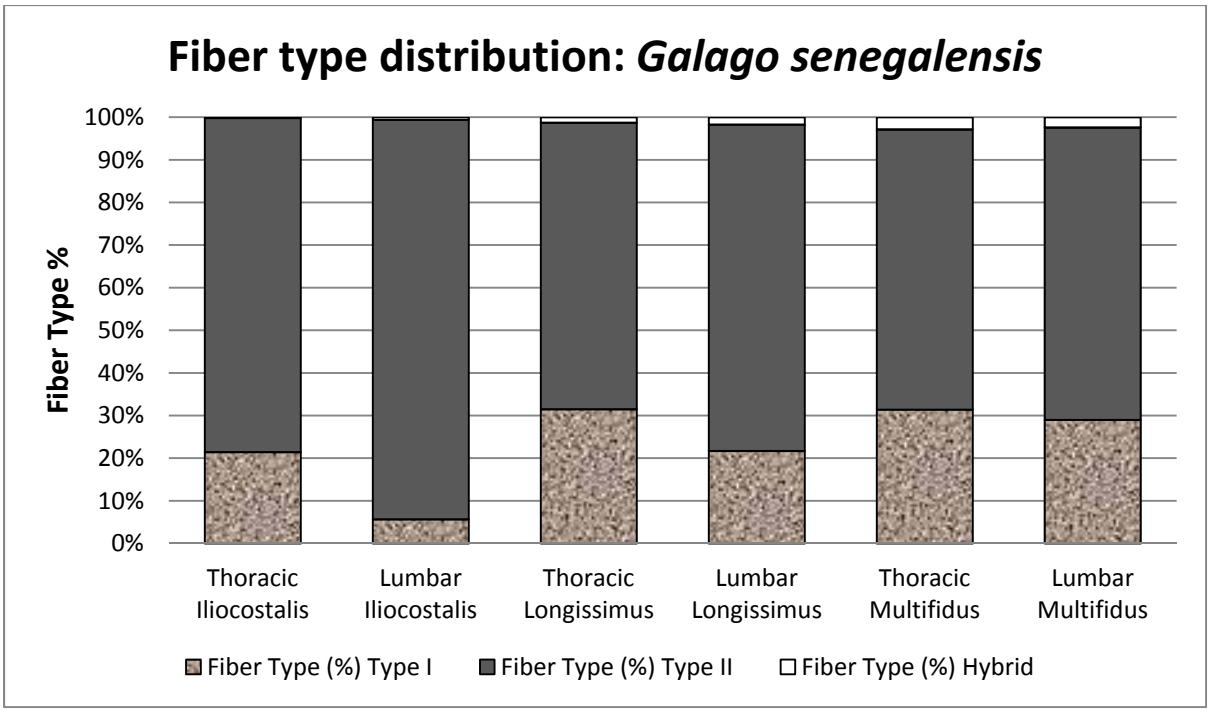

Fig. 49: Fiber type distribution in *G. senegalensis*

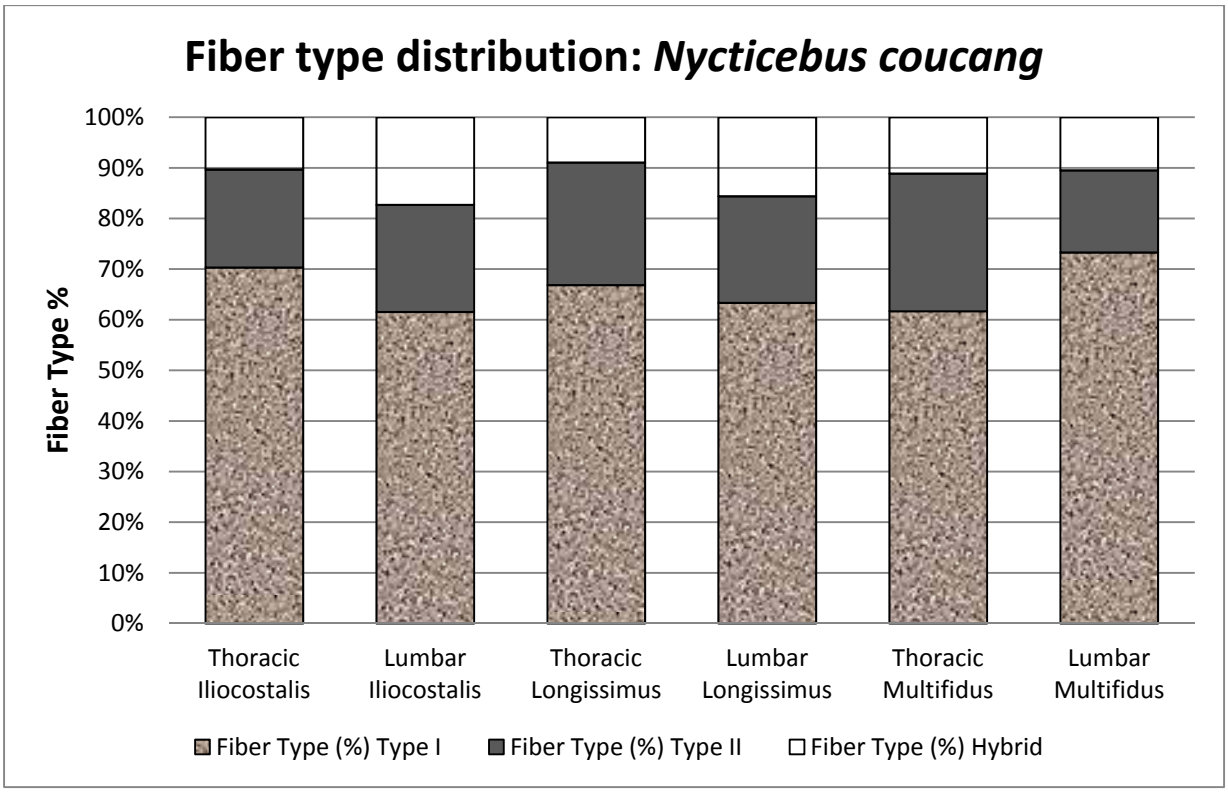

Fig. 50: Fiber type distribution in *N. coucang*

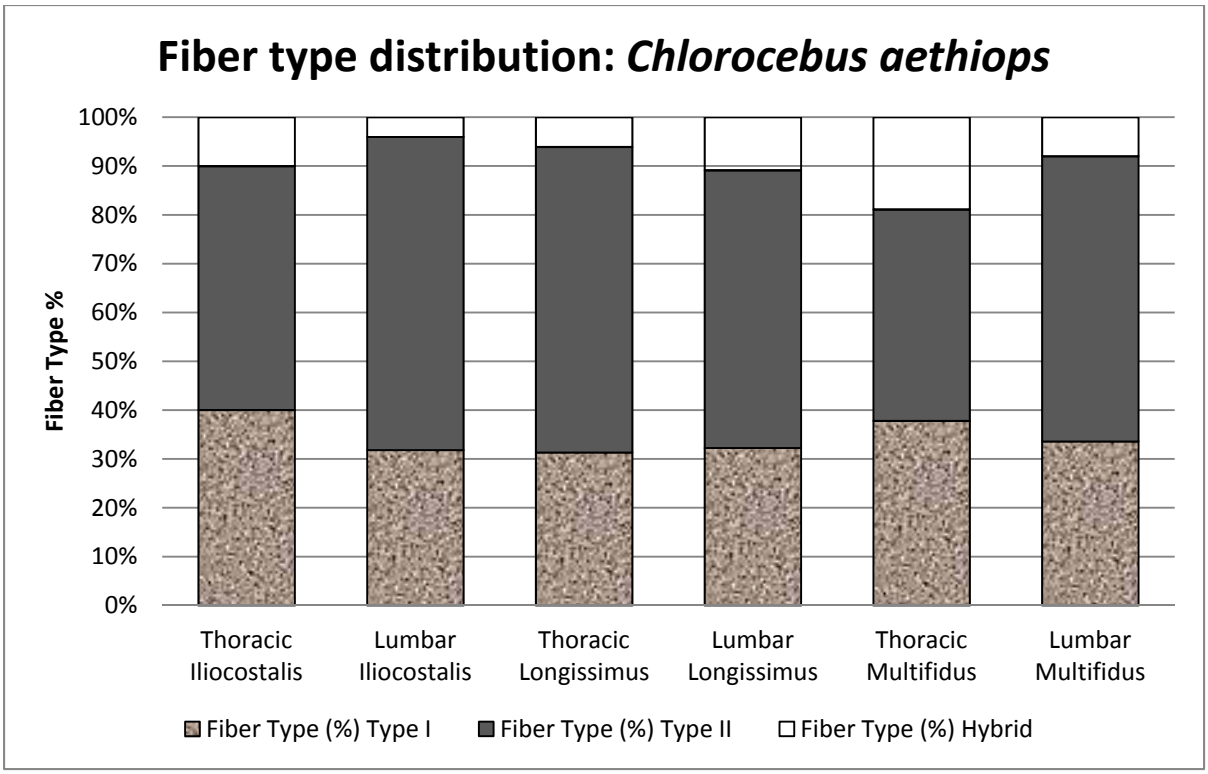

Fig. 51: Fiber type distribution in *C. aethiops*

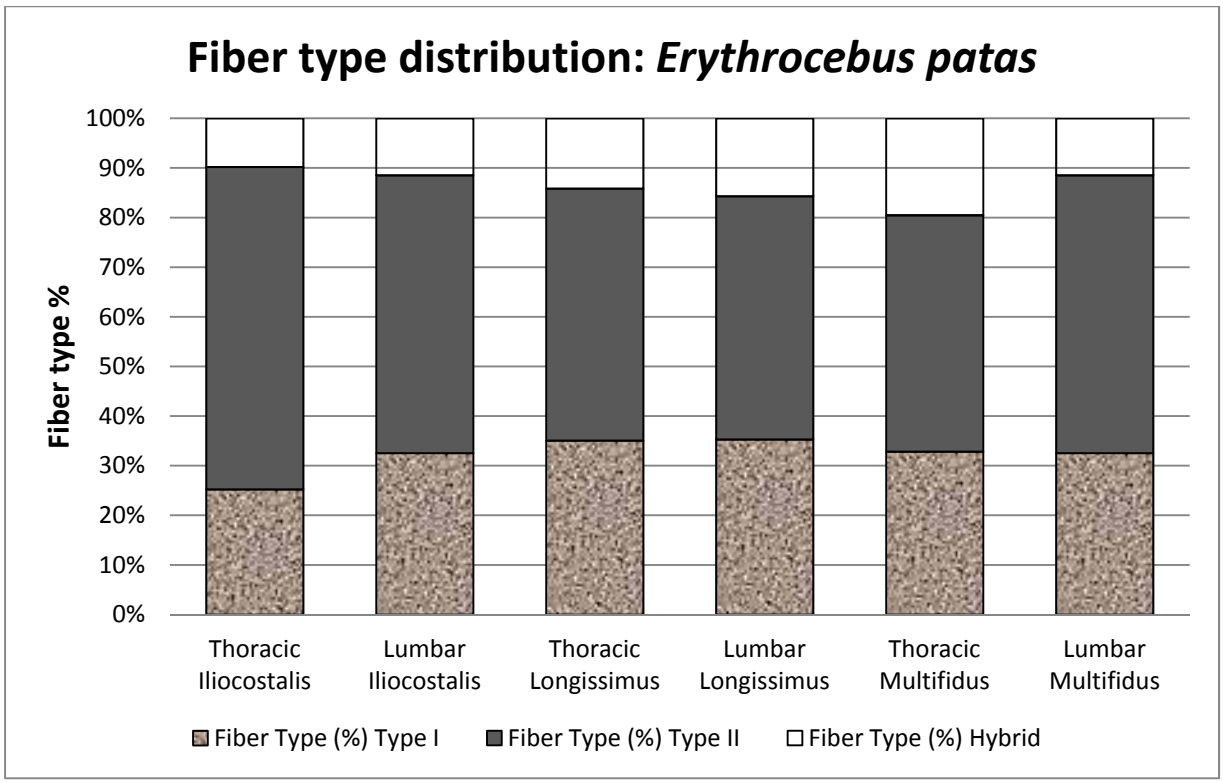

Fig. 52: Fiber type distribution in *E. patas*

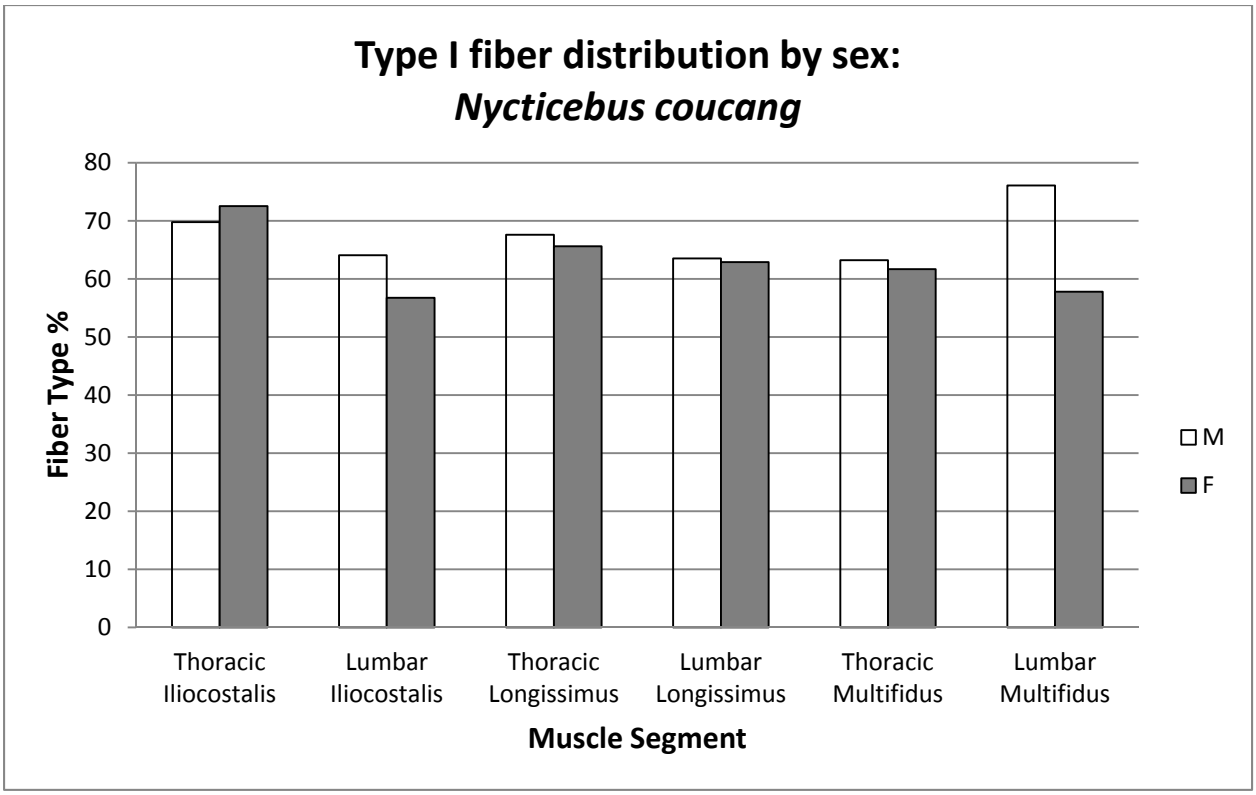

Fig. 53: Type I fiber proportion by sex: *N. coucang*

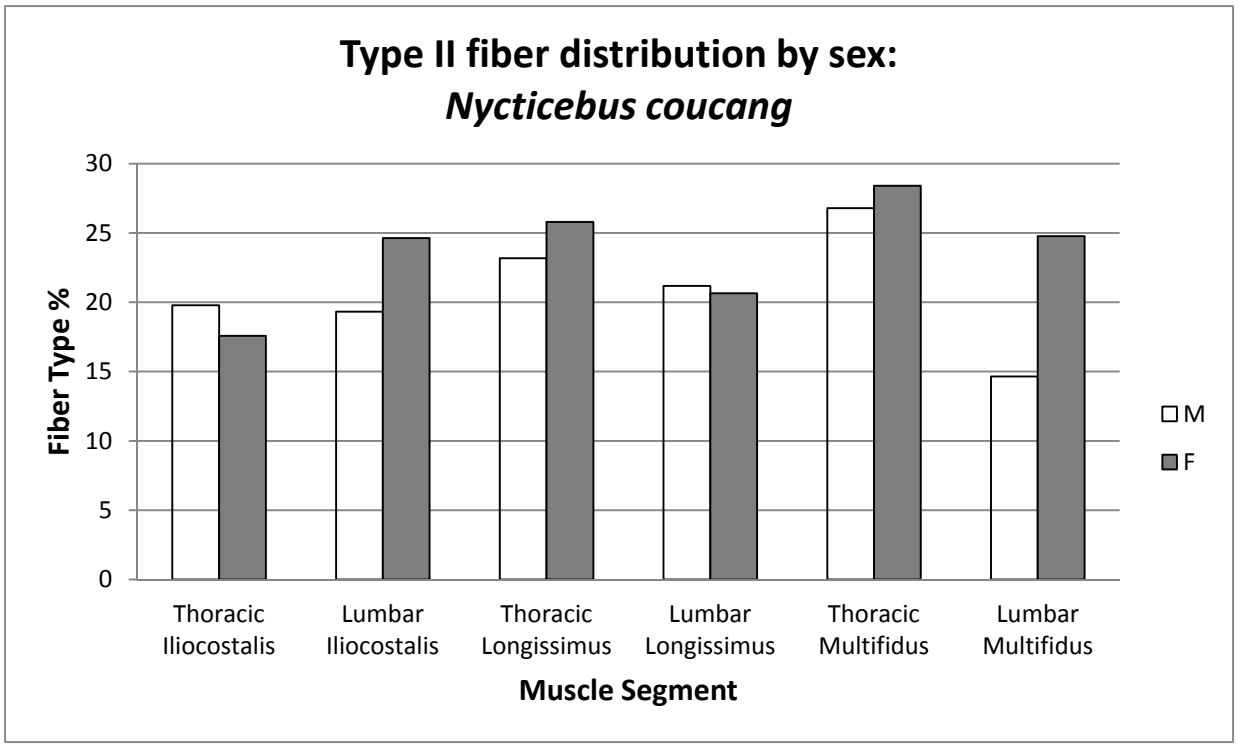

Fig. 54: Type II fiber proportion by sex: *N. coucang*

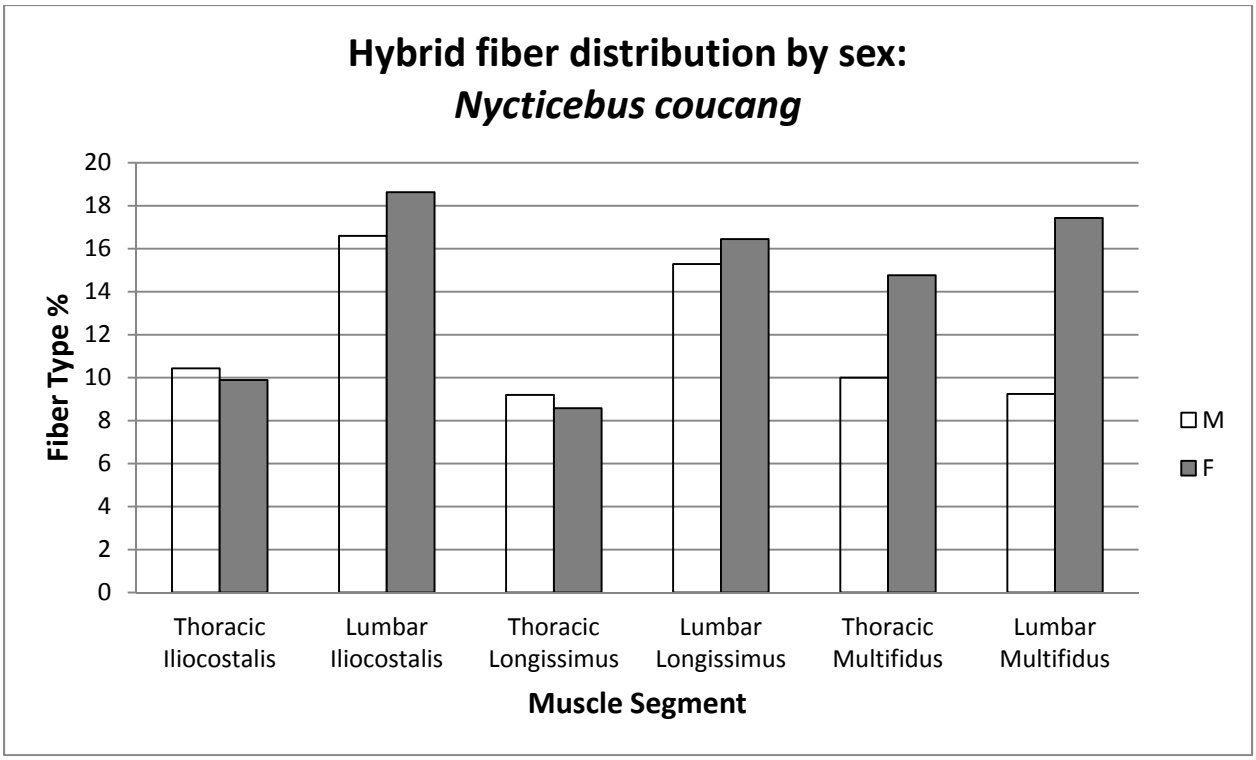

Fig. 55: Hybrid fiber proportion by sex: *N. coucang*

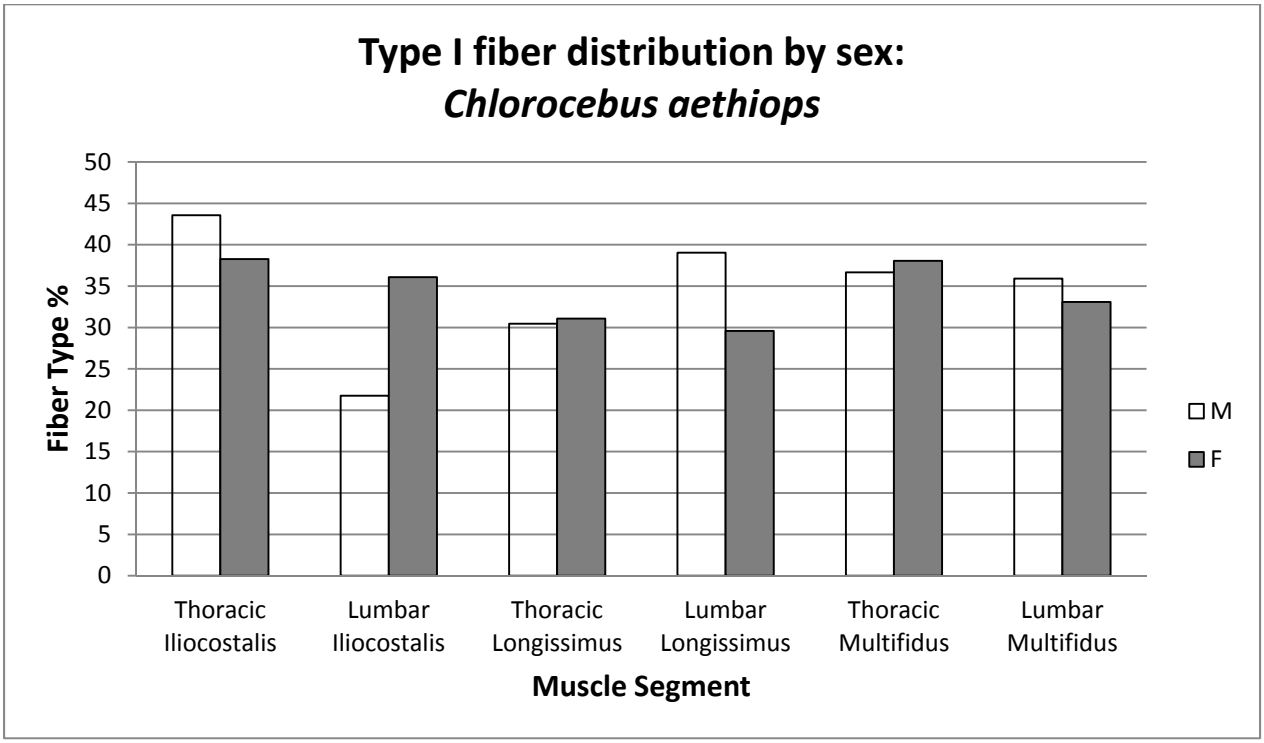

Fig. 56: Type I fiber proportion by sex: *C. aethiops*

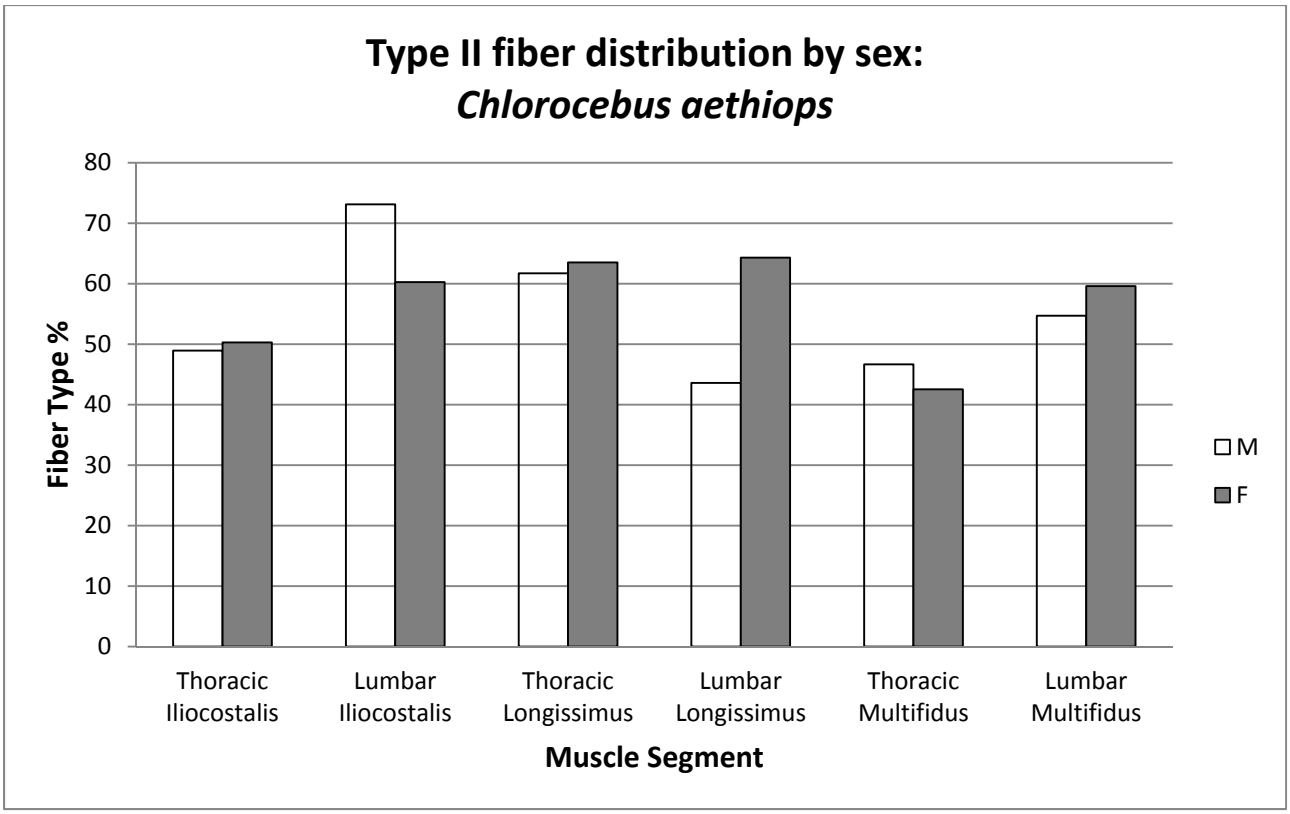

Fig. 57: Type II fiber proportion by sex: *C. aethiops*

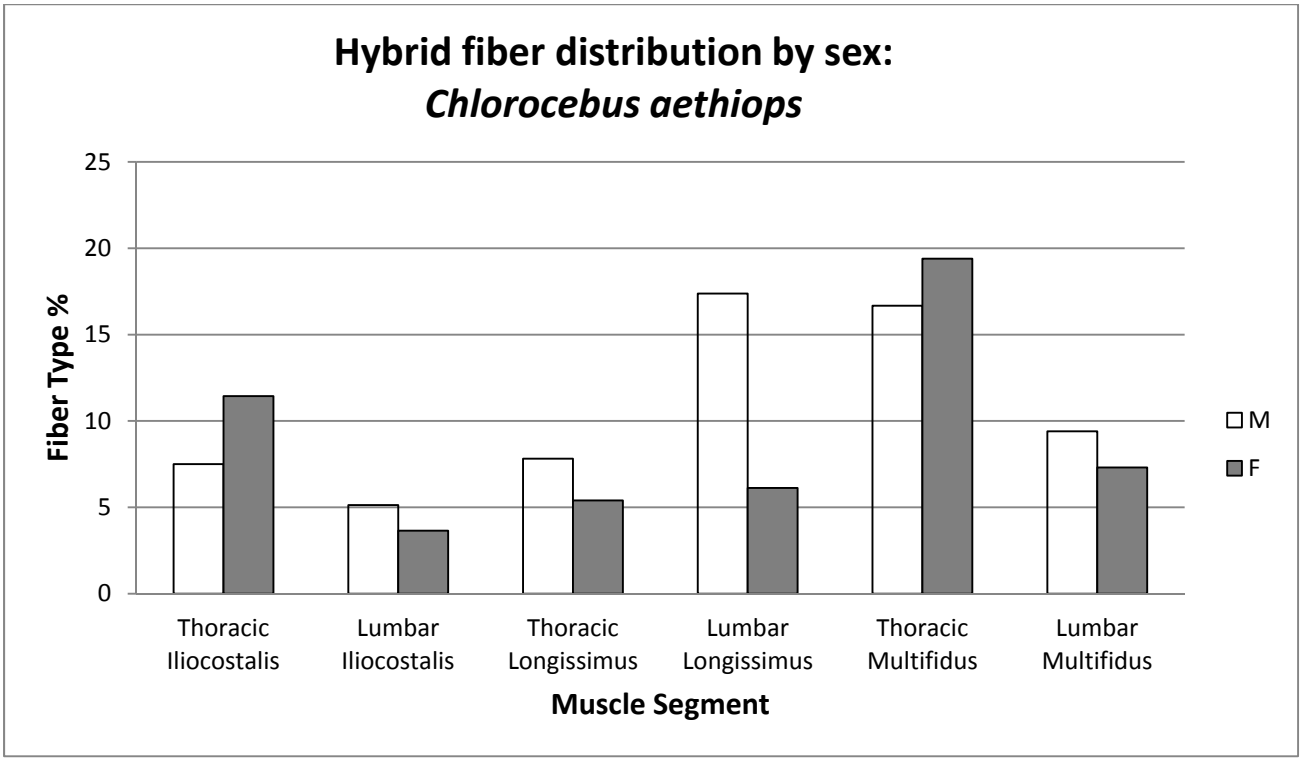

Fig. 58: Hybrid fiber proportion by sex: *C. aethiops*

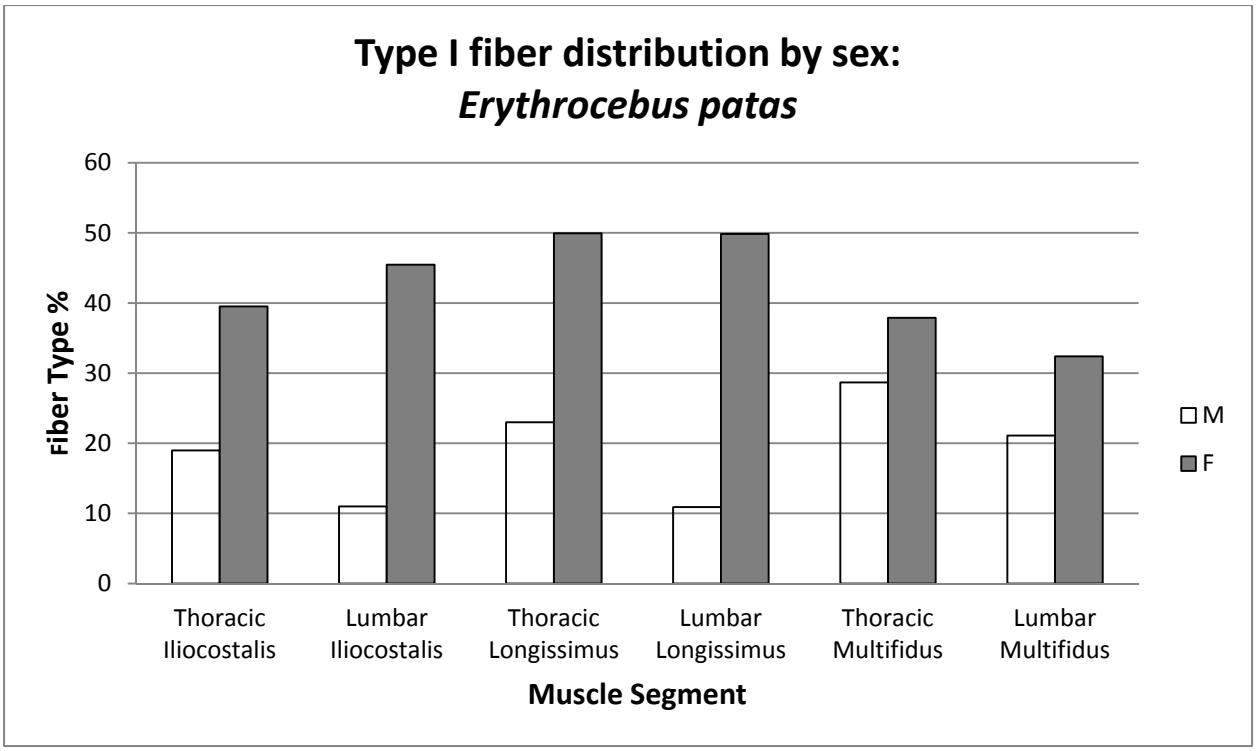

Fig. 59: Type I fiber proportion by sex: *E. patas*

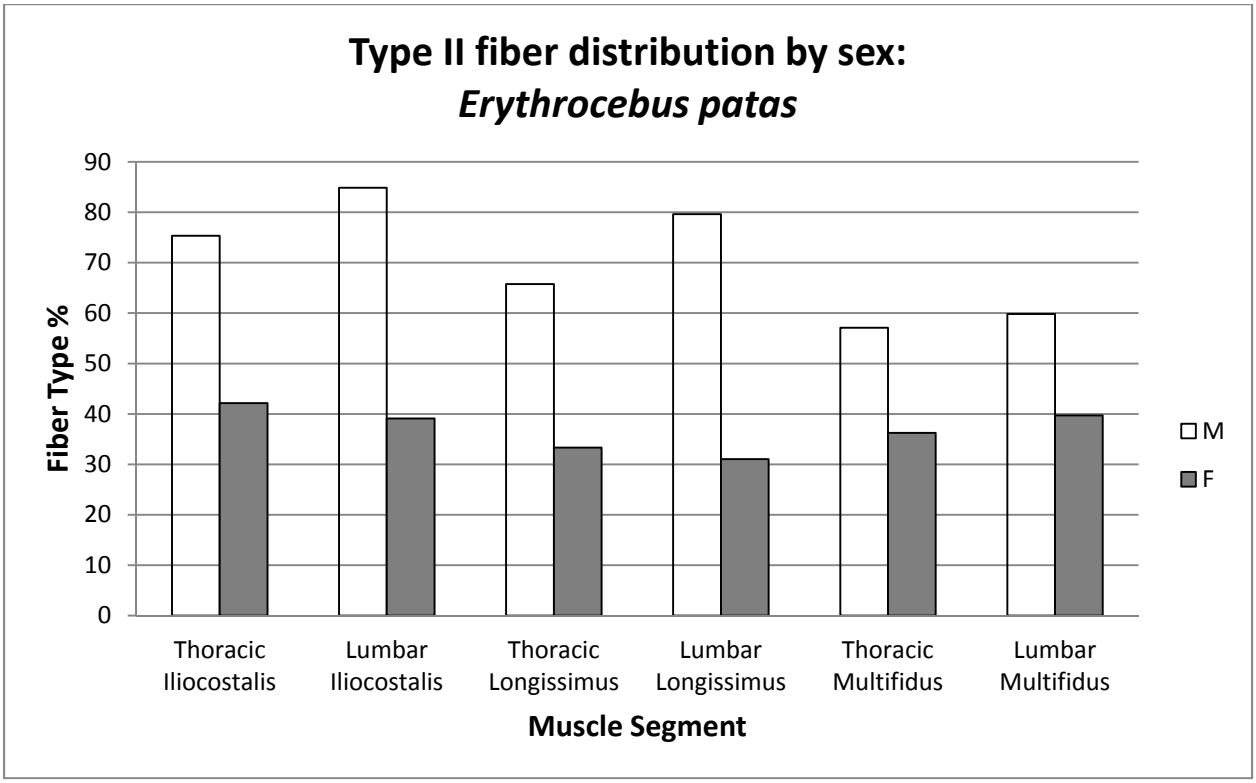

Fig. 60: Type II fiber proportion by sex: *E. patas*

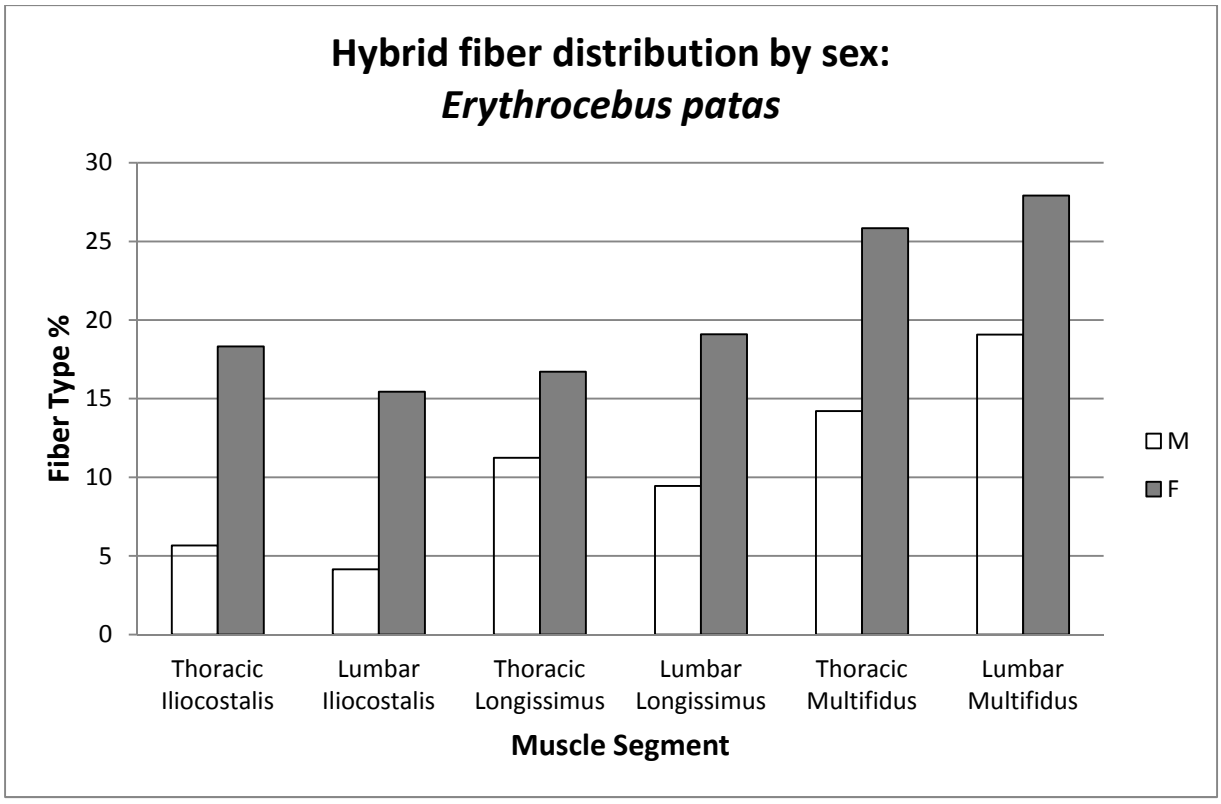

Fig. 61: Hybrid fiber proportion by sex: *E. patas*

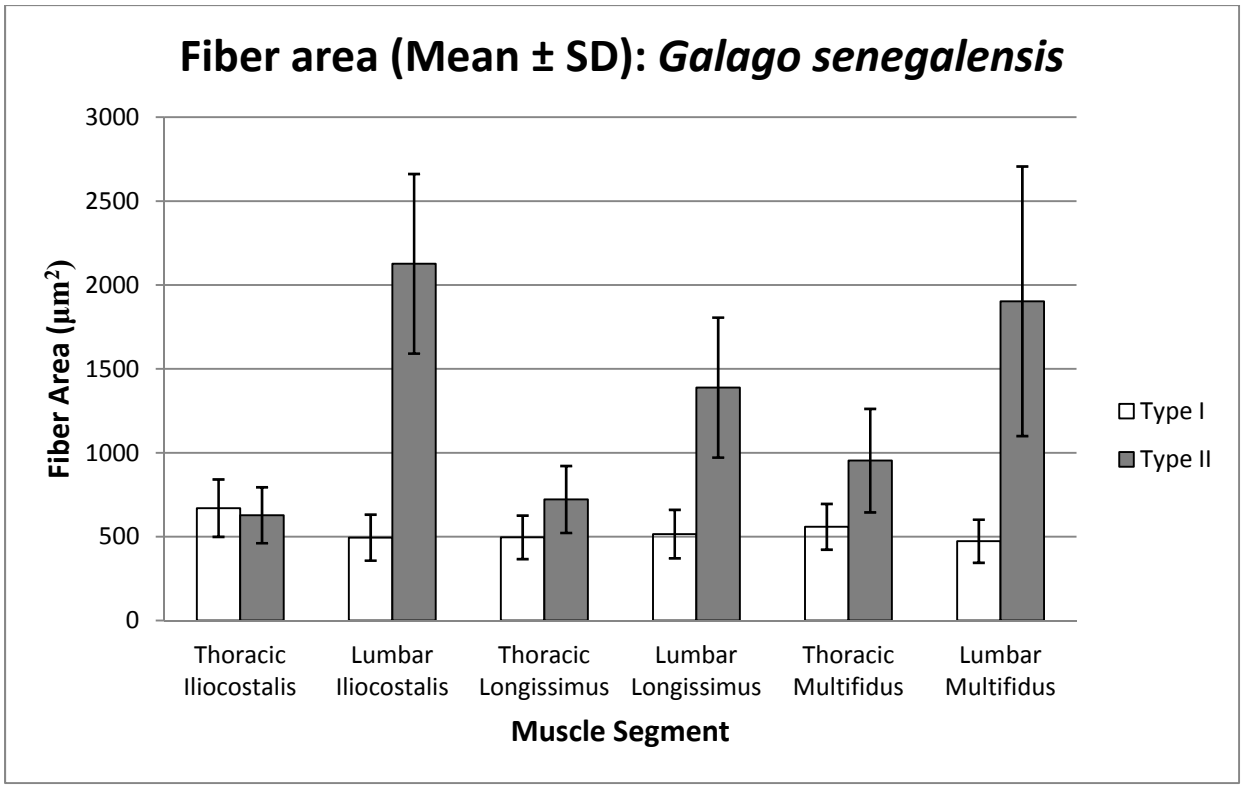

Fig. 62: Area for different fiber types: *G. senegalensis*

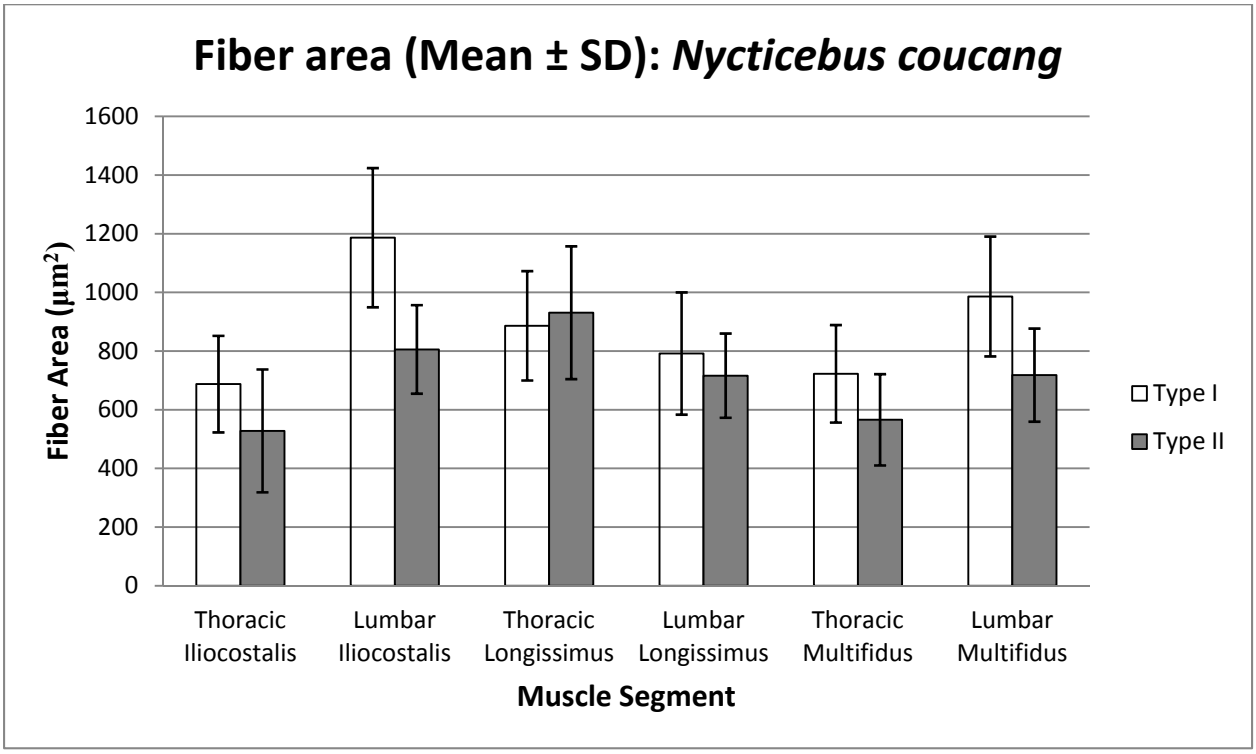

Fig. 63: Area for different fiber types: *N. coucang*

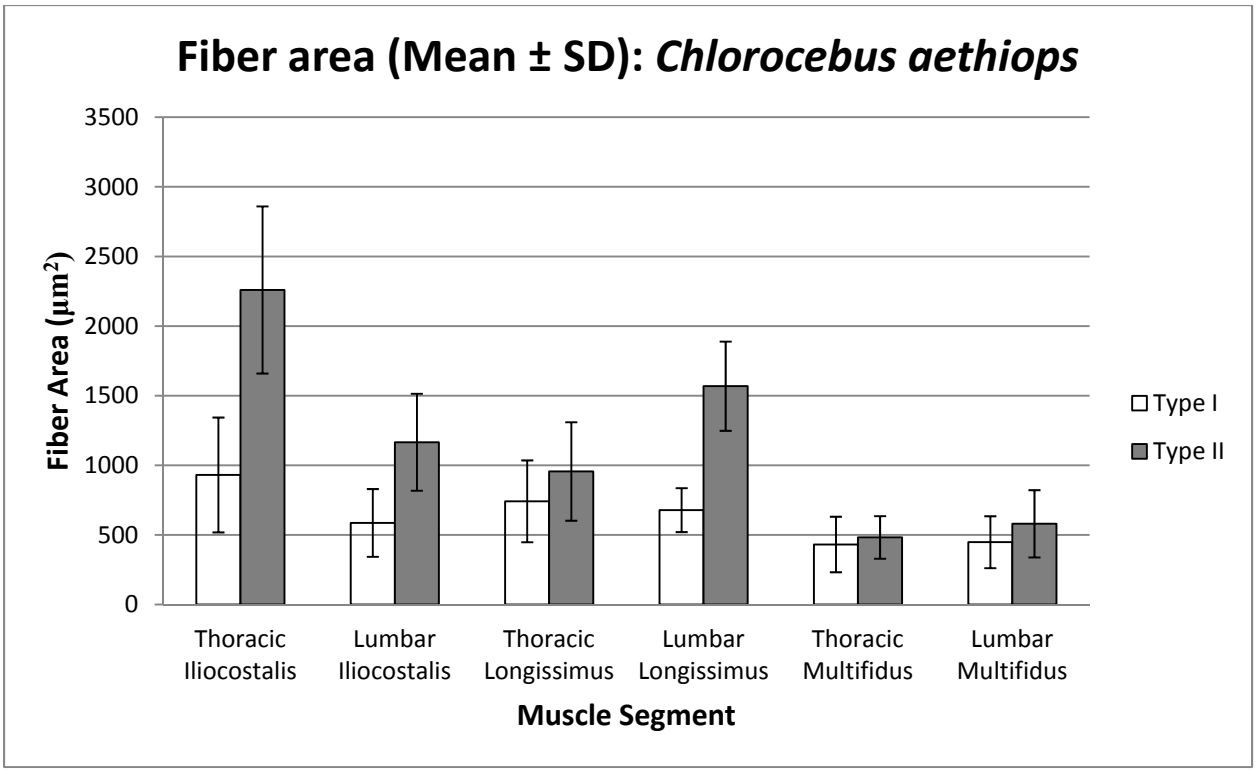

Fig. 64: Area for different fiber types: *C. aethiops*

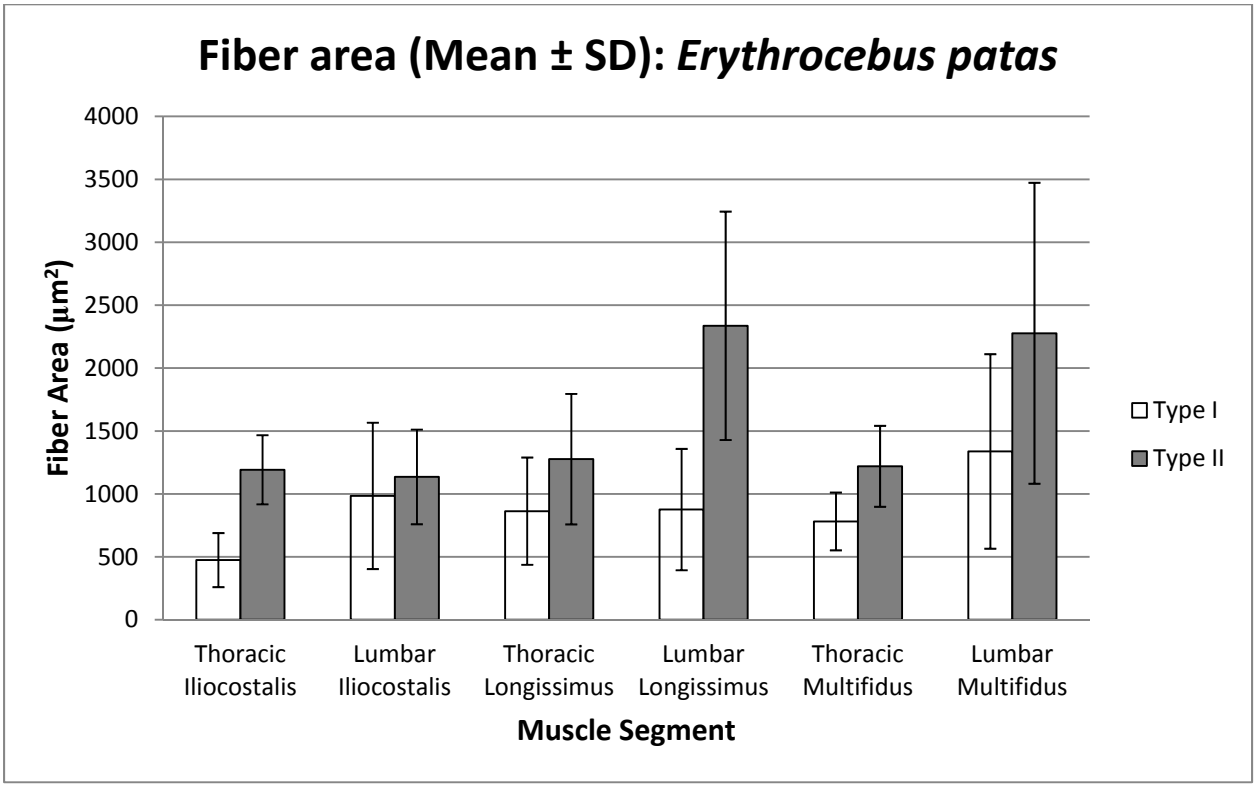

Fig. 65: Area for different fiber types: *E. patas*

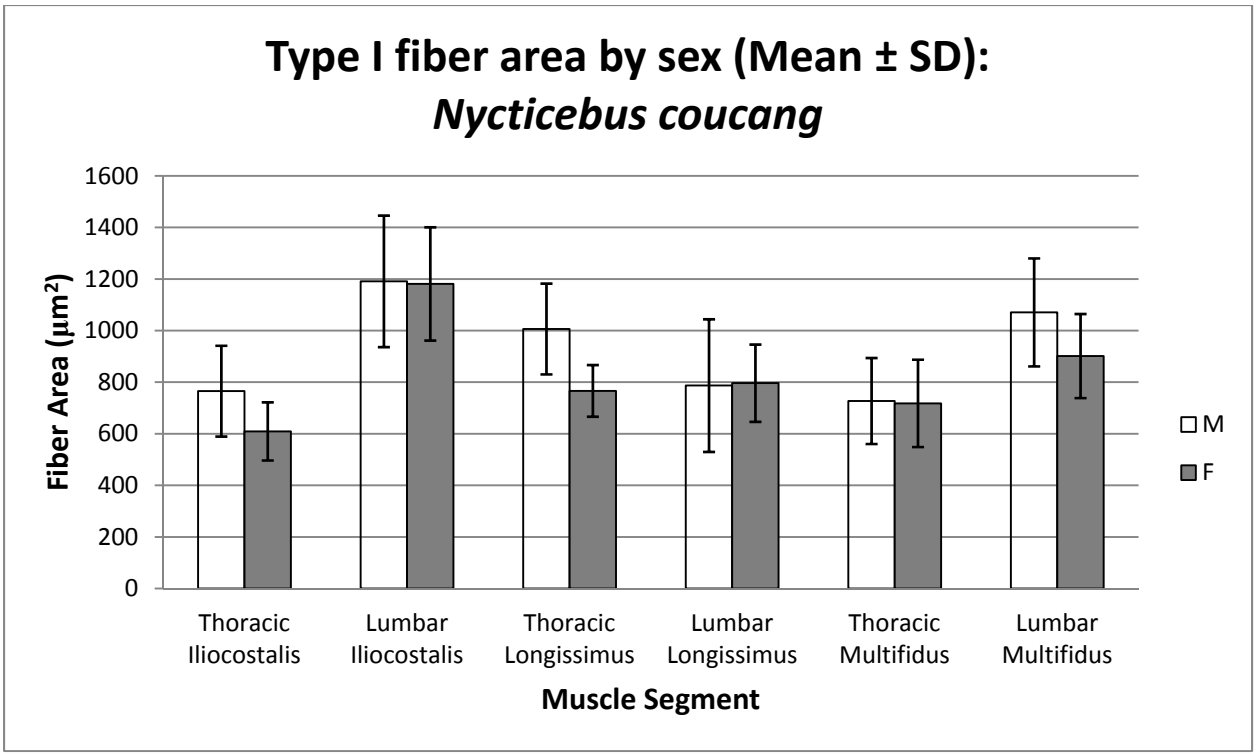

Fig. 66: Type I fiber area by sex: *N. coucang*

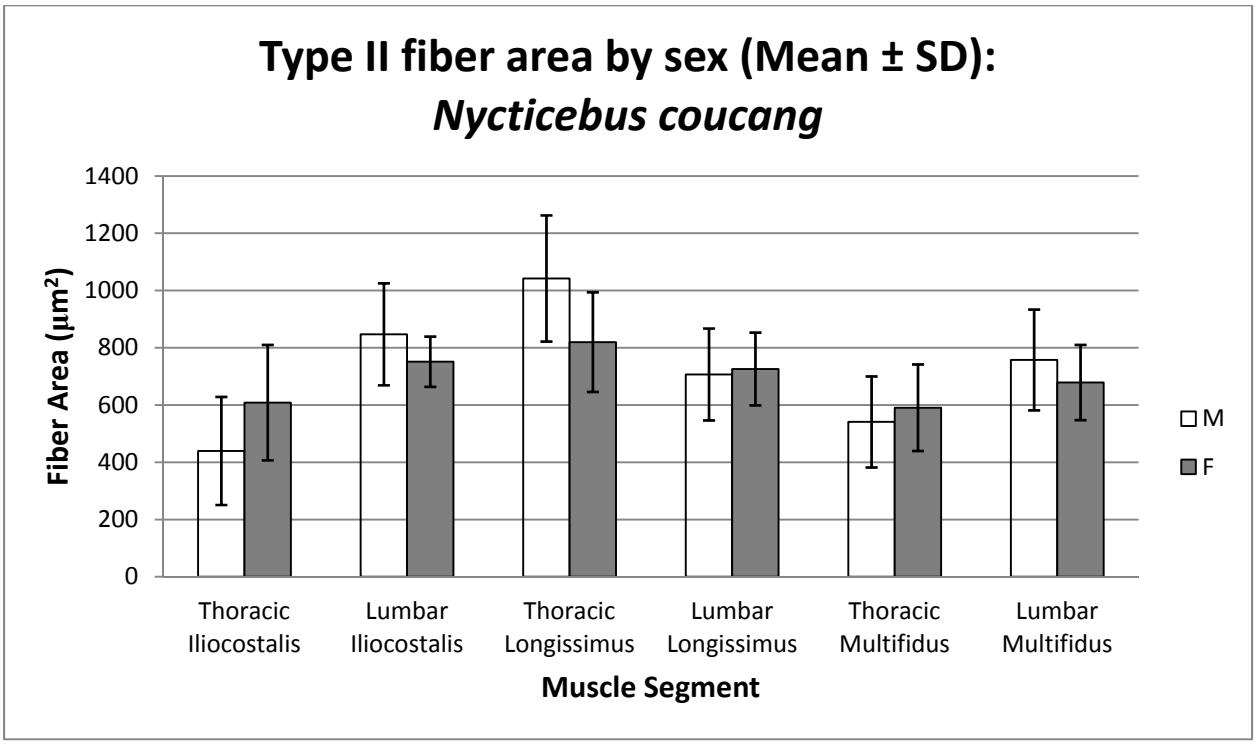

Fig. 67: Type II fiber area by sex: *N. coucang*

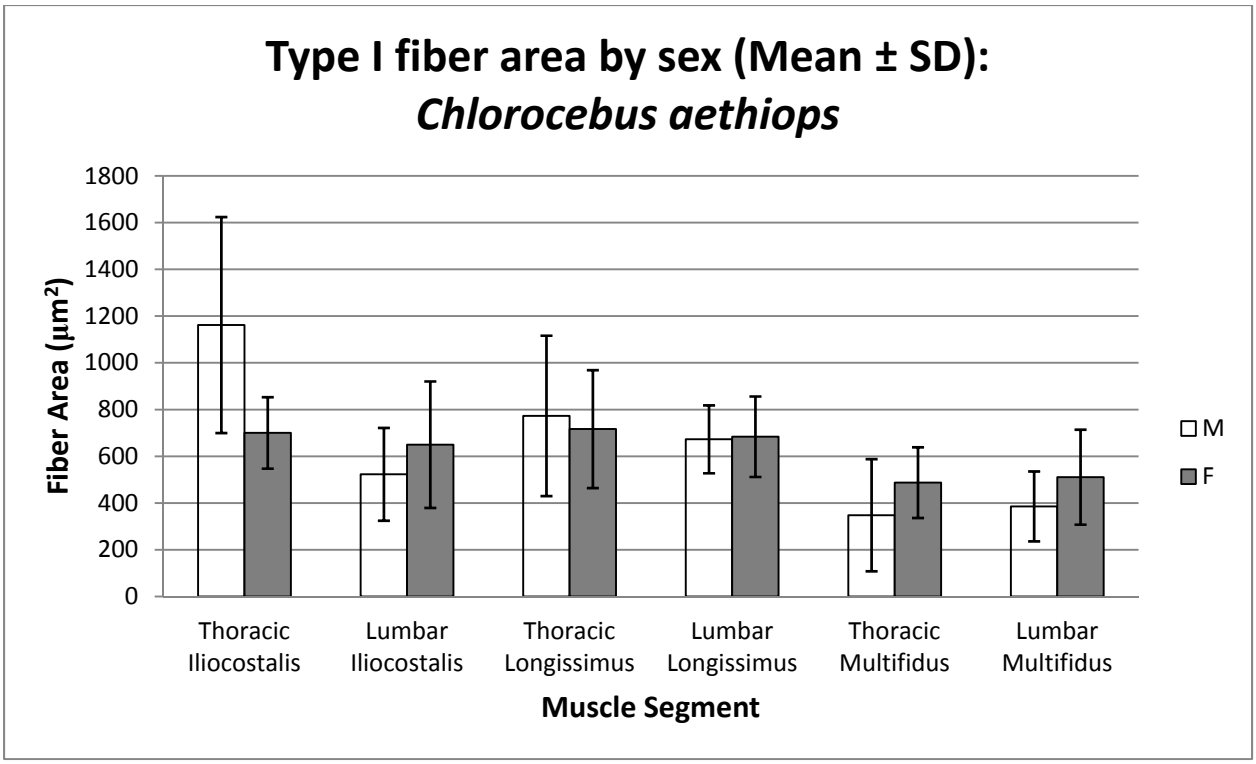

Fig. 68: Type I fiber area by sex: *C. aethiops*

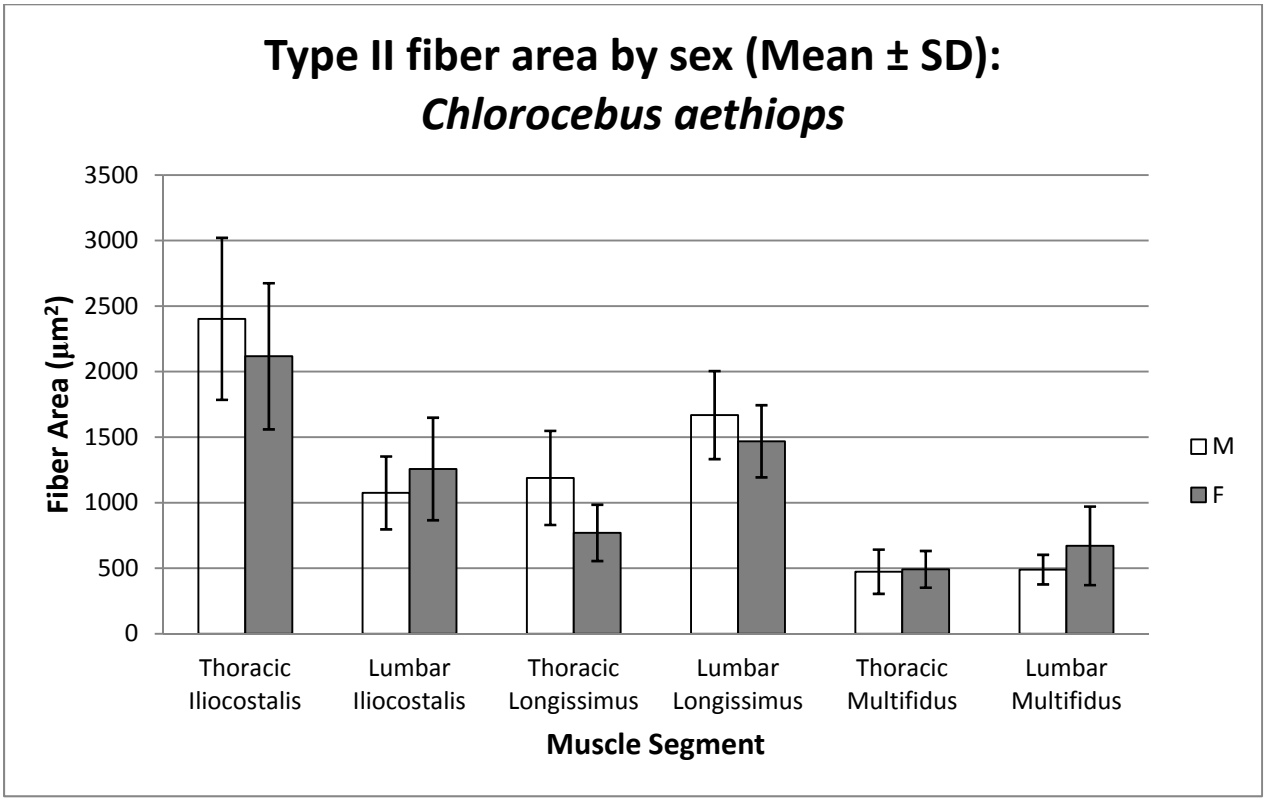

Fig. 69: Type II fiber area by sex: *C. aethiops*

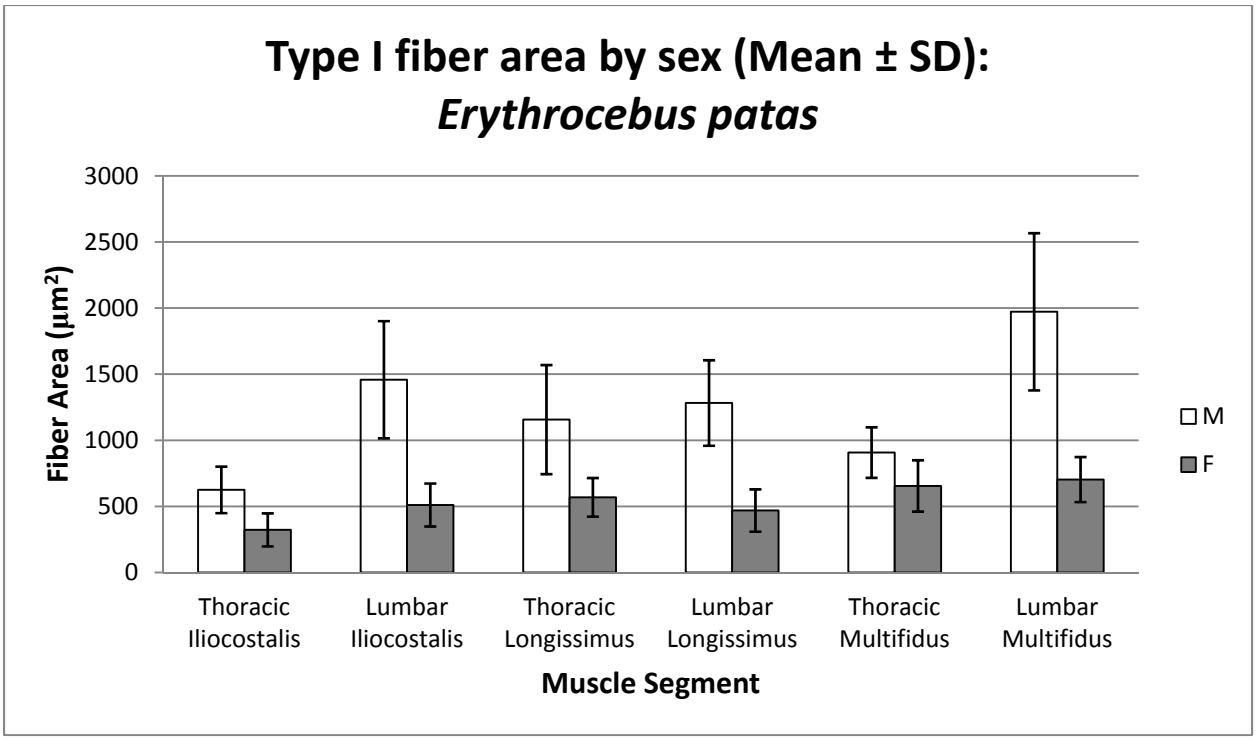

Fig. 70: Type I fiber area by sex: *E. patas*

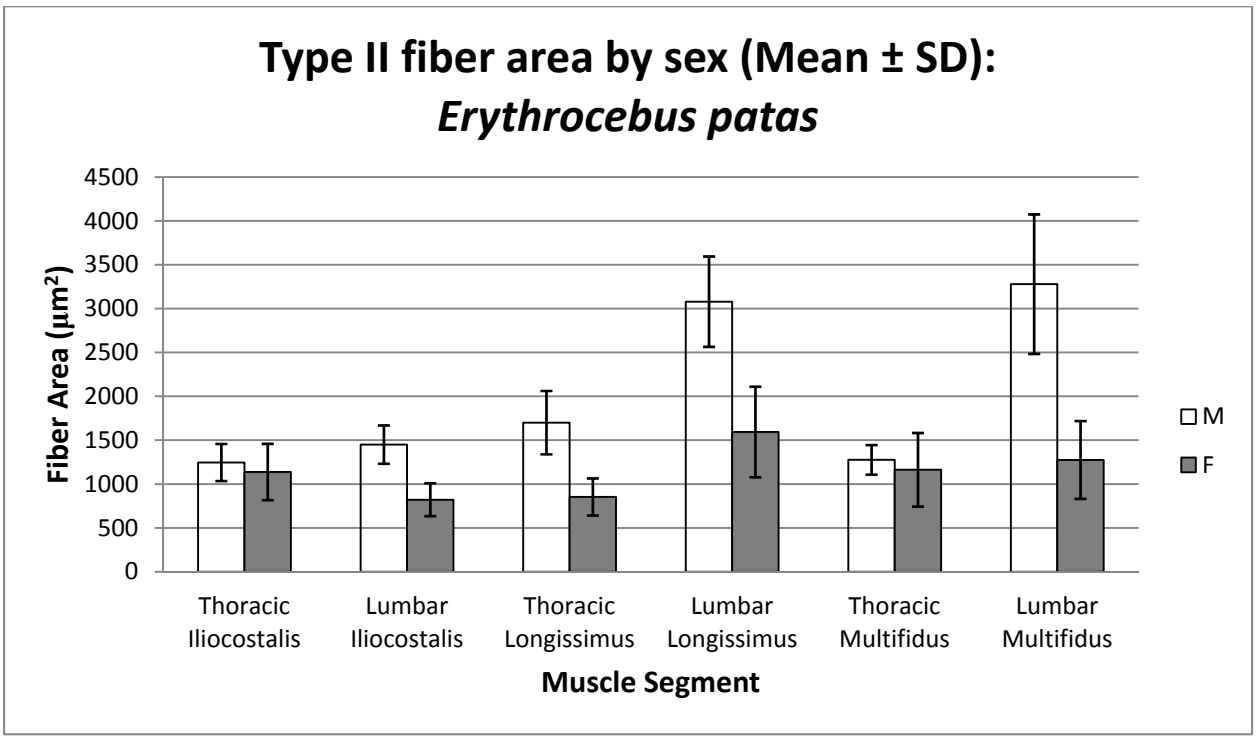

Fig. 71: Type II fiber area by sex: *E. patas*

Chapter 4

Vertebral Morphology and Muscle Leverage

4.1 Introduction

As the link between head and limbs, the spine's role in locomotion has been recognized in studies on its morphological variation in primates utilizing different positional behaviors (see references in Chapter 1). Although investigators have identified many important and functionally relevant distinctions in vertebral anatomy among various groups of primates (e.g., Keith, 1902, 1923; Schultz, 1938, 1961; Washburn and Buettner-Janusch, 1952; Erikson, 1960, 1963; Ankel, 1972; Sanders, 1990, 1991), less attention has been given to vertebral diversity within these groups. However, with the development of novel research methodologies, investigators have renewed their interest in the diversity of primate vertebral morphology (e.g., Sanders and Bodenbender, 1994; Johnson and Shapiro, 1998; Sanders, 1998; Shapiro and Simons, 2002; Shapiro et al., 2001, 2005; Shapiro, 2007; Russo and Shapiro, 2011).

It has been noted that each region of the vertebral column tends to vary morphologically among primates (e.g., Schultz, 1961; Ankel, 1972). Morphological specializations of each type of vertebra are for the most part functionally associated with posture and locomotion, but they may also be related to respiration (thoracic; Kapandji, 1974) or obstetrics (sacrum; e.g., Tague and Lovejoy, 1986; Abitbol, 1987a, b).

Despite the functional importance of all regions of the vertebral column, the lumbar region is characterized by the greatest diversity in the primate spine (Shapiro, 1993a). Accordingly, this chapter will focus on the comparative functional morphology of the lumbar vertebrae in the study species. The emphasis on lumbar vertebrae does not imply that other regions are unimportant. Instead, this analysis is intended to illustrate the complexity of the

vertebral function when considering only one of its constituting sections, and is meant to stimulate further research on all aspects of the vertebral column.

Hypothesis and predictions

It has been observed that the mass of spinal extensor muscles tends to be higher in leaping primates relative to non-leaping ones (Fleagle, 1977a; Emerson, 1985; Johnson and Shapiro, 1998), which is presumably an adaptation for rapid back extension during leaping. This argument is further supported by theoretical observations that muscles ideally suited to produce high velocity of movement of a limb segment to a given position may not always be best designed to bring that segment to that position most quickly (Stern, 1974). In fact, Stern (1974) argues that muscles with relatively smaller lever arms act by contracting at somewhat lower velocities but over longer periods of time, which is useful for producing high velocity at a determined position and retaining the ability to further torque during a greater range of motion. On the other hand, muscles with larger lever arms are beneficial for movements of short duration that must be accomplished relatively quickly; this is because the most important requirement for movements of short duration is high average velocity, accomplished by initial high acceleration. This latter arrangement seems to be consistent with the musculoskeletal configuration of animals that use the axial movement at the lumbar region (flexion – extension) to accelerate and enhance step length utilizing the lumbar vertebral column and the pelvic girdle as the most proximal element of the hindlimb (e.g. vervet monkeys, Hurov, 1987). Hall-Craggs (1965) also observed that at the beginning of leaping, the lesser galago progressively extends its back and trunk from a crouched position, followed by a gradual extension of hind limbs. As the animal takes off, the back, trunk, and hind limbs lies almost along a straight line (Hall-Craggs, 1965; see Fig. 1 in Chapter 1). In a similar fashion, *Pithecia pithecia* rapidly extends its back from a crouched

position to initiate take-off; and immediately after take-off, the back is almost completely extended in these monkeys (Walker, 2005). These observations provide theoretical, qualitative support to the notion that a larger lever arm for the epaxial muscles would facilitate back extension at the beginning of the take-off phase of the leaping cycle. I, therefore, hypothesize that the lever arm for epaxial muscles will be larger in dorsomobile primates (lesser galago and vervet monkey) relative to that in dorsostable primates (slow loris and patas monkey). It should also be mentioned here that because the sagittal movement of the spine takes places in the lumbar region, this hypothesis will be tested only in the lumbar region of the spine.

4.2 Materials and methods

To understand vertebral morphology and muscle leverage, i.e., lever arm, a number of functional aspects of lumbar vertebrae were investigated in the four study taxa. The sample size is presented in Table 1. Only adult individuals without any obvious pathology were included in the analysis; adulthood was determined by the eruption of the M3, and/or the epiphyseal fusion of the long bones. Sexes were pooled.

Counts and measurements

Lumbar vertebrae were determined based on the zygapophyseal orientation, which is considered more functionally relevant because it is based on the types of movements permitted at the intervertebral joints (Washburn and Buettner-Janusch, 1952; Erikson, 1960, 1963; Clauser, 1975, 1980). Functionally relevant measurements taken on the lumbar vertebrae are listed in Table 2, and illustrated in Fig. 1a-f. These measurements and their relationships with spinal mobility are also briefly described below.

Cranio-caudal length of the lumbar vertebral body.

An increase in the cranio-caudal length of the lumbar vertebral body increases the functional length of the lumbar column. Primates with the most numerous lumbar vertebrae tend to be habitual leapers (*Lepilemur*, *Indri*, *Propithecus*, and *Avahi*) (Shapiro, 1993a, 1995). Although the number of lumbar vertebrae is fairly uniform in the Old World monkeys, the frequent leapers (e.g., *Presbytis* and *Colobus*; Fleagle, 1977a, b; Rose, 1978) have relatively elongated lumbar regions compared to their more exclusively quadrupedal counterparts. This elongation has been caused by an increase of the cranio-caudal length of each lumbar vertebral body (Ward, 1991; Shapiro, 1993a). Rapid sagittal movement of a long lumber region could be expected to aid the propulsion needed for leaping (Erikson, 1963; Fleagle and Meldrum, 1988),

which would increase the leap length, especially in conjunction with the increase in back muscle mass that characterizes leaping primates (Fleagle, 1977a; Emerson, 1985). Similarly, by facilitating enhanced sagittal mobility, a long lumbar region might be helpful for the vervet monkey to increase its stride length during galloping. Therefore, I predict that relative cranio-caudal length of the lumbar vertebral body will be greater in *G. senegalensis* and *C. aethiops*, compared to *N. coucang* and *E. patas*, respectively.

Interzygapophyseal distance (cranio-caudal)

This characteristic is a morphological by-product of the cranio-caudal length of the lumbar vertebral body. A greater interzygapophyseal distance would provide a wider range of motion in sagittal plane for spinal flexion/extension (Shapiro and Simons, 2002; Shapiro et al., 2005; Shapiro, 2007). Therefore, I predict that the relative interzygapophyseal distance will be greater in *G. senegalensis* and *C. aethiops*, compared to *N. coucang* and *E. patas*, respectively.

Spinous process length

The lumbar spinous processes act as bony levers for the muscles capable of extending the lower back. The most prominent muscle that acts on the spinous processes in the lumbar region is multifidus (Shapiro, 1993a). The principal action of (lumbar) multifidus is extension of the lower back (Macintosh and Bogduk, 1986; Shapiro, 1991, 1993a). The lever arm for multifidus, as expressed by the dorsal projection of the spinous processes, is relatively longer in indriids than it is in strepsirrhines who leap less frequently, or when compared to hominoids or atelines (Shapiro, 1991, 1995). This indicates more effective back muscle leverage in indriids, and is more likely attributable to the capability of rapidly extending the back during leaping (Fleagle, 1977a; Shapiro, 1995). An increased leverage via an elongated spinous process would also help sagittal movement for the vervet monkey. Therefore, I predict that the relative spinous process

length will be greater in *G. senegalensis* and *C. aethiops*, compared to *N. coucang* and *E. patas*, respectively.

Transverse process position and orientation

As with the spinous processes, transverse processes of lumbar vertebrae act as bony levers for muscles that move the lumbar column. Due to their location, longissimus and iliocostalis can effect extension (bilateral recruitment) or lateral flexion (unilateral recruitment) of the lumbar region. The lumbar transverse processes of most primates are oriented ventrally (i.e., the distal tips lie ventral relative to the base of the process), which is also the case for most mammals. On the other hand, in atelines, great apes, and humans, lumbar transverse processes are oriented dorsally (Mivart, 1865; Benton, 1967; Gambaryan, 1974; Filler, 1986; Kelley, 1986; Shapiro, 1991, 1995).

Generally, the ventral position and orientation of transverse processes characterizing most primates creates a relatively deep compartment for the erector spinae muscles (i.e., the compartment that is formed by the spinous process, lamina, and transverse process). Therefore, the erector spinae muscles tend to be more massive in cross section (relative to body size) in primates with ventrally oriented transverse processes than in atelines or hominoids (Keith, 1940; Benton, 1967, 1974; Shapiro, 1993a, 1995). I predict that the lumbar transverse processes of *G. senegalensis* and *C. aethiops* will be relatively more ventrally positioned and oriented, compared to those of *N. coucang* and *E. patas*, respectively.

Statistical analyses

Means were computed for each variable at each vertebral level across all individuals within a species. In order to generate a relative measure of muscle leverage for comparison among primates with different body sizes, it was necessary to choose a consistent size variable

by which to divide the lever arm value. An obvious choice would be the cube root of body weight. However, body weights were not known for each individual. Therefore, an alternative size variable was chosen – the geometric mean of all non-angular variables at each vertebral level in each individual. The geometric mean is equivalent to the n-th root of the product of "n" variables (Sokal and Rohlf, 1995: Jungers et al., 1995). In this study, the geometric mean was a more accurate estimator of overall body size than body weight because it could be calculated for each individual. Non-angular variables were size-standardized by the geometric mean of all non-angular variables. The size-standardized variables were logged (Sokal and Rohlf, 1995), and one-way analysis of variance (ANOVA, one-tailed) was conducted. Level of significance was set at $p \leq 0.05$. All statistical tests were performed on MS-Excel 2007 (Microsoft, Inc.), and SPSS v.16 software (IBM-SPSS, Inc.).

4.3 Results

Strepsirrhines

Within species, across vertebral level

Cranio-caudal height of vertebral body

Relative cranio-caudal height of the lumbar vertebral body (ventral and dorsal) in *G. senegalensis* showed a steady increase from L1 to L6 level, and then a decline for L7-L8 vertebrae (Tables 3-4; Figs. 2-3). ANOVA results for differences across vertebrae (both ventral and dorsal heights) were significant (Tables 3-4).

In *N. coucang*, cranio-caudal height of the vertebral body (ventral) showed a general decrease from L1 to L9 level (Table 3; Fig. 2). However, the dorsal height was more variable. L2 had shorter body than L1; but the height increased from L3 to L5, and then declined from L6 to L9 (Table 4; Fig. 3). ANOVA results were not significant across vertebrae (ventral and dorsal heights) (Tables 3-4).

Interzygapophyseal distance

Relative interzygapophyseal distance in the lumbar vertebrae of the lesser galago remained quite steady from L1-L4; then it increased from L5-L6, and declined again from L7-L8 (Table 5; Fig. 4). Differences across vertebrae were not significant (Table 5).

In the slow loris, there was no consistent pattern in the relative interzygapophyseal distance from L1-L5. However, relative interzygapophyseal distance steadily increased from L6-L9 (Table 5; Fig. 4). Differences across vertebrae were not significant (Table 5).

Spinous process length

Relative spinous process length in the lesser galago declined from L1 to L5, and increased from L6 to L8 (Table 6; Fig. 5). The differences across vertebrae were significant

(Table 6). A somewhat similar pattern was observed in the slow loris, with relative spinous process length decreasing from L1 to L5, and then increasing from L6 to L9 (Table 6; Fig. 5). However, for the loris vertebrae, the differences in relative spinous process length were not significant (Table 6).

Position of transverse process

Relative ventro-dorsal position of the transverse process in *G. senegalensis* increased from L2-L4, and then again, from L6-L8 (Table 7; Fig. 6). Differences across vertebrae were significant (Table 7).

In *N. coucang*, there was no consistent pattern from L1-L5; there was an increase in the relative ventro-dorsal position of the transverse process from L5-L8, which declined again at L9 (Table 7; Fig. 6). No significant difference was noticed across vertebrae (Table 7).

Orientation of transverse process

Ventro-dorsal orientation of the transverse process in the lesser galago increased from L6-L8; there was no consistent pattern in more cranially located vertebrae (L1-L5) (Table 8; Fig. 7). Differences across vertebrae were not significant (Table 8).

No consistent pattern was observed in the transverse process orientation of the slow loris (Table 8; Fig. 7). There was no significant difference across vertebrae either (Table 8).

Between species, within vertebral level

Cranio-caudal height of vertebral body (Tables 3-4; Figs. 2-3)

Differences between the strepsirrhine species in relative cranio-caudal height of the vertebral bodies were significant at L1 (ventral height) and L6-L7 (ventral and dorsal heights) levels. Differences in heights at L4 (ventral) and L3 and L5 (dorsal) were virtually indistinguishable between species.

Interzygapophyseal distance (Table 5; Fig. 4)

Differences in relative interzygapophyseal distance between species were significant at all vertebral levels, except L8, with the vertebrae of lesser galago having greater distance compared to those of the slow loris.

Spinous process length (Table 6; Fig. 5)

Although relative length of the spinous process was greater in the lesser galago (at all vertebral levels), none of the differences were significant.

Ventro-dorsal position of transverse process (Table 7; Fig. 6)

Apart from L1, differences in relative transverse process position between species were significant at all vertebral levels, with the vertebrae of lesser galago having smaller values (i.e., more ventrally positioned transverse process) than those of slow loris.

Ventro-dorsal orientation of transverse process (Table 8; Fig. 7)

Although the lumbar transverse processes were more ventrally oriented (i.e., narrower angles) in the lesser galago, the differences were significant only at L3-L4 and L6-L8 levels.

Cercopithecoids

Within species, across vertebral level

Cranio-caudal height of vertebral body

Relative cranio-caudal height of the lumbar vertebral body (ventral and dorsal) in *C. aethiops* showed a steady increase from L1 to L5 level, and then a decline from L7-L9 (ventral) and L6-L9 (dorsal) (Tables 9-10; Figs. 8-9). ANOVA results for differences across vertebrae (both ventral and dorsal heights) were significant (Tables 9-10). Similar trends were also observed across vertebrae in *E. patas*, where relative vertebral body height increased from L1-

L6, and decreased from L7-L9 (Tables 9-10; Figs. 8-9). Differences across vertebrae were significant both relative ventral and dorsal heights (Tables 9-10).

Interzygapophyseal distance

Relative interzygapophyseal distance in both *C. aethiops* and *E. patas* increased from L1-L5, and declined from L6-L9 (Table 11; Fig. 10). Significant differences were noticed across vertebrae within each species (Table 11).

Spinous process length

In the vervet monkey, relative spinous process length increased from L2-L7, and then declined (Table 12; Fig. 11). On the other hand, in the patas monkey, relative spinous process length increased from L2-L9 (Table 12: Fig. 11). Differences across vertebrae were significant within each species as well (Table 12).

Ventro-dorsal position of transverse process

Lumbar transverse processes from L2-L7 were progressively more ventrally positioned (i.e. ratios became smaller) in the vervet monkey; however, the transverse processes in this species became more dorsally placed at L8-L9 compared to those of the more cranial vertebrae (Table 13: Fig. 12). A somewhat similar pattern was observed in the patas monkey as well, with transverse processes of L2-L6 were more ventrally positioned than those of L7-L9 (Table 13: Fig. 12). Significant differences were noticed across vertebrae within each species (Table 13).

Ventro-dorsal orientation of transverse process

In the vervet monkey, lumbar transverse processes from L2-L5 were progressively more ventrally oriented (i.e. narrower angles) than those of L6-L9 (Table 14; Fig. 13). In the patas monkey, transverse processes from L2-L7 were more ventrally oriented than those of L8-L9

(Table 14; Fig. 13). Differences across vertebrae within each species were also significant (Table 14).

Between species, within vertebral level

Cranio-caudal height of vertebral body (Tables 9-10; Figs. 8-9)

Relative ventral heights were greater in the vervet monkey from L5-L9. Differences between the cercopithecoid species in ventral body height were significant at all vertebral levels, except L4, L6, and L9.

Relative dorsal body heights were significantly greater in the vervet monkey at all vertebral levels.

Interzygapophyseal distance (Table 11; Fig. 10)

Relative interzygapophyseal distances were greater in the vervet monkey compared to those of the patas monkey at all vertebral levels. However, the differences were significant only from L2-L9.

Spinous process length (Table 12: Fig. 11)

Relative spinous process lengths between the monkeys were significantly different at all vertebral levels, with the patas monkey having relatively longer spinous proceeses than the vervet monkey.

Ventro-dorsal position of transverse process (Table 13: Fig. 12)

At all levels, lumbar transverse processes were significantly more ventrally positioned (i.e. smaller relative values) in the vervet monkey than those of the patas monkey.

Ventro-dorsal orientation of transverse process (Table 14; Fig. 13)

Although the lumbar transverse processes were generally more ventrally oriented (i.e. narrower angles) in the vervet monkey, the differences were significant only at L3-L6.

Especially at L7-L9, although the angles were narrower for the vervet monkey, they were graphically indistinguishable from those of the patas monkey.

4.4 Discussion

The results generally confirm predictions of differences in lumbar morphology between *G. senegalensis* and *N. coucang*, and to a lesser extent, between *C. aethiops* and *E. patas*. The modal number of lumbar vertebrae is 8 in both of the strepsirrhine species, although some *N. coucang* individuals have 9 lumbar vertebrae (this study). An important implication of these observations relates to the proportion length of the lumbar region. Given the same number of lumbar vertebrae, if each vertebra had a cranio-caudally shorter body in the slow loris, then it would have a relatively shorter lumbar region than the lesser galago. An elongated lumbar region would facilitate rapid sagittal mobility required for leaping in the latter group. However, the data show that relative cranio-caudal length of the vertebral body is greater in the lesser galago only in the three caudalmost lumbar vertebrae (L6-L8) (Tables 3-4; Figs. 2-3). Although it has been argued that rapid flexion-extension of a long lumbar region could be expected to assist leaping (Erikson, 1963; Shapiro, 1993a), data in this study suggest that because of their relatively greater length, L6-L8 vertebrae in the lesser galago would make a greater contribution to an overall elongation of the lumbar region (and consequently, to leaping).

Compared to the lesser galago, lumbar vertebral bodies of the slow loris are characterized by a general decline in their respective relative cranio-caudal length from L1-L9 (Tables 3-4; Figs. 2-3). This characteristic possibly reflects the influence of body size on their specialized positional behavior. Negative allometry of lumbar vertebral body and/or region lengths is not uncommon within primate taxonomic groups, e.g., cercopithecoids, hominoids, subfossil lemurs (e.g, *Palaeopropithecus* and *Babakotia*) etc. (Jungers, 1984; Sanders and Bodenbender, 1994; Shapiro, 1993a; Shapiro and Simons, 2002; Shapiro et al., 2005; Ward, 1993). Reduction of the height of the lumbar body and/or lumbar region promotes lumbar stability by reducing potential

bending moments (Ward, 1993). Although it has been argued that compared to the more generalized quadrupedal strepsirrhines, all lorisids share these characteristics; they seem to be accentuated in the larger-bodied *Nycticebus* (Shapiro, 2007). Cartmill and Milton (1977) have observed that along with a reduced lumbar region (owing to a reduction in the cranio-caudal height of individual vertebral bodies), the axial skeleton of the lorisids is characterized by a wide rib cage, ventral displacement of the thoracic vertebrae, and by an elongated sacrum. Moreover, although there is no reduction in the number of lumbar vertebrae in the lorisids, their thorax is quite elongated, and "contributes disproportionately to the total trunk length" (Cartmill and Milton, 1977: 268). It is possible that lumbar reduction enables these primates to control movements between the thorax and pelvis during bridging behaviors employed to cross gaps in trees. Specifically, with a reduced lower back, and a relatively elongated, stiff thoracic region, the trunks of these primates are long enough to facilitate reaching across gaps, but rigid enough for the maintenance of controlled movements (cf. Cartmill and Milton, 1977).

Both cercopithecoid species have 9 lumbar vertebrae. The patterns of changes in vertebral body height are practically identical between the cercopithecoid monkeys (Tables 9-10; Figs. 8-9). However, the vervet is characterized by relatively taller lumbar bodies, and consequently a relatively longer lumbar region compared to that of the patas (Tables 9-10; Figs. 8-9). Compared to the apes, the cercopithecoids have a relatively long lumbar region that most likely facilitates leaping or running by increasing sagittal mobility (Jungers, 1984; Ward, 1991; Shapiro, 1993a). On the other hand, within cercopithecoids, the lumbar region shows negative alloemtry in length, i.e., larger cercopithecoids have relatively shorter lumbar regions (Jungers, 1984). Jungers' (1984) suggestion, and the observation in the present study that relative shortening of the lumbar region may be associated with the rigidity of the spine are consistent

with Hurov's (1987) observation that vervets use spinal flexibility to increase stride length, while larger-bodied patas monkeys (with their relatively reduced lumbar segments) do not.

Although not part of my current study, Hurov (1987) noted another distinctive feature in the axial skeletons of both vervet and patas monkeys. He observed that the intervertebral discs of the vervet monkey were thicker than those of the patas monkey. The insertion of thicker and flexible cartilaginous discs into the vertebral column of the vervet monkey would further elongate its spinal column and impart greater flexibility. Therefore, in vervets, thicker discs facilitate greater range of spinal motion that eventually permits increased hindlimb step length during galloping (Hurov, 1987).

Interzygapophyseal distance

Greater interzygapophyseal distance in the lumbar region (with the para-sagittally oriented lumbar interzygapophyses) would promote a greater range of sagittal plane mobility (flexion-extension; Shapiro, 2007). Interzygapophyseal distance may also be a morphological by-product of the cranio-caudal length of the vertebral body. In the case of *G. senegalensis*, *C. aethiops*, and *E. patas*, the patterns of changes in interzygapophyseal distance across vertebrae roughly mirror that of the cranio-caudal length of the vertebral body (Tables 5 and 11; Figs. 4 and 10). On the other hand, this is not the case with *N. coucang* (Table 5; Fig. 4).

The significantly greater relative interzygapophyseal distance for the lesser galago (apart from L8), compared to that of the slow loris, supports my prediction, and provides evidence that this characteristic is useful for a habitual leaper with rapid spinal extension. Likewise, vervet lumbar vertebrae with their greater interzygapophyseal distance would promote rapid sagittal movement that this monkey makes for increasing hindlimb stride length during galloping (Hurov, 1987). On the other hand, reduced interzygapophyseal distance in both slow loris and

patas monkey would also contribute to a reduced range of sagittal-plane movement, and correspondingly, to greater sagittal-plane stability.

Spinous process length

The lumbar spinous processes act as bony levers capable of extending the lower back. The most prominent muscle that acts on the spinous processes in the lumbar region is multifidus. In humans, this muscle consists of fascicles that form overlapping groups. At each level, a fascicle arises from the base and caudolateral edge of the spinous process, while several fascicles arise together from the caudal tip of the spine. The fascicles in each group diverge caudally to the transverse elements, the iliac crest, and the sacrum (Bogduk and Twomey, 1987; Stern, 2005). The attachments of multifidus in primates dissected in this study did not differ noticeably from those described for humans (see also Howell and Straus, 1933; Kumakura and Inokuchi, 1992; Curtis, 1995).

The principal action of multifidus is extension of the lower back (Macintosh and Bogduk, 1986). It was reported that the lever arm for multifidus, as expressed by the dorsal projection of the spinous process, was longer (relative to body size) in indriids than it was in strepsirrhines who leaped less frequently, or in more dorsostable primates (hominoids and atelines; Shapiro, 1991). This indicates more effective back muscle leverage in indriids, and is most likely attributable to the rapid spinal extension during leaping (Fleagle, 1977a; Shapiro, 1991), and possibly also galloping. It was therefore expected in the present study that primates with a rapid sagittal movement of the back would exhibit relatively longer lumbar spinous process compared to those with less sagittally mobile back.

Data for relative spinous process length provide inconsistent support for this expectation. Although lumbar vertebrae of the habitual leaper *G. senegalensis* had relatively longer spinous

processes than those of *N. coucang* (slow-moving quadruped), the differences were not significant at any vertebral level between the species (Table 6; Fig. 5). This observation most likely suggests that the role of multifidus may not be as important in spinal extension during leaping (of lesser galago) as thought by other investigators (e.g. Shapiro, 1991, 1993a). Similarly, in the cercopithecoid pair, relative length of lumbar spinous processes is significantly reduced in the more dorsomobile vervet than in the dorsostable patas (Table 12: Fig. 11). Once again, this observation contradicts the expectation that a longer spinous process (and the consequently greater lever arm for multifidus) would be characteristic of primates with rapid sagittal spinal mobility.

A number of explanations can be offered for the rejection of the original prediction regarding the differences in relative spinous process length between dorsomobile (lesser galago and vervet) and dorsostable (slow loris and patas) monkeys. It is possible that any difference between dorsomobile and dorsostable primates with respect to spinous process is reflected in its shape and orientation, and not necessarily in its contribution to the extensor lever arm. In other words, it may not be muscle leverage that is important, but the direction of "pull" of a muscle (Slijper, 1946; Shapiro, 1991, 1993a), or the ability of the spines to "lock" in order to prevent hyperextension (Erikson, 1963; Kelley, 1986). Shapiro (2007) observed that the spinous process of lorisid primates was more perpendicular to caudally oriented (relative to that of the galagids, which had more cranially oriented lumbar spinous process), resembling that of primates (e.g., apes, atelines, some subfossil lemurs) whose positional behavior relies on sagittal-plane spinal stability and/or orthograde/antipronograde postures (Sanders and Bodenbender, 1994; Shapiro, 1993a, 1995; Shapiro et al., 2005). On the other hand, there have been no previous attempts to quantify the shape or orientation of the spinous process in cercopithecoid monkeys. A future

analysis involving the quantification of these characteristics in the cercopithecoid monkeys should provide additional insights on the results reported here.

Secondly, it is possible that there truly are no differences between dorsomobile and dorsostable primates with respect to the extensor leverage of the multifidus (as reflected in the relative spinous process length). In other words, and more specifically, multifidus activity might be equally important in rapid sagittal movement during leaping, as it is in locomotor behaviors requiring a stable spine. Although this possibility might explain the absence of significant differences in relative spinous process length between strepsirrhines, it does not explain the differences in relative fiber length between the strepsirrhines (with the lumbar multifidus of lesser galago having significantly longer fibers. See chapter 2. Tables 13, 16, 19), nor does it explain why there were significant differences in this characteristic (at each vertebral level) between the cercopithecoid monkeys. Future work on the in vivo analysis of multifidus activity in the species in this study should clarify this issue.

Position and orientation of transverse process

Values for the ventro-dorsal position of lumbar transverse processes reported here reflect the placement of the tips of the transverse processes (in a transverse plane) relative to the ventral aspect of the vertebral body (Fig. 1d). Although prior studies have identified distinctive differences among primates in transverse process morphology (e.g., Benton, 1967, 1974; Ankel, 1972; Filler, 1986; Kelley, 1986), their focus on the site of origin of transverse process (its "root") can be misleading with respect to muscle leverages. Because of the angular orientation of transverse process, the bony structure itself may be far removed from the root with respect to a transverse plane. Therefore, in order to consider the leverages of muscles which attach to the tranverse processes (longissimus or quadrates lumborum), it is more important to establish how

far ventrally or dorsally the bony structure lies in relation to the ventral (or dorsal) aspect of the vertebral body, than to determine where the transverse process originates (body, pedicle, or lamina).

In this study, a value of zero (0) for the ratio "ventro-dorsal position of transverse process/GM" indicates that the tip of the bony process lies in line with the ventral aspect of the vertebral body; while a value of one (1) indicates that the tip lies along the dorsal aspect of the vertebral body . A value greater than 1 indicates that the tip lies dorsal to the dorsalmost aspect of the vertebral body, while a value less than 1 indicates that the tip lies ventral to the dorsal aspect of the vertebral body. These are true regardless of the site of the root of the transverse process.

The results show values closer to or greater than 1.0 for slow loris at all vertebral levels, with significant differences between those of the lesser galago (whose values are well below 1.0) (Table 7; Fig. 6). These distinctions indicate that the transverse processes are more ventrally positioned in the lumbar vertebrae of lesser galago. Orientations of transverse process are also more acute in the lesser galago than in the slow loris (Table 8; Fig. 7). A similar pattern was also noticed in the cercopithecoid monkeys, with more ventrally positioned and acute-angled transverse processes in the vervet than in the patas (Tables 13-14; Figs. 12-13). These results suggest a larger compartment for the erector spinae muscle mass in the lesser galago and the vervet than in the slow loris and the patas. Because primates in the former group are characterized by rapid sagittal spinal movement, it is plausible that more ventrally positioned and acute-angled transverse process facilitate such movement.

Some authors have argued that transverse process morphology (ventro-dorsal position and orientation) is related to body size. Halpert et al. (1987) found that in African bovids, larger

species had more perpendicularly oriented transverse process relative to a sagittal plane. In this study, within each pair of primates, the larger species (*N. coucang* and *E. patas*) exhibits more dorsally oriented transverse process (Tables 8 and 14; Figs. 7 and 13). This characteristic is similar to that in other dorsostable primates (e.g., hominoids, atelines), and appears to confer spinal stability in conjunction with a larger body size (Ward, 1993; Sanders and Bodenbender, 1994; Shapiro, 1993a). Therefore, size-related differences between lesser galago and slow loris on the one hand; and between vervet and patas monkeys on the other make it difficult to ascertain whether transver process position and orientation specifically reflect differences in spinal movement pattern. Further research on this aspect of transverse process morphology, and utilizing a larger sample size, is needed in order to test the hypothesis that the position and orientation of transverse process are somehow related to body size.

Table 1: Sample size

Taxon	Number of specimens	Sources of specimens
Galago senegalensis	9	Dept. of Mammalogy, American Museum of Natural History.
Nycticebus coucang	9	Dept. of Mammalogy, US National Museum of Natural History.
Chlorocebus aethiops	50	
Erythrocebus patas	50	Caribbean Primate Research Center, University of Puerto Rico.

Table 2: Functional relevance of the lumbar vertebral measurements

Measurements	Functional relevance[a]		Measuring device
Vertebral body: craniocaudal length	**Longer**: greater lumbar flexibility	**Shorter**: greater lumbar stability; resistance to bending	Caliper measurement
Spinous process: length	**Longer**: increased muscular leverage for sagittal plane spinal extension	**Shorter**: reduced muscular leverage for sagittal plane spinal extension	Caliper measurement
Transverse process: ventrodorsal position and orientation	**More ventral**: larger compartment for epaxial muscle mass.	**More dorsal**: reduced compartment for epaxial muscle mass.	Digital measurement on ImageJ
Interzygapophyseal distance: craniocaudal	**Zygapophyses farther apart**: wider range of motion in sagittal plane spinal flexion/extension	**Zygapophyses closer together**: decreased range of motion in sagittal plane spinal flexion/extension	Digital measurement on ImageJ

[a]Functional relevance of the lumbar vertebral measurements are compiled from Ankel (1967), Benton (1967), Gambaryan (1974), Jenkins (1974), Hurov (1987), Godfrey and Jungers (2003), Sanders and Bodenbender (1994), Sanders (1998), Shapiro (1993, 1995, 2007), Shapiro and Simons (2002), Shapiro et al (2005), Ward (1993).

Table 3: Cranio-caudal length of vertebral body (ventral)/GM: Strepsirrhines (Mean ± SD)

Vertebral level	*G. senegalensis* (n = 9)	*N. coucang* (n = 9)	ANOVA (between species, within vertebral level)	
			F	p
L1	0.813775 ± 0.133002	0.995287 ± 0.248057	3.743	0.036
L2	0.861824 ± 0.154353	0.938447 ± 0.118185	1.398	NS (0.127)
L3	0.883024 ± 0.132683	0.955425 ± 0.171954	1.000	NS (0.166)
L4	0.929504 ± 0.093734	0.935456 ± 0.084257	0.020	NS (0.445)
L5	0.974684 ± 0.07518	0.938646 ± 0.077119	1.008	NS (0.165)
L6	1.110823 ± 0.165223	0.916382 ± 0.094784	9.378	0.004
L7	1.063166 ± 0.191762	0.913482 ± 0.119656	3.947	0.032
L8	0.909768 ± 0.078377	0.859558 ± 0.061121	2.082	NS (0.086)
L9	---	0.859676 ± 0.154024	---	---
ANOVA (within species, across vertebral level)	F = 5.639	F = 0.790	---	
	p = 0.000	NS (p = 0.307)		

Table 4: Cranio-caudal length of vertebral body (dorsal)/GM: Strepsirrhines (Mean ± SD)

Vertebral level	*G. senegalensis* (n = 9)	*N. coucang* (n = 9)	ANOVA (between species, within vertebral level)	
			F	p
L1	0.830263 ± 0.199599	1.014621 ± 0.255186	2.914	NS (0.054)
L2	0.887856 ± 0.201142	0.93776 ± 0.122226	0.405	NS (0.267)
L3	0.955097 ± 0.211154	0.9865 ± 0.174206	0.118	NS (0.368)
L4	0.938456 ± 0.088508	0.990317 ± 0.113875	1.164	NS (0.149)
L5	1.009332 ± 0.087234	1.018902 ± 0.109013	0.042	NS (0.420)
L6	1.191497 ± 0.179387	0.964247 ± 0.095294	11.265	0.002
L7	1.109038 ± 0.222257	0.941677 ± 0.124626	3.882	0.033
L8	0.96618 ± 0.113582	0.888919 ± 0.1035	2.017	NS (0.089)
L9	---	0.849198 ± 0.200594	---	---
ANOVA (within species, across vertebral level)	F = 5.014	F = 1.159	---	
	p = 0.000	NS (p = 0.169)		

Table 5: Interzygapophyseal distance/GM: Strepsirrhines (Mean ± SD)

Vertebral level	*G. senegalensis* (n = 9)	*N. coucang* (n = 9)	ANOVA (between species, within vertebral level)	
			F	p
L1	2.405865 ± 0.362599	1.55387 ± 0.555859	13.184	0.002
L2	2.380576 ± 0.64314	1.734029 ± 0.623126	4.406	0.027
L3	2.370382 ± 0.690447	1.648644 ± 0.51085	6.355	0.012
L4	2.393524 ± 0.713147	1.523593 ± 0.474531	9.282	0.004
L5	2.432284 ± 0.76114	1.714094 ± 0.584321	5.042	0.020
L6	2.721859 ± 0.993287	1.703979 ± 0.657435	6.572	0.011
L7	2.609008 ± 0.686957	1.729774 ± 0.545292	8.040	0.007
L8	2.377073 ± 0.666343	1.86441 ± 0.649933	2.397	NS (0.072)
L9	---	2.389697 ± 0.229721	---	---
ANOVA (within species, across vertebral level)	F = 0.179	F = 0.936	---	
	NS (p = 0.495)	NS (p = 0.247)		

Table 6: Spinous process length/GM: Strepsirrhines (Mean ± SD)

Vertebral level	*G. senegalensis* (n = 9)	*N. coucang* (n = 9)	ANOVA (between species, within vertebral level)	
			F	p
L1	0.9235 ± 0.317552	0.732587 ± 0.214988	1.853	NS (0.098)
L2	0.806251 ± 0.319781	0.648421 ± 0.245173	1.165	NS (0.15)
L3	0.687017 ± 0.246273	0.582034 ± 0.20247	0.831	NS (0.189)
L4	0.642609 ± 0.193003	0.574176 ± 0.17416	0.538	NS (0.238)
L5	0.615277 ± 0.137786	0.571891 ± 0.142034	0.408	NS (0.267)
L6	0.643603 ± 0.126328	0.617199 ± 0.138306	0.169	NS (0.344)
L7	0.682472 ± 0.109708	0.630663 ± 0.157667	0.603	NS (0.225)
L8	0.750768 ± 0.145902	0.638251 ± 0.177394	1.839	NS (0.099)
L9	---	0.65605 ± 0.143205	---	---
ANOVA (within species, across vertebral level)	F = 2.049	F = 0.548	---	
	p = 0.032	NS (p = 0.408)		

Table 7: Ventro-dorsal position of transverse process/GM: Strepsirrhines (Mean ± SD)

Vertebral level	*G. senegalensis* (n = 9)	*N. coucang* (n = 9)	ANOVA (between species, within vertebral level)	
			F	p
L1	0.610684 ± 0.441483	0.961504 ± 0.295086	1.309	NS (0.158)
L2	0.331919 ± 0.064164	1.421048 ± 0.130845	111.709	0.005
L3	0.449276 ± 0.23127	1.277283 ± 0.174746	21.545	0.01
L4	0.695482 ± 0.074821	1.44832 ± 0.265541	37.688	0.000
L5	0.638779 ± 0.118573	1.170157 ± 0.248157	21.889	0.001
L6	0.415662 ± 0.18127	1.225232 ± 0.260603	40.776	0.000
L7	0.498052 ± 0.110924	1.256867 ± 0.309092	36.597	0.000
L8	0.644741 ± 0.1098	1.348988 ± 0.293014	30.392	0.000
L9	---	1.196556 ± 0.09134	---	---
ANOVA (within species, across vertebral level)	F = 2.689	F = 1.169	---	
	p = 0.015	NS (p = 0.177)		

Table 8: Ventro-dorsal orientation of transverse process: Strepsirrhines (Mean ± SD)

Vertebral level	*G. senegalensis* (n = 9)	*N. coucang* (n = 9)	ANOVA (between species, within vertebral level)	
			F	p
L1	69.12933 ± 14.28638	83.971 ± 8.850655	2.34	NS (0.101)
L2	60.855 ± 2.934493	79.01133 ± 10.44076	2.61	NS (0.124)
L3	68.62767 ± 1.323271	81.14867 ± 4.395989	22.316	0.005
L4	64.77967 ± 10.05841	76.2975 ± 7.65416	3.737	0.045
L5	68.46267 ± 10.57475	74.35683 ± 8.955283	1.086	NS (0.161)
L6	61.41043 ± 5.290322	82.3274 ± 2.785604	64.137	0.000
L7	69.722 ± 4.829634	80.63225 ± 3.841363	14.803	0.002
L8	72.364 ± 3.996857	82.786 ± 6.644973	11.195	0.004
L9	---	80.21933 ± 2.930437	---	---
ANOVA (within species, across vertebral level)	F = 1.42	F = 1.031	---	
	NS (p = 0.116)	NS (p = 0.218)		

Table 9: Cranio-caudal length of vertebral body (ventral)/GM: Cercopithecoids (Mean ± SD)

Vertebral level	*C. aethiops* (n = 50)	*E. patas* (n = 50)	ANOVA (between species, within vertebral level)	
			F	p
L1	0.897525 ± 0.090783	0.9379 ± 0.057581	7.13	0.005
L2	0.927638 ± 0.125329	0.982804 ± 0.0669	7.602	0.004
L3	1.134734 ± 0.134966	1.204166 ± 0.092569	9.110	0.002
L4	1.263482 ± 0.133202	1.297899 ± 0.087271	2.362	NS (0.064)
L5	1.392699 ± 0.158972	1.330021 ± 0.111971	5.229	0.012
L6	1.38358 ± 0.137383	1.358776 ± 0.150478	0.75	NS (0.195)
L7	1.385243 ± 0.139003	1.306322 ± 0.131619	8.655	0.002
L8	1.254296 ± 0.142913	1.172224 ± 0.116055	9.766	0.001
L9	1.065314 ± 0.098787	1.051711 ± 0.087918	0.447	NS (0.253)
ANOVA (within species, across vertebral level)	F = 112.049	F = 112.097	---	
	p = 0.000	p = 0.000		

Table 10: Cranio-caudal length of vertebral body (dorsal)/GM: Cercopithecoids (Mean ± SD)

Vertebral level	*C. aethiops* (n = 50)	*E. patas* (n = 50)	ANOVA (between species, within vertebral level)	
			F	p
L1	0.970678 ± 0.103635	0.798832 ± 0.053979	109.013	0.000
L2	1.007473 ± 0.113152	0.826487 ± 0.055858	103.611	0.000
L3	1.239268 ± 0.163495	0.997386 ± 0.081259	88.413	0.000
L4	1.379908 ± 0.147198	1.094759 ± 0.126776	109.513	0.000
L5	1.493026 ± 0.190815	1.138422 ± 0.094685	139.081	0.000
L6	1.486702 ± 0.182772	1.171313 ± 0.131252	98.172	0.000
L7	1.47195 ± 0.178933	1.13764 ± 0.125027	118.761	0.000
L8	1.338015 ± 0.190438	1.032473 ± 0.09944	98.292	0.000
L9	1.135424 ± 0.121588	0.947687 ± 0.081381	68.938	0.000
ANOVA (within species, across vertebral level)	F = 84.542	F = 94.633	---	
	p = 0.000	p = 0.000		

Table 11: Interzygapophyseal distance/GM: Cercopithecoids (Mean ± SD)

Vertebral level	*C. aethiops* (n = 50)	*E. patas* (n = 50)	ANOVA (between species, within vertebral level)	
			F	p
L1	1.436059 ± 0.176147	1.415105 ± 0.07026	0.613	NS (0.218)
L2	1.606239 ± 0.20886	1.538934 ± 0.075447	4.612	0.017
L3	1.898609 ± 0.287604	1.786804 ± 0.11297	6.578	0.006
L4	2.038626 ± 0.287324	1.855991 ± 0.115412	17.484	0.000
L5	2.112537 ± 0.352801	1.840752 ± 0.161359	24.62	0.000
L6	2.049142 ± 0.343633	1.826669 ± 0.220301	14.801	0.000
L7	2.031736 ± 0.345551	1.719892 ± 0.197195	31.005	0.000
L8	1.798307 ± 0.31382	1.580237 ± 0.149274	19.037	0.000
L9	1.58536 ± 0.217188	1.436851 ± 0.130722	14.326	0.000
ANOVA (within species, across vertebral level)	F = 36.607	F = 70.698	---	
	p = 0.000	p = 0.000		

Table 12: Spinous process length/GM: Cercopithecoids (Mean ± SD)

Vertebral level	*C. aethiops* (n = 50)	*E. patas* (n = 50)	ANOVA (between species, within vertebral level)	
			F	p
L1	0.818969 ± 0.085646	0.956679 ± 0.128988	40.643	0.000
L2	0.742455 ± 0.072134	0.826034 ± 0.104122	22.353	0.000
L3	0.813784 ± 0.098145	0.878178 ± 0.115828	9.202	0.002
L4	0.855052 ± 0.102827	0.911332 ± 0.121072	6.421	0.007
L5	0.95231 ± 0.137153	1.007092 ± 0.144722	3.814	0.027
L6	0.988665 ± 0.135885	1.103992 ± 0.189167	12.491	0.001
L7	1.020515 ± 0.144504	1.156408 ± 0.154625	20.833	0.000
L8	1.011218 ± 0.115039	1.187194 ± 0.137265	48.005	0.000
L9	1.011818 ± 0.137454	1.19997 ± 0.116273	46.084	0.000
ANOVA (within species, across vertebral level)	F = 41.914	F = 50.75	---	
	p = 0.000	p = 0.000		

Table 13: Ventro-dorsal position of transverse process/GM: Cercopithecoids (Mean ± SD)

Vertebral level	*C. aethiops* (n = 50)	*E. patas* (n = 50)	ANOVA (between species, within vertebral level)	
			F	p
L2	0.439874 ± 0.084462	0.632318 ± 0.116219	6.292	0.027
L3	0.418601 ± 0.086101	0.539745 ± 0.084841	46.052	0.000
L4	0.333334 ± 0.070039	0.430601 ± 0.07509	44.864	0.000
L5	0.260057 ± 0.095233	0.375197 ± 0.092141	37.75	0.000
L6	0.251242 ± 0.091009	0.337405 ± 0.083554	24.052	0.000
L7	0.247298 ± 0.088131	0.361744 ± 0.097361	37.973	0.000
L8	0.339849 ±0.105567	0.46694 ± 0.12627	28.621	0.000
L9	0.522948 ± 0.13174	0.600761 ± 0.104162	8.802	0.002
ANOVA (within species, across vertebral level)	F = 43.77	F = 41.945	---	
	p = 0.000	p = 0.000		

Table 14: Ventro-dorsal orientation of transverse process: Cercopithecoids (Mean ± SD)

Vertebral level	*C. aethiops* (n = 50)	*E. patas* (n = 50)	ANOVA (between species, within vertebral level)	
			F	p
L2	67.134 ± 6.539024	70.205 ± 4.23557	0.356	NS (0.288)
L3	63.79791 ± 5.518487	69.90306 ± 5.218338	29.707	0.000
L4	59.2816 ± 6.312256	64.3264 ± 4.343763	21.673	0.000
L5	57.3418 ± 7.527514	63.7112 ± 6.315005	21.011	0.000
L6	57.9318 ± 7.494618	61.81612 ± 5.165872	8.98	0.002
L7	60.177 ± 7.568133	60.9036 ± 6.706725	0.258	NS (0.307)
L8	67.71083 ± 7.105933	68.85625 ± 7.052299	0.628	NS (0.215)
L9	77.51733 ± 4.401315	78.56049 ± 6.17007	0.789	NS (0.189)
ANOVA (within species, across vertebral level)	F = 44.287	F = 41.31	---	
	p = 0.000	p = 0.000		

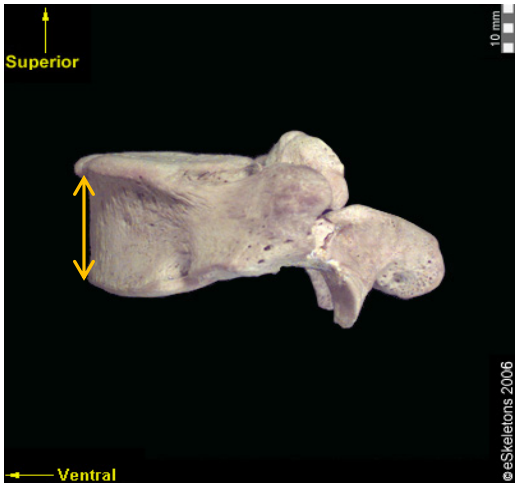

Fig. 1a: Cranio-caudal length of the vertebral body, measured at the midline of the ventral surface of the vertebral body.

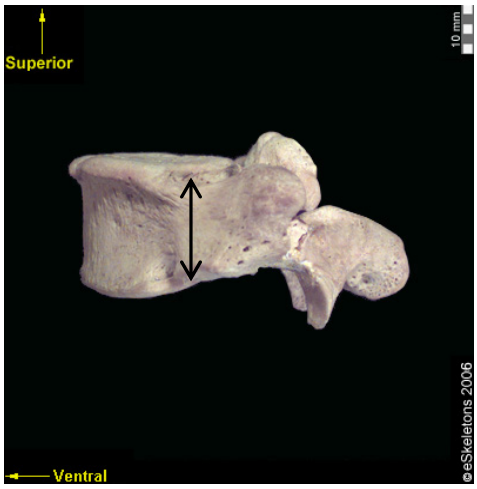

Fig. 1b: Cranio-caudal length of the vertebral body, measured at the lateral aspect of the dorsal surface of the vertebral body.

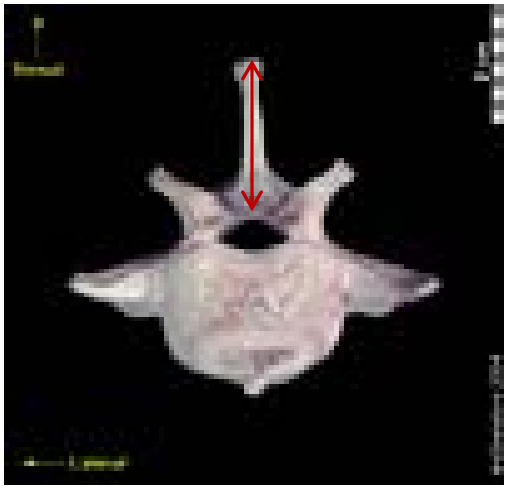

Fig. 1c: Length of the spinous process: distance from the dorsal edge of the neural canal to the tip of the spinous process.

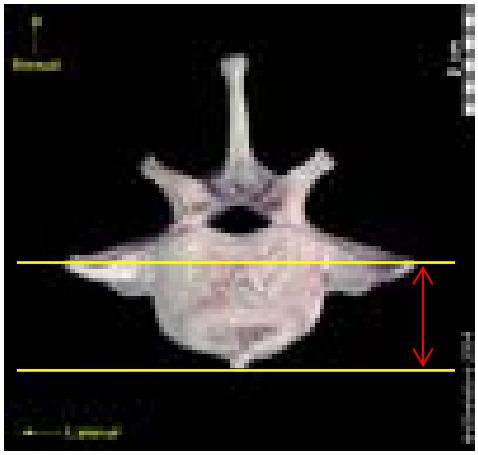

Fig. 1d: Ventro-dorsal position of the transverse process: perpendicular distance between a line drawn through the tips of the transverse processes and line drawn tangent to the most ventral point of the cranial surface of the vertebral body. The shorter the distance between the two horizontal lines, the more ventral is the position of the transverse process.

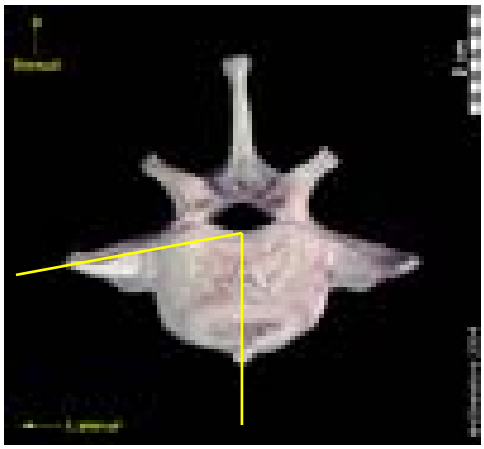

Fig. 1e: Ventro-dorsal orientation of the transverse process: orientation in a coronal plane, measured as the angle formed between the long axis of the transverse process and the midline of the vertebral body. The smaller the angle, the more ventral is the orientation of the transverse process.

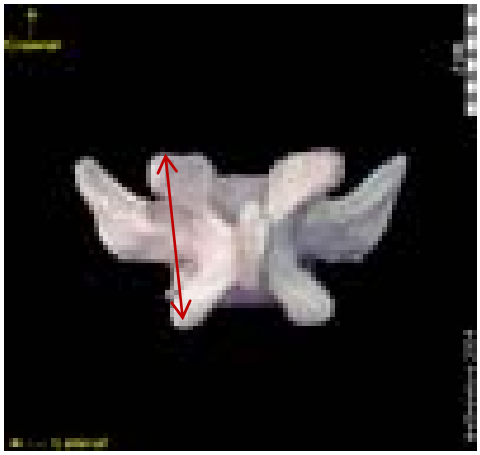

Fig. 1f: Interzygapophyseal distance: distance between tips of pre- and postzygapophyses

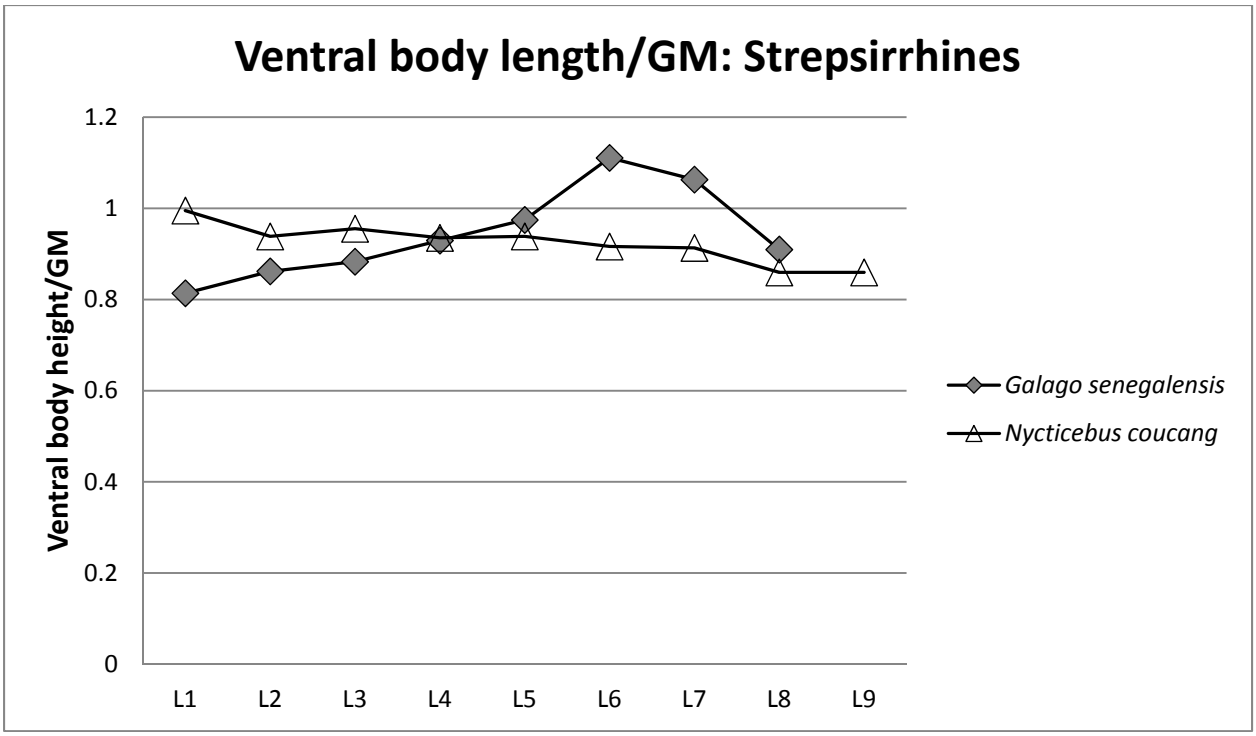

Fig. 2: Cranio-caudal vertebral body length (ventral)/GM: Strepsirrhines

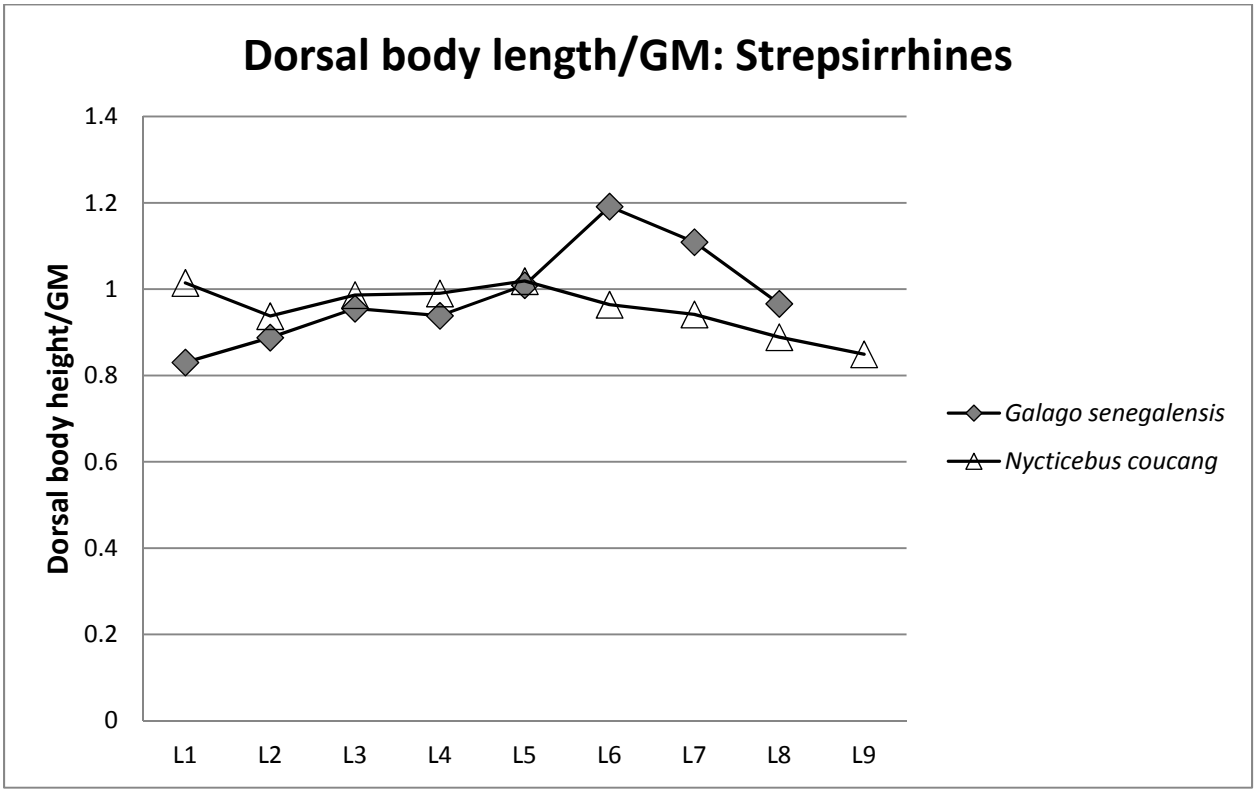

Fig. 3: Cranio-caudal vertebral body length (dorsal)/GM: Strepsirrhines

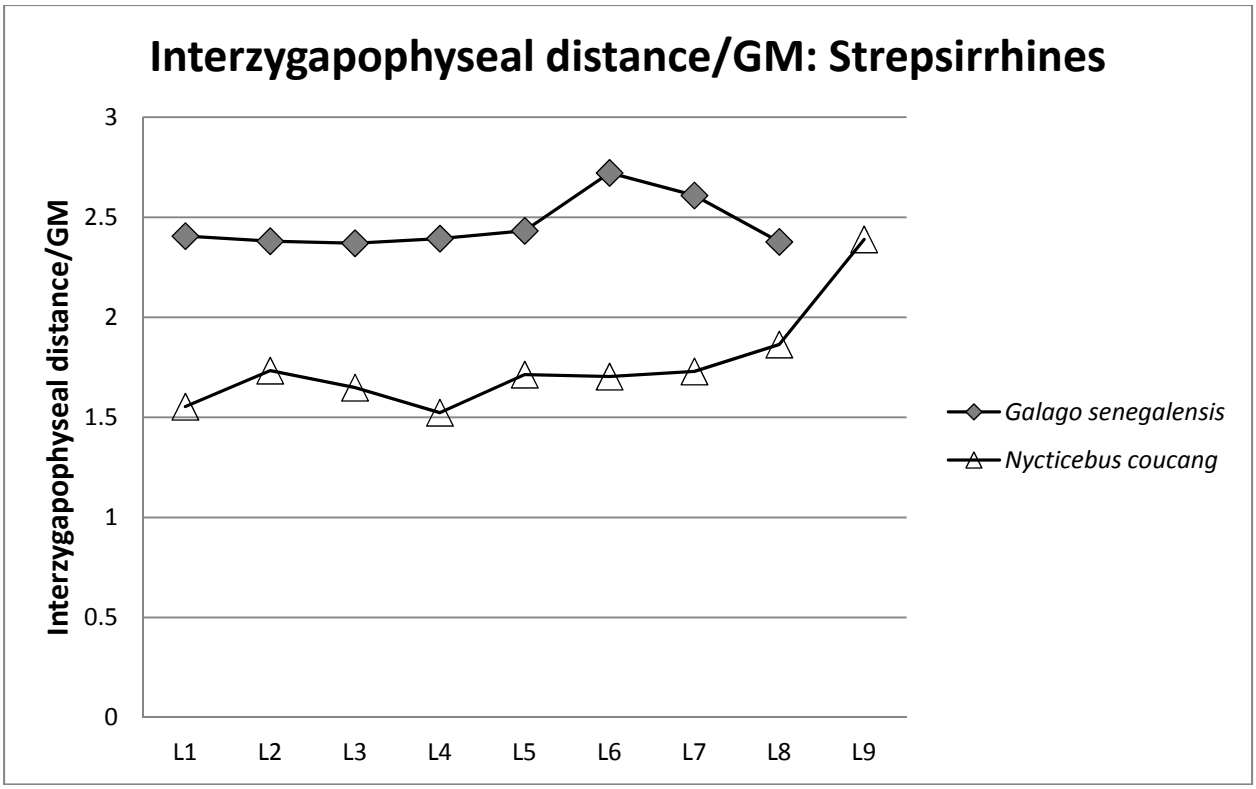

Fig. 4: Interzygapophyseal distance/GM: Strepsirrhines

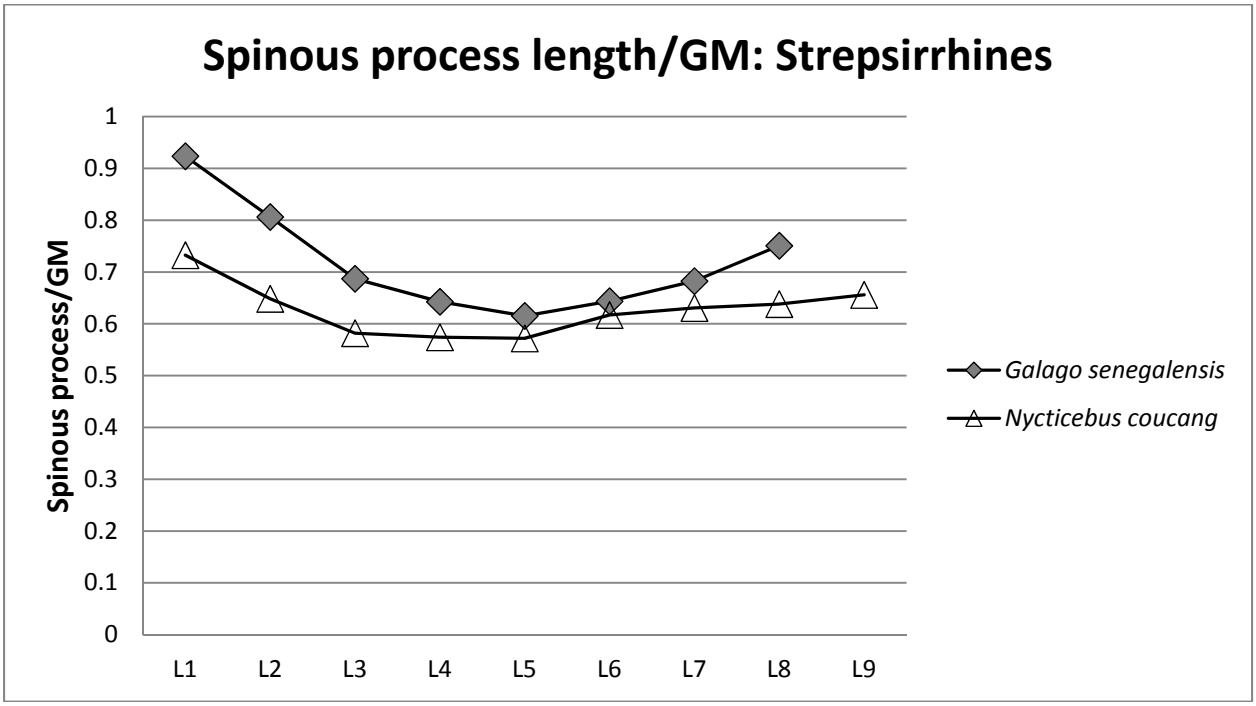

Fig. 5: Spinous process length/GM: Strepsirrhines

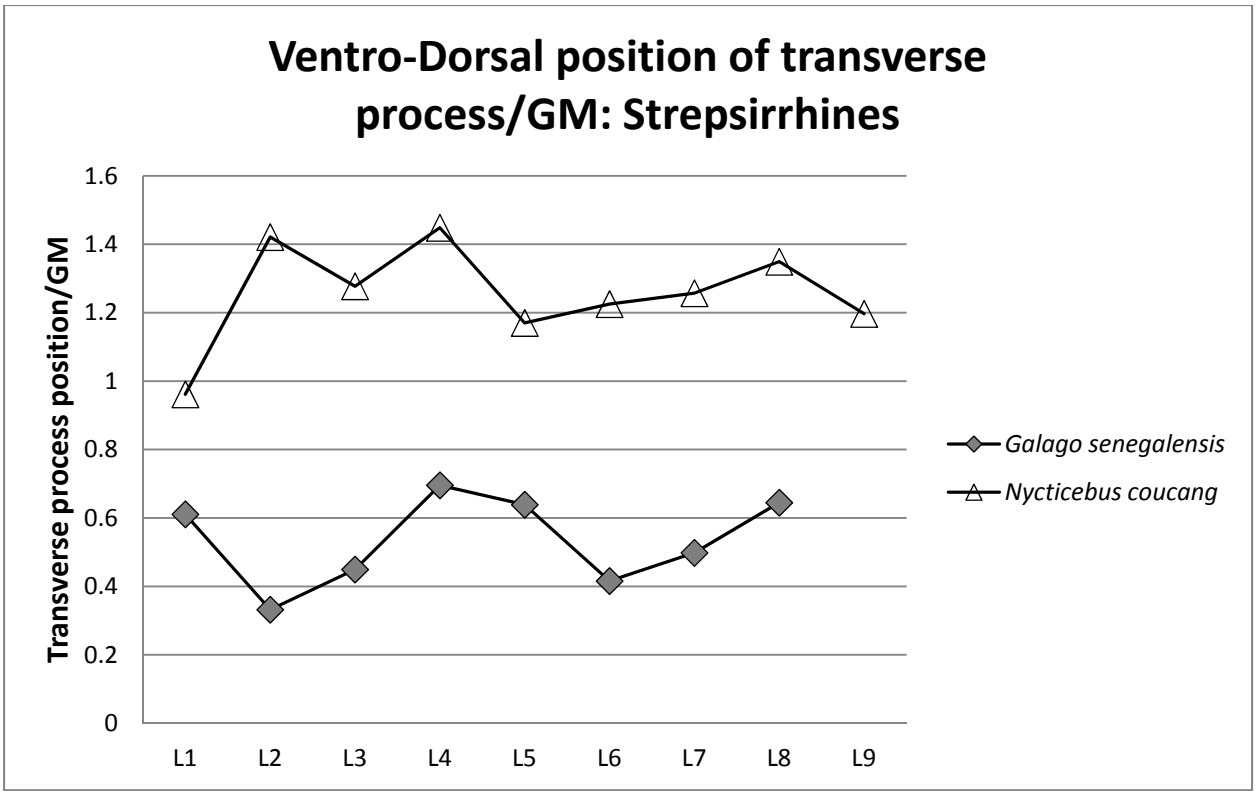

Fig. 6: Ventro-dorsal position of transverse process/GM: Strepsirrhines

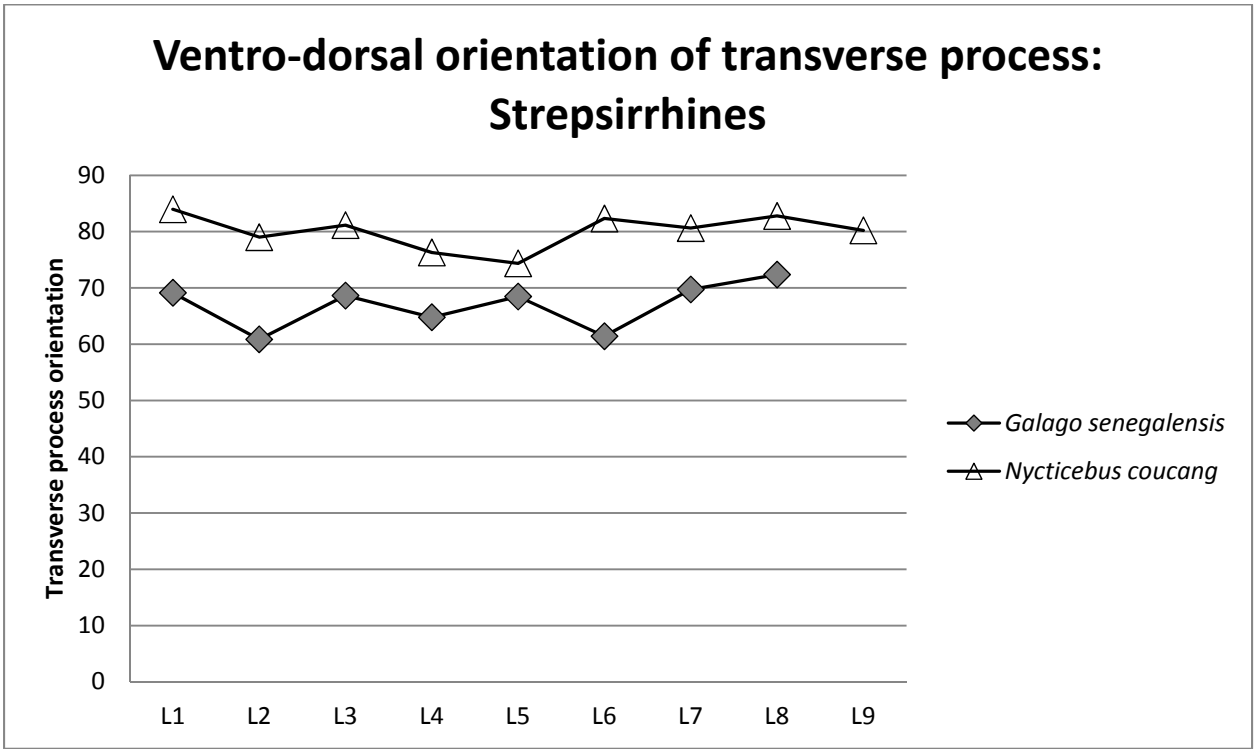

Fig. 7: Ventro-dorsal orientation of transverse process: Strepsirrhines

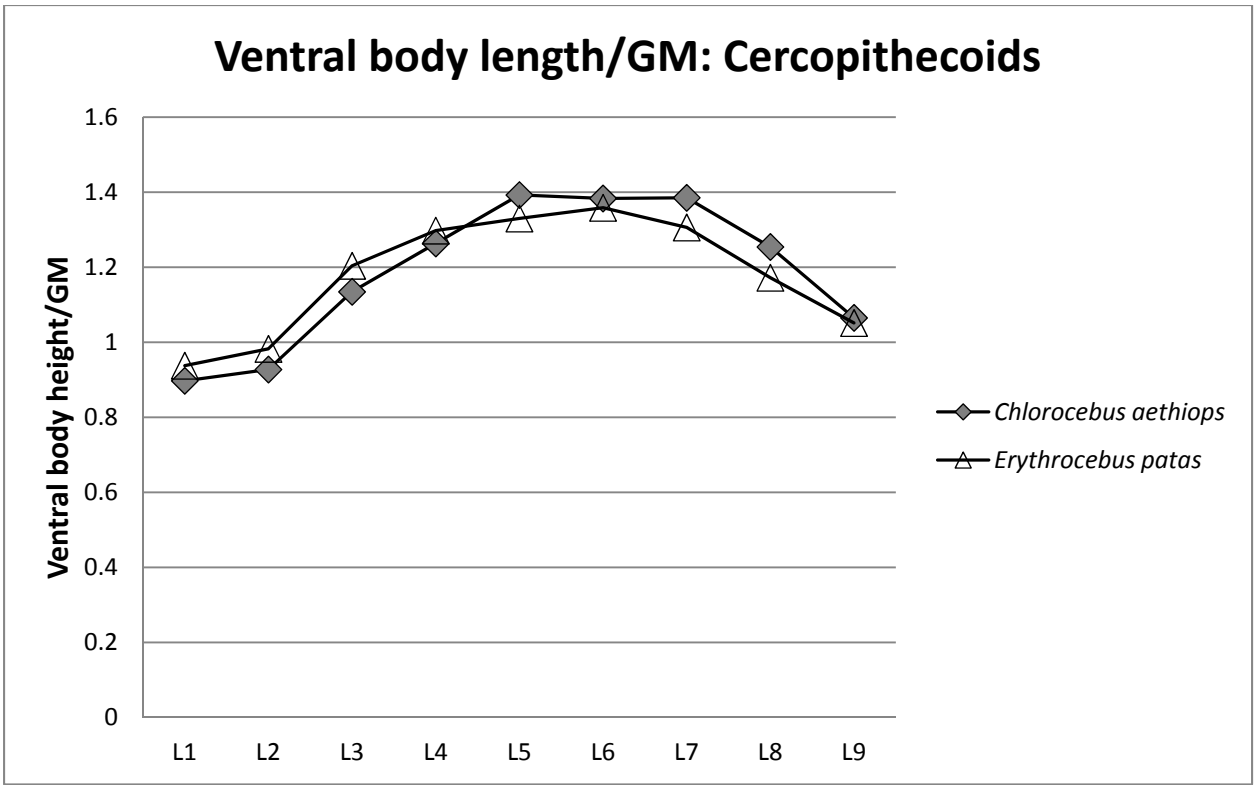

Fig. 8: Cranio-caudal vertebral body length (ventral)/GM: Cercopithecoids

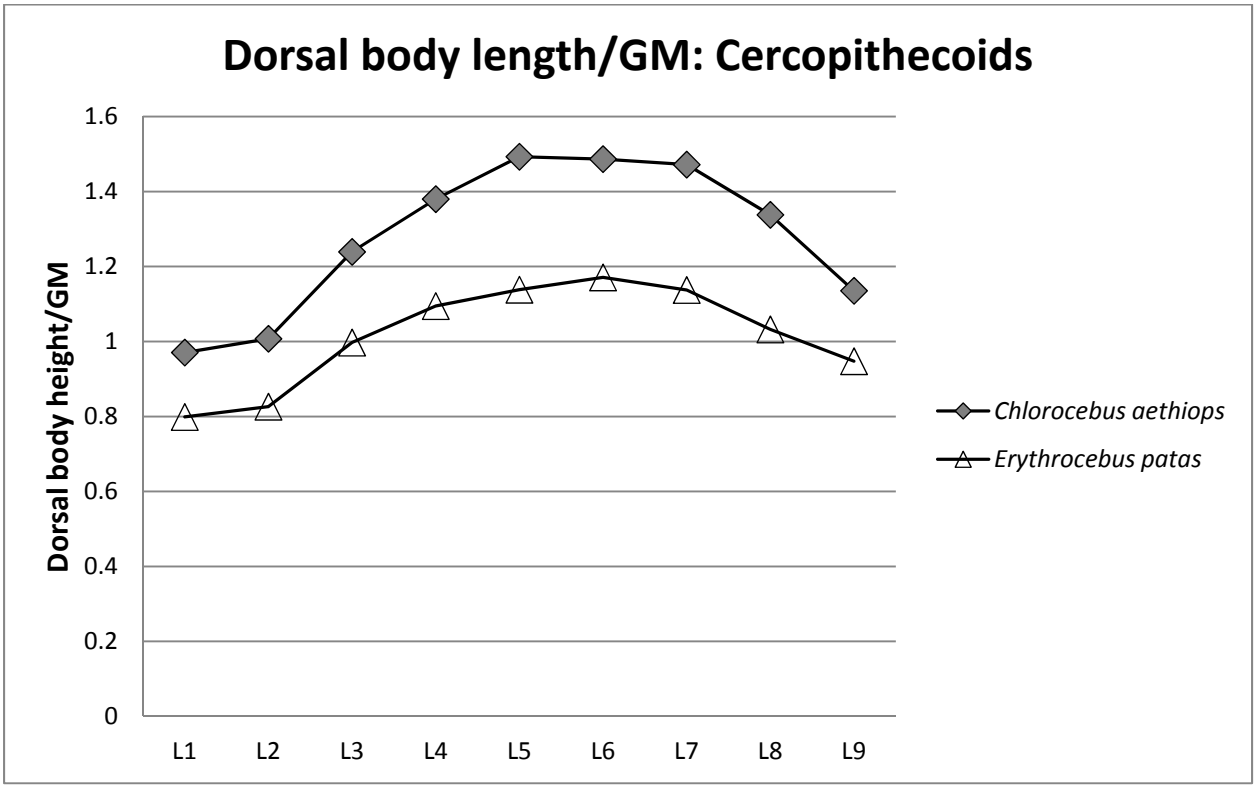

Fig. 9: Cranio-caudal body length (dorsal)/GM: Cercopithecoids

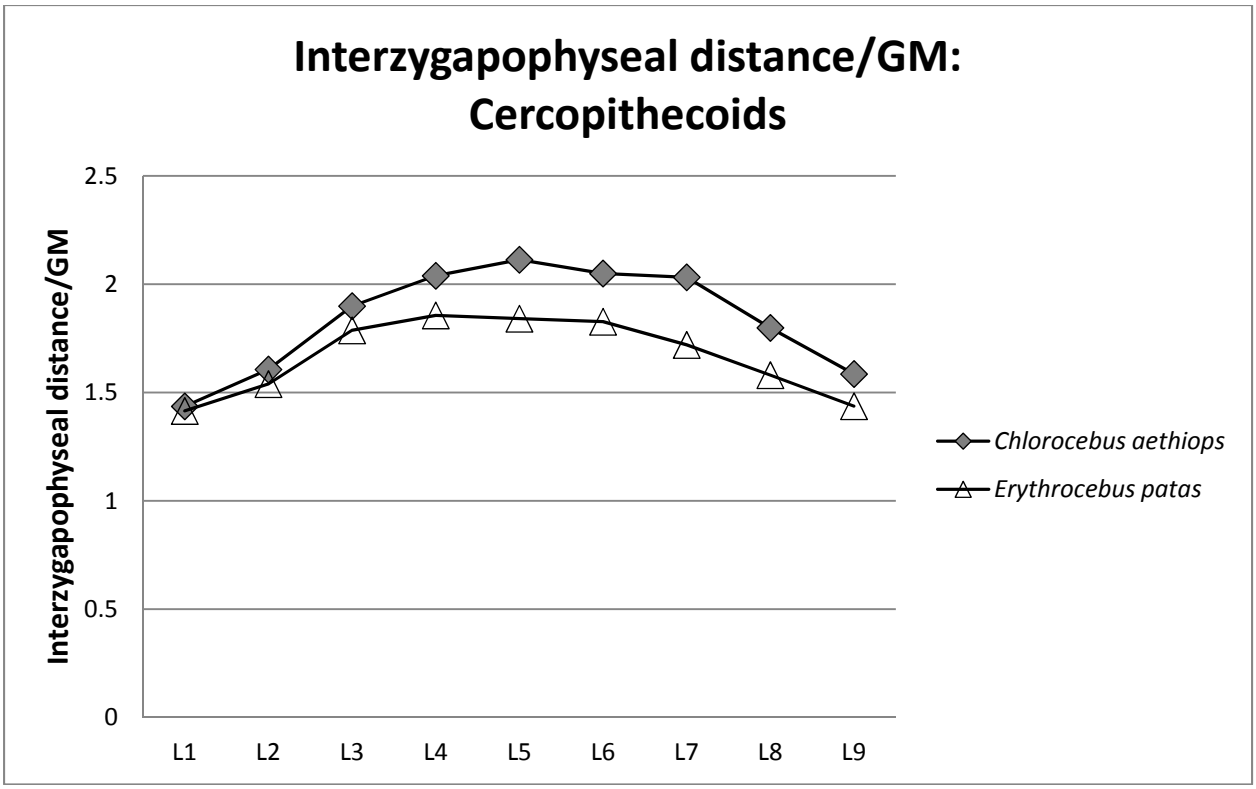

Fig. 10: Interzygapophyseal distance/GM: Cercopithecoids

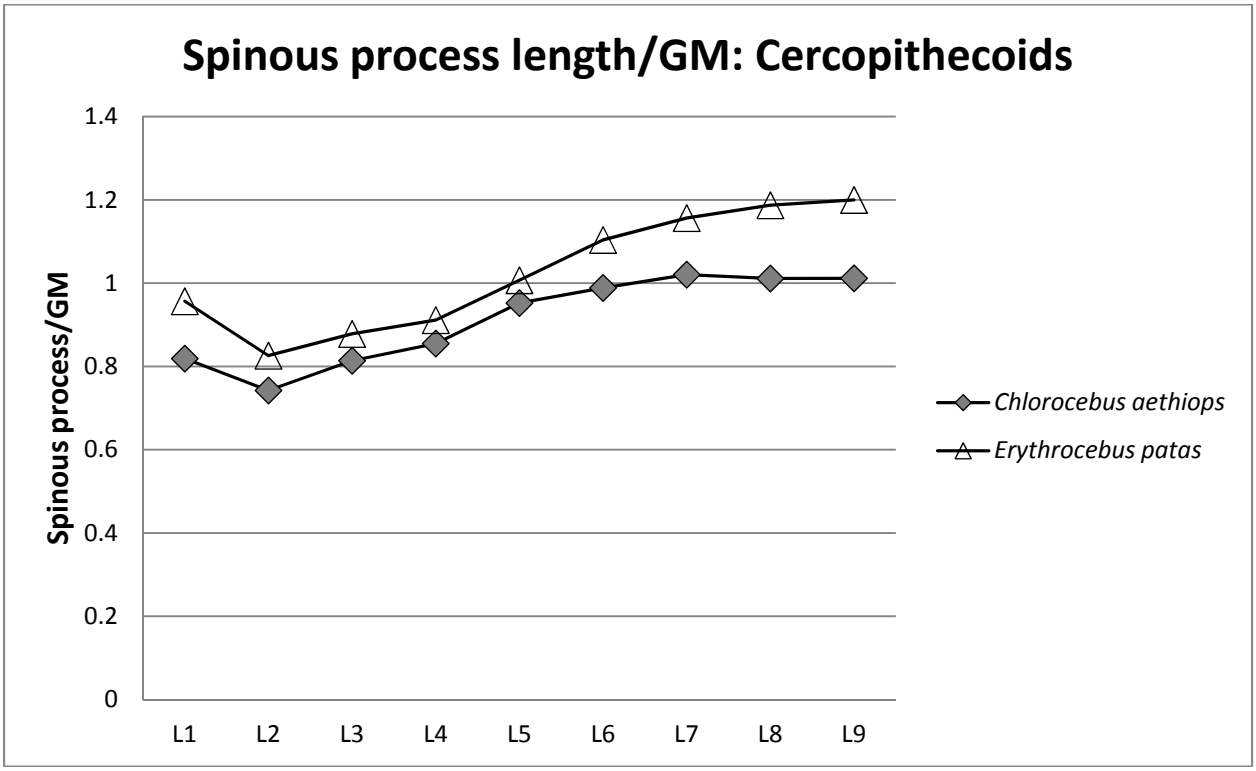

Fig. 11: Spinous process length/GM: Cercopithecoids

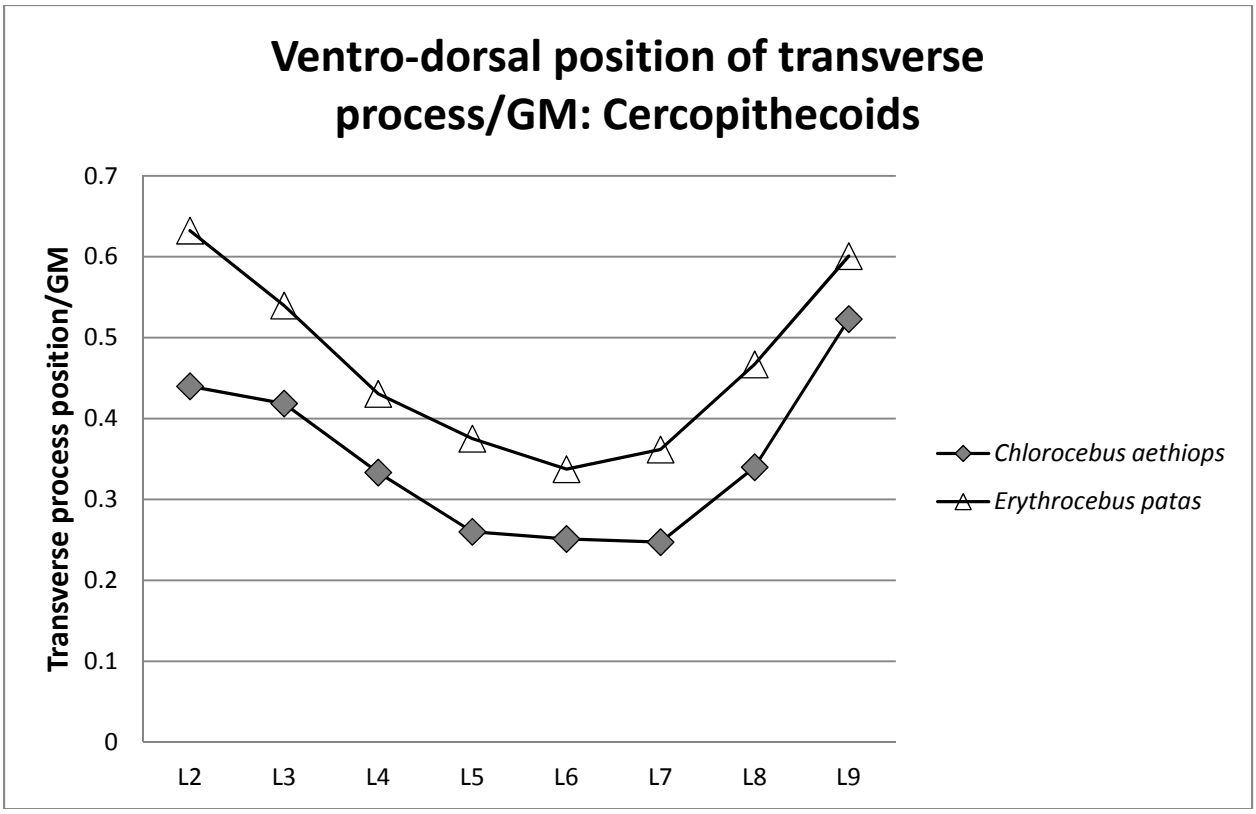

Fig. 12: Ventro-dorsal position of transverse process/GM: Cercopithecoids

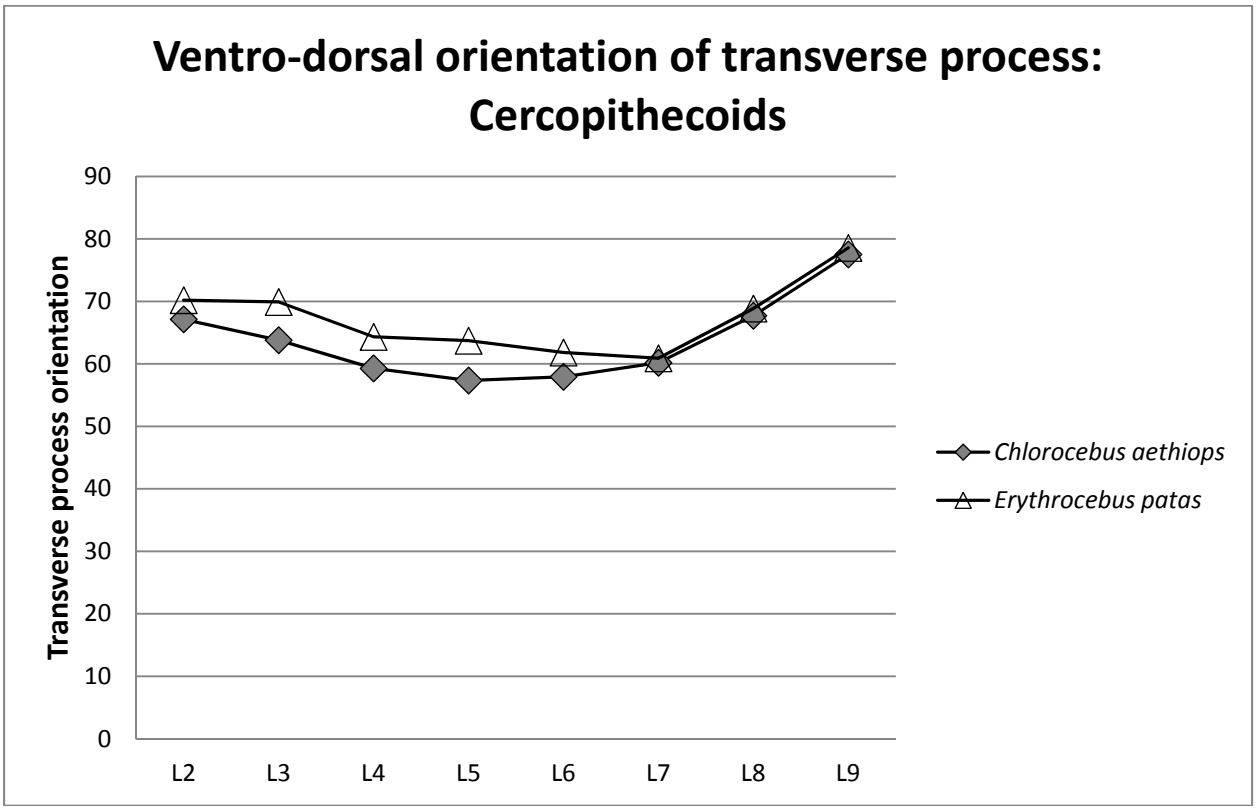

Fig. 13: Ventro-dorsal orientation of transverse process: Cercopithecoids

Chapter 5

Summary and Conclusions

5.1 Synthesis of epaxial muscle characteristics

The present study was undertaken to examine the relationships between the spinal movement patterns and physiological (i.e. architectural), histological, and mechanical (i.e. lever arm) characteristics of selected epaxial muscles in primates. The hypotheses were:

1) Epaxial muscles of primates with a rapid spinal extension pattern will be physiologically suited to producing higher contraction velocities compared to those that do not engage in a similar pattern of spinal extension. I, therefore, predicted that epaxial muscles of *G. senegalensis* and *C. aethiops* would exhibit relatively longer, less pinnate fibers, and relatively smaller PCSAs compared to those of *N. coucang* and *E. patas*, respectively.
2) Epaxial muscles of primates with rapid spinal extension (*G. senegalensis* and *C. aethiops*) will contain more fast-twitch (Type II) fibers; while slow-twitch (Type I) fibers will predominate in those of the dorsostable primates (*E. patas*) and those without rapid back extension (*N. coucang*).
3) The lever arm for epaxial muscles will be larger in dorsomobile primates (*G. senegalensis* and *C. aethiops*) relative to that in dorsostable primates (*N. coucang* and *E. patas*). I predicted that compared to *N. coucang* and *E. patas*, *G. senegalensis* and *C. aethiops* would have relatively taller (lumbar) vertebral bodies, relatively greater interzygapophyseal distance, relatively longer spinous processes, and relatively more ventrally positioned transverse processes.

A summary of the findings of epaxial muscle characteristics for each species is presented below, as well as in Table 1.

Galago senegalensis. Epaxial muscles of the lesser galago are adapted for generating high contraction velocity, as evinced by their smaller pinnation angle, relatively longer fibers, and preponderance of Type II (fast-twitch) fibers. Relatively smaller PCSAs in the majority of the muscle segments are indicative of the fact that the epaxial muscles of the galago have increased velocity at some expense to force. On the other hand, lumbar iliocostalis has relatively longer fibers, relatively larger PCSA, and a high proportion of Type II fibers, suggesting that this muscle is simultaneously capable of generating high tension and increasing excursion and contraction velocity. It is, therefore, possible that lumbar iliocostalis plays a special role in leaping of the lesser galago. Osteological data also show that the lumbar vertebrae of the lesser galago, with their progressively (relatively) taller bodies, relatively greater interzygapophyseal distance, relatively long spinous processes, and relatively more ventrally positioned transverse processes, are well-suited to elongating the lumbar segment of the spine, increasing the lever arm of the epaxial muscles, and facilitating rapid movement on a sagittal plane. These observations suggest that the epaxial muscles of the lesser galago would be employed to augment propulsive locomotor activities requiring rapid muscle recruitment.

Nycticebus coucang. In almost every respect of muscle characteristics, the slow loris, with larger pinnation angles, relatively shorter fibers, and predominance of Type I (slow-twitch) fibers is the mirror opposite of the lesser galago. Relatively larger muscle PCSAs (except for lumbar iliocostalis) are evidence that the epaxial muscles of the slow loris are adapted for force generation, instead of rapid acceleration. The lumbar vertebrae of the slow loris, with their declining (relative) cranio-caudal length, relatively smaller interzygapophyseal distance,

relatively short spinous processes, and relatively more dorsally positioned transverse processes, would reduce the length of the lumbar vertebral column itself, and decrease the lever arm for epaxial muscles. These muscular and skeletal characteristics would be less likely to generate high velocity and rapid sagittal mobility; instead they would facilitate higher force generation, and movements that require stabilizing the trunk for an extended period of time, such as anti-pronograde suspension and bridging.

Chlorocebus aethiops. Epaxial muscles of the vervet monkey tend to be more parallel-fibered. However, contrary to the prediction, these fibers also tend to be relatively shorter than those of the patas monkey. On the other hand, relatively longer tendons indicate a greater capacity for elastic storage in the vervet epaxial muscles. Higher PCSA values suggest that the epaxial muscles of the vervet monkey are adapted for force-generation. However, Type II fibers generally predominate in the lumbar segments relative to the thoracic segments of the vervet epaxial muscles. In addition, osteological data show that the lumbar vertebrae of vervet monkeys have short spinous process, tall vertebral bodies, greater interzygapophyseal distance, and more ventrally positioned transverse processes. It has also been observed that they have thicker intervertebral discs (Hurov, 1987). These osteological characteristics would increase the length of the vertebral column, especially in the lumbar region, thereby increasing the range for sagittal movement. A reduced lever arm for multifidus caused by short spinous processes might be offset by the preponderance of Type II fibers in the lumbar segments of the epaxial muscles. An elongated spinal column (especially the lumbar region), with its accompanying osteological features, would facilitate an enhanced range of sagittal movement for the vertebral column. Epaxial muscles with relatively longer tendons (thus greater elastic storage capacity), and composed primarily of Type II fibers would be useful for active spinal flexion, and increase

rapid accelerating capacity of the epaxial muscles during galloping on the ground by the vervet monkey. In fact, the two characteristics of vervet epaxial muscles, relatively longer tendons and relatively greater PCSA, would seem to be important if the muscles were producing force in order to store strain energy. On the other hand, higher PCSA would allow the epaxial muscles to generate greater force needed to stabilize the trunk against gravity during arboreal locomotion.

Erythrocebus patas. Patas monkeys have more pinnate-fibered epaxial muscles, which also happen to have longer fibers (and relatively shorter tendons) relative to those of the vervet monkey. Smaller PCSA relative to those of the vervet monkeys, while being contrary to the prediction, suggests a trade-off between force and velocity, and possibly indicates the relatively reduced importance of maintaining trunk stability on the stable ground for this habitually terrestrial animal. On the other hand, only 3 segments (out of 6) – lumbar iliocostalis, thoracic longissimus, lumbar longissimus – of the epaxial muscles of the patas monkey tend to contain more Type I fibers relative to those of the vervet monkeys – a characteristic which is expected to impart greater stabilizing potential. Bony morphology of lumbar vertebrae include a relatively longer spinous process, shorter vertebral bodies, short interzygapophyseal distance, and more dorsally positioned transverse processes. Along with thinner intervertebral discs, reduction in vertebral body height and interzygapophyseal distance would make for a shorter lumbar region in the patas monkey relative to that in the vervet monkey. A short lumbar region would reduce the range of sagittal mobility. It is possible that the spinal movement in patas monkeys is determined primarily by the osseo-ligamentous and/or cartilaginous characteristics of the vertebral column (e.g., thickness of intervertebral disc; Hurov, 1987), with the epaxial muscles playing a limited role.

5.2 Limitations of the study

The present work attempts to associate the physiological, histological, and mechanical characteristics of epaxial muscles with documented patterns of spinal movement in two pairs of primates. The one obvious limitation of this work is the small sample size, which, one might argue, would limit the general applicability of its findings. However, studies that involve destructive tissue sampling, and which require access to rare animals in museum collections, are likely to be constrained by a small sample size. Another issue with individual specimens was that all of them had been pre-dissected, and organs/tissues had been removed from each one of them. This condition precluded the collection of accurate measurements of individual body mass. In addition, the choice of study species might also invite questions. Because the present study did not involve any experimental documentation of spinal mobility, I had to rely on works by other investigators who had made observations (quantitative and/or qualitative) on the spinal movement patterns of primates. Each of the four study species had its back movement examined and/or commented on during prior experimental works (*G. senegalensis*: Hall-Craggs, 1965; *N. coucang*: Shapiro et al., 2001; *C. aethiops* and *E. patas*: Vangor, 1979; Hurov, 1987).

Apart from the small sample size in each species, there are a number of limitations of comparative biological studies on adaptation based on only two species (Garland and Adolph, 1994). For example, phenotypic differences could have been outcomes of genetic differentiation caused by speciation (although for certain traits, such as muscle fiber type, it has been observed that the phenotypic response is "plastic", i.e., permitted by the genetic background, but largely determined by the ways in which the muscles are used during ontogeny; see Pette, 2001 for a review). Secondly, it is possible there has been little or no genetic exchange between the two species in question since their evolutionary divergence; and so, at a minimum, they have

diverged somewhat because of random genetic drift alone. Thirdly, two species may have experienced different environmental and developmental conditions, selective pressures, and activity regimes, and consequently have adapted differently. This is, of course, the principal reason for investigating adaptation by comparing species. While uniform selection pressure can offset random genetic drift, it is highly unlikely to envision perfectly identical selection pressure for different species. Even under uniform selection pressure, an identical genetic and phenotypic response is not guaranteed (Hill and Caballero, 1992; Garland and Adolph, 1994). In other words, trying to understand adaptation based on a two-species comparison tends to confound independent variables, such as species membership and environmental factor (presumed selective regime).

To address these problems with two-species comparison, some investigators (e.g., Purvis and Webster, 1999) have suggested that comparison of a phenotypic variable (musculoskeletal, behavioral, etc.) be made within a clade rather than between them. They argue that a comparison between a pair of species belonging to the same clade is more likely to ensure the independence of phenotypic variables.

In the present study, I compared two pairs of primates. The first pair (*G. senegalensis* and *N. coucang*) belongs to the infraorder Lorisiformes (Nekaris and Bearder, 2011), while the second (*C. aethiops* and *E. patas*) belongs to the tribe Cercopithecini (Perelman et al., 2011). Clearly, in none of the pairs, did the species belong to the same genus. The divergence within the lorisiform clade took place 40.34 million years ago (Perelman et al., 2011); while in the cercopithecini clade, the divergence is less than 5 million years old (4.47 million years; Perelman et al., 2011). It may, therefore, be argued that phenotypic differences (positional behavior, musculoskeletal anatomy, etc.) between the lesser galago and slow loris are so extreme because

these characteristics had evolved over a longer period of time; while the reason for subtle phenotypic differences between vervet and patas monkeys is that there was less time for differentiation in anatomy and positional behavior between the the two species.

Each epaxial muscle was divided into thoracic and lumbar segments. Because the muscles of the erector spinae group (iliocostalis and longissimus) are organized as columns (iliocostalis attaches caudally to the iliac crest and sacro-iliac joint, and terminates cranially at the first rib; longissimus cranially extends upto the skull, and caudally into the tail as m. extensor caudae lateralis; Howell and Straus, 1933; Kumakura and Inokuchi, 1992), this was an artificial division based on bony landmarks (zygapophyseal orientation of vertebrae). In addition, the presence of ribs and the caudally oriented spinous processes of thoracic vertebrae reduce the range of movements possible in the thoracic region; thus making the lumbar region the most mobile part of the spinal column between the cervical and sacral regions. In addition, because of the para-sagittaly oriented zygapophyses, sagittal movement takes place only in the lumbar region. As for the characteristics of epaxial muscle tissues, the study design presumes the association of specific physiological phenomena with behavioral characteristics (i.e. spinal movement pattern) of the study-species. Consequently, the interpretation of the results was limited by the "correctness" of the underlying assumptions.

There is no foolproof method to infer dynamic properties from static anatomical data. Of the architectural parameters that were considered, PCSA is an estimate of the effective *maximum* force available to an animal from each muscle. Therefore, the "working ranges" of force during normal activity must be assumed (in this study) to be of the same relative proportion among muscles as is the maximum.

It is well documented that the histological profile of a muscle is a reflection of specific physiological parameters (e.g., time to maximum tension, resistance to "fatigue") (Burke et al., 1971; McDonagh et al., 1980; Burke, 1981). However, for a given fiber type, the values of these parameters appear to vary among muscles (Burke, 1981). Although the hierarchy of contraction times and fatigue-resistance among slow (Type I) and fast (Type II) motor units is consistent in vertebrate skeletal muscles, the degree to which motor units differ from one another is not. In addition, the function of hybrid fibers is poorly understood. The physiological properties of motor units in the epaxial muscles were not directly analyzed in this study. As a result, conclusions based on the physiological nature of the constituent motor units are necessarily implied from the histological profile which associates reactions to slow and fast antibodies with relatively slow and fast rates of tension development.

Intramuscular variability with regard to morphology may also affect the interpretation of results. Because intramuscular variation was not the focus of this study, a mean value was obtained with which the muscle as a whole could be characterized.

With respect to muscle architecture, the extent to which differences in fiber length, pinnation angle, etc., reflect functional variation or whether they are merely accommodations to the geometry of the whole muscle is unclear. A basic problem with muscle immunohistochemistry involved the use of tissues collected from preserved, as opposed to fresh cadavers. The duration of preservation affected the persistence of antibodies. Finally, it would have been ideal to include measurements of intervertebral discs in the analysis of bony vertebrae and muscle lever arms. However, the use of museum osteological collections precluded that possibility.

5.3 Further implications

Results of the present study, which attempted to explain positional behavior in terms of physiological, histological, and mechanical characteristics of epaxial muscles, generally support prior works which associated locomotion with similar features (see Chapter 1). As for observations in this study that have contradicted predictions, it may be argued that the adaptability of a species to a particular locomotory behavior could be affected by neuromuscular adaptation. The interpretation of musculoskeletal function would encounter further difficulties with regard to the plasticity of features such as fiber types. The impact on the interpretability of fossil bones is obvious.

Another point that should be emphasized is a reconfirmation of the necessity of comprehensive documentation regarding both the substrates and the adaptive behavior of the species in question. General designations for primate environments (e.g., terrestrial, arboreal) as well as gross designations for locomotor behaviors (e.g., quadrupedalism, vertical clinging and leaping) may be useful in gross morphological comparisons. However, the interpretation of physiologically-based morphological traits, such as those presented in this study, must be based on more analytical approaches to the interaction between animals and their respective habitats, i.e., *how* the organism adapts to the variety of physical obstacles provided by the unique locality within which it resides. In this regard, the "three-dimensionality" as well as the requisite speed of the animal demands serious consideration. Oxnard (1979) has argued that comparisons in morphological and locomotor behavior should be made *within* a series of primate species differing consistently in their use of habitats. Additionally, a serial "observational design" could be extended to non-primate mammals. *Parallel comparisons between series* would presumably

provide the strongest possible control over spurious, superficial associations between positional behavior and morphology.

Further studies on the locomotor role of the back in primates should quantify the contribution of back motion to hindlimb step length at different speeds. It has been argued, using segmented models adjusted to eliminate back motion while maintaining angular excursions and limb segment lengths, that back movement contributed 5%-12% to hindlimb step length in mammals (terrestrial and arboreal) such as dogs and chipmunks (Hurov, 1987). In addition, comparative EMG studies of recruitment of epaxial muscles as a function of rapid acceleration would provide an ideal independent check of theories related to neural control of interlimb coordination during gait transitions (English and Lennard, 1982).

Another extension of the current study would be to collect comparable data for taxa with similar positional behavior but different size. The lemurid primates include species with a diverse array of positional behavior, such as terrestrial quadrupedalism, arboreal quadrupedalism, and leaping. For example, although both *Lemur catta* and *Eulemur fulvus* are closely related, behavioral studies have distinguished the former from the latter by the former's greater terrestriality, and the latter's greater arboreality/leaping tendency (Tattersall, 1982; Anapol, 1984). This distinction has already been associated with some differences in their respective gross morphological comparisons (Ward and Sussman, 1979). Whether the architectural and histological characteristics of their respective epaxial musculature are substantive of gross locomotor differences remain to be tested. It would be interesting to see in which respect of muscle morphology (architecture and/or fiber histochemistry) these two forms would differ. Thus the epaxial muscles of *L. catta* might contain a higher proportion of Type I

fibers. High proportion of Type I fibers appear to be present in animals that spend a considerable amount of time on the ground (e.g., dog, cat, patas monkeys; Anapol, 1984; this study).

Among monkeys, the locomotor behavior and musculoskeletal anatomy of *Pithecia pithecia* and *Chiropotes satanas* on the one hand; and *Presbytis obscura* and *Presbytis melalophos* on the other are well documented (Fleagle, 1977a, b; Fleagle and Meldrum, 1988; Walker, 2005). *P. pithecia* and *P. melalophos* are leapers, while *C. satanas* and *P. obscura* are arboreal quadrupeds. The behavioral differences are reflected by significant differences in their skeletal configurations and propulsive musculature (Fleagle, 1977a, b; Fleagle and Meldrum, 1988). With regard to muscle morphology, the additional dimension of considerable leaping behavior while retaining a substantial proportion of quadrupedalism in *P. melalophos* may require a higher degree of architectural disparity and a heterogeneous fiber type population chatacterized by a high proportion of Type IIA (Fast-Oxidative) fibers.

The fiber-type composition of epaxial muscles in species that rely on vertical climbing (e.g., apes) has not been investigated. Despite the variety of locomotor repertoires which are found among the apes, it seems reasonable to predict that a bipolar distribution of fiber types would be found in their epaxial muscles. Among the more arboreal species (gibbons, siamangs, chimpanzees, bonobos, and orang-utans), high preponderance of Type I (slow-twitch) fibers would seem to be the most ideal arrangement for large-bodied animals that climb in and out of trees. Climbing probably requires considerable resistance to joint flexion, in addition to rather "deliberate" phasic activity. Gorillas, although largely terrestrial, move about cautiously with quadrupedal walking and climbing. All the great apes, therefore, may exhibit a preponderance of Type I fibers. In addition, for certain strenuous tasks (e.g., escape from predators), one may expect to find a sizeable proportion of fast-oxidative (Type IIB) fibers as well. In addition, the

presence of pinnate-fibered epaxial muscles with large PCSA might allow the large-bodied, dorsostable apes (orang-utans and gorillas) to maintain trunk stability during vertical climbing and cautious arboreal locomotion in general.

The present study was an attempt to investigate the differences in the morphology of a number of epaxial muscles in two pairs of primates in terms of their respective spinal movement patterns. The results of these comparisons generally support the hypothesis that the architectural, histological, and mechanical characteristics of a muscle are associated with the pattern of movement of the part of body it is attached to. Whether the interpretation of these results retains its validity with regard to mammalian (or even tetrapod) locomotion in general remains to be examined.

Table 1: Synthesis of epaxial muscle characteristics

Taxon	Muscle Characteristics		
	Physiology (Architecture)	Histochemistry	Osteology
G. senegalensis	• Pinnation: Narrow • Fiber length: Long • PCSA: Small	• Primarily composed of Type II (fast-twitch) fibers.	• Vertebral body: Progressively taller • Interzygapophyseal distance: Large • Spinous process: Long • Transverse process position/orientation: Ventral
N. coucang	• Pinnation: Wide • Fiber length: Short • PCSA: Large	• Predominance of Type I (slow-twitch) fibers.	• Vertebral body: Progressively shorter • Interzygapophyseal distance: Small • Spinous process: Short • Transverse process position/orientation: Dorsal
C. aethiops	• Pinnation: Narrow • Fiber length: Short • PCSA: Large	• Higher proportion of Type II (fast-twitch) fibers in the lumbar segments of epaxial muscles, relative to those of *E. patas*.	• Vertebral body: Tall • Interzygapophyseal distance: Large • Spinous process: Short • Transverse process position/orientation: Ventral
E. patas	• Pinnation: Wide • Fiber length: Long • PCSA: Small	• Lower proportion of Type II (fast-twitch) fibers in the lumbar segments of epaxial muscles, relative to those of *C. aethiops*.	• Vertebral body: Short • Interzygapophyseal distance: Small • Spinous process: Short • Transverse process position/orientation: Dorsal

Bibliography

Aagaard P, Andersen JL, Dyhre-Poulsen P, Leffers A-M, Wagner A, Magnusson SP, Halkjaer-Kristensen J, Simonsen EB. 2001. A mechanism for increased contractile strength of human pennate muscle in response to strength training: Changes in muscle architecture. J Physiol 534: 613-623.

Abitbol M. 1987a. Evolution of the lumbosacral angle. Am J Phys Anthropol 72: 361-372.

Abitbol 1987b. Evolution of the sacrum in hominoids. Am J Phys Anthropol 74: 65-81.

Abramoff MD, Magelhaes PJ, Ram SJ. 2004. Image processing with ImageJ. Biophotonics International 11: 36-42.

Aerts P. 1998. Vertical jumping in *Galago senegalensis*: the quest for an obligate mechanical power amplifier. Phil Trans R Soc Lond B 353: 1607-1620.

Aerts P, De Clercq D, Plompen H, De Vree F. 1994. "Thigh-powered" jumping in the bushbaby (*Galago senegalensis)*. J Morph 220: 319.

Alexander RM, Bennet-Clark HC. 1977. Storage of elastic strain energy in muscle and other tissue. Nature 265: 114-117.

Alexander RM, Dimery NJ, Ker RF. 1985. Elastic structures in the back and their role in galloping in some mammals. J Zool 207: 467-482.

Alexander RM, Vernon A. 1975. The dimensions of knee and ankle muscles and the forces they exert. J Hum Movmt Stud 1: 115-123.

Anapol FC. 1984. Morphological and functional diversity within the quadriceps femoris in *Lemur fulvus*: architectural, histochemical, and histochemical considerations. PhD dissertation. Stony Brook: State University of New York.

Anapol FC, Barry K. 1996. Fiber architecture of the extensor of the hindlimb in semiterrestrial and arboreal guenons. Am J Phys Anthropol 99: 429-447.

Anapol FC, Gray JP. 2003. Fiber architecture of the intrinsic muscles of the shoulder and arm in semiterrestrial and arboreal guenons. Am J Phys Anthropol 122: 51-65.

Anapol FC, Herring SW. 1989. Length-tension relationships of masseter and digastric muscles of miniature swine during ontogeny. J Exp Biol 143: 1-16.

Anapol FC, Jungers WL. 1986. Architectural and histochemical diversity within the quadriceps femoris of brown lemur (*Lemur fulvus*). Am J Phys Anthropol 69: 355-375.

Anapol FC, Jungers WL. 1987. Telemetered electromyography of the fast and slow extensors of the leg of the brown lemur (*Lemur fulvus*). J Exp Biol 130: 341-358.

Anapol FC, Muhl ZF, Fuller JH. 1987. The force-velocity relation of the rabbit digastric muscle. Arch Oral Biol 32: 93-99.

Anapol F, Shahnoor N, Gray JP. 2004. Fiber architecture, muscle function, and behavior: gluteal and hamstring muscles of semiterrestrial and arboreal guenons. In: Anapol F, German RZ, Jablonski NG, editors. Shaping primate evolution. Cambridge: Cambridge University Press. pp. 99-133.

Andersen JL, Klitgaard H, Saltin B. 1994. Myosin heavy chain isoforms in single fibers from m. vastus lateralis of sprinters: influence of training. Acta Physiol Scand 151: 135-142.

Anemone RL. 1993. The functional anatomy of the hip and thigh in primates. In: Gebo DL, editor. Postcranial Adaptations in Nonhuman Primates. DeKalb: Northern Illinois University Press. pp. 150-174.

Ankel F. 1962. Vergleichende untersuchungen über die skelettmorhologie des greifschwanzes südamerikanischer affen (Platyrrhina). Zeitschrift für Morphologie und Oekologie der Tiere 52: 131-170.

Ankel F. 1965. Der canalis sacralis als indikator für die länge der caudalregion der primate. Folia Primatol 3: 263-276.

Ankel F. 1967. Morphologie von wirbelsäule und brustkorb. Primatologia IV: 1-120.

Ankel F. 1972. Vertebral morphology of fossil and extant primates. In: Tuttle RH, editor. The Functional and Evolutionary Biology of Primates. Chicago: Aldine-Atherton. pp. 223-240.

Anthony MRL, Kay RF. 1993. Tooth form and diet in ateline and alouattine primates: reflections on the comparative method. Am J Sci 293A: 356-382.

Ariano MA, Armstrong RB, Edgerton VR. 1973. Hindlimb muscle fiber populations of five mammals. J Histochem Cytochem 21: 51-55.

Armstrong RB. 1980. Properties and distributions of the fiber types in the locomotory muscles of mammals. In: Schmidt-Nielsen K, Bolis L, Taylor CR, editors. Comparative physiology: primitive mammals. Cambridge: Cambridge University Press. pp. 243-254.

Armstrong RB, Marum P, Saubert CW, Seeherman HJ, Taylor CR. 1977. Muscle fiber activity as a function of speed and gait. J Appl Physiol 43: 672-677.

Armstrong RB, Saubert CW, Seeherman HJ, Taylor CR. 1982. Distribution of fiber types in locomotory muscles of dogs. Am J Anat 163: 87-98.

Asmussen E. 1959. The weight-carrying function of the human spine. Acta Orthop 29: 276-290.

Ausoni S, Gorza L, Schiaffino S, Gunderson K, Lomo T. 1990. Expression of myosin heavy chain isoforms in stimulates fast and slow rat muscles. J Neurosci 10: 153-155.

Avis V. 1962. Brachiation: The crucial issue for man's ancestry. Southwestern Journal of Anthropology 18: 119-148.

Badoux DM. 1965. Some notes on the functional anatomy of *Macropus giganteus* Zimm. With general remarks on the mechanics of bipedal leaping. Acta Anat 62: 418-433.

Bagnall KM, Ford DM, McFadden KD, Greenhill BJ, Raso VJ. 1983. A comparison of vertebral muscle fiber characteristics between human and monkey tissue. Acta Anat 117: 51-57.

Bang ML, Li X, Littlefield R, Bremner S, Thor A, Knowlton KU, Lieber RL, Chen J. 2006. Nebulin-deficient mice exhibit shorter thin filament lengths and reduced contractile function in skeletal muscle. J Cell Biol 173: 905-916.

Bär A, Pette D. 1988. Three fast myosin heavy chain in adult rat skeletal muscle. FEBS Letters 235: 153-155.

Barany M. 1967. ATPase activity of myosin correlated with speed of muscle shortening. J Gen Physiol 50: 197-216.

Baum DA, Larson A. 1991. Adaptation reviewed: A phylogenetic methodology for studying character macroevolution. Syst Zool 40: 1-18.

Bennett-Clark HC. 1977. Scale effects in jumping animals. In: Pedley T, editor. Scale effects in animal locomotion. London: Academic Press. pp. 185-201.

Benton RS. 1967. Morphological evidence for adaptations within the epaxial region of the primates. In: Vagtborg H, editor. The baboon in medical research, vol. 2. Austin: University of Texas Press. pp. 201-216.

Benton RS. 1974. Structural patterns in the pongidae and cercopithecidae. Ybk Phys Anthropol 18: 65-88.

Biewener A. 1998. Muscle function in vivo: a comparison of muscles used for elastic energy savings versus muscles used to generate mechanical power. Amer Zool 38: 703-717.

Biewener A, Alexander RM, Heglund NC. 1981. Elastic energy storage in the hopping of kangaroo rats (*Dipodomys spectabilis*). J Zool 195: 369-383.

Bloch JI, Boyer DM. 2002. Grasping primate origins. Science 298: 1606-1610.

Bock WJ. 1980. The definition and recognition of biological adaptation. Am Zool 20: 217-227.

Bock WJ, Von Wahlert G. 1965. Adaptation and the form-function complex. Evolution 19: 269-299.

Bodine SC, Roy RR, Meadows DA, Zernicke RF, Sacks RD, Fournier M, Edgerton VR. 1982. Architectural, histochemical, and contractile characteristics of a unique biarticular muscle: the cat semitendinosus. J Neurophysiol 48: 192-201.

Bodine SC, Roy RR, Eldred E, Edgerton VR. 1987. Maximal force as a function of anatomical features of motor units in the cat tibialis anterior. J Neurophysiol 6: 1730-1745.

Bogduk N, Twomey L. 1987. Clinical anatomy of the lumbar spine. New York: Churchill Livingstone.

Botterman BR, Binder MD, Stuart DG. 1978. Functional anatomy of the association between motor units and muscle receptors. Am Zool 18: 135-152.

Bottinelli R, Betto R, Schiaffino S, Reggiani C. 1994. Maximum shortening velocity and coexistence of myosin heavy chains isoforms in single skinned fast fibers of rat skeletal muscles. J Musc Res Cell Motil 15: 413-419.

Bottinelli R, Canepari M, Pellegrino MA, Reggiani C. 1996. Force-velocity properties of human skeletal muscle fibers: myosin heavy chain isoform and temperature dependence. J Physiol 495: 573-586.

Brandon R. 1990. Adaptation and environment. Princeton: Princeton University Press.

Brandon-Jones D, Eudey AA, Geissman T, Groves CP, Melnick DJ, Morales JC, Shekelle M, Stewart C-B. 2004. Asian primate classification. Int J Primatol 25: 97-164.

Brooke MH, Kaiser KK. 1970. Muscle fiber types. How many and what kind? Arch Neurol 23: 369-379.

Burke RE. 1975. A comment on the existence of motor unit types. In: Brady RO, editor. The nervous system. The basic neuroscience. New York: Raven. Vol. I, pp. 611-619.

Burke RE. 1980. Motor unit types: functional specialization in motor control. Trends in Neurosciences 3: 255-258.

Burke RE. 1981. Motor units: anatomy, physiology, and functional organization. In: Peachy LD, editor, Handbook of physiology. Bethesda, MD: American Physiological Society. pp. 345-422.

Burke RE. 1986. Physiology of motor units. In: Engel AG, Banker QB, editors. Myology. New York: McGraw Hill. pp. 419-443.

Burke RE, Tsairis P. 1973. Anatomy and innervation ratios in motor units of cat gastrocnemius. J Physiol 234: 749-765.

Burke RE, Tsairis P. 1974. The correlation of physiological properties with histochemical characteristics in single muscle units. Ann NY Acad Sci 228: 145-159.

Burke RE, Tsairis P. 1977. Histochemical and physiological profile of a skeletofusimotor (β) unit in cat soleus muscle. Brain Res 129: 341-345.

Burke RE, Levine DN, Zajac FE, Tsairis P, Engel WK. 1971. Mammalian motor units: physiological-histochemical correlation in three types in cat gastrocnemius. Science 174: 709-712.

Burke RE, Levine DN, Tsairis P, Zajac FE. 1973. Physiological types and histochemical profiles in motor units of the cat gastrocnemius. J Physiol 234: 723-748.

Burke RE, Reymar WZ, Walsh JV. 1976. Relative strength of synaptic input from short-latency pathways to motor units of defined type in cat medial gastrocnemius. J Neurophysiol 39: 447-458.

Burkholder TJ, Fingado B, Baron S, Lieber RL. 1994. Relationship between muscle fiber types and sizes and muscle architectural properties in the mouse hindlimb. J Morph 220: 1-14.

Burkholder TJ, Lieber RL. 2001. Sarcomere length operating range of vertebrate muscles during movement. J Exp Biol 204: 1529-1536.

Burr DB, Ruff CB, Johnson C. 1989. Structural adaptations of the femur and humerus to arboreal and terrestrial environments in three species of macaque. Am J Phys Anthropol 79: 357-367.

Butler-Brown GS, Whalen RG. 1984. Myosin isozyme transitions occurring during the postnatal development of the rat soleus muscle. Dev Biol 102: 324-334.

Cant JGH. 1986. Locomotion and feeding postures of spider and howler monkeys: Field study and evolutionary interpretations. Folia Primatol 46: 1-14.

Carlson H, Halbertsma J, Zomlefer M. 1979. Control of the trunk during walking in the cat. Acta Physiol Scand 105: 251-253.

Carpenter CR, Durham NM. 1969. A preliminary description of suspensory behavior in non-human primates. In: Hofer HO, editor, Proceedings of 2nd International Congress of Primatology 2: 147-154.

Carrier DR. 1990. Activity of the hypaxial muscles during walking in the lizard *Iguana iguana*. J Exp Biol 152: 453-470.

Cartmill M, Milton K. 1977. The lorisiform wrist joint and the evolution of brachiating adaptation in the Hominoidea. Am J Phys Anthropol 47: 249-272.

Cartmill M, Lemelin P, Schmitt D. 2002. Support polygons and symmetrical gaits in mammals. Zool J Linn Soc 136: 401-420.

Chanaud CM, Pratt CA, Loeb GE. 1991. Functionally complex muscles of the cat hindlimb. V. The roles of histochemical fiber-type regionalization and mechanical heterogeneity in differential muscle activation. Exp Brain Res 85: 300-313.

Charles-Dominique P. 1977. Ecology and behavior of nocturnal primates. London: Duckworth Press.

Charles-Dominique P, Bearder SK. 1979. Field studies of lorisid behavior: methodological aspects. In: Doyle GA, Martin RD, editors. The study of prosimian behavior. London: Academic Press. pp. 567-629.

Clauser DA. 1975. The numbers of vertebrae in three African cercopithecine species. Folia Primatol 23: 308-319.

Clauser DA. 1980. Functional and comparative anatomy of the primate spinal column: some postural and locomotor adaptations. PhD dissertation. Milwaukee: University of Wisconsin.

Coddington JA. 1988. Cladistic test of adaptational hypotheses. Cladistics 4: 3-22.

Collatos TC, Edgerton VR, Smith JL, Botterman BR. 1977. Contractile properties and fiber type compositions of flexors and extensors of elbow joint in cat: implications for motor control. J Neurophysiol 40: 1292-1300.

Curtis DJ. 1995. Functional anatomy of the trunk musculature in the slow loris (*Nycticebus coucang*). Am J Phys Anthropol 97: 367-379.

Dammeijer PFM, van Mameren H, van Dijk P, Moorman AFM, Habets P, Manni JJ, Drukker J. 2000. Stapedius muscle fiber composition in the rat. Hear Res 141: 169-179.

Demes B, Fleagle JG, Jungers WL. 1999. Take-off and landing forces of leaping strepsirrhine primates. J Hum Evol 37: 279-292.

Demes B, Fleagle JG, Lemelin P. 1998. Myological correlates of prosimian leaping. J Hum Evol 34: 385-399.

Demes B, Jungers WL, Fleagle JG, Wunderlich RE, Richmond BG, Lemelin P. 1996. Body size and leaping kinematics in Malagasy vertical clingers and leapers. J Hum Evol 31: 367-388.

Demes B, Jungers WL, Gross TS, Fleagle JG. 1995. Kinetics of primate leaping: Influence of substrate orientation and compliance. Am J Phys Anthropol 96: 419-429.

Demes B, Jungers WL, Nieschalk U. 1990. Size- and speed-related aspects of quadrupedal walking in slender and slow lorises. In: Jouffroy FK, Stack MH, Niemitz C, editors. Gravity, Posture and Locomotion in Primates. Firenze: Editrice “I1 Sedicesimo”. pp. 175-197.

Demes B, Larson SG, Stern JT, Jungers WL, Biknevicius AR, Schmitt D. 1994. The kinematics of primate quadrupedalism: “hindlimb drive’ reconsidered. J Hum Evol 26: 353-374.

Dolphin K, Belshaw R, Orme CDL, Quicke DLJ. 2000. Noise and incongruence: interpreting results of the incongruence length difference test. Mol Phylogenet Evol 17: 401-406.

Donisch E. 1973. A comparative study of the back muscles of gibbon and man. In: Rumbaugh DM, editor. Gibbon and siamang, vol. 2. Basel: Karger. pp. 96-120.

Dum RP, Kennedy TT. 1980. Physiological and histochemical characteristics of motor units in cat tibialis anterior and extensor digitorum longus muscles. J Neurophysiol 43: 1615-1630.

Dunbar DC. 1994. The influence of segmental movements and design on whole body rotations during the airborne phase of primate leaps. Z Morphol Anthropol 80: 109-124.

Dunbar DC, Badam GL. 1998. Development of posture and locomotion in free-ranging primates. Neurosci Biobehav Rev 22: 541-546.

Dykyj D. 1980. Locomotion of a slow loris in a designed substrate context. Am J Phys Anthropol 52: 577-586.

Edman K. 1966. The relation between sarcomere length and active tension in isolated semitendinosus fibers of the frog. J Physiol 183: 407-417.

Edström L, Kugelberg E. 1968. Histochemical composition, distribution of fibers, and fatigability of single motor units. Anterior tibial muscle of the rat. J Neurol Neurosurg Psychiatry 31: 424-433.

Eisenberg BR. 1983. Quantitative ultrastructure of mammalian skeletal muscle. In: Peachy LD, Adrian RH, Geiger SR, editors. Skeletal muscle (vol. 10). Baltimore, MD: American Physiological Society. pp. 73-112.

Emerson S. 1985. Jumping and leaping. In: Hildebrand M, Bramble D, Liem K, Wake D, editors. Functional vertebrate morphology. Cambridge: Harvard University Press. pp. 58-72.

English AW. 1980. The functions of the lumbar spine during stepping in cat. J Morphol 165: 55-66.

English AW, Lennard PR. 1982. Interlimb coordination during stepping in the cat: in-phase stepping and gait transitions. Brain Res 245: 353-364.

English AW, Letbetter 1982. Anatomy and innervation patterns of cat lateral gastrocnemius and plantaris muscles. Anat Rec 146: 67-77.

Enstam KL, Isbell LA. 2004. Microhabitat preference and vertical use of space by patas monkeys (*Erythrocebus patas*) in relation to predation risk and habitat structure. Folia Primatol 75: 70-84.

Erikson GE. 1960. The vertebral column of New World primates. Anat Rec 138: 346.

Erikson GE. 1963. Brachiation in New World monkeys and in anthropoid apes. Symp Zool Soc Lond 10: 135-164.

Farrell BD. 1998. "Inordinate fondness" explained: Why are there so many beetles? Science 281: 555-559.

Felder A, Ward SR, Lieber RL. 2005. Sarcomere length measurement permits high resolution normalization of muscle fiber length in architectural studies. J Exp Biol 208: 3275-3279.

Filler AG. 1986. Axial character seriation in mammals: A historical and morphological exploration of the origin, development, use, and current collapse of the homology paradigm. PhD dissertation. Cambridge: Harvard University Press.

Fischer MS. 1999. Kinematics, EMG, and inverse dynamics of the therian forelimb – a synthetic approach. Zool Anz 238: 41-54.

Fischer MS, Lehmann R. 1998. Application of cineradiography for metric and kinematic study of in-phase gaits during locomotion of pika (*Ochotona rufescens*, Mammalia: Lagomorpha). Zoology 101: 148-173.

Fischer MS, Schilling N, Schmidt M, Haarhaus D, Witte HF. 2002. Basic limb kinematics of small therian mammals. J Exp Biol 205: 1315-1338.

Fisher DC. 1985. Evolutionary morphology: beyond the analogous, the anecdotal, and the ad hoc. Paleobiology 11: 120-138.

Fleagle JG. 1977a. Locomotor behavior and muscular anatomy of sympatric Malaysian leaf-monkeys (*Presbytis obscura* and *Presbytis melalophos*). Am J Phys Anthropol 46: 297-307.

Fleagle JG. 1977b. Locomotor behavior and skeletal anatomy of sympatric Malaysian leaf monkeys (*Presbytis obscura* and *Presbytis melalophos*). Ybk Phys Anthropol 20: 440-453.

Fleagle JG. 1978. Locomotion, posture, and habitat utilization in two sympatric Malaysian leaf-monkeys (*Presbytis obscura* and *Presbytis melalophos*). In: Montgomery GG, editor. Ecology of Arboreal Folivores. Washington, DC: Smithsonian Institution Press. pp. 243-251.

Fleagle, JG. 1979. Primate positional behavior and anatomy: naturalistic and experimental approaches. In: Morbeck ME, Preuschoft H, Gomberg N, editors. Environment, behavior, and morphology: dynamic interactions in primates. New York: Fischer. pp. 313-325.

Fleagle JG. 1999. Primate adaptation and evolution. San Diego, CA: Academic Press.

Fleagle JG, Meldrum DJ. 1988. Locomotor behavior and skeletal morphology of two sympatric pitheciine monkeys, *Pithecia pithecia* and *Chiropotes satanas*. Am J Primatol 16: 227-249.

Fleagle JG, Mittermeier RA. 1980. Locomotor behavior, body size, and comparative ecology of seven Surinam monkeys. Am J Phys Anthropol 52: 301-314.

Fleagle JG, Stern JT, Jungers WL, Susman RL, Vangor AK, Wells JP. 1981. Climbing: A biomechanical link with brachiation and with bipedalism. Symp Zool Soc Lond 48: 359-375.

Ford DM, Bagnall KM, McFadden KD, Reid DC. 1986. A comparison of muscle fiber characteristics at different levels of vertebral column in the rhesus monkey. Acta Anat 126: 163-166.

Frolich LM, Biewener A. 1992. Kinematic and electromyographic analysis of the functional role of the body axis during terrestrial and aquatic locomotion in the salamander *Ambystoma tigrinum*. J Exp Biol 162: 107-130.

Fulton JF. 1940. Experimental studies on the functions of the frontal lobes in monkeys, chimpanzees, and man. In: Baitsell GA, editor. Science in Progress. New Haven: Yale University Press. pp. 55-77.

Gál JM. 1993a. Mammalian spinal biomechanics. I. Static and dynamic mechanical properties of intact intervertebral joints. J Exp Biol 174: 247-280.

Gál JM. 1993b. Mammalian spinal biomechanics. II. Intervertebral lesion experiments and mechanisms of bending resistance. J Exp Biol 174: 281-293.

Galat-Luong A, Galat G, Durand J-P, Pourrut X. 1996. Sexual weight dimorphism and social organization in green and patas monkeys in Senegal. Fol Primatol 67: 92-93.

Gambaryan PP. 1974. How mammals run. New York: John Wiley.

Gans C. 1982. Fiber architecture and muscle function. Exerc Spt Sci Rev 10: 160-207.

Gans C, Bock WJ. 1965. IV. The functional significance of muscle architecture – a theoretical analysis. Ergeb Anat Entwickl 38: 115-142.

Gans C, de Vree F. 1987. Functional bases of fiber length and angulation in muscle. J Morphol 192: 63-85.

Garland T, Adolph SC. 1994. Why not to do two-species comparative studies: limitations on inferring adaptation. Physiol Zool 67: 797-828.

Gauthier GF. 1986. Skeletal muscle fiber types. In: Engel AG, Franzini-Armstrong C, editors. Myology. New York: McGraw-Hill. pp. 255-283.

Gauthier GF, Lowey S. 1977. Polymorphism of myosin among skeletal muscle fiber types. J Cell Biol 74: 760-779.

Gauthier GF, Lowey S. 1979. Distribution of myosin isoenzymes among skeletal muscle fiber types. J Cell Biol 81: 10-25.

Gebo DL. 1993. Functional morphology of the foot in primates. In: Gebo DL, editor. Postcranial Adaptations in Nonhuman Primates. DeKalb: Northern Illinois University Press. pp. 175-196.

Gebo DL, Chapman CA. 1995. Positional behavior in five sympatric old world monkeys. Am J Phys Anthropol 97: 49-76.

Gillespie CA, Simpson DR, Edgerton VR. 1974. Motor unit recruitment as reflected by muscle fiber glycogen loss in a prosimian (bushbaby) after running and jumping. J Neurol Neurosurg Psychiat 37: 817-824.

Godfrey LR, Jungers WL. 2003. The extinct sloth lemurs of Madagascar. Evol Anthropol 12: 252-263.

Gollnick PD, Piehl K, Saltin B. 1974a. Selective glycogen depletion pattern in human muscle fibers after exercise of varying intensity and at varying pedaling rates. J Physiol 241: 45-57.

Gollnick PD, Karlsson K, Piehl K, Saltin B. 1974b. Selective glycogen depletion in skeletal muscle fiber of man following sustained contractions. J Physiol 241: 59-67.

Gonyea WJ, Ericson GC. 1977. Morphological and histochemical organization of the flexor carpi radialis muscle in the cat. Am J Anat 148: 329-344.

Gordon T, Thomas CK, Stein RB, Erdebil S. 1988. Comparison of physiological and histochemical properties of motor units after cross-reinnervation of antagonistic muscles in the cat hindlimb. J Neurophysiol 60: 365-378.

Gorza L. 1990. Identification of a novel type 2 fiber population in mammalian skeletal muscle by combined use of histochemical myosin ATPase and anti-myosin monoclonal antibodies. J Histochem Cytochem 38: 257-265.

Gorza L, Gunderson K, Lomo T, Schiaffino T, Westgaard RH. 1988. Slow-to-fast transformation of denerveted soleus muscles by chronic high frequency stimulation in the rat. J Physiol 402: 627-649.

Grand TI. 1972. A mechanical interpretation of terminal branch feeding. J Mammal 53: 198-201.

Grand TI. 1976. Differences in terrestrial velocity in *Macaca* and *Presbytis*. Am J Phys Anthropol 45: 101-108.

Grand TI. 1977. Body weight: Its relation to tissue composition, segment distribution, and motor function. I. Interspecific comparisons. Am J Phys Anthropol 47: 211-240.

Grand TI. 1978. Adaptation of tissue and limb segments to facilitate moving and feeding in Arboreal folivores. In: Montgomery GG, editor, Ecology of Arboreal Folivores. Washington, DC, Smithsonian Institution Press. pp. 231-241.

Grand TI. 1984. Motion economy within the canopy: Four strategies for mobility. In: Rodman PS, Cant JGH, editors. Adaptations to Foraging in Non-human Primates. New York: Columbia University Press. pp. 54-72.

Gray J. 1968. Animal locomotion. New York: W. W. Norton.

Graziotti GH, Rios CM, Rivero JL. 2001. Evidence for three fast myosin heavy chain isoforms in type II skeletal muscle fibers in the adult llama (*Lama glama*) J Histochem Cytochem 49: 1033-1044.

Gregor RJ, Edgerton VR, Perrine JJ, Campion DS, DeBus C. 1979. Torque-velocity relationships and muscle fiber composition in elite female athletes. J Appl Physiol 47: 388-392.

Grubb P, Butynski TM, Oates JF, Bearder SK, Disotell TR, Groves CP, Struhsaker TT. 2003. Assessment of the diversity of African primates. Int J Primatol 24: 1301-1357.

Goslow GE, Cameron WE, Stuart DG. 1977. Ankle flexor muscles in the cat: length-active tension and muscle unit properties as related to locomotion. J Morphol 153: 23-37.

Goslow GE, Reinking RM, Stuart DG. 1973. The cat step cycle: Hindlimb joint angles and muscle lengths during unrestrained locomotion. J Morphol 141: 1-41.

Gunn HM. 1978. Differences in the histochemical properties of skeletal muscle of different breeds of horses and dogs. J Anat 127: 615-634.

Hall KRL. 1966. Behaviour and ecology of the wild patas monkey, *Erythrocebus patas*, in Uganda. J Zool 148: 15-87.

Hall-Craggs ECB. 1965. An analysis of the jump of the lesser galago (*Galago senegalensis*). J Zool 147: 20-29.

Hall-Craggs ECB. 1974. Physiological and histochemical parameters in comparative locomotor studies. In: Martin RD, Doyle GA, Walker AC, editors. Prosimian biology. London: Duckworth. pp. 829-845.

Halpert AP, Jenkins FA, Franks H. 1987. Structure and scaling of the lumbar vertebrae in African bovids (Mammalia: Artiodactyla). J Zool 211: 239-258.

Hämäläinen N, Pette D. 1993. The histochemical profiles of fast fiber IIB, IID, and IIA in skeletal muscle of mouse, rat, and rabbit. J Histochem Cytochem 41: 733-743.

Hämäläinen N, Pette D. 1995. Patterns of myosin isoforms in mammalian skeletal muscle fibers. Micros Res Tech 30: 381-389.

Hanna JB, Chan LK, Schmitt D. 2011. Loris locomotor behavior in relation to skeletal morphology: Disjunction between assumed mobility and utilized range of motion. Am J Phys Anthropol 144 (S52): 155-156.

Hannerz J, Grimby L. 1973. Recruitment order of motor units in man: significance of pre-existing state of facilitation. J Neurol Neurosurg Psychiat 36: 275-281.

Harrison T. 2010. Later tertiary lorisiformes. In: Werdelin L, Saunders WJ, editors. Cenozoic mammals of Africa. Berkeley: University of California Press. pp. 333-349.

Harvey PH, Pagel MD. 1991. The comparative method in evolutionary biology. Oxford: Oxford University Press.

Haxton HA. 1944. Absolute muscle force in the ankle flexors of man. J Physiol Lond 103: 267-273.

Haxton HA. 1947. Muscles of the pelvic limb: a study of the differences between bipeds and quadrupeds. Anat Rec 98: 337-346.

Hermanson JW, Cobb MA, Schutt WA, Muradali F, Ryan JM. 1993. Histochemical and myosin composition of vampire bat (*Desmodus rotundus*) pectoralis muscle targets a unique locomotory niche. J Morphol 217: 347-356.

Herrel A, Adriaens D, Verraes W, Aerts P. 2002. Bite performance in clariid fishes with s hypertrophied jaw adductors as deduced by bite modeling. J Morphol 253: 196-205.

Herring SW, Grimm A, Grimm BR. 1979. Functional heterogeneity in a multipennate muscle. Am J Anat 154: 563-575.

Herring SW, Grimm AF, Grimm BR. 1984. Regulation of sarcomere number in skeletal muscle: A comparison of hypotheses. Muscle Nerve 7: 161-173.

Herzog W, Leonard T, Joumaa V, DuVall M, Panchangam A. 2012. The three filament model of skeletal muscle stability and force production. Mol Cell Biom 9: 175-191.

Hildebrand M. 1959. Motions of the running cheetah and horse. J Mammal 40: 481-495.

Hildebrand M. 1967. Symmetrical gait in primates. Am J Phys Anthropol 26: 18-27.

Hildebrand M. 1974. Analysis of vertebrate structure. New York: John Wiley.

Hill AV. 1938. The heat of shortening and the dynamic constants of muscle. Proc R Soc Lond B 126: 136-194.

Hill WG, Caballero A. 1992. Artificial selection experiments. Ann Rev Ecol Syst 23: 287-310.

Hoffer JA, Loeb GE, Marks WB, O'donovan MJ, Pratt CA, Sugano N. 1987. Cat hindlimb motoneurons during locomotion. I. Destination, axonal conduction velocity, and recruitment threshold. J Neurophysiol 57: 510-573.

Howell AB. 1932. The saltatorial rodent Dipodomys. Proc Am Acad Arts Sci 67: 377-536.

Howell AB. 1938. Morphogenesis of the architecture of hip and thigh. J Morphol 62: 177-218.

Howell AB. 1944. Speed in Animals: their Specializations for Running and Leaping. Chicago: University of Chicago Press.

Howell AB, Straus WL. 1933. The muscular system. In: Hartman CG, Straus WL, editors. The anatomy of the rhesus monkey. New York: Hafner. pp. 89-175.

Hunter JP, Jernvall J. 1995. The hypocone as a key innovation in mammalian evolution. Proc Nat Acad Sci 92: 10718-10722.

Hurov JR. 1987. Terrestrial locomotion and back anatomy in vervets (*Cercopithecus aethiops*) and patas monkeys (*Erythrocebus patas*). Am J Primatol 13: 297-311.

Isbell LA, Pruetz JD, Lewis M, Young TP. 1998. Locomotor activity differences between sympatric patas monkeys (*Erythrocebus patas*) and vervet monkeys (*Cercopithecus aethiops*): implications for the evolution of long hindlimb length in *Homo*. Am J Phys Anthropol 105: 199-207.

Izumo S, Nadal-Ginard B, Mahdavi V. 1986. All members of the MHC multigene family respond to thyroid hormone in highly tissue-specific manner. Science 231: 594-600.

James RS, Navas CA, Herrel A. 2007. How important are skeletal muscle mechanics in setting limits on jumping performance? J Exp Biol 210: 923-933.

Jenkins FA. 1974. Tree shrew locomotion and the origins of primate arborealism. In: Jenkins FA, editor. Primate locomotion. New York: Academic Press. pp. 85-115.

Jenkins FA, Camazine SM. 1977. Hip structure and locomotion in ambulatory and cursorial carnivores. J Zool 181: 351-370.

Johnson SE, Shapiro LJ. 1998. Positional behavior and vertebral morphology in atelines and cebines. Am J Phys Anthropol 105: 333-354.

Jones CL. 1979. The morphogenesis of the thigh of the mouse Mus musculus with special reference to tetrapod muscle homologies. J Morphol 162: 275-310.

Jouffroy FK, Gasc JP, Decombas M, Oblin S. 1974. Biomechanics of vertical leaping from the ground in *Galago alleni*: a cineradiographic analysis. In: Martin RD, Doyle GA, Walker AC, editors. Prosimian biology. London: Duckworth. pp. 817-827.

Jouffroy FK, Médina MF. 1996. Developmental changes in the fiber composition of elbow, knee, and ankle extensor muscles in cercopithecoid monkeys. Folia Primatol 66: 55-67.

Jouffroy FK, Médina MF. 2004. Comparative fiber-type composition and size in the antigravity muscles of primate limbs. In: Anapol F, German RZ, Jablonski NG, editors. Shaping primate evolution. Cambridge: Cambridge University Press. pp. 134-161.

Jouffroy FK, Médina MF, Renous S, Gasc J-P. 2003. Immunocytochemical characteristics of elbow, knee, and ankle muscles of the five-toed jerboa (*Allactaga elater*). J Anat 202: 373-386.

Jouffroy FK, Petter A. 1990. Gravity-related kinematic changes in lorisine horizontal locomotion in relation to position of the body. In: Jouffroy FK, Stack MH, Niemitz C, editors. Gravity, posture, and locomotion in primates. Firenze: Il Sedicesimo. pp. 199-208.

Jouffroy, FK, Stern JT, Médina MF, Larson SG. 1999. Functional and cytochemical characteristics of postural limb muscles of the rhesus monkey: a telemetered EMG and immunofluorescence study. Folia Primatol 70: 235-253.

Jungers WL. 1984. Scaling of the hominoid locomotor skeleton with special reference to lesser apes. In: Preuschoft H, Chivers D, Brockelman W, Creel N, editors. The lesser apes. Edinburgh: Edinburgh University Press. pp. 146-169.

Jungers WL. Colson TR. 1985. Relative brain size in galagos and lorises. In: Duncker HR, Fleischer G, editors. Functional morphology in vertebrates. Stuttgart and New York: Gustav Fischer Verlag. pp. 537-540.

Jungers WL, Falsetti AB, Wall CE. 1995. Shape, relative size, and size-adjustments in morphometrics. Yrbk Phys Anthropol 38: 137-161.

Jungers WL, Godfrey LR, Simons EL, Chatrath PS, Rakotosamimanana B. 1995. Phylogenetic and functional affinities of *Babakotia* (Primates), a fossil lemur from northern Madagascar. Proc Nat Acad Sci 88: 9082-9086.

Kapandji IA. 1974. The physiology of the joints, vol. 3. The trunk and the vertebral column. London: Churchill Livingstone.

Kay RF, Cartmill M. 1977. Cranial morphology and adaptations of *Palaechthon nacimienti* and other Paromomyidae (Plesiadapoidea, ?Primates), with description of a new genus and species. J Hum Evol 6: 19-53.

Keith A. 1902. The extent to which the posterior segments of the body have been transmuted and suppressed in the evolution of man and allied primates. J Anat Lond 37: 18-40.

Keith A. 1923. Man's posture: its evolution and disorders. 2. The evolution of the orthograde spine. British Medical Journal 1: 499-502.

Keith A. 1940. Fifty years ago. Am J Phys Anthropol 26: 251-267.

Kelley JJ. 1986. Paleobiology of Miocene hominoids. PhD dissertation. New Haven: Yale University.

Kimura T, Inokuchi S. 1985. Distribution pattern of muscle fiber type in muscles biceps brachii of white-handed gibbon. J Anthrop Soc Nippon 93: 371-380.

Kimura T, Okada M, Ishida H. 1979. Kinesiological characteristics of primate walking: its significance in human walking. In: Morbeck ME, Preuschoft H, Gomberg N, editors. Environment, behavior, and morphology: dynamic interactions in primates. New York: Fischer. pp. 297-311.

Kischel P, Stevens V, Montel F, Picquet F, Mounier Y. 2001. Plasticity of monkey triceps muscles fibers in microgravity conditions. J Appl Physiol 90: 1825-1832.

Kojima R, Okada M. 1996. Distribution of muscle fiber types in thoracic and lumbar epaxial muscles of Japanese macaques (*Macaca fuscata*). Folia Primatol 66: 38-43.

Kugelberg E, Edström L. 1968. Differential histochemical effects of muscle contractions on phosphorylase and glycogen in various types of fibers: relation to fatigue. J Neurol Neurosurg Psychiatry 31: 415-423.

Kumakura H, Hirasaki E, Nakano Y. 1996. Organization of epaxial muscles in terrestrial and arboreal primates. Folia Primatol 66: 25-37.

Kumakura H, Inokuchi S. 1992. Morphological diversity of the lorisoid epaxial muscles. In: Matano S, Tuttle RH, Ishida H, Goodman M, editors. Topics in primatology (vol. 3): evolutionary biology, reproductive endocrinology, and virology. Tokyo: University of Tokyo Press. pp. 83-93.

Larson SG. 1993. Functional morphology of the shoulder in primates. In: Gebo DL, editor. Postcranial Adaptations in Nonhuman Primates. DeKalb: Northern Illinois University Press. pp. 45-69.

Larson SG. 1998. Parallel evolution in hominoid trunk and forelimbs. Evol Anthropol 6: 87-99.

Larson SG, Stern JT. 2006. Maintenance of above-branch balance during primate arboreal quadrupedalism: coordinated use of forearm rotators and tail motion. Am J Phys Anthropol 129: 71-81.

Larsson L, Ansved T, Edstrom L, Gorza L, Schiaffino S. 1991. Effects of age on physiological, immunohistochemical, and biochemical properties of fast-twitch single motor units in the rat. J Physiol 443: 257-275.

Lauder GV. 1996. The argument for design. In: Rose MR, Lauder GV, editors. Adaptation. San Diego and London: Academic Press. pp. 55-91.

Lee PC. 1995. Comparative ecology of postnatal growth and weaning among haplorhine primates. In: Lee PC, editor. Comparative primate socioecology. Cambridge: Cambridge University Press. pp. 111-139.

Lemelin P. 1995. Comparative and functional myology of the prehensile tail in new world monkeys. J Morph 224: 351-368.

Lemelin P, Schmitt D, Cartmill M. 2003. Footfall patterns and interlimb co-ordination in opossums (Family Didelphidae): evidence for the evolution of diagonal-sequence walking gaits in primates. J Zool 260: 423-429.

Lieber RL. 2010. Skeletal muscle structure, function, and plasticity. Baltimore: Lippincoat Williams & Wilkins.

Lieber RL, Yeh Y, Baskin RJ. 1984. Sarcomere length determination using laser diffraction: effect of beam and fiber diameter. Biophys J 45: 1007-1016.

Linari M, Woledge RC, Curtin NA. 2003. Energy storage during stretch of active single fibers from frog skeletal muscle. J Physiol 548: 461-474.

Lockwood CA, Fleagle JG. 1999. The recognition and evaluation of homoplasy in primate and human evolution. Am J Phys Anthropol 110: 189-232.

Loeb GE, Gans C. 1986. Electromyography for experimentalists. Chicago: The University of Chicago Press.

Loughna PT, Izumo S, Goldspink G, Nadal-Ginard B. 1990. Disuse and passive stretch cause rapid alteration in expression of developmental and adult contractile protein genes in skeletal muscle. Development 109: 217-223.

Macintosh J, Bogduk N. 1986. The biomechanics of the lumbar multifidus. Clin Biomech 1: 205-213.

MacLatchy L, Gebo D, Kityo R, Pilbeam D. 2000. Postcranial functional morphology of *Morotopithecus bishopi*, with implications for the evolution of modern ape locomotion. J Hum Evol 39: 159-183.

Magid A, Law DJ. 1985. Myofibrils bear most of the resting tension in frog skeletal muscle. Science 230: 1280-1282.

Mannion AF, Dumas GA, Cooper RG, Espinosa FJ, Faris MW, Stevenson JM. 1997. Muscle fiber size and type distribution in thoracic and lumbar regions of erector spinae in healthy subjects without low back pain: Normal values and sex differences. J Anat 190: 505-513.

Marden JH. 1990. Maximum load lifting and induced power output of Harris' hawks are general functions of flight muscle mass. J Exp Biol 149: 511-514.

Marechal G, Goffart M, Reznik M, Gerebtzoff MA. 1976. The striated muscles in a slow-mover *Perodicticus potto* (Prosimii, Lorisidae, Lorisinae). Comp Biochem Physiol 54A: 81-93.

Masters JC, Boniotto M, Crovella S, Roos C, Pozzi L, Delpero M. 2007. Phylogenetic relationships among the Lorisoidea as indicated by craniodental morphology and mitochondrial sequence data. Am J Primatol 69: 6-15.

Maton B. 1980. Fast and slow motor units: their recruitment for tonic and phasic contraction in normal man. Eur J Appl Physiol 43: 45-55.

McConathy D, Giddings CJ, Gonyea WJ. 1983. Structure-function relationships of the flexor carpi radialis muscle compared among four species of mammals. J Morphol 175: 279-292.

McDonagh JS, Binder MD, Reinking RM, Stuart DG. 1980a. Tetrapartite classification of motor units of cat tibialis posterior. J Neurophysiol 44: 696-712.

McDonagh JS, Binder MD, Reinking RM, Stuart DG. 1980b. A commentary on muscle unit properties in cat hindlimb muscles. J Morphol 166: 217-230.

McGraw WS. 1996. Cercopithecid locomotion, support use, and support availability in the Tai Forest, Ivory Coast. Am J Phys Anthropol 100: 507-522.

McGraw WS. 1998. Comparative locomotion and habitat use of six monkeys in the Tai Forest, Ivory Coast. Am J Phys Anthropol 105: 493-510.

Médina MF, Jouffroy FK. 1998. Immunocytochemical approach to the study of postural limb muscles in reptiles. Biona Rep 13: 252-253.

Meldrum DJ, Dagosto M, White J. 1997. Hindlimb suspension and hindfoot reversal in *Varecia variegata* and other arboreal mammals. Am J Phys Anthropol 103: 85-102.

Mivart St. G. 1865. Contributions toward a more complete knowledge of the axial skeleton in the primates. Proc Zool Soc Lond 33: 545-592.

Monster AW, Chan HC, O'Connor D. 1978. Activity patterns of human skeletal muscles: relation of muscle fiber type composition. Science 200: 314-317.

Morton DJ. 1924. Evolution of the longitudinal arch of the human foot. J Bone Joint Surg Am 6: 56-90.

Muhl ZF. 1982. Active length-tension relation and the effect of muscle pinnation on fiber lengthening. J Morphol 173: 285-292.

Murphy RA, Beardsley AC. 1974. Mechanical properties of the cat soleus muscle in situ. Am J Physiol 227: 1008-1013.

Napier JR, Napier PH. 1967. A handbook of living primates. New York: Academic Press.

Napier JR, Walker AC. 1967. Vertical clinging and leaping: a newly recognized category of locomotor behaviour of primates. Folia Primatol 6: 204-219.

Nekaris KAI. 2001. Activity budget and positional behavior of the Mysore slender loris (*Loris tardigradus lydekkarianus*): implications for "slow climbing locomotion. Folia Primatol 72: 228-241.

Nekaris KAI, Bearder SK. 2011. The lorisiform primates of Asia and Mainland Africa: diversity shrouded in darkness. In: Campbell CJ, Fuentes A, MacKinnon KC, Bearder SK, Stumpf RM, editors. Primates in perspective (2nd edition). Oxford: Oxford University Press. pp. 24-45.

Nekaris KAI, Stevens NJ. 2007. Not all lorises are slow: rapid arboreal locomotion in *Loris tardigradus* of Southwestern Sri Lanka. Am J Primatol 69: 113-121.

Off EC, Gebo DL. 2005. Galago locomotion in Kibale National Park, Uganda. Am J Primatol 66: 189-195.

Organ JM, Teaford MF, Taylor AB. 2009. Functional correlates of fiber architecture of the lateral caudal musculature in prehensile and nonprehensile tails of the Platyrrhini (Primates) and Procyonidae (Carnivora). Anat Rec 292: 827-841.

Organ JM. 2010. Structure and function of platyrrhine caudal vertebrae. Anat Rec 293-730-745.

Oxnard CE. 1975. Primate locomotor classifications for evaluating fossils: Their inutility and an alternative. In: Kondo S, Kawai M, Ehara A, Kawamura S, editors. Proceedings from the Symposia of the Fifth Congress of the International Primatological Society. Tokyo: Japan Science Press. pp. 269-286.

Oxnard CE. 1979. Some methodological factors in studying the morphological-behavioral interface. In: Morbeck ME, Preuschoft H, Gomberg N, editors. Environment, behavior, and morphology: Dynamic interactions in primates. New York: Gustav Fischer. pp. 183-207.

Pal GP, Routal RV. 1987. Transmission of weight through the lower thoracic and lumbar regions of the vertebral column in man. J Anat 152: 93-105.

Perelman P, Johnson WE, Roos C, Seuanez HN, Horvath JE, Moreira MAM, Kessing B, Pontius J, Roelke M, Rumpler Y, Schneider MPC, Silva A, O'Brien SJ, Pecon-Slattery J. 2011. A molecular phylogeny of living primates. PLoS Genet 7: e1001342.

Peter JB, Barnard RJ, Edgerton VR, Gillespie CA, Stempel KE. 1972. Metabolic profiles of three fiber types of skeletal muscle in guinea pigs and rabbits. Biochemistry 11: 2627-2633.

Peters SE. 1989. Structure and function in vertebrate skeletal muscle. Am Zool 29: 221-234.

Pette D. 2001. Historical perspectives: Plasticity of mammalian skeletal muscle. J Appl Physiol 90: 1119-1124.

Pette D, Staron RS. 1997. Mammalian skeletal muscle fiber type transitions. Int Rev Cytol 170: 143-223.

Pette D, Staron RS. 2000. Myosin isoforms, muscle fiber types, and transitions. Microsc Res Tech 50: 500-509.

Pette D, Staron RS. 2001. Transitions of muscle fiber phenotypic profiles. Histochem Cell Biol 115: 359-372.

Pette D, Vrbova G. 1985. Neural control of phenotypic expression in mammalian muscle fibers. Muscle Nerve 8: 676-689.

Petter A, Jouffroy FK. 1993. Fiber type population in limb muscles of *Microcebus murinus*. Primates 34: 181-196.

Pilbeam D. 2004. The anthropoid postcranial axial skeleton: Comments on development, variation, and evolution. J Exp Zool 302: 241-267.

Plaghki L, Goffart M, Beckers-Bleukx G, Moureau-Lebbe A. 1981. Some characteristics of the hindlimb muscles in the leaping night monkey *Aotus trivirgatus* (Primates, Anthropoidae, Cebidae). Comp Biochem Physiol 70A: 341-349.

Powell PL, Roy RR, Kanim P, Bello MA, Edgerton VR. 1984. Predictability of skeletal muscle tension from architectural determinations in guinea pig hind-limbs. J Appl Physiol Respir Environ Exercise Physiol 57: 1715-1721.

Pridmore PA. 1992. Trunk movements during locomotion in the marsupial *Monodelphis domestica* (Didelphidae). J Morphol 211: 137-146.

Purvis A, Webster AJ. 1999. Phylogenetically independent comparisons and primate phylogeny. In: Lee PC, editor. Comparative Primate Socioecology. Cambridge: Cambridge University Press. pp. 44-70.

Rayne J, Crawford GNC. 1972. The relationship between fiber length, muscle excursion, and jaw movements in the rat. Arch Oral Biol 17: 859-872.

Reeve HK, Sherman PW. 1993. Adaptation and the goals of evolutionary research. Quart Rev Biol 68: 1-32.

Ripley S. 1967. The leaping of langurs: a problem in the study of locomotor adaptation. Am J Phys Anthropol 26: 149-170.

Ritter D. 1995. Epaxial muscle function during locomotion in a lizard (Varamus salvator) and the proposal of a key innovation in the vertebrate axial musculoskeletal system. J Exp Biol 198: 2477-2490.

Ritter D. 1996. Axial muscle function during lizard locomotion. J Exp Biol 199: 2499-2510.

Roberts TJ, Azizi E. 2011. Flexible mechanisms: the diverse role of biological springs in vertebrate movement. J Exp Biol 214: 353-361.

Roberts TJ, Marsh RL, Weyand PG, Taylor CR. 1997. Muscular force in running turkeys: the economy of minimizing work. Science 275: 1113-1115.

Rockwell H, Gaynor Evans F, Pheasant H. 1938. The comparative morphology of the vertebral spinal column. Its form as related to function. J Morph 63: 87-117.

Rodman PS. 1979. Skeletal differentiation in *Macaca fascicularis and Macaca nemestrina* in relation to arboreal and terrestrial quadrupedalism. Am J Phys Anthropol 51: 51-62.

Rollinson J, Martin RD. 1981. Comparative aspects of primate locomotion, with special reference to arboreal cercopithecines. In: Day MH, editor. Vertebrate Locomotion. Symposium of Zoological Society of London 48: 377-427.

Roos PJ. 1964. Lateral bending in newt locomotion. Proc Koniglike Ned Akad Wetenschappen C 67: 223-232.

Rose MD. 1973. Quadrupedalism in primates. Primates 14: 337-357.

Rose MD. 1974. Postural adaptations in new and old world monkeys. In: Jenkins FA, editor. Primate Locomotion. New York: Academic Press. pp. 201-222.

Rose MD. 1978. Feeding and associated positional behavior of black and white colobus monkeys (*Colobus guereza*). In: Montgomery GG, editor. The ecology of arboreal folivores. Washington, DC: Smithsonian Institution Press. pp. 253-262.

Rose MD. 1979. Positional behavior of natural populations: some quantitative results of a field study of *Colobus guereza* and *Cercopithecus aethiops*. In: Morbeck ME, Preuschoft H, Gomberg N, editors. Environment, behavior, and morphology: dynamic interactions in primates. New York: Fischer. pp. 75-93.

Rose MD. 1993. Functional anatomy of the elbow and forearm in primates. In: Gebo DL, editor. Postcranial Adaptation in Nonhuman Primates. DeKalb: Northern Illinois University Press. pp. 70-95.

Ross C, Jones KE. 1995. Socioecology and the evolution of primate reproductive trees. In: Lee PC, editor. Comparative primate socioecology. Cambridge: Cambridge University Press. pp. 73-110.

Ross CF, Lockwood CA, Fleagle JG, Jungers WL. 2002. Adaptation and behavior in the primate fossil record. In: Plavcan JM, Kay RF, Jungers WL, Van Schaik CP, editors. Reconstructing behavior in primate fossil record. New York: Kluwer/Plenum. pp. 1-41.

Roy RR, Bello MA, Powell PL, Simpson DR. 1984. Architectural design and fiber-type distribution of the major elbow flexors and extensors of the monkey (*Cynomolgus*). Am J Anat 171: 285-293.

Rubinstein NA, Hoh JFY. 2000. The distribution of myosin heavy chain isoforms among rat extraocular muscle fiber types. Invest Opthalmol Vis Sci 41: 3391-3398.

Russo GA, Shapiro LJ. 2011. Morphological correlates of tail length in the catarrhine sacrum. J Hum Evol 61: 223-232.

Salmons S. 1980. The response of skeletal muscle to different patterns of use: Some new developments and concepts. In: Pette D, editor. Plasticity of muscle. Berlin: Walter de Gruyter. pp. 387-399.

Sanders WJ. 1990. Weight transmission through the lumbar vertebrae and sacrum in australopithecines. Am J Phys Anthropol S81: 289.

Sanders WJ. 1991. Comparative study of hominoid lumbar neural canal dimensions. Am J Phys Anthropol S12: 157.

Sanders WJ. 1998. Comparative morphometric study of the australopithecine vertebral series Stw-H8/H41. J Hum Evol 34: 249-302.

Sanders WJ, Bodenbender BE. 1994. Morphometric analysis of lumbar vertebra UMP 67-28: Implications for spinal function and phylogeny of the Miocene Moroto hominoid. J Hum Evol 26: 203-237.

Sargis EJ. 2001. A preliminary qualitative analysis of the axial skeleton of tupaiids (Mammalia, Scandentia): functional morphology and phylogenetic implications. J Zool 253: 473-483.

Sartorius CA, Lu BD, Acakpo-Satchivi L, Jacobsen RP, Byrnes WC, Leinwand LA. 1998. Myosin heavy chains IIa and IId are functionally distinct in the mouse. J Cell Biol 141: 943-953.

Schiaffino S, Gorza L, Sartore S, Saggin L, Ausoni S, Vianello M, Gundersen K, Lomo T. 1989. Three myosin heavy chain isoforms in type 2 skeletal muscle fibers. J Musc Res Cell Motil 10: 197-205.

Schilling N. 2009. Metabolic profile of the perivertebral muscles in small therian mammals: implications for the evolution of mammalian trunk musculature. Zoology 112: 279-304.

Schilling N, Fischer M. 1999. Kinemtaic analysis of treadmill locomotion of tree shrews, *Tupaia glis* (Scandentia: Tupaiidae). Mamm Biol 64: 129-153.

Schmidt M, Fischer MS. 2000. Cineradiographic study of forelimb movements during quadrupedal walking in the brown lemur (*Eulemur fulvus*, Primates, Lemuridae). Am J Phys Anthropol 111: 245-262.

Schmidt M, Schilling N. 2007. Fiber type distribution in the shoulder muscles of the tree shrew, the cotton-top tamarin, and the squirrel monkey related to shoulder movements and forelimb loading. J Hum Evol 52: 401-419.

Schmitt D. 1998. Forelimb mechanics during arboreal and terrestrial quadrupedalism in Old World monkeys. In: Strasser E, Fleagle J, Rosenberger A, McHenry H, editors. Primate Locomotion: Recent Advances. New York: Plenum Press. pp. 175-204.

Schmitt D, Lemelin P. 2002. Origins of primate locomotion: gait mechanics of the woolly opossum. Am J Phys Anthropol 118: 231-238.

Schultz AH. 1938. The relative length of the regions of the spinal column in Old World primates. Am J Phys Anthropol 24: 1-22.

Schultz AH. 1961. Vertebral column and thorax. Primatologia, vol. 4. Basel: Karger. pp. 1-66.

Schumacher GH. 1961. Funktionelle morphologie der kaumuskulatur. (Trans. Muhl Z). Jena: Gustav Fischer.

Sciote JJ, Morris TJ. 2000. Skeletal muscle function and fiber types: the relationship between occlusal function and the phenotype of jaw-closing muscles in humans. J Orthodont 27: 15-30.

Sellers W. 1996. A biomechanical investigation into the absence of leaping in the locomotor repertoire of the slender loris (*Loris tardigradus*). Folia Primatol 67: 1-14.

Serrano AL, Perez M, Lucia A, Chicharro JL, Quiroz-Roth E, Rivero JL. 2001. Immunolabeling, histochemistry, and in situ hybridization in human skeletal muscle fibers to detect myosin chain expression at the protein and mRNA level. J Anat 199: 329-337.

Shapiro LJ. 1991. Functional morphology of the primate spine with special reference to orthograde posture and bipedal locomotion. PhD dissertation. Stony Brook: State University of New York.

Shapiro LJ. 1993a. Functional morphology of the vertebral column in primates. In: Gebo DL, editor. Postcranial Adaptation in Nonhuman Primates. DeKalb: Northern Illinois University Press. pp. 121-149.

Shapiro LJ. 1993b. Evaluation of "unique" aspects of human vertebral bodies and pedicles with a consideration of *Australopithecus africanus*. J Hum Evol 433-470.

Shapiro LJ. 1995. Functional morphology of indriid lumbar vertebrae. Am J Phys Anthropol 98: 323-342.

Shapiro LJ. 2007. Morphological and functional differentiation in the lumbar spine of lorisids and galagids. Am J Primatol 69: 86-102.

Shapiro LJ, Demes B. 1996. Spinal kinematics in lorids and cheirogaleids. Am J Phys Anthropol suppl. 22: 213.

Shapiro LJ, Demes B, Cooper J. 2001. Lateral bending of the lumbar spine during quadrupedalism in primates. J Hum Evol 40: 231-259.

Shapiro LJ, Jungers WL. 1988. Back muscle function during bipedal walking in chimpanzee and gibbon: implications for the evolution of human locomotion. Am J Phys Anthropol 77: 201-212.

Shapiro LJ, Jungers WL. 1994. Electromyography of back muscles during quadrupedal and bipedal walking in primates. Am J Phys Anthropol 93: 491-504.

Shapiro LJ, Seiffert CVM, Godfrey LR, Jungers WL, Simons EL, Randria GFN. 2005. Morphometric analysis of lumbar vertebrae in extinct Malagasy strepsirrhines. Am J Phys Anthropol 128: 823-839.

Shapiro LJ, Simons CVM. 2002. Functional aspects of strepsirrhine lumbar vertebral bodies and spinous processes. J Hum Evol 42: 753-783.

Sickles DW, Pinkstaff CA. 1980. Are fast glycolytic fibers present in slow loris (*Nycticebus coucang*) hindlimb muscles? J Histochem Cytochem 28: 57-59.

Sickles DW, Pinkstaff CA. 1981a. Comparative histochemical study of prosimian primate hindlimb muscles. I. Muscle fiber types. Am J Anat 160: 175-186.

Sickles DW, Pinkstaff CA. 1981b. Comparative histochemical study of prosimian primate hindlimb muscles. II. Populations of fiber types. Am J Anat 160: 175-186.

Singh K, Melis EH, Richmond JR, Scott SH. 2002. Morphometry of *Macaca mulatta* forelimb. II. Fiber-type composition in shoulder and elbow muscles. J Morphol 251: 323-332.

Slijper E. 1946. Comparative biologic-anatomical investigations on the vertebral column and spinal musculature of mammals. Verh K Ned Akad Wet 42: 1-128.

Smerdu V, Karsch-Mizrachi I, Campione M, Leinwand L, Schiaffino S. 1994. Type IIx myosin heavy chain transcripts are expressed in type IIb fibers of human skeletal muscle. Am J Physiol Cell Physiol 267: C1723-C1728.

Smith JL, Betts B, Edgerton VR, Zernicke RF. 1980. Rapid ankle extension during paw shakes: selective recruitment of fast ankle extensors. J Neurophysiol 43: 612-620.

Smith JM, Savage RJG. 1956. Some locomotory adaptations in mammals. J Linn Soc Lond Zool 42: 603-622.

Smith RJ, Jungers WL. 1997. Body mass in comparative primatology. J Hum Evol 32: 523-559.

Sober E. 1984. The nature of selection. Cambridge, MA: MIT Press.

Sokal RR, Rohlf FJ. 1995. Biometry (3rd edition). New York: W. H. Freeman.

Starck D. 1978. Vergleichende anatomie der wirbeltiere auf evolutionbiologischer grundlage. Bd 3: Organe des aktiven bewegungsapparates, der koordination, der umweltbeziehung, des stoffwechsels und der fortpflanzung. Berlin: Springer.

Staron RS, Pette D. 1986. Correlation between myofibrillar ATPase activity and myosin heavy chain composition in rabbit muscle fibers. Histochemistry 86: 19-23.

Staron RS, Pette D. 1993. The continuum of pure and hybrid myosin heavy chain-based fiber types in rat skeletal muscle. Histochemistry 100: 149-153.

Stein JM, Padykula HA. 1962. Histochemical classification of individual skeletal muscle fibers of the rat. Am J Anat 110: 103-123.

Stephens JA, Stuart DG. 1974. Proceedings: the classification of motor units in cat medial gastrocnemius muscle. J Physiol 240: 43-44.

Stephenson GMM. 2001. Hybrid skeletal muscle fibers: a rare or common phenomenon? Clin Exp Pharm Physiol 28: 692-702.

Stern JT. 1970. The meaning of "adaptation" and its relation to the phenomenon of natural selection. Evol Biol 4: 39-66.

Stern JT. 1971. Functional myology of the hip and thigh of cebid monkeys and its implications for the evolution of erect posture. Bibliotheca Primatologica 14: 1-318.

Stern JT. 1974. Computer modeling of gross muscle dynamics. J Biomech 7: 411-428.

Stern JT. 1975. Before bipedality. Yrbk Phys Anthropol 19: 59-68.

Stern JT. 2005. Core concepts of anatomy (2nd edition).

Strasser E. 1992. Hindlimb proportions, allometry, and biomechanics in Old World monkeys (Primates, Cercopithecidae). Am J Phys Anthropol 87: 187-213.

Straus WL, Wislocki GB. 1932. On certain similarities between sloths and slow lemurs. Bull Mus Comp Zool Harv 74: 45-56.

Stuart DG, Enoka RM. 1983. Motoneurons, motor units, and the size principle. In: Rosenberg RN, editor. The clinical neurosciences, Sect. 5: neurobiology. New York: Churchill Livingstone. pp. 471-517.

Sukhanov VB. 1974. General system of symmetrical locomotion of terrestrial vertebrates and some features of movement of lower tetrapods (translated by Hague MM). New Delhi: Amerind Publishing Co. Pvt. Ltd.

Sullivan TE, Armstrong RB. 1978. Rat locomotory muscle fiber activity during trotting and galloping. J Appl Physiol 44: 358-363.

Suzuki A. 1977. A comparative histochemical study of the masseter muscle of the cattle, sheep, swine, dog, guinea pig, and rat. Histochem 51: 121-131.

Tague RG, Lovejoy CO. 1986. The obstetric pelvis of A.L. 288-1 (Lucy). J Hum Evol 15: 237-255.

Tam PP. 1986. A study on the pattern of prospective somites in the presomitic mesoderm of mouse embryos. J Embryol Exp Morphol 92: 269-285.

Tattersall I. 1982. The primates of Madagascar. New York: Columbia University Press.

Taylor AB, Eng CM, Anapol FC, Vinyard CJ. 2009. The functional correlates of jaw-muscle fiber architecture in tree-gouging and nongouging callitrichid monkeys. Am J Phys Anthropol 139: 353-367.

Taylor AB, Jones KE, Kunwar R, Ravosa MJ. 2006. Dietary consistency and plasticity of masseter fiber architecture in postweaning rabbits. Anat Rec 288A: 1105-1111.

Taylor AB, Vinyard CJ. 2004. Comparative analysis of masseter fiber architecture in tree-gouging (*Callithrix jacchus*) and nongouging (*Saguinus oedipus*) callitrichids. J Morphol 261: 276-285.

Taylor AB, Vinyard CJ. 2007. Jaw-muscle fiber architecture in *Cebus*. Am J Phys Anthropol S44: 229.

Taylor AB, Vinyard CJ. 2008. The relationship between jaw muscle architecture and feeding behavior in primates: tree-gouging and nongouging gummivorous callitrichids as a natural experiment. In: Vinyard CJ, Ravosa MJ, Wall CE, editors. Primate craniofacial function and biology. New York: Springer. pp. 241-262.

Taylor AB, Vinyard CJ. 2009. Jaw muscle fiber architecture in tufted capuchins favors generating relatively large muscle forces without compromising jaw gape. J Hum Evol 57: 710-720.

Taylor CR. 1978. Why change gaits? Recruitment of muscles and muscle fibers as a function of speed and gait. Am Zool 18: 153-161.

Telley IA, Stehle R, Ranatunga KW, Pfitzer G, Stüssi E, Denoth J. 2006. Dynamic behavior of half-sarcomeres during and after stretch in activated rabbit psoas myofibrils: sarcomere asymmetry but no 'sarcomere popping'. J Physiol 573: 173-185.

ter Keurs HEDJ, Iwazumi T, Pollack GH. 1978. The sarcomere length-tension relation in skeletal muscle. J Gen Physiol 72: 565-592.

Termin A, Staron RS, Pette D. 1989. Changes in myosin heavy chain isoforms during chronic low-frequency stimulation of rat fast hindlimb muscles. Eur J Biochem 186-749-754.

Thorpe SKS, Crompton RH, Gunther MM, Key RF, Alexander RM. 1999. Dimensions and moment arms of the hind- and forelimb muscles of common chimpanzees (*Pan troglodytes*). Am J Phys Anthropol 110: 179-199.

Thorstensson A, Carlson H. 1987. Fiber types in human lumbar back muscles. Acta Physiol Scand 131: 195-202.

Tokuriki M. 1973a. Electromyographic and joint-mechanical studies in quadrupedal locomotion. I. Walk. Jap J Vet Sci 35: 433-446.

Tokuriki M. 1973b. Electromyographic and joint-mechanical studies in quadrupedal locomotion. I. Trot. Jap J Vet Sci 35: 525-533.

Tokuriki M. 1979. Cinematographic and electromyographic analysis of vertical standing jump in the dog. J Exp Biol 83: 271-282.

Tosi AJ, Melnick DJ, Disotell TR. 2004. Sex chromosome phylogenetics indicate a single transition to terrestriality in the guenons (tribe Cercopithecini). J Hum Evol 46: 223-237.

Turner TR, Anapol FC, Jolly CJ. 1994. Body weights of adult vervet monkeys (*Cercopithecus aethiops*) at four sites in Kenya. Fol Primatol 63: 177-179.

Tuttle RH. 1972. Relative mass of cheiridial muscles in catarrhine primates. In: Tuttle RH, editor. The Functional and Evolutionary Biology of Primates. Chicago: Aldine Atherton. pp. 262-291.

van de Graff KM, Harper J, Goslow GEJ. 1982. Analysis of posture and gait selection during locomotion in the striped skunk (*Mephitis mephitis*). J Mammal 63: 582-590.

van der Meij MAA, Bout RG. 2004. Scaling of jaw-muscle size and maximal bite force in finches. J Exp Biol 207: 2745-2753.

van der Meij MAA, Bout RG. 2006. Seed husking time and maximal bite force in finches. J Exp Biol 209: 3329-3335.

Vangor AK. 1979. Electromyography of gait in non-human primates and its significance for the evolution of bipedality. PhD dissertation. Stony Brook: State University of New York.

van Wassenberg S, Aerts P, Adriaens D, Herrel A. 2005. A dynamic model of mouth closing movements in clariid catfishes: the role of enlarged jaw adductors. J Theor Biol 234: 49-65.

Vijayan K, Thompson JL, Norenberg KM, Fitts RH, Riley DA. 2001. Fiber-type susceptibility to eccentric contraction-induced damage of hindlimb-unloaded rat AL muscles. J Appl Physiol 90: 770-776.

Vilensky JA. 1987. Locomotor behavior and control in human and non-human primates: Comparisons with cats and dogs. Neurosci Biobehav Rev 11: 263-274.

Vilensky JA. 1989. Primate quadrupedalism: how and why does it differ from that of typical quadrupeds? Brain Behav Evol 34: 357-364.

Vilensky JA, O'Connor BL. 1997. Stepping in human with complete spinal cord transaction: a phylogenetic evaluation. Motor Control 1: 248-292.

Vilensky JA, Libii JN, Moore AM. 1991. Trot-gallop gait transitions in quadrupeds. Physiol Behav 50: 835-842.

Vilensky JA, Moore AM, Libii JN. 1994. Squirrel monkey locomotion on an inclined treadmill: implications for the evolution of gaits. J Hum Evol 26: 375-386.

Vinyard CJ, Wall CE, Williams SH, Hylander WL. 2003. Comparative functional analysis of skull morphology of tree-gouging primates. Am J Phys Anthropol 120: 153-170.

von Mering F, Fischer MS. 1999. Fiber type regionalization of forelimb muscles in two mammalian species, *Galea musteloides* (Rodentia, Caviidae) and *Tupaia belangeri* (Scandentia, Tupaiidae), with comments on postnatal myogenesis. Zoomorphology 119: 117-126.

Wainright SA. 1988. Form and functions in organism. Amer Zool 28: 671-680.

Walker A. 1969. The locomotion of the lorises, with special reference to the Potto. Afr J Ecol 7: 1-5.

Walker AC. 1974. Locomotor adaptations in past and present prosimian primates. In: Jenkins FA, editor. Primate locomotion. New York: Academic Press. pp. 349-381.

Walker SE. 2005. Leaping behavior of *Pithecia pithecia* and *Chiropotes satanas* in eastern Venezuela. Am J Primatol 66: 369-387.

Walker SM, Schrodt GR. 1974. I segment lengths and thin filament periods in skeletal muscle fibers of the Rhesus monkey and the human. Anat Rec 178: 63-82.

Wallace IJ, Demes B. 2008. Symmetrical gaits of *Cebus apella*: implications for the functional significance of diagonal sequence gait in primates. J Hum Evol 54: 783-794.

Walmsley B, Hodgson JA, Burke RE. 1978. Forces produced by medial gastrocnemius and soleus muscles during locomotion in freely moving cats. J Neurophysiol 41: 1203-1216.

Washburn SL, Buettner-Janusch J. 1952. The definition of thoracic and lumbar vertebrae. Am J Phys Anthropol 10: 251.

Watson RR, Miller TA, Davis RW. 2003. Immunohistochemical fiber typing of harbor seal skeletal muscle. J Exp Biol 206: 4105-4111.

Ward CV. 1990. The lumbar region of the Miocene hominoid Proconsul nyanzae. Am J Phys Anthropol S81: 314.

Ward CV. 1991. Functional anatomy of the lower back and pelvis of the Miocene hominoid *Proconsul nyanzae* from Mfangano Island, Kenya. PhD dissertation. Baltimore: Johns Hopkins University.

Ward CV. 1993. Torso morphology and locomotion in *Proconsul nyanzae.* Am J Phys Anthropol 92: 291-328.

Ward SC, Sussman RW. 1979. Correlates between locomotor anatomy and behavior in two sympatric species of *Lemur*. Am J Phys Anthropol 50: 575-590.

Weiss A, Leinwand LA. 1996. The mammalian myosin heavy chain gene family. Ann Rev Cell Dev Biol 12: 417-439.

Weiss A, McDonough D, Wertman B, Acakpo-Satchivi L, Montgomery K, Kucherlapati R, Leinwand L, Krauter K. 1999. Organization of human and mouse myosin heavy chain gene clusters is highly conserved. Proc Natl Acad Sci USA 96: 2958-2963.

Whalen RG, Johnstone D, Bryers PS, Butler-Brown MS, Ecob MS, Jaros E. 1984. A developmentally regulated disappearance of slow myosin in fast type muscles of the mouse. FEBS Letters 177: 51-56.

Whitcome KK, Shapiro LJ, Lieberman DE. 2007. Fetal load and the evolution of lumbar lordosis in bipedal hominins. Nature 450: 1075-1078.

Williams GC. 1966. Adaptation and natural selection. Princeton: Princeton University Press.

Williamson DL, Godard MP, Porter D, Costill DL, Trappe SW. 2000. Progressive resistance training reduces myosin heavy chain co-expression in single muscle fibers from older men. J Appl Physiol 88: 627-633.

Williamson DL, Gallagher PM, Carroll CC, Raue U, Trappe SW. 2001. Reduction in hybrid single muscle fiber proportions with resistance training in humans. J Appl Physiol 91: 1955-1961.

Willemse JJ. 1977. Morphological and functional aspects of the arrangement of connective tissue and muscle fibers in the tail of the Mexican axolotl, *Siredon mexicanum* (Shaw) (Amphibia, Urodela). Acta Anat 97: 266-285.

Wilson DR. 1972. Tail reduction in *Macaca*. In: Tuttle RH, editor. The functional and evolutionary biology of primates. Chicago: Aldine-Atherton. pp. 241-261.

Wineski L, Gans C. 1984. Morphological basis of the feeding mechanics in the shingleback lizard *Trachydosaurus rugosus* (Scincidae: Reptilia). J Morphol 181: 271-295.

Wolpert L. 1981. Positional information, pattern formation, and morphogenesis. In: Connelly TG, Brinkley LL, Carlson BM, editors. Morphogenesis and pattern formation. New York: Raven Press. pp. 5-20.

Yoder AD, Irwin JD, Payseur BA. 2001. Failure of the ILD to determine data compatibility for slow loris phylogeny. Syst Biol 50: 408-424.

Yoon SJ, Seller SH, Kucherlapati R, Leinwand LA. 1992. Organization of the human myosin heavy chain gene cluster. Proc Natl Acad Sci USA 89: 12078-12082.

Zar JH. 1999. Biostatistical analysis. Upper Saddle River, NJ: Prentice Hall.

Zumwalt A. 2006. The effect of endurance exercise on the morphology of muscle attachment sites. J Exp Biol 209: 444-454.

Appendix

Individual data for muscle physiological variables

Table 1: *G. senegalensis*: Absolute muscle mass (g)

Individual	Sex	Thoracic Iliocostalis	Lumbar Iliocostalis	Thoracic Longissimus	Lumbar Longissimus	Thoracic Multifidus	Lumbar Multifidus
1	M	0.1495	0.1443	0.5813	0.7017	0.0247	0.0241
2	M	0.4437	0.7349	0.4078	0.2987	0.0284	0.0936
3	M	0.2849	0.2651	0.3623	0.2815	0.0537	0.0979
4	M	0.1235	0.9493	0.7919	0.4931	0.0576	0.0920

Table 2: *G. senegalensis*: Relative muscle mass

Individual	Sex	Thoracic Iliocostalis	Lumbar Iliocostalis	Thoracic Longissimus	Lumbar Longissimus	Thoracic Multifidus	Lumbar Multifidus
1	M	0.0702	0.0677	0.2729	0.3294	0.0116	0.0113
2	M	0.2083	0.3450	0.1915	0.1402	0.0133	0.0439
3	M	0.1338	0.1245	0.1701	0.1322	0.0252	0.0460
4	M	0.0580	0.4457	0.3718	0.2315	0.0270	0.0432

Table 3: *N. coucang*: Absolute muscle mass (g)

Individual	Sex	Thoracic Iliocostalis	Lumbar Iliocostalis	Thoracic Longissimus	Lumbar Longissimus	Thoracic Multifidus	Lumbar Multifidus
1	F	0.1519	0.1822	0.4619	0.4047	0.1282	0.1044
2	M	1.0138	0.8306	2.1240	1.8185	0.1633	0.2199
3	M	0.2560	0.1766	0.6975	0.3593	0.0108	0.0130
4	M	0.7708	0.2148	1.9988	0.7233	0.4996	0.0524

Table 4: *N. coucang*: Relative muscle mass

Individual	Sex	Thoracic Iliocostalis	Lumbar Iliocostalis	Thoracic Longissimus	Lumbar Longissimus	Thoracic Multifidus	Lumbar Multifidus
1	F	0.0258	0.0309	0.0784	0.0687	0.0218	0.0177
2	M	0.1721	0.1410	0.3606	0.3087	0.0277	0.0373
3	M	0.0435	0.0300	0.1184	0.0610	0.0018	0.0022
4	M	0.1309	0.0365	0.3394	0.1228	0.0848	0.0089

Table 5: *G. senegalensis*: Resting pinnation angle

Individual	Sex	Thoracic Iliocostalis	Lumbar Iliocostalis	Thoracic Longissimus	Lumbar Longissimus	Thoracic Multifidus	Lumbar Multifidus
1	M	4.65	2.21	4.03	5.20	2.84	8.35
2	M	5.58	3.98	7.06	6.15	2.84	1.99
3	M	3.72	4.42	6.05	4.73	3.31	5.36
4	M	2.79	1.77	5.75	3.60	3.09	1.99

Table 6: *N. coucang*: Resting pinnation angle

Individual	Sex	Thoracic Iliocostalis	Lumbar Iliocostalis	Thoracic Longissimus	Lumbar Longissimus	Thoracic Multifidus	Lumbar Multifidus
1	F	6.13	8.86	8.65	7.61	6.48	4.98
2	M	7.44	6.53	8.65	3.81	4.16	3.98
3	M	6.13	5.13	6.30	5.92	4.16	4.98
4	M	11.69	3.11	12.55	8.79	6.94	3.49

Table 7: *G. senegalensis*: Raw fiber length (Lf) (mm)

Individual	Sex	Thoracic Iliocostalis	Lumbar Iliocostalis	Thoracic Longissimus	Lumbar Longissimus	Thoracic Multifidus	Lumbar Multifidus
1	M	9.62	24.07	14.59	19	8.51	14.9
2	M	17.02	14.67	15.12	25.5	9.33	11.24
3	M	18.16	9.64	12.77	21.07	13.52	10.02
4	M	10.94	11.39	12.88	19.57	8.08	15.14

Table 8: *N. coucang*: Raw fiber length (Lf) (mm)

Individual	Sex	Thoracic Iliocostalis	Lumbar Iliocostalis	Thoracic Longissimus	Lumbar Longissimus	Thoracic Multifidus	Lumbar Multifidus
1	F	9.86	6.82	8.36	8.03	6.64	3.36
2	M	5.17	7.94	6.43	4.73	2.45	4.06
3	M	9.75	7.57	10.23	7.01	6.64	2.87
4	M	12.48	7.14	8.55	5.84	6.68	4.77

Table 9: Summary of Lf (mm) for the strepsirrhines (Mean ± SD)

Species	Iliocostalis		Longissimus		Multifidus	
	Thoracic	Lumbar	Thoracic	Lumbar	Thoracic	Lumbar
G. senegalensis	13.94 ± 4.2801	14.94 ± 6.4323	13.84 ± 1.1927	21.29 ± 2.9425	9.86 ± 2.4945	12.83 ± 2.5849
N. coucang	9.32 ± 3.04	7.37 ± 0.49	8.39 ± 1.55	6.40 ± 1.43	5.60 ± 2.10	3.77 ± 0.83
Mann-Whitney U test result	NS (p = 0.17)	p = 0.01	p = 0.01	p = 0.01	p = 0.01	p = 0.01

Table 10: *G. senegalensis*: Resting fiber length (NLf) (mm)

Individual	Sex	Thoracic Iliocostalis	Lumbar Iliocostalis	Thoracic Longissimus	Lumbar Longissimus	Thoracic Multifidus	Lumbar Multifidus
1	M	10.35	27.24	14.47	20.08	9.00	12.51
2	M	18.31	16.59	14.99	26.95	9.86	9.44
3	M	19.54	10.90	12.66	22.26	14.29	8.41
4	M	11.78	12.89	12.77	20.69	8.55	12.71

Table 11: *N. coucang*: Resting fiber length (NLf) (mm)

Individual	Sex	Thoracic Iliocostalis	Lumbar Iliocostalis	Thoracic Longissimus	Lumbar Longissimus	Thoracic Multifidus	Lumbar Multifidus
1	F	11.27	7.31	10.60	9.49	7.09	3.38
2	M	5.91	8.51	8.15	5.59	2.61	4.08
3	M	11.13	8.11	12.98	8.28	7.08	2.88
4	M	14.26	7.65	10.85	6.90	7.12	4.79

Table 12: *G. senegalensis*: Relative NLf-1

Individual	Sex	Thoraco-lumbar spine length (mm)	Thoracic Iliocostalis	Lumbar Iliocostalis	Thoracic Longissimus	Lumbar Longissimus	Thoracic Multifidus	Lumbar Multifidus
1	M	89.1	11.6162	30.5724	16.2402	22.5365	10.1010	14.0404
2	M	112	16.3482	14.8125	13.3839	24.0625	8.8036	8.4286
3	M	97	20.1443	11.2371	13.0515	22.9485	14.7320	8.6701
4	M	104	11.3269	12.3942	12.2788	19.8942	8.2212	12.2212

Table 13: *N. coucang*: Relative NLf-1

Individual	Sex	Thoraco-lumbar spine length (mm)	Thoracic Iliocostalis	Lumbar Iliocostalis	Thoracic Longissimus	Lumbar Longissimus	Thoracic Multifidus	Lumbar Multifidus
1	F	151.8	7.4242	4.8155	6.9829	6.2516	4.6706	2.2266
2	M	165	3.5818	5.1576	4.9394	3.3879	1.5818	2.4727
3	M	154	7.2273	5.2662	8.4286	5.3766	4.5974	1.8701
4	M	160	8.9125	4.7813	6.7813	4.3125	4.4500	2.9938

Table 14: *G. senegalensis*: Relative NLf-2

Individual	Sex	Thoracic Iliocostalis	Lumbar Iliocostalis	Thoracic Longissimus	Lumbar Longissimus	Thoracic Multifidus	Lumbar Multifidus
1	M	21.9568	61.9980	22.9303	44.1876	42.0043	80.3153
2	M	36.1106	41.3886	24.1341	51.2424	51.6817	56.2496
3	M	41.7323	31.1283	23.8656	48.5650	66.5270	43.2856
4	M	27.8021	36.8622	22.3146	42.4981	37.7144	75.7262

Table 15: *N. coucang*: Relative NLf-2

Individual	Sex	Thoracic Iliocostalis	Lumbar Iliocostalis	Thoracic Longissimus	Lumbar Longissimus	Thoracic Multifidus	Lumbar Multifidus
1	F	18.1624	19.6525	11.4807	19.7395	22.0430	11.7951
2	M	8.6796	19.0166	8.7330	9.4719	7.8596	13.8371
3	M	16.1933	18.7422	14.3614	14.9433	22.8450	11.8944
4	M	22.3365	19.8844	12.5743	11.9861	22.2282	14.6010

Table 16: *G. senegalensis*: Raw muscle length (ML) (mm)

Individual	Sex	Thoracic Iliocostalis	Lumbar Iliocostalis	Thoracic Longissimus	Lumbar Longissimus	Thoracic Multifidus	Lumbar Multifidus
1	M	46.19	39.82	63.26	44.04	20.79	18.68
2	M	49.03	37.59	62.28	50.71	18.39	19.12
3	M	45.03	33.38	53.19	44.29	20.48	21.52
4	M	41.28	33.02	57.37	47.23	22.06	19.94

Table 17: *N. coucang*: Raw muscle length (ML) (mm)

Individual	Sex	Thoracic Iliocostalis	Lumbar Iliocostalis	Thoracic Longissimus	Lumbar Longissimus	Thoracic Multifidus	Lumbar Multifidus
1	F	60.22	36.56	89.42	46.18	31.58	28.63
2	M	67.13	44.01	91.09	57.9	33.00	29.46
3	M	66.94	42.57	86.81	53.76	30.42	24.2
4	M	61.53	37.81	83.3	56.19	31.46	32.78

Table 18: Summary of ML (mm) for the strepsirrhines (Mean ± SD)

Species	Iliocostalis		Longissimus		Multifidus	
	Thoracic	Lumbar	Thoracic	Lumbar	Thoracic	Lumbar
G. senegalensis	45.38 ± 3.21	35.95 ± 3.31	59.03 ± 4.67	46.57 ± 3.12	20.43 ± 1.52	19.82 ± 1.25
N. coucang	63.96 ± 3.60	40.24 ± 3.61	87.66 ± 3.40	53.51 ± 5.17	31.62 ± 1.06	28.77 ± 3.53
Mann-Whitney U test result	p = 0.01	NS (p = 0.1)	p = 0.01	NS (p = 0.06)	p = 0.01	p = 0.01

Table 19: *G. senegalensis*: Resting muscle length (Lb) (mm)

Individual	Sex	Thoracic Iliocostalis	Lumbar Iliocostalis	Thoracic Longissimus	Lumbar Longissimus	Thoracic Multifidus	Lumbar Multifidus
1	M	47.14	43.94	63.10	45.44	21.43	15.58
2	M	50.71	40.08	62.11	52.59	19.08	16.78
3	M	46.82	35.02	53.05	45.84	21.48	19.43
4	M	42.37	34.97	57.23	48.68	22.67	16.78

Table 20: *N. coucang*: Resting muscle length (Lb) (mm)

Individual	Sex	Thoracic Iliocostalis	Lumbar Iliocostalis	Thoracic Longissimus	Lumbar Longissimus	Thoracic Multifidus	Lumbar Multifidus
1	F	62.05	37.20	92.33	48.08	32.16	28.66
2	M	68.09	44.75	93.32	59.02	33.21	29.49
3	M	68.73	43.27	90.38	55.41	30.99	24.21
4	M	63.84	38.47	86.29	57.57	32.03	32.81

Table 21: *G. senegalensis*: Potential excursion of whole muscle (*h*)

Individual	Sex	Thoracic Iliocostalis	Lumbar Iliocostalis	Thoracic Longissimus	Lumbar Longissimus	Thoracic Multifidus	Lumbar Multifidus
1	M	2.4010	6.2993	3.3522	4.6631	2.0826	2.9301
2	M	4.2566	3.8439	3.4965	6.2710	2.2816	2.1821
3	M	4.5257	2.5268	2.9450	5.1645	3.3070	1.9532
4	M	2.7251	2.9792	2.9691	4.7900	1.9781	2.9380

Table 22: *N. coucang*: Potential excursion of whole muscle (*h*)

Individual	Sex	Thoracic Iliocostalis	Lumbar Iliocostalis	Thoracic Longissimus	Lumbar Longissimus	Thoracic Multifidus	Lumbar Multifidus
1	F	2.6228	1.7152	2.4848	2.2172	1.6511	0.7844
2	M	1.3804	1.9820	1.9105	1.2949	0.6051	0.9453
3	M	2.5902	1.8831	3.0220	1.9259	1.6413	0.6684
4	M	3.3864	1.7699	2.5866	1.6190	1.6606	1.1088

Table 23: *G. senegalensis*: Relative *h*

Individual	Sex	Thoracic Iliocostalis	Lumbar Iliocostalis	Thoracic Longissimus	Lumbar Longissimus	Thoracic Multifidus	Lumbar Multifidus
1	M	0.05093	0.14337	0.05312	0.10261	0.09720	0.18811
2	M	0.08395	0.09590	0.05629	0.11924	0.11959	0.13002
3	M	0.09666	0.07216	0.05552	0.11268	0.15396	0.10053
4	M	0.06432	0.08520	0.05188	0.09839	0.08726	0.17505

Table 24: *N. coucang*: Relative *h*

Individual	Sex	Thoracic Iliocostalis	Lumbar Iliocostalis	Thoracic Longissimus	Lumbar Longissimus	Thoracic Multifidus	Lumbar Multifidus
1	F	0.04227	0.04611	0.02691	0.04612	0.05133	0.02737
2	M	0.02027	0.04429	0.02047	0.02194	0.01822	0.03206
3	M	0.03769	0.04352	0.03344	0.03476	0.05296	0.02760
4	M	0.05304	0.04601	0.02998	0.02812	0.05184	0.03380

Table 25: *G. senegalensis*: Tendon length (TL) (mm)

Individual	Sex	Thoracic Iliocostalis	Lumbar Iliocostalis	Thoracic Longissimus	Lumbar Longissimus	Thoracic Multifidus	Lumbar Multifidus
1	M	36.41	31.5	33.49	39.18	11.03	11.91
2	M	32.48	32.06	36.8	42.3	12.69	10.7
3	M	42.69	20.55	41.78	35.93	12.19	8.36
4	M	31.54	22.97	36.03	33.82	11.71	12.02

Table 26: *N. coucang*: Tendon length (TL) (mm)

Individual	Sex	Thoracic Iliocostalis	Lumbar Iliocostalis	Thoracic Longissimus	Lumbar Longissimus	Thoracic Multifidus	Lumbar Multifidus
1	F	7.88	7.27	7.99	8.01	5.75	3.05
2	M	4.93	7.83	6.34	6.09	2.24	2.99
3	M	8.30	6.45	10.33	6.25	5.89	2.54
4	M	10.57	6.00	8.16	5.17	5.96	3.89

Table 27: *G. senegalensis*: TL/(TL + NLf)

Individual	Sex	Thoracic Iliocostalis	Lumbar Iliocostalis	Thoracic Longissimus	Lumbar Longissimus	Thoracic Multifidus	Lumbar Multifidus
1	M	0.7787	0.5363	0.6983	0.6612	0.5507	0.4877
2	M	0.6395	0.6590	0.7106	0.6108	0.5627	0.5313
3	M	0.6860	0.6534	0.7675	0.6175	0.4603	0.4985
4	M	0.7281	0.6405	0.7383	0.6204	0.5779	0.4860

Table 28: *N. coucang*: TL/(TL + NLf)

Individual	Sex	Thoracic Iliocostalis	Lumbar Iliocostalis	Thoracic Longissimus	Lumbar Longissimus	Thoracic Multifidus	Lumbar Multifidus
1	F	0.4114	0.4986	0.4298	0.4577	0.4478	0.4743
2	M	0.4548	0.4792	0.4375	0.5214	0.4619	0.4229
3	M	0.4272	0.4430	0.4432	0.4301	0.4541	0.4686
4	M	0.4257	0.4396	0.4292	0.4283	0.4557	0.4482

Table 29: *G. senegalensis*: PCSA (cm^2)

Individual	Sex	Thoracic Iliocostalis	Lumbar Iliocostalis	Thoracic Longissimus	Lumbar Longissimus	Thoracic Multifidus	Lumbar Multifidus
1	M	0.1363	0.0501	0.3793	0.3294	0.0259	0.018
2	M	0.2283	0.4183	0.2556	0.1043	0.0272	0.0938
3	M	0.1377	0.2295	0.2694	0.1193	0.0355	0.1097
4	M	0.0991	0.6968	0.5841	0.2252	0.0637	0.0685

Table 30: *N. coucang*: PCSA (cm^2)

Individual	Sex	Thoracic Iliocostalis	Lumbar Iliocostalis	Thoracic Longissimus	Lumbar Longissimus	Thoracic Multifidus	Lumbar Multifidus
1	F	0.1269	0.2331	0.4078	0.4001	0.1701	0.2913
2	M	1.6101	0.9179	2.4389	3.0726	0.2178	0.509
3	M	0.2165	0.2053	0.5056	0.4086	0.0144	0.0426
4	M	0.5011	0.2654	1.7022	0.9806	0.6594	0.1034

Table 31: *G. senegalensis*: Relative PCSA-1 (PCSA/Species mean body mass$^{0.67}$)

Individual	Sex	Thoracic Iliocostalis	Lumbar Iliocostalis	Thoracic Longissimus	Lumbar Longissimus	Thoracic Multifidus	Lumbar Multifidus
1	M	0.003754	0.001380	0.010446	0.009072	0.000713	0.000496
2	M	0.006288	0.011521	0.007040	0.002873	0.000749	0.002583
3	M	0.003792	0.006321	0.007420	0.003286	0.000978	0.003021
4	M	0.002729	0.019191	0.016087	0.006202	0.001754	0.001887

Table 32: *N. coucang*: Relative PCSA-1 (PCSA/Species mean body mass$^{0.67}$)

Individual	Sex	Thoracic Iliocostalis	Lumbar Iliocostalis	Thoracic Longissimus	Lumbar Longissimus	Thoracic Multifidus	Lumbar Multifidus
1	F	0.001768	0.003248	0.005682	0.005574	0.002370	0.004058
2	M	0.022432	0.012788	0.033979	0.042808	0.003034	0.007092
3	M	0.003016	0.002860	0.007044	0.005693	0.000201	0.000594
4	M	0.006981	0.003698	0.023716	0.013662	0.009187	0.001441

Table 33: *G. senegalensis*: Relative PCSA-2 (PCSA/Upper estimate of body mass$^{0.67}$)

Individual	Sex	Thoracic Iliocostalis	Lumbar Iliocostalis	Thoracic Longissimus	Lumbar Longissimus	Thoracic Multifidus	Lumbar Multifidus
1	M	0.003418	0.001256	0.009511	0.008260	0.000649	0.000451
2	M	0.005725	0.010489	0.006409	0.002615	0.000682	0.002352
3	M	0.003453	0.005755	0.006755	0.002992	0.000890	0.002751
4	M	0.002485	0.017473	0.014647	0.005647	0.001597	0.001718

Table 34: *N. coucang*: Relative PCSA-2 (PCSA/Upper estimate of body mass$^{0.67}$)

Individual	Sex	Thoracic Iliocostalis	Lumbar Iliocostalis	Thoracic Longissimus	Lumbar Longissimus	Thoracic Multifidus	Lumbar Multifidus
1	F	0.001528	0.002808	0.004912	0.004819	0.002049	0.003508
2	M	0.019392	0.011055	0.029375	0.037007	0.002623	0.006130
3	M	0.002608	0.002473	0.006090	0.004921	0.000173	0.000513
4	M	0.006035	0.003197	0.020502	0.011811	0.007942	0.001245

Table 35: *G. senegalensis*: Relative PCSA-3 (PCSA/Lower estimate of body mass$^{0.67}$)

Individual	Sex	Thoracic Iliocostalis	Lumbar Iliocostalis	Thoracic Longissimus	Lumbar Longissimus	Thoracic Multifidus	Lumbar Multifidus
1	M	0.004187	0.001539	0.011650	0.010118	0.000796	0.000553
2	M	0.007012	0.012848	0.007851	0.003204	0.000835	0.002881
3	M	0.004230	0.007049	0.008275	0.003664	0.001090	0.003369
4	M	0.003044	0.021402	0.017941	0.006917	0.001957	0.002104

Table 36: *N. coucang*: Relative PCSA-3 (PCSA/Lower estimate of body mass$^{0.67}$)

Individual	Sex	Thoracic Iliocostalis	Lumbar Iliocostalis	Thoracic Longissimus	Lumbar Longissimus	Thoracic Multifidus	Lumbar Multifidus
1	F	0.002130	0.003913	0.006845	0.006716	0.002855	0.004890
2	M	0.027027	0.015408	0.040939	0.051576	0.003656	0.008544
3	M	0.003634	0.003446	0.008487	0.006859	0.000242	0.000715
4	M	0.008411	0.004455	0.028573	0.016460	0.011069	0.001736

Table 37: *C. aethiops*: Absolute muscle mass (g)

Individual	Sex	Thoracic Iliocostalis	Lumbar Iliocostalis	Thoracic Longissimus	Lumbar Longissimus	Thoracic Multifidus	Lumbar Multifidus
1	F	1.1883	2.881	10	10	0.0974	0.1423
2	F	1.0592	5	6	17*	0.0746	0.5449
3	M	1.8187	6	21*	10	0.0930	0.5019
4	F	1.6038	4	11	5	0.0856	0.436
5	F	0.7806	8	5	7	---	---

Asterisk (*) indicates outlier.

Table 38: *C. aethiops*: Relative muscle mass

Individual	Sex	Thoracic Iliocostalis	Lumbar Iliocostalis	Thoracic Longissimus	Lumbar Longissimus	Thoracic Multifidus	Lumbar Multifidus
1	F	0.0399	0.0967	0.3356	0.3356	0.0033	0.0048
2	F	0.0355	0.1678	0.2013	0.5705*	0.0025	0.0183
3	M	0.0427	0.1408	0.4930	0.2347	0.0022	0.0118
4	F	0.0538*	0.1342	0.3691	0.1678	0.0029	0.0146
5	F	0.0262	0.2685*	0.1678	0.2349	---	---

Asterisk (*) indicates outlier.

Table 39: *E. patas*: Absolute muscle mass (g)

Individual	Sex	Thoracic Iliocostalis	Lumbar Iliocostalis	Thoracic Longissimus	Lumbar Longissimus	Thoracic Multifidus	Lumbar Multifidus
1	M	2.0806	3.8671	20	17	0.3156	0.1715
2	M	3.6630	2.1275	15	29	0.2216	0.1055
3	F	0.3181	0.889	2	1	0.0217	0.139
4	F	4	1.9064	6	9	0.2405	0.1436
5	F	0.6843	4	6	8	---	---

Table 40: *E. patas*: Relative muscle mass

Individual	Sex	Thoracic Iliocostalis	Lumbar Iliocostalis	Thoracic Longissimus	Lumbar Longissimus	Thoracic Multifidus	Lumbar Multifidus
1	M	0.0168	0.0312	0.1613	0.1371	0.0025	0.0014
2	M	0.0295	0.0172	0.1210	0.2339*	0.0018	0.0009
3	F	0.0049	0.0137	0.0308*	0.0154*	0.0003	0.0021
4	F	0.0615*	0.0293	0.0923	0.1385	0.0037	0.0022
5	F	0.0105	0.0615*	0.0923	0.1231	---	---

Asterisk (*) indicates outlier.

Table 41: *C. aethiops*: Resting pinnation angle

Individual	Sex	Thoracic Iliocostalis	Lumbar Iliocostalis	Thoracic Longissimus	Lumbar Longissimus	Thoracic Multifidus	Lumbar Multifidus
1	F	3.79	2.16	3.22	4.01*	1.15	1.91
2	F	4.69	2.37	2.42	2.49	2.77	1.91
3	M	3.92	2.67	3.22	2.83	2.00	2.49
4	F	4.92	2.42	2.62	2.45	2.49	1.00
5	F	3.35	2.04	3.70	2.08	---	---

Asterisk (*) indicates outlier.

Table 42: *E. patas*: Resting pinnation angle

Individual	Sex	Thoracic Iliocostalis	Lumbar Iliocostalis	Thoracic Longissimus	Lumbar Longissimus	Thoracic Multifidus	Lumbar Multifidus
1	M	4.20	5.33	5.41	5.47	3.50	5.00
2	M	7.65*	5.28	10.12*	5.35	3.33	4.04
3	F	2.55*	3.56	2.61	3.65	3.10	4.47
4	F	4.35	2.41	4.58	4.01	3.23	3.59
5	F	3.90	4.36	2.96	3.10	---	---

Asterisk (*) indicates outlier.

Table 43: *C. aethiops*: Raw fiber length (Lf) (mm)

Individual	Sex	Thoracic Iliocostalis	Lumbar Iliocostalis	Thoracic Longissimus	Lumbar Longissimus	Thoracic Multifidus	Lumbar Multifidus
1	F	31.24	19.29	18.36	34.43	8.75	4.63
2	F	21.86	25.66	30.46	26.29	8.72	8.62
3	M	35.9	26.88	44.47	37.87	6.37	4.42
4	F	34.09	30.54	40.37	22.19	11.48	8.23
5	F	25.55	33.9	25.21	25.6	---	---

Table 44: *E. patas*: Raw fiber length (Lf) (mm)

Individual	Sex	Thoracic Iliocostalis	Lumbar Iliocostalis	Thoracic Longissimus	Lumbar Longissimus	Thoracic Multifidus	Lumbar Multifidus
1	M	21.62	28.3	16.06	23.79	10.9	13.19
2	M	26.58	22.92	20.59	34.07	12.98	8.39
3	F	24.6	25.17	34.68	25.82	10.36	10.67
4	F	37.65	31.23	21.99	32.47	12.51	10.37
5	F	32.72	26.64	37.87	43.1	---	---

Table 45: Summary of Lf (mm) for the cercopithecoid monkeys (Mean ± SD)

Species	Iliocostalis		Longissimus		Multifidus	
	Thoracic	Lumbar	Thoracic	Lumbar	Thoracic	Lumbar
C. aethiops	29.73 ± 5.89	27.25 ± 5.50	31.77 ± 10.72	29.28 ± 6.58	8.83 ± 2.09	6.48 ±2.26
E. patas	28.63 ± 6.47	26.85 ± 3.15	26.24 ± 9.49	31.85 ± 7.64	11.69 ± 1.26	10.66 ± 1.97
Mann-Whitney U test result	NS (p = 0.42)	NS (p = 0.42)	NS (p = 0.21)	NS (p = 0.42)	NS (p = 0.06)	p = 0.03

Table 46: *C. aethiops*: Resting fiber length (NLf) (mm)

Individual	Sex	Thoracic Iliocostalis	Lumbar Iliocostalis	Thoracic Longissimus	Lumbar Longissimus	Thoracic Multifidus	Lumbar Multifidus
1	F	23.31	25.27	18.99	38.60	8.30	4.85
2	F	16.31	33.61	31.50	29.47	8.27	9.03
3	M	26.79	35.21	46.00	42.45	6.04	4.63
4	F	25.44	40.00	41.76	24.87	10.89	8.62
5	F	19.06	44.41	26.08	28.70	---	---

Table 47: *E. patas*: Resting fiber length (NLf) (mm)

Individual	Sex	Thoracic Iliocostalis	Lumbar Iliocostalis	Thoracic Longissimus	Lumbar Longissimus	Thoracic Multifidus	Lumbar Multifidus
1	M	24.06	41.09	15.36	32.58	11.47	16.30
2	M	29.52	33.28	19.69	46.65	13.66	10.37
3	F	27.32	36.54	33.17	35.36	10.90	13.19
4	F	41.82	45.34	21.03	44.46	13.17	12.82
5	F	36.34	38.68	36.22	59.02	---	---

Table 48: *C. aethiops*: Relative NLf-1

Individual	Sex	Thoraco-lumbar spine length (mm)	Thoracic Iliocostalis	Lumbar Iliocostalis	Thoracic Longissimus	Lumbar Longissimus	Thoracic Multifidus	Lumbar Multifidus
1	F	263	8.8631	9.6084	7.2205	14.6768	3.1559	1.8441
2	F	252	6.4722	13.3373	12.5000	11.6944	3.2817	3.5833
3	M	311	8.6141	11.3215	14.7910	13.6495	1.9421	1.4887
4	F	286	8.8951	13.9860	14.6014	8.6958*	3.8077	3.0140
5	F	242	7.8760	18.3512*	10.7769	11.8595	---	---

Asterisk (*) indicates outlier.

Table 49: *E. patas*: Relative NLf-1

Individual	Sex	Thoraco-lumbar spine length (mm)	Thoracic Iliocostalis	Lumbar Iliocostalis	Thoracic Longissimus	Lumbar Longissimus	Thoracic Multifidus	Lumbar Multifidus
1	M	237	10.1519	17.3376	6.4810	13.7468	4.8397	6.8776
2	M	341	8.6569	9.7595	5.7742	13.6804	4.0059	3.0411
3	F	255	10.7137	14.3294	13.0078	13.8667	4.2745	5.1725
4	F	237	17.6456*	19.1308	8.8734	18.7595	5.5570	5.4093
5	F	302	12.0331	12.8079	11.9934	19.5430	---	---

Asterisk (*) indicates outlier.

Table 50: *C. aethiops*: Relative NLf-2

Individual	Sex	Thoracic Iliocostalis	Lumbar Iliocostalis	Thoracic Longissimus	Lumbar Longissimus	Thoracic Multifidus	Lumbar Multifidus
1	F	24.1701	19.0378*	14.6507	26.7303	56.0221	24.0575
2	F	17.9780	24.6435	30.3964	20.6909	45.3897	40.9107
3	M	24.3172	22.6230	34.9978	24.8772	31.4069	25.6937
4	F	24.7432	24.5616	35.2449	15.9229	48.6813	43.9572
5	F	20.7939	28.7799*	24.8381	22.1406	---	---

Asterisk (*) indicates outlier.

Table 51: *E. patas*: Relative NLf-2

Individual	Sex	Thoracic Iliocostalis	Lumbar Iliocostalis	Thoracic Longissimus	Lumbar Longissimus	Thoracic Multifidus	Lumbar Multifidus
1	M	27.0098	38.1911	16.2762	22.5022	57.4930	62.1925
2	M	33.3981	26.7902	17.5036	19.7529	70.6194	45.8821
3	F	26.1154	26.9934	28.0439	24.6825	35.7245	49.1198
4	F	23.3663	41.1865	24.9901	28.3164	45.8771	44.2652
5	F	29.4439	22.6243	24.9231	31.2101	---	---

Table 52: *C. aethiops*: Raw muscle length (ML) (mm)

Individual	Sex	Thoracic Iliocostalis	Lumbar Iliocostalis	Thoracic Longissimus	Lumbar Longissimus	Thoracic Multifidus	Lumbar Multifidus
1	F	106.74	124.97	128.8	138.99	15.4	20.16
2	F	97.93	126.06	102.28	138.3	18.22	21.54
3	M	122	144.82	129.45	164.69	19.66	18.02
4	F	114.05	150.57	116.68	152.71	22.37	19.61
5	F	100.09	140.66	103.87	125.6	---	---

Table 53: *E. patas*: Raw muscle length (ML) (mm)

Individual	Sex	Thoracic Iliocostalis	Lumbar Iliocostalis	Thoracic Longissimus	Lumbar Longissimus	Thoracic Multifidus	Lumbar Multifidus
1	M	85.91	90.98	95.28	133.37	19.21	22.17
2	M	84.57	110.77	113.66	219.83	18.46	20.03
3	F	101.08	120.6	120.24	130.87	29.81	23.58
4	F	173.56*	91.76	85.4	141.44	27.85	25.78
5	F	118.72	155.33	147.47	168.43	---	---

Asterisk (*) indicates outlier.

Table 54: Summary of ML (mm) for the cercopithecoid monkeys (Mean ± SD)

Species	Iliocostalis		Longissimus		Multifidus	
	Thoracic	Lumbar	Thoracic	Lumbar	Thoracic	Lumbar
C. aethiops	108.16 ± 9.98	137.42 ± 11.43	116.22 ± 13.04	144.06 ± 15.00	18.91 ± 2.91	19.83 ± 1.46
E. patas	112.77 ± 36.69	113.89 ± 26.39	112.41 ± 24.06	158.79 ± 37.23	23.83 ± 5.83	22.89 ± 2.42
Mann-Whitney U test result	NS (p = 0.42)	NS (p = 0.08)	NS (p = 0.35)	NS (p = 0.35)	NS (p = 0.17)	NS (p = 0.06)

Table 55: *C. aethiops*: Resting muscle length (Lb) (mm)

Individual	Sex	Thoracic Iliocostalis	Lumbar Iliocostalis	Thoracic Longissimus	Lumbar Longissimus	Thoracic Multifidus	Lumbar Multifidus
1	F	96.44	132.74	129.62	144.41	14.82	20.16
2	F	90.72	136.38	103.63	142.43	18.22	22.07
3	M	110.17	155.64	131.44	170.64	19.23	18.02
4	F	102.82*	162.86	118.49	156.19	22.37	19.61
5	F	91.66	154.31	105.00	129.63	---	---

Asterisk (*) indicates outlier.

Table 56: *E. patas*: Resting muscle length (Lb) (mm)

Individual	Sex	Thoracic Iliocostalis	Lumbar Iliocostalis	Thoracic Longissimus	Lumbar Longissimus	Thoracic Multifidus	Lumbar Multifidus
1	M	89.08	107.59	94.37	144.79	19.95	26.21
2	M	88.39	124.22	112.49	236.17	19.34	22.60
3	F	104.61	135.37	118.28	143.26	30.51	26.85
4	F	178.98	110.08	84.15	157.01	28.71	28.96
5	F	123.42	170.97	145.33	189.11	---	---

Table 57: *C. aethiops*: Potential excursion of whole muscle (*h*)

Individual	Sex	Thoracic Iliocostalis	Lumbar Iliocostalis	Thoracic Longissimus	Lumbar Longissimus	Thoracic Multifidus	Lumbar Multifidus
1	F	5.3995	5.8421	4.3954	8.9462	1.9168	1.1208
2	F	3.7846	7.7700	7.2842	6.8167	1.9126	2.0867
3	M	6.2082	8.1443	10.6471	9.8202	1.3962	1.0710
4	F	5.9047	9.2498	9.6581	5.7511	2.5190	1.9910
5	F	4.4122	10.2685	6.0404	6.6332	---	---

Table 58: *E. patas*: Potential excursion of whole muscle (*h*)

Individual	Sex	Thoracic Iliocostalis	Lumbar Iliocostalis	Thoracic Longissimus	Lumbar Longissimus	Thoracic Multifidus	Lumbar Multifidus
1	M	5.5770	9.5447	3.5679	7.5688	2.6551	3.7838
2	M	6.8979	7.7316	4.6416	10.8346	3.1621	2.4031
3	F	6.3185	8.4632	7.6736	8.1910	2.5219	3.0594
4	F	9.6962	10.4847	4.8778	10.3044	3.0483	2.9680
5	F	8.4189	8.9681	8.3825	13.6550	---	---

Table 59: *C. aethiops*: Relative *h*

Individual	Sex	Thoracic Iliocostalis	Lumbar Iliocostalis	Thoracic Longissimus	Lumbar Longissimus	Thoracic Multifidus	Lumbar Multifidus
1	F	0.05599	0.04401*	0.03391	0.06195	0.12937	0.05559
2	F	0.04172	0.05697	0.07029	0.04786	0.10497	0.09454
3	M	0.05635	0.05233	0.08101	0.05755	0.07260	0.05943
4	F	0.05743	0.05680	0.08151	0.03682	0.11261	0.10153
5	F	0.04814	0.06654*	0.05753	0.05117	---	---

Asterisk (*) indicates outlier.

Table 60: *E. patas*: Relative *h*

Individual	Sex	Thoracic Iliocostalis	Lumbar Iliocostalis	Thoracic Longissimus	Lumbar Longissimus	Thoracic Multifidus	Lumbar Multifidus
1	M	0.06261	0.08871	0.03781	0.05228	0.13309	0.14437
2	M	0.07804	0.06224	0.04126	0.04588	0.16348	0.10632
3	F	0.06040	0.06252	0.06488	0.05718	0.08265	0.11393
4	F	0.05418	0.09524	0.05796	0.06563	0.10619	0.10248
5	F	0.06821	0.05246	0.05768	0.07221	---	----

Table 61: *C. aethiops*: Tendon length (TL) (mm)

Individual	Sex	Thoracic Iliocostalis	Lumbar Iliocostalis	Thoracic Longissimus	Lumbar Longissimus	Thoracic Multifidus	Lumbar Multifidus
1	F	56.84	49.85*	62.6	47.72	9.76	14.44
2	F	86.58*	60.47	47.66*	66.27	8.41	11.72
3	M	52.89	69.44	66.88	65.45	11.28	8.69
4	F	62.51	65.46	64	55.13	9.85	10.38
5	F	42.43	62.43	69.25	61.64	---	---

Asterisk (*) indicates outlier.

Table 62: *E. patas*: Tendon length (TL) (mm)

Individual	Sex	Thoracic Iliocostalis	Lumbar Iliocostalis	Thoracic Longissimus	Lumbar Longissimus	Thoracic Multifidus	Lumbar Multifidus
1	M	43.02	38.97	34.76	55.24	9.66	12.3
2	M	44.8	43.92	45.4	74.91	9.98	11.19
3	F	55.45	72.63	73.93*	60.44	10.71	8.7
4	F	67.58	36.68	43.66	70.54	8.92	8.25
5	F	69.52	63.81	52.17	85.31	---	---

Asterisk (*) indicates outlier.

Table 63: *C. aethiops*: TL/(TL + NLf)

Individual	Sex	Thoracic Iliocostalis	Lumbar Iliocostalis	Thoracic Longissimus	Lumbar Longissimus	Thoracic Multifidus	Lumbar Multifidus
1	F	0.70917	0.66360	0.76725	0.55283	0.54042	0.74861
2	F	0.84148*	0.64275	0.60207	0.69219	0.50420	0.56482
3	M	0.66378	0.66355	0.59249	0.60658	0.65127	0.65240
4	F	0.71074	0.62071	0.60514	0.68913	0.47493	0.54632
5	F	0.69003	0.58433	0.72642	0.68231	---	---

Asterisk (*) indicates outlier.

Table 64: *E. patas*: TL/(TL + NLf)

Individual	Sex	Thoracic Iliocostalis	Lumbar Iliocostalis	Thoracic Longissimus	Lumbar Longissimus	Thoracic Multifidus	Lumbar Multifidus
1	M	0.64132	0.48676	0.69354	0.62901	0.45717	0.43007
2	M	0.60280	0.56891	0.69750	0.61624	0.42217	0.51902
3	F	0.66993	0.66529	0.69029	0.63090	0.49560	0.39744
4	F	0.61773	0.44721	0.67491	0.61339	0.40380	0.39155
5	F	0.65672	0.62260	0.59023*	0.59108	---	---

Asterisk (*) indicates outlier.

Table 65: *C. aethiops*: PCSA (cm^2)

Individual	Sex	Thoracic Iliocostalis	Lumbar Iliocostalis	Thoracic Longissimus	Lumbar Longissimus	Thoracic Multifidus	Lumbar Multifidus
1	F	0.4815	1.0785	4.9769	2.4464	0.1111	0.2776
2	F	0.6127	1.407	1.8015	5.4554*	0.0853	0.5709
3	M	0.6411	1.6113	4.3147	2.2272	0.1457	1.0252
4	F	0.5946	0.9458	2.4909	1.9014	0.0743	0.4787
5	F	0.387	1.7041	1.811	2.3073	---	---

Asterisk (*) indicates outlier.

Table 66: *E. patas*: PCSA (cm^2)

Individual	Sex	Thoracic Iliocostalis	Lumbar Iliocostalis	Thoracic Longissimus	Lumbar Longissimus	Thoracic Multifidus	Lumbar Multifidus
1	M	0.8164	0.887	12.2708	4.9169	0.26	0.0992
2	M	1.1642	0.6026	7.0992	5.859	0.1533	0.0961
3	F	0.1101	0.2299	0.5702	0.2672	0.0188	0.0994
4	F	0.9028	0.3977	2.6921	1.9115	0.1726	0.1058
5	F	0.1778	0.9761	1.566	1.2812	---	---

Table 67: *C. aethiops*: Relative PCSA-1 (PCSA/Species mean body mass$^{0.67}$)

Individual	Sex	Thoracic Iliocostalis	Lumbar Iliocostalis	Thoracic Longissimus	Lumbar Longissimus	Thoracic Multifidus	Lumbar Multifidus
1	F	0.002264	0.005071	0.023401	0.011503	0.000522	0.001305
2	F	0.002881	0.006616	0.008471	0.025651*	0.000401	0.002684
3	M	0.002373	0.005963	0.015968	0.008242	0.000539	0.003794
4	F	0.002796	0.004447	0.011712	0.008940	0.000349	0.002251
5	F	0.001820	0.008013	0.008515	0.010849	---	---

Asterisk (*) indicates outlier.

Table 68: *E. patas*: Relative PCSA-1 (PCSA/Species mean body mass$^{0.67}$)

Individual	Sex	Thoracic Iliocostalis	Lumbar Iliocostalis	Thoracic Longissimus	Lumbar Longissimus	Thoracic Multifidus	Lumbar Multifidus
1	M	0.001477	0.001604	0.022196	0.008894	0.000470	0.000179
2	M	0.002106	0.001090	0.012842	0.010598	0.000277	0.000174
3	F	0.000307	0.000641	0.001590	0.000745	0.000052	0.000277
4	F	0.002517	0.001109	0.007507	0.005330	0.000481	0.000295
5	F	0.000496	0.002722*	0.004367	0.003572	---	---

Asterisk (*) indicates outlier.

Table 69: *C. aethiops*: Relative PCSA-2 (PCSA/Upper estimate of body mass$^{0.67}$)

Individual	Sex	Thoracic Iliocostalis	Lumbar Iliocostalis	Thoracic Longissimus	Lumbar Longissimus	Thoracic Multifidus	Lumbar Multifidus
1	F	0.002068	0.004633	0.021380	0.010509	0.000477	0.001193
2	F	0.002632	0.006044	0.007739	0.023436*	0.000366	0.002453
3	M	0.002148	0.005400	0.014460	0.007464	0.000488	0.003436
4	F	0.002554	0.004063	0.010701	0.008168	0.000319	0.002056
5	F	0.001663	0.007321	0.007780	0.009912	---	---

Asterisk (*) indicates outlier.

Table 70: *E. patas*: Relative PCSA-2 (PCSA/Upper estimate of body mass$^{0.67}$)

Individual	Sex	Thoracic Iliocostalis	Lumbar Iliocostalis	Thoracic Longissimus	Lumbar Longissimus	Thoracic Multifidus	Lumbar Multifidus
1	M	0.001250	0.001358	0.018790	0.007529	0.000398	0.000152
2	M	0.001783	0.000923	0.010871	0.008972	0.000235	0.000147
3	F	0.000279	0.000582	0.001445	0.000677	0.000048	0.000252
4	F	0.002287	0.001008	0.006820	0.004843	0.000437	0.000268
5	F	0.000450	0.002473	0.003967	0.003246	---	---

Table 71: *C. aethiops*: Relative PCSA-3 (PCSA/Lower estimate of body mass$^{0.67}$)

Individual	Sex	Thoracic Iliocostalis	Lumbar Iliocostalis	Thoracic Longissimus	Lumbar Longissimus	Thoracic Multifidus	Lumbar Multifidus
1	F	0.002513	0.005629	0.025976	0.012769	0.000580	0.001449
2	F	0.003198	0.007344	0.009403	0.028474*	0.000445	0.002980
3	M	0.002666	0.006700	0.017941	0.009261	0.000606	0.004263
4	F	0.003103	0.004936	0.013001	0.009924	0.000388	0.002499
5	F	0.002020	0.008894	0.009452	0.012043	---	---

Asterisk (*) indicates outlier.

Table 72: *E. patas*: Relative PCSA-3 (PCSA/Lower estimate of body mass$^{0.67}$)

Individual	Sex	Thoracic Iliocostalis	Lumbar Iliocostalis	Thoracic Longissimus	Lumbar Longissimus	Thoracic Multifidus	Lumbar Multifidus
1	M	0.001844	0.002004	0.027719	0.011107	0.000587	0.000224
2	M	0.002630	0.001361	0.016037	0.013235	0.000346	0.000217
3	F	0.000343	0.000717	0.001778	0.000833	0.000059	0.000310
4	F	0.002815	0.001240	0.008396	0.005961	0.000538	0.000330
5	F	0.000554	0.003044	0.004884	0.003996	---	---

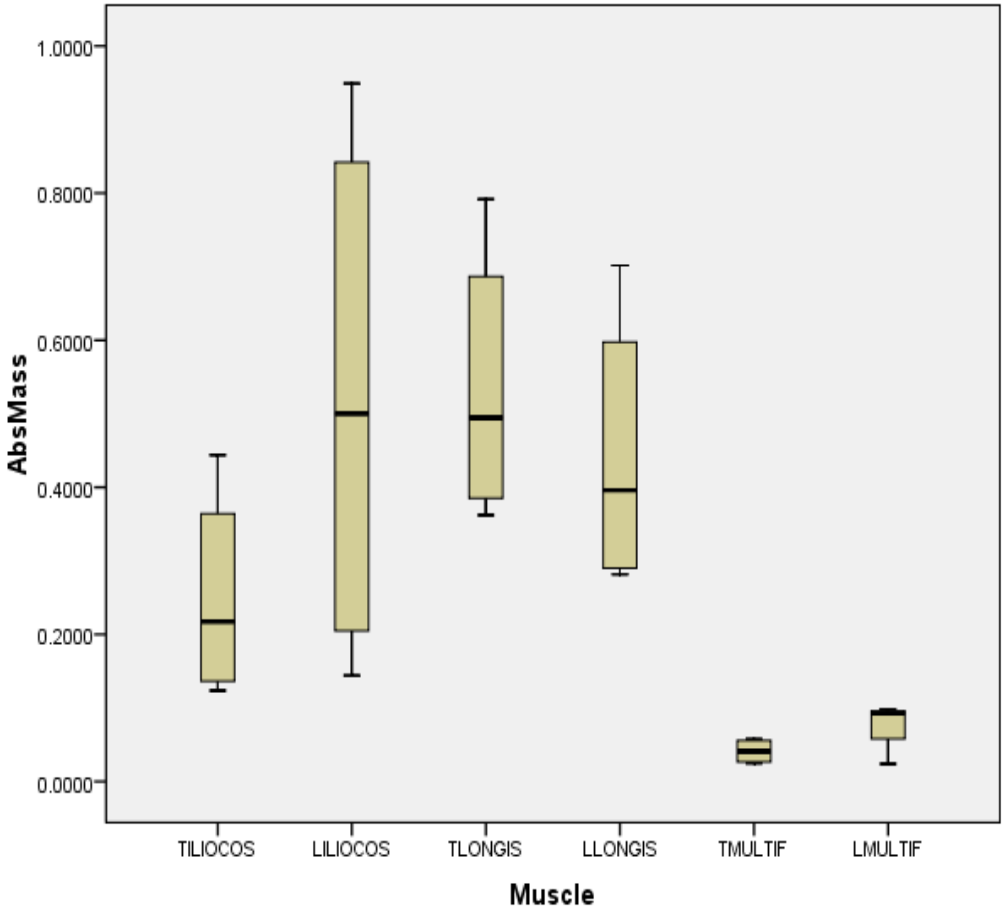

Fig. 1: *G. senegalensis*: Absolute muscle mass

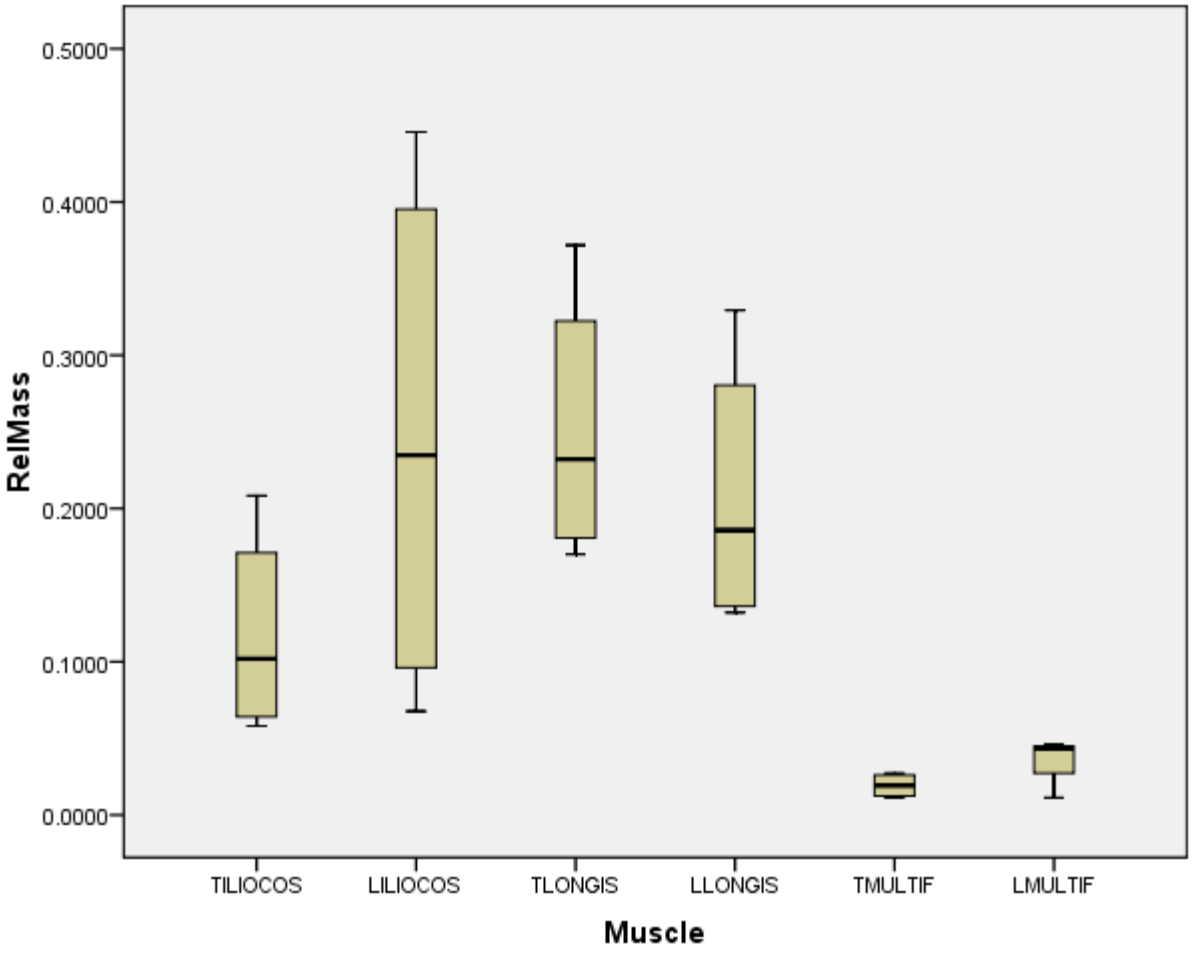

Fig. 2: *G. senegalensis*: Relative muscle mass

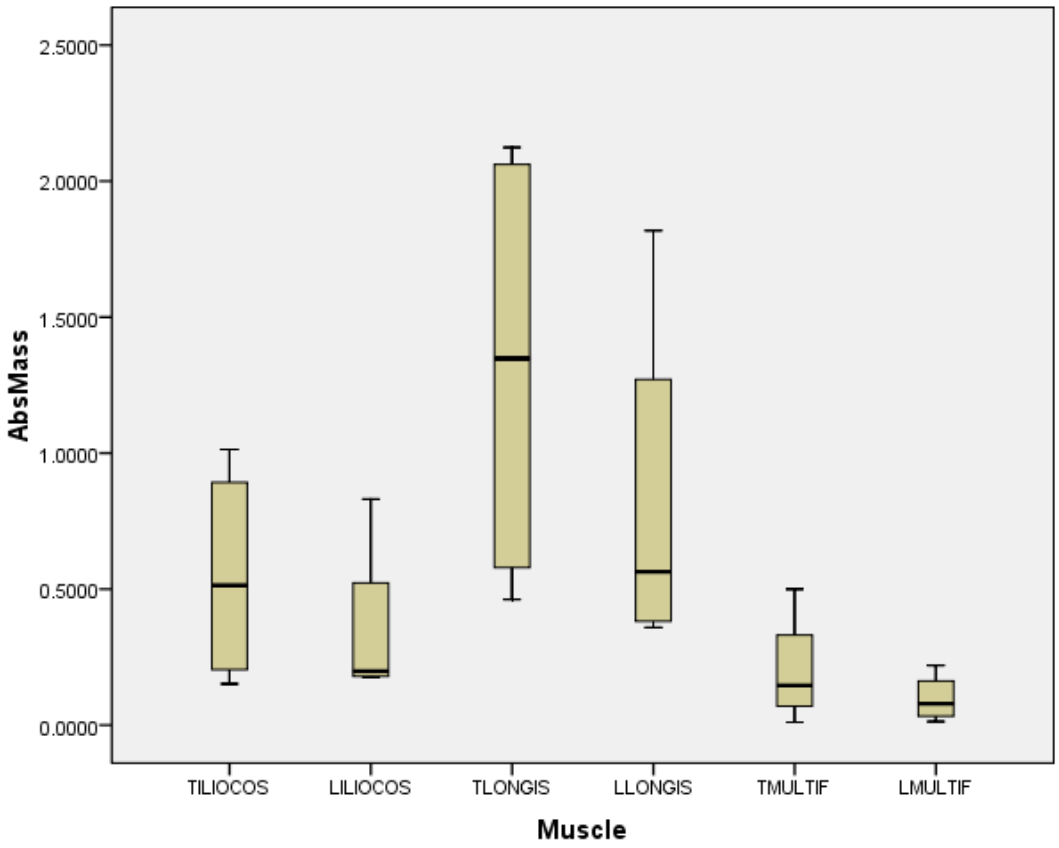

Fig. 3: *N. coucang*: Absolute muscle mass

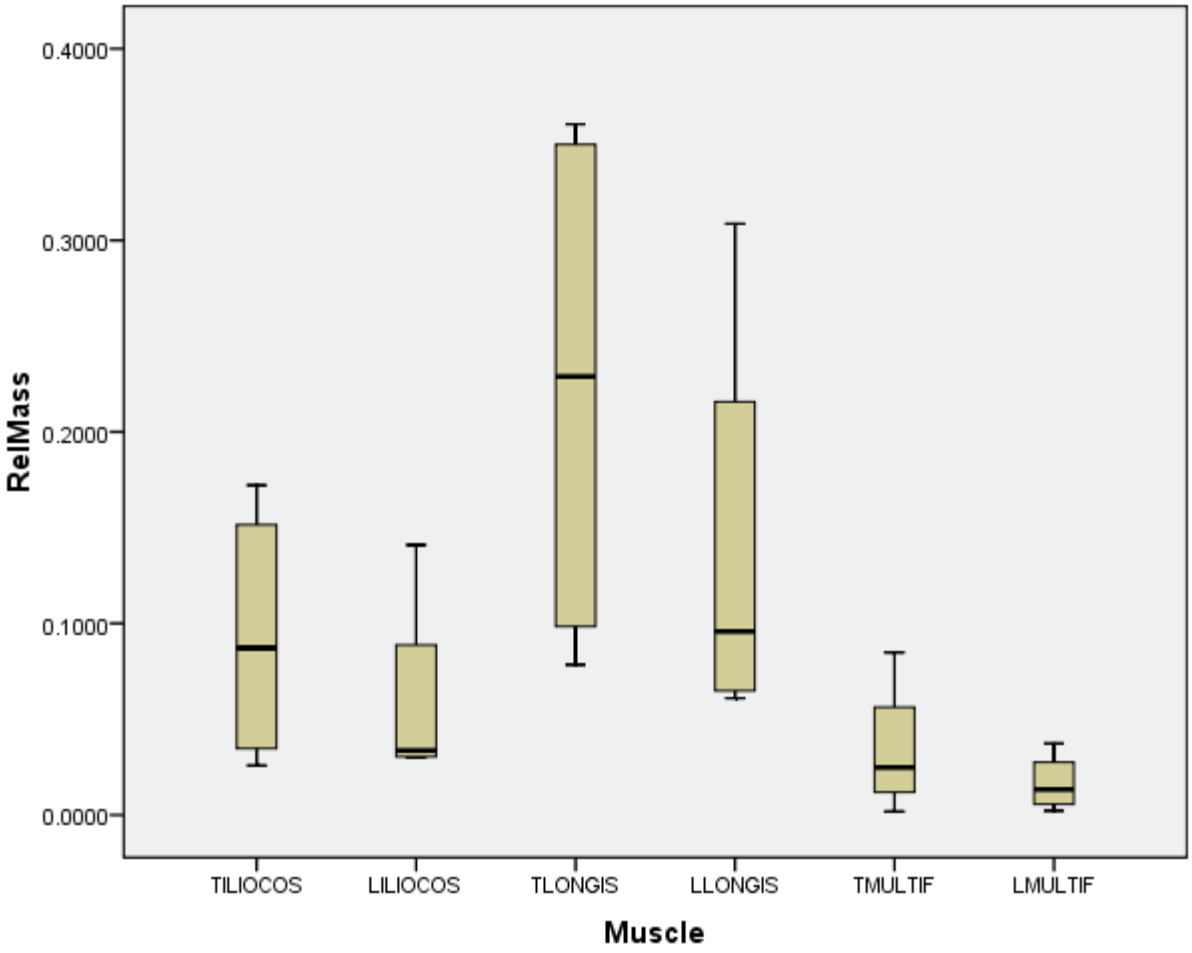

Fig. 4: *N. coucang*: Relative muscle mass

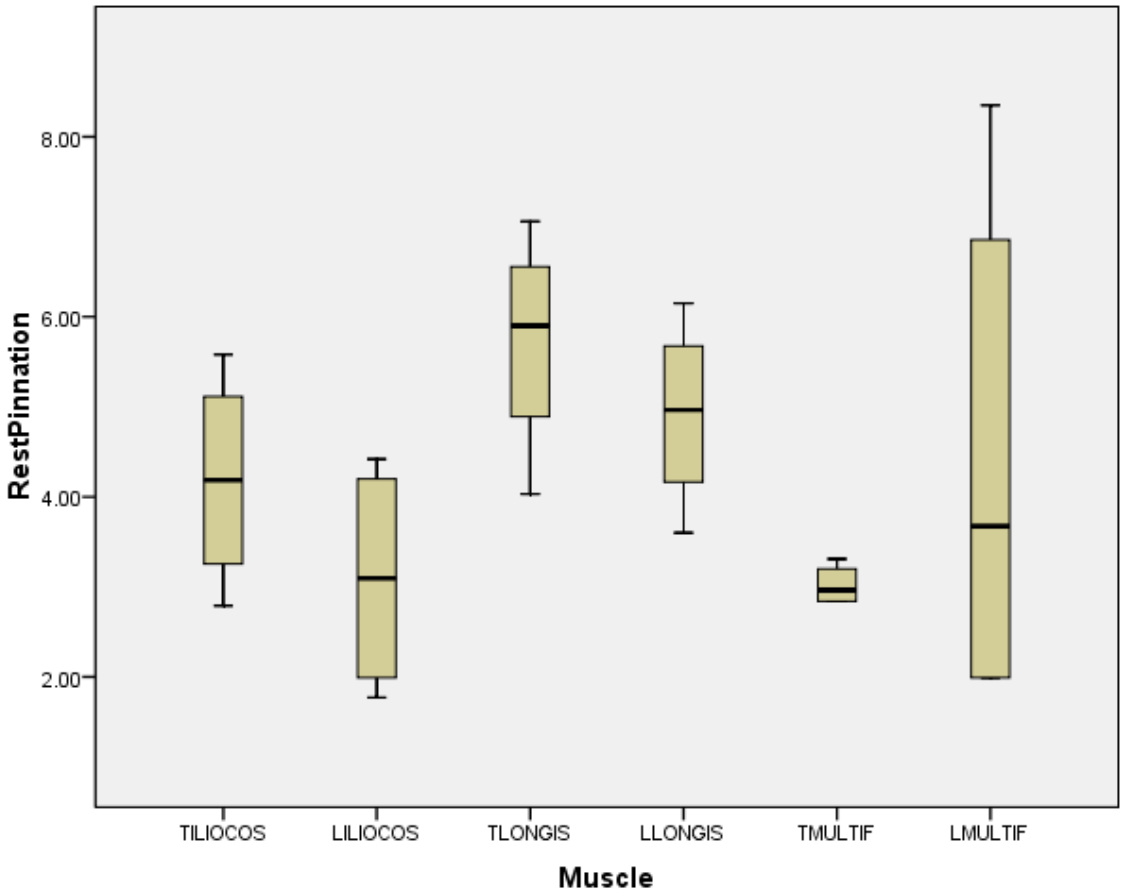

Fig. 5: *G. senegalensis*: Resting pinnation angle

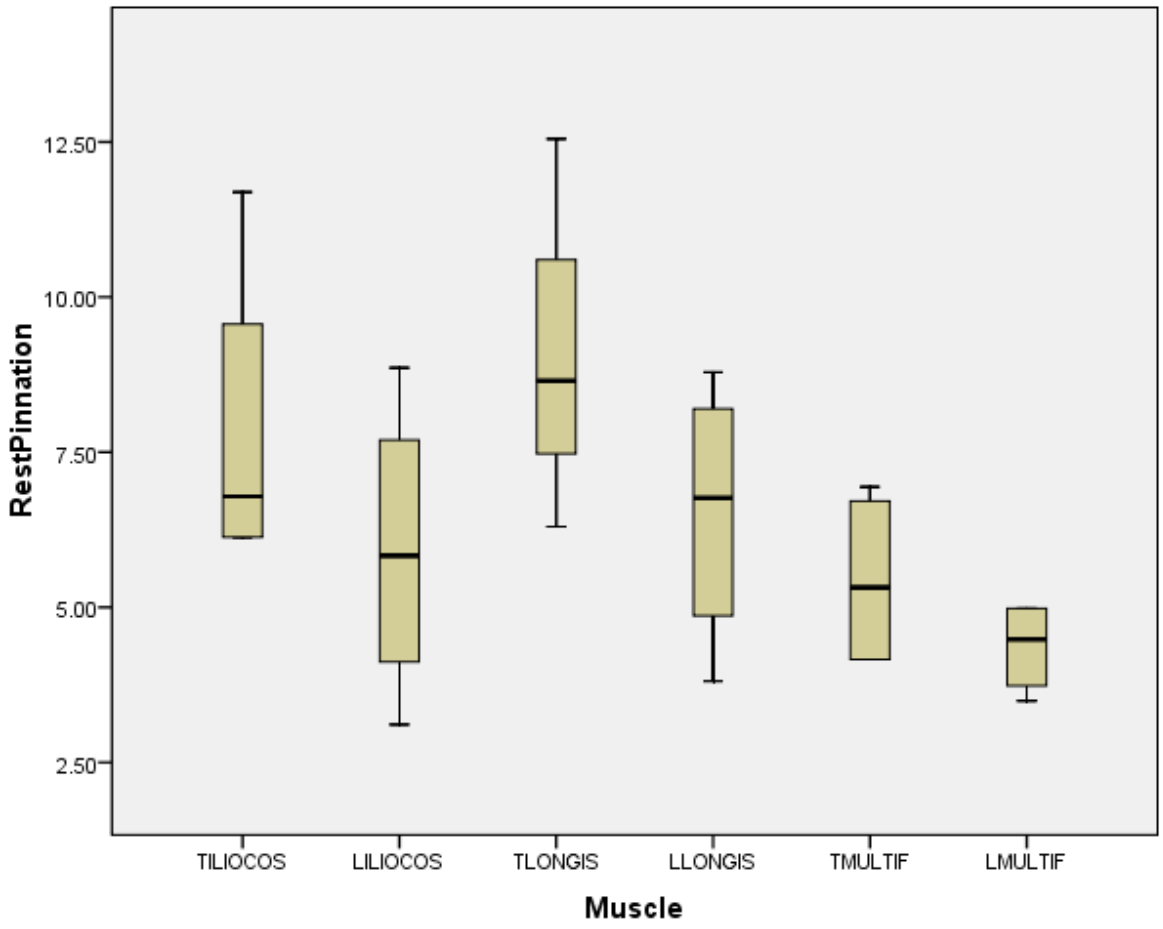

Fig. 6: *N. coucang*: Resting pinnation angle

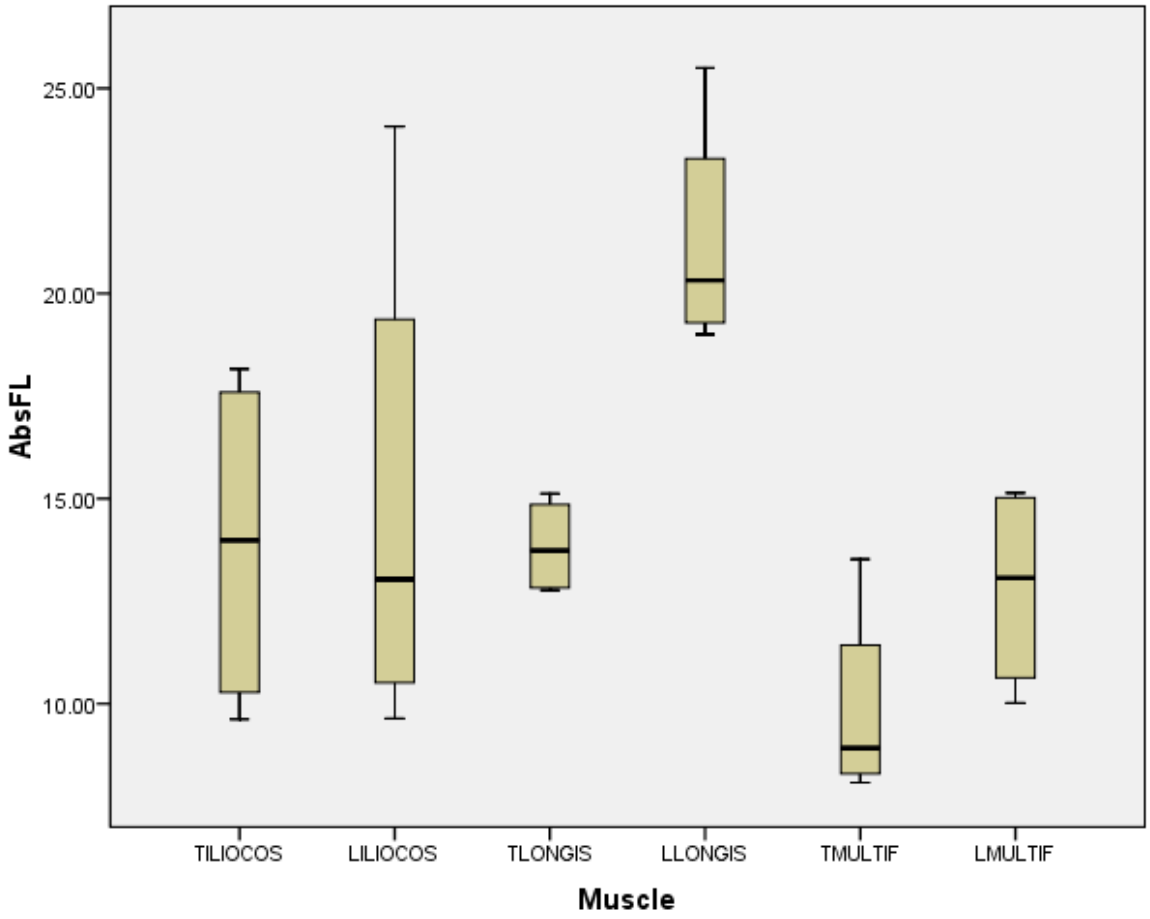

Fig. 7: *G. senegalensis*: Raw fiber length (Lf)

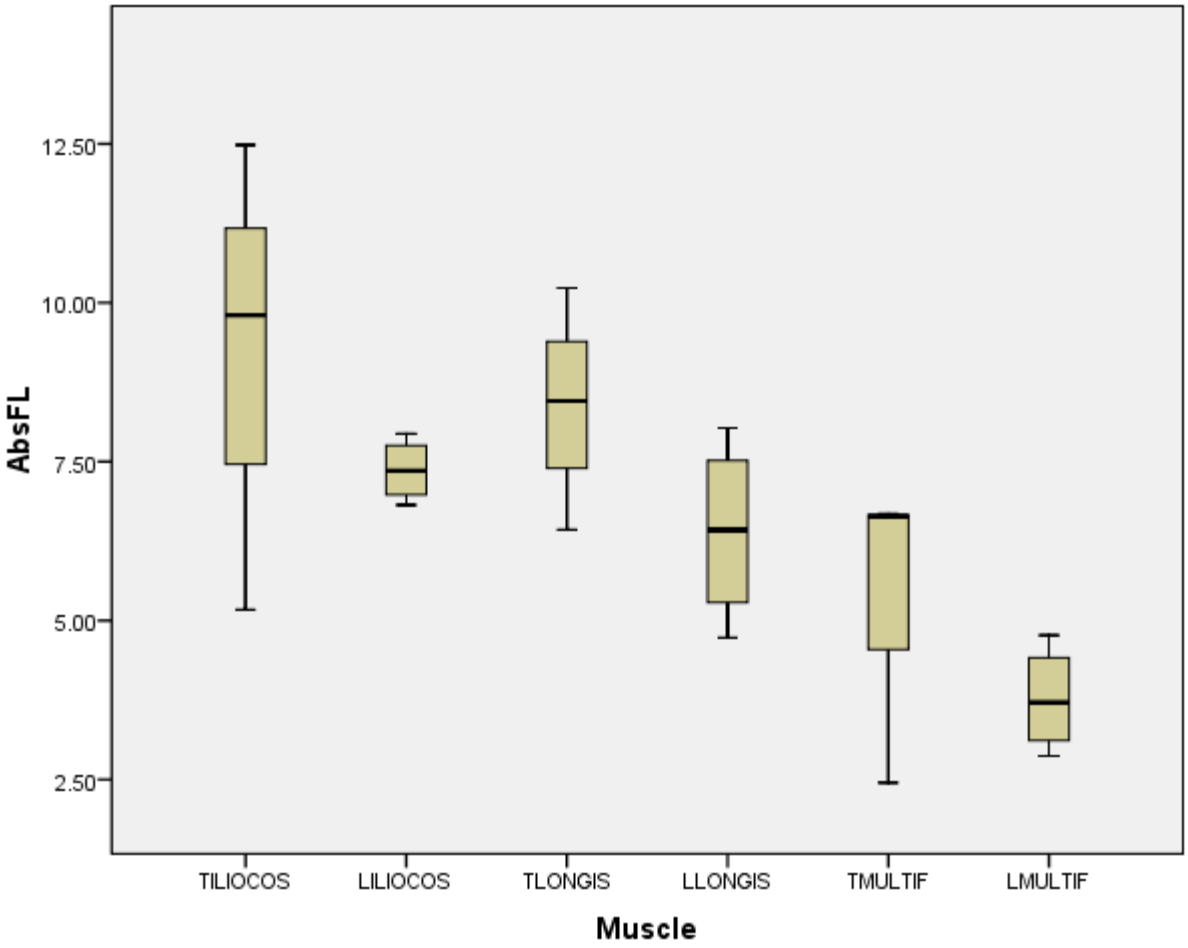

Fig. 8: *N. coucang*: Raw fiber length (Lf)

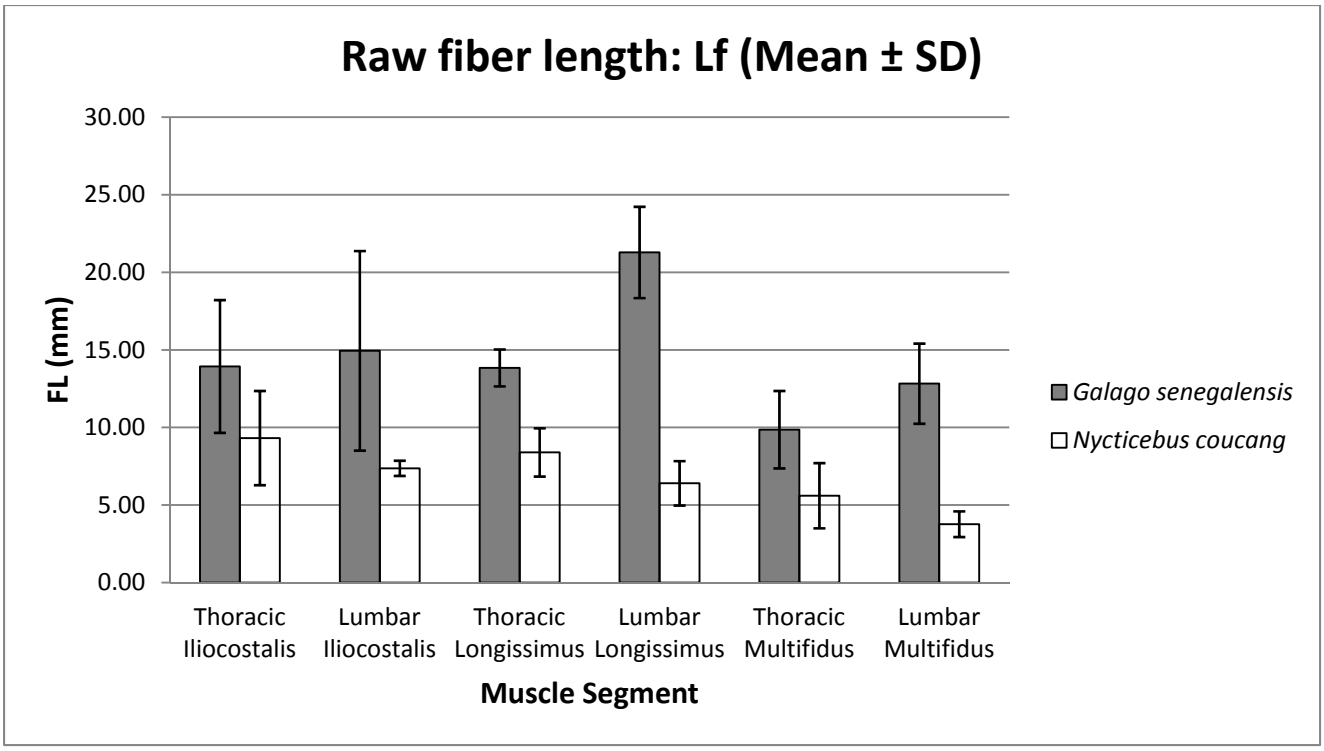

Fig. 9: Mean (± SD) of raw fiber length (Lf) for *G. senegalensis* and *N. coucang*

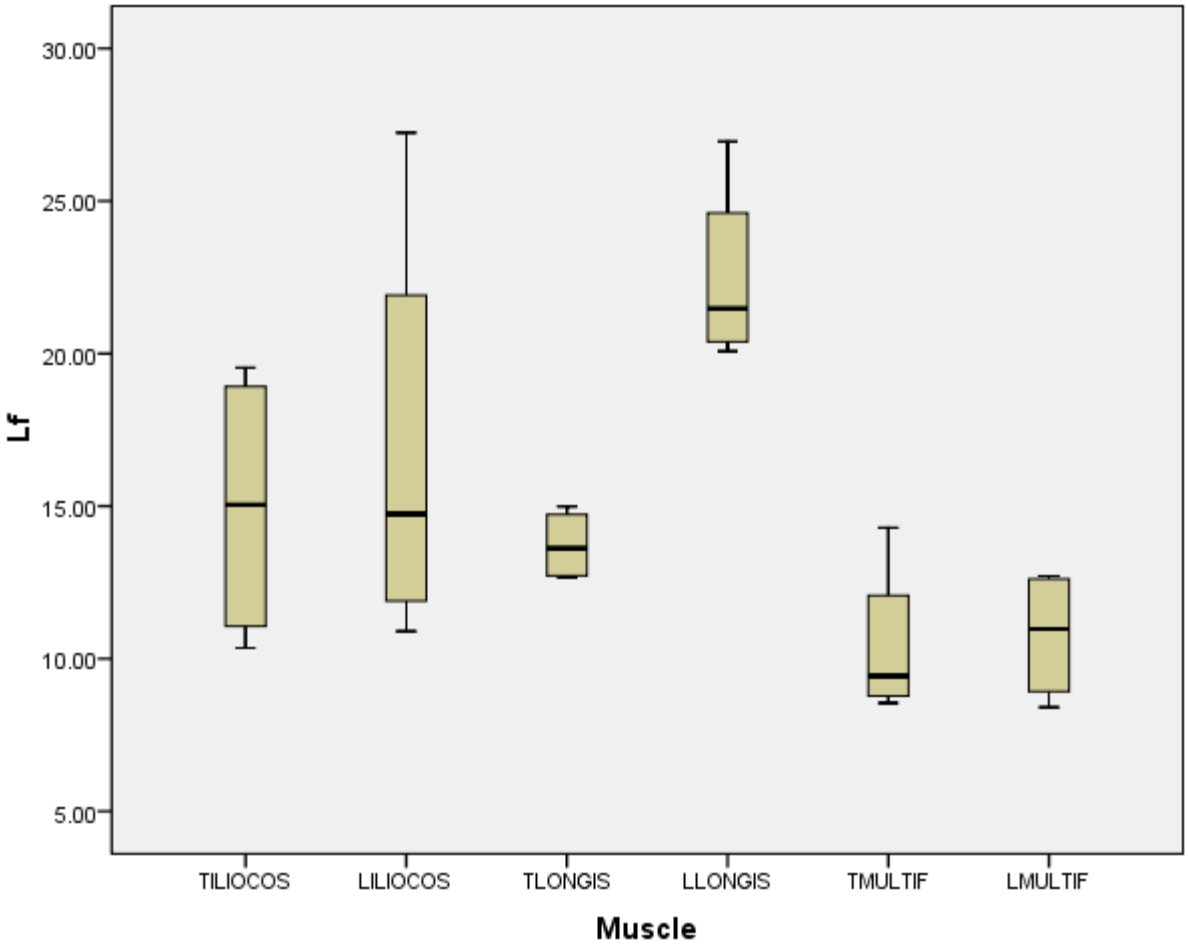

Fig. 10: *G. senegalensis*: Resting fiber length (NLf)

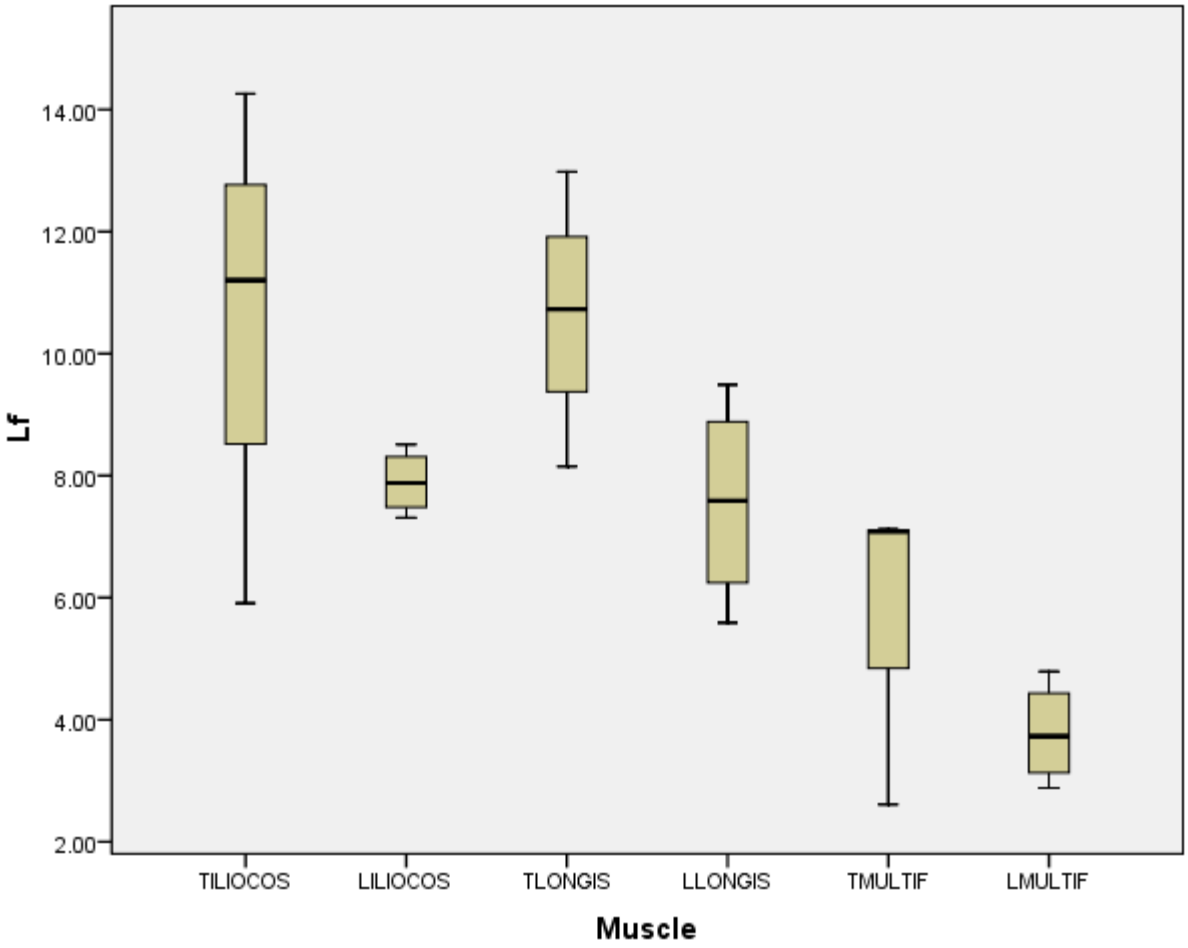

Fig. 11: *N. coucang*: Resting fiber length (NLf)

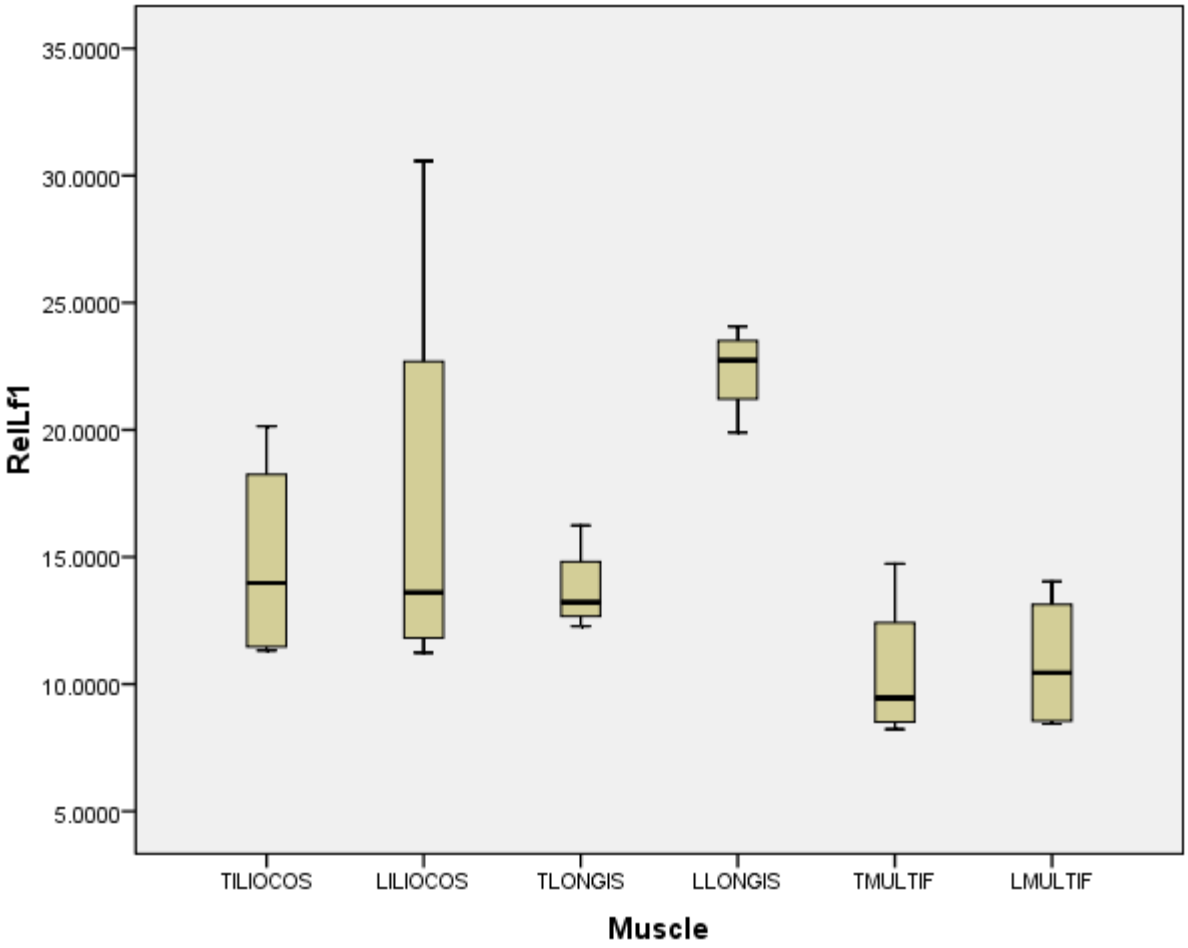

Fig. 12: *G. senegalensis*: Relative NLf-1 (to thoraco-lumbar spine length)

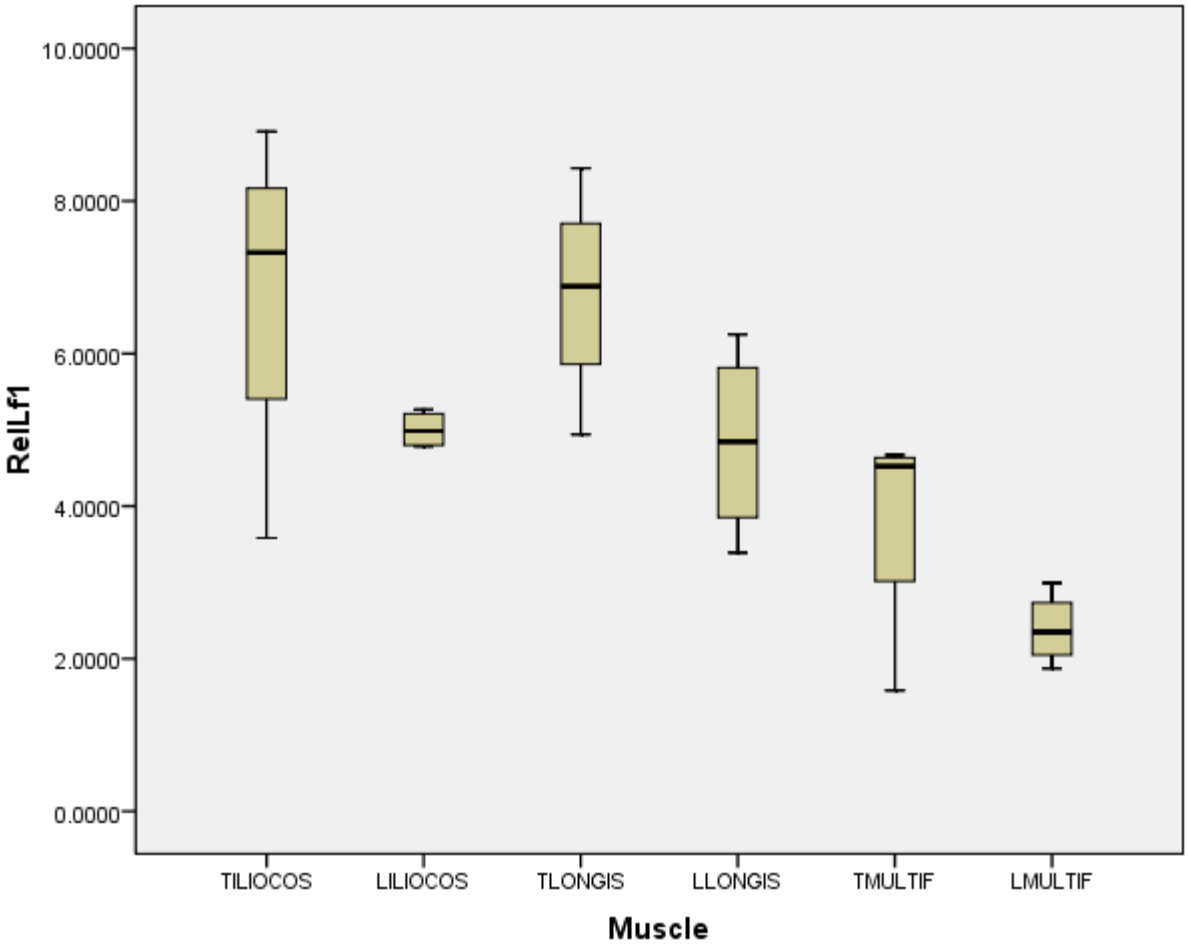

Fig. 13: *N. coucang*: Relative NLf-1 (to thoraco-lumbar spine length)

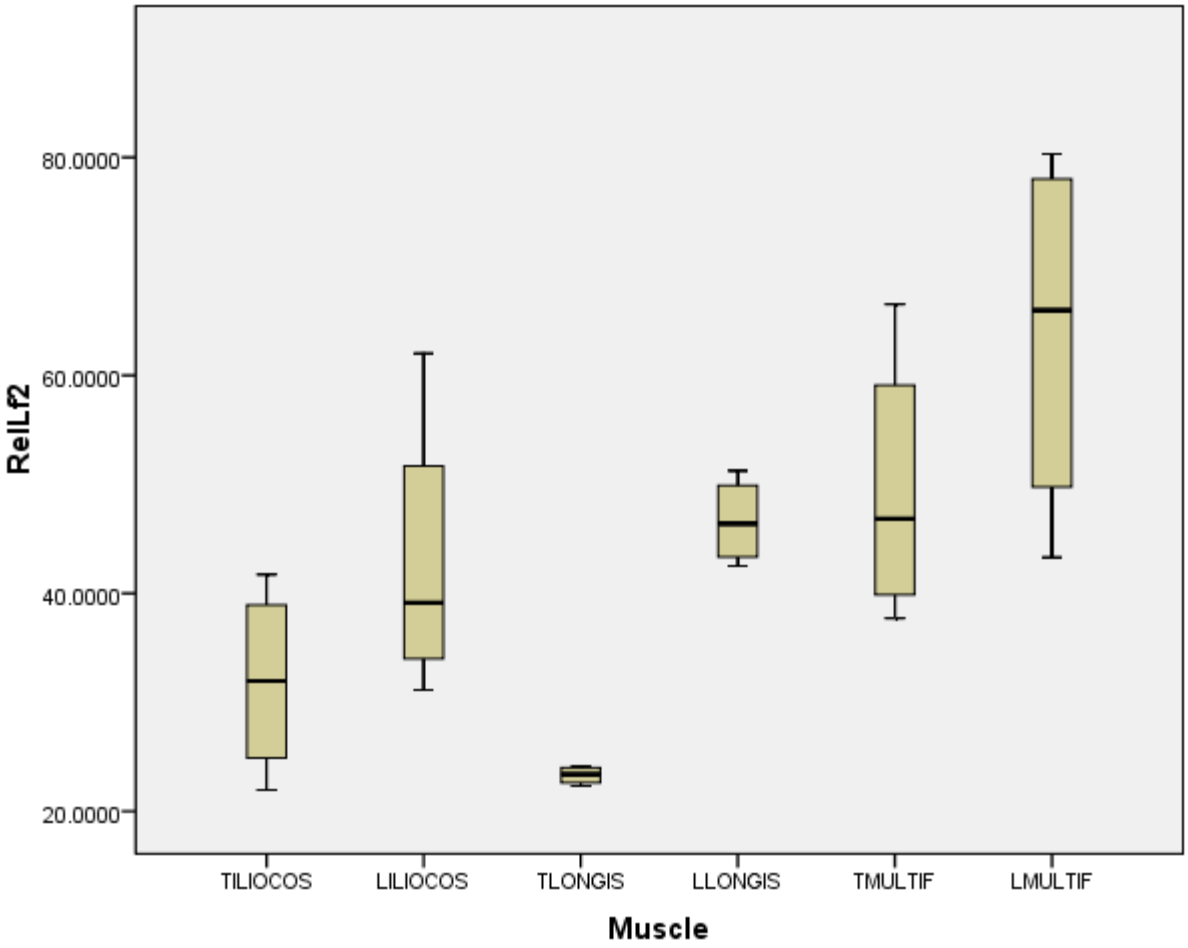

Fig. 14: *G. senegalensis*: Relative NLf-2 (to resting muscle length)

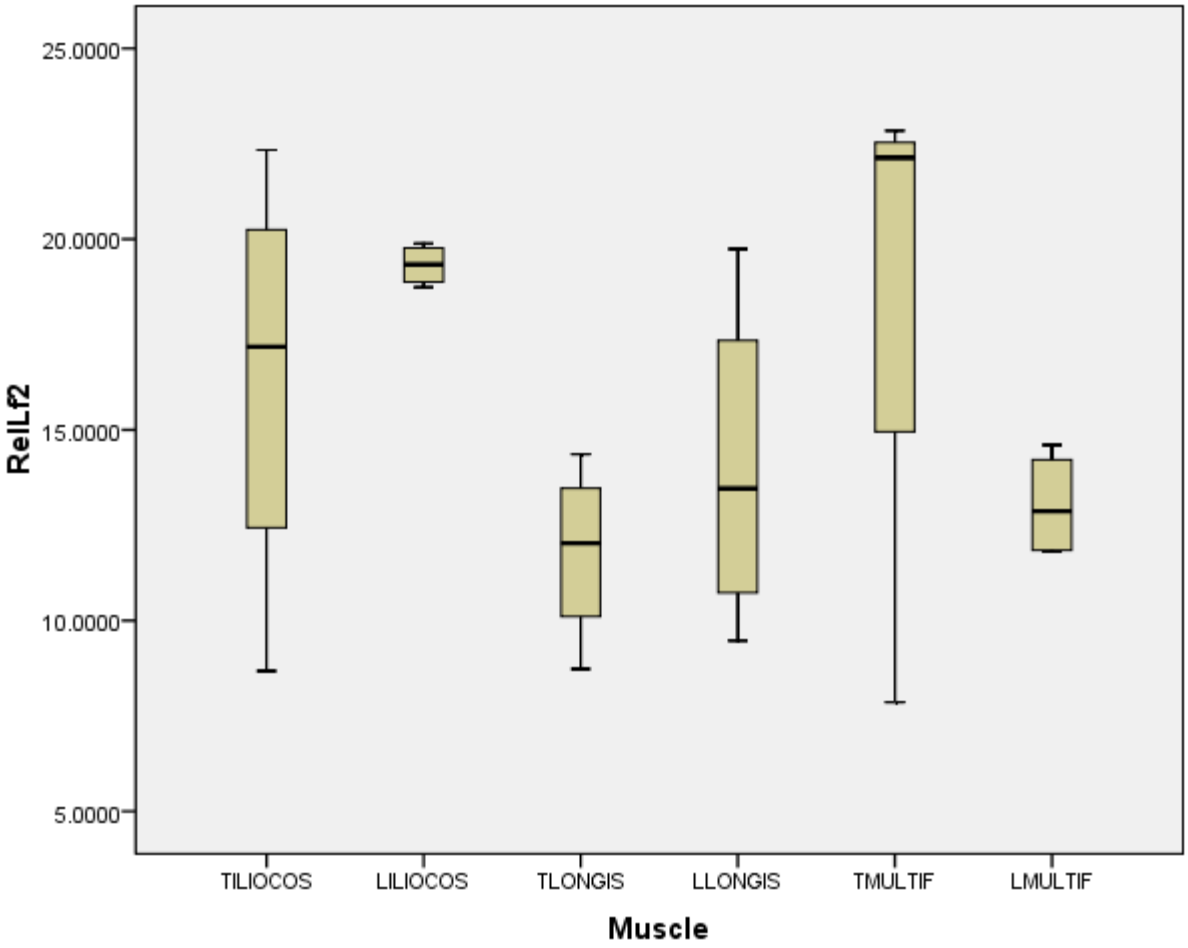

Fig. 15: *N. coucang*: Relative NLf-2 (to resting muscle length)

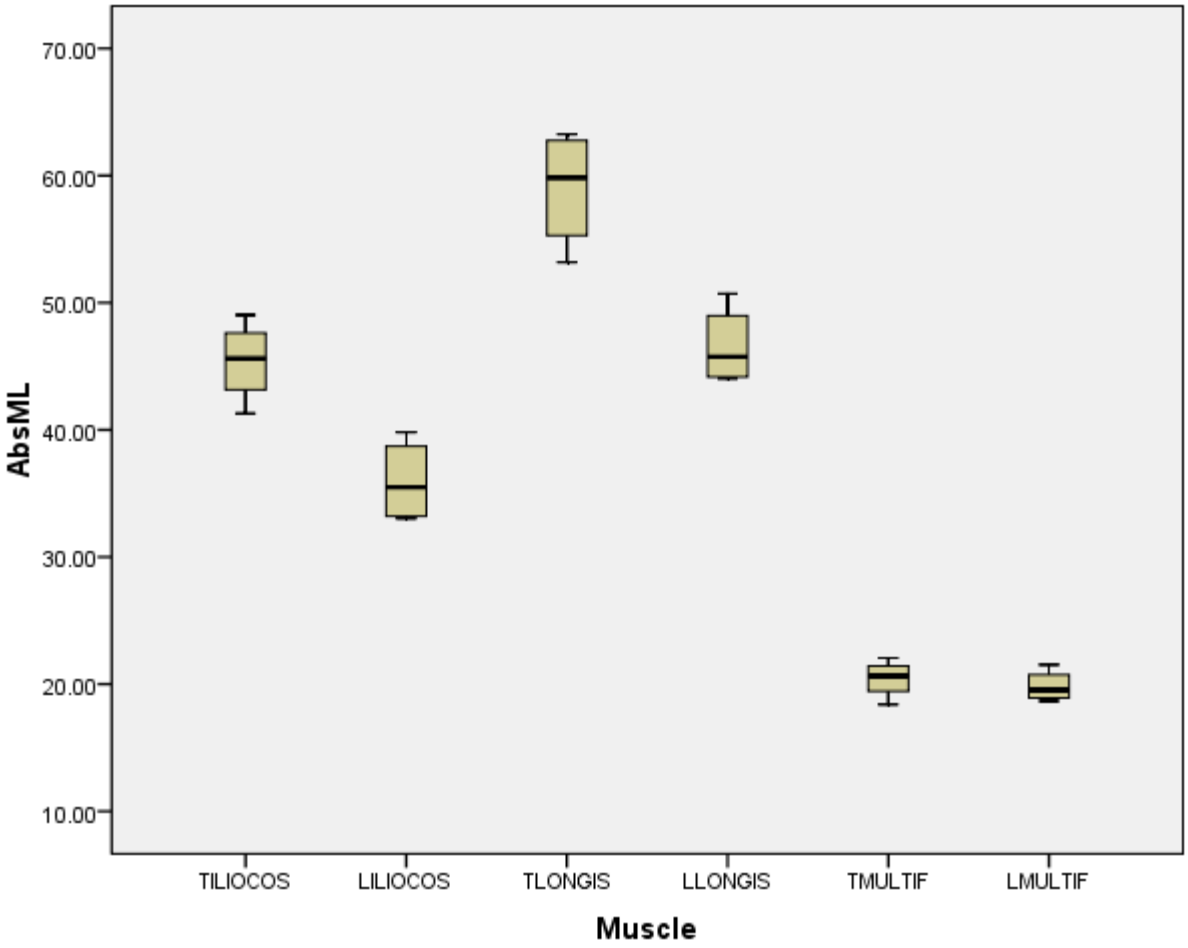

Fig. 16: *G. senegalensis*: Raw muscle length (ML)

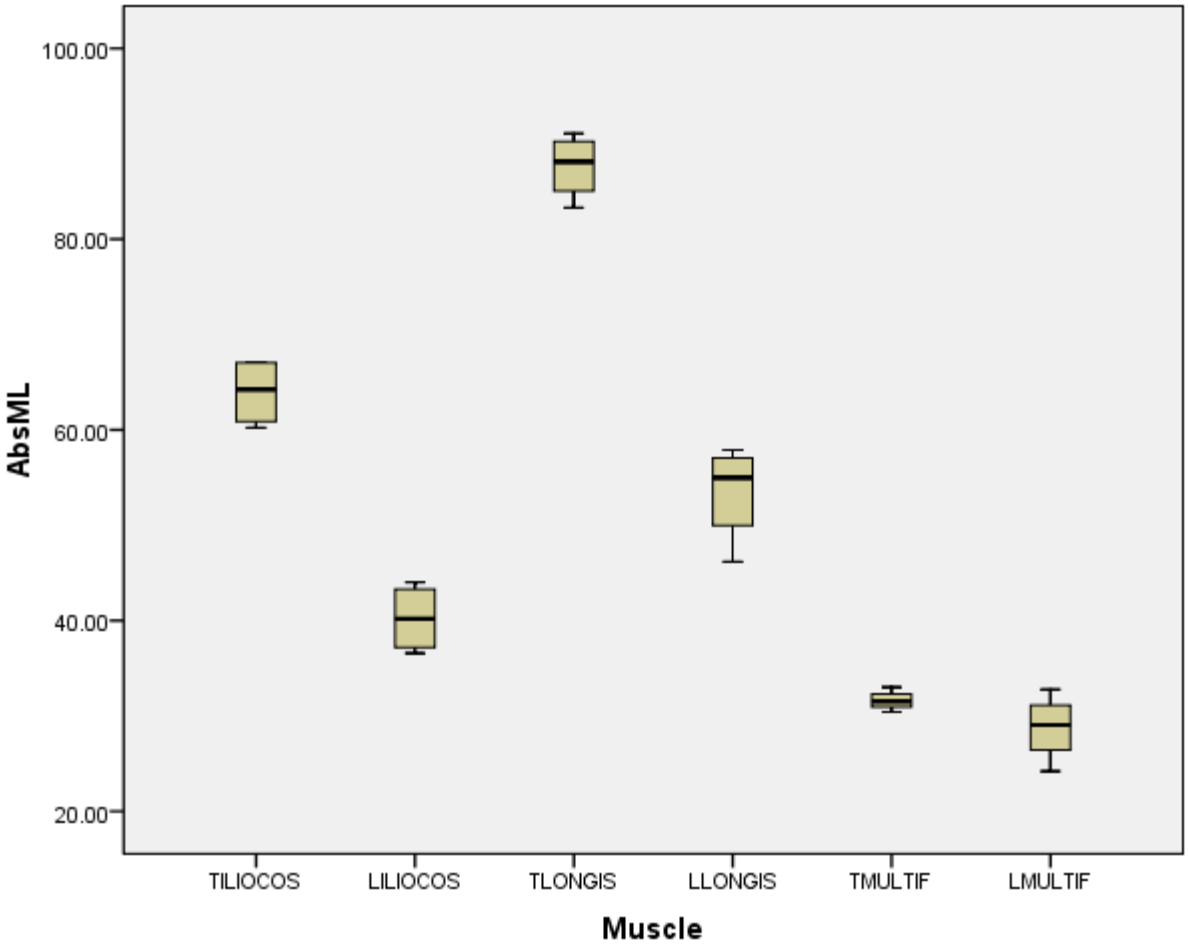

Fig. 17: *N. coucang*: Raw muscle length (ML)

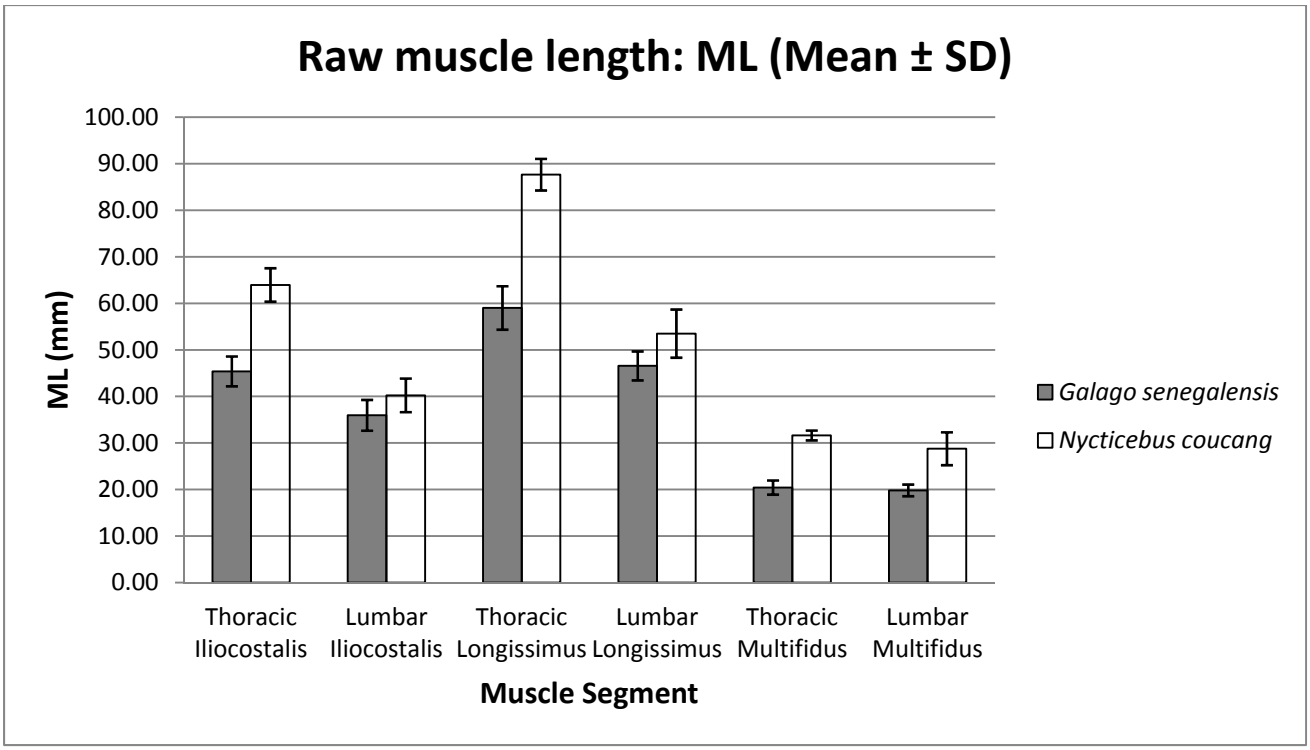

Fig. 18: Mean (± SD) of ML for *G. senegalensis* and *N. coucang*

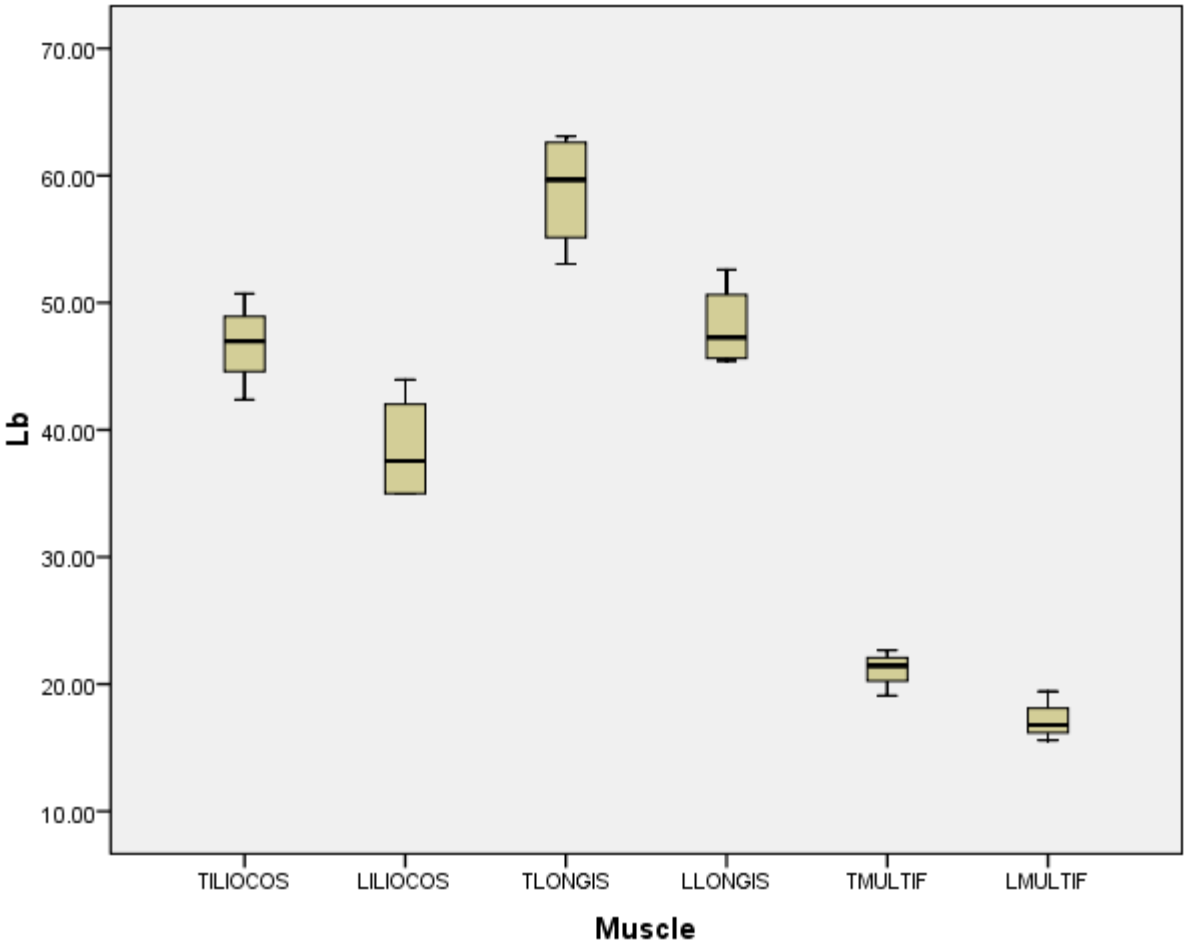

Fig. 19: *G. senegalensis*: Resting muscle length (Lb)

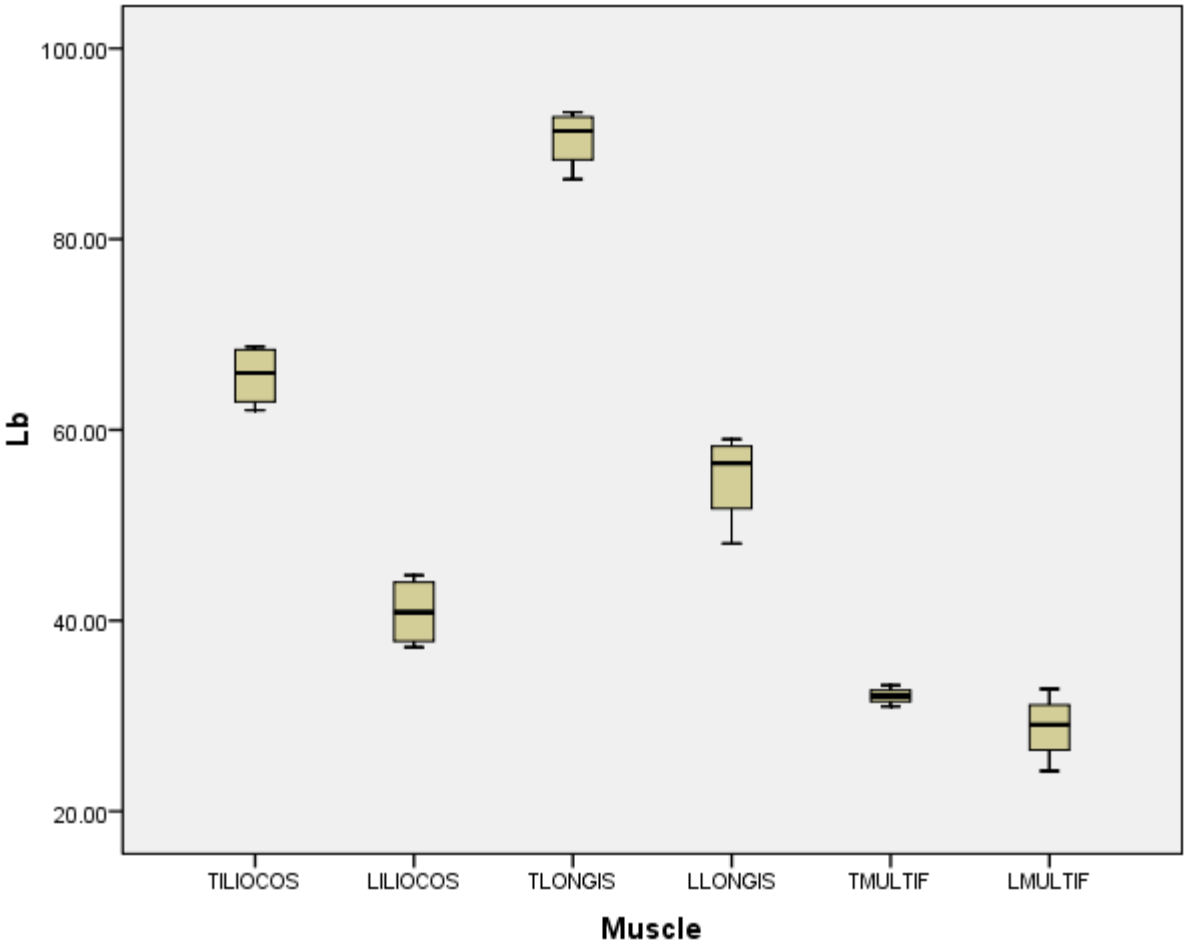

Fig. 20: *N. coucang*: Resting muscle length (Lb)

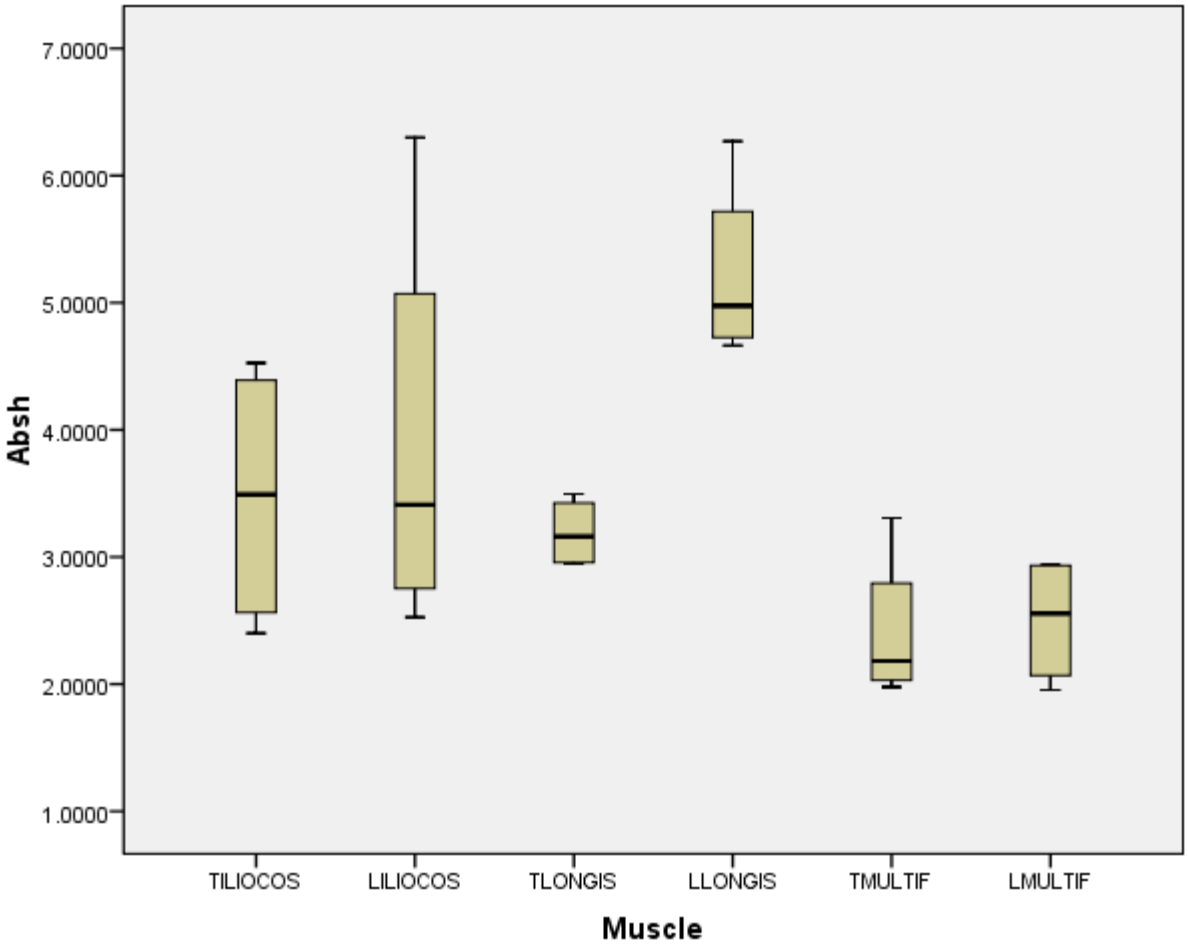

Fig. 21: *G. senegalensis*: Potential excursion of whole muscle (*h*)

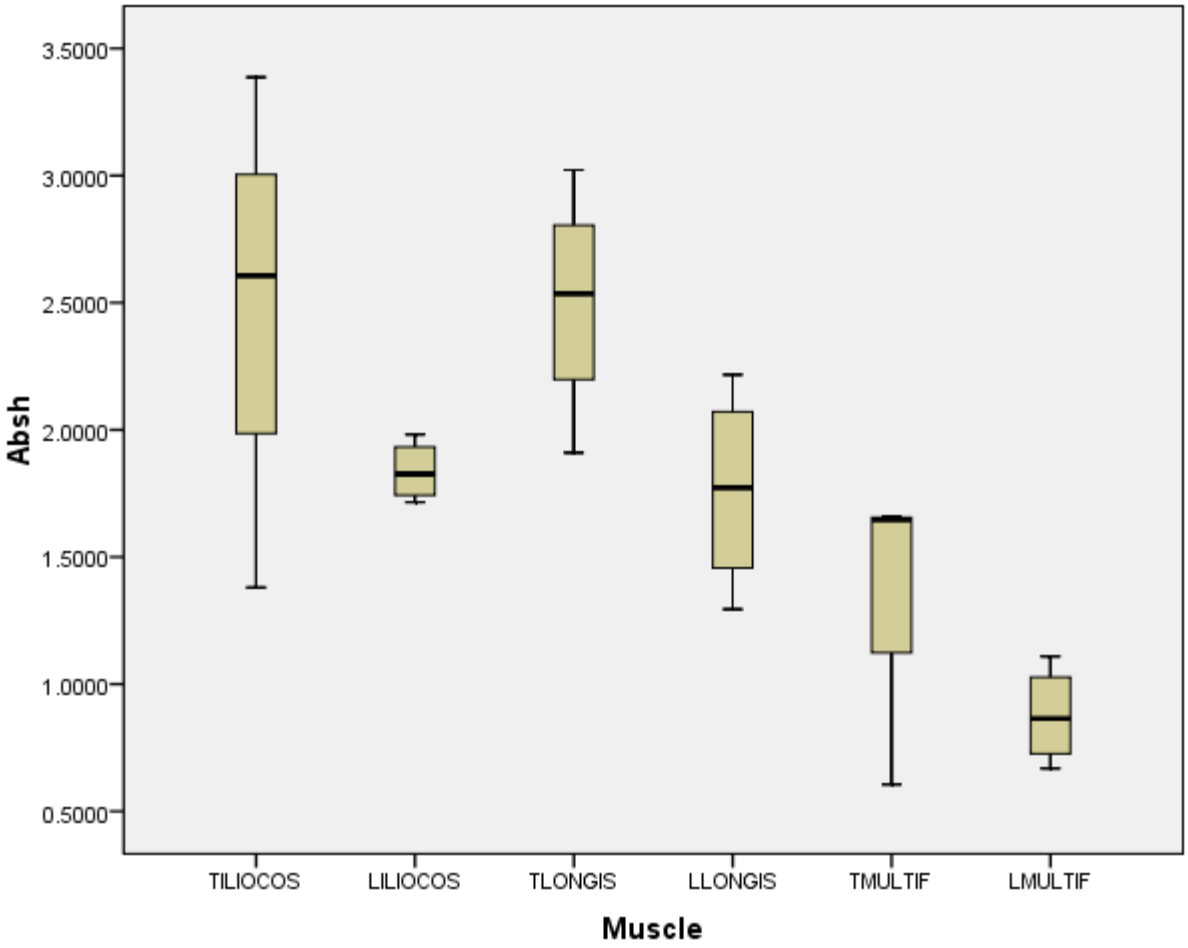

Fig. 22: *N. coucang*: Potential excursion of whole muscle (*h*)

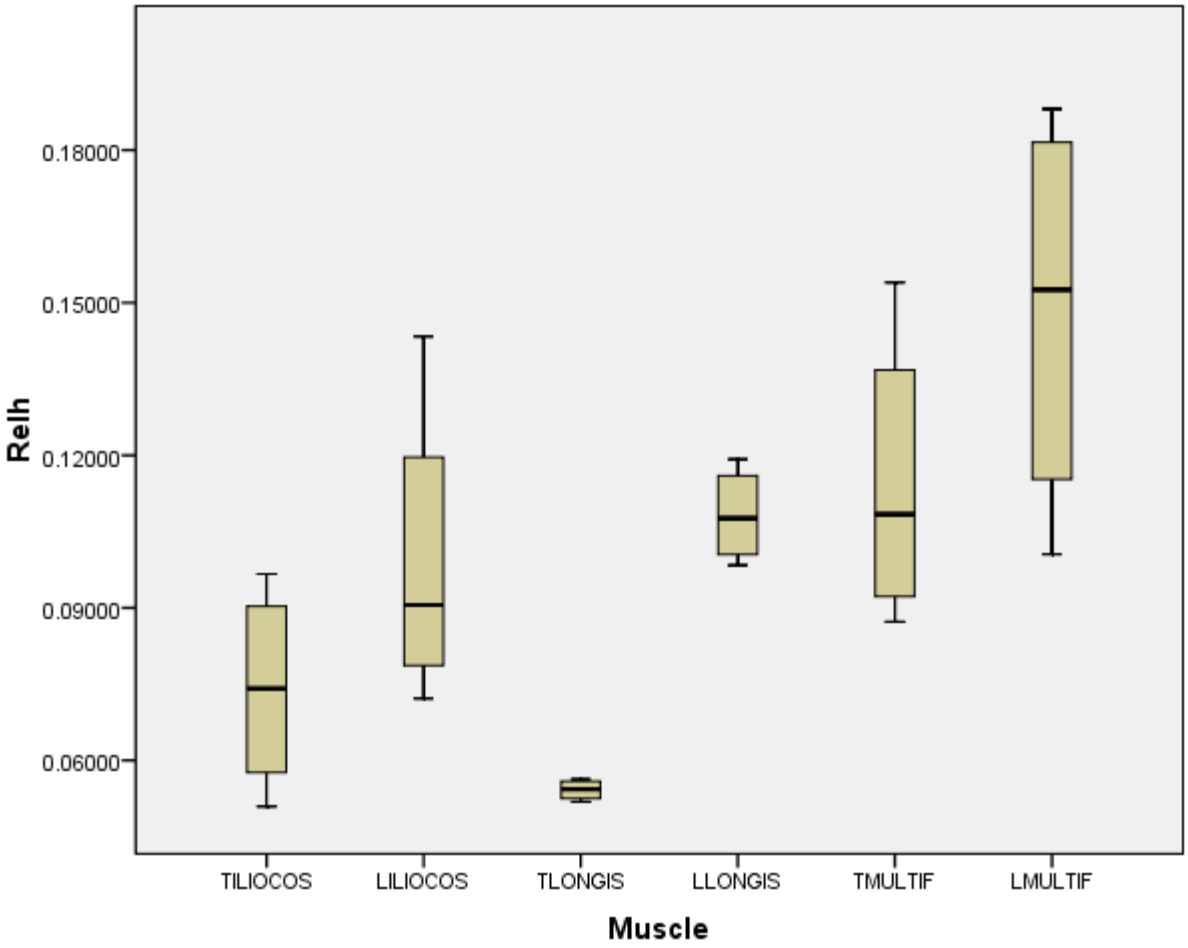

Fig. 23: *G. senegalensis*: Relative *h*

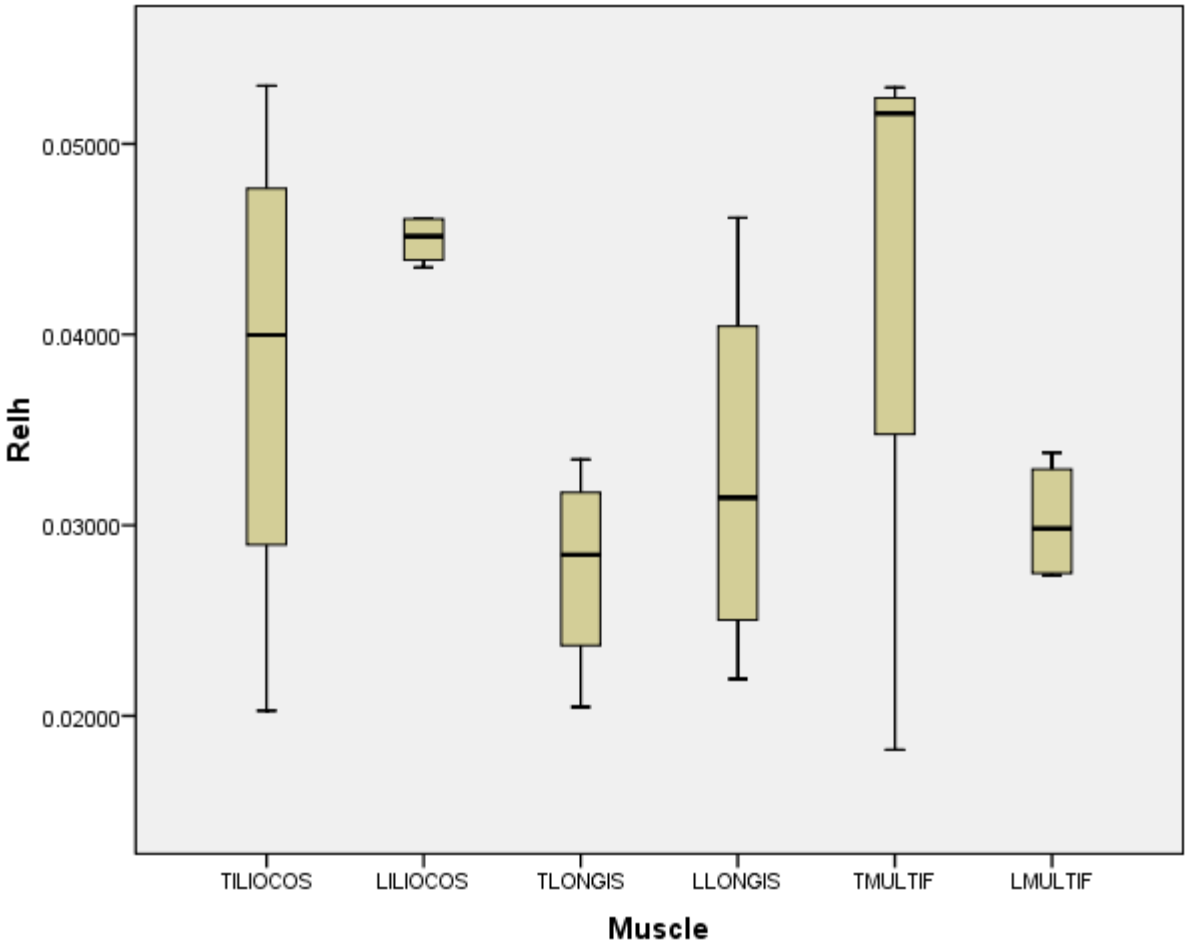

Fig. 24: *N. coucang*: Relative *h*

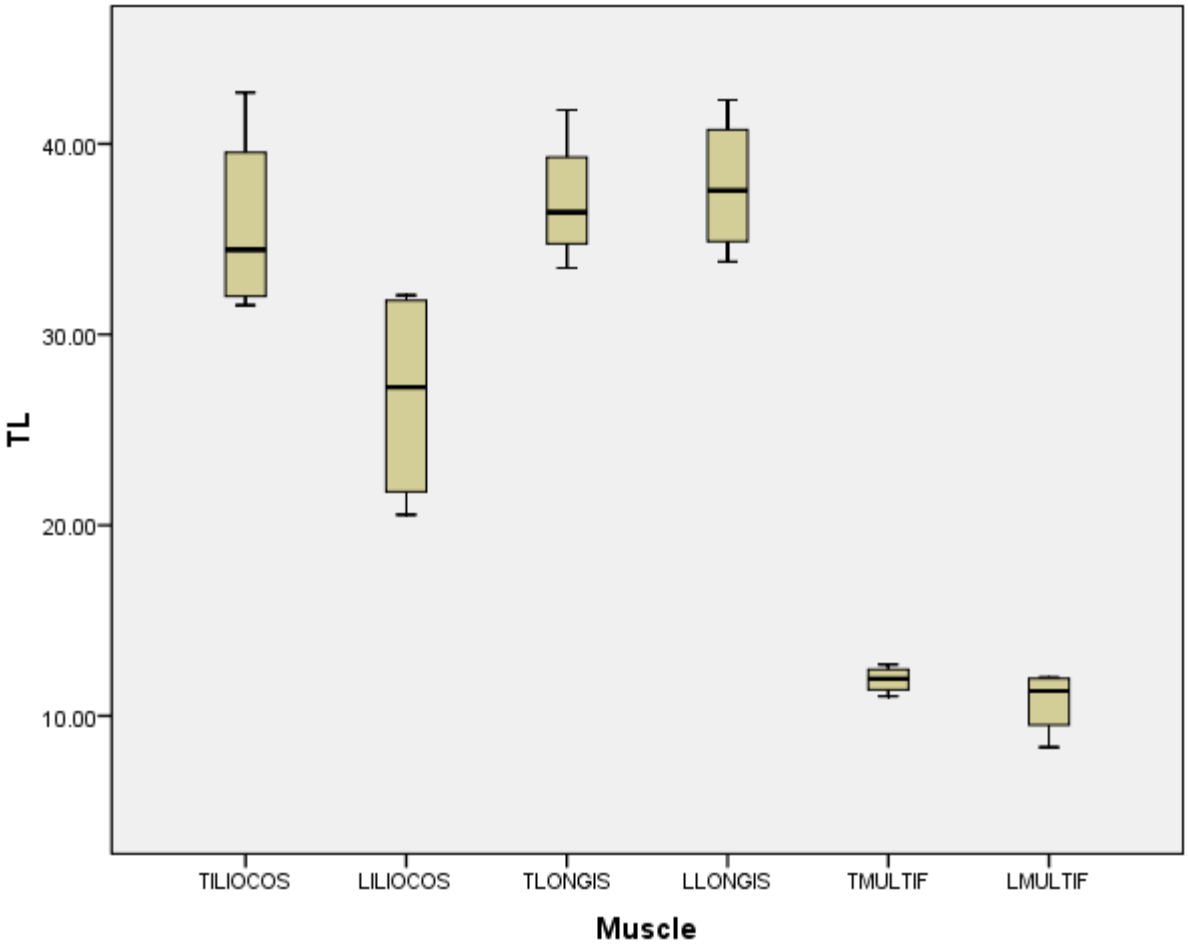

Fig. 25: *G. senegalensis*: Tendon length (TL)

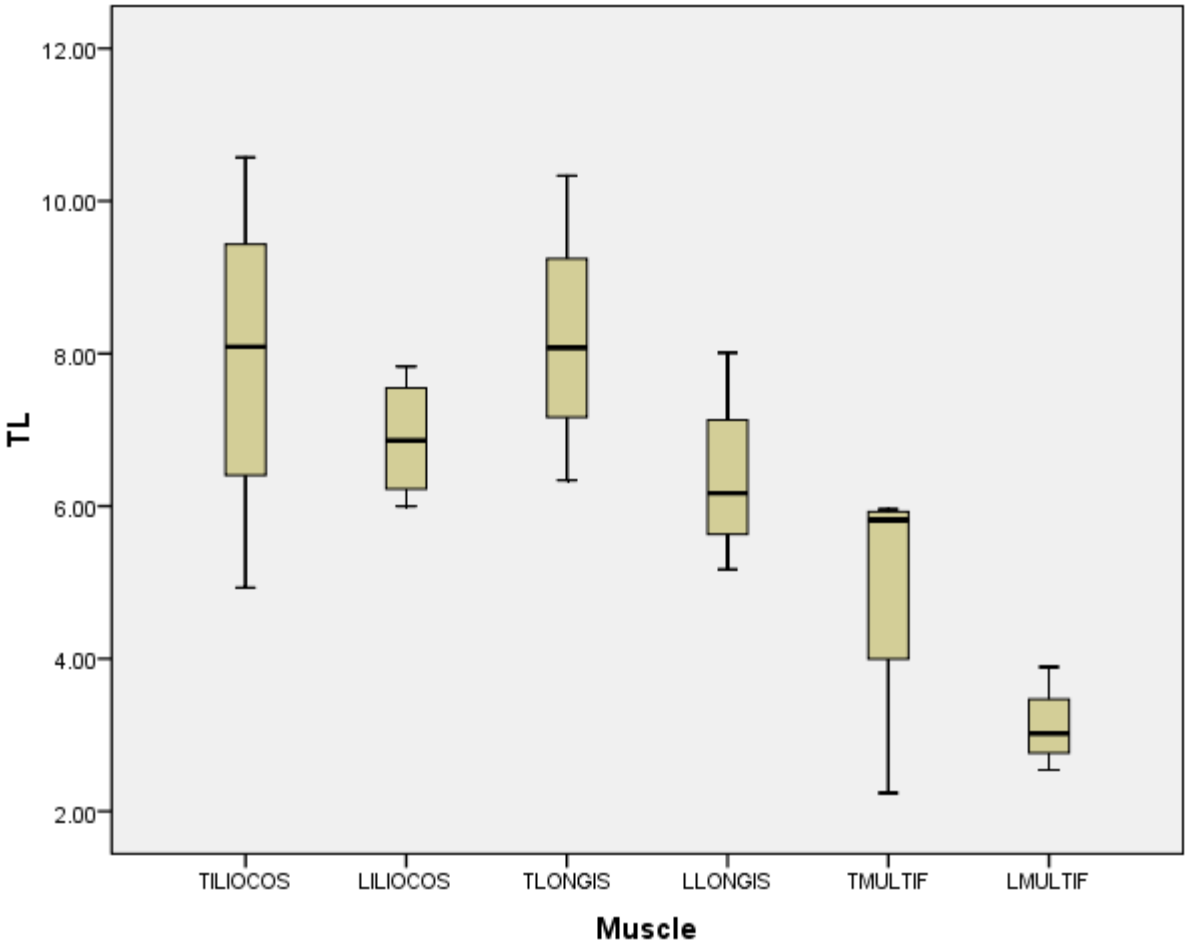

Fig. 26: *N. coucang*: Tendon length (TL)

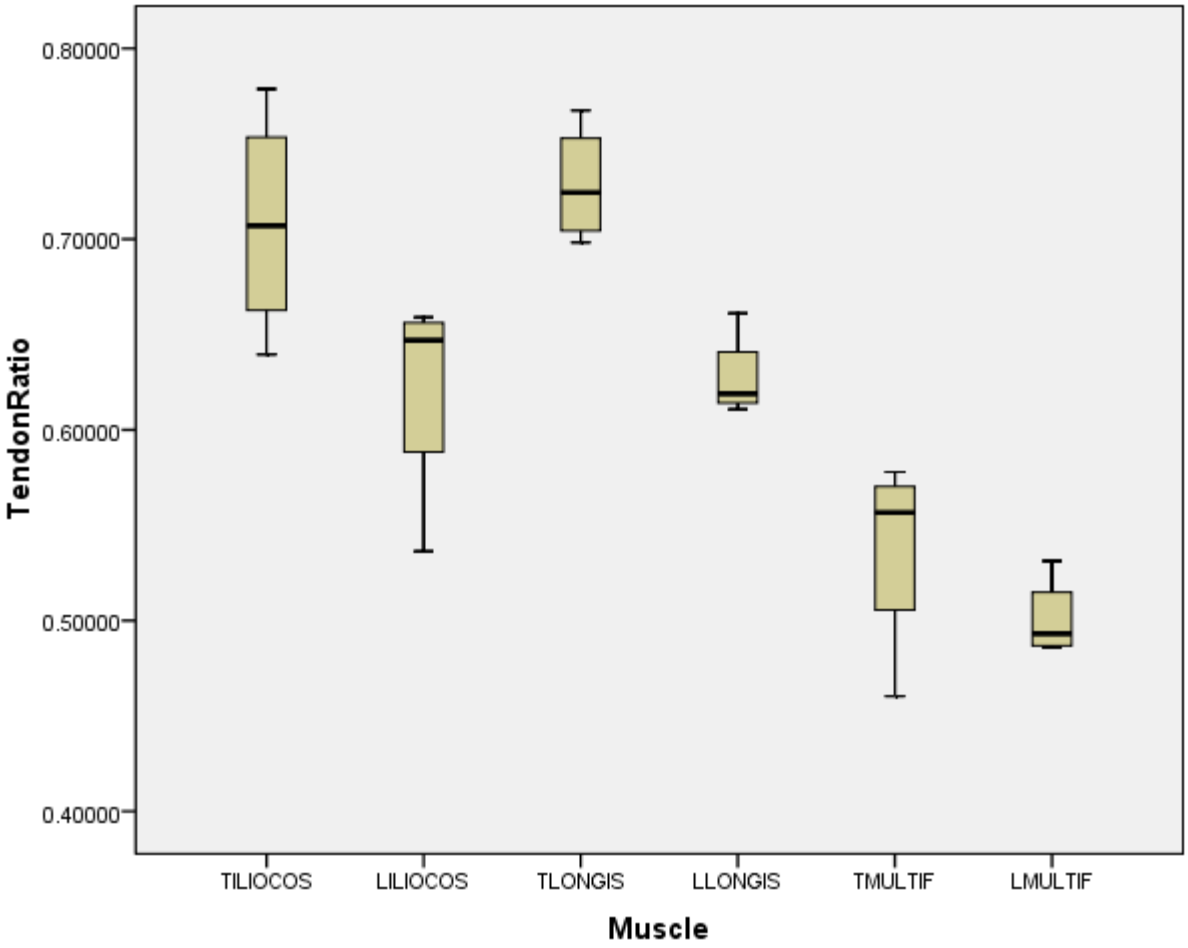

Fig. 27: *G. senegalensis*: TL/(TL + NLf)

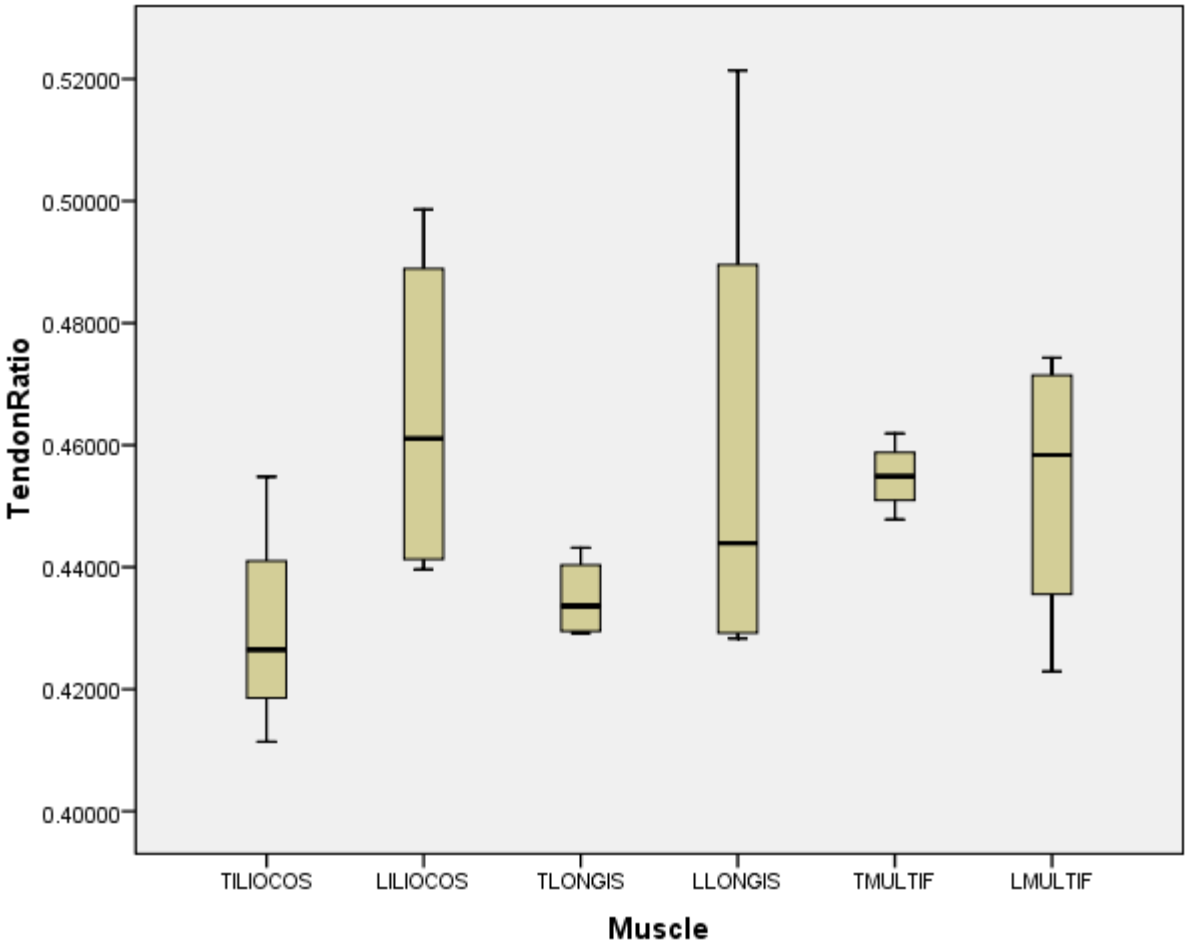

Fig. 28: *N. coucang*: TL/(TL + NLf)

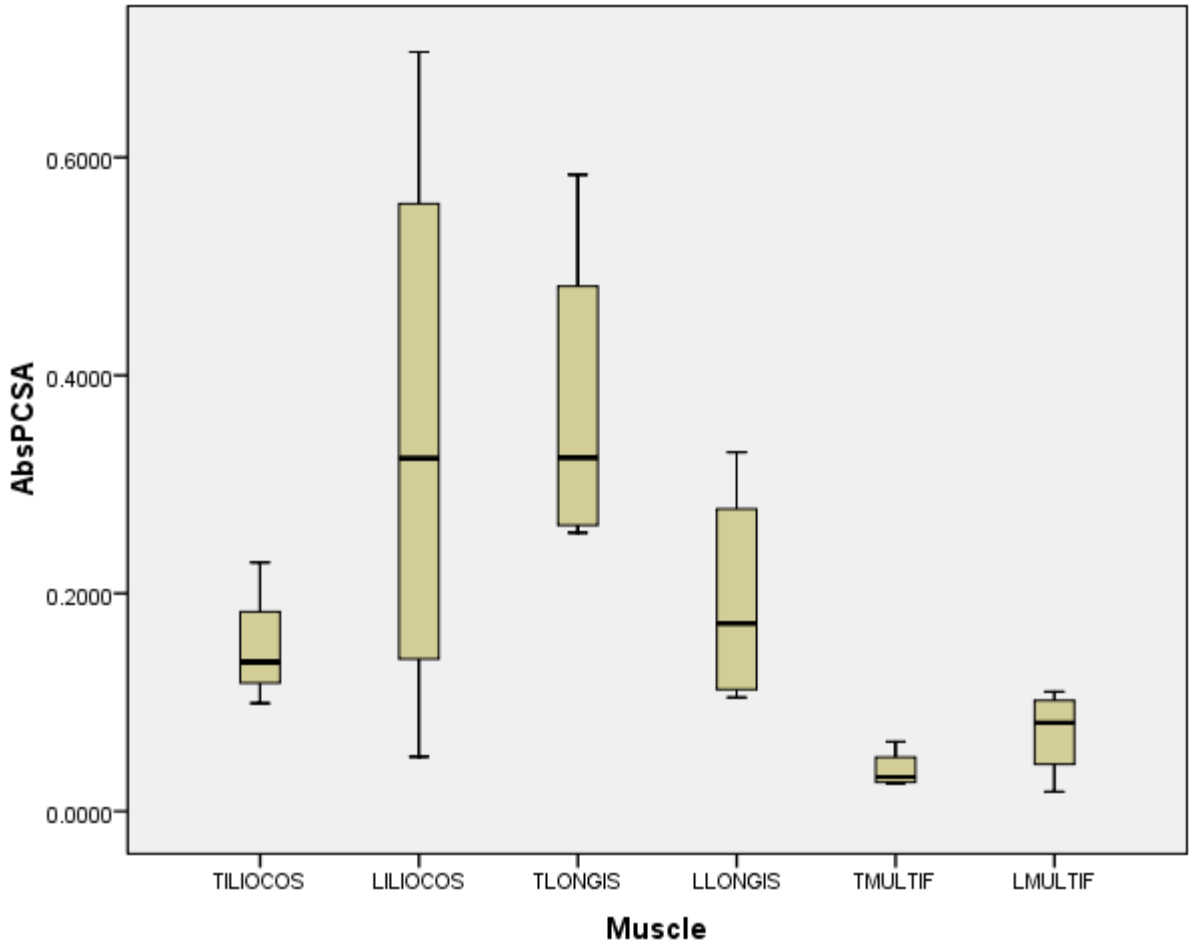

Fig. 29: *G. senegalensis*: PCSA

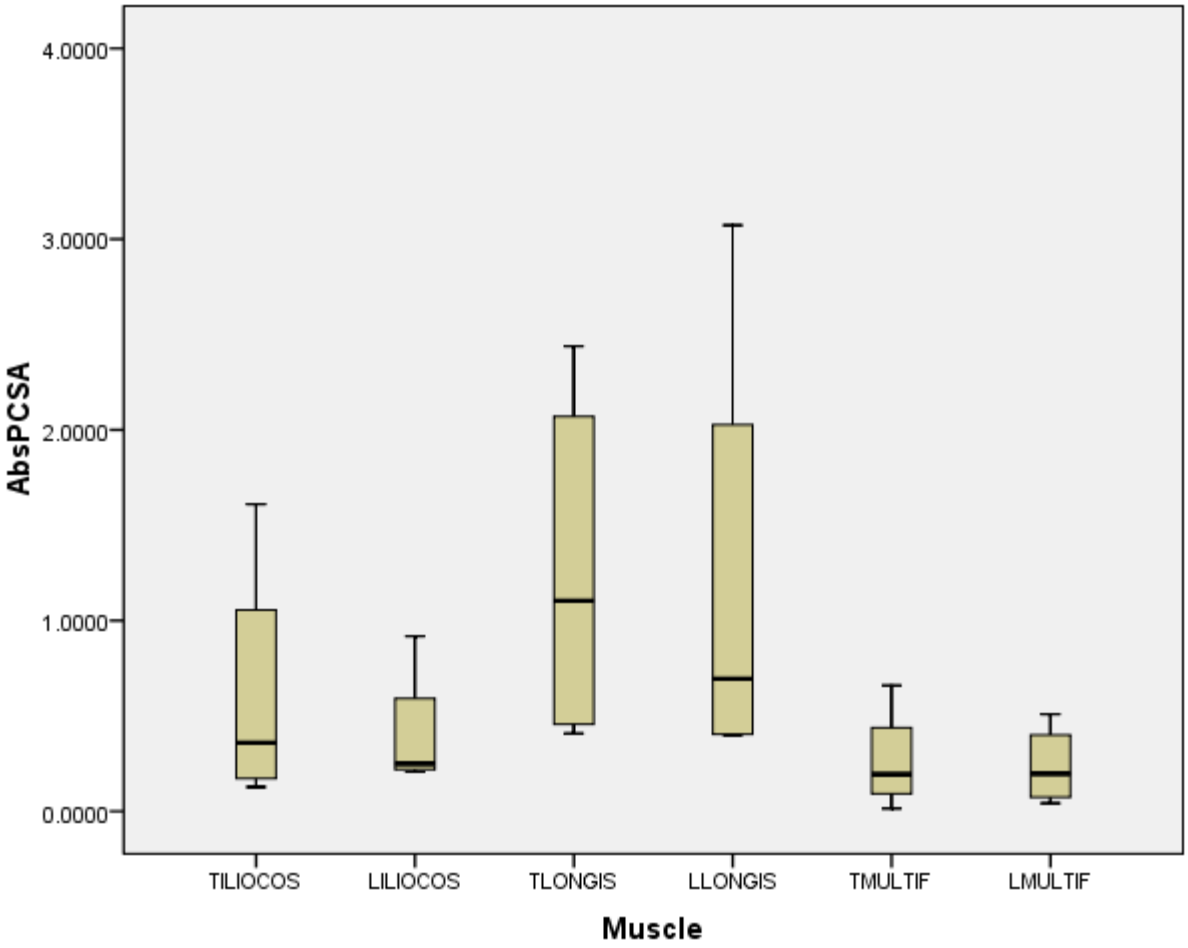

Fig. 30: *N. coucang*: PCSA

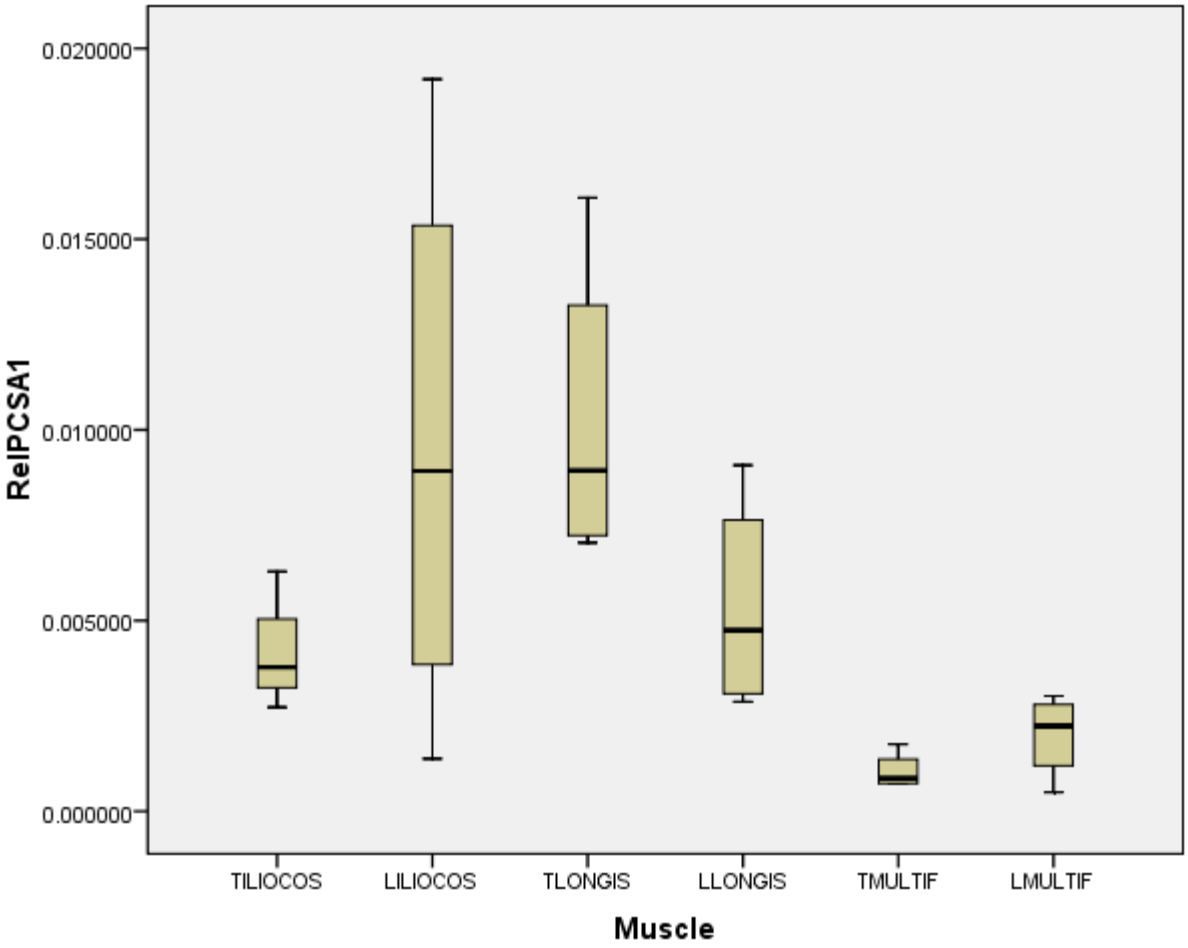

Fig. 31: *G. senegalensis*: Relative PCSA-1 (to species mean body mass$^{0.67}$)

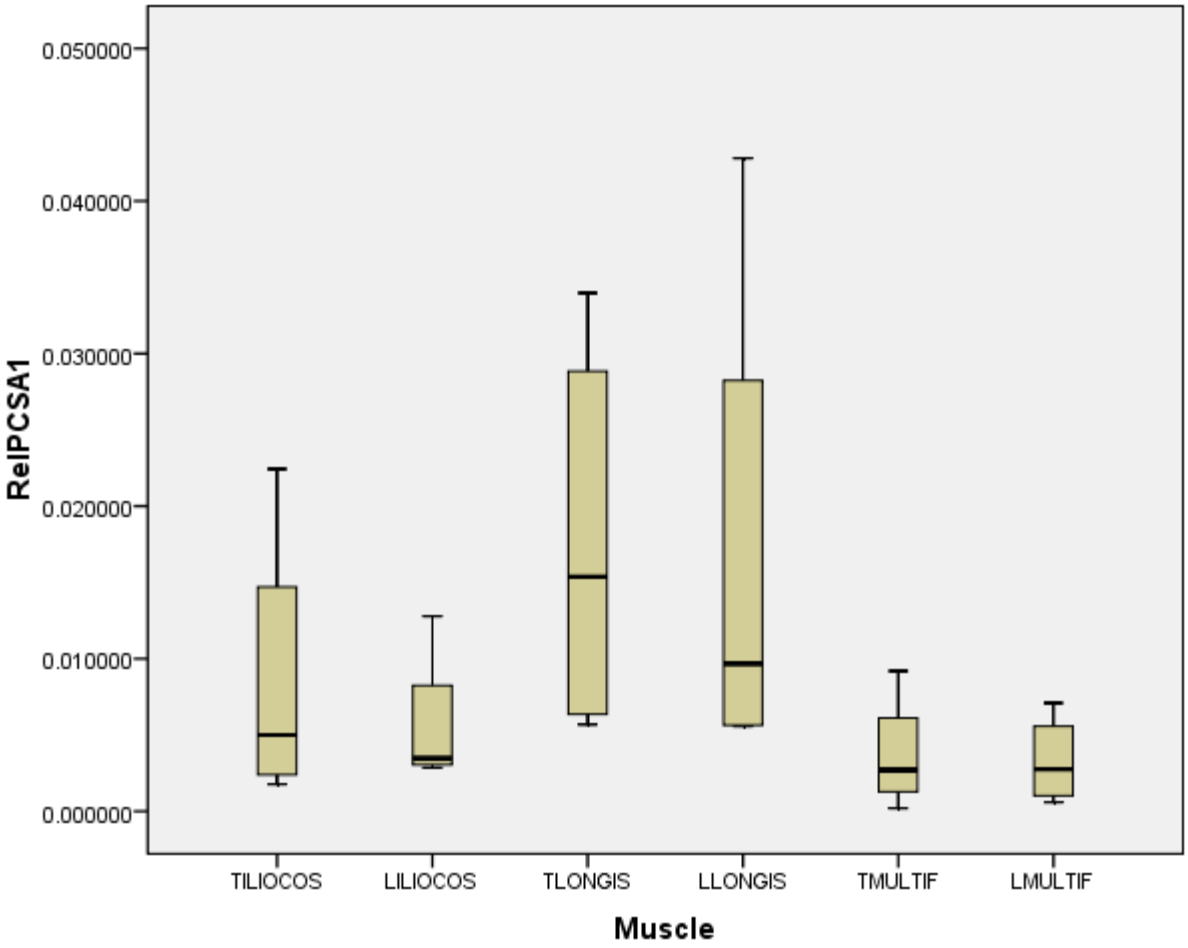

Fig. 32: *N. coucang*: Relative PCSA-1 (to species mean body mass$^{0.67}$)

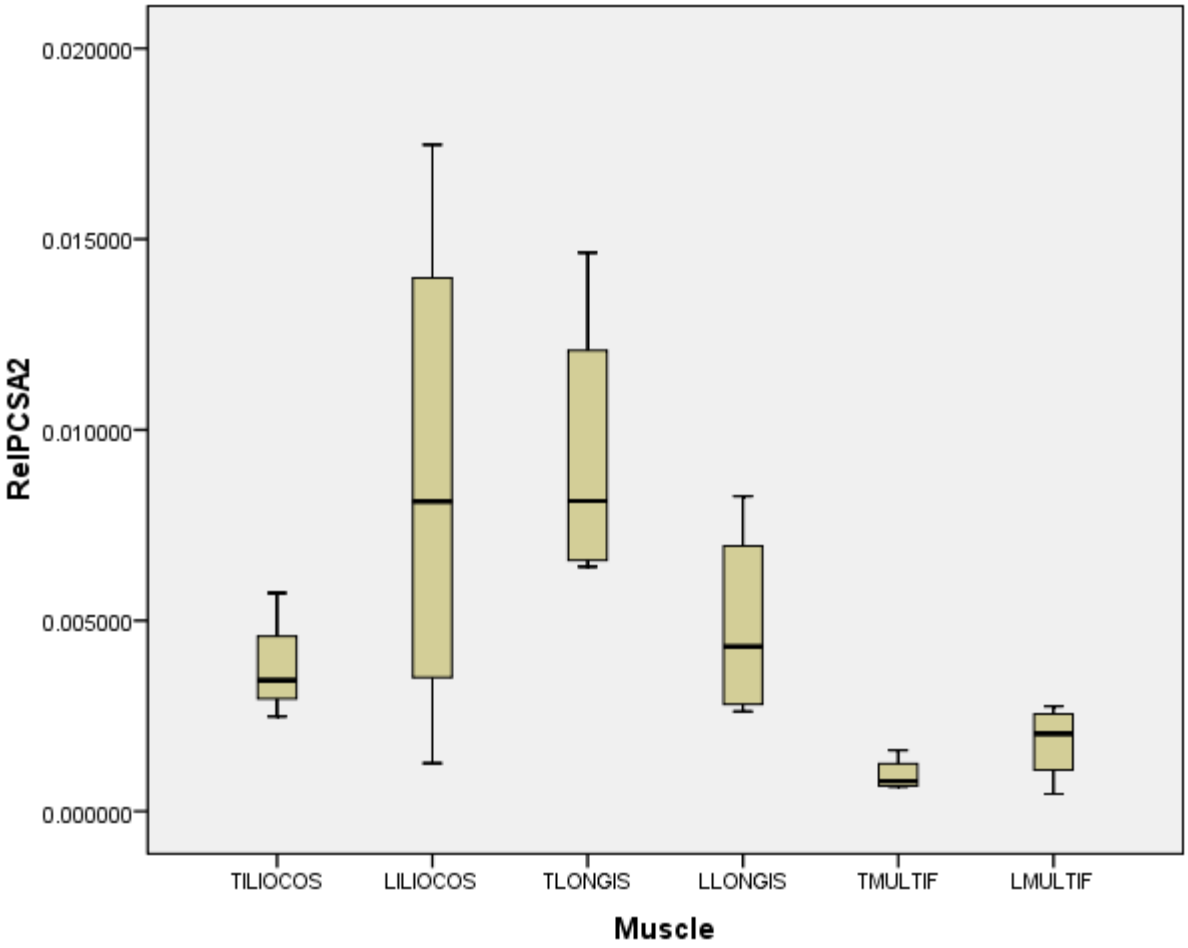

Fig. 33: *G. senegalensis*: Relative PCSA-2 (to upper estimate of body mass$^{0.67}$)

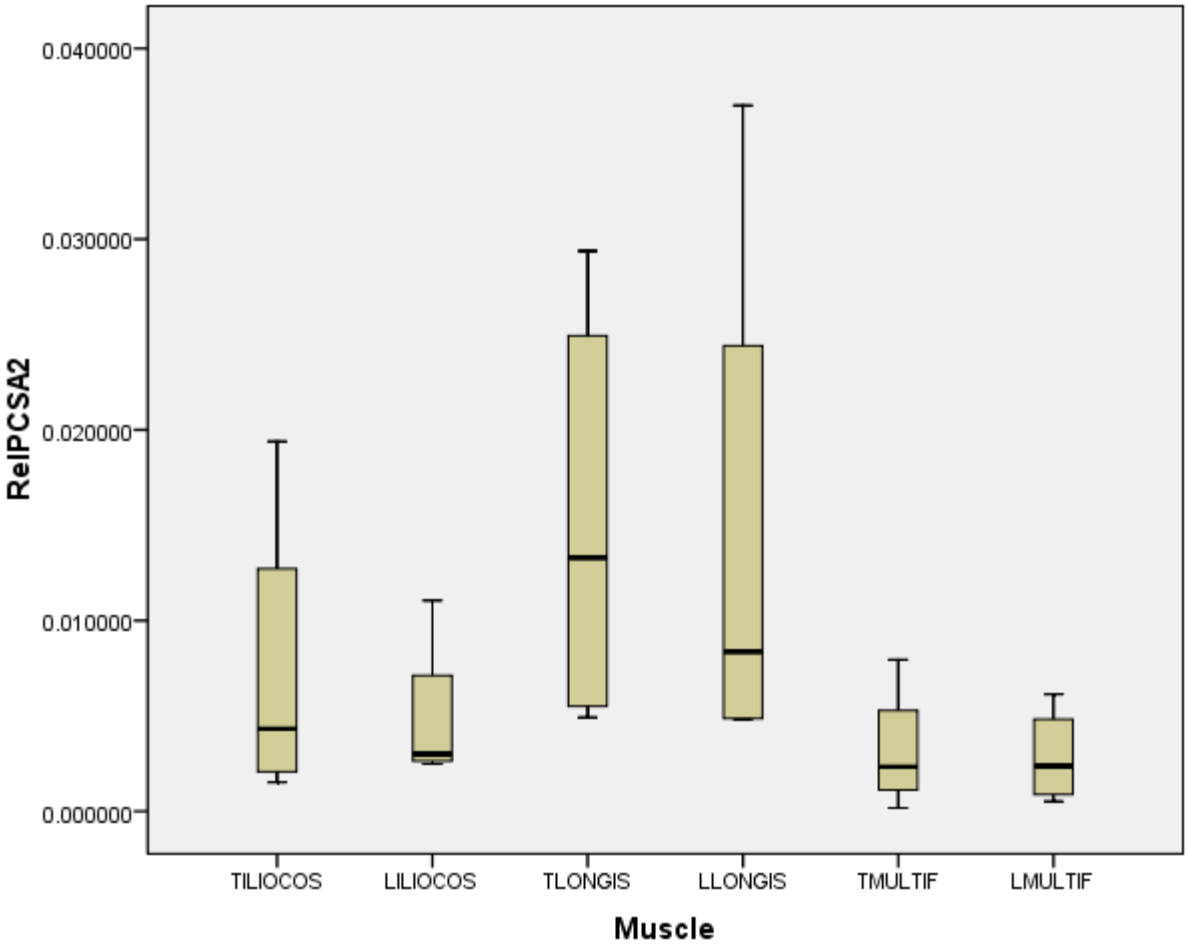

Fig. 34: *N. coucang*: Relative PCSA-2 (to upper estimate of body mass$^{0.67}$)

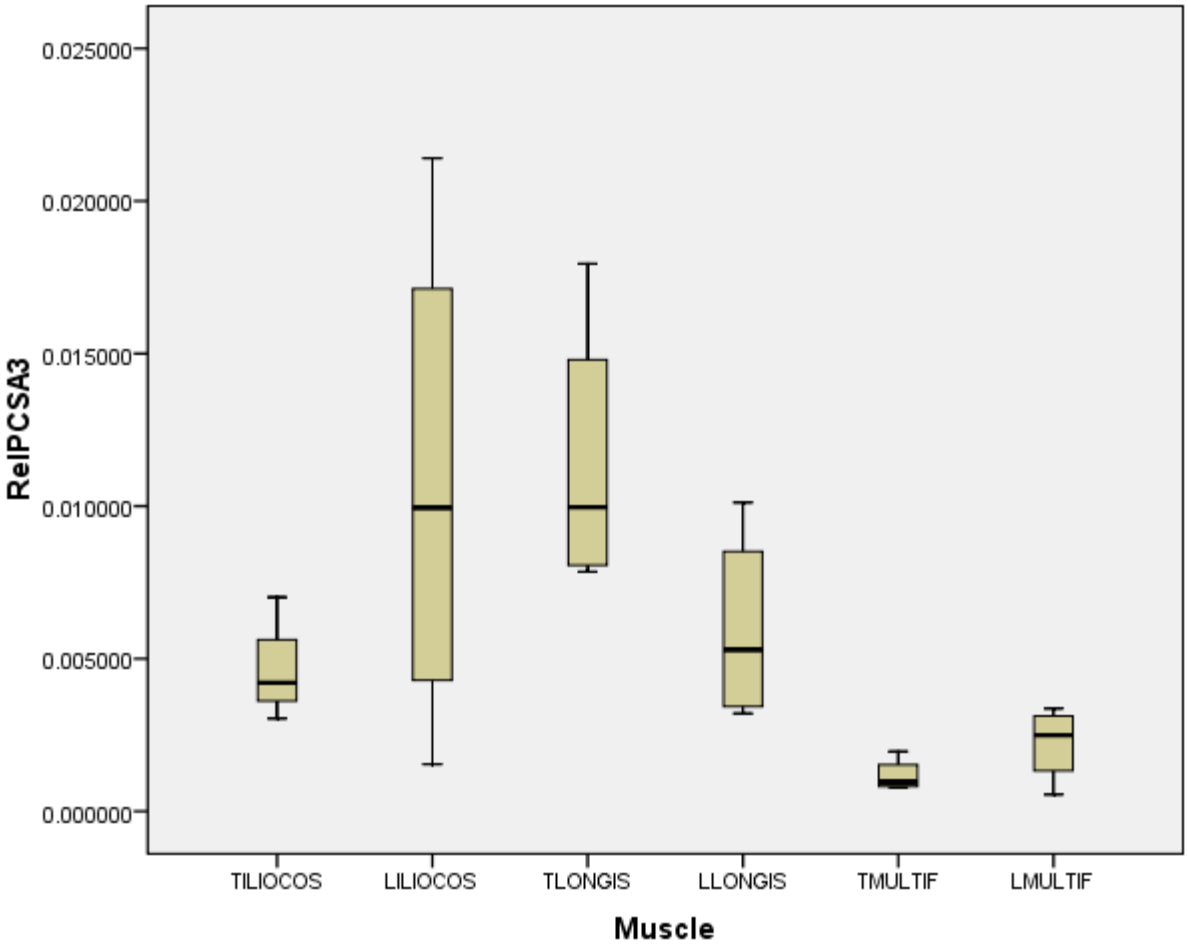

Fig. 35: *G. senegalensis*: Relative PCSA-3 (to lower estimate of body mass$^{0.67}$)

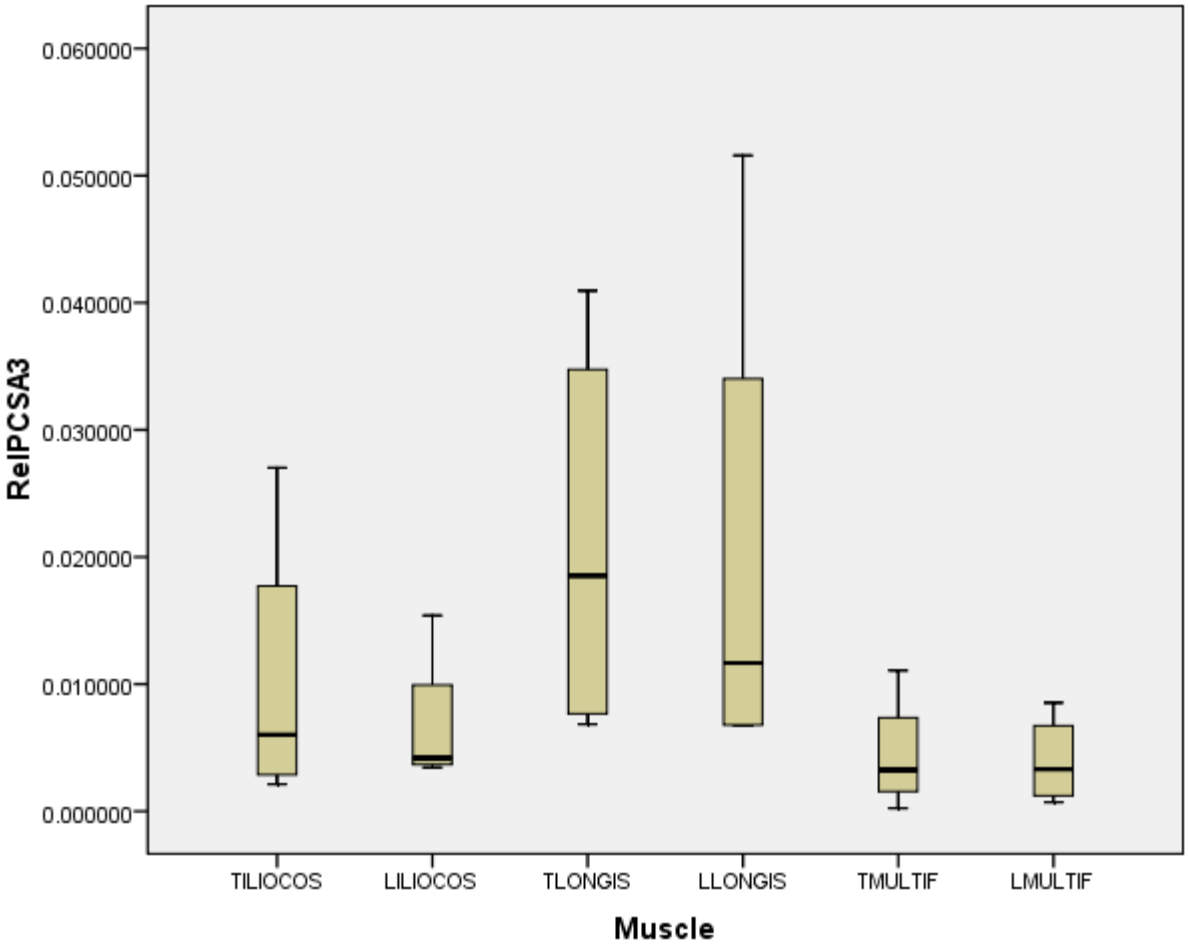

Fig. 36: *N. coucang*: Relative PCSA-3 (to lower estimate of body mass$^{0.67}$)

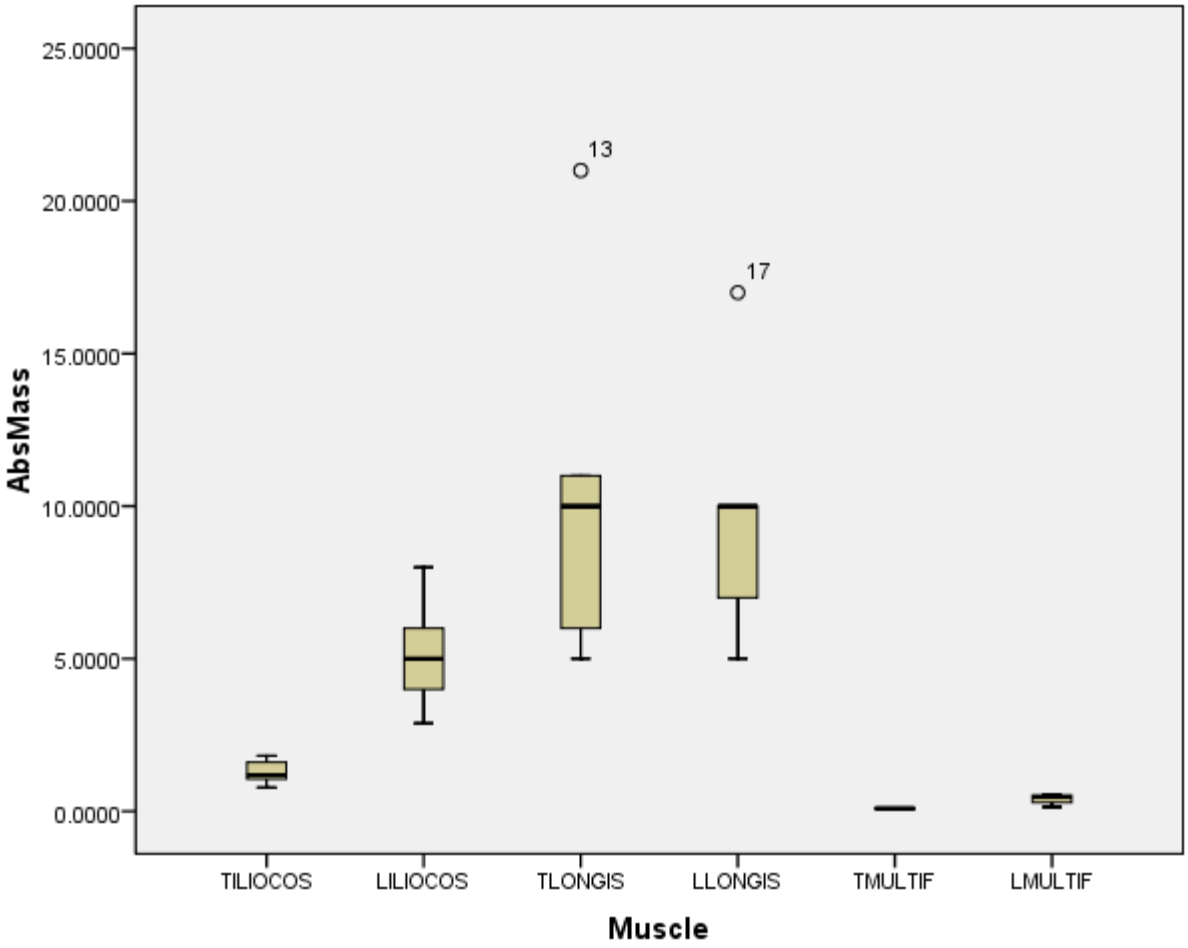

Fig. 37: *C. aethiops*: Absolute muscle mass

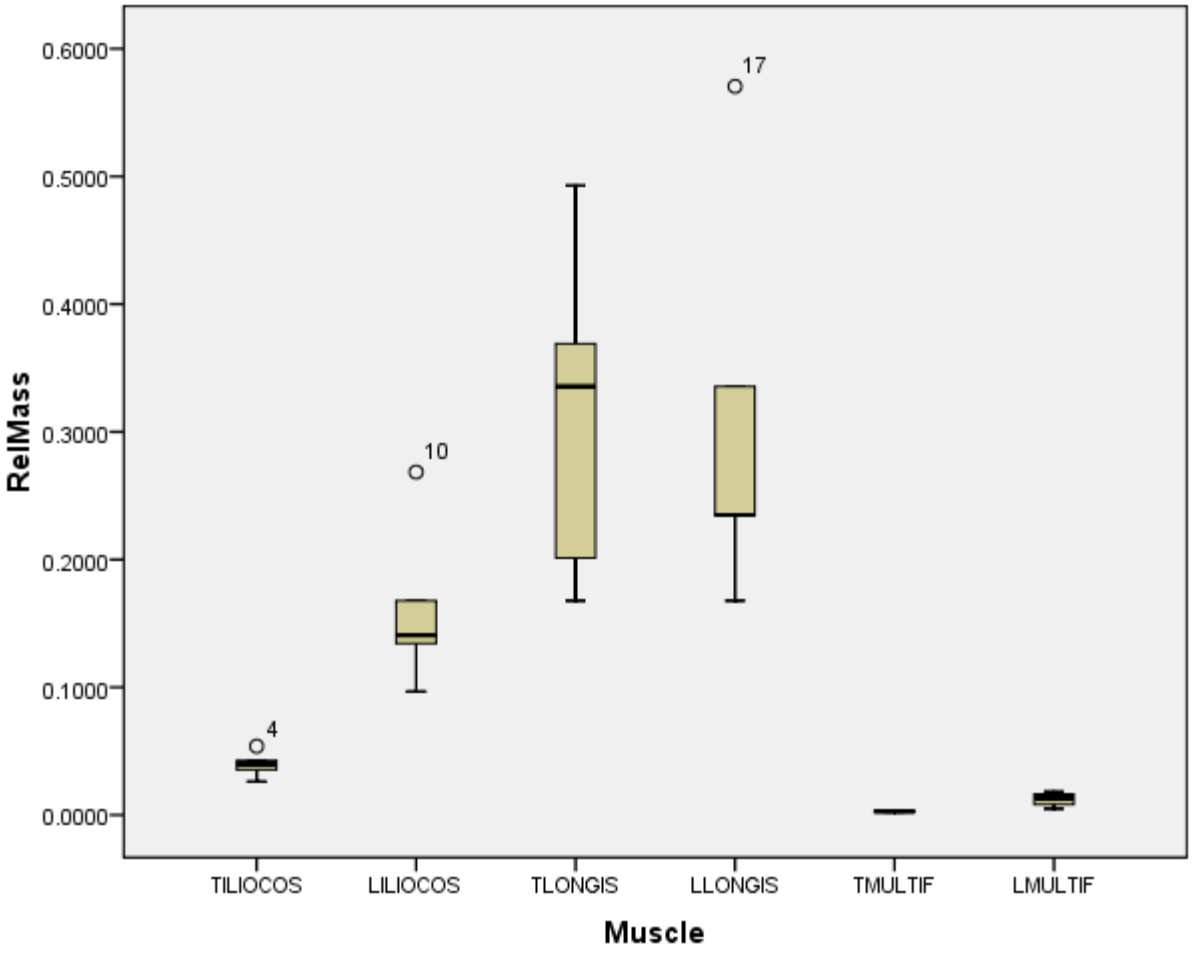

Fig. 38: *C. aethiops*: Relative muscle mass

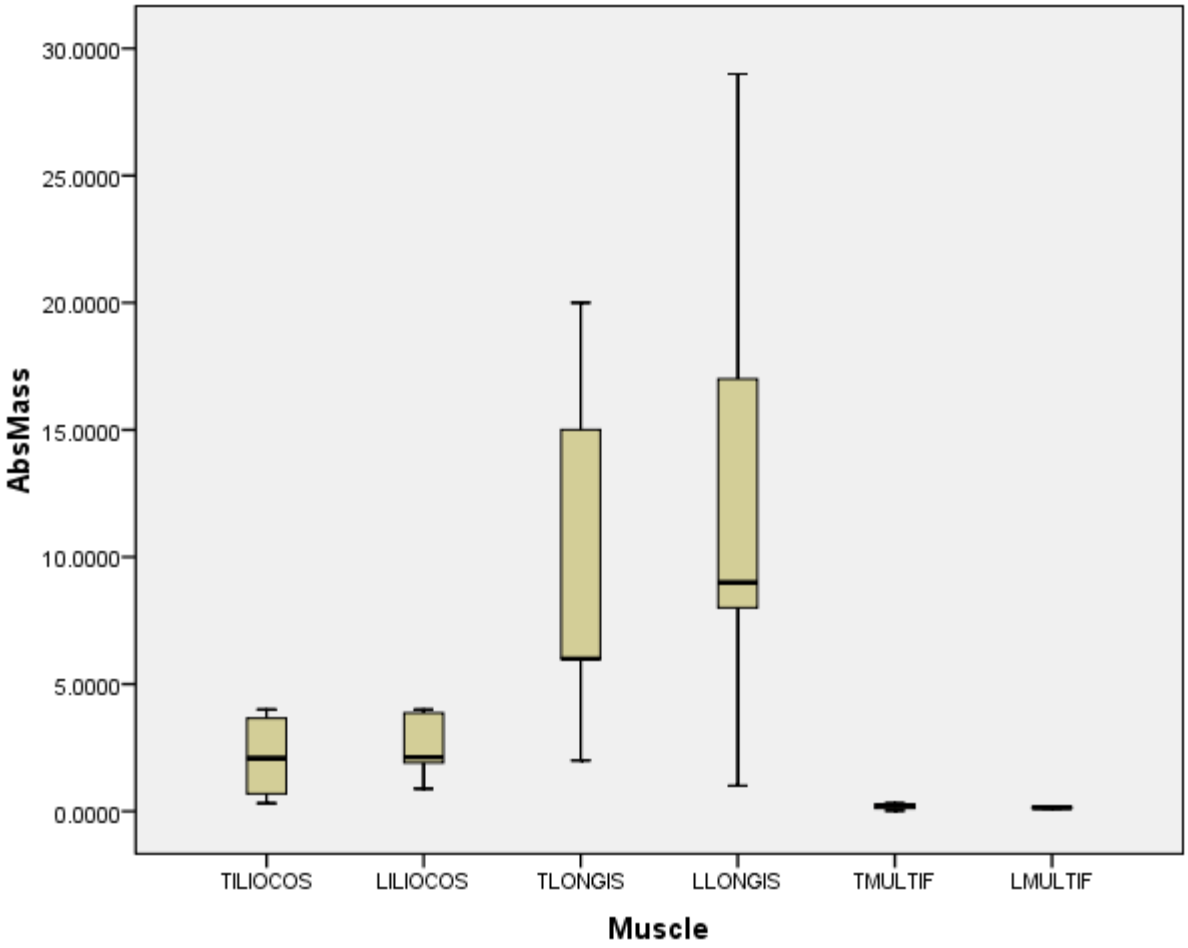

Fig. 39: *E. patas*: Absolute muscle mass

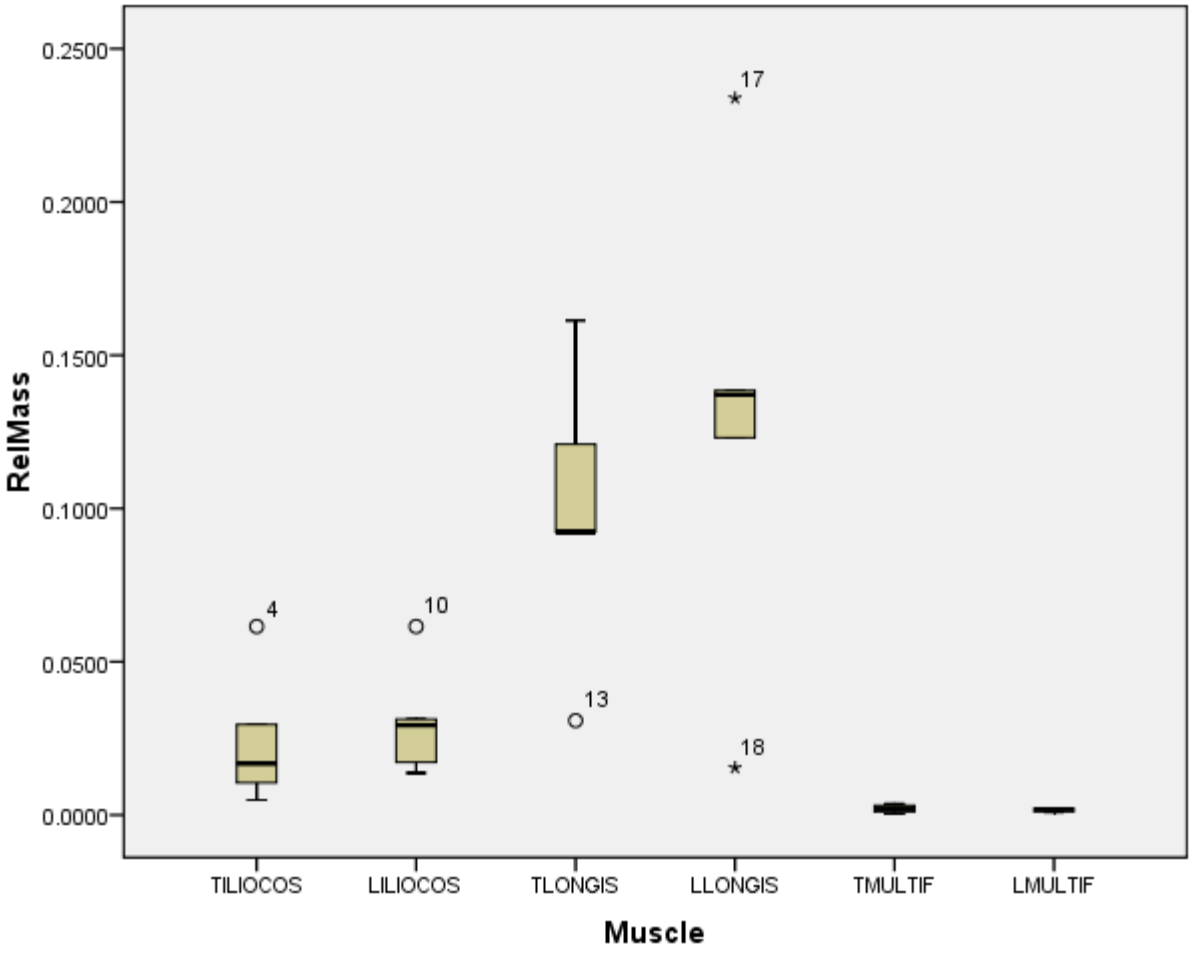

Fig. 40: *E. patas*: Relative muscle mass

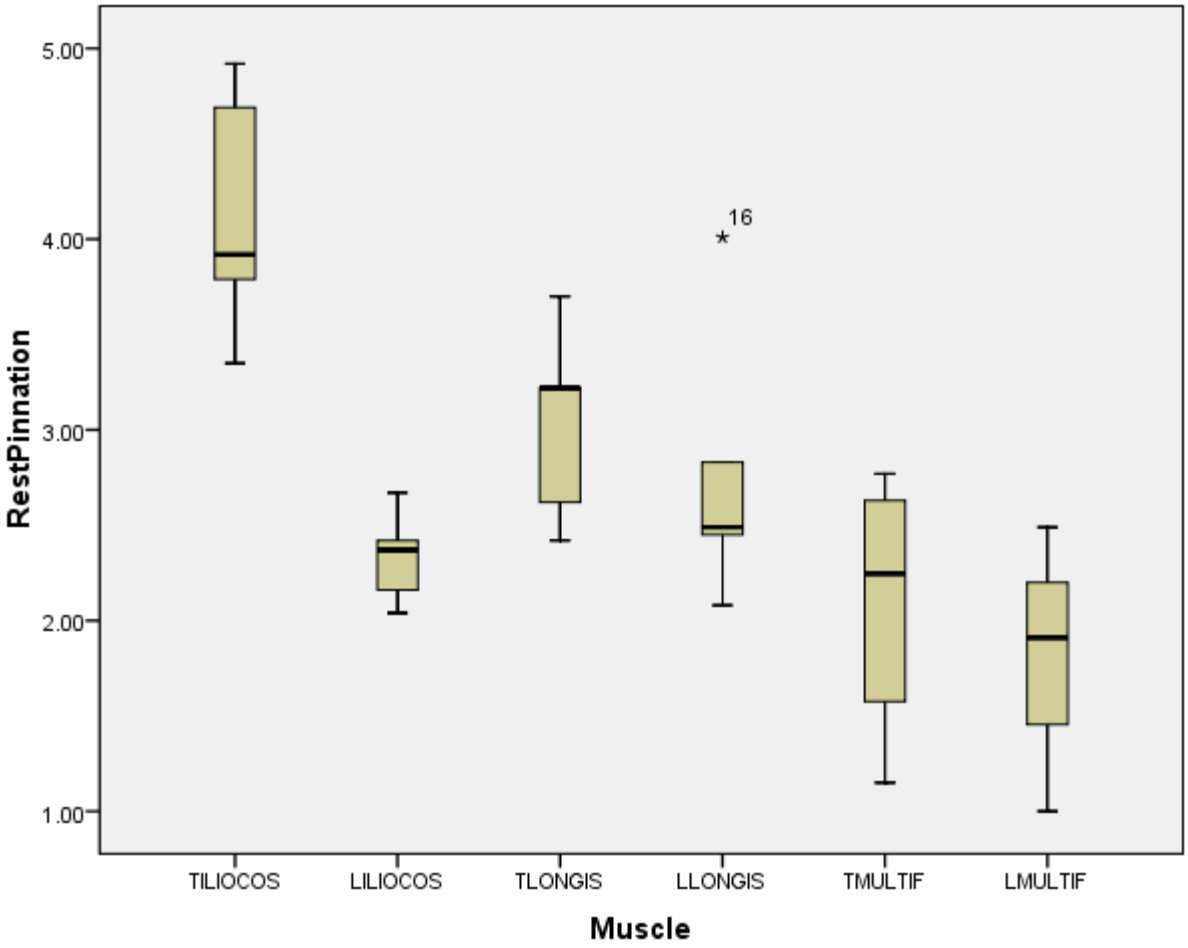

Fig. 41: *C. aethiops*: Resting pinnation angle

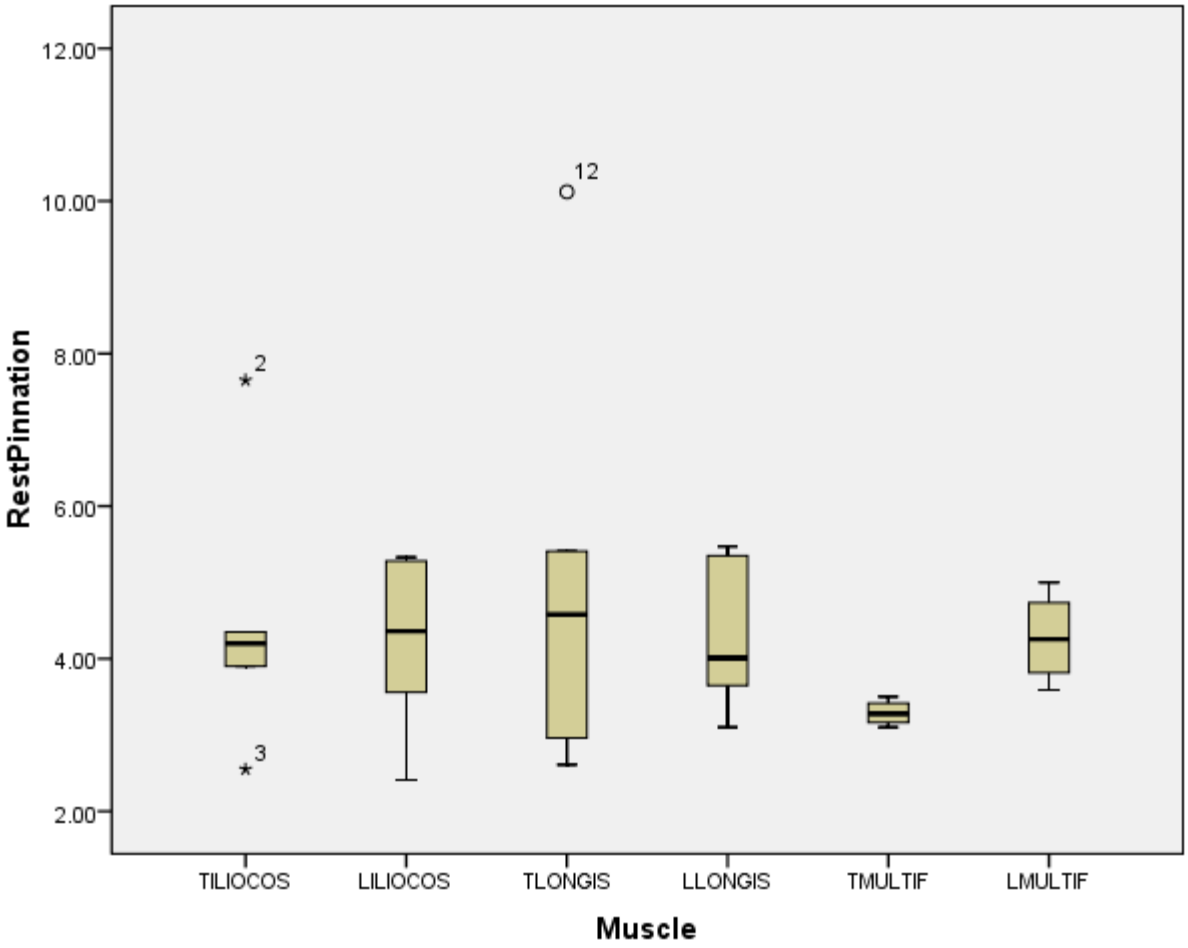

Fig. 42: *E. patas*: Resting pinnation angle

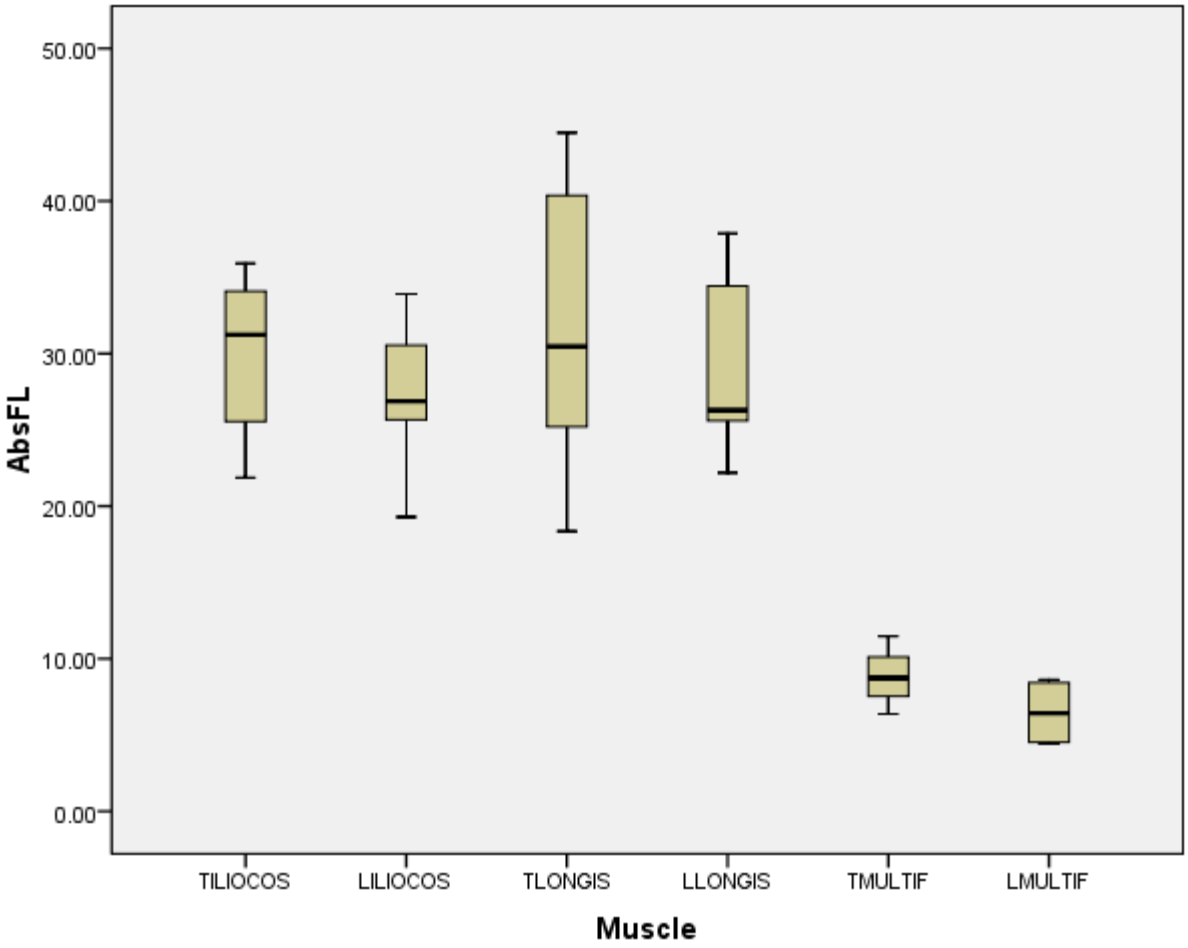

Fig. 43: *C. aethiops*: Raw fiber length (Lf)

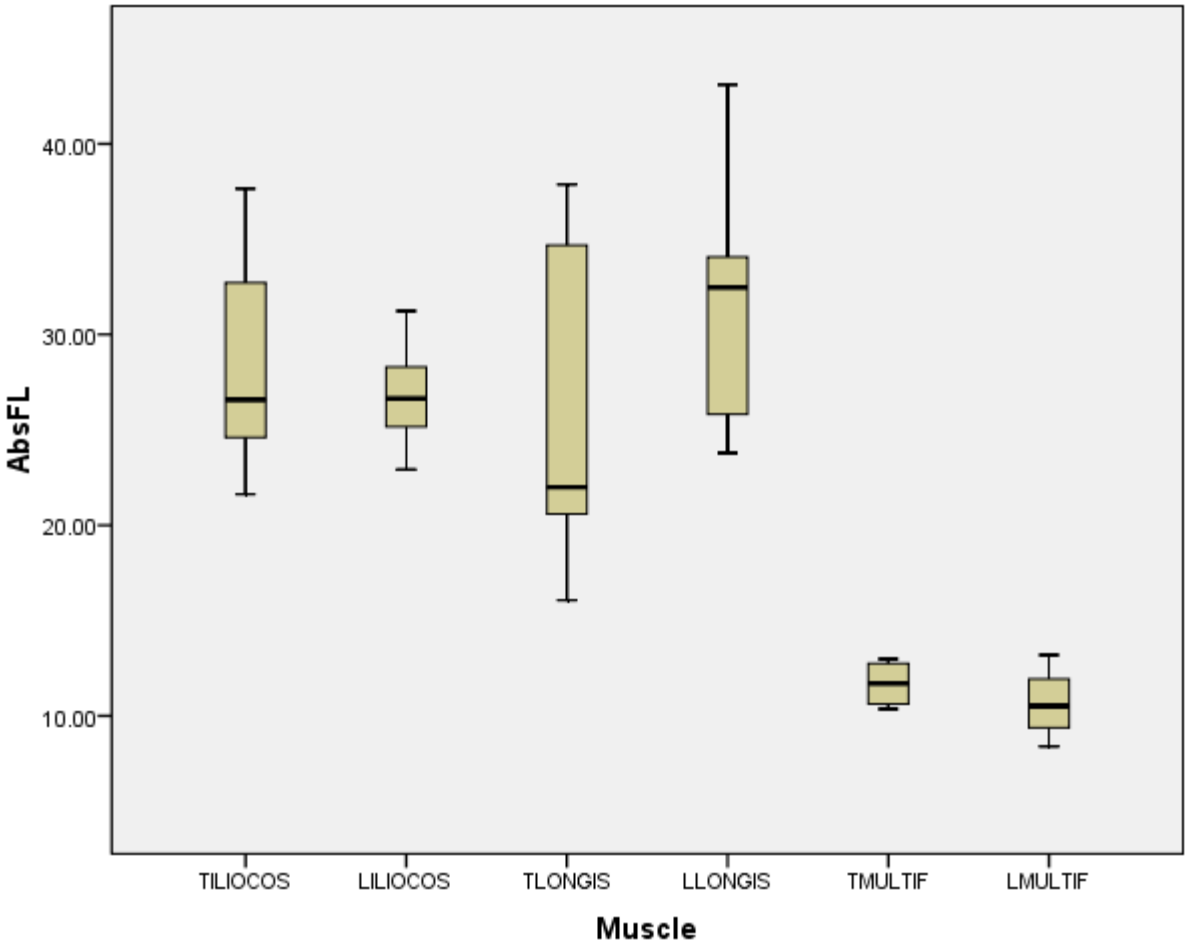

Fig. 44: *E. patas*: Raw fiber length (Lf)

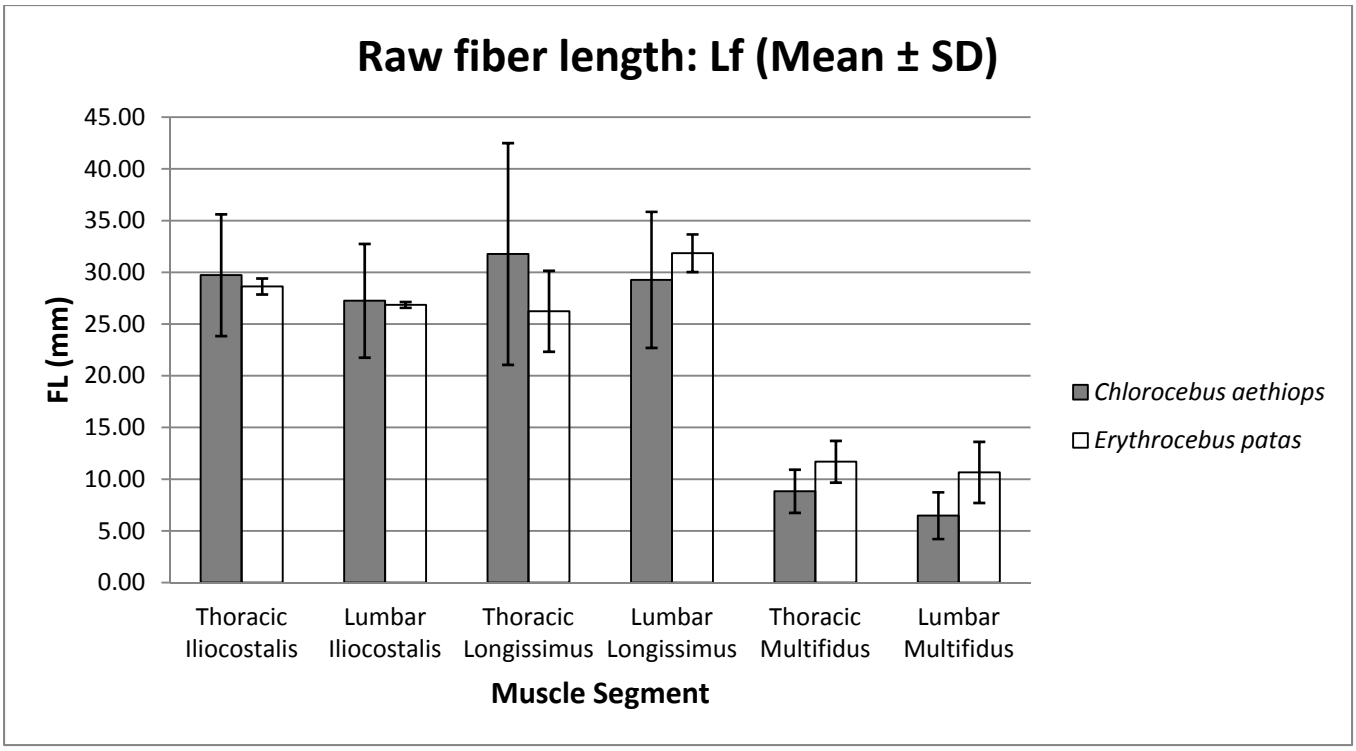

Fig. 45: Mean (± SD) of raw fiber length (Lf) for *C. aethiops* and *E. patas*

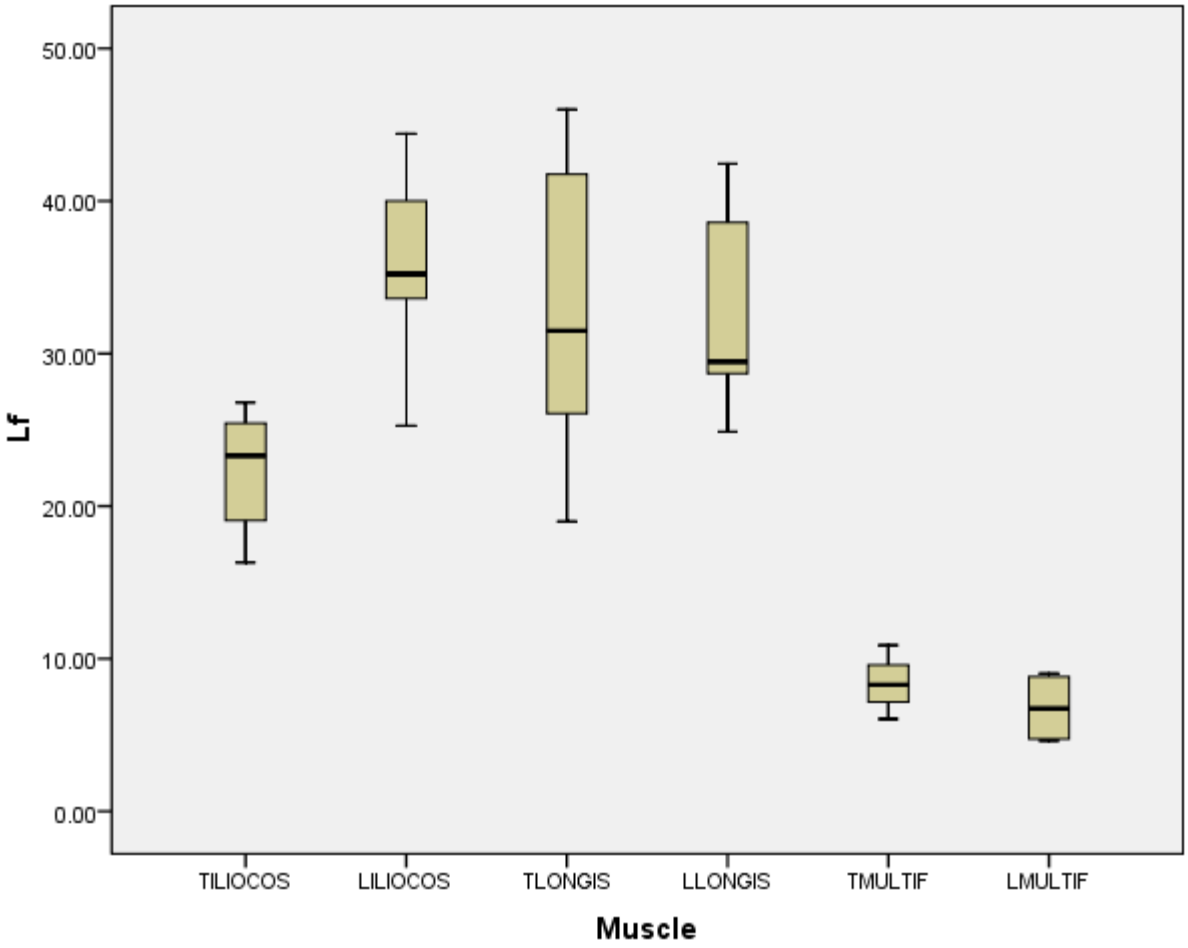

Fig. 46: *C. aethiops*: Resting fiber length (NLf)

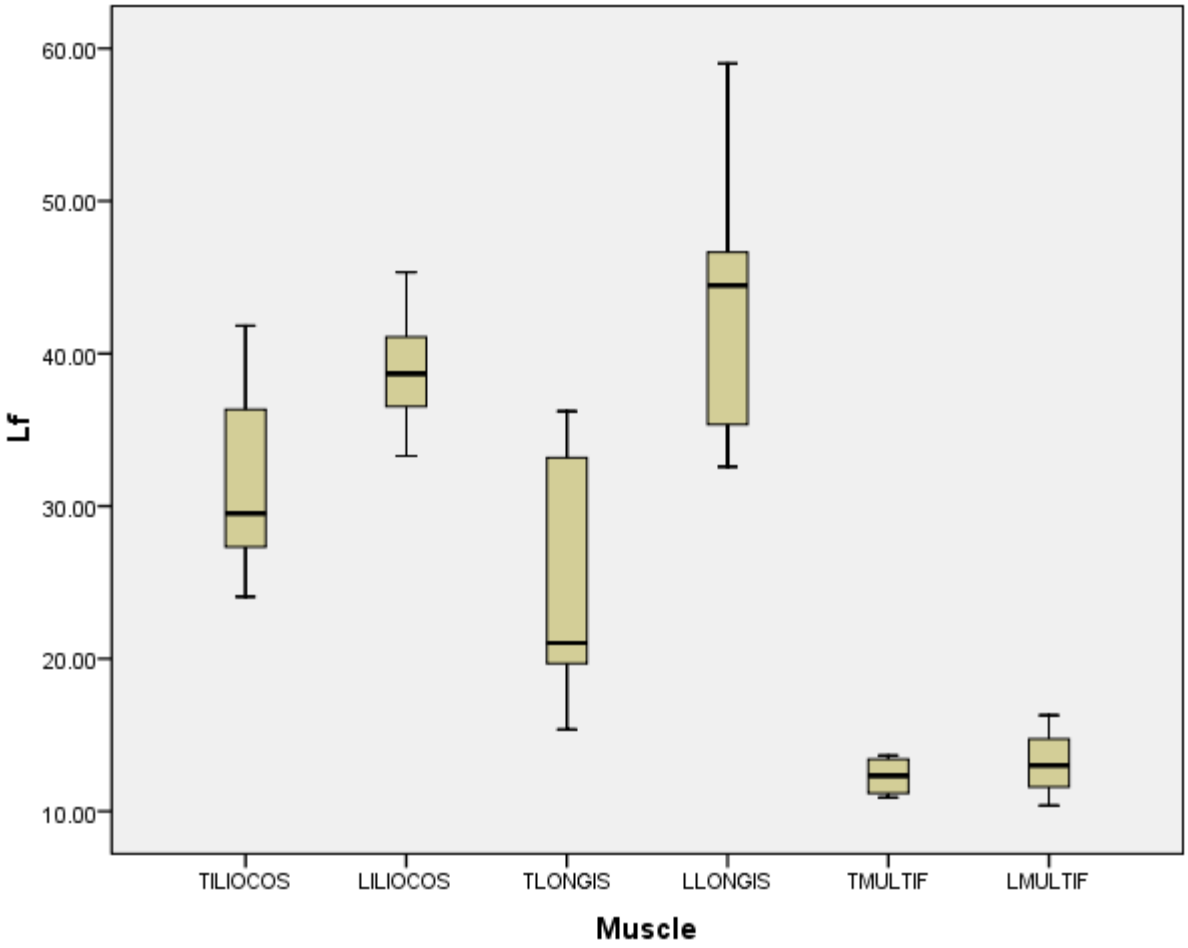

Fig. 47: *E. patas*: Resting fiber length (NLf)

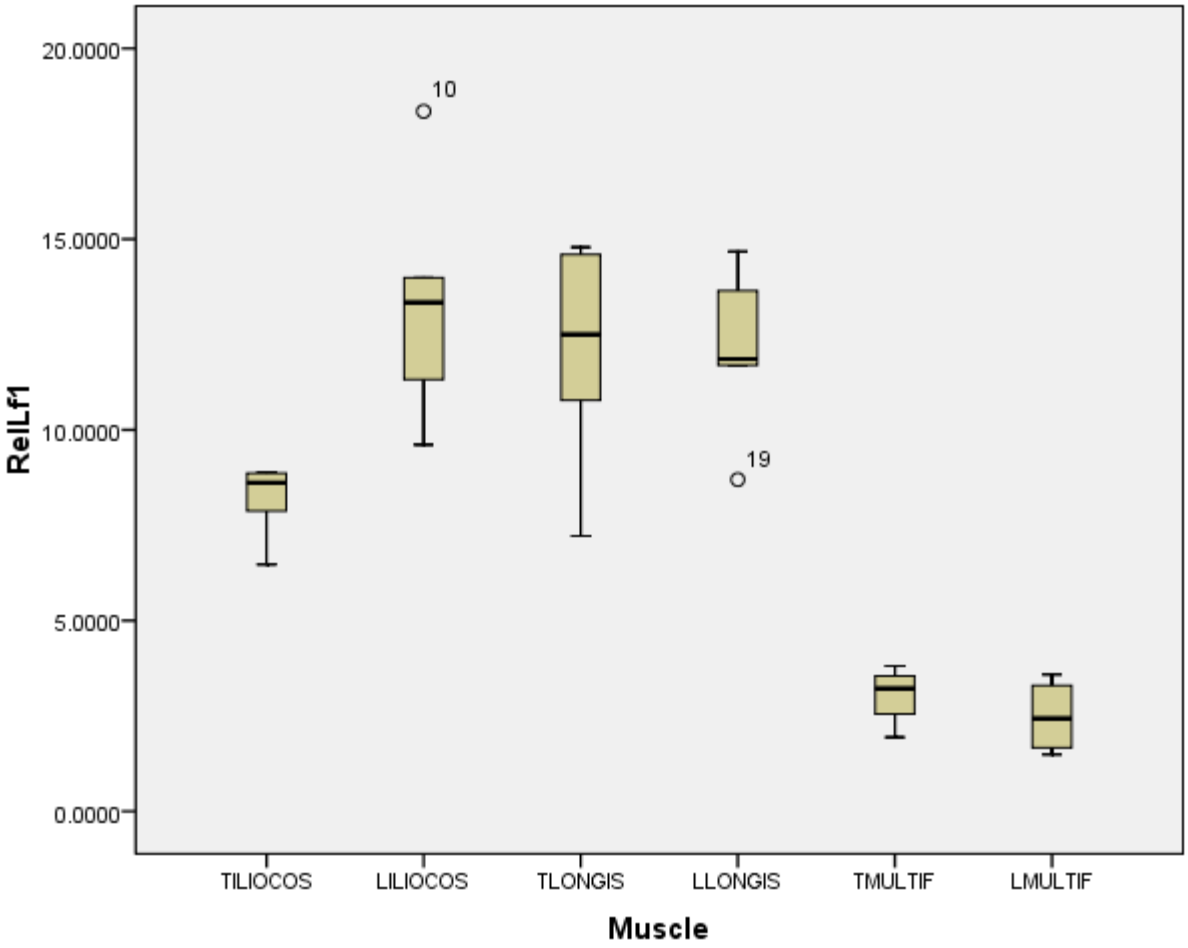

Fig. 48: *C. aethiops*: Relative NLf-1 (to thoraco-lumbar spine length)

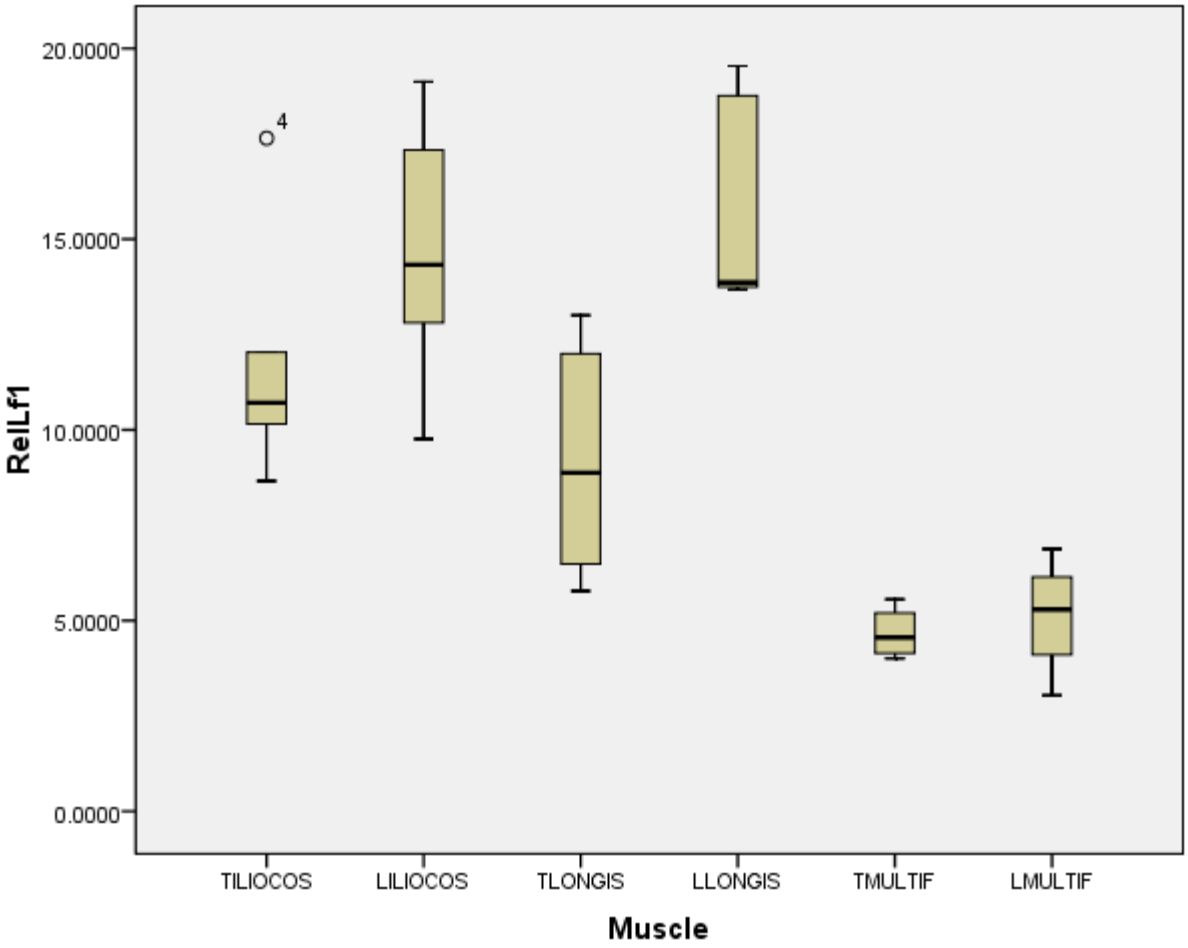

Fig. 49: *E. patas*: Relative NLf-1 (to thoraco-lumbar spine length)

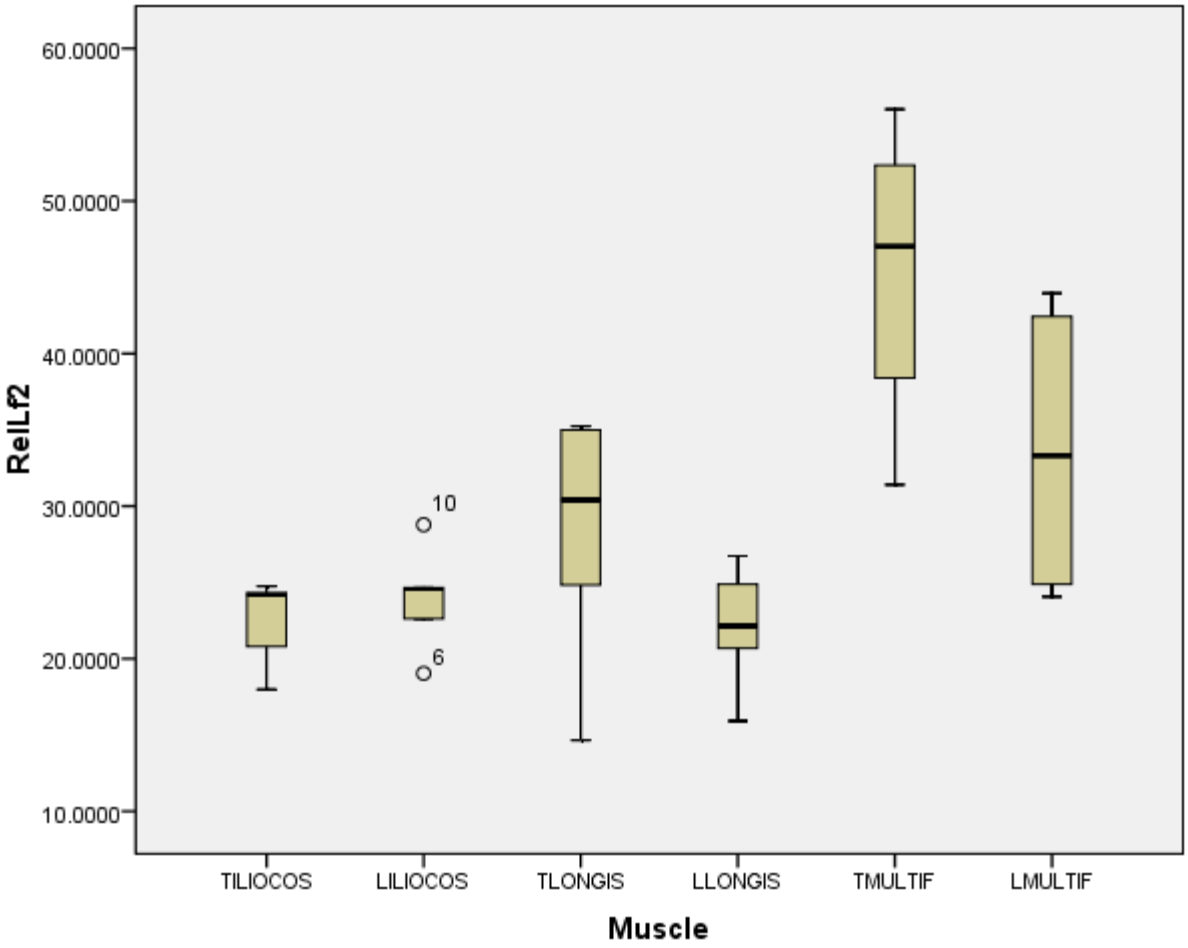

Fig. 50: *C. aethiops*: Relative NLf-2 (to resting muscle length)

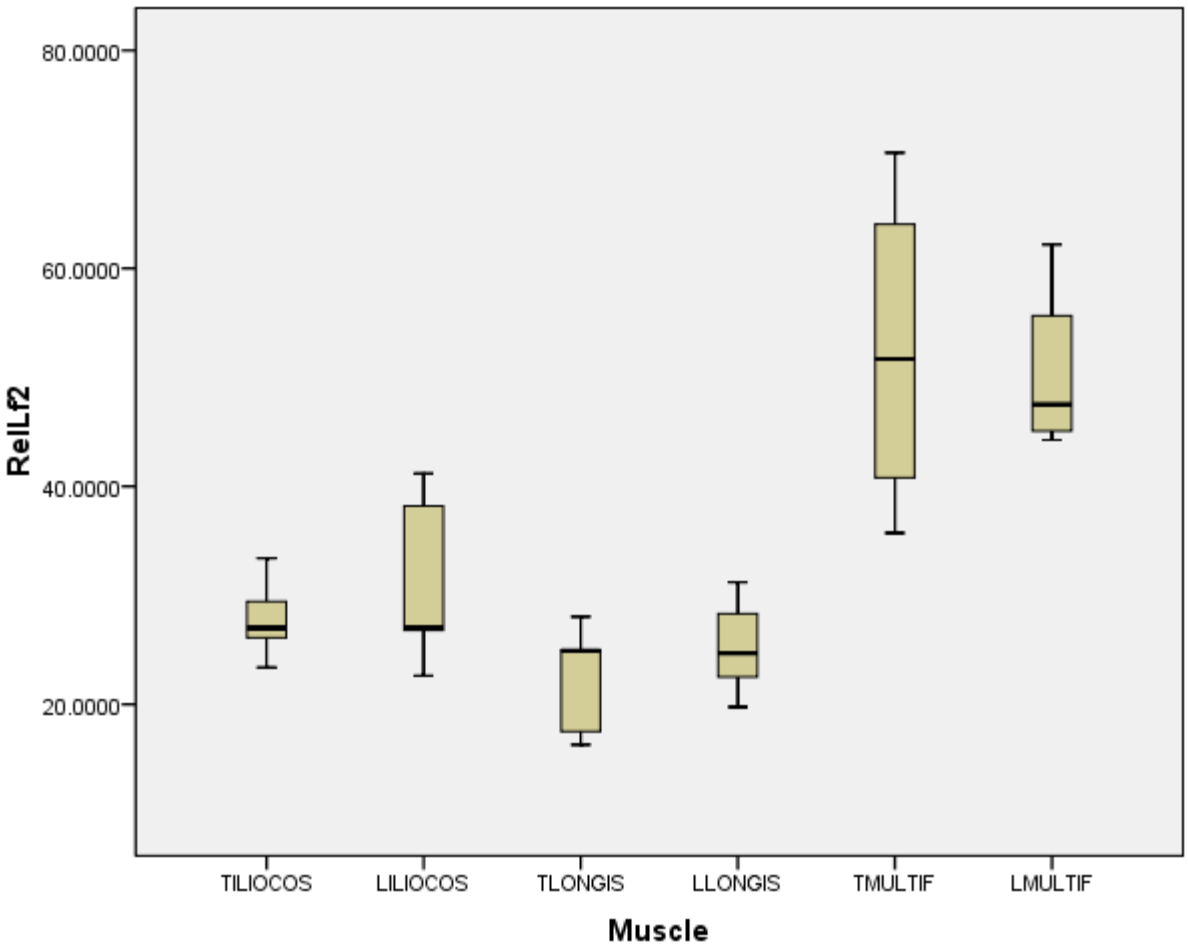

Fig. 51: *E. patas*: Relative NLf-2 (to resting muscle length)

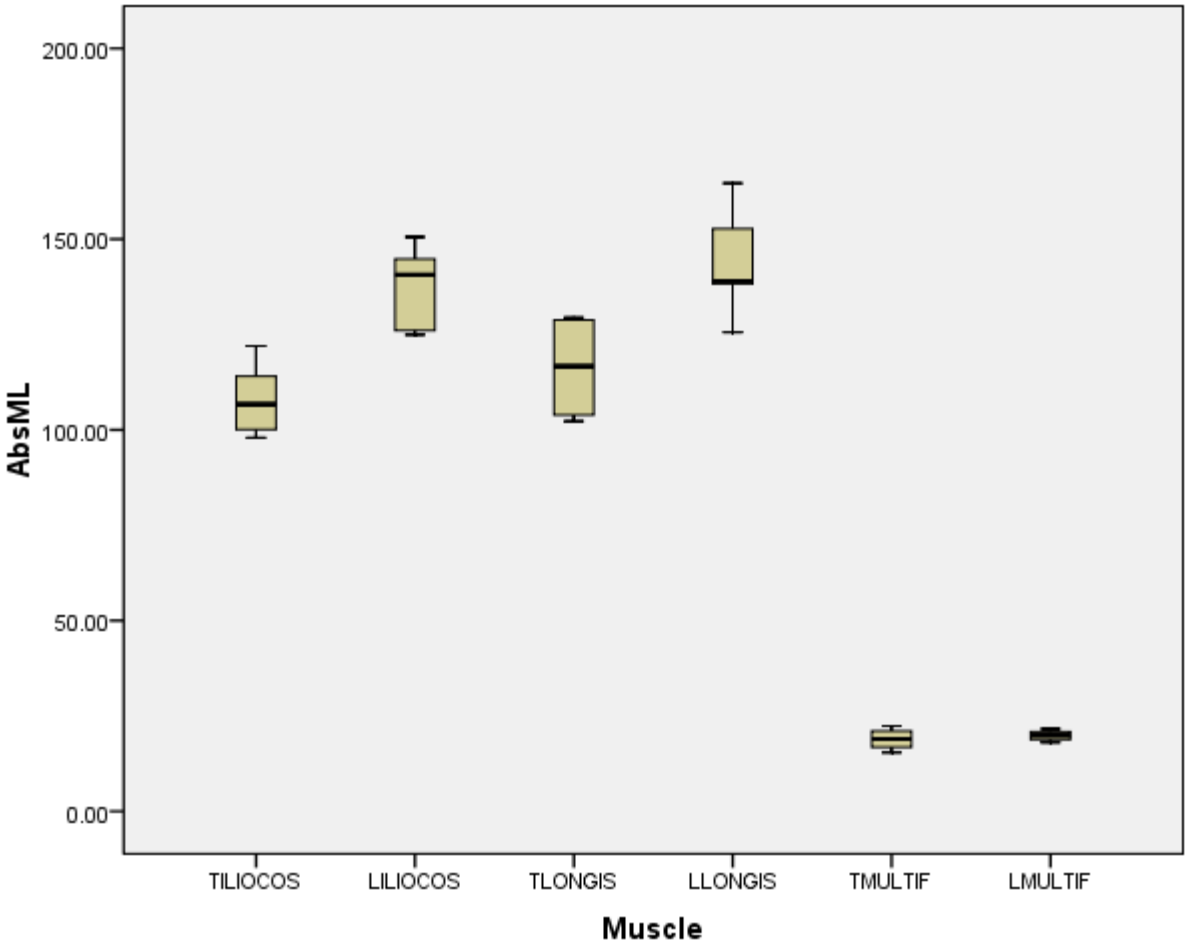

Fig. 52: *C. aethiops*: Raw muscle length (ML)

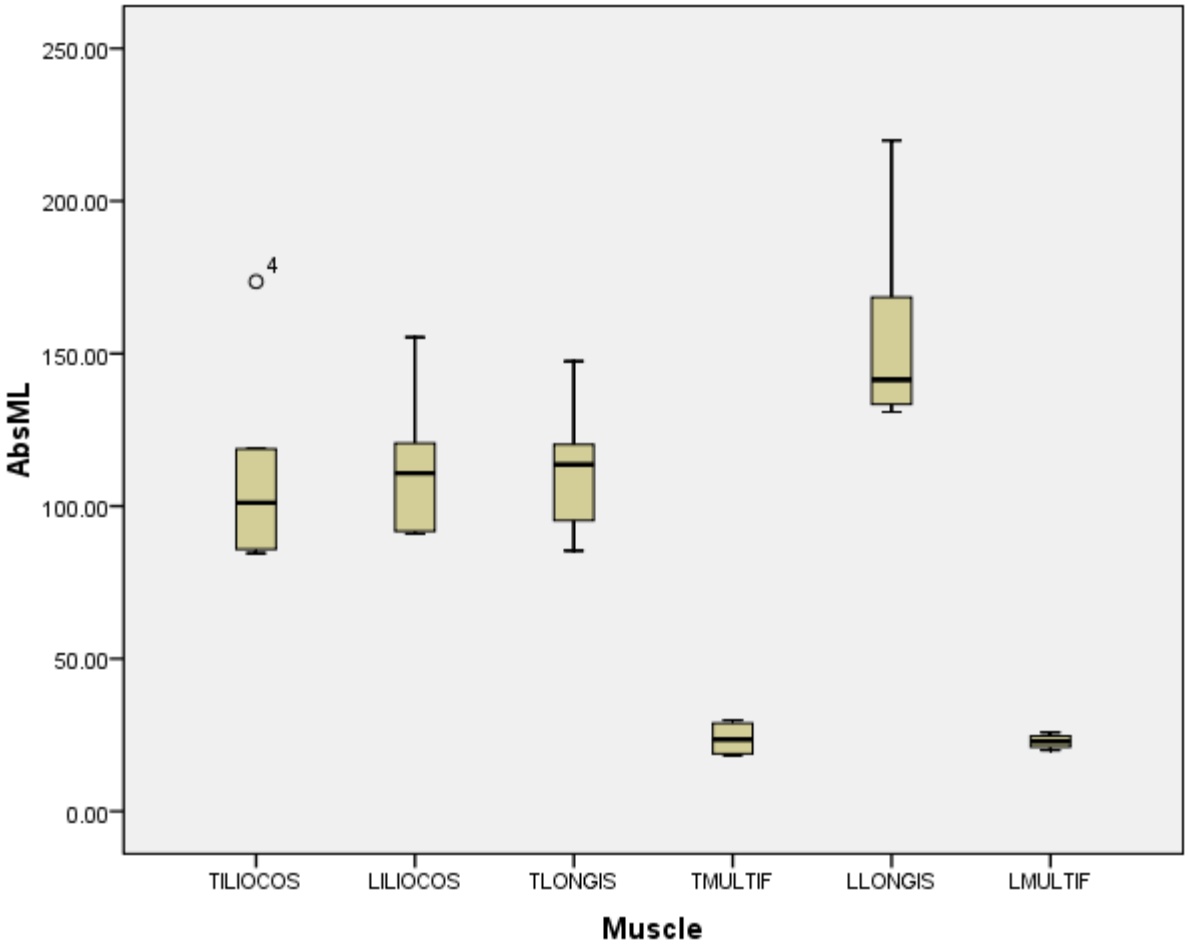

Fig. 53: *E. patas*: Raw muscle length (ML)

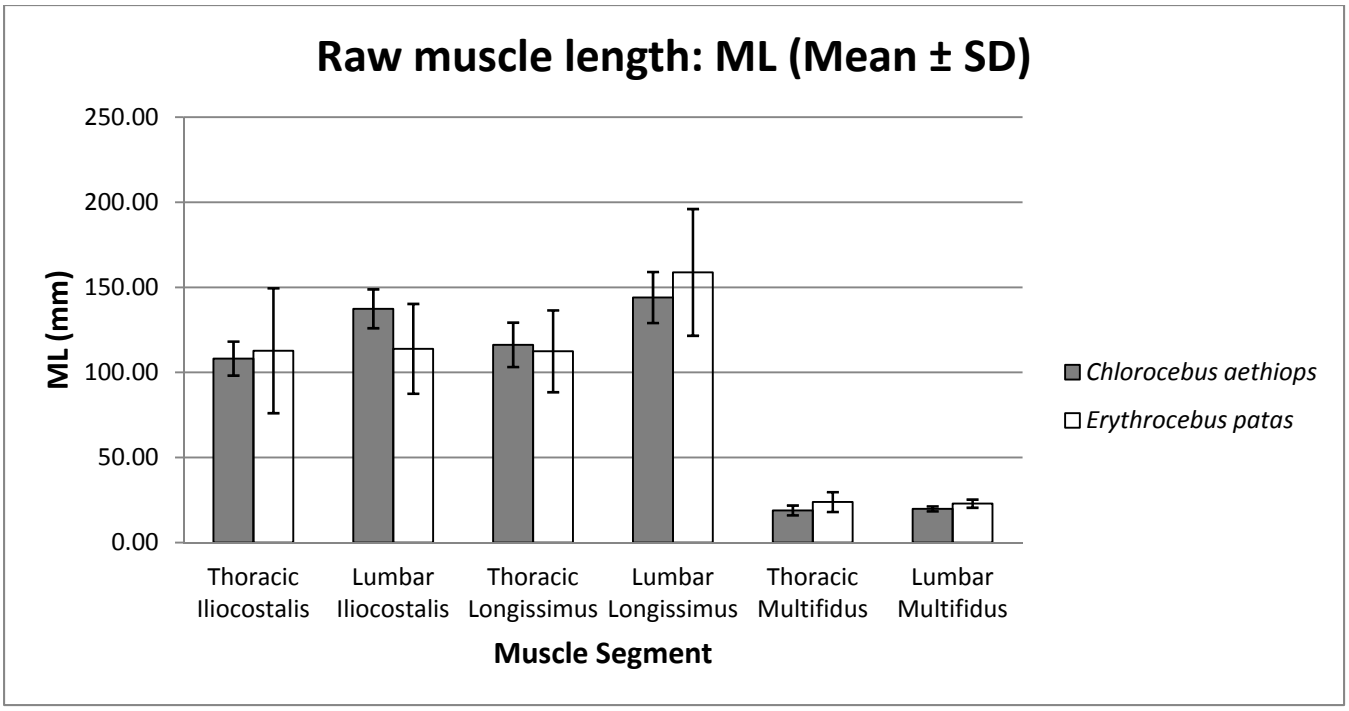

Fig. 54: Mean (± SD) of ML for *C. aethiops* and *E. patas*

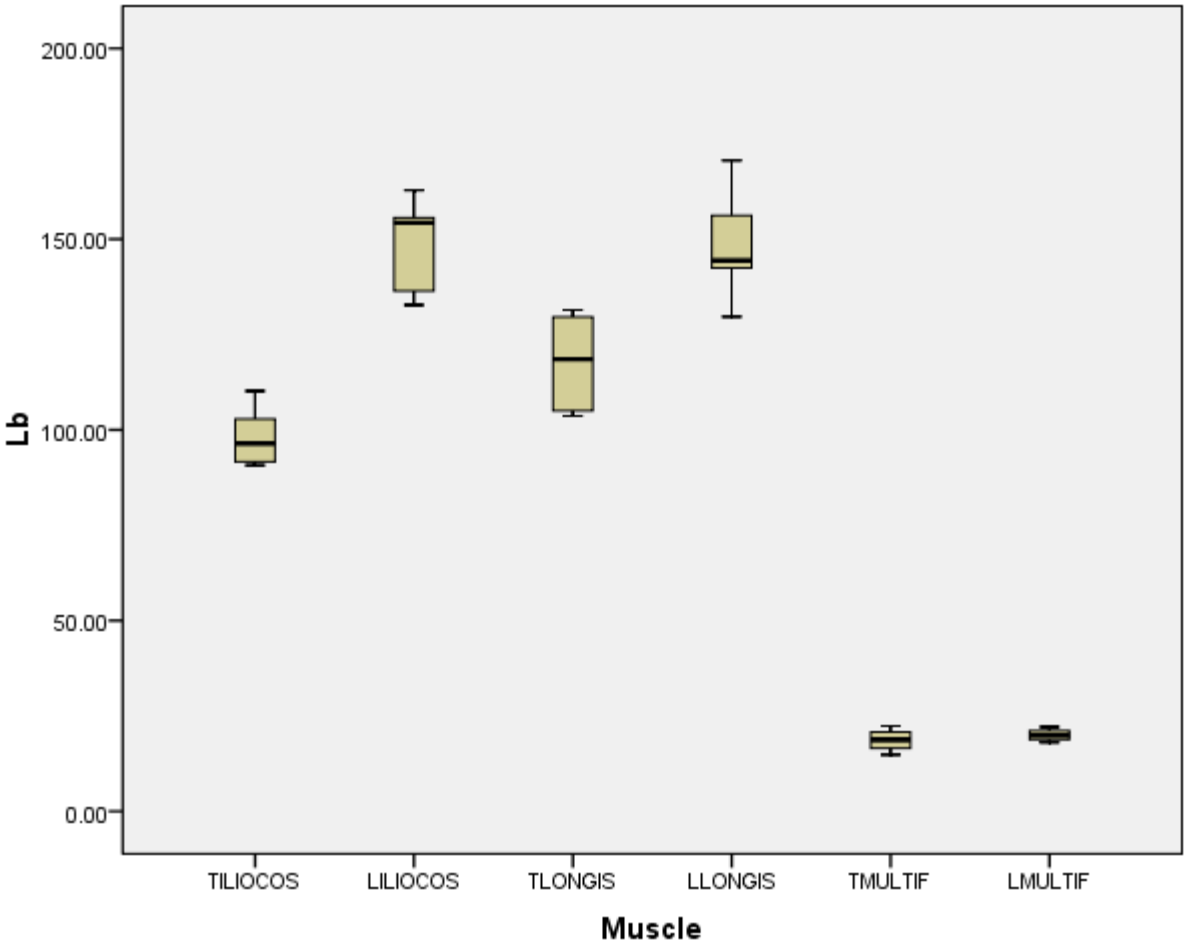

Fig. 55: *C. aethiops*: Resting muscle length (Lb)

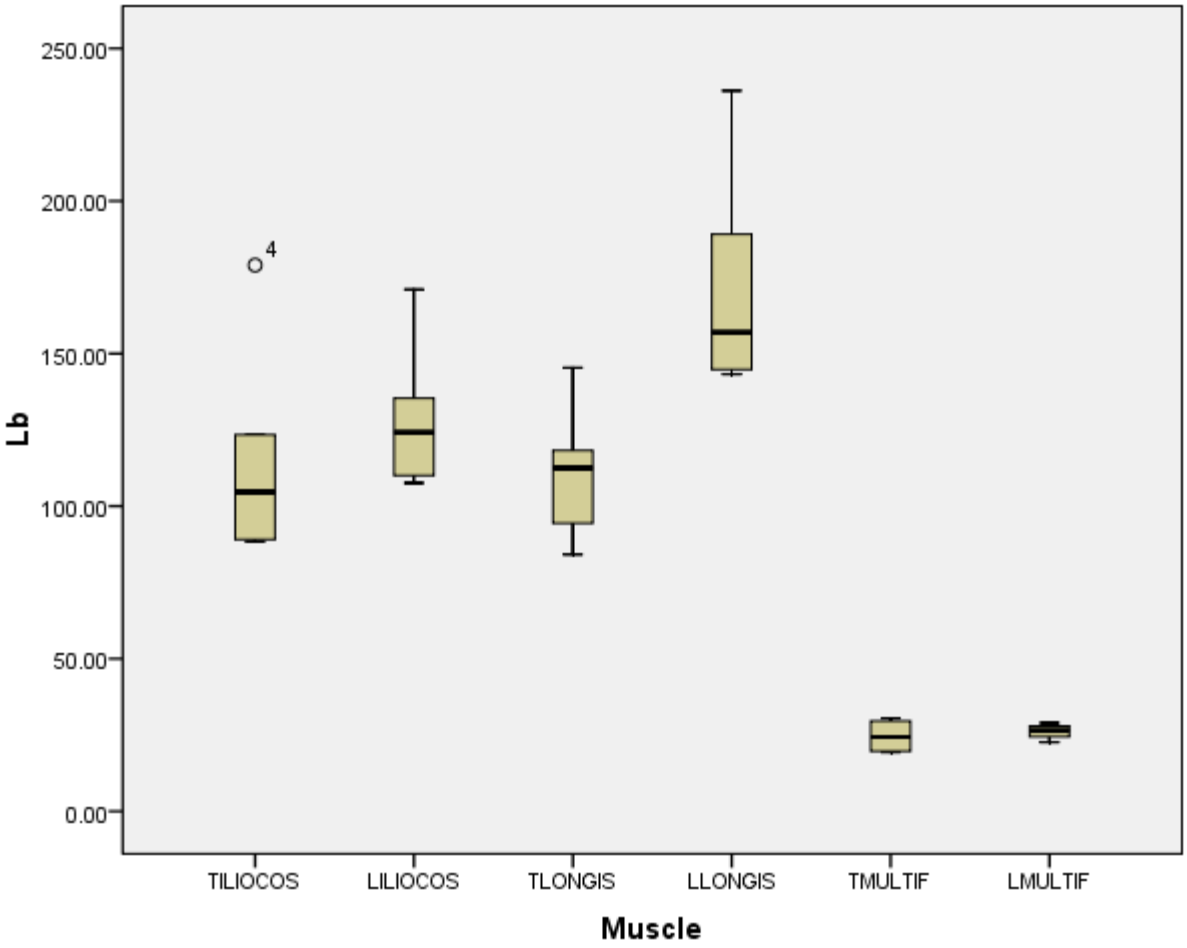

Fig. 56: *E. patas*: Resting muscle length (Lb)

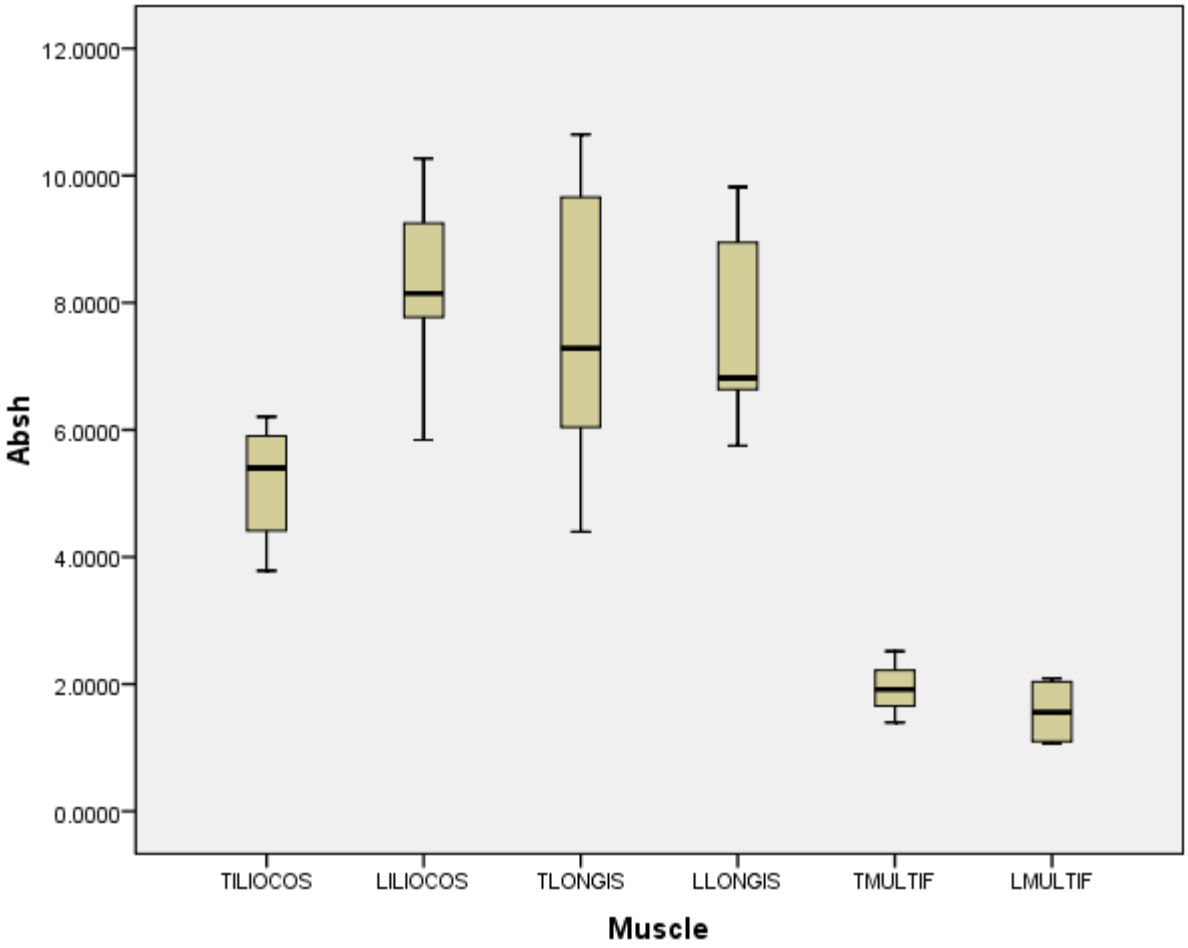

Fig. 57: *C. aethiops*: Potential excursion of whole muscle (*h*)

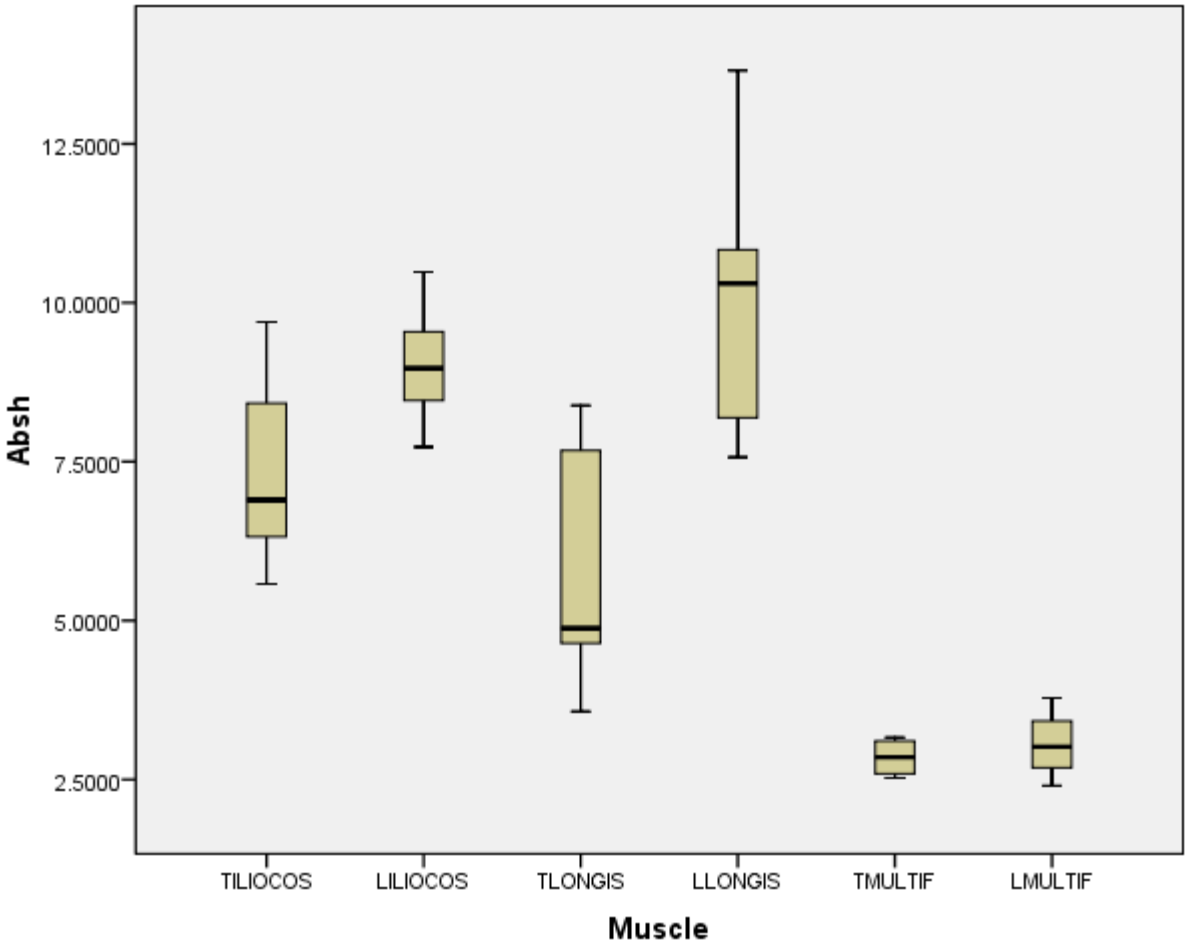

Fig. 58: *E. patas*: Potential excursion of whole muscle (*h*)

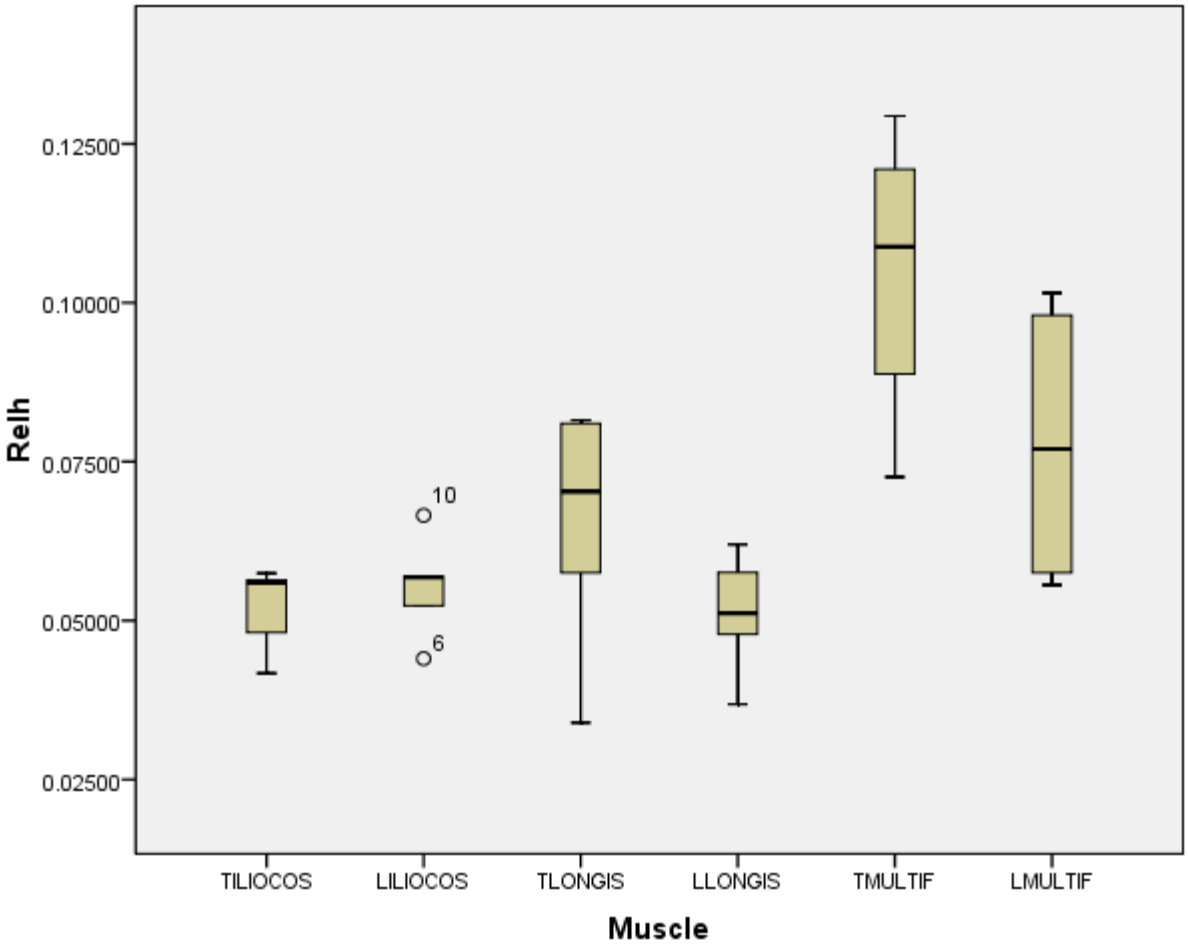

Fig. 59: *C. aethiops*: Relative *h*

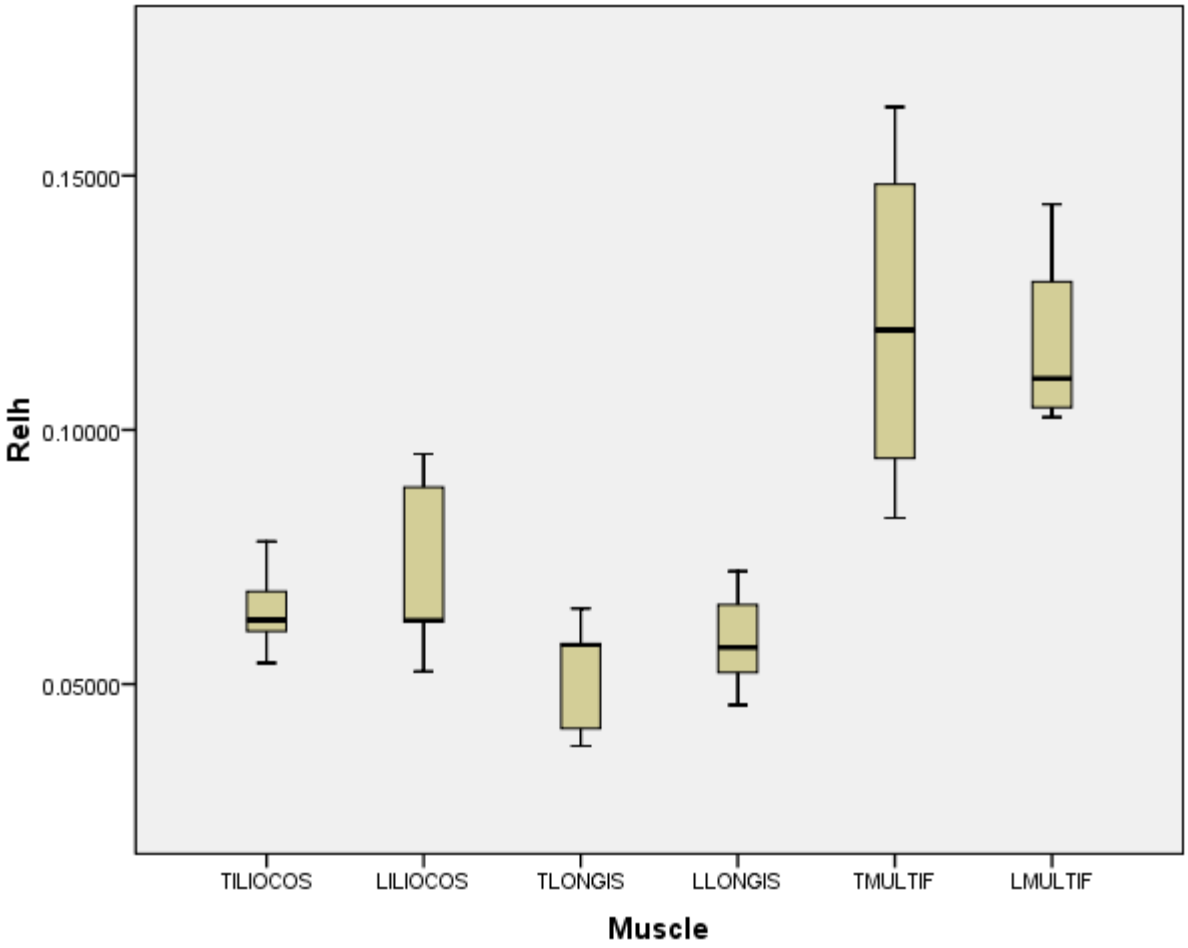

Fig. 60: *E. patas*: Relative *h*

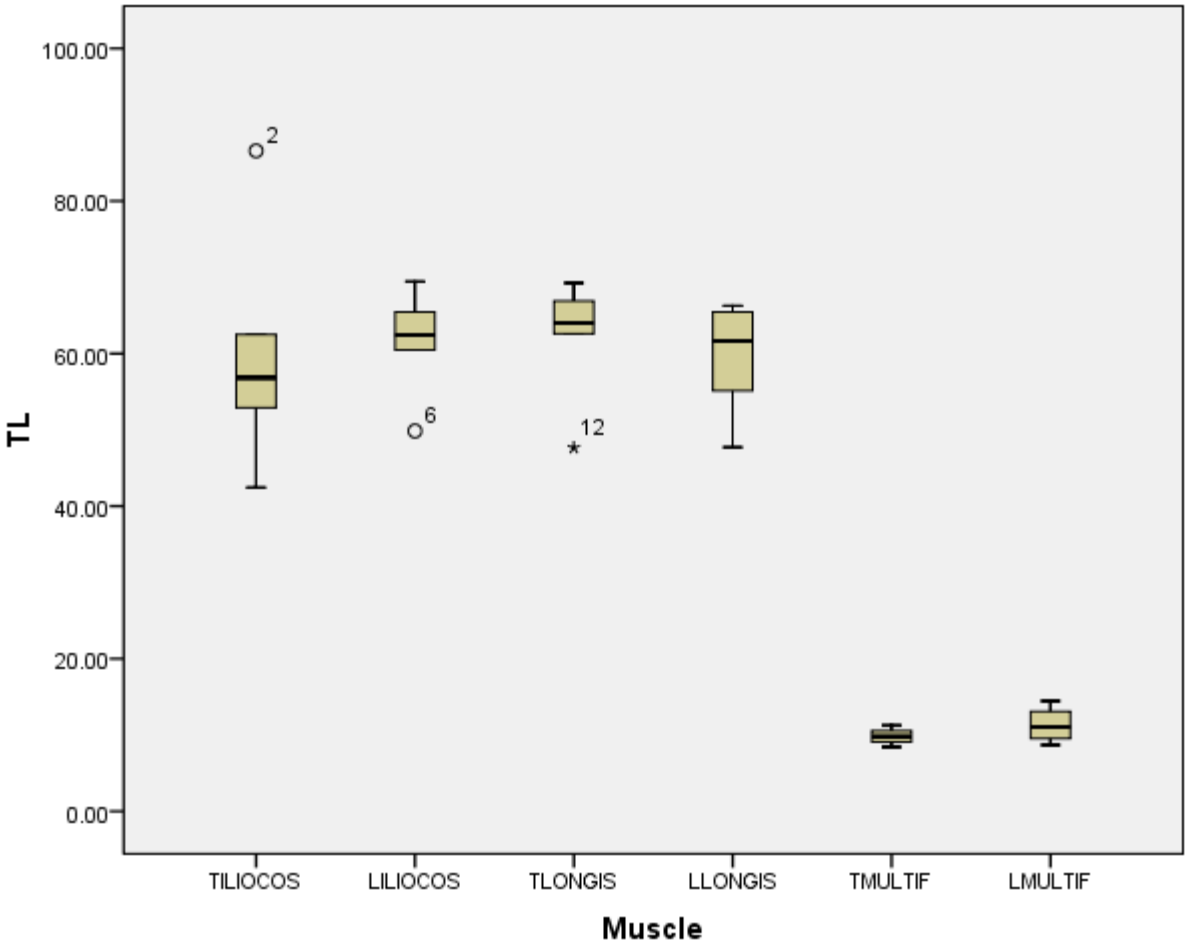

Fig. 61: *C. aethiops*: Tendon length (TL)

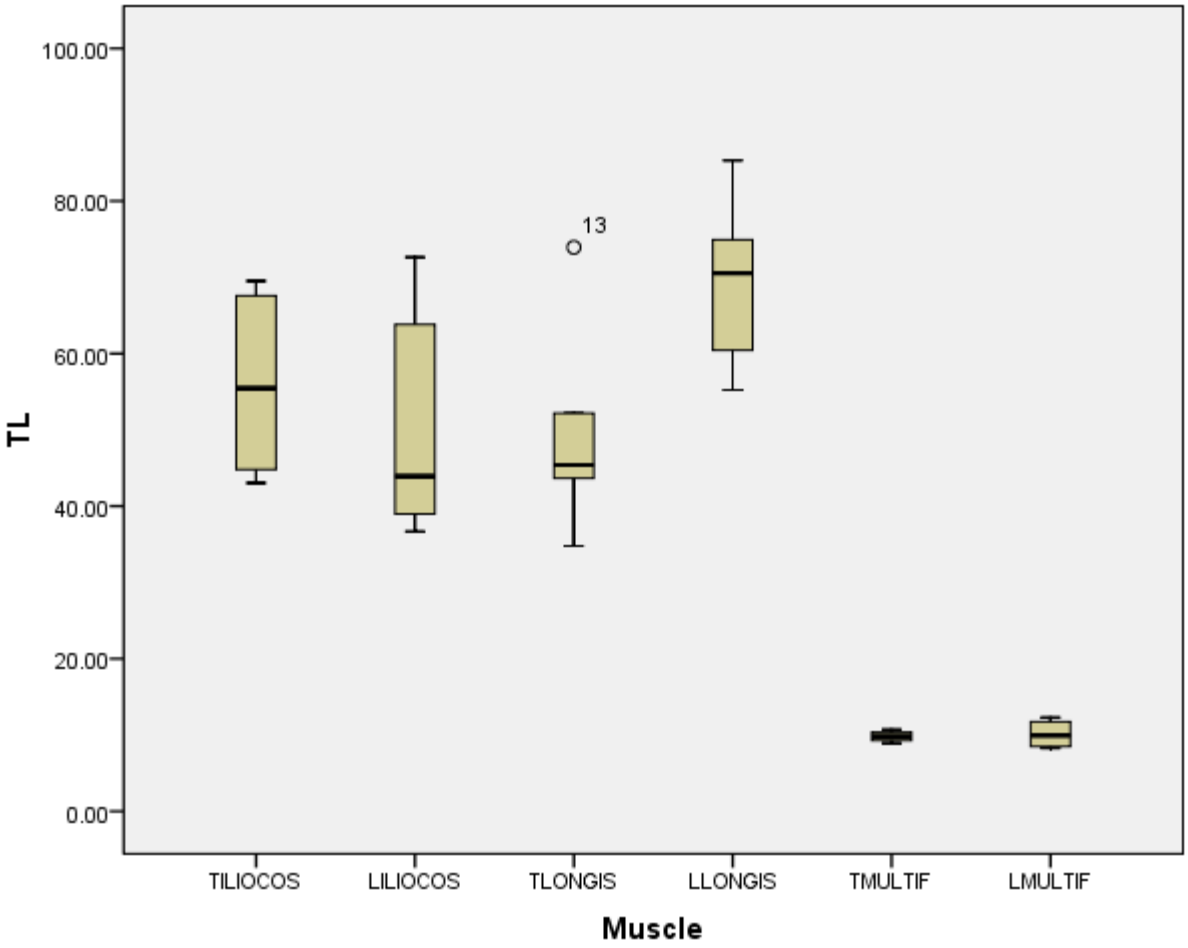

Fig. 62: *E. patas*: Tendon length (TL)

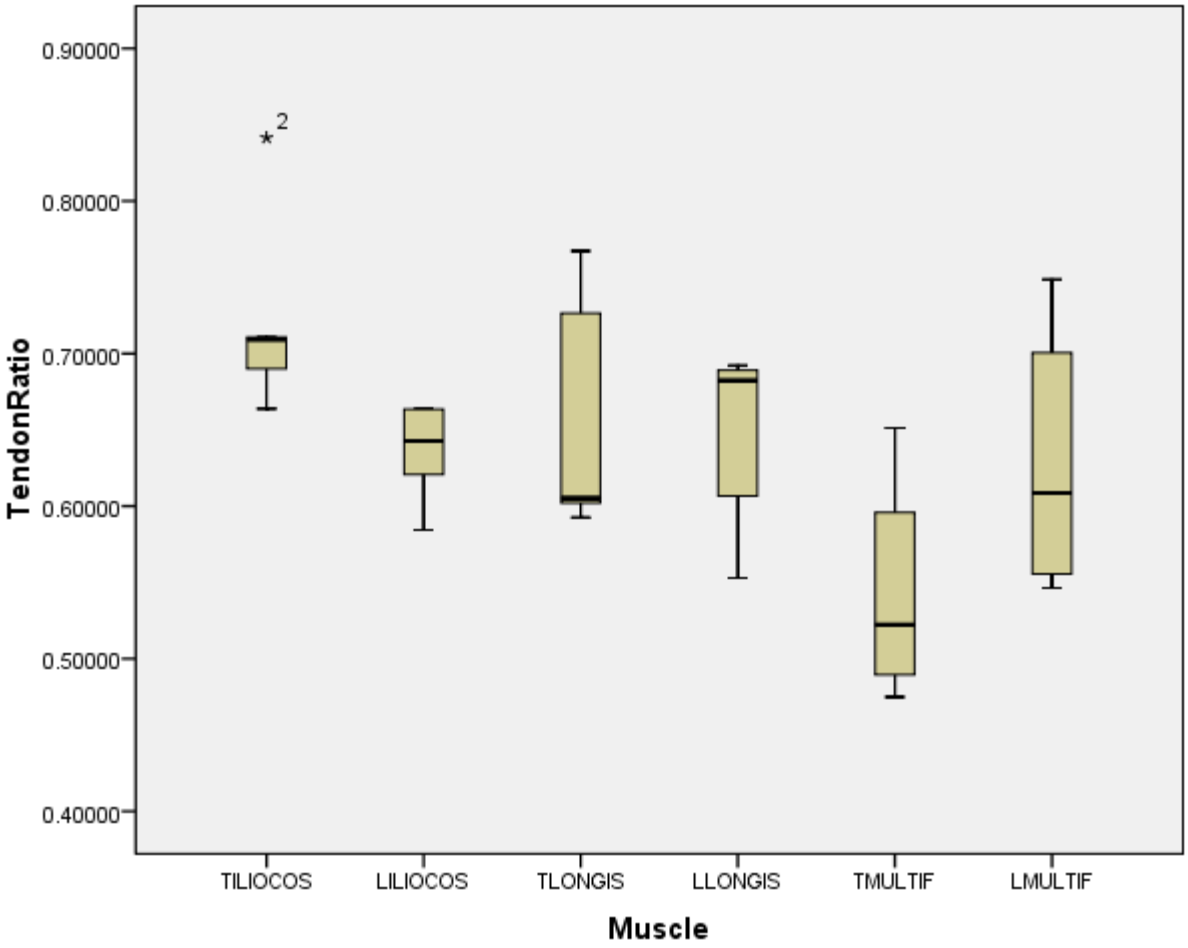

Fig. 63: *C. aethiops*: TL/(TL + NLf)

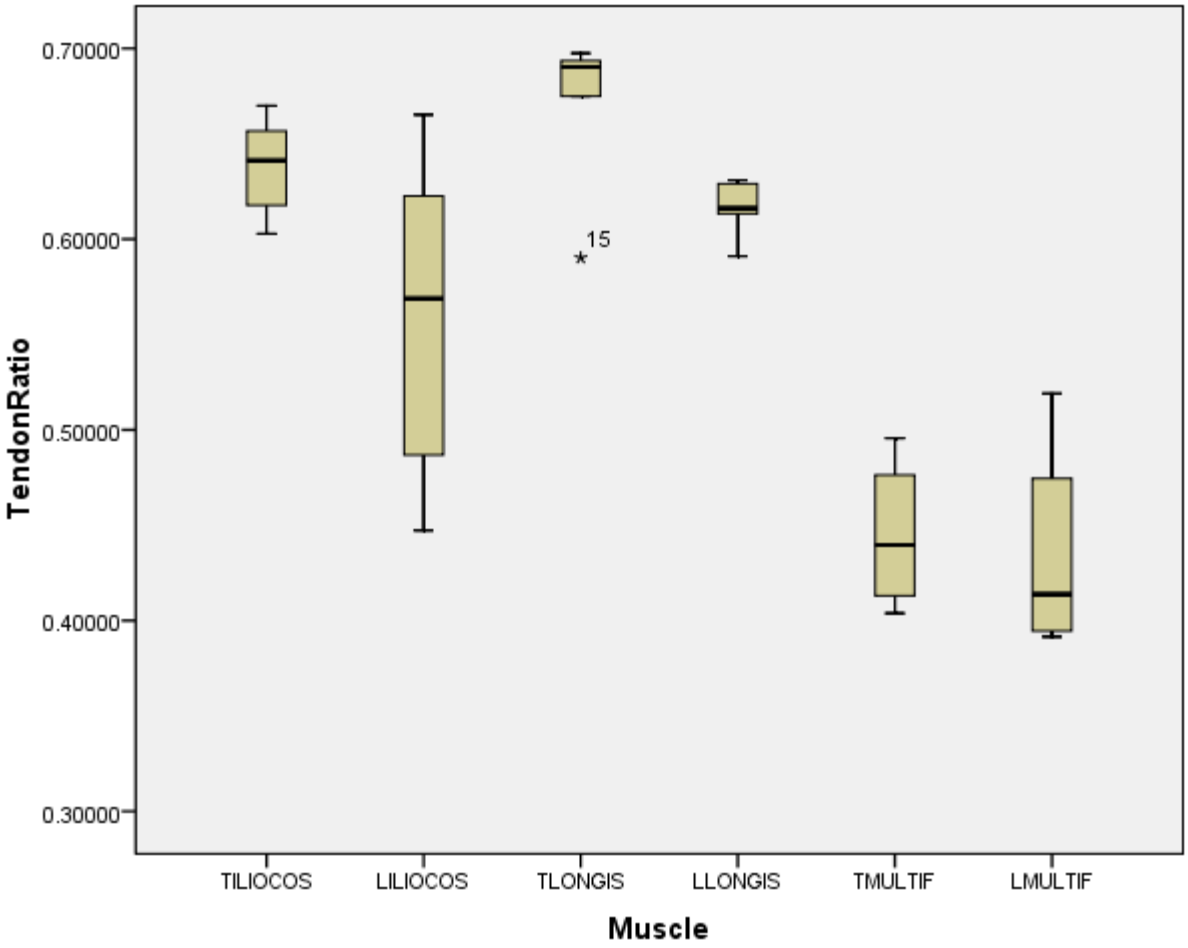

Fig. 64: *E. patas*: TL/(TL + NLf)

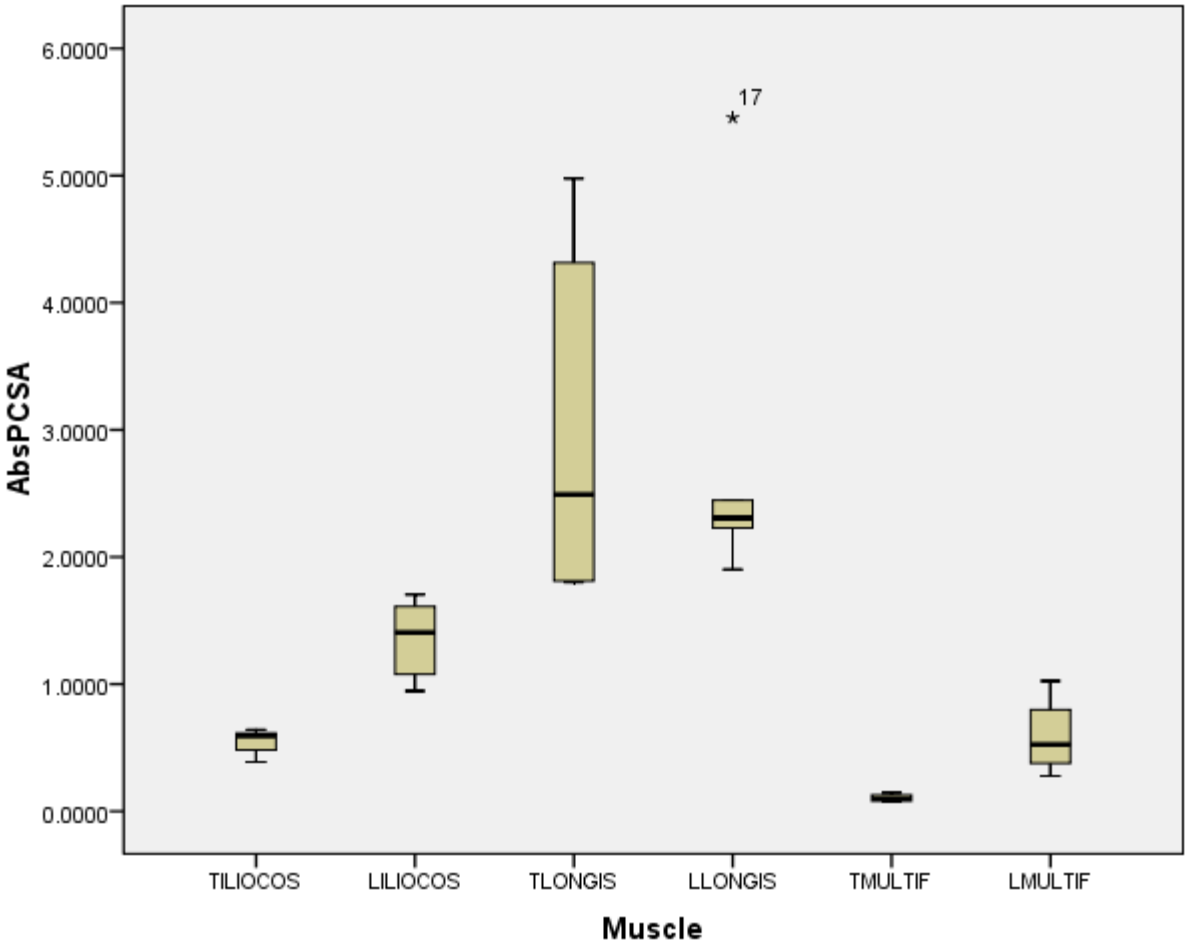

Fig. 65: *C. aethiops*: PCSA

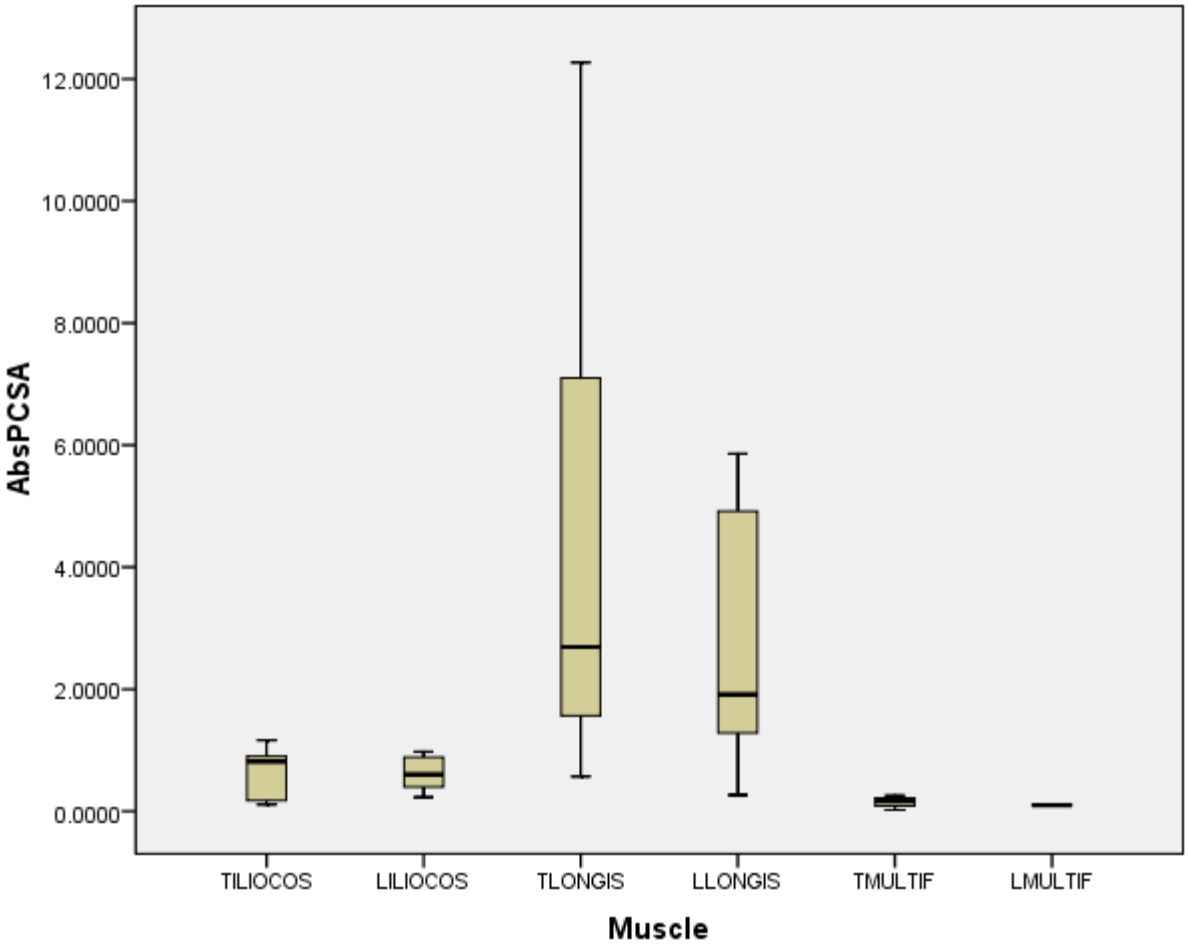

Fig. 66: *E. patas*: PCSA

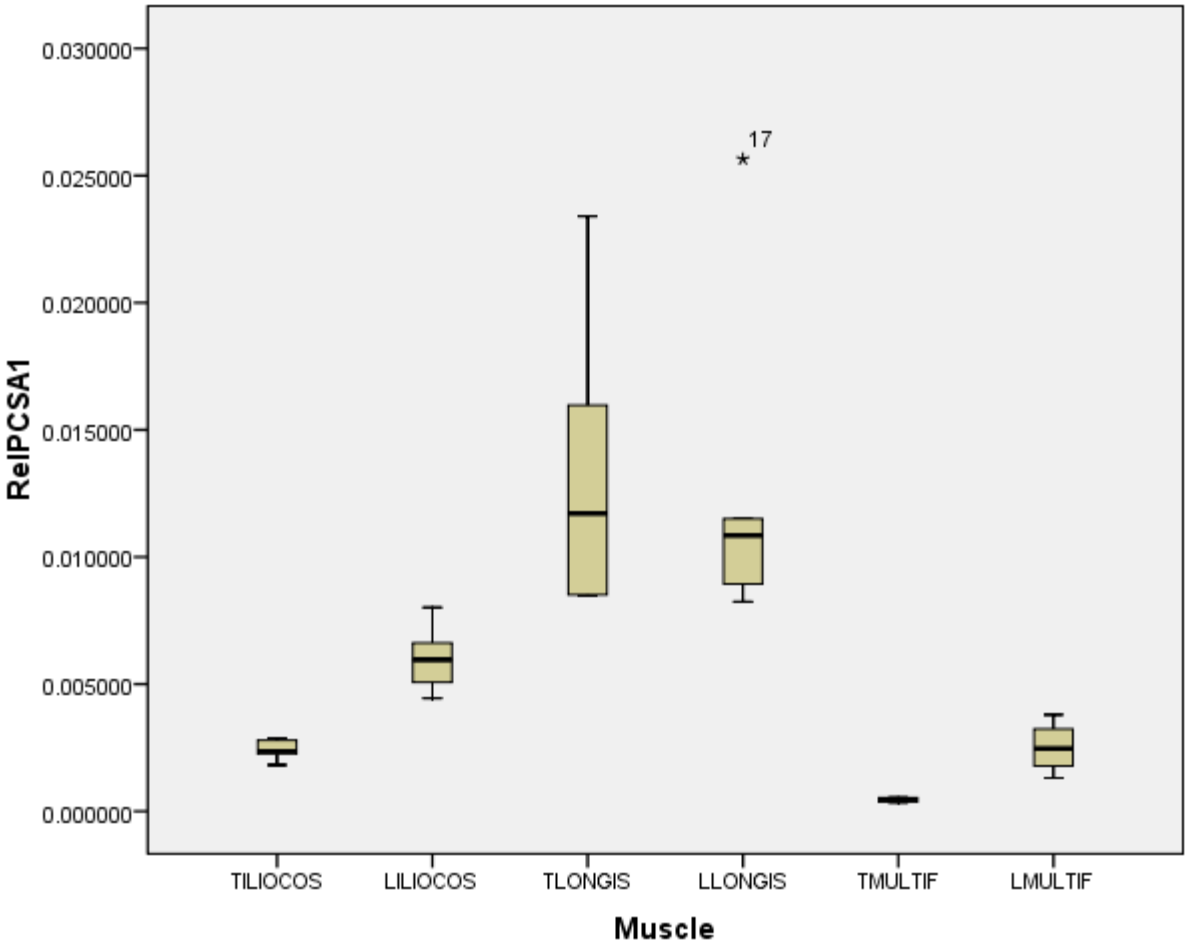

Fig. 67: *C. aethiops*: Relative PCSA-1 (to species mean body mass$^{0.67}$)

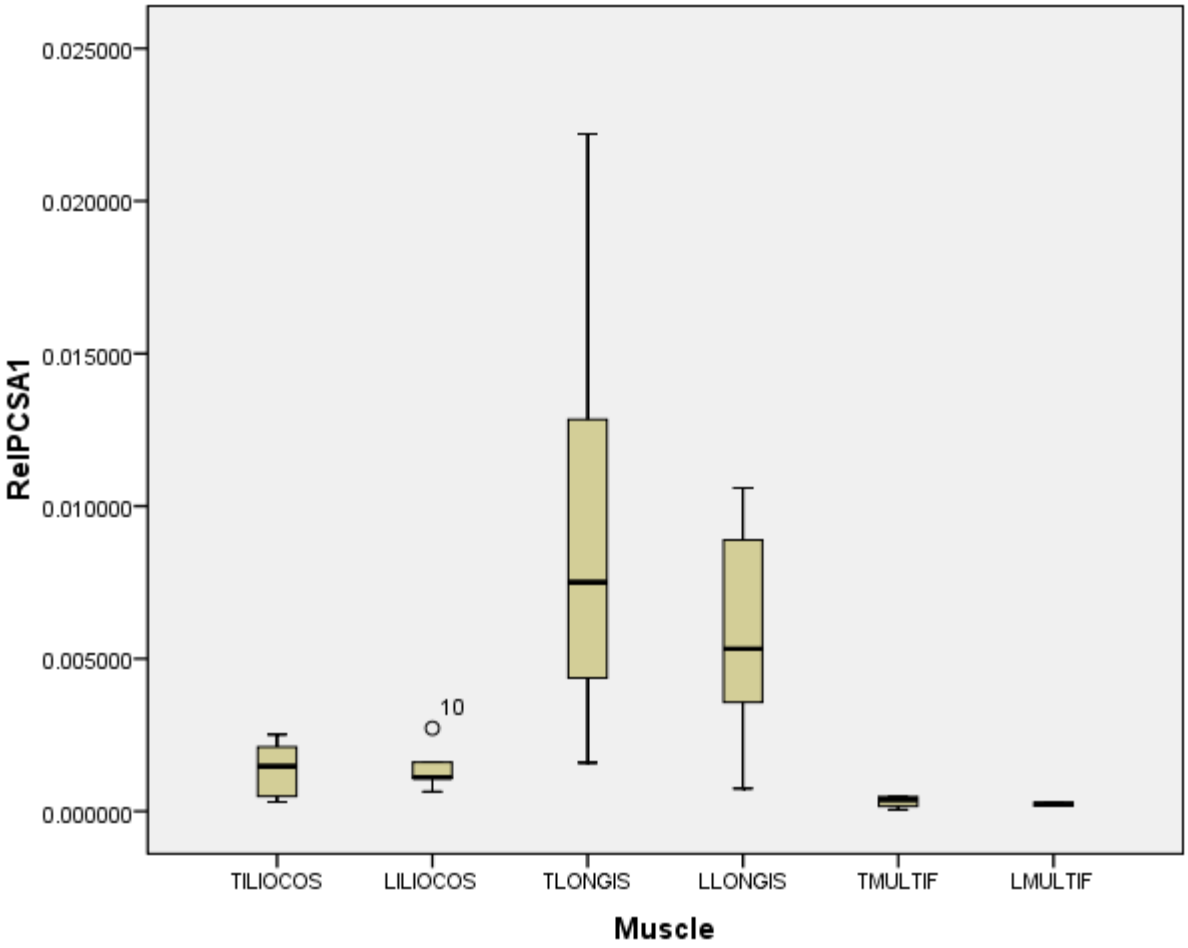

Fig. 68: *E. patas*: Relative PCSA-1 (to species mean body mass$^{0.67}$)

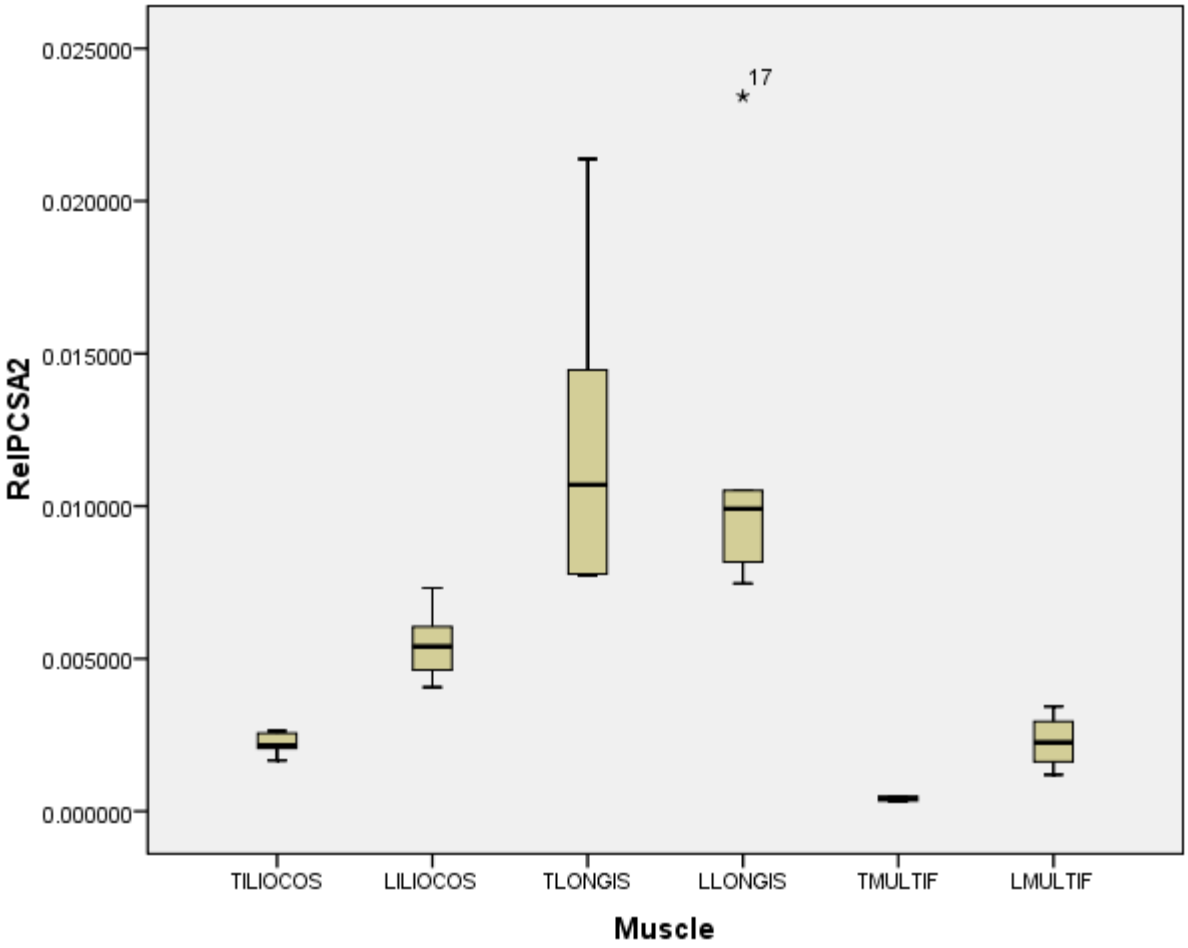

Fig. 69: *C. aethiops*: Relative PCSA-2 (to upper estimate of body mass$^{0.67}$)

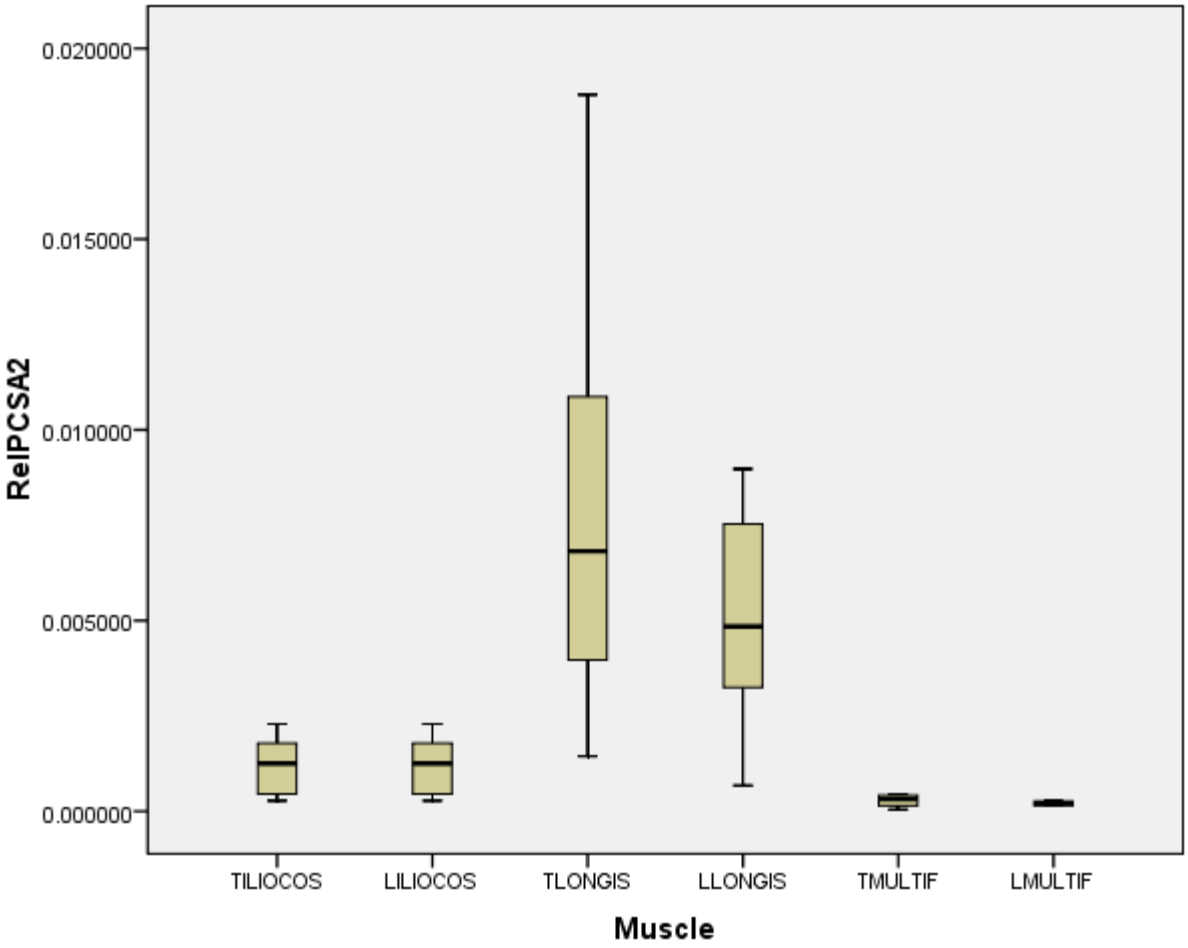

Fig. 70: *E. patas*: Relative PCSA-2 (to upper estimate of body mass$^{0.67}$)

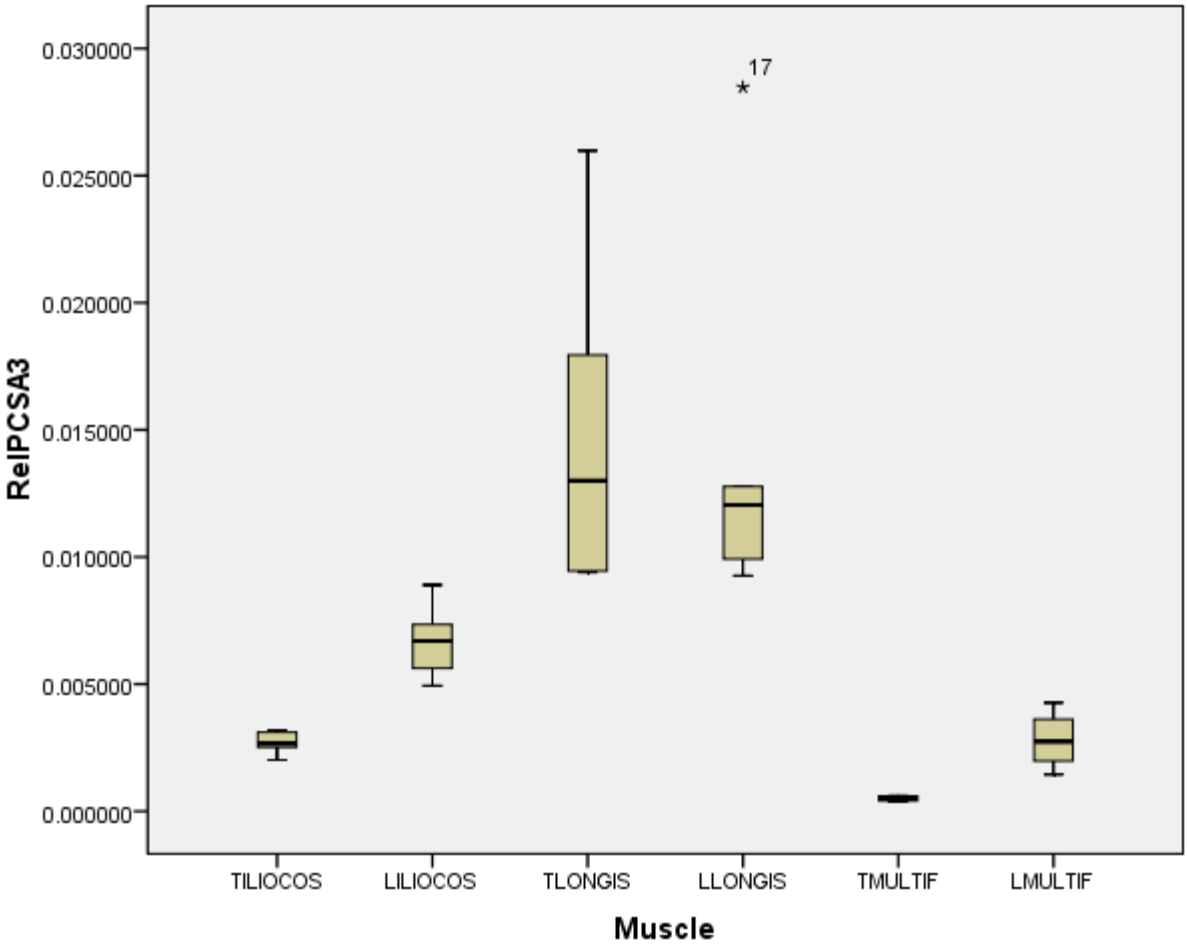

Fig. 71: *C. aethiops*: Relative PCSA-3 (to lower estimate of body mass$^{0.67}$)

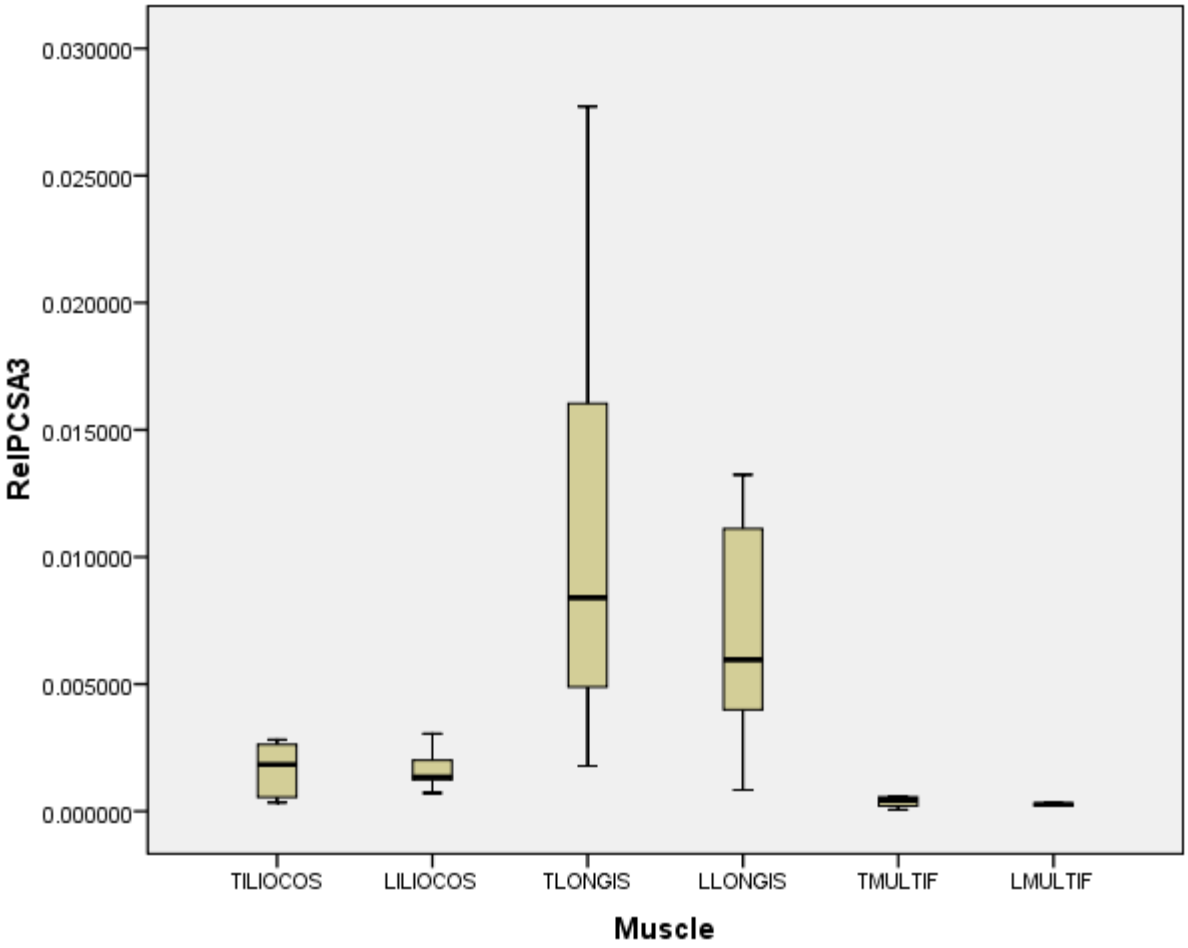

Fig. 72: *E. patas*: Relative PCSA-3 (to lower estimate of body mass$^{0.67}$)